



ISTANBUL  
UNIVERSITY  
PRESS

Indexed in  
Web of Science



# Istanbul Journal of Pharmacy

## Original Articles

**Clinical characteristics of patients undergoing coronary artery bypass surgery: Focus on gender differences**  
Gülsev Özen, Khadija Aljesri, Öznur Kızar, Gökçe Topal, Gülsüm Türkyılmaz, Saygın Türkyılmaz

**Ameliorative effects of melatonin on intestinal oxidative damage in streptozotocin-induced diabetic rats**  
Zatiye Ayça Çevikelli Yakut, Gizem Buse Akçay, Özge Çevik, Gökşel Şener

***Lactobacillus plantarum* and *Lactobacillus helveticus* modulate SIRT1, Caspase3 and Bcl-2 in the testes of high-fructose-fed rats**  
Onur Gökhan Yıldırım, Gökhan Sadi, Fatma Akar

**Anticancer and antituberculosis effects of 5-fluoro-1*H*-indole-2,3-dione 3-thiosemicarbazones**  
Zekiye Şeyma Sevinçli, Zerrin Cantürk, Miriç Dikmen, Nilgün Karalı

**Cytochrome P450 2A13 3375C>T gene polymorphism in a Turkish population**  
Zuhal Uçkun Şahinoğulları

**Evaluation of the hepatotoxic potential of citalopram in rats**  
Sinem Ilgin, Fulya Dağasan, Dilek Burukoğlu Dönmez, Merve Baysal, Özlem Atlı Eklioğlu

**Liquid chromatographic determination of citrinin residues in various meat products: A pioneer survey in Turkey**  
Fatih Mehmet Sarı, Ezgi Öztas, Sibel Özden, Gül Özhan

**Interaction of curcumin on cisplatin cytotoxicity in HeLa and HepG2 carcinoma cells**  
Merve Becit, Sevtap Aydın Dilsiz, Nursen Başaran

**Study of the beneficial effect of vanadium sulfate on the liver of experimental diabetic rats**  
Sevim Tunali, Ayşegül Peksel, İnci Arisan, Refiye Yanardağ

**Effect of gel formulation obtained from *Fomes fomentarius* on bleeding and clotting time: A pilot study**  
Gülşah Gedik, Hülya Asan, Anıl Özyurt, Hakan Allı, Ahmet Asan, Hakan Nazlı, Önder Sarp

**Development of inhalable cubosome nanoparticles of nystatin for effective management of invasive pulmonary aspergillosis**  
Marzuka Kazi, Mohamed Hassan Dehghan

**Chitosan films and chitosan/pectin polyelectrolyte complexes encapsulating silver sulfadiazine for wound healing**  
Gökçen Yaşayan

**Enhancing the antibacterial activity of the biosynthesized silver nanoparticles by "püse"**  
Arzu Özgen, Sinem Gürkan Aydın, Erdi Bilgiç

**Evaluation of Caco-2 cell permeability of ritonavir nanosuspensions**  
Alptuğ Karaküçük, Naile Öztürk, Nevin Çelebi

**Natural pigment of red-fleshed pitaya (*Hylocereus polyrhizus*) as dental plaque disclosing agent: A preliminary study**  
Amaliya Amaliya, Regi Taufik Firdaus, Nunung Rusminah

**Investigation of the effect of some plant aqueous extracts on calcium phosphate precipitation as a simulation of initial dental calculus formation *in vitro***  
Büşra Selmi Çepis, Serap Akyüz, Özlem Saçan, Refiye Yanardağ, Aysen Yarat

**Tyrosinase and cholinesterase inhibitory activities and molecular docking studies on apigenin and vitexin**  
Esen Sezen Karaoğlan, Mehmet Koca

**Isolation and characterization of antimicrobial compounds from *Cotinus coggygria* Scop. ethyl acetate extract**  
Ali Şen, Ayşe Seher Birteksöz Tan, Sükran Kültür, Leyla Bitiş

**Antispasmodic activities of the methanolic extract from aerial parts of *Origanum* species on excised rat ileum**  
Muhammet Emin Çam, Ayşe Nur Hazar Yavuz, Levent Kabasakal, Turgut Taşkın, Leyla Bitiş, Hatice Kübra Elçioğlu

***In vitro* adenosine deaminase inhibitory activity of some selected plant extracts and chemical compounds**  
Aris Tercan, Özlem Saçan

**Investigation of *in vitro* anti-hyperpigmentation, antidiabetic, neuroprotective and antioxidant potential of *Medicago murex* Willd. (Fabaceae)**  
Damla Pamukcu, Volkan Aylanc, Bülent Eskin, Gökhan Zengin, Mehmet Dursun, Yavuz Selim Çakmak

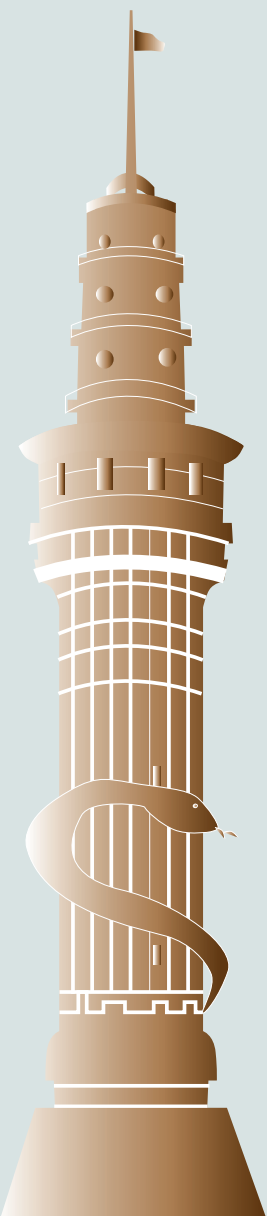
**Phenolic compounds and bioactivity of *Scorzonera pygmaea* Sibth. & Sm. aerial parts: *In vitro* antioxidant, anti-inflammatory and antimicrobial activities**  
Hasan Şahin, Aynur Sarı, Nurten Özsoy, Berna Özbek Çelik

**About the presence of *Pulmonaria angustifolia* L. (Boraginaceae) in Turkey**  
Bülent Olcay, Hüseyin Onur Tuncay

**Review Articles**

**Reshaping cytoskeleton: different acts of modulatory compounds**  
Pelin Zobaroğlu, Gamze Bora

**Vitamin-anticancer drug conjugates: a new era for cancer therapy**  
Ritesh P. Bhole, Shradha Jadhav, Yogesh B. Zambare, Rupesh V. Chikhale, Chandrakant G. Bonde





# Istanbul Journal of Pharmacy

## OWNER

Erdal CEVHER, Department of Pharmaceutical Technology, İstanbul University, Turkey

## EDITOR in CHIEF

Emine AKALIN, Department of Pharmaceutical Botany, İstanbul University, Turkey

## EDITORIAL ASSISTANT

Bahar GÜRDAL ABAMOR, Department of Pharmaceutical Botany, İstanbul University, Turkey

Gülsev ÖZEN, Department of Pharmacology, İstanbul University, Turkey

## EDITORS

Nuriye AKEV, Department of Biochemistry, İstanbul University, Turkey

Nilgün KARALI, Department of Pharmaceutical Chemistry, İstanbul University, Turkey

Yıldız ÖZSOY, Department of Pharmaceutical Technology, İstanbul University, Turkey

B.Sönmez UYDEŞ DOĞAN, Department of Pharmacology, İstanbul University, Turkey

## LANGUAGE EDITOR

Elizabeth Mary EARL, İstanbul University, Turkey

Alan James NEWSON, İstanbul University, Turkey

## STATISTICAL EDITOR

Abdulbari Bener, Department of Biostatistics & Medical Informatics, İstanbul University, Turkey

## EDITORIAL BOARD

Afife MAT, Department of Pharmacognosy, İstanbul University, Turkey

Berna ÖZBEK-ÇELİK, Department of Pharmaceutical Microbiology, İstanbul University, Turkey

Bilge ŞENER, Department of Pharmacognosy, Gazi University, Turkey

Carsten EHRHARDT, Panoz Institute, Trinity College Dublin, Ireland

Claudio T. SUPURAN, Neurofarba Department, University of Florence, Italy

Erden BANOĞLU, Department of Pharmaceutical Chemistry, Gazi University, Turkey

Fatma AKAR, Department of Pharmacology, Gazi University, Turkey

Gianniantonio DOMINA, University of Palermo, Italy

İlkay KÜÇÜKGÜZEL, Department of Pharmaceutical Chemistry, Marmara University, Turkey

Johan Van de VOORDE, Department of Pharmacology, Ghent University, Belgium

Melih ALTAN, Department of Pharmacology, Bezmialem University, Turkey

Meral ÖZALP, Department of Pharmaceutical Microbiology, Hacettepe University, Turkey

Müberra KOŞAR, Department of Pharmacognosy, Eastern Mediterranean University, Northern Cyprus

Nilüfer YÜKSEL, Department of Pharmaceutical Technology, Ankara University, Turkey

Nurşen BAŞARAN, Department of Pharmaceutical Toxicology, Hacettepe University, Turkey

Oya ALPAR, Department of Pharmaceutical Technology, Altınbaş University, Turkey and Department of Pharmaceutical Technology, UCL, UK

Özlem Nazan ERDOĞAN, Department of Pharmacy Management, İstanbul University, Turkey

Sıdıka TOKER, Department of Analytical Chemistry, İstanbul University, Turkey

Sibel ÖZDEN, Department of Pharmaceutical Toxicology, İstanbul University, Turkey

Stephen R. DOWNIE, Department of Plant Biology, University of Illinois, USA

Tao CHEN, Soochow University, China

Ufuk KOLAK, Department of Analytical Chemistry, İstanbul University, Turkey

Zeliha YAZICI, Department of Pharmacology, Biruni University, Turkey

• Sorumlu Yazı İşleri Müdürü / Responsible Manager: Münevver Bahar Gürdal • Yayın türü / Publication Type: Yaygın süreli / Periodical  
İstanbul Üniversitesi Eczacılık Fakültesi'nin yayınıdır / The journal is a publication of İstanbul University Faculty of Pharmacy. Yayıncı /  
Publisher: İstanbul University Press





# Istanbul Journal of Pharmacy

## AIMS AND SCOPE

Istanbul Journal of Pharmacy (Istanbul J Pharm) is an international, scientific, open access periodical published in accordance with independent, unbiased, and double-blinded peer-review principles. The journal is the official publication of İstanbul University Faculty of Pharmacy and it is published triannually on April, August, and December. The publication language of the journal is English.

Istanbul Journal of Pharmacy (Istanbul J Pharm) aims to contribute to the literature by publishing manuscripts at the highest scientific level on all fields of pharmaceutical sciences. The journal publishes original articles, short reports, letters to the editor and reviews.

The target audience of the journal includes specialists and professionals working and interested in all disciplines of pharmaceutical, also medicinal, biological and chemical sciences.

The editorial and publication processes of the journal are shaped in accordance with the guidelines of the International Committee of Medical Journal Editors (ICMJE), World Association of Medical Editors (WAME), Council of Science Editors (CSE), Committee on Publication Ethics (COPE), European Association of Science Editors (EASE), and National Information Standards Organization (NISO). The journal is in conformity with the Principles of Transparency and Best Practice in Scholarly Publishing (doaj.org/bestpractice).

Istanbul Journal of Pharmacy is currently indexed in Web of Science-Emerging Sources Citation Index, TUBITAK ULAKBIM TR Index and CAS database.

Processing and publication are free of charge with the journal. No fees are requested from the authors at any point throughout the evaluation and publication process. All manuscripts must be submitted via the online submission system, which is available at <http://dergipark.gov.tr/iujp>. The journal guidelines, technical information, and the required forms are available on the journal's web page.

All expenses of the journal are covered by the İstanbul University Faculty of Pharmacy. Potential advertisers should contact the Editorial Office. Advertisement images are published only upon the Editor-in-Chief's approval.

Statements or opinions expressed in the manuscripts published in the journal reflect the views of the author(s) and not the opinions of the İstanbul University Faculty of Pharmacy, editors, editorial board, and/or publisher; the editors, editorial board, and publisher disclaim any responsibility or liability for such materials.

Istanbul Journal of Pharmacy is an open access publication and the journal's publication model is based on Budapest Open Access Initiative (BOAI) declaration. Journal's archive is available online, free of charge at <http://ijp.istanbul.edu.tr>. İstanbul Journal of Pharmacy's content is licensed under a Creative Commons Attribution-NonCommercial 4.0 International License.



**Editor in Chief:** (Prof. Dr.) Emine AKALIN

**Address:** İstanbul University, Faculty of Pharmacy, Department of Pharmaceutical Botany, Beyazıt, 34116, Fatih İstanbul

**Phone:** +90 212 440 02 75

**Fax:** +90 212 440 02 52

**E-mail:** [akaline@istanbul.edu.tr](mailto:akaline@istanbul.edu.tr)

**Publisher:** İstanbul University Press

**Address:** İstanbul University Central Campus, 34452 Beyazıt, Fatih / İstanbul - Turkey

**Phone:** +90 212 440 00 00



## INSTRUCTIONS TO AUTHORS

### Context

Istanbul Journal of Pharmacy (Istanbul J Pharm) is an international, scientific, open access periodical published in accordance with independent, unbiased, and double-blinded peer-review principles. The journal is the official publication of İstanbul University Faculty of Pharmacy and it is published triannually on April, August, and December. The publication language of the journal is English.

Istanbul Journal of Pharmacy (Istanbul J Pharm) aims to contribute to the literature by publishing manuscripts at the highest scientific level on all fields of pharmaceutical sciences. The journal publishes original articles, short reports, letters to the editor and reviews.

### Editorial Policy

The editorial and publication processes of the journal are shaped in accordance with the guidelines of the International Council of Medical Journal Editors (ICMJE), the World Association of Medical Editors (WAME), the Council of Science Editors (CSE), the Committee on Publication Ethics (COPE), the European Association of Science Editors (EASE), and National Information Standards Organization (NISO). The journal conforms to the Principles of Transparency and Best Practice in Scholarly Publishing ([doaj.org/bestpractice](http://doaj.org/bestpractice)).

Originality, high scientific quality, and citation potential are the most important criteria for a manuscript to be accepted for publication. Manuscripts submitted for evaluation should not have been previously presented or already published in an electronic or printed medium. The journal should be informed of manuscripts that have been submitted to another journal for evaluation and rejected for publication. The submission of previous reviewer reports will expedite the evaluation process. Manuscripts that have been presented in a meeting should be submitted with detailed information on the organization, including the name, date, and location of the organization.

### Peer-Review Policy

Manuscripts submitted to İstanbul Journal of Pharmacy will go through a double-blind peer-review process. Each submission will be reviewed by at least two external, independent peer reviewers who are experts in their fields in order to ensure an unbiased evaluation process. The

editorial board will invite an external and independent editor to manage the evaluation processes of manuscripts submitted by editors or by the editorial board members of the journal. The Editor in Chief is the final authority in the decision-making process for all submissions.

### Ethical Principles

An approval of research protocols by the Ethics Committee in accordance with international agreements (World Medical Association Declaration of Helsinki "Ethical Principles for Medical Research Involving Human Subjects," amended in October 2013, [www.wma.net](http://www.wma.net)) is required for experimental, clinical, and drug studies. If required, ethics committee reports or an equivalent official document will be requested from the authors. For manuscripts concerning experimental research on humans, a statement should be included that shows that written informed consent of patients and volunteers was obtained following a detailed explanation of the procedures that they may undergo. For studies carried out on animals, the measures taken to prevent pain and suffering of the animals should be stated clearly. Information on patient consent, the name of the ethics committee, and the ethics committee approval number should also be stated in the Materials and Methods section of the manuscript. It is the authors' responsibility to carefully protect the patients' anonymity. For photographs that may reveal the identity of the patients, signed releases of the patient or of their legal representative should be enclosed.

### Plagiarism

All submissions are screened by a similarity detection software (iThenticate by CrossCheck) at any point during the peer-review or production process. Even if you are the author of the phrases or sentences, the text should not have unacceptable similarity with the previously published data.

When you are discussing others' (or your own) previous work, please make sure that you cite the material correctly in every instance.

In the event of alleged or suspected research misconduct, e.g., plagiarism, citation manipulation, and data falsification/fabrication, the Editorial Board will follow and act in accordance with COPE guidelines





## Authorship

Each individual listed as an author should fulfill the authorship criteria recommended by the International Committee of Medical Journal Editors (ICMJE - [www.icmje.org](http://www.icmje.org)). The ICMJE recommends that authorship be based on the following 4 criteria:

1. Substantial contributions to the conception or design of the work; or the acquisition, analysis, or interpretation of data for the work; AND
2. Drafting the work or revising it critically for important intellectual content; AND
3. Final approval of the version to be published; AND
4. Agreement to be accountable for all aspects of the work in ensuring that questions related to the accuracy or integrity of any part of the work are appropriately investigated and resolved.

In addition to being accountable for the parts of the work he/she has done, an author should be able to identify which co-authors are responsible for specific other parts of the work. In addition, authors should have confidence in the integrity of the contributions of their co-authors.

All those designated as authors should meet all four criteria for authorship, and all who meet the four criteria should be identified as authors. Those who do not meet all four criteria should be acknowledged in the title page of the manuscript.

Istanbul Journal of Pharmacy requires corresponding authors to submit a signed and scanned version of the authorship contribution form (available for download through <http://ijp.istanbul.edu.tr/en/>) during the initial submission process in order to act appropriately on authorship rights and to prevent ghost or honorary authorship. If the editorial board suspects a case of "gift authorship," the submission will be rejected without further review. As part of the submission of the manuscript, the corresponding author should also send a short statement declaring that he/she accepts to undertake all the responsibility for authorship during the submission and review stages of the manuscript.

## Conflict of Interest

Istanbul Journal of Pharmacy requires and encourages

the authors and the individuals involved in the evaluation process of submitted manuscripts to disclose any existing or potential conflicts of interests, including financial, consultant, and institutional, that might lead to potential bias or a conflict of interest. Any financial grants or other support received for a submitted study from individuals or institutions should be disclosed to the Editorial Board. To disclose a potential conflict of interest, the ICMJE Potential Conflict of Interest Disclosure Form should be filled in and submitted by all contributing authors. Cases of a potential conflict of interest of the editors, authors, or reviewers are resolved by the journal's Editorial Board within the scope of COPE and ICMJE guidelines.

The Editorial Board of the journal handles all appeal and complaint cases within the scope of COPE guidelines. In such cases, authors should get in direct contact with the editorial office regarding their appeals and complaints. When needed, an ombudsperson may be assigned to resolve cases that cannot be resolved internally. The Editor in Chief is the final authority in the decision-making process for all appeals and complaints.

## Copyright and Licensing

Istanbul Journal of Pharmacy requires each submission to be accompanied by a Copyright Agreement Form (available for download at <http://ijp.istanbul.edu.tr/en/>). When using previously published content, including figures, tables, or any other material in both print and electronic formats, authors must obtain permission from the copyright holder. Legal, financial and criminal liabilities in this regard belong to the author(s). By signing the Copyright Agreement Form, authors agree that the article, if accepted for publication by the Istanbul Journal of Pharmacy, will be licensed under a Creative Commons Attribution-NonCommercial 4.0 International License (CC-BY-NC).

## Disclaimer

Statements or opinions expressed in the manuscripts published in Istanbul Journal of Pharmacy reflect the views of the author(s) and not the opinions of the editors, the editorial board, or the publisher; the editors, the editorial board, and the publisher disclaim any responsibility or liability for such materials. The final responsibility in regard to the published content rests with the authors.



## MANUSCRIPT PREPARATION

The manuscripts should be prepared in accordance with ICMJE-Recommendations for the Conduct, Reporting, Editing, and Publication of Scholarly Work in Medical Journals (updated in December 2015 - <http://www.icmje.org/icmje-recommendations.pdf>). Authors are required to prepare manuscripts in accordance with the CONSORT guidelines for randomized research studies, STROBE guidelines for observational original research studies, STARD guidelines for studies on diagnostic accuracy, PRISMA guidelines for systematic reviews and meta-analysis, ARRIVE guidelines for experimental animal studies, and TREND guidelines for non-randomized public behavior.

Manuscripts can only be submitted through the journal's online manuscript submission and evaluation system, available at <http://ijp.istanbul.edu.tr/en/>. Manuscripts submitted via any other medium will not be evaluated.

Manuscripts submitted to the journal will first go through a technical evaluation process where the editorial office staff will ensure that the manuscript has been prepared and submitted in accordance with the journal's guidelines. Submissions that do not conform to the journal's guidelines will be returned to the submitting author with technical correction requests.

Authors are required to submit the following:

- Copyright Agreement Form
- Author Form
- Title Page

during the initial submission.

The manuscript should be prepared in MS Word format by using Times New Roman font (12 pt) and double-spaced on one side of the paper with adequate margins (2.5 cm).

### Preparation of the Manuscript

**Title page:** A separate title page should be submitted with all submissions and this page should include:

- The full title of the manuscript as well as a short title (running head) of no more than 50 characters,

- Name(s), affiliations, and highest academic degree(s) and ORCID ID(s) of the author(s),
- Grant information and detailed information on the other sources of support,
- Name, address, telephone (including the mobile phone number) and fax numbers, and email address of the corresponding author,
- Acknowledgment of the individuals who contributed to the preparation of the manuscript but who do not fulfill the authorship criteria.

**Abstract:** An structured abstract should be submitted with Original Articles (Background and Aims, Methods, Results, Conclusion). Please check Table 1 below for word count specifications.

**Keywords:** Each submission must be accompanied by a minimum of three to a maximum of six keywords for subject indexing at the end of the abstract. The keywords should be listed in full without abbreviations. The keywords should be selected from the National Library of Medicine, Medical Subject Headings database (<https://www.nlm.nih.gov/mesh/MBrowser.html>).

### Manuscript Types

**Original Articles:** This is the most important type of article since it provides new information based on original research. The main text of original articles should be structured with Introduction, Materials and Methods, Results, Discussion, and Conclusion subheadings. Results and Discussion sections can be combined under "Result and Discussion" heading. Please check Table 1 for the limitations for Original Articles.

Statistical analysis to support conclusions is usually necessary. Statistical analyses must be conducted in accordance with international statistical reporting standards (Altman DG, Gore SM, Gardner MJ, Pocock SJ. Statistical guidelines for contributors to medical journals. *Br Med J* 1983; 7; 1489-93). Information on statistical analyses with specified statistical software and descriptive details of the chemical used should be provided with a separate subheading under the Materials and Methods section.

Units should be prepared in accordance with the International System of Units (SI).



**Editorial Comments:** Editorial comments aim to provide a brief critical commentary by reviewers with expertise or with high reputation in the topic of the research article published in the journal. Authors are selected and invited by the journal to provide such comments. Abstract, Keywords, and Tables, Figures, Images, and other media are not included.

**Review Articles:** Reviews prepared by authors who have extensive knowledge on a particular field and whose scientific background has been translated into a high volume of publications with a high citation potential are welcomed. These authors may even be invited by the journal. Reviews should describe, discuss, and evaluate the current level of knowledge of a topic in clinical practice and should guide future studies. Please check Table 1 for the limitations for Review Articles.

**Short Papers:** Please check Table 1 for the limitations for Short Papers.

**Letters to the Editor:** This type of manuscript discusses important parts, overlooked aspects, or lacking parts of a previously published article. Articles on subjects within the scope of the journal that might attract the readers' attention, particularly educative cases, may also be submitted in the form of a "Letter to the Editor." Readers can also present their comments on the published manuscripts in the form of a "Letter to the Editor." Abstract, Keywords, and Tables, Figures, Images, and other media should not be included. The text should be unstructured. The manuscript that is being commented on must be properly cited within this manuscript.

## Tables

Tables should be included in the main document, pre-

ented after the reference list, and they should be numbered consecutively in the order they are referred to within the main text. A descriptive title must be placed above the tables. Abbreviations used in the tables should be defined below the tables by footnotes (even if they are defined within the main text). Tables should be created using the "insert table" command of the word processing software and they should be arranged clearly to provide easy reading. Data presented in the tables should not be a repetition of the data presented within the main text but should be supporting the main text.

## Figures and Figure Legends

Figures, graphics, and photographs should be submitted as separate files (in TIFF or JPEG format) through the submission system. The files should not be embedded in a Word document or the main document. When there are figure subunits, the subunits should not be merged to form a single image. Each subunit should be submitted separately through the submission system. Images should not be labeled (a, b, c, etc.) to indicate figure subunits. Thick and thin arrows, arrowheads, stars, asterisks, and similar marks can be used on the images to support figure legends. Like the rest of the submission, the figures too should be blind. Any information within the images that may indicate an individual or institution should be blinded. The minimum resolution of each submitted figure should be 300 DPI. To prevent delays in the evaluation process, all submitted figures should be clear in resolution and large in size (minimum dimensions: 100 × 100 mm). Figure legends should be listed at the end of the main document.

All acronyms, abbreviations, and symbols used in the manuscript must follow international rules and should be defined at first use, both in the abstract and in the

**Table 1. Limitations for each manuscript type**

Type of manuscript	Word limit	Abstract word limit	Table limit	Figure limit
Original Article	3500	250 (Structured)	6	7 or total of 15 images
Review Article	5000	250 (Unstructured)	6	10 or total of 20 images
Short Paper	1000	200	No tables	10 or total of 20 images
Letter to the Editor	500	No abstract	No tables	No media



main text. The abbreviation should be provided in parentheses following the definition.

For plant materials, herbarium name (or acronym), number, name and surname of the person who identified the plant materials should be indicated in the Materials and Methods section of the manuscript.

When a drug, product, hardware, or software program is mentioned within the main text, product information, including the name of the product, the producer of the product, and city and the country of the company (including the state if in USA), should be provided in parentheses in the following format: "Discovery St PET/CT scanner (General Electric, Milwaukee, WI, USA)"

All references, tables, and figures should be referred to within the main text, and they should be numbered consecutively in the order they are referred to within the main text. Limitations, drawbacks, and the shortcomings of original articles should be mentioned in the Discussion section before the conclusion paragraph.

## REFERENCES

### Reference Style and Format

Istanbul Journal of Pharmacy complies with APA (American Psychological Association) style 6th Edition for referencing and quoting. For more information:

- American Psychological Association. (2010). Publication manual of the American Psychological Association (6<sup>th</sup> ed.). Washington, DC: APA.
- <http://www.apastyle.org>

Accuracy of citation is the author's responsibility. All references should be cited in text. Reference list must be in alphabetical order. Type references in the style shown below

### Citations in the Text

Citations must be indicated with the author surname and publication year within the parenthesis.

If more than one citation is made within the same parenthesis, separate them with (;).

### Samples:

#### **More than one citation;**

(Esin et al., 2002; Karasar, 1995)

#### **Citation with one author;**

(Akyolcu, 2007)

#### **Citation with two authors;**

(Sayiner & Demirci, 2007)

#### **Citation with three, four, five authors;**

First citation in the text: (Ailen, Ciambune, & Welch, 2000) Subsequent citations in the text: (Ailen et al., 2000)

#### **Citations with more than six authors;**

(Çavdar et al., 2003)

### Citations in the Reference

All the citations done in the text should be listed in the References section in alphabetical order of author surname without numbering. Below given examples should be considered in citing the references.

### Basic Reference Types

#### Book

##### **a) Turkish Book**

Karasar, N. (1995). *Araştırmalarda rapor hazırlama* (8<sup>th</sup> ed.) [Preparing research reports]. Ankara, Turkey: 3A Eğitim Danışmanlık Ltd.

##### **b) Book Translated into Turkish**

Mucchielli, A. (1991). *Zihniyetler* [Mindsets] (A. Kotil, Trans.). İstanbul, Turkey: İletişim Yayınları.

##### **c) Edited Book**

Ören, T., Üney, T., & Çölkesen, R. (Eds.). (2006). *Türkiye bilişim ansiklopedisi* [Turkish Encyclopedia of Informatics]. İstanbul, Turkey: Papatya Yayıncılık.

##### **d) Turkish Book with Multiple Authors**

Tonta, Y., Bitirim, Y., & Sever, H. (2002). *Türkçe arama motorlarında performans değerlendirme* [Performance evaluation in Turkish search engines]. Ankara, Turkey: Total Bilişim.

##### **e) Book in English**

Kamien R., & Kamien A. (2014). *Music: An appreciation*. New York, NY: McGraw-Hill Education.

##### **f) Chapter in an Edited Book**

Bassett, C. (2006). Cultural studies and new media. In G. Hall & C. Birchall (Eds.), *New cultural studies: Adventures in theory* (pp. 220-237). Edinburgh, UK: Edinburgh University Press.



## **g) Chapter in an Edited Book in Turkish**

Erkmen, T. (2012). Örgüt kültürü: Fonksiyonları, öğeleri, işletme yönetimi ve liderlikteki önemi [Organization culture: Its functions, elements and importance in leadership and business management]. In M. Zencirkıran (Ed.), *Örgüt sosyolojisi* [Organization sociology] [pp. 233–263]. Bursa, Turkey: Dora Basım Yayın.

## **h) Book with the same organization as author and publisher**

American Psychological Association. (2009). *Publication manual of the American psychological association* (6<sup>th</sup> ed.). Washington, DC: Author.

## **Article**

### **a) Turkish Article**

Mutlu, B., & Savaşer, S. (2007). Çocuğu ameliyat sonrası yoğun bakımda olan ebeveynlerde stres nedenleri ve azaltma girişimleri [Source and intervention reduction of stress for parents whose children are in intensive care unit after surgery]. *Istanbul University Florence Nightingale Journal of Nursing*, 15(60), 179–182.

### **b) English Article**

de Cillia, R., Reisigl, M., & Wodak, R. (1999). The discursive construction of national identity. *Discourse and Society*, 10(2), 149–173. <http://dx.doi.org/10.1177/0957926599010002002>

### **c) Journal Article with DOI and More Than Seven Authors**

Lal, H., Cunningham, A. L., Godeaux, O., Chlibek, R., Diez-Domingo, J., Hwang, S.-J. ... Heineman, T. C. (2015). Efficacy of an adjuvanted herpes zoster subunit vaccine in older adults. *New England Journal of Medicine*, 372, 2087–2096. <http://dx.doi.org/10.1056/NEJMoa1501184>

### **d) Journal Article from Web, without DOI**

Sidani, S. (2003). Enhancing the evaluation of nursing care effectiveness. *Canadian Journal of Nursing Research*, 35(3), 26–38. Retrieved from <http://cjr.mcgill.ca>

### **e) Journal Article with DOI**

Turner, S. J. (2010). Website statistics 2.0: Using Google Analytics to measure library website effectiveness. *Technical Services Quarterly*, 27, 261–278. <http://dx.doi.org/10.1080/07317131003765910>

## **f) Advance Online Publication**

Smith, J. A. (2010). Citing advance online publication: A review. *Journal of Psychology*. Advance online publication. <http://dx.doi.org/10.1037/a45d7867>

## **g) Article in a Magazine**

Henry, W. A., III. (1990, April 9). Making the grade in today's schools. *Time*, 135, 28–31.

## **Doctoral Dissertation, Master's Thesis, Presentation, Proceeding**

### **a) Dissertation/Thesis from a Commercial Database**

Van Brunt, D. (1997). *Networked consumer health information systems* [Doctoral dissertation]. Available from ProQuest Dissertations and Theses database. [UMI No. 9943436]

### **b) Dissertation/Thesis from an Institutional Database**

Yaylı-Yıldız, B. (2014). *University campuses as places of potential publicness: Exploring the political, social and cultural practices in Ege University* [Doctoral dissertation]. Retrieved from Retrieved from: <http://library.iyte.edu.tr/tr/hizli-erisim/iyte-tez-portali>

### **c) Dissertation/Thesis from Web**

Tonta, Y. A. (1992). *An analysis of search failures in online library catalogs* [Doctoral dissertation, University of California, Berkeley]. Retrieved from <http://yunus.hacettepe.edu.tr/~tonta/yayinlar/phd/ickapak.html>

### **d) Dissertation/Thesis abstracted in Dissertations Abstracts International**

Appelbaum, L. G. (2005). Three studies of human information processing: Texture amplification, motion representation, and figure-ground segregation. *Dissertation Abstracts International: Section B. Sciences and Engineering*, 65(10), 5428.

### **e) Symposium Contribution**

Krinsky-McHale, S. J., Zigman, W. B., & Silverman, W. (2012, August). Are neuropsychiatric symptoms markers of prodromal Alzheimer's disease in adults with Down syndrome? In W. B. Zigman (Chair), *Predictors of mild cognitive impairment, dementia, and mortality in adults with Down syndrome*. Symposium conducted at the meeting of the American Psychological Association, Orlando, FL.

### **f) Conference Paper Abstract Retrieved Online**

Liu, S. (2005, May). *Defending against business crises with the help of intelligent agent based early warning solutions*. Paper presented at the Seventh



International Conference on Enterprise Information Systems, Miami, FL. Abstract retrieved from [http://www.iceis.org/iceis2005/abstracts\\_2005.htm](http://www.iceis.org/iceis2005/abstracts_2005.htm)

#### **g) Conference Paper - In Regularly Published Proceedings and Retrieved Online**

Herculano-Houzel, S., Collins, C. E., Wong, P., Kaas, J. H., & Lent, R. (2008). The basic nonuniformity of the cerebral cortex. *Proceedings of the National Academy of Sciences*, 105, 12593–12598. <http://dx.doi.org/10.1073/pnas.0805417105>

#### **h) Proceeding in Book Form**

Parsons, O. A., Pryzwansky, W. B., Weinstein, D. J., & Wiens, A. N. (1995). Taxonomy for psychology. In J. N. Reich, H. Sands, & A. N. Wiens (Eds.), *Education and training beyond the doctoral degree: Proceedings of the American Psychological Association National Conference on Postdoctoral Education and Training in Psychology* (pp. 45–50). Washington, DC: American Psychological Association.

#### **i) Paper Presentation**

Nguyen, C. A. (2012, August). *Humor and deception in advertising: When laughter may not be the best medicine*. Paper presented at the meeting of the American Psychological Association, Orlando, FL.

#### **Other Sources**

##### **a) Newspaper Article**

Browne, R. (2010, March 21). This brainless patient is no dummy. *Sydney Morning Herald*, 45.

##### **b) Newspaper Article with no Author**

New drug appears to sharply cut risk of death from heart failure. (1993, July 15). *The Washington Post*, p. A12.

##### **c) Web Page/Blog Post**

Bordwell, D. (2013, June 18). David Koepf: Making the world movie-sized [Web log post]. Retrieved from <http://www.davidbordwell.net/blog/page/27/>

##### **d) Online Encyclopedia/Dictionary**

Ignition. (1989). In *Oxford English online dictionary* (2<sup>nd</sup> ed.). Retrieved from <http://dictionary.oed.com>

Marcoux, A. (2008). Business ethics. In E. N. Zalta (Ed.). *The Stanford encyclopedia of philosophy*. Retrieved from <http://plato.stanford.edu/entries/ethics-business/>

##### **e) Podcast**

Dunning, B. (Producer). (2011, January 12). *inFact: Conspiracy theories* [Video podcast]. Retrieved from <http://itunes.apple.com/>

##### **f) Single Episode in a Television Series**

Egan, D. (Writer), & Alexander, J. (Director). (2005). Failure to communicate. [Television series episode]. In D. Shore (Executive producer), *House*; New York, NY: Fox Broadcasting.

##### **g) Music**

Fuchs, G. (2004). Light the menorah. On *Eight nights of Hanukkah* [CD]. Brick, NJ: Kid Kosher.

#### **REVISIONS**

When submitting a revised version of a paper, the author must submit a detailed “Response to the reviewers” that states point by point how each issue raised by the reviewers has been covered and where it can be found (each reviewer’s comment, followed by the author’s reply and line numbers where the changes have been made) as well as an annotated copy of the main document. Revised manuscripts must be submitted within 30 days from the date of the decision letter. If the revised version of the manuscript is not submitted within the allocated time, the revision option may be cancelled. If the submitting author(s) believe that additional time is required, they should request this extension before the initial 30-day period is over.

Accepted manuscripts are copy-edited for grammar, punctuation, and format. Once the publication process of a manuscript is completed, it is published online on the journal’s webpage as an ahead-of-print publication before it is included in its scheduled issue. A PDF proof of the accepted manuscript is sent to the corresponding author and their publication approval is requested within 2 days of their receipt of the proof.

**Editor in Chief:** Emine AKALIN

**Address:** İstanbul University Faculty of Pharmacy, İstanbul, Turkey

**Phone:** +90 212 440 02 75

**Fax:** +90 212 440 02 52

**E-mail:** [jfacpharm@istanbul.edu.tr](mailto:jfacpharm@istanbul.edu.tr)

**Publisher:** İstanbul University Press

**Address:** İstanbul University Central Campus, 34452 Beyazıt, Fatih / İstanbul - Turkey

**Phone:** +90 212 440 00 00





## CONTENTS

### ORIGINAL ARTICLES

- Clinical characteristics of patients undergoing coronary artery bypass surgery:  
Focus on gender differences** .....153  
Gülsev Özen, Khadija Aljesri, Öznur Kızar, Gökçe Topal, Gülsüm Türkyılmaz, Saygın Türkyılmaz
- Ameliorative effects of melatonin on intestinal oxidative damage in streptozotocin-induced  
diabetic rats** .....160  
Zatiye Ayça Çevikelli Yakut, Gizem Buse Akçay, Özge Çevik, Göksel Şener
- Lactobacillus plantarum* and *Lactobacillus helveticus* modulate SIRT1, Caspase3 and Bcl-2  
in the testes of high-fructose-fed rats** .....168  
Onur Gökhan Yıldırım, Gökhan Sadı, Fatma Akar
- Anticancer and antituberculosis effects of 5-fluoro-1*H*-indole-2,3-dione 3-thiosemicarbazones** .....176  
Zekiye Şeyma Sevinçli, Zerrin Cantürk, Miriş Dikmen, Nilgün Karalı
- Cytochrome P450 2A13 3375C>T gene polymorphism in a Turkish population** .....181  
Zuhal Uçkun Şahinoğulları
- Evaluation of the hepatotoxic potential of citalopram in rats** .....188  
Sinem İlgin, Fulya Dağaşan, Dilek Burukoğlu Dönmez, Merve Baysal, Özlem Atlı Eklioğlu
- Liquid chromatographic determination of citrinin residues in various meat products:  
A pioneer survey in Turkey** .....195  
Fatih Mehmet Sarı, Ezgi Öztaş, Sibel Özden, Gül Özhan
- Interaction of curcumin on cisplatin cytotoxicity in HeLa and HepG2 carcinoma cells** .....202  
Merve Becit, Sevtap Aydın Dilsiz, Nurşen Başaran
- Study of the beneficial effect of vanadium sulfate on the liver of experimental diabetic rats** .....211  
Sevim Tunalı, Ayşegül Peksel, İnci Arısan, Refiye Yanardağ
- Effect of gel formulation obtained from *Fomes fomentarius* on bleeding and clotting time:  
A pilot study** .....216  
Gülşah Gedik, Hülya Asan, Anıl Özyurt, Hakan Allı, Ahmet Asan, Hakan Nazlı, Önder Sarp
- Development of inhalable cubosome nanoparticles of nystatin for effective management of  
invasive pulmonary aspergillosis** .....224  
Marzuka Kazi, Mohamed Hassan Dehghan
- Chitosan films and chitosan/pectin polyelectrolyte complexes encapsulating silver sulfadiazine  
for wound healing** .....238  
Gökçen Yaşayan
- Enhancing the antibacterial activity of the biosynthesized silver nanoparticles by “püse”** .....245  
Arzu Özgen, Sinem Gürkan Aydın, Erdi Bilgiç





## CONTENTS

### ORIGINAL ARTICLES

- Evaluation of Caco-2 cell permeability of ritonavir nanosuspensions .....251  
Alptuğ Karaküçük, Naile Öztürk, Nevin Çelebi
- Natural pigment of red-fleshed pitaya (*Hylocereus polyrhizus*) as dental plaque disclosing agent:  
A preliminary study .....256  
Amaliya Amaliya, Regi Taufik Firdaus, Nunung Rusminah
- Investigation of the effect of some plant aqueous extracts on calcium phosphate precipitation  
as a simulation of initial dental calculus formation *in vitro* .....262  
Büşra Selmi Çepiş, Serap Akyüz, Özlem Saçan, Refiye Yanardağ, Aysen Yarat
- Tyrosinase and cholinesterase inhibitory activities and molecular docking studies on apigenin and vitexin .....268  
Esen Sezen Karaoğlan, Mehmet Koca
- Isolation and characterization of antimicrobial compounds from *Cotinus coggygia* Scop. ethyl  
acetate extract .....272  
Ali Şen, Ayşe Seher Birteksöz Tan, Şükran Kültür, Leyla Bitiş
- Antispasmodic activities of the methanolic extract from aerial parts of *Origanum* species on excised  
rat ileum .....277  
Muhammet Emin Çam, Ayşe Nur Hazar Yavuz, Levent Kabasakal, Turgut Taşkın, Leyla Bitiş, Hatice Kübra Elçioğlu
- In vitro* adenosine deaminase inhibitory activity of some selected plant extracts and chemical compounds .....283  
Aris Tercan, Özlem Saçan
- Investigation of *in vitro* anti-hyperpigmentation, antidiabetic, neuroprotective and antioxidant potential of  
*Medicago murex* Willd.. (Fabaceae) .....289  
Damla Pamukcu, Volkan Aylaç, Bülent Eskin, Gökhan Zengin, Mehmet Dursun, Yavuz Selim Çakmak
- Phenolic compounds and bioactivity of *Scorzonera pygmaea* Sibth. & Sm. aerial parts:  
*In vitro* antioxidant, anti-inflammatory and antimicrobial activities .....294  
Hasan Şahin, Aynur Sarı, Nurten Özsoy, Berna Özbek Çelik
- About the presence of *Pulmonaria angustifolia* L. (Boraginaceae) in Turkey .....300  
Bülent Olçay, Hüseyin Onur Tuncay

### REVIEW ARTICLES

- Reshaping cytoskeleton: different acts of modulatory compounds .....304  
Pelın Zobaroğlu, Gamze Bora
- Vitamin-anticancer drug conjugates: a new era for cancer therapy .....312  
Ritesh P. Bhole, Shradha Jadhav, Yogesh B. Zambare, Rupesh V. Chikhale, Chandrakant G. Bonde



## IN THE MEMORY AND HONOR OF PROF. DR. KASIM CEMAL GÜVEN

### Prof. Dr. Kasım Cemal Güven



Professor Prof. Dr. Kasım Cemal Güven was born in Trabzon, Beşikdüzü in 1925, graduated from Istanbul University College of Pharmacy in 1946 and assigned as a research assistant in pharmaceutical chemistry at the same college in 1947. He worked as a pharmacist in Elbistan, Kahramanmaraş between 1948 and 1950. He returned back to Istanbul University Faculty of Pharmacy in 1950. After receiving his PhD degree on Pharmaceutical Technology (formerly named as Galenic) in 1953, he gained the academic degree of Associate Professor in 1956 and Professor in 1965. Prof. Dr. Güven was the Dean of Faculty of Pharmacy of Istanbul University in between 1965 and 1969.

Prof. Dr. Güven conducted research projects at Munich University (Germany) with a DAAD fellowship in 1964 and at Münster University in 1984.

Prof. Dr. Güven's main research interest was on galenical pharmacy/pharmaceutical technology. In addition to his main research area, he has published over 300 national and international publications and scientific papers covering topics such as synthesis and stability of drugs, chemistry of land plants, chemistry of sea animals (enzymes, insulin, heparin), chemistry of land and marine algae, and sea pollution. His publications have been cited in over 45 books and over 200 research papers. One of his most popular book was "**The Medical Formulary**" which aimed to give a detailed information related to the properties and preparation of majistral products as well as to give some scales that frequently used in Medicine and Pharmaceutics and also to give some examples of cosmetic preparations. For many years, this book served as a valuable guide for the Pharmacy students educated in different Faculties of Pharmacy in Turkey.







He was also the author of many scientific and vocational books dealing with pharmaceutical technology and pharmaceutical sciences. During his academic career, he was the advisor of more than 50 PhD and master theses.

In 1953, Professor Güven initiated publication of *Acta Pharm.Scientia* (formerly *Pharmaceutical Bulletin*), and as editor, he ensured continued publication of the journal until 2011. In addition, he was the editor of scientific journals such as *Journal of the Black Sea / Mediterranean Environment*.

After retiring from Istanbul University Faculty of Pharmacy Department of Pharmaceutical Technology in 1991, he gave doctorate lectures about chemical carcinogens at Istanbul University Oncology Institute, he served as a consultant for Istanbul Public Health Institute, and he continued his research at Istanbul University Institute of Marine Sciences and Management for many years.

Prof. Dr. Yıldız Özsoy

# Clinical characteristics of patients undergoing coronary artery bypass surgery: Focus on gender differences

Gülsev Özen<sup>1</sup> , Khadija Aljesri<sup>1</sup> , Öznur Kızır<sup>2</sup> , Gökçe Topal<sup>1</sup> , Gülsüm Türkyılmaz<sup>3</sup> ,  
Saygın Türkyılmaz<sup>3</sup> 

<sup>1</sup>Istanbul University, Faculty of Pharmacy, Department of Pharmacology, Istanbul, Turkey

<sup>2</sup>Istanbul University, Faculty of Pharmacy, Istanbul, Turkey

<sup>3</sup>Bakirkoy Dr Sadi Konuk Education and Research Hospital, Department of Cardiovascular Surgery, Istanbul, Turkey

**ORCID IDs of the authors:** G.Ö 0000-0002-8862-383X; K.A. 0000-0002-8527-5438; Ö.K. 0000-0002-4903-3677;  
G.T. 0000-0001-7196-3179; G.T. 0000-0001-6910-7664; S.T. 0000-0003-2165-6853

**Cite this article as:** Ozen, G., Aljesri, K., Kizar, O., Topal, G., Turkyilmaz G., & Turkyilmaz, S. (2020). Clinical characteristics of patients undergoing coronary artery bypass surgery: Focus on gender differences. *Istanbul Journal of Pharmacy*, 50 (3), 153-159.

## ABSTRACT

**Background and Aims:** The aim of the present study is to investigate whether the clinical characteristics of patients undergoing coronary artery bypass surgery (CABG) differ by sex.

**Methods:** This study was performed with a total of 58 patients who underwent CABG. The age, weight, height, systolic and diastolic blood pressure, HbA1c, high-density lipoprotein (HDL), low-density lipoprotein (LDL) and total cholesterol values together with the demographic characteristics of patients undergoing CABG were collected and compared between male and female patients.

**Results:** In the present study, 71% of patients undergoing CABG were men and 29% of them were women. There was no significant difference in weight, systolic and diastolic blood pressure, HbA1c, and total cholesterol values between male and female patients. Body mass index, LDL and HDL levels, the ratios of LDL/total cholesterol and HDL/total cholesterol were higher while height was lower in females compared to male patients.

**Conclusion:** Our study highlights the need for sex-specific approaches in the prevention of coronary artery diseases. Risk factors including obesity, diabetes, hypertension, and dyslipidemia influence the outcome of death in patients undergoing CABG. Correct management of controllable risk factors with the focus on gender differences could be beneficial in reducing mortality and morbidity rates by altering the prognosis of coronary artery diseases.

**Keywords:** Coronary artery bypass surgery, patient characteristics, gender differences, cardiovascular risk factors

## INTRODUCTION

Cardiovascular diseases are the most common cause of death globally and are the major contributor to the burden of premature mortality and morbidity. According to the WHO, cardiovascular diseases are responsible for approximately 17.9 million deaths every year (World Health Organization, 2017, [https://www.who.int/health-topics/cardiovascular-diseases/#tab=tab\\_1](https://www.who.int/health-topics/cardiovascular-diseases/#tab=tab_1)). More than 75% of these deaths occur in low or middle income countries (Roth et al., 2017).

Among cardiovascular diseases, coronary artery disease (CAD), occurs primarily as a result of atherosclerosis of coronary arteries where plaque builds up inside them. Generally, patients with CAD are classified into two types according to their symptoms

### Address for Correspondence:

Gülsev ÖZEN, e-mail: [gulsevozen@istanbul.edu.tr](mailto:gulsevozen@istanbul.edu.tr)

This work is licensed under a Creative Commons Attribution 4.0 International License.



Submitted: 29.06.2020  
Revision Requested: 18.07.2020  
Last Revision Received: 21.07.2020  
Accepted: 10.08.2020

(Cowell, Newby, & Boon, 2004; Quertermous & Ingelsson, 2016). The first type is patients with chronic stable angina characterized by myocardial ischemia, which develops as a result of an imbalance between the oxygen demand of myocardium and the oxygen supply, and is often accompanied by chest pain (Kabakçı et al., 1990). The second type is acute coronary syndrome which is also known as acute myocardial infarction (MI) and unstable angina (Cowell et al., 2004), where a plaque rupture, plaque erosion and coronary thrombosis may develop and sudden coronary death may occur (Otsuka et al., 2015). The severity of CAD and treatment options are determined by the type and number of coronary arteries where stenosis occurs. Pharmacological therapy in the treatment of CAD is applied in order to reduce myocardial oxygen demand and increase myocardial blood flow to the heart. This treatment is carried out with various agents including nitrates, beta-blockers, angiotensin converting enzyme inhibitors, antiplatelets, and anticoagulation agents (Willerson & Helmes, 2015). Coronary revascularization is another frequently preferred safe and effective treatment method that improves myocardial perfusion and relieves myocardial ischemia symptoms (Wilson, 2015). Percutaneous coronary intervention (PCI) or coronary angioplasty is a widely used invasive treatment (Madhavan, Gersh & Alexander, 2018). In severe cases where patients are not responding to other pharmacological treatment methods, a coronary artery bypass graft operation (CABG) represents a superior surgical intervention for myocardial revascularization (Samak et al., 2016).

CABG is an important surgical procedure that improves blood flow to the heart by using venous or arterial grafts to bypass the part of the coronary artery where occlusion due to atherosclerosis occurs (Jannati, Navaei, & Ronizi, 2019). The CABG is known to be one of the most common surgical procedures worldwide with approximately 400,000 CABGs performed annually in the United States (Alexander & Smith, 2016). The success of a CABG depends on the long-term patency of venous or arterial grafts (Goldman et al., 2004). However, surgical trends have decreased as the use of alternative options such as medical treatment and PCI have increased (Bachar & Manna, 2020).

Hypertension, dyslipidemia, diabetes, kidney dysfunction, age, gender, lifestyle, cigarette smoking, diet, obesity, and family history have been found to be common risk factors for CAD in patients. Controlling these risk factors through lifestyle changes and, when necessary, through medical treatment can help to prevent CAD (Madhavan et al., 2018; Shao, Wang & Tian, 2020). Development of CAD in women when they are younger occurs less than in men because of the protective effects of oestrogen. A long-term follow up study indicated that high levels of total cholesterol and low-density lipoprotein (LDL), as well as diabetes eliminate the female advantage (Koch, Khandwala & Nussmeier, 2003; Bonow, Smaha & Smith 2002; Kannel & Wilson, 1995). Furthermore, in the post-menopausal period, the same frequency of CAD was detected for both genders (Ahmad et al., 2010).

Several studies have indicated that female gender is an independent predictor of poor post-operative outcome after CABG and this could be due to differences in clinical characteristics between female and male patients (Nicolini et al., 2016; Em-

mert et al., 2010; Bukkapatnam, Yeo & Li, 2010). In the present study, age, weight, height, systolic and diastolic blood pressure, HbA1c (glycated haemoglobin), high-density lipoprotein (HDL), LDL, and total cholesterol values together with the demographic characteristics of patients undergoing CABG were collected and compared between male and female patients.

## MATERIALS AND METHODS

### Subjects

This study was performed with a total of 58 patients who underwent CABG in Bakirkoy Dr Sadi Konuk Education and Research Hospital between November 2018 and August 2019. Personal information and the pre-operative worksheet were used to obtain patients' clinical characteristics. Subjects in all age groups who underwent CABG surgery were included in the study. Exclusion criteria were as follows: Previous cardiac surgery (open), aortic and mitral disease, concomitant procedures (e.g., aortic annulus enlargement, ascending aorta replacement, more than single-valve surgery) and tricuspid annuloplasty. Patient's gender, age, weight, height, systolic and diastolic blood pressure, HbA1c, HDL, LDL and total cholesterol values together with their demographic characteristics were collected and recorded. The study was approved by the Institutional Review Board of Istanbul University, Institute of Cardiology (no: İ.Ü.E.50.0.05.00/8). Patients enrolled in this study gave informed consent for all investigations.

### Statistical analysis

The patients' age, weight, height, systolic and diastolic blood pressure, HbA1c, HDL, LDL and total cholesterol values were expressed in terms of their mean  $\pm$  standard error of mean (SEM). Body mass index (BMI) was calculated by dividing weight in kg by height in meter squared. Statistical analysis was performed using the Student's t-test. P value  $<0.05$  indicated that data is significantly different. The statistical analysis was performed by using Graph Pad (Prism 7) software.

## RESULTS AND DISCUSSION

Increased rates of in-hospital morbidity after CABG were observed in women (Koch et al., 2003). Furthermore, a meta analysis study including 966,492 patients reported that women had an increased risk for short-term, mid-term and long-term mortality compared with men undergoing CABG (Alam et al., 2013). This could be due to an unfavorable preoperative risk profile in women. In order to investigate this hypothesis, in the present study we compared several risk factors for CAD between women and men undergoing CABG in Turkey.

In the present study, 71% of the patients undergoing CABG were men and 29% of them were women. In accordance with our results, several studies indicated that the majority of patients who had undergone CABG were males (Ahmad et al., 2010; Koch et al., 2003; Varma et al., 2014; Elbardissi et al., 2012; Seccareccia et al., 2006; Dinh et al., 2008; McNeely, Markwell, & Vassileva, 2016). Our study demonstrated that the mean age was 61 years for both men ( $61 \pm 1.96$ ) and women ( $61 \pm 1.38$ ). The age distribution of both genders is presented in Figure 1. The majority (47%) of women were between 60-70 years-old

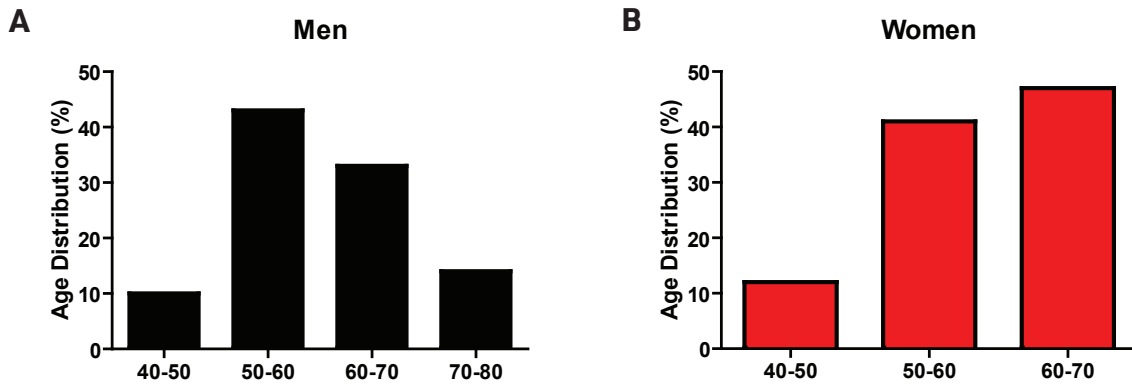


**Figure 1.** Age distribution of patients who underwent coronary artery bypass surgery. Age distribution is presented as percentage of number of patients (n value for men: 41, for women: 17).

while the majority of men (43%) were between 50-60 years-old. A different study performed on stable outpatients with suspected CAD demonstrated that mean age was 59 years for men and 62 years for women (Hemal et al., 2016). In accordance with that study, another study performed on patients undergoing CABG in Saudi Arabia demonstrated that women were significantly older than men (Ahmad et al., 2010). The discrepancy between these studies and our current results could be due to different ethnic groups included in these studies. In fact, Varma *et al.* compared the findings obtained from Indian and Western populations undergoing CABG (Varma et al., 2014). The mean age of Indian patients was 57 years while it was greater than 65 years in Western patients (Varma et al., 2014). This result is in accordance with the high risk profile of CAD in Asian-Indians (Ajay & Prabhakaran, 2010). Furthermore, a recent study investigated the ages of patients undergoing

CABG from 1997 to 2011 in the United States and reported an increase in the mean of patient age with time (Cornwell, Omer & Rosengart, 2015). Also, another study demonstrated an increase in mean age among US patients undergoing CABG from 2000 to 2009 (Elbardissi et al., 2012). These studies emphasized that ethnic groups and also the year when the studies were conducted could affect the results.

Obesity is an important risk factor for the development of CAD (Ades & Savage, 2017). Furthermore, obesity is found to be a significant independent predictor for adverse outcomes and prolonged hospitalization after CABG (Prabhakar et al., 2002; Terada et al., 2016). BMI values are frequently used for the estimation of obesity degree. In the present study, the average height of women was significantly lower than men while there was no difference in weight between both genders (Figure 2).

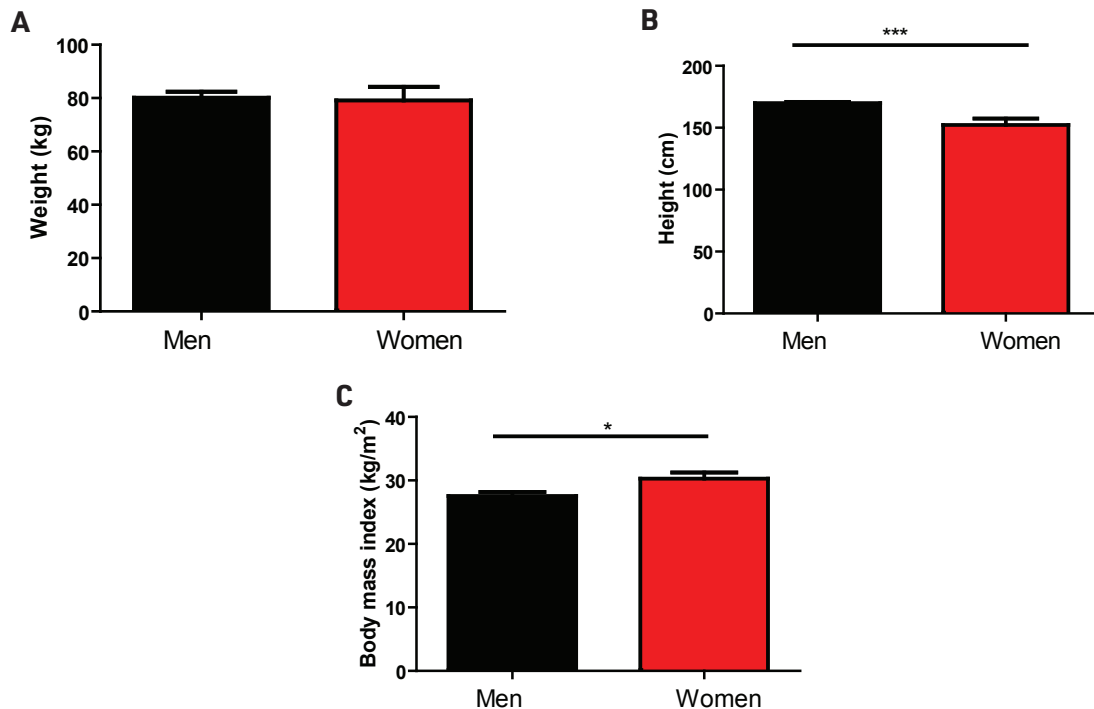


**Figure 2.** Weight, height and body mass index values of patients who underwent coronary artery bypass surgery. Body mass index is calculated by dividing weight in kg by height in meter squared. Values are means  $\pm$  s.e.mean derived from (n) different patients (n value for women: 17, for men: 41). \* indicates values significantly different  $p < 0.05$ , \*\*\* indicates  $p < 0.001$  (student's t test).

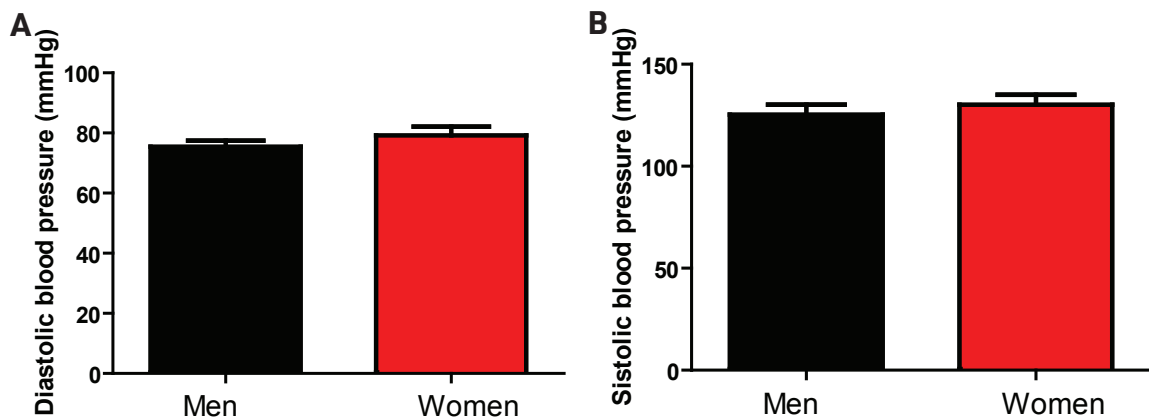


**Figure 3.** Diastolic and systolic blood pressure values of patients who underwent coronary artery bypass surgery. Values are means  $\pm$  s.e.mean derived from (n) different patients (n value for women: 17, for men: 41).

Furthermore, BMI values were significantly higher in women (Figure 2). In accordance with our results, another study indicated that the prevalence of morbid obesity is higher in those women undergoing CABG than men (Ahmad et al., 2010). On the other hand, another study performed on patients undergoing CABG demonstrated that women were shorter, weighed less and had a lower BMI compared to men (Koch et al., 2003; Terada et al., 2016).

It is important to note that diet and exercise lifestyle modifications could have a potentially significant role in improving cardiovascular risk factors in patients who undergo CABG. Several gender differences were noted in diet and sedentary life habits. Men are more likely than women to exercise multiple times with higher intensity levels while women are more likely to adhere to long-term dietary advice. Moreover, exercise could have more beneficial effects on women than men in regards to quality of life and functional outcomes. Further studies are necessary in order to elucidate reasons for these differences between gender (Coyan, Reeder, & Vacek, 2014; Markou, Evers & van Swieten, 2008).

Hypertension is associated with an increase in cardiovascular morbidity of CABG patients during the perioperative period (Aronson, Boisvert, & Lapp, 2002). Hypertension stage 1 is defined as systolic/diastolic blood pressure equal to 130/80 mmHg or above (Whelton et al., 2018). In our study, we indicated no difference in systolic and diastolic blood pressure between men and women (Figure 3). However, several studies reported that women with CAD were more likely to be hypertensive than men (Hemal et al., 2016; Ahmad et al., 2010).

The Framingham Heart Study reported that the presence of diabetes doubled the age-adjusted risk for CAD in men and tripled it in women (Kannel & McGee, 1979). The HbA1c value is used for long-term glycemic control in diabetic patients and correlates best with mean blood glucose over the previous 8 to 12 weeks (Rohlfing et al., 2002). In our study, no differences in HbA1c values between men and women undergoing CABG were observed (Figure 4). In accordance with our results, the prevalence of diabetes in both women and men was similar (Hemal et al., 2016). However, in another

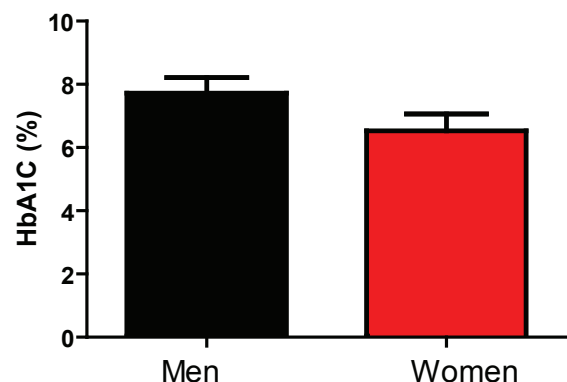


**Figure 4.** HbA1C values of patients who underwent coronary artery bypass surgery. The term HbA1c refers to glycated haemoglobin. Values are means  $\pm$  s.e.mean derived from (n) different patients (n value for women: 17, for men: 41).

study, female patients had an increased incidence of diabetes mellitus (Ahmad et al., 2010).

The incidence of CAD in several studies was inversely related to HDL concentrations and positively related to LDL concentrations. The Framingham Heart Study indicated that the risk of MI increases by 25% for every 5 mg/dL decrease in HDL levels for both men and women. On the other hand, lowering LDL levels is associated with a reduction in CAD (Castelli, 1983; Di Angelantonio et al., 2009; Praticò, Tangirala & Rader, 1998; Ference et al., 2017). In the present study, we indicated higher HDL and LDL levels in women compared to men (Figure 5). Furthermore, the ratios of HDL/total cholesterol and LDL/total cholesterol were greater in women than men (Figure 5). In accordance with our findings, another study indicated that women undergoing CABG had higher HDL, LDL and cholesterol values (Terada et al., 2016). Furthermore, several studies showed that female patients with CAD were more likely to have dyslipidemia than male patients (Ahmad et al., 2010). Higher LDL values observed in female patients could contribute to the progression of atherosclerotic CAD. In accordance with our results, a study performed in six countries reported that women have higher HDL values than men (Davis et al., 1996).

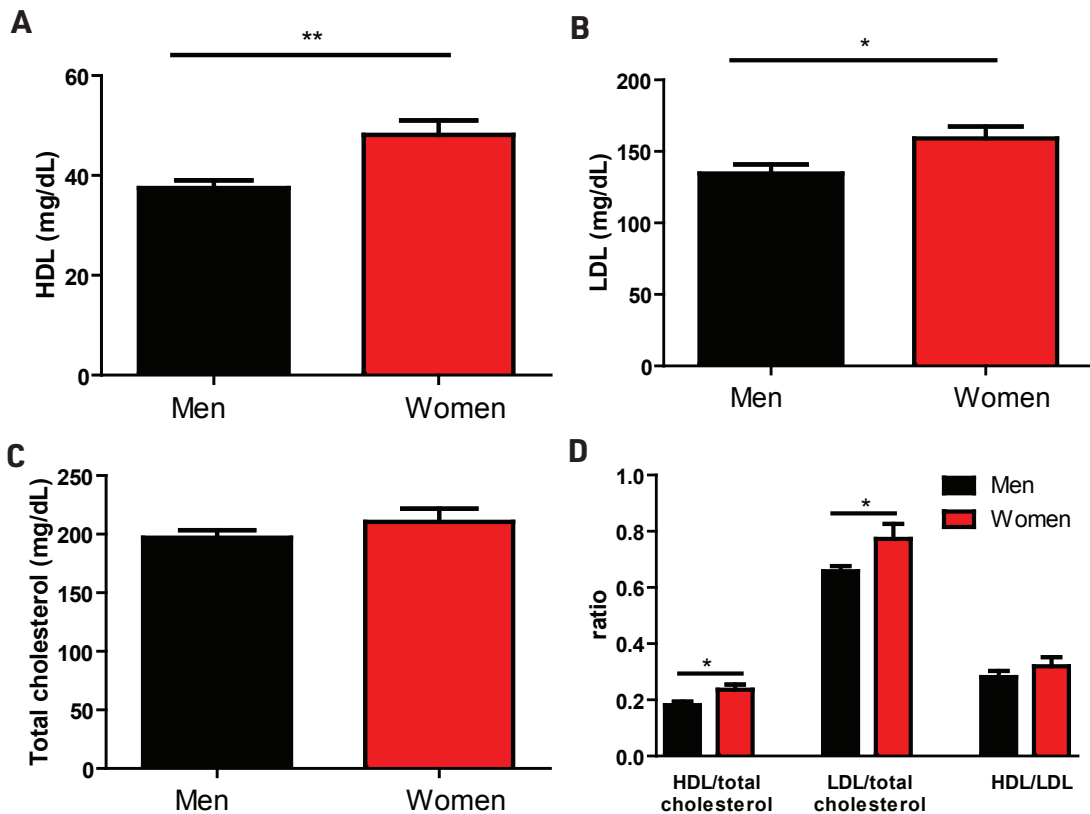


**Figure 5.** High-density lipoprotein (HDL), low-density lipoprotein (LDL), total cholesterol values and their ratios derived from patients who underwent coronary artery bypass surgery. Values are means  $\pm$  s.e.mean derived from (n) different patients (n value for women: 17, for men: 41). \* indicates values significantly different  $p < 0.05$ , \*\* indicates  $p < 0.01$  (student's t test).

In conclusion, the present study reported a significant difference in lipid profile and BMI between women and men undergoing CABG and highlighted the need for sex-specific approaches for the prevention of CAD. Several studies investigated a gender difference in clinical characteristics of patients undergoing CABG. Our study has both consistent as well as opposing results with those previous studies. This could be due to genetic predisposition, differences in ethnic groups, access to healthcare for diagnosis, and awareness of patients for cardiovascular risk factors. Risk factors including obesity, diabetes, hypertension and dyslipidemia influence the outcome of death in patients undergoing CABG. Correct management of controllable risk factors significantly reduces mortality and morbidity rates by altering the prognosis of CAD and is important for reducing hospital costs of these patients. Therefore, major socioeconomic education and preventive measures are needed to reduce the burden of major co-morbidities in patients with CAD and to seek early cardiac advice and care. A relatively low number of patients were included in the present study and this is one limitation of the study. Further multi-center studies including higher numbers of Turkish patients undergoing CABG with the focus on gender differences are needed.

**Ethics Committee Approval:** This study was approved by the Institutional Review Board of the Istanbul University Institute of Cardiology (no: 50.0.05.00/8).

**Informed Consent:** Written consent was obtained from the participants.

**Peer-review:** Externally peer-reviewed.

**Author Contributions:** Conception/Design of Study- G.Ö., S.T., G.T., G.T.; Data Acquisition- G.Ö., K.A., Ö.K.; Data Analysis/Interpretation- G.Ö.; Drafting Manuscript- G.Ö., K.A.; Critical Revision of Manuscript- G.T., S.T., G.T.; Final Approval and Accountability- G.Ö., K.A., Ö.K., G.T., G.T., S.T.; Technical or Material Support- Ö.K.; Supervision- G.Ö.

**Conflict of Interest:** The authors have no conflict of interest to declare.

**Financial Disclosure:** This study was supported by Scientific Research Projects Coordination Unit of Istanbul University. (Project number: TSA-2018-31849)

## REFERENCES

- Ades, P. A., & Savage, P. D. (2017). Obesity in coronary heart disease: An unaddressed behavioral risk factor. *Preventive Medicine, 104*, 117–119. <https://doi.org/10.1016/j.ypmed.2017.04.013>
- Ahmad, M., Arifi, A. A., Onselen, R. van, Alkodami, A. A., Zaibag, M., Khaldi, A. A. A., & Najm, H. K. (2010). Gender differences in the surgical management and early clinical outcome of coronary artery disease: Single centre experience. *Journal of the Saudi Heart Association, 22*(2), 47–53. <https://doi.org/10.1016/j.jsha.2010.02.004>



- Ajay, V. S., & Prabhakaran, D. (2010). Coronary heart disease in Indians: Implications of the INTERHEART study. *Indian Journal of Medical Research*, 132(5), 561–566. <https://doi.org/10.4103/0971-5916.73396>
- Alam, M., Bandedali, S. J., Kayani, W. T., Ahmad, W., Shahzad, S. A., Jneid, H. ... Virani, S. S. (2013). Comparison by meta-analysis of mortality after isolated coronary artery bypass grafting in women versus men. *American Journal of Cardiology*, 112(3), 309–317. <https://doi.org/10.1016/j.amjcard.2013.03.034>
- Alexander, J. H., & Smith, P. K. (2016). Coronary-artery bypass grafting. *The New England Journal of Medicine*, 375(10), 22–33. <https://doi.org/10.1056/NEJMc1608042>
- Aronson, S., Boisvert, D., & Lapp, W. (2002). Isolated systolic hypertension is associated with adverse outcomes from coronary artery bypass grafting surgery. *Anesthesia and Analgesia*, 94(5), 1079–1084. <https://doi.org/10.1097/00005539-200205000-00005>
- Bachar, B. J., & Manna, B. (2020). *Coronary artery bypass graft. statpearls*. Retrieved from <http://www.ncbi.nlm.nih.gov/pubmed/29939613>
- Bonow, R. O., Smaha, L. A., Smith, S. C., Mensah, G. A., & Lenfant, C. (2002). World Heart Day 2002: The international burden of cardiovascular disease: Responding to the emerging global epidemic. *Circulation*, 106(13), 1602–1605. <https://doi.org/10.1161/01.CIR.0000035036.22612.2B>
- Bukkapatnam, R. N., Yeo, K. K., Li, Z., & Amsterdam, E. A. (2010). Operative Mortality in Women and Men Undergoing Coronary Artery Bypass Grafting (from the California Coronary Artery Bypass Grafting Outcomes Reporting Program). *American Journal of Cardiology*, 105(3), 339–342. <https://doi.org/10.1016/j.amjcard.2009.09.035>
- Castelli, W. P. (1983). Cardiovascular disease and multifactorial risk: Challenge of the 1980s. *American Heart Journal*, 106(5), 1191–1200. [https://doi.org/10.1016/0002-8703\(83\)90174-6](https://doi.org/10.1016/0002-8703(83)90174-6)
- Cornwall, L. D., Omer, S., Rosengart, T., Holman, W. L., & Bakaeen, F. G. (2015). Changes over time in risk profiles of patients who undergo coronary artery bypass graft surgery: The Veterans Affairs Surgical Quality Improvement Program (VASQIP). *Journal of the American Medical Association (JAMA)*, 150(4), 308–315. <https://doi.org/10.1001/jamasurg.2014.1700>
- Cowell, S. J., Newby, D. E., & Boon, N. A. (2004). Coronary artery disease in the elderly patient. *Reviews in Clinical Gerontology*, 14(2), 105–118. <https://doi.org/10.1017/S095925980400139X>
- Coyn, G. N., Reeder, K. M., & Vacek, J. L. (2014). Diet and exercise interventions following coronary artery bypass graft surgery: A review and call to action. *Physician and Sportsmedicine*, 42(2), 119–129. <https://doi.org/10.3810/psm.2014.05.2064>
- Davis, C. E., Williams, D. H., Oganov, R. G., Tao, S. C., Rywik, S. L., Stein, Y., & Little, J. A. (1996). Sex difference in high density lipoprotein cholesterol in six countries. *American Journal of Epidemiology*, 143(11), 1100–1106. <https://doi.org/10.1093/oxfordjournals.aje.a008686>
- Di Angelantonio, E., Sarwar, N., Perry, P., Kaptoge, S., Ray, K. K., Thompson, A., ... Danesh, J. (2009). Major lipids, apolipoproteins, and risk of vascular disease. *Journal of the American Medical Association (JAMA)*, 302(18), 1993–2000. <https://doi.org/10.1001/jama.2009.1619>
- Dinh, D. T., Lee, G. A., Billah, B., Smith, J. A., Shardey, G. C., & Reid, C. M. (2008). Trends in coronary artery bypass graft surgery in Victoria, 2001–2006: findings from the Australasian society of cardiac and thoracic surgeons' database project. *The Medical Journal of Australia*, 188, 214–217. <https://doi.org/10.5694/j.1326-5377.2008.tb01587.x>
- Elbardissi, A. W., Aranki, S. F., Sheng, S., O'Brien, S. M., Greenberg, C. C., & Gammie, J. S. (2012). Trends in isolated coronary artery bypass grafting: An analysis of the Society of Thoracic Surgeons adult cardiac surgery database. *Journal of Thoracic and Cardiovascular Surgery*, 143(2), 273–281. <https://doi.org/10.1016/j.jtcvs.2011.10.029>
- Emmert, M. Y., Salzberg, S. P., Seifert, B., Schurr, U. P., Odavic, D., Reuthebuch, O., & Genoni, M. (2010). Despite modern off-pump coronary artery bypass grafting women fare worse than men☆. *Interactive Cardiovascular and Thoracic Surgery*, 10(5), 737–741. <https://doi.org/10.1510/icvts.2009.220277>
- Ference, B. A., Ginsberg, H. N., Graham, I., Ray, K. K., Packard, C. J., Bruckert, E. ... Catapano, A. L. (2017). Low-density lipoproteins cause atherosclerotic cardiovascular disease. 1. Evidence from genetic, epidemiologic, and clinical studies. A consensus statement from the European Atherosclerosis Society Consensus Panel. *European Heart Journal*, 38(32), 2459–2469. <https://doi.org/10.1093/eurheartj/ehx144>
- Goldman, S., Zadina, K., Moritz, T., Ovitt, T., Sethi, G., Copeland, J. G. ... Henderson, W. (2004). Long-term patency of saphenous vein and left internal mammary artery grafts after coronary artery bypass surgery: Results from a Department of Veterans Affairs Cooperative Study. *Journal of the American College of Cardiology*, 44(11), 2149–2156. <https://doi.org/10.1016/j.jacc.2004.08.064>
- Hemal, K., Pagidipati, N. J., Coles, A., Dolor, R. J., Mark, D. B., Pellikka, P. A. ... Douglas, P. S. (2016). Sex differences in demographics, risk factors, presentation, and noninvasive testing in stable outpatients with suspected coronary artery disease insights from the PROMISE Trial. *Journal of the American College of Cardiology (JACC): Cardiovascular Imaging*, 9(4), 337–346. <https://doi.org/10.1016/j.jcmg.2016.02.001>
- Jannati, M., Navaei, M., & Ronizi, L. (2019). A comparative review of the outcomes of using arterial versus venous conduits in coronary artery bypass graft (CABG). *Journal of Family Medicine and Primary Care*, 8(9), 2768. [https://doi.org/10.4103/jfmpc.jfmpc\\_367\\_19](https://doi.org/10.4103/jfmpc.jfmpc_367_19)
- Kabakçı, M. G., Oto, A., Oram, E., Karamhmetoğlu, A., Oram, A., & Uğurlu, Ş. (1990). Dilitiazem Therapy in Stable Angina Pectoris: A Placebo-Controlled Study. *Türk Kardiyoloji Derneği Arşivi*, 18(3), 170–175. Retrieved from: <https://archivestsc.com/tr/jvi.aspx?pdire=tkd&plng=tur&un=TKDA-53458&look4=>
- Kannel, W. B., & McGee, D. L. (1979). Diabetes and cardiovascular risk factors: The Framingham study. *Circulation*, 59(1), 8–13. <https://doi.org/10.1161/01.CIR.59.1.8>
- Koch, C. G., Khandwala, F., Nussmeier, N., & Blackstone, E. H. (2003). Gender profiling in coronary artery bypass grafting. *Journal of Thoracic and Cardiovascular Surgery*, 126(6), 2044–2051. [https://doi.org/10.1016/S0022-5223\(03\)00955-3](https://doi.org/10.1016/S0022-5223(03)00955-3)
- Madhavan, M. V., Gersh, B. J., Alexander, K. P., Granger, C. B., & Stone, G. W. (2018). Coronary Artery Disease in Patients ≥80 Years of Age. *Journal of the American College of Cardiology*, 71(18), 2015–2040. <https://doi.org/10.1016/j.jacc.2017.12.068>
- Markou, A. L. P., Evers, M., van Swieten, H. A., & Noyez, L. (2008). Gender and physical activity one year after myocardial revascularization for stable angina. *Interactive Cardiovascular and Thoracic Surgery*, 7(1), 96–101. <https://doi.org/10.1510/icvts.2007.160382>
- McNeely, C., Markwell, S., & Vassileva, C. (2016). Trends in Patient Characteristics and Outcomes of Coronary Artery Bypass Grafting in the 2000 to 2012 Medicare Population. *Annals of Thoracic Surgery*, 102(1), 132–138. <https://doi.org/10.1016/j.athoracsurg.2016.01.016>
- Nicolini, F., Vezzani, A., Fortuna, D., Contini, G. A., Pacini, D., Gabbieri, D., ... Gherli, T. (2016). Gender differences in outcomes following isolated coronary artery bypass grafting: Long-term results. *Journal of Cardiothoracic Surgery*, 11(1), 144–150. <https://doi.org/10.1186/s13019-016-0538-4>
- Otsuka, F., Byrne, R. A., Yahagi, K., Mori, H., Ladich, E., Fowler, D. R. ... Joner, M. (2015). Neoatherosclerosis: Overview of histopathologic findings and implications for intravascular imaging assessment. *European Heart Journal*, 36(32), 2147–2159.

- Prabhakar, G., Haan, C. K., Peterson, E. D., Coombs, L. P., Cruzza-vala, J. L., & Murray, G. F. (2002). The risks of moderate and extreme obesity for coronary artery bypass grafting outcomes: A study from the society of thoracic surgeons' database. *Annals of Thoracic Surgery*, *74*, 1125–1131. [https://doi.org/10.1016/S0003-4975\(02\)03899-7](https://doi.org/10.1016/S0003-4975(02)03899-7)
- Praticò, D., Tangirala, R. K., Rader, D. J., Rokach, J., & FitzGerald, G. A. (1998). Vitamin E suppresses isoprostane generation in vivo and reduces atherosclerosis in ApoE-deficient mice. *Nature Medicine*, *4*(10), 1189–1192. <https://doi.org/10.1038/2685>
- Quertermous, T., & Ingelsson, E. (2016). Coronary Artery Disease and Its Risk Factors: Leveraging Shared Genetics to Discover Novel Biology. *Circulation Research*, *118*(1), 14–16. <https://doi.org/10.1161/CIRCRESAHA.115.307937>
- Rohlfing, C. L., Wiedmeyer, H. M., Little, R. R., England, J. D., Tennill, A., & Goldstein, D. E. (2002). Defining the relationship between plasma glucose and HbA1c: Analysis of glucose profiles and HbA1c in the Diabetes Control and Complications Trial. *Diabetes Care*, *25*(2), 275–278. <https://doi.org/10.2337/diacare.25.2.275>
- Roth, G. A., Johnson, C., Abajobir, A., Abd-Allah, F., Abera, S. F., Abyu, G., ... Murray, C. (2017). Global, Regional, and National Burden of Cardiovascular Diseases for 10 Causes, 1990 to 2015. *Journal of the American College of Cardiology*, *70*(1), 1–25. <https://doi.org/10.1016/j.jacc.2017.04.052>
- Samak, M., Fatullayev, J., Sabashnikov, A., Zeriuoh, M., Schmack, B., Ruhparwar, A., ... Weymann, A. (2016). Total Arterial Revascularization: Bypassing Antiquated Notions to Better Alternatives for Coronary Artery Disease. *Medical Science Monitor Basic Research*, *22*, 107–114. <https://doi.org/10.12659/MSMBR.901508>
- Seccareccia, F., Perucci, C. A., D'Errigo, P., Arcà, M., Fusco, D., Rosato, S., & Greco, D. (2006). The Italian CABG Outcome Study: Short-term outcomes in patients with coronary artery bypass graft surgery. *European Journal of Cardio-Thoracic Surgery*, *29*(1), 56–62. <https://doi.org/10.1016/j.ejcts.2005.07.017>
- Shao, C., Wang, J., Tian, J., & Tang, Y. D. (2020). Coronary Artery Disease: From Mechanism to Clinical Practice. *Advances in Experimental Medicine and Biology*, *1177*, 1–36. [https://doi.org/10.1007/978-981-15-2517-9\\_1](https://doi.org/10.1007/978-981-15-2517-9_1)
- Terada, T., Johnson, J. A., Norris, C., Padwal, R., Qiu, W., Sharma, A. M., ... Forhan, M. (2016). Severe obesity is associated with increased risk of early complications and extended length of stay following coronary artery bypass grafting surgery. *Journal of the American Heart Association*, *5*(6), e003282. <https://doi.org/10.1161/JAHA.116.003282>
- Varma, P. K., Kundan, S., Ananthanarayanan, C., Panicker, V. T., Pillai, V. V., Sarma, P. S., & Karunakaran, J. (2014). Demographic profile, clinical characteristics and outcomes of patients undergoing coronary artery bypass grafting—retrospective analysis of 4,024 patients. *Indian Journal of Thoracic and Cardiovascular Surgery*, *30*(4), 272–277. <https://doi.org/10.1007/s12055-014-0318-5>
- Kannel, W. B. & Wilson, P. W. F. (1995). Risk Factors That Attenuate the Female Coronary Disease Advantage. *Archives of Internal Medicine*, *155*(1), 57–61. <https://doi.org/10.1001/archinte.1995.00430010063008>
- Whelton, P. K., Carey, R. M., Aronow, W. S., Casey, D. E., Collins, K. J., Dennison Himmelfarb, C., ... Wright, J. T. (2018). 2017 ACC/AHA/AAPA/ABC/ACPM/AGS/APHA/ASH/ASPC/NMA/PCNA Guideline for the Prevention, Detection, Evaluation, and Management of High Blood Pressure in Adults: A Report of the American College of Cardiology/American Heart Association Task Force on Clinical Practice Guidelines. *Circulation*, *138*(17), e484–e594. <https://doi.org/10.1161/CIR.0000000000000596>
- World Health Organization. (2017, 17 May). Cardiovascular diseases. [Web log post]. Retrieved from: [https://www.who.int/health-topics/cardiovascular-diseases/#tab=tab\\_1](https://www.who.int/health-topics/cardiovascular-diseases/#tab=tab_1)
- Willerson, J. T., & Holmes D. R. (2015). Coronary artery disease. Switzerland, AG: Springer Nature.
- Wilson, J. M. (2015). Coronary Artery bypass surgery and percutaneous coronary revascularization: Impact on morbidity and mortality in patients with coronary artery disease. London, UK: Springer.

# Ameliorative effects of melatonin on intestinal oxidative damage in streptozotocin-induced diabetic rats

Zatiye Ayça Çevikelli Yakut<sup>1,2</sup> , Gizem Buse Akçay<sup>1</sup> , Özge Çevik<sup>3</sup> , Göksel Şener<sup>1</sup> 

<sup>1</sup>Marmara University, Faculty of Pharmacy, Department of Pharmacology, Istanbul, Turkey

<sup>2</sup>Trakya University, Faculty of Pharmacy, Department of Pharmacognosy, Edirne, Turkey

<sup>3</sup>Adnan Menderes University, Faculty of Medicine, Department of Biochemistry, Aydın, Turkey

**ORCID IDs of the authors:** Z.A.Ç.Y. 0000-0002-6697-6781; G.B.A.0000-0002-0163-5708; Ö.Ç.0000-0002-9325-3757; G.Ş. 0000-0001-7444-6193

**Cite this article as:** Çevikelli Yakut, Z. A., Akçay, G. B., Çevik, O., & Şener, G. (2020). Ameliorative effects of melatonin on intestinal oxidative damage in streptozotocin-induced diabetic rats. *Istanbul Journal of Pharmacy*, 50 (3), 160-167.

## ABSTRACT

**Background and Aims:** The potential therapeutic effects of melatonin on changes in intestinal tissue of diabetic rats were investigated.

**Methods:** Male Sprague-Dawley rats were assigned into 5 groups (10 rats in each): Control, diabetes, diabetes+insulin, diabetes+melatonin, and diabetes+insulin+melatonin groups. Streptozotocin (60 mg/kg) was administered intraperitoneally to the rats to induce diabetes. At the end of 8 weeks of treatment, after blood glucose measurement and subsequent decapitation, glutathione (GSH) and malondialdehyde (MDA) levels and caspase-3, myeloperoxidase (MPO), and superoxide dismutase (SOD) activities in the intestinal tissue were investigated.

**Results:** In diabetic animals, elevated blood glucose levels caused oxidant damage in the intestinal tissue that was demonstrated with increased MDA levels, caspase and MPO activities, and decreased GSH levels and SOD activities. Although melatonin demonstrated more significant results than insulin, separate administration of both melatonin and insulin improved the oxidative damage parameters compared to the diabetes group. In the combined treatment group, all parameters were back to control levels statistically more significant when compared with the treatment-alone.

**Conclusion:** Melatonin has been shown to protect intestinal tissue from diabetic oxidant damage. With insulin treatment in type I diabetes, melatonin supplements may increase the quality of life through reducing complications.

**Keywords:** Diabetes mellitus, oxidative damage, intestine, insulin, melatonin

## INTRODUCTION

Diabetes Mellitus (DM) is characterized by high blood glucose levels which are caused by the impaired effect and/or release of insulin. Since hyperglycemia triggers the oxidative stress that plays a role in many diabetes complications (Garcia, Rodrigues, Alonso, Rodrigues-Ochoa, & Aguilar, 2015), whether antioxidants have positive effects on DM is an object of interest.

Free radicals that are necessary for many signals in physiological processes, such as differentiation and migration in cells (Bansal & Bilaspuri, 2011), trigger the cell damage through the passage of unpaired electrons into proteins and DNAs (Vural, Sabuncu, Arslan, & Aksoy, 2001). While antioxidants found endogenously or taken exogenously provide defense against this damage, several factors, such as aging, various drugs, and diseases, make the body prone to oxidative stress by disrupting the balance between

**Address for Correspondence:**  
Göksel ŞENER, e-mail: gsener@marmara.edu.tr

Submitted: 01.08.2020  
Revision Requested: 04.09.2020  
Last Revision Received: 04.09.2020  
Accepted: 11.09.2020  
Published Online: 16.10.2020

This work is licensed under a Creative Commons Attribution 4.0 International License.



antioxidants and pro-oxidants (Ullah, Khan, & Khan, 2016). Hyperglycemia triggers oxidative stress by increasing free radical formation and suppressing the antioxidant defense system (Ighodaro, 2018). The oxidative stress in diabetes damages almost all organs in the body, such as the heart, kidneys, eyes, neurons, liver, small and large vessels, and gastrointestinal (GI) system (Kochar & Umathe, 2009). Diabetes mellitus can affect all regions of GI tract, such as the esophagus, intestines, and anorectum (Wolosin & Edelman, 2000), due to the elevated free radical levels. Diabetes mellitus generates morphological and functional changes in the intestinal mucosa; for instance, hyperplasia and hypertrophy occur in epithelial cells (Bhor, Raghuram, & Sivakami, 2004).

Antioxidants are molecules that can prevent tissue damage by reducing the amount and effectiveness of reactive oxygen species (ROS) (Vural et al., 2001). In recent reports, free radical scavenging and antioxidant properties of melatonin, which is a pineal hormone regulating circadian rhythm, have been indicated, in addition to its positive effects on glucose metabolism (Alikhani, Keshavarzi, Hadjzadeh, & Karimi, 2015; Hadjzadeh, Alikhani, Hosseinian, Zarei, & Keshavarzi, 2018; Yang et al., 2016). Melatonin protects against oxidant damage because melatonin stimulates the antioxidant enzyme production, neutralizes the reactive oxygen and nitrogen species, reduces the proinflammatory cytokine levels, and stabilizes the cell membrane (Esposito & Cuzzocrea, 2010). Moreover, curative effects of melatonin on gastric and intestinal problems in different experimental studies of DM throw light on our study (Alikhani et al., 2015; Hadjzadeh et al., 2018; Yang et al., 2016).

The present study aims to determine the possible benefits of melatonin supplementation to protect the intestinal tissues from oxidative injury in streptozotocin (STZ)-induced diabetic rats.

## MATERIALS AND METHODS

### Animals and ethics

Three months old male Sprague-Dawley rats (250-300 grams) were obtained from Marmara University Research Center for Experimental Animals. All experimental protocols were performed according to the Marmara University Animal Care and Use Committee (Protocol: 33.2015.mar).

### Experimental protocol

The rats were randomly assigned into five groups (10 rats in each): Control group (C), diabetes group (D), insulin-treated diabetes group (D+I), melatonin-treated diabetes group (D+M), and insulin-and-melatonin-treated diabetes group (D+I+M). In the diabetes groups, STZ (60 mg/kg) was applied intraperitoneally (ip) to induce diabetes. The rats demonstrating blood glucose levels above 200 mg/dL were regarded as diabetic (Husni, Anggaara, Isnansetyo, & Nugroho, 2016). Following the diabetes induction, rats were treated with insulin (sc, 6U/kg) (Paskaloğlu, Şener, & Ayanoğlu-Dülger, 2004) and/or melatonin (ip, 10 mg/kg) (Alikhani et al., 2015; Hadjzadeh et al., 2018; Yang et al., 2016). Treatments were continued for 8 weeks (Paskaloğlu et al., 2004). 3 ml of 0.9% NaCl solution was also applied daily to all groups for fluid replacement. Body weights and blood glucose levels were recorded after the diabetes in-

duction and at the end of the 8<sup>th</sup> week. Blood glucose levels were measured with a glucometer (Accu-Chek, F. Hoffman-La Roche Ltd, Basel, Switzerland) by taking blood samples from the orbital vein under mild ether anesthesia. Eight weeks later, intestinal tissue specimens of the animals were removed to detect malondialdehyde (MDA) and glutathione (GSH) levels, myeloperoxidase (MPO), superoxide dismutase (SOD), and caspase-3 activities. In addition, western blotting was performed to evaluate caspase-3 protein expression.

### Measurements in intestinal tissue samples

#### Malondialdehyde (MDA) and glutathione (GSH) levels

To evaluate the MDA and GSH levels, intestinal tissue specimens were homogenized in an ice-cold medium containing 150 mM KCl. Beuge and Aust's method was used for MDA assay (Beuge & Aust, 1978). A solution containing thiobarbituric acid (0.375, TBA) and trichloroacetic acid (15%, TCA) in 0.25 N HCl was added to 0.5 mL homogenate. The absorbance of the color of the samples cooled and centrifuged after being kept in a hot water bath for 15 minutes was read at 532 nm. The unit used was nmol/g tissue.

The Beutler method was used to investigate the GSH levels (Beutler, Duron, & Kelly, 1963). 0.4 mL 10% homogenate was mixed with 0.2 mL 20% TCA and centrifuged for 15 minutes at 3000 rpm. Supernatant (0.5 mL) was collected and added to a 0.3 mol/L Na<sub>2</sub>HPO<sub>4</sub>·2H<sub>2</sub>O solution (2 mL). Afterwards a 0.2 mL dithiobisnitrobenzoate solution (0.4 mg/mL) in 1% sodium citrate was added. The absorbance was recorded at 412 nm after mixing. Glutathione levels were calculated by the aid of the extinction coefficient of 1.36×10<sup>4</sup> M<sup>-1</sup> cm<sup>-1</sup>. The unit used was µmol/g tissue.

#### Superoxide dismutase (SOD) activity

According to the method of Mylroie et al., the absorbance of color formed in samples kept in the fluorescence light and at 37 °C with the buffer prepared by using 50 mM potassium phosphate buffer-EDTA, 0.2 mM riboflavin, and 6mM o-dianisidine was read at 460 nm. The unit used was U/g tissue (Mylroie, Collins, Umbles, & Kyle, 1986).

#### Myeloperoxidase (MPO) activity

Tissue specimens were homogenized in a 50 mM potassium phosphate buffer (PB) (pH 6.0). For 10 min, centrifugation was carried out at 41,400 g. Afterwards the pellets were suspended in a 50 mM PB solution which contained 0.5% hexadecyltrimethylammonium bromide. Centrifugation was carried out at 41,400 g for 10 min after three freeze-thaw cycles. Sonication was performed between the cycles. 0.3 mL of aliquots were added to a 2.3 mL reaction mixture (o-dianisidine, 50 mM PB, and 20 mM H<sub>2</sub>O<sub>2</sub> solution). The absorbance change at 460 nm for 3 min on a spectrophotometer was used to calculate the MPO activity (DU-73 Spectrophotometer, Beckman Coulter Inc, Fullerton, CA, USA). The unit used was U/g tissue (Hillegas, Griswold, Brickson, & Winslow, 1990).

#### Caspase-3 activity

Caspase-3 activities in the tissue samples were investigated in accordance with the kit procedure, using Colorimetric Protease Assay Kit of Caspase-3 (Caspase-3 Colorimetric Kit-200

Tests Biosource (TM), Thermo Fisher Scientific Inc, Waltham, MA, USA). Formation of chromophore p-nitroanilide from caspase-3 substrate N-Acetyl-Asp-Glu-Val-Asp p-nitroanilide was evaluated spectrophotometrically. The absorbance of released p-nitroanilide was determined in an ELISA reader at 405 nm (Çevik et al., 2012).

A cell blasting buffer was added to the tissue homogenate and suspended in a cold environment, and the supernatant was used after centrifugation at 10,000 g. The supernatant was loaded onto the wells. After adding 50 µL of reaction buffer, 4 mM N-Acetyl-Asp-Glu-Val-Asp p-nitroanilide substrate was added. After the incubation for 2 hours at 37°C, the results were calculated according to the standards by reading in the ELISA reader at 405 nm.

#### **Caspase-3 protein expression analysis with western blot method**

Samples were blasted with 70% amplitude in ice ultrasonic homogenizer for 15 seconds by using a cell blasting buffer. In the upper phase obtained with centrifugation at 12,000 g at 40°C, western blotting studies were carried out (Bradford, 1976).

The protein (25 µg) was resolved on the 12% SDS-PAGE. Next, it was transferred to a nitrocellulose membrane (Santa Cruz Biotechnology Inc, CA, USA). In order to block the nitrocellulose membrane, 5% nonfat skim milk powder in tris-buffered saline (TBS) was used (Sigma-Aldrich, St. Louis, Missouri, USA). Then the nitrocellulose membrane was washed twice with 0.1% Tween-20 in TBS, followed by incubation overnight with a primary antibody. 1:500 monoclonal rat anti-caspase-3, anti-b-actin (Santa Cruz Biotechnology Inc, CA, USA), and cleaved-caspase-3 (Cell Signaling Technology Inc, Danvers, Massachusetts, USA) were used. The incubation of the membrane was performed with HRP conjugated secondary antibody for two hours. Next, the membrane was developed with chemiluminescence reagents (Santa Cruz Biotechnology Inc, CA, USA). Afterwards, the membrane was exposed to Fuji Super RX film (Fujifilm Corporation, Tokyo, Japan). For the analysis of protein bands, "Image J Programme OD Analysis Software" was used (NIH, Bethesda, Maryland, USA). To normalize the signals, a respective β-actin signal was used (Çevik et al., 2012).

#### **Statistical analysis**

The Graphpad Prism 5.0 program was used for the statistical analysis (GraphPad Software, San Diego, CA, USA). All data were expressed as mean±SD. Biochemical data were analyzed with variance analysis (ANOVA) followed by Tukey multiple comparison tests. Statistical significance was accepted as p<0.05.

## **RESULTS**

#### **Body weight and fasting blood glucose levels**

In the control group, body weight levels measured in the 8<sup>th</sup> week were significantly increased as compared to basal values (p<0.05) (Table 1). In the diabetes group, the 8<sup>th</sup> week body weight decreased significantly as compared to the baseline values (p<0.001). In other groups, body weight levels did not demonstrate any significant difference.

The beginning (t1) blood glucose levels of all diabetic groups were significantly elevated with respect to that of control group (p<0.001) (Table 2). Insulin, melatonin, and combined treatments reduced blood glucose levels at the end of the experiment (t2) with respect to t1 levels (p<0.001).

#### **Intestinal tissue malondialdehyde (MDA) levels**

Intestinal tissue MDA levels were found to be significantly higher in the diabetes group as compared to the control group values (p<0.001) (Figure 1). Insulin-alone administration did not improve the MDA levels with respect to the diabetes group and did not reduce the MDA levels to the control group levels (p<0.05). Melatonin treatment given to diabetic rats abolished the increase in intestinal tissue MDA levels (p<0.001). Combined treatment provided similar results (p<0.001). In the combined treatment group, MDA levels were also demonstrated to be lower (p<0.05) than insulin treatment alone.

#### **Intestinal tissue glutathione (GSH) levels**

Diabetes mellitus decreased intestinal tissue GSH levels significantly as compared to the control group levels (p<0.001) (Figure 2). In the insulin treatment group, the GSH levels tended to increase with respect to the diabetes group; however, it was not statistically significant. Treatment of diabetic rats with either melatonin or insulin+melatonin elevated intestinal tissue GSH levels (p<0.01-0.001).

#### **Intestinal tissue superoxide dismutase (SOD) levels**

Intestinal tissue SOD activity was decreased in diabetes and insulin-treated diabetes groups with respect to the control group (p<0.01 and p<0.05) (Figure 3). Treatment with melatonin and insulin+melatonin increased the intestinal tissue SOD activity in the diabetic rats (p<0.05).

#### **Intestinal tissue myeloperoxidase (MPO) activity levels**

In the diabetes group, intestinal tissue MPO activity was higher than that of the control group (p<0.001) (Figure 4). Myeloperoxidase activity was reduced in the insulin-treated group, but this decrease was not significant. Treatment of diabetic rats with either melatonin or melatonin+insulin abolished the MPO activity elevations (p<0.001).

#### **Intestinal tissue caspase-3 activity levels**

Intestinal tissue caspase-3 activity was elevated in the diabetes group compared with the control group (p<0.01) (Figure 5). Insulin-alone administration did not significantly change caspase-3 activity levels. Melatonin and insulin+melatonin treatments decreased the intestinal tissue caspase-3 activity of diabetic animals (p<0.05).

#### **Caspase-3 protein expression in intestinal tissue**

Caspase-3 bands increased significantly in the diabetic and insulin-treated animals with respect to the control group (p<0.001). These bands decreased with the co-administration of melatonin and insulin (p<0.001) (Figure 6). The combination of insulin and melatonin protected the cells against diabetes-induced damage through reducing cell death and increasing cell proliferation.



**Table 1. Body weights of the groups at the beginning and at the end of the experiment.**

	C	D	D+I	D+M	D+I+M
t <sub>1</sub> (g)	265±17	257±15	279±28.1	266±15	286±13
t <sub>2</sub> (g)	312±9*	205±13 <sup>+++</sup>	285±19	288±21	311±24

C: Control, D: Diabetes, I: Insulin, M: Melatonin. t<sub>1</sub>: at the beginning (after diabetes induction), t<sub>2</sub>: at 8<sup>th</sup> week. Each group consists of 10 animals. Data are expressed as mean ± SD. DATA are analyzed with variance analysis (ANOVA) followed by Tukey multiple comparison tests. \*p<0.05, <sup>+++</sup>p<0.001: versus t<sub>1</sub>.

**Table 2. Fasting blood glucose levels of the groups at the beginning and at the end of the experiment.**

	C	D	D+I	D+M	D+I+M
t <sub>1</sub> (mg/dL)	98±12	342±32 <sup>+++</sup>	362±32 <sup>+++</sup>	328±22 <sup>+++</sup>	346±22 <sup>+++</sup>
t <sub>2</sub> (mg/dL)	93±10	356±41	116±18 <sup>+++</sup>	181±16 <sup>+++</sup>	102±10 <sup>+++</sup>

C: Control, D: Diabetes, I: Insulin, M: Melatonin. t<sub>1</sub>: at the beginning (after diabetes induction), t<sub>2</sub>: at 8<sup>th</sup> week. Each group consists of 10 animals. Data are expressed as mean ± SD. DATA are analyzed with variance analysis (ANOVA) followed by Tukey multiple comparison tests. <sup>+++</sup>p<0.001: versus control group at t<sub>1</sub>, <sup>+++</sup>p<0.001: versus t<sub>1</sub>.

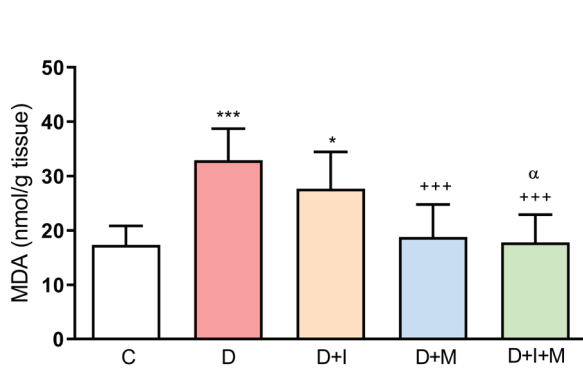


**Figure 1.** Malondialdehyde (MDA) levels in intestinal tissue of rats. \*p<0.05, <sup>+++</sup>p<0.001: versus control group, <sup>+++</sup>p<0.001: versus diabetes group, α p<0.05: versus insulin treated diabetes group. C: Control. D: Diabetes. I: Insulin. M: Melatonin. Each group consists of 10 animals. Data are expressed as mean ± SD. DATA are analyzed with variance analysis (ANOVA) followed by Tukey multiple comparison tests.

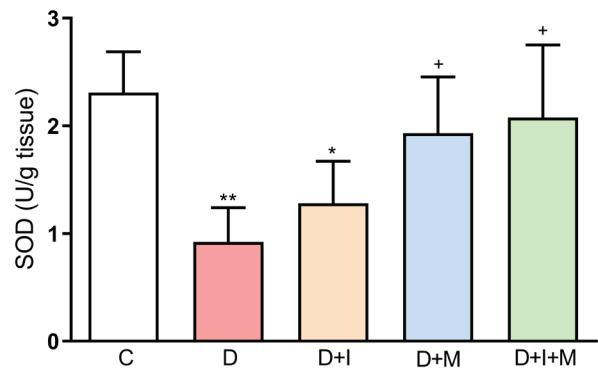


**Figure 3.** Superoxide dismutase (SOD) activities in intestinal tissues of rats. \*p<0.05, <sup>\*\*</sup>p<0.01: versus control group, <sup>+</sup>p<0.05: versus diabetes group. C: Control. D: Diabetes. I: Insulin. M: Melatonin. Each group consists of 10 animals. Data are expressed as mean ± SD. DATA are analyzed with variance analysis (ANOVA) followed by Tukey multiple comparison tests.

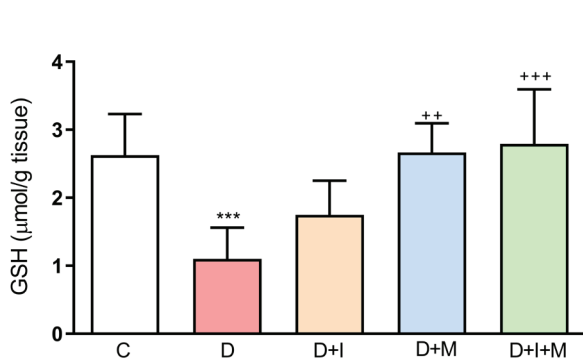


**Figure 2.** Glutathione (GSH) levels in intestinal tissues of rats. <sup>\*\*\*</sup>p<0.001: versus control group, <sup>++</sup>p<0.01, <sup>+++</sup>p<0.001: versus diabetes group. C: Control. D: Diabetes. I: Insulin. M: Melatonin. Each group consists of 10 animals. Data are expressed as mean ± SD. DATA are analyzed with variance analysis (ANOVA) followed by Tukey multiple comparison tests.

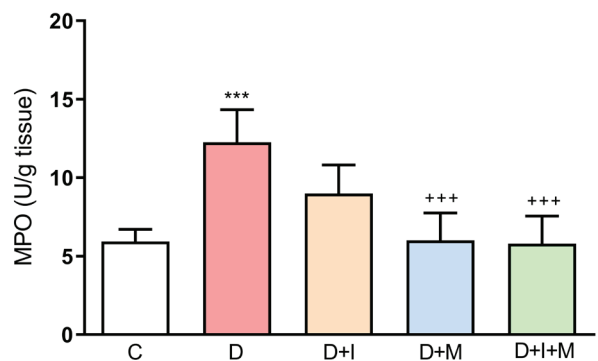


**Figure 4.** Myeloperoxidase (MPO) activities in intestinal tissues of rats. <sup>\*\*\*</sup>p<0.001: versus control group, <sup>+++</sup>p<0.001: versus diabetes group. C: Control. D: Diabetes. I: Insulin. M: Melatonin. Each group consists of 10 animals. Data are expressed as mean ± SD. DATA are analyzed with variance analysis (ANOVA) followed by Tukey multiple comparison tests.

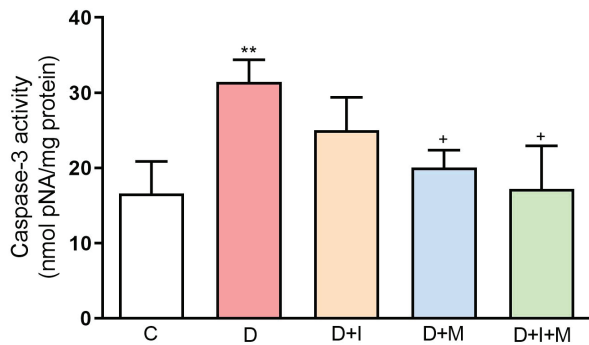


**Figure 5.** Caspase-3 activities in intestinal tissues of rats. \*\* $p < 0.01$ : versus control group, + $p < 0.05$ : versus diabetes group. C: Control. D: Diabetes. I: Insulin. M: Melatonin. Each group consists of 10 animals. Data are expressed as mean  $\pm$  SD. DATA are analyzed with variance analysis (ANOVA) followed by Tukey multiple comparison tests.

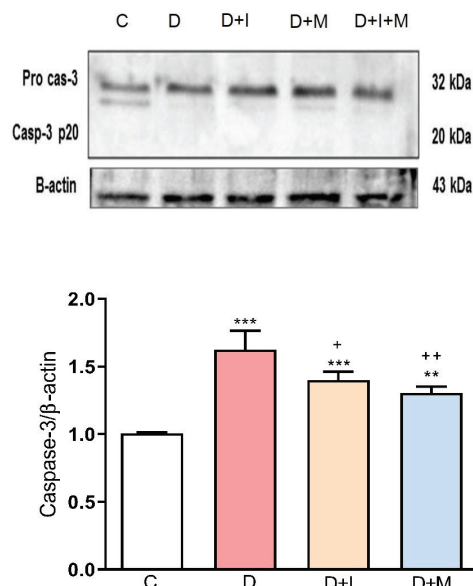


**Figure 6.** Caspase-3 protein expression in the intestinal tissues of rats determined by Western blotting. \*\* $p < 0.01$ , \*\*\* $p < 0.001$ : versus control group, + $p < 0.05$ , ++ $p < 0.01$ , +++ $p < 0.001$ : versus diabetes group,  $\alpha\alpha$ :  $p < 0.01$  versus insulin treated diabetes group,  $\gamma$   $p < 0.05$ : versus melatonin treated diabetes group. C: Control. D: Diabetes. I: Insulin. M: Melatonin. Each group consists of 10 animals. Data are expressed as mean  $\pm$  SD. DATA are analyzed with variance analysis (ANOVA) followed by Tukey multiple comparison tests.

## DISCUSSION

Melatonin is a hormone secreted from the pineal gland, the main function of which is to regulate the circadian rhythm. Due to its lipophilic structure, melatonin is not stored in the pineal gland and diffuses into the blood. According to previous *in vitro* and *in vivo* experimental studies and clinical studies, melatonin has positive effects on glucose metabolism in DM (Owino, Buonfiglio, Tchio & Tosini, 2019). In the culture study with pancreatic islet cells of type 2 diabetic patients, melatonin increased insulin release through repairing the  $\beta$  cells (Costes, Boss, Thomas, & Matveyenko, 2015). In the STZ-induced dia-

betes model, melatonin reduced fasting blood glucose levels (Alikhani et al., 2015). Additionally animals undergoing pinealectomy exhibited glucose tolerance impairment, insulin resistance, and DM, and these were repaired with melatonin treatment (Nogueira et al., 2011). In a clinical trial in type 2 diabetic patients, melatonin treatment reduced plasma glucose levels and provided glycemic control (Hussain et al., 2006). In accordance with previous reports, in our study, melatonin treatment significantly reduced the blood glucose levels in diabetic groups. Moreover, it potentialized the hypoglycemic effect of insulin in combined treatment group.

In DM, since glucose is spent for lipolysis and gluconeogenesis, the need of other cells for glucose is not adequately met and body weight decreases significantly (Alikhani et al., 2015; Husni et al., 2016). In our study, at the end of the experiment, it was demonstrated that the body weight levels were significantly lower in the diabetes group than the values at the beginning of the study. Insulin and melatonin treatments prevented the decrease in body weight.

Oxidative stress leads to serious complications in DM. In this regard, free radical formation are elevated, and antioxidant enzyme levels decrease in DM. Glucose oxidation produces radical anions, such as reactive ketoaldehydes and superoxide anions. Moreover, glucose reacts with proteins and generates advanced glycation end products that bind to their receptors and change the cellular functions (Vural et al., 2001; Hussain et al., 2006). The gastrointestinal tract is affected seriously by oxidative stress in DM. For instance, sensitivity of gastric mucosa to ulcers is elevated, gastric acid secretion is inhibited, or gastric mucosal atrophy arises (Alikhani et al., 2015).

Recent studies have drawn attention to melatonin as a free radical scavenger. In addition to directly neutralizing the free radicals, melatonin increases the effectiveness of antioxidants. It has been reported that melatonin possesses antioxidant activity in DM models through decreasing lipid peroxidation products and increasing antioxidant enzyme levels (Vural et al., 2001). Apart from the pineal gland, melatonin is also created in other organs, including the retina, GI tract, and skin. The amount of GI melatonin is 400 times higher than in the pineal gland (Yang et al., 2016). In addition to the introduction of circulating melatonin into the GI tract, it is synthesized in the intestinal mucosa enterochromaphine cells of the GI tract. All GI tract tissues also have melatonin binding sites. Previously, Alikhani et al. showed that melatonin improved gastric mucus secretion and gastric motility in diabetic rats (Alikhani et al., 2015). Yang et al. demonstrated that melatonin restored elevated intestinal permeability in STZ-induced diabetic rats (Yang et al., 2016).

Malondialdehyde that is the final product of lipid peroxidation triggers atherosclerosis and atherotrombosis through oxidizing the LDL. In clinical researches, elevated plasma MDA levels were detected in diabetic patients (Mandal, Varghese, Gaviraju, Talwar, & Malini, 2019). Hadjzadeh et al. demonstrated that melatonin treatment lowered gastric MDA levels and prevented gastric oxidative damage in STZ-induced diabetic rats (Hadjzadeh et al., 2018). Moreover, various studies exhibited positive effects of melatonin on elevated MDA levels in differ-



ent tissues. For instance, Montilla et al. administered melatonin to the rats before triggering diabetes with STZ (Montilla, Tunes, de Agueda, Gascon, & Soria, 1998). They detected that hyperglycemia and elevated MDA levels in plasma and renal tissue were prevented with melatonin treatment. In agreement with previous reports, in our study, melatonin-treated diabetic rats had significantly lower intestinal MDA levels compared to diabetic rats. In the combined treatment group, the MDA level also decreased significantly. Melatonin lifted the effectiveness of insulin in the combined treatment group.

With the thiol group, GSH eliminates the free radicals (Vural et al., 2001). According to experimental and clinical studies, DM affects GSH levels negatively due to its elevated oxidation or reduced synthesis. For instance, the clinical studies have shown that serum GSH concentration is reduced in DM patients (Mandal et al., 2019). Moreover, decreased intestinal GSH levels were determined with high glucose concentrations in the experimental studies (Bolkent, Bolkent, Yanardag, Mutlu, & Yıldırım, 2006). The results of our study demonstrated that intestinal tissue GSH levels were significantly lower in the diabetes group than the control group. Both melatonin and combined treatments increased GSH levels compared to the diabetes group. Similarly, Vural et al. determined in their study conducted on STZ-induced diabetic rats that melatonin treatment brought decreased erythrocytes GSH levels to control group levels (Vural et al., 2001).

Superoxide dismutase, which is known as the antioxidant enzyme, catalyzes superoxide anion dismutation into oxygen and hydrogen peroxide. Loven et al. demonstrated in the experimental study that STZ-induced diabetic rats had reduced SOD levels in intestinal tissues (Loven et al., 1982). In various clinical studies, SOD levels were found to be low in DM patients due to SOD glucosylation and increased free radicals (Djordjević, Djurić, Djordjević, Apostolski, & Živković, 2011). The results of our study demonstrated that diabetes reduced the SOD activity with respect to the control group. Superoxide dismutase activity was also lower in the insulin-treated group compared to the control group. However, SOD activity increased in the melatonin and combined treatment groups. Supportively, Hadjzadeh et al. demonstrated that melatonin treatment in STZ-induced diabetic rats improved gastric SOD activities (Hadjzadeh et al., 2018).

Myeloperoxidase is released from activated leukocytes in the inflammatory area and generates ROS (Garcia et al., 2015; Santhi, Shaik, & Mahendran, 2017). Studies in diabetic patients have found that serum MPO levels increase with elevated blood glucose levels (Song et al., 2015). High glucose levels increase hydrogen peroxide formation, and MPO uses hydrogen peroxide as a biological substrate to create highly reactive hypochlorid acid (Garcia et al., 2015). Furthermore, MPO triggers the formation of foam cells and plaque rupture through LDL modification. Supportively, it was demonstrated that coronary artery disease elevated plasma MPO concentration in diabetic patients (Song et al., 2015). Hardin et al. demonstrated elevated intestinal MPO activity in rats with Type 1 DM (Hardin, Donegan, Woodman, Trevenen, & Gall, 2002). In different experimental studies, melatonin

treatment has been shown to reduce MPO activity that was elevated in various tissues due to DM. For instance, Onk et al. found that melatonin treatment significantly reduced MPO levels in lung tissue that were elevated due to the STZ-induced diabetes in rats (Onk et al., 2018). Gurel-Gokmen et al. reported that melatonin treatment in STZ-induced diabetic rats potentiates the effect of insulin to reduce MPO levels in brain tissue (Gurel-Gokmen et al., 2018). In our study, the diabetes group had significantly elevated MPO activity when compared to the control group. With melatonin and melatonin + insulin treatments, MPO activity decreased significantly.

Caspase-3, which is the mediator of cell apoptosis, is an enzyme member of the cysteine protease family (Ghosh et al., 2009). Various experimental studies suggested that high caspase-3 activity contributes to both diabetes development and its complications. Liadis et al. found that diabetes did not occur in caspase-3 knockout mice with STZ administration because apoptosis did not develop in  $\beta$  cells (Liadis et al., 2005). In different diabetes studies, increased caspase-3 activity was demonstrated to damage the hippocampus, kidneys, and retina through triggering apoptosis (Ghosh et al., 2009; Anarkooli, Sankian, Ahmadpor, Varasteh, & Haghair, 2008; Kowluru & Koppolu, 2002). In limited experimental studies, it has been shown that apoptosis due to high caspase-3 activity caused by hyperglycemia is alleviated with melatonin treatment (Onk et al., 2018). In our study, in diabetes group, intestinal caspase-3 activity was elevated significantly compared to control group. Melatonin treatment reduced caspase-3 activity compared to the diabetes group. This effect was not achieved with insulin therapy.

With the western blot method, it is possible to determine whether certain proteins specific to apoptosis are expressed or broken, such as caspase-3. In our study, when the expression of caspase-3 proteins were examined with western blot, it was demonstrated that diabetes and insulin treatment groups had increased caspase-3 bands with respect to the control group. The reduction in these bands was observed with the co-administration of melatonin and insulin. It can be said that co-administration of insulin and melatonin decreases cell death and increases cell proliferation.

## CONCLUSION

Our results demonstrate that melatonin treatment prevents the intestinal tissue damage in DM. Additionally antioxidant effects of melatonin on intestinal tissues are more obvious than insulin-alone therapy. As a consequence, melatonin could be used as a potential therapeutic supplement in diabetes-induced intestinal damage.

**Acknowledgement:** This study was funded by Marmara University Scientific Research Projects Committee with the grant number SAG-C-YLP-091215-0532.

**Peer-review:** Externally peer-reviewed.

**Ethics Committee Approval:** All experimental protocols were performed according to the Marmara University Animal Care and Use Committee (Protocol number: 33.2015.mar).

**Author Contributions:** Conception/Design of Study- Z.A.Ç.Y., G.B.A., Ö.Ç., G.Ş.; Data Acquisition- Z.A.Ç.Y., G.Ş.; Data Analysis/Interpretation- Z.A.Ç.Y., G.Ş.; Drafting Manuscript- Z.A.Ç.Y., G.Ş.; Critical Revision of Manuscript- Z.A.Ç.Y., G.B.A., Ö.Ç., G.Ş.; Final Approval and Accountability- Z.A.Ç.Y., G.B.A., Ö.Ç., G.Ş.; Technical or Material Support- Z.A.Ç.Y., G.B.A., Ö.Ç., G.Ş.; Supervision- G.Ş.

**Conflict of Interest:** The authors have no conflict of interest to declare.

**Financial Disclosure:** This study was supported by Marmara University Scientific Research Projects Committee (Grant number: SAG-C-YLP-091215-0532).

## REFERENCES

- Alikhani, V., Keshavarzi, Z., Hadjzadeh, M. A. R., & Karimi, S. (2015). The effect of melatonin on gastric parameters following diabetes induction in male rats. *Acta Endocrinologica (Buc)*, 11(2), 155–161. <https://doi.org/10.4183/aeb.2015.155>
- Anarkooli, I. J., Sankian, M., Ahmadpour, S., Varasteh, A. R., & Haghiri, H. (2008). Evaluation of Bcl-2 family gene expression and caspase-3 activity in hippocampus STZ- induced diabetic rats. *Experimental Diabetes Research*, 2008, 638467. <https://doi.org/10.1155/2008/638467>
- Bansal, A. K., & Bilaspuri, G. S. (2011). Impact of oxidative stress and antioxidants on semen functions. *Veterinary Medicine International*, 2011, 686137. <https://doi.org/10.4061/2011/686137>
- Beuge, J. A., & Aust, S. D. (1978). Microsomal lipid peroxidation. *Methods in Enzymology*, 52, 302–311. [https://doi.org/10.1016/s0076-6879\(78\)52032-6](https://doi.org/10.1016/s0076-6879(78)52032-6)
- Beutler, E., Duron, O., & Kelly, B. M. (1963). Improved method for the determination of blood glutathione. *Journal of Laboratory and Clinical Medicine*, 61, 882–888.
- Bhor, V. M., Raghuram, N., & Sivakami, S. (2004). Oxidative damage and altered antioxidant enzyme activities in the small intestine of streptozotocin-induced diabetic rats. *The International Journal of Biochemistry & Cell Biology*, 36, 89–97.
- Bolkent, S., Bolkent, S., Yanardag, R., Mutlu, O., & Yildirim, S. (2006). Alterations in somatostatin cells and biochemical parameters following zinc supplementation in gastrointestinal tissue of streptozotocin-induced diabetic rats. *Acta Histochem Cytochem*, 39(1), 9–15. <https://doi.org/10.1267/ahc.05054>
- Bradford, M. M. (1976). A rapid and sensitive method for the quantitation of microgram quantities of protein utilizing the principle of protein-dye binding. *Analytical Biochemistry*, 72(2), 248–254. <https://doi.org/10.1006/abio.1976.9999>
- Costes, S., Boss, M., Thomas, A. P., & Matveyenko, A. V. (2015). Activation of Melatonin Signaling Promotes  $\beta$ -Cell Survival and Function. *Molecular Endocrinology*, 29(5), 682–692. <https://doi.org/10.1210/me.2014-1293>
- Çevik, Ö., Oba, R., Macit, Ç., Çetinel, Ş., Çilingir-Kaya, Ö.T., Şener, E., & Şener, G. (2012). Lycopene inhibits caspase-3 activity and reduces oxidative organ damage in a rat model of thermal injury. *Burns*, 38(6), 861–871. <https://doi.org/10.1016/j.burns.2012.01.006>
- Djordjevic, G. M., Djuric, S. S., Djordjevic, V. B., Apostolski, S., & Zivkovic, M. (2011). The role of oxidative stress in pathogenesis of diabetic neuropathy: Erythrocyte superoxide dismutase, catalase and glutathione peroxidase level in relation to peripheral nerve conduction in diabetic neuropathy patients. Dr. Colleen Croniger (Ed.), *Role of the Adipocyte in Development of Type 2 Diabetes* (pp. 153-178). Rijeka, Croatia: InTech. Retrieved from <https://www.intechopen.com/books/role-of-the-adipocyte-in-development-of-type-2-diabetes/the-role-of-oxidative-stress-in-pathogenesis-of-diabetic-neuropathy-erythrocyte-superoxide-dismutase>
- Esposito, E., & Cuzzocrea, S. (2010). Antiinflammatory activity of melatonin in central nervous system. *Current Neuropharmacology*, 8(3), 228–242. <https://doi.org/10.2174/157015910792246155>
- Garcia, A. G., Rodrigues, M. R., Alonso, C. G., Rodrigues-Ochoa, D. Y., & Aguilar, C. A. (2015). Myeloperoxidase is associated with insulin resistance and inflammation in overweight subjects with first-degree relatives with Type 2 diabetes mellitus. *Diabetes & Metabolism Journal*, 39(1), 59–65. <https://doi.org/10.4093/dmj.2015.39.1.59>
- Ghosh, S., Khazaei, M., Moien-Afshari, F., Ang, L. S., Granville, D. J., Verchere, C. B. ... Laher, I. (2009). Moderate exercise attenuates caspase-3 activity, oxidative stress, and inhibits progression of diabetic renal disease in db/db mice. *American Journal of Physiology-Renal Physiology*, 296(4), 700–708. <https://doi.org/10.1152/ajprenal.90548.2008>
- Gurel-Gokmen, B., Ipekci, H., Oktay, S., Alev, B., Ustundag, U. V., Ak, E., Tunali-Akbay, T. (2018). Melatonin improves hyperglycemia induced damages in rat brain. *Diabetes Metabolism Research and Reviews*, 34(8), e3060. <https://doi.org/10.1002/dmrr.3060>
- Hadjzadeh, M. A. R., Alikhani, V., Hosseini, S., Zarei, B., & Keshavarzi, Z. (2018). The effect of melatonin against gastric oxidative stress and dyslipidemia in streptozotocin-induced diabetic rats. *Acta Endocrinologica (Buchar)*, 14(4), 453–458. <https://doi.org/10.4183/aeb.2018.453>
- Hardin, J. A., Donegan, L., Woodman, R. C., Trevenen, C., & Gall, D. G. (2002). Mucosal inflammation in a genetic model of spontaneous type I diabetes mellitus. *Canadian Journal of Physiology and Pharmacology*, 80(11), 1064–1070. <https://doi.org/10.1139/y02-138>
- Hillegas, L. M., Griswold, D. E., Brickson, B., & Winslow, C. A. (1990). Assessment of myeloperoxidase activity in whole rat kidney. *Journal of Pharmacological Methods*, 24(4), 285–295. [https://doi.org/10.1016/0160-5402\(90\)90013-b](https://doi.org/10.1016/0160-5402(90)90013-b)
- Husni, A., Anggara, F. P., Isnansetyo, A., & Nugroho, A. E. (2016). Blood glucose level and lipid profile of streptozotocin-induced diabetic rats treated with *Sargassum polystum* extract. *International Journal of Pharmaceutical and Clinical Research*, 8(5), 445–450. <https://doi.org/10.3923/jbs.2016.58.64>
- Hussain, S. A., Khadim, H. M., Khalaf, B. H., Ismail, S. H., Hussein, K. I., & Sahib, A. S. (2006). Effects of melatonin and zinc on glycemic control in Type 2 diabetic patients poorly controlled with metformin. *Saudi Medical Journal*, 27(10), 1483–1488.
- Ighodaro, O. M. (2018). Molecular pathways associated with oxidative stress in diabetes mellitus. *Biomedicine & Pharmacotherapy*, 108, 656–662.
- Kochar, N. I., & Umathe, S. N. (2009). Beneficial effects of L-arginine against diabetes-induced oxidative stress in gastrointestinal tissues in rats. *Pharmacological Reports*, 61, 665–672. [https://doi.org/10.1016/s1734-1140\(09\)70118-5](https://doi.org/10.1016/s1734-1140(09)70118-5)
- Kowluru, R., & Koppolu, P. (2002). Diabetes-induced activation of caspase-3 in retina: effect of antioxidant therapy. *Free Radical Research*, 36(9), 993–999. <https://doi.org/10.1080/1071576021000006572>
- Liadis, N., Murakami, K., Eweida, M., Elford, A. R., Sheu, L., Gaisano, H. Y. ... Woo, M. (2005). Caspase-3-dependent  $\beta$ -cell apoptosis in the initiation of autoimmune diabetes Mellitus. *Molecular and Cellular Biology*, 25(9), 3620–3629. <https://doi.org/10.1128/MCB.25.9.3620-3629.2005>
- Loven, D. P., Scheld, H. P., Oberley, L. W., Wilson, H. D., Bruch, L., Niehaus, C. L. (1982). Superoxide dismutase activity in the intestine of the streptozotocin-diabetic rat. *Endocrinology*, 111(3), 737–742. <https://doi.org/10.1210/endo-111-3-737>
- Mandal, M., Varghese, A., Gaviraju, V. K., Talwar, S. N., Malini, S. S. (2019). Impact of hyperglycaemia on molecular markers of oxidative stress and antioxidants in type 2 diabetes mellitus. *Clinical Diabetology*, 8(4), 215–222. <https://doi.org/10.5603/DK.2019.0015>

- Montilla, P. L., Tunez, I. F., de Agueda, C. M., Gascon, F. L., Soria, J. V. (1998). Protective role of melatonin and retinol palmitate in oxidative stress and hyperlipidemic nephropathy induced by adriamycin in rats. *Journal of Pineal Research*, 25(2), 86–93. <https://doi.org/10.1111/j.1600-079x.1998.tb00544.x>
- Mylroie, A. A., Collins, H., Umbles, C., Kyle, J. (1986). Erythrocyte superoxide dismutase activity and other parameters of copper status in rats ingesting lead acetate. *Toxicology and Applied Pharmacology*, 82(3), 512–520. [https://doi.org/10.1016/0041-008x\(86\)90286-3](https://doi.org/10.1016/0041-008x(86)90286-3)
- Nogueira, T. C., Lellis-Santos, C., Jesus, D. S., Taneda, M., Rodrigues, S. C., Amaral, F. G. ... Anhe, G. F. (2011). Absence of melatonin induces night-time hepatic insulin resistance and increased gluconeogenesis due to stimulation of nocturnal unfolded protein response. *Endocrinology*, 152(4), 1253–1263. <https://doi.org/10.1210/en.2010-1088>
- Onk, D., Onk, O. A., Erol, H. S., Özkara, M., Çomaklı, S., Ayazoğlu, T. A., ... Ünver, S. (2018). Effect of melatonin on antioxidant capacity, inflammation and apoptotic cell death in lung tissue of diabetic rats. *Acta Cirurgica Brasileira*, 33(4), 375–385. <https://doi.org/10.1590/s0102-865020180040000009>
- Owino, S., Buonfiglio, D. D. C., Tchio, C., Tosini, G. (2019). Melatonin signaling a key regulator of glucose homeostasis and energy metabolism. *Frontiers in Endocrinology*, 10, 488. <https://doi.org/10.3389/fendo.2019.00488>
- Paskaloğlu, K., Şener, G., Ayanoğlu-Dülger, G. (2004). Melatonin treatment protects against diabetes-induced functional and biochemical changes in rat aorta and corpus cavernosum. *European Journal of Pharmacology*, 499(3), 345–354. <https://doi.org/10.1016/j.ejphar.2004.08.002>
- Santhi, T., Shaik, J. B., Mahendran, B. (2017). Myeloperoxidase levels predicts the vascular dysfunction in patients with Type 2 Diabetes Mellitus. *Journal of Dental and Medical Sciences*, 16(3), 30–34.
- Song, P., Xu, J., Song, Y., Jiang, S., Yuan, H., Zhang, X. (2015). Association of plasma myeloperoxidase level with risk of coronary artery disease in patients with Type 2 diabetes. *Disease Markers*, 2015, 761939. <https://doi.org/10.1155/2015/761939>
- Ullah, A., Khan, A., Khan, I. (2016). Diabetes mellitus and oxidative stress—A concise review. *Saudi Pharmaceutical Journal*, 24, 547–553. <https://doi.org/10.1016/j.jsps.2015.03.013>
- Vural, H., Sabuncu, T., Arslan, S.O., Aksoy, N. (2001). Melatonin inhibits lipid peroxidation and stimulates the antioxidant status of diabetic rats. *Journal of Pineal Research*, 31, 193–198. <https://doi.org/10.1034/j.1600-079x.2001.310301.x>
- Wolosin, J. D., & Edelman, S. V. (2000). Diabetes and the gastrointestinal tract. *Clinical Diabetes*, 18(4), 148.
- Yang, X., Zou, D., Tang, S., Fan, T., Su, H., Hu, R. ... Wang, Y. (2016). Ameliorative effect of melatonin against increased intestinal permeability in diabetic rats: possible involvement of MLCK-dependent MLC phosphorylation. *Molecular Cellular Biochemistry*, 416(1-2), 23–32. <https://doi.org/10.1007/s11010-016-2691-4>.

# *Lactobacillus plantarum* and *Lactobacillus helveticus* modulate SIRT1, Caspase3 and Bcl-2 in the testes of high-fructose-fed rats

Onur Gökhan Yıldırım<sup>1</sup> , Gökhan Sadi<sup>2</sup> , Fatma Akar<sup>3</sup> 

<sup>1</sup>Artvin Coruh University, Vocational School of Health Services, Department of Pharmacy Services, Artvin, Turkey

<sup>2</sup>Karamanoglu Mehmetbey University, K.Ö. Science Faculty, Department of Biology, Karaman, Turkey

<sup>3</sup>Gazi University, Faculty of Pharmacy, Department of Pharmacology, Ankara, Turkey

**ORCID IDs of the authors:** O.G.Y. 0000-0003-0090-7369; G.S. 0000-0002-6422-1203; F.A. 0000-0002-5432-0304

**Cite this article as:** Yıldırım, O. G., Sadi, G., & Akar, F. (2020). *Lactobacillus plantarum* and *Lactobacillus helveticus* modulate SIRT1, Caspase3 and Bcl-2 in the testes of high-fructose-fed rats. *Istanbul Journal of Pharmacy*, 50 (3), 168-175.

## ABSTRACT

**Background and Aims:** The influence of a high-fructose diet and probiotics on the male reproductive system and the testicular apoptotic pathway has been poorly documented. In this study, we aimed to investigate the influence of *Lactobacillus plantarum* and *Lactobacillus helveticus* supplementation on apoptotic factors such as sirtuin1, caspase3 and bcl-2 on the testicular tissue of high-fructose-fed rats.

**Methods:** Fructose was given to the rats as a 20% solution in drinking water for 15 weeks. Gene expressions were established by real-time PCR. Protein levels were determined by Western blot analysis.

**Results:** Fructose consumption did not change mRNA expression of SIRT1, but did result in a decreased protein level. Dietary fructose reduced bcl-2 mRNA and protein expressions, whereas no changes were observed in the gene and protein expression levels of factor caspase-3. Both *Lactobacillus* supplementations increased SIRT1 protein expression without changing the mRNA levels in fructose-fed rats. The supplementations with both probiotics produced a significant down-regulation on caspase3 mRNA and protein levels. Bcl-2 protein level increases with both probiotics supplementation while, mRNA level did not show difference in *L. plantarum*, but increased in *L. helveticus* supplementation.

**Conclusion:** Treatments with *L. plantarum* and *L. helveticus* can reduce testicular apoptosis induced by dietary high-fructose in rats via suppressing caspase3 and promoting sirt1 and bcl-2 protein expressions.

**Keywords:** Dietary fructose, *Lactobacillus plantarum*, *Lactobacillus helveticus*, apoptosis, testes

## INTRODUCTION

Metabolic syndrome (MetS), which can be promoted by excessive fructose consumption, is the main health problem that affects people life quality along with the worldwide due to its many complications such as glucose intolerance, central adiposity, hyperlipidemia, hypertension, fatty liver disease and chronic low-grade inflammation (Dandona & Dhindsa, 2011; Morrison & Brannigan, 2015; Rastrelli, Filippi, Sforza, Maggi, & Corona, 2018; Tsai, Matsumoto, Fujimoto, & Boyko, 2004). In recent studies, it has been shown that low testosterone levels, one of the several factors responsible for male infertility, is commonly associated with metabolic syndrome, obesity, and Type-2 diabetes (Caldas, Porto, Motta, & Casulari, 2009; Dhindsa et al., 2010; Ebrahimi et al., 2017). Studies have shown that low testosterone levels may enhance oxidative stress and also trigger apoptosis of Germ cells and Sertoli cells (Chaki et al., 2006; Simoes et al., 2013). However, the roles of apoptosis in fructose-related MetS and testicular homeostasis has not been investigated. In recent years, studies in rodents showed that diabetes causes increased inflammation and testicular oxidative stress as well as elevat-

### Address for Correspondence:

Onur Gökhan YILDIRIM, e-mail: ogyildirim@artvin.edu.tr

This work is licensed under a Creative Commons Attribution 4.0 International License.



Submitted: 09.08.2020  
Revision Requested: 29.09.2020  
Last Revision Received: 30.09.2020  
Accepted: 14.10.2020

ed Bax/Bcl2 ratio and caspase-dependent apoptosis (Nna, Bakar, Ahmad, & Mohamed, 2018; L. Zhao et al., 2017). The consumption of 10% fructose in drinking water for 8 weeks significantly increased apoptosis-associated speck-like protein (ASC) and caspase-1 levels of rat kidneys (Hu, Zhang, Pan, Li, & Kong, 2012). A recent study demonstrated that a high consumption of fructose (35% of daily calories) increased Bax / Bcl2 ratio and the number of apoptotic cells compared to the control in the liver of mice (Choi, Abdelmegeed, & Song, 2017). It has been reported that rats fed with a fructose diet have the activation of pro-apoptotic c-Jun N-terminal kinase (JNK) and apoptotic caspase3 in the liver and pancreatic tissues (Balakumar et al., 2016). We have previously shown that a high-fructose diet causes down-regulation of SIRT1 and up-regulation of iNOS protein expressions in the aorta of rats (Akar et al., 2012; Babacanoglu, Yildirim, Sadi, Pektas, & Akar, 2013). In rats administered with 30% fructose in drinking water, an induction of apoptosis was found and an increase in Bax/Bcl2 ratio and caspase-3 levels in the aorta were detected (Lu, Zhao, Yao, & Zhang, 2017). The consumption of 10% fructose in drinking water initiated apoptosis with increased Tumor necrosis factor- $\alpha$  (TNF- $\alpha$ ) and p53 levels, while it suppressed SIRT1 of rat liver (L. Song et al., 2019). In another study, the administration of 30% fructose in drinking water caused structural abnormalities and increased apoptotic cell number in the testes of rats (Meydanli et al., 2018). In our previous study, dietary high-fructose enhanced mitogenic protein IGF-1R and inflammatory markers such as iNOS, IL-1 $\beta$ , and TNF- $\alpha$  expressions which are accompanied by low testosterone in the testes of rats. Besides, our histological examination demonstrated intratubular degeneration in the testes of fructose-fed rats (Yildirim et al., 2019).

Probiotics are living microorganisms that benefit their host and are used to prepare fermented products (Hotel & Cordoba, 2001; Rosa et al., 2016). The beneficial effects of probiotics on health are accepted worldwide. Probiotics may be useful in reducing cardiovascular risk factors from pathological conditions such as type 2 diabetes (Hendijani & Akbari, 2018; Markowiak & Slizewska, 2017). Increased adipocyte inflammation, liver fat accumulation, and apoptosis due to high-fat and fructose diets were significantly suppressed by *Lactobacillus* (*L.* *rhamnosus*) supplementation (Q. Liu et al., 2020). Another study reported that high-fructose-induced increases in plasma glucose, insulin and triglyceride levels, oxidative stress, and hepatic lipogenesis were reduced with *L. curvatus* and *L. plantarum* supplementations (Park, Ahn, Huh, McGregor, & Choi, 2013). In our recent study, an *L. plantarum* and *L. helveticus* supplementation in high-fructose-fed rats reduced plasma insulin levels and improved kidney antioxidant parameters (Korkmaz et al., 2019a). Also, the consumption of these probiotics improved the insulin signaling pathway in the kidney and liver of rats fed with fructose (Korkmaz et al., 2019b; Sumlu, Bostanci, Sadi, Alcigir, & Akar, 2020). In this study, we aimed to find the effectiveness of *L. plantarum* and *L. helveticus* on the apoptotic targets in the testes of high-fructose-fed rats.

## MATERIALS AND METHODS

### Animal and diets

The Ethical Animal Research Committee of Afyon Kocatepe University (Akuhadyek-49533702), in compliance with the

Guide for the Care and Use of Laboratory Animals (National Research Council Committee 2011) approved the protocol for animal use. Three-week-old male Wistar rats were housed in temperature- and humidity-controlled rooms (20-22°C, 40-50% relative humidity) with a 12-h light-dark cycle. The rats were fed with a standard rodent chow diet composed of 62% starch, 23% protein, 4% fat, 7% cellulose, standard vitamins, and salt mixture. After acclimation for 1 week, the rats were randomly divided into 4 groups: control, fructose Fruc, fructose + *L. plantarum* (Fruc + LP), and fructose + *L. helveticus* (Fruc + LH). Fructose (Danisco Sweeteners OY, Finland) was given to the rats as a 20% solution (w/v) in drinking water, which was freshly prepared every day, *ad libitum* for 15 weeks. *L. helveticus* and *L. plantarum* were given by gastric gavage once a day for the final six weeks in 2 ml saline solution at appropriate dosing ( $1 \times 10^9$  CFU per 100 g of body weight of animal). The same volume of saline was given to the control and fructose groups by the gavage for the same period. At the end of the experiment, the animals were anesthetized with a mixture of ketamine-xylazine (100 and 10 mg/kg, respectively, i.p.). The testicular tissues were immediately dissected and blotted dry. Then they were frozen in liquid nitrogen and stored at -85 °C until the gene and protein expression studies.

### Preparation of *Lactobacillus plantarum* and *Lactobacillus helveticus*

*Lactobacillus helveticus* and *L. plantarum* were cultured in De Man, Rogosa and Sharpe broth (MRS; Oxoid; Unipath Ltd., Basingstoke, Hampshire, England) at 30 °C in a rotary shaker at 150 rpm. Stock cultures were stored at -80 °C in MRS broth including 20% (v/v) glycerol. Erlenmeyer flasks containing 20 ml of MRS were inoculated with 1.5 ml of glycerol stock culture. The cultures were incubated at 35 °C  $\pm$  1 °C on a rotary shaker at 150 rpm and grown to an optical density of 1.0 at 600 nm (cell density corresponding to  $1 \times 10^8$  CFU/ml). The culture was divided into 10 ml tubes ( $1 \times 10^9$  CFU), then cells were harvested at 5000 g for 5 min at 4 °C. The cell pellets were washed by isotonic saline solution and lyophilized under a freeze dryer.

### Determination of gene expressions with quantitative real-time polymerase chain reaction (qRT-PCR)

Total RNAs were isolated from the testicular tissues using RNeasy total RNA isolation kit (Qiagen, Venlo, The Netherlands) as described in the manufacturer's protocol. After isolation, the amount and the quality of the total RNA were determined by spectrophotometry at 260/280nm and agarose gel electrophoresis. Then, 1  $\mu$ g total RNA was reverse transcribed to cDNA with a commercial first-strand cDNA synthesis kit (Thermo Fisher Scientific, USA). Sirt1, caspase3 and bcl-2 gene expression levels were determined by a real-time quantitative polymerase chain reaction (qRT-PCR, LightCycler480 II, Roche, Basel, Switzerland). mRNA expressions were determined by mixing 1  $\mu$ l cDNA, 5  $\mu$ l 2X SYBR Green Master Mix (Roche, Basel, Switzerland) and 2  $\mu$ l primer pairs each (Table 1) at 0.5  $\mu$ M final concentrations in a total volume of 10  $\mu$ l. qRT-PCR was performed as follows: initial denaturation at 95 °C for 10 min, denaturation at 95 °C for 10 s, annealing at 58 °C for 15 s and extension at 72 °C for 15 s with 40 repeated thermal cycles measuring the green fluorescence at the end of each extension step. All samples were performed in



**Table 1. Primer sequences of sirt1, caspase3, bcl-2 and internal standard gapdh used for the mRNA expression determination.**

Gene	Forward Primer Sequence (5'→3')	Reverse Primer Sequence (5'→3')
<i>sirt1</i>	CGGTCTGTTCAGCATCATCTTCC	CGCCTTATCTCTAGTTCCTGTG
<i>caspase3</i>	GAGCTTGAACGCGAAGAAA	CTCTGAGGTTAGTGCATCG
<i>bcl-2</i>	TTCCTGCATCTCATGCCAAG	TACCAATAGCACTTCGCGTC
<i>gapdh</i>	TGATGACATCAAGAAGGTGGTGAAG	TCCTTGAGGCCATGTGGGCCAT

triplicate and the specificity of the PCR products was confirmed using melt analysis. The relative expression of genes with respect to the internal control; glyceraldehyde 3-phosphate dehydrogenase (*gapdh*) was measured with the efficiency corrected advance relative quantification tool provided by the LightCycler® 480 SW 1.5.1 software.

#### Determination of protein expressions by Western blot

Testicular tissues were homogenized in 4-fold volumes of homogenization medium (50 mM Tris, 150 mM sodium chloride, 5 mM ethylenediaminetetraacetic acid, 1%(w/w) Triton X-100, 0.26% (w/v) sodium deoxycholate, 50 mM sodium fluoride, 0.1 mM sodium orthovanadate and 0.2 mM phenylmethylsulfonyl fluoride, pH:7.4) with Tissue Ruptor™ (Qiagen, Venlo, Netherlands) homogenizer and then the homogenates were centrifuged at 1500g for 10 min at +4 °C. Then, the supernatants were collected and protein levels were determined using the Lowry method (Lowry, Rosebrough, Farr, & Randall, 1951).

All groups total proteins (50–100 µg) were separated by the SDS-PAGE method using Mini Protean Tetra electrophoresis (Bio-Rad Laboratories, Hercules CA, USA). The separated proteins were transferred onto the polyvinylidene fluoride membrane with a semi-dry electroblotting apparatus (TransBlot Turbo, BioRad, Germany) after which the membranes were blocked with 5% bovine serum albumin for 1 h. Primary antibodies were utilized for priming the respective SIRT1 (Anti-SIRT1 Rabbit IgG, Scbt sc-15404 1/500), Caspase3 (Anti-Caspase-3 Rabbit IgG, Sigma C8487 1/1000) and Bcl-2 (Anti-Bcl-2 Rabbit IgG, Scbt 1/ 1000) proteins overnight at +4 °C.

Membranes for normalization were labeled with an internal control *Gapdh* protein [Anti-*Gapdh* Rabbit IgG, Scbt sc-25778, 1/2000]. After the primary antibody incubation and washing step, Horse Radish Peroxidase (HRP) conjugated secondary antibody (Goat anti-rabbit IgG-HRP conjugate, Scbt sc-2030, 1/10000) was incubated for 1 hour. Then the blots were treated with Clarity™ Western ECL (Bio-Rad Laboratories, Hercules, USA) substrate solution for 5 min. Images of the blots were obtained using the ChemiDoc™ MP Chemiluminescence detection system (Bio-Rad Laboratories, USA) equipped with a CCD camera. The relative expression of the proteins with respect to *Gapdh* was calculated using the ImageLab 4.1 software.

#### Statistical analysis

The results are given as mean ± standard error of the mean (SEM); n is the number of rats. Statistical analyses were performed using the Student's t-test for unpaired data or one-way ANOVA followed by the Bonferroni post-hoc analysis. Values were evaluated with GraphPad Prism (version 6, GraphPad

Software, La Jolla, CA). Data were considered to be significantly different when the P-value was less than 0.05.

#### RESULTS

Expression levels of genes related to testicular apoptosis *sirt1*, *caspase3* and *bcl-2* were measured by qRT-PCR. As shown in Figure 1a, neither dietary fructose nor the probiotic supplementations altered expression levels of SIRT1mRNA in the

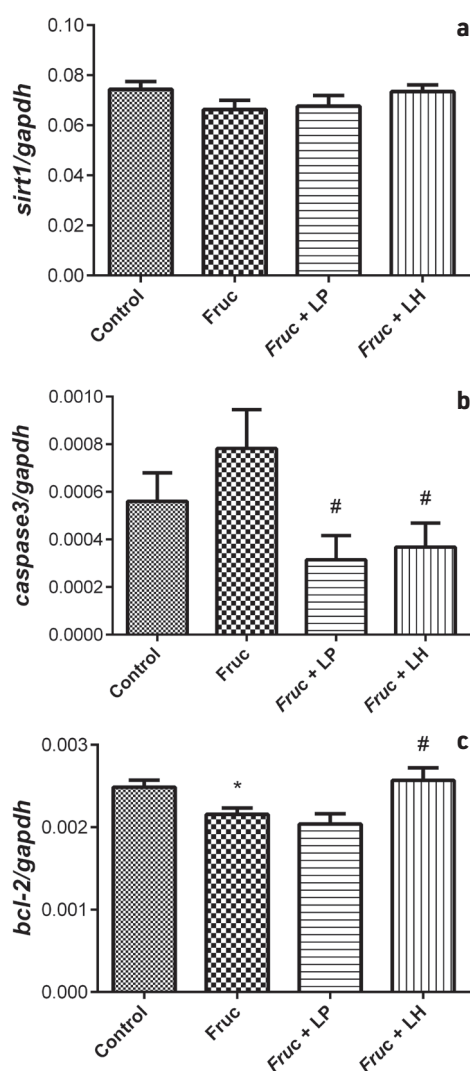


**Figure 1.** The mRNA expression levels of *sirt1* (a), *caspase3* (b) and *bcl-2* (c) in the testes of Control, Fruc, Fruc + LP, and Fruc + LH groups. Data were normalized using *gapdh*. Values are expressed as mean ± SEM, n=6–8. \*p<0.05 versus control group; #p<.05, significantly different from fructose group. Fruc: Fructose; LP: *L. plantarum*; LH: *L. helveticus*.

testicular samples of rats. There was a tendency toward an increase in the expression level of caspase3 mRNA in the fructose-treated rats compared to the controls, but the differences did not achieve a significance level. However, *L. plantarum* and *L. helveticus* supplementations decreased the expression of caspase3 mRNA in fructose-treated rats (Figure 1b). Importantly, the anti-apoptotic bcl-2 mRNA level was markedly decreased in fructose-fed rats, which was improved only with *L. helveticus* supplementation (Figure 1c).

The protein expression levels of SIRT1, caspase3 and bcl-2 in testes samples of rats were determined by Western Blot analysis. Dietary fructose did not change the level of caspase3. However, *L. helveticus* and *L. plantarum* supplementations decreased this protein in the testicular tissue of high-fructose-fed rats. The expressions of SIRT1 and bcl-2 proteins were signifi-

cantly decreased with a high-fructose diet, however, *L. helveticus* and *L. plantarum* supplementations markedly upregulated these proteins (Figure 2).

## DISCUSSION

A high-fructose diet may cause glucose intolerance, hypertension, hyperlipidemia, and chronic low-grade inflammation. The development of metabolic disorders might be worsened by the activation of proinflammatory cytokine and oxidative stress. We have previously shown that high-fructose consumption enhances the expression of inflammatory factors in the testis, blood vessels, liver or adipose tissue accompanied by low testosterone level in the rats (Akar et al., 2012; Babacanoglu et al., 2013; Pektas, Koca, Sadi, & Akar, 2016; Pektas, Sadi, & Akar, 2015; Pektas et al., 2017; Sadi et al., 2015; Yildirim et al.,

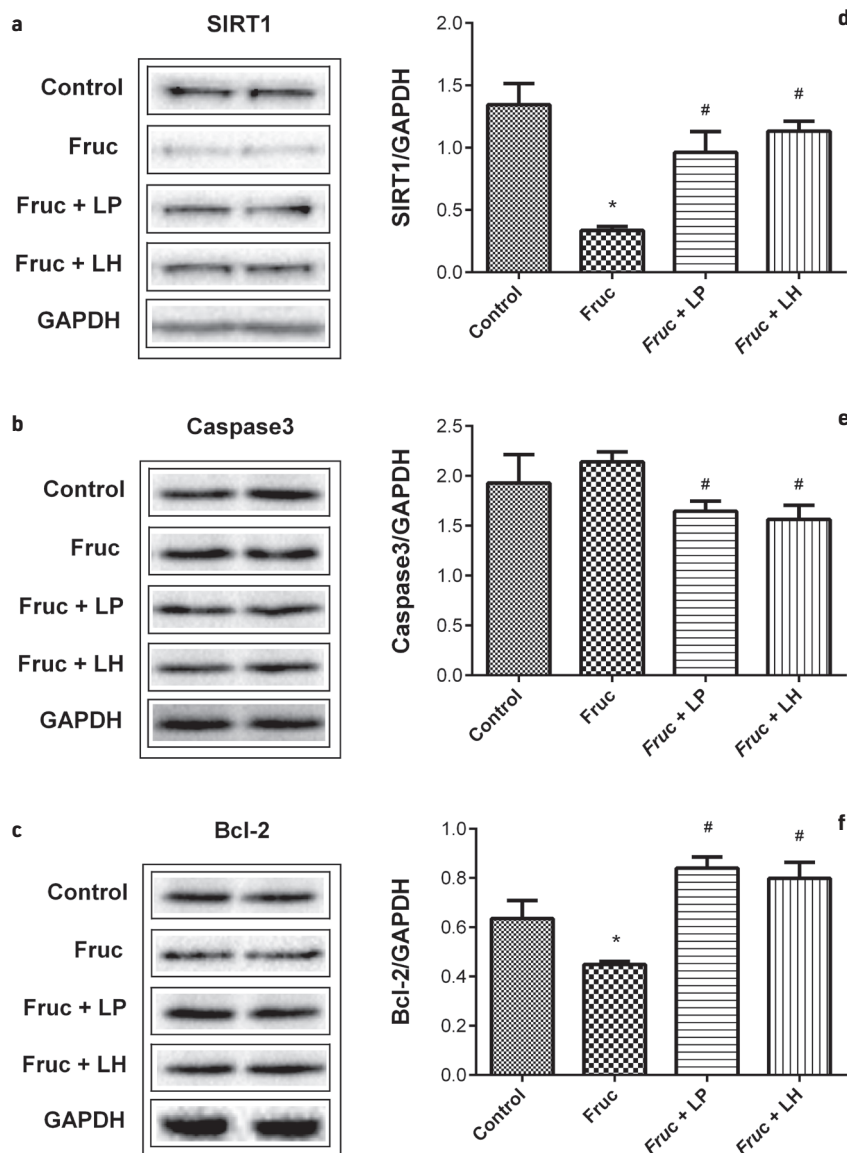


**Figure 2.** Representative Western blot bands (a-c) and relative protein expressions of SIRT1 (d), Caspase3 (e) and Bcl-2 (f) in the testes of Control, Fruc, Fruc + LP, and Fruc + LH groups. Data were normalized using Gapdh. Values are expressed as mean  $\pm$  SEM, n=6-8. \*p<0.05 versus control group; #p<.05, significantly different from fructose group; Fructose; LP: *L. plantarum*; LH: *L. helveticus*.



2019). Diseases such as MetS, type 2 diabetes, and obesity are associated with hypogonadism in men (Caldas et al., 2009; Dhindsa et al., 2010; Ebrahimi et al., 2017).

Apoptotic pathways are evolutionarily maintained and play a pivotal role in homeostasis in the testicular tissue. Although regular apoptosis of spermatogenic cells is necessary to maintain testicular homeostasis, excessive cell death can cause infertility due to damaged spermatogenesis (Passos et al., 2007). When cells are exposed to irreparable oxidative stress, the cells force proapoptotic signals to eliminate the damaging materials (Green & Llambi, 2015). Caspases and bcl-2 play important roles in cellular apoptotic processes. Previous studies showed that cell apoptosis can be suppressed due to caspase-3 inhibition with specific protease inhibitors (Creagan, Dawson, & Slack, 2004; Hayashi, Kojima, & Ito, 2006). SIRT1, which is a member of the nicotinamide adenine dinucleotide (NAD)-dependent protein deacetylase family is associated with the regulatory control of diverse cellular process including energy homeostasis, inflammation, cell survival, apoptosis and DNA repair (Vachharajani et al., 2016; X.-l. Wang et al., 2016). Recent studies show that SIRT1 deficiency cause reproductive disorder due to diminished spermatogenesis and germ cell functions (Cousens, Maresh, Yanagimachi, Maeda, & Allsopp, 2008; McBurney et al., 2003). SIRT1 and bcl-2 have an inhibitory effect on cell apoptosis playing an important role in apoptosis. Bax belongs to the same protein family as the bcl-2 gene but has an opposite function, and their equilibrium determines the degree of cell apoptosis (Brady & Gil-Gomez, 1998; Cory, Huang, & Adams, 2003; H. Liu et al., 2018; W. Song et al., 2016).

Low testosterone levels in animals may cause oxidative stress and also trigger Germ and Sertoli cells (SCs) apoptosis by increasing Bax/Bcl-2 ratio and caspase3 activities (Chaki et al., 2006; Simoes et al., 2013). Streptozotocin-induced diabetes increases pro-apoptotic proteins, whereas Bax and Bad decrease the levels of SIRT1, bcl-2 and bcl-XL, which are antiapoptotic proteins in the rat testis. Besides, the weight of reproductive organs (testis and epididymis) and level of serum testosterone were decreased in the same diabetic rats compared to the control group (Koh, 2007a, 2007b; Tsounapi et al., 2012; Xu et al., 2014; Y. Zhao et al., 2012). In animal models, diabetes increases the expression of p53 and initiates apoptosis by activating caspase3 in rat testes (Alsemeh, Samak, & El-Fatah, 2020; Faid, Al-Hussaini, & Kilarkaje, 2015; Koh, 2007a; Y. Zhao et al., 2011). Additionally, the studies showed that diabetes increases testicular caspase3 mRNA expression and suppresses bcl-2 mRNA and protein levels (Du, Qiu, Wang, & Wang, 2018; Nna et al., 2018). Recent studies demonstrated that fructose consumption in rodents initiates apoptosis in several organs such as the kidney, pancreas, aorta, liver, and testes (Balakumar et al., 2016; Choi et al., 2017; Hu et al., 2012; Lu et al., 2017; Meydanli et al., 2018). In the present study, dietary fructose did not change testicular caspase3 mRNA and protein levels. However, this dietary intervention decreased anti-apoptotic bcl-2 mRNA expression and protein level. In addition, the testicular SIRT1 protein level, but not mRNA expression, was dramatically decreased in the fructose-fed group. In a study on mice, increased testicular oxidative and nitrosative stress were shown to induce apoptosis by

stimulating the p53-mediated Bax/caspase3 pathway (Shahin, Singh, & Chaturvedi, 2018). In a previous study, we also showed that dietary high-fructose increased expression of iNOS, TNF- $\alpha$ , and Nfkb mRNAs and caused testicular degeneration (Yildirim et al., 2019). All these results revealed that high-fructose consumption could activate testicular oxidative stress, inflammation and apoptosis in the rodents.

Studies in human and experimental animals proposed a link between metabolic diseases and intestinal microbiota (Backhed, Ley, Sonnenburg, Peterson, & Gordon, 2005; Ley et al., 2005). Supplementation with *Lactobacillus* (L.) species, which is one of the primary components of human intestinal microbiota, was shown to produce antioxidant, antihyperlipidemic, antidiabetic, antiapoptotic, and anti-inflammatory activities in the experimental studies (Choi et al., 2017; Honda, Moto, Uchida, He, & Hashizume, 2012; Korkmaz et al., 2019a; Mohammadi et al., 2019; Plaza-Diaz, Ruiz-Ojeda, Vilchez-Padial, & Gil, 2017; Sumlu et al., 2020; H. F. Wang et al., 2012; Y. Wang et al., 2017). Metabolic irregularities including hyperglycemia, hyperinsulinemia, and dyslipidemia due to high-fructose consumption in rats were found to improve with *L. acidophilus* and *L. casei* supplements (Yadav, Jain, & Sinha, 2007). Moreover, supplementations with *L. plantarum* and *L. helveticus* improved the insulin signaling pathway in the kidney and liver of rats fed with a high-fructose diet (Korkmaz et al., 2019a ; 2019b; Sumlu et al., 2020). The experiments experiments with probiotics, *L. helveticus* and *L. plantarum* supplementations were able to suppress apoptosis by decreasing caspase3 and improving bcl-2 levels in different organs of the animals (Bouhafs, Moudilou, Exbrayat, Lahouel, & Idoui, 2015; Girard et al., 2009; Huang et al., 2019; Mohammadi et al., 2019). Recently, a study showed that high-fat diet-induced adiposity, glucose intolerance and dyslipidemia were ameliorated by *L. plantarum* supplementation by increasing the expression of SIRT1 and PPAR $\alpha$  in the liver and adipose tissues (Kwon et al., 2020). In our previous studies using *L. plantarum* and *L. helveticus* supplementations we determined that oral administration of these probiotics (1x10<sup>9</sup> CFU per 100 g of body weight of animal doses) for 6 weeks improved the deleterious effects of dietary fructose in the kidney and the liver (Korkmaz et al., 2019a; 2019b ; Sumlu et al., 2020). Therefore, in the current study we applied these two probiotics at the same dose for the same period. In this investigation, supplementation with *L. plantarum* and *L. helveticus* produced a marked downregulation on caspase3 mRNA and protein levels in testicular samples of high-fructose-fed rats. Also, the testicular protein level of SIRT1 was significantly increased by both prebiotic supplementations in fructose-fed rats. Moreover, the decline in testicular bcl-2 mRNA and protein levels due to high-fructose consumption was improved by *L. helveticus* supplementation. However, while *L. plantarum* supplementation increased bcl-2 protein level, it did not change mRNA expression, showing a posttranslational improving effect on the antiapoptotic factor.

In conclusion, our data indicated that treatment with *L. plantarum* and *L. helveticus* species can reduce testicular apoptosis induced by dietary high-fructose in rats by suppressing

caspase3 and promoting SIRT1 and bcl-2 protein expressions. In practice, formulations containing these probiotics could show beneficial effects in certain reproductive irregularities of males.

**Peer-review:** Externally peer-reviewed.

**Ethics Committee Approval:** The experiments reported here complied with the current laws and regulations of the Turkish Republic on the care and handling of experimental animals and the local ethics committee of experimental animals of Afyon Kocatepe University (Akuhadyek-49533702).

**Informed Consent:** Written consent was obtained from the participants.

**Author Contributions:** Conception/Design of Study- F.A.; Data Acquisition- O.G.Y., G.S.; Data Analysis/Interpretation- G.S., F.A.; Drafting Manuscript- O.G.Y., F.A.; Critical Revision of Manuscript- G.S., F.A.; Final Approval and Accountability- O.G.Y., F.A.; Technical or Material Support- O.G.Y., G.S.; Supervision- F.A.

**Conflict of Interest:** The authors have no conflict of interest to declare.

**Financial Disclosure:** This work was supported by the Gazi University Research Fund under Grant [BAP 02/2017-20].

## REFERENCES

- Akar, F., Uludag, O., Aydin, A., Aytekin, Y. A., Elbeg, S., Tuzcu, M., & Sahin, K. (2012). High-fructose corn syrup causes vascular dysfunction associated with metabolic disturbance in rats: protective effect of resveratrol. *Food and Chemical Toxicology*, *50*(6), 2135–2141.
- Alsemeh, A. E., Samak, M. A., & El-Fatah, S. S. A. (2020). Therapeutic prospects of hydroxytyrosol on experimentally induced diabetic testicular damage: potential interplay with AMPK expression. *Cell and Tissue Research*, *380*(1), 173–189.
- Babacanoglu, C., Yildirim, N., Sadi, G., Pektas, M. B., & Akar, F. (2013). Resveratrol prevents high-fructose corn syrup-induced vascular insulin resistance and dysfunction in rats. *Food and Chemical Toxicology*, *60*, 160–167.
- Backhed, F., Ley, R. E., Sonnenburg, J. L., Peterson, D. A., & Gordon, J. I. (2005). Host-bacterial mutualism in the human intestine. *Science*, *307*(5717), 1915–1920.
- Balakumar, M., Raji, L., Prabhu, D., Sathishkumar, C., Prabu, P., Mohan, V., & Balasubramanyam, M. (2016). High-fructose diet is as detrimental as high-fat diet in the induction of insulin resistance and diabetes mediated by hepatic/pancreatic endoplasmic reticulum (ER) stress. *Molecular and Cellular Biochemistry*, *423*(1-2), 93–104.
- Bouhafs, L., Moudilou, E. N., Exbrayat, J. M., Lahouel, M., & Idoui, T. (2015). Protective effects of probiotic *Lactobacillus plantarum* BJ0021 on liver and kidney oxidative stress and apoptosis induced by endosulfan in pregnant rats. *Renal Failure*, *37*(8), 1370–1378.
- Brady, H. J. M., & Gil-Gomez, G. (1998). Molecules in focus - Bax. The pro-apoptotic Bcl-2 family member, Bax. *International Journal of Biochemistry and Cell Biology*, *30*(6), 647–650.
- Caldas, A. D., Porto, A. L., Motta, L. D., & Casulari, L. A. (2009). Relationship between insulin and hypogonadism in men with metabolic syndrome. *Arquivos Brasileiros de Endocrinologia e Metabologia*, *53*(8), 1005–1011.
- Chaki, S. P., Misro, M. M., Gautam, D. K., Kaushik, M., Ghosh, D., & Chainy, G. B. (2006). Estradiol treatment induces testicular oxidative stress and germ cell apoptosis in rats. *Apoptosis*, *11*(8), 1427–1437.
- Choi, Y., Abdelmegeed, M. A., & Song, B. J. (2017). Diet high in fructose promotes liver steatosis and hepatocyte apoptosis in C57BL/6J female mice: Role of disturbed lipid homeostasis and increased oxidative stress. *Food and Chemical Toxicology*, *103*, 111–121.
- Cory, S., Huang, D. C., & Adams, J. M. (2003). The Bcl-2 family: roles in cell survival and oncogenesis. *Oncogene*, *22*(53), 8590–8607.
- Coussens, M., Maresh, J. G., Yanagimachi, R., Maeda, G., & Allsopp, R. (2008). Sirt1 deficiency attenuates spermatogenesis and germ cell function. *PLoS One*, *3*(2), e1571.
- Cregan, S. P., Dawson, V. L., & Slack, R. S. (2004). Role of AIF in caspase-dependent and caspase-independent cell death. *Oncogene*, *23*(16), 2785–2796.
- Dandona, P., & Dhindsa, S. (2011). Update: Hypogonadotropic hypogonadism in type 2 diabetes and obesity. *Journal of Clinical Endocrinology and Metabolism*, *96*(9), 2643–2651.
- Dhindsa, S., Miller, M. G., McWhirter, C. L., Mager, D. E., Ghanim, H., Chaudhuri, A., & Dandona, P. (2010). Testosterone concentrations in diabetic and nondiabetic obese men. *Diabetes Care*, *33*(6), 1186–1192.
- Du, Z., Qiu, Z., Wang, Z., & Wang, X. (2018). The inhibitory effects of soybean isoflavones on testicular cell apoptosis in mice with type 2 diabetes. *Experimental and Therapeutic Medicine*, *15*(1), 305–309.
- Ebrahimi, F., Schuetz, P., Mueller, B., Urwyler, S. A., Donath, M. Y., & Christ-Crain, M. (2017). Effects of IL-1 [beta] on the hypothalamic-pituitary-gonadal axis in men with obesity and metabolic syndrome-A randomized, double-blind, placebo-controlled trial. Paper presented at the 19th European Congress of Endocrinology. Endocrine Abstracts (2017) 49 EP687.
- Faid, I., Al-Hussaini, H., & Kilarkaje, N. (2015). Resveratrol alleviates diabetes-induced testicular dysfunction by inhibiting oxidative stress and c-Jun N-terminal kinase signaling in rats. *Toxicology and Applied Pharmacology*, *289*(3), 482–494.
- Girard, S. A., Bah, T. M., Kaloustian, S., Lada-Moldovan, L., Rondeau, I., Tompkins, T. A., . . . Rousseau, G. (2009). *Lactobacillus helveticus* and *Bifidobacterium longum* taken in combination reduce the apoptosis propensity in the limbic system after myocardial infarction in a rat model. *British Journal of Nutrition*, *102*(10), 1420–1425.
- Green, D. R., & Llambi, F. (2015). Cell Death Signaling. *Cold Spring Harbor Perspectives in Biology*, *7*(12), a006080.
- Hayashi, K., Kojima, R., & Ito, M. (2006). Strain differences in the diabetogenic activity of streptozotocin in mice. *Biological and Pharmaceutical Bulletin*, *29*(6), 1110–1119.
- Hendijani, F., & Akbari, V. (2018). Probiotic supplementation for management of cardiovascular risk factors in adults with type II diabetes: A systematic review and meta-analysis. *Clinical Nutrition*, *37*(2), 532–541.
- Honda, K., Moto, M., Uchida, N., He, F., & Hashizume, N. (2012). Anti-diabetic effects of lactic acid bacteria in normal and type 2 diabetic mice. *Journal of Clinical Biochemistry and Nutrition*, *51*(2), 96–101.
- Hotel, A. C. P., & Cordoba, A. (2001). Health and nutritional properties of probiotics in food including powder milk with live lactic acid bacteria. *Prevention*, *5*(1), 1–10.
- Hu, Q. H., Zhang, X., Pan, Y., Li, Y. C., & Kong, L. D. (2012). Allopurinol, quercetin and rutin ameliorate renal NLRP3 inflammasome activation and lipid accumulation in fructose-fed rats. *Biochemical Pharmacology*, *84*(1), 113–125.
- Huang, L., Zhao, Z., Duan, C., Wang, C., Zhao, Y., Yang, G., . . . Li, S. (2019). *Lactobacillus plantarum* C88 protects against aflatoxin B 1-induced liver injury in mice via inhibition of NF-κB-mediated inflammatory responses and excessive apoptosis. *BMC Microbiology*, *19*(1), 170.
- Koh, P. O. (2007a). Streptozotocin-induced diabetes increases apoptosis through JNK phosphorylation and Bax activation in rat testes. *Journal of Veterinary Medical Science*, *69*(9), 969–971.

- Koh, P. O. (2007b). Streptozotocin-induced diabetes increases the interaction of Bad/Bcl-XL and decreases the binding of pBad/14-3-3 in rat testis. *Life Sciences*, 81(13), 1079–1084.
- Korkmaz, O. A., Sadi, G., Kocabas, A., Yildirim, O. G., Sumlu, E., Koca, H. B., . . . Akar, F. (2019a). Lactobacillus helveticus and Lactobacillus plantarum modulate renal antioxidant status in a rat model of fructose-induced metabolic syndrome. *Archives of Biological Sciences*, 71(2), 265–273.
- Korkmaz, O. A., Sumlu, E., Koca, H. B., Pektas, M. B., Kocabas, A., Sadi, G., & Akar, F. (2019b). Effects of Lactobacillus Plantarum and Lactobacillus Helveticus on Renal Insulin Signaling, Inflammatory Markers, and Glucose Transporters in High-Fructose-Fed Rats. *Medicina (Kaunas, Lithuania)*, 55(5), 207.
- Kwon, J., Kim, B., Lee, C., Joung, H., Kim, B.-K., Choi, I. S., & Hyun, C.-K. (2020). Comprehensive amelioration of high-fat diet-induced metabolic dysfunctions through activation of the PGC-1 $\alpha$  pathway by probiotics treatment in mice. *PLoS One*, 15(2), e0228932.
- Ley, R. E., Backhed, F., Turnbaugh, P., Lozupone, C. A., Knight, R. D., & Gordon, J. I. (2005). Obesity alters gut microbial ecology. *Proceedings of the National Academy of Sciences of the United States of America*, 102(31), 11070–11075.
- Liu, H., Zhang, S., Liu, C., Wu, J., Wang, Y., Yuan, L., . . . Zhuang, D. (2018). Resveratrol ameliorates microcystin-LR-induced testis germ cell apoptosis in rats via SIRT1 signaling pathway activation. *Toxins*, 10(6), 235.
- Liu, Q., Liu, Y., Li, F., Gu, Z., Liu, M., Shao, T., . . . Feng, W. (2020). Probiotic culture supernatant improves metabolic function through FGF21-adiponectin pathway in mice. *The Journal of Nutritional Biochemistry*, 75, 108256.
- Lowry, O. H., Rosebrough, N. J., Farr, A. L., & Randall, R. J. (1951). Protein measurement with the Folin phenol reagent. *Journal of Biological Chemistry*, 193(1), 265–275.
- Lu, X. L., Zhao, C. H., Yao, X. L., & Zhang, H. (2017). Quercetin attenuates high fructose feeding-induced atherosclerosis by suppressing inflammation and apoptosis via ROS-regulated PI3K/AKT signaling pathway. *Biomedicine and Pharmacotherapy*, 85, 658–671.
- Markowiak, P., & Slizewska, K. (2017). Effects of Probiotics, Prebiotics, and Synbiotics on Human Health. *Nutrients*, 9(9), 1021.
- McBurney, M. W., Yang, X., Jardine, K., Hixon, M., Boekelheide, K., Webb, J. R., . . . Lemieux, M. (2003). The mammalian SIR2 $\alpha$  protein has a role in embryogenesis and gametogenesis. *Molecular and cellular biology*, 23(1), 38–54.
- Meydanli, E. G., Gumusel, A., Ozkan, S., Tanriverdi, G., Balci, M. B. C., Develi Is, S., . . . Bekpinar, S. (2018). Effects of resveratrol on high-fructose-induced testis injury in rats. *Ultrastructural Pathology*, 42(1), 65–73.
- Mohammadi, G., Dargahi, L., Naserpour, T., Mirzanejad, Y., Alizadeh, S. A., Peymani, A., & Nassiri-Asl, M. (2019). Probiotic mixture of Lactobacillus helveticus R0052 and Bifidobacterium longum R0175 attenuates hippocampal apoptosis induced by lipopolysaccharide in rats. *International Microbiology*, 22(3), 317–323.
- Morrison, C. D., & Brannigan, R. E. (2015). Metabolic syndrome and infertility in men. *Best Practice & Research: Clinical Obstetrics & Gynaecology*, 29(4), 507–515.
- Nna, V. U., Bakar, A. B. A., Ahmad, A., & Mohamed, M. (2018). Diabetes-induced testicular oxidative stress, inflammation, and caspase-dependent apoptosis: the protective role of metformin. *Archives of Physiology and Biochemistry*, 1–12.
- Park, D. Y., Ahn, Y. T., Huh, C. S., McGregor, R. A., & Choi, M. S. (2013). Dual probiotic strains suppress high fructose-induced metabolic syndrome. *World Journal of Gastroenterology*, 19(2), 274–283.
- Passos, J. F., Saretzki, G., Ahmed, S., Nelson, G., Richter, T., Peters, H., . . . von Zglinicki, T. (2007). Mitochondrial dysfunction accounts for the stochastic heterogeneity in telomere-dependent senescence. *PLoS Biology*, 5(5), e110.
- Pektas, M. B., Koca, H. B., Sadi, G., & Akar, F. (2016). Dietary Fructose Activates Insulin Signaling and Inflammation in Adipose Tissue: Modulatory Role of Resveratrol. *BioMed Research International*, 2016, 8014252.
- Pektas, M. B., Sadi, G., & Akar, F. (2015). Long-Term Dietary Fructose Causes Gender-Different Metabolic and Vascular Dysfunction in Rats: Modulatory Effects of Resveratrol. *Cellular Physiology and Biochemistry*, 37(4), 1407–1420.
- Pektas, M. B., Yucel, G., Koca, H. B., Sadi, G., Yildirim, O. G., Ozturk, G., & Akar, F. (2017). Dietary Fructose-Induced Hepatic Injury in Male and Female Rats: Influence of Resveratrol. *Drug Research (Stuttg)*, 67(2), 103–110.
- Plaza-Diaz, J., Ruiz-Ojeda, F. J., Vilchez-Padial, L. M., & Gil, A. (2017). Evidence of the Anti-Inflammatory Effects of Probiotics and Synbiotics in Intestinal Chronic Diseases. *Nutrients*, 9(6), 555.
- Rastrelli, G., Filippi, S., Sforza, A., Maggi, M., & Corona, G. (2018). Metabolic syndrome in male hypogonadism. In *Metabolic Syndrome Consequent to Endocrine Disorders* (Vol. 49, pp. 131–155): Karger Publishers.
- Rosa, D. D., Grzeskowiak, L. M., Ferreira, C. L., Fonseca, A. C., Reis, S. A., Dias, M. M., . . . Peluzio Mdo, C. (2016). Kefir reduces insulin resistance and inflammatory cytokine expression in an animal model of metabolic syndrome. *Food & Function*, 7(8), 3390–3401.
- Sadi, G., Ergin, V., Yilmaz, G., Pektas, M. B., Yildirim, O. G., Menevse, A., & Akar, F. (2015). High-fructose corn syrup-induced hepatic dysfunction in rats: improving effect of resveratrol. *European Journal of Nutrition*, 54(6), 895–904.
- Shahin, S., Singh, S. P., & Chaturvedi, C. M. (2018). 2.45 GHz microwave radiation induced oxidative and nitrosative stress mediated testicular apoptosis: Involvement of a p53 dependent bax-caspase-3 mediated pathway. *Environmental Toxicology*, 33(9), 931–945.
- Simoes, V. L., Alves, M. G., Martins, A. D., Dias, T. R., Rato, L., Socorro, S., & Oliveira, P. F. (2013). Regulation of apoptotic signaling pathways by 5 $\alpha$ -dihydrotestosterone and 17 $\beta$ -estradiol in immature rat Sertoli cells. *Journal of Steroid Biochemistry and Molecular Biology*, 135, 15–23.
- Song, L., Chen, T. Y., Zhao, X. J., Xu, Q., Jiao, R. Q., Li, J. M., & Kong, L. D. (2019). Pterostilbene prevents hepatocyte epithelial-mesenchymal transition in fructose-induced liver fibrosis through suppressing miR-34a/Sirt1/p53 and TGF- $\beta$ 1/Smads signalling. *British journal of pharmacology*, 176(11), 1619–1634.
- Song, W., Liu, M. G., Zhang, J. B., Zhang, J. J., Sun, M. M., & Yu, Q. K. (2016). Mechanism of action of EBV, Bcl-2, p53, c-Myc and Rb in non-Hodgkin's lymphoma. *European Review for Medical and Pharmacological Sciences*, 20(6), 1093–1097.
- Sumlu, E., Bostanci, A., Sadi, G., Alcigir, M. E., & Akar, F. (2020). Lactobacillus plantarum improves lipogenesis and IRS-1/AKT/eNOS signalling pathway in the liver of high-fructose-fed rats. *Archives of Physiology and Biochemistry*, 1–9.
- Tsai, E. C., Matsumoto, A. M., Fujimoto, W. Y., & Boyko, E. J. (2004). Association of bioavailable, free, and total testosterone with insulin resistance: influence of sex hormone-binding globulin and body fat. *Diabetes Care*, 27(4), 861–868.
- Tsounapi, P., Saito, M., Dimitriadis, F., Koukos, S., Shimizu, S., Satoh, K., . . . Sofikitis, N. (2012). Antioxidant treatment with edaravone or taurine ameliorates diabetes-induced testicular dysfunction in the rat. *Molecular and Cellular Biochemistry*, 369(1-2), 195–204.
- Vachharajani, V. T., Liu, T., Wang, X., Hoth, J. J., Yoza, B. K., & McCall, C. E. (2016). Sirtuins link inflammation and metabolism. *Journal of Immunology Research*, 8167273.
- Wang, H. F., Tseng, C. Y., Chang, M. H., Lin, J. A., Tsai, F. J., Tsai, C. H., . . . Tsai, C. C. (2012). Anti-inflammatory effects of probiotic Lactobacillus paracasi on ventricles of BALB/C mice treated with ovalbumin. *Chinese Journal of Physiology*, 55(1), 37–46.

- Wang, X.-l., Wu, L.-y., Zhao, L., Sun, L.-n., Liu, H.-y., Liu, G., & Guan, G.-j. (2016). SIRT1 activator ameliorates the renal tubular injury induced by hyperglycemia in vivo and in vitro via inhibiting apoptosis. *Biomedicine & Pharmacotherapy*, *83*, 41–50.
- Wang, Y., Wu, Y., Wang, Y., Xu, H., Mei, X., Yu, D., . . . Li, W. (2017). Antioxidant Properties of Probiotic Bacteria. *Nutrients*, *9*(5), 521.
- Xu, Y., Lei, H., Guan, R., Gao, Z., Li, H., Wang, L., . . . Xin, Z. (2014). Studies on the mechanism of testicular dysfunction in the early stage of a streptozotocin induced diabetic rat model. *Biochemical and Biophysical Research Communications*, *450*(1), 87–92.
- Yadav, H., Jain, S., & Sinha, P. R. (2007). Antidiabetic effect of probiotic dahi containing *Lactobacillus acidophilus* and *Lactobacillus casei* in high fructose fed rats. *Nutrition*, *23*(1), 62–68.
- Yildirim, O. G., Sumlu, E., Aslan, E., Koca, H. B., Pektas, M. B., Sadi, G., & Akar, F. (2019). High-fructose in drinking water initiates activation of inflammatory cytokines and testicular degeneration in rat. *Toxicology Mechanisms and Methods*, *29*(3), 224–232.
- Zhao, L., Gu, Q., Xiang, L., Dong, X., Li, H., Ni, J., . . . Chen, G. (2017). Curcumin inhibits apoptosis by modulating Bax/Bcl-2 expression and alleviates oxidative stress in testes of streptozotocin-induced diabetic rats. *Therapeutics and Clinical Risk Management*, *13*, 1099–1105.
- Zhao, Y., Tan, Y., Dai, J., Li, B., Guo, L., Cui, J., . . . Cai, L. (2011). Exacerbation of diabetes-induced testicular apoptosis by zinc deficiency is most likely associated with oxidative stress, p38 MAPK activation, and p53 activation in mice. *Toxicology Letters*, *200*(1-2), 100–106.
- Zhao, Y., Tan, Y., Dai, J., Wang, B., Li, B., Guo, L., . . . Cai, L. (2012). Zinc deficiency exacerbates diabetic down-regulation of Akt expression and function in the testis: essential roles of PTEN, PTP1B and TRB3. *Journal of Nutritional Biochemistry*, *23*(8), 1018–1026.

# Anticancer and antituberculosis effects of 5-fluoro-1H-indole-2,3-dione 3-thiosemicarbazones

Zekiye Şeyma Sevinçli<sup>1,2,3</sup> , Zerrin Cantürk<sup>4</sup> , Miriř Dikmen<sup>5</sup> , Nilgün Karalı<sup>2</sup> 

<sup>1</sup>Van Yuzuncu Yil University, Faculty of Pharmacy, Department of Pharmaceutical Chemistry, Van, Turkey

<sup>2</sup>Istanbul University, Faculty of Pharmacy, Department of Pharmaceutical Chemistry, Istanbul, Turkey

<sup>3</sup>Istanbul University, Institute of Health Sciences, Department of Pharmaceutical Chemistry, Istanbul, Turkey

<sup>4</sup>Anadolu University, Faculty of Pharmacy, Department of Pharmaceutical Microbiology, Eskiřehir, Turkey

<sup>5</sup>Anadolu University, Faculty of Pharmacy, Department of Pharmacology, Eskiřehir, Turkey

**ORCID IDs of the authors:** Z.Ş.S. 0000-0001-7821-6854; Z.C. 0000-0001-7709-4285; M.D. 0000-0002-9856-3148; N.K. 0000-0002-6916-122X

**Cite this article as:** Sevinçli, Z. S., Canturk, Z., Dikmen, M., & Karali, N. (2020). Anticancer and antituberculosis effects of 5-fluoro-1H-indole-2,3-dione 3-thiosemicarbazones. *Istanbul Journal of Pharmacy*, 50 (3), 176-180.

## ABSTRACT

**Background and Aims:** The aim of this study was to screen the *in vitro* anticancer/antituberculosis activities of 5-fluoro-1-methyl/ethyl-1H-indole-2,3-dione 3-thiosemicarbazones.

**Methods:** A549/U-87MG cell lines were used for the anticancer activity of the compounds, while CCD-19Lu cell line was used to determine their cytotoxic effects. In antituberculosis activity studies using MTB H37Rv cell line, BJ cell line was used to determine the cytotoxic effects. MTT assay was used to obtain IC<sub>50</sub> values.

**Results:** **6a**, **6b**, **6g**, **6h**, **6l**, **6n**, **7c**, **7k** and **7l** were found to be highly effective against A549 cell line compared to cisplatin whereas **6d**, **6h**, **6l**, **6n**, **7d** and **7f** were found to be effective against U-87MG cell line compared to cisplatin. It was also determined that **6a**, **6b** and **7l** did not show cytotoxic effects on CCD-19Lu cell line. The antituberculosis effects of the compounds were investigated against MTB H37Rv cell groups using rifampicin as standard. It was determined that **6b**, **6c**, **6g-k**, **6n**, **7b**, **7j** and **7l** have near-standard activity and **6b**, **7b** and **7l** were not cytotoxic on BJ cell line.

**Conclusion:** While determining effective compounds in anticancer studies, it was concluded that active compounds can be reached by modifications in compounds in antituberculosis studies.

**Keywords:** Anticancer activity, antituberculosis activity, 5-fluoro-1H-indole-2,3-diones

## INTRODUCTION

1H-Indole-2,3-dione and its derivatives have a broad spectrum of biological properties including anticancer, antiviral and antimicrobial activities. There are several reports on the anticancer activities of 1H-indole-2,3-dione 3-thiosemicarbazone derivatives (Karalı, 2002; Hall et al., 2009; Hall et al., 2011; Priyanka, Manasa & Sammaiah, 2014; Pape et al. 2016; Karalı et al., 2017). A pharmacophore analysis of the active compounds revealed that 1H-indole-2,3-dione 3-thiosemicarbazone moiety, aromatic/ hydrophobic features at the N4 position of the thiosemicarbazone, introduction of electron-withdrawing groups at position 5 of 1H-indole-2,3-dione and alkylation of position 1 of 1H-indole-2,3-dione were essential for anticancer activity (Vine, Locke, Ranson, Pyne & Bremner, 2007; Matesic et al., 2008; Sabet, Mohammadpour, Sadeghi & Fassihi, 2010, Pervez, Saira, Iqbal, Yaqub, & Khan, 2011; Pervez, Saira, Iqbal, Yaqub, & Khan, 2013; Lin et al. 2013). Researchs also showed that N<sup>4</sup>-phenyl substituted thiosemicarbazone derivatives were significantly more active than N<sup>4</sup>-alkyl and N<sup>4</sup>-cycloalkyl thiosemicarbazone derivatives (Hall et al., 2009; Hall et al., 2011). 5-Fluoro-1H-indole-2,3-dione 3-[4-(4-methoxyphenyl)thiosemicarbazone] have been reported as selective MDR1 activity (Hall et

## Address for Correspondence:

Zekiye Şeyma SEVINÇLİ, e-mail: seymasevincli@yyu.edu.tr

This work is licensed under a Creative Commons Attribution 4.0 International License.



Submitted: 08.09.2020  
Revision Requested: 14.10.2020  
Last Revision Received: 27.10.2020  
Accepted: 18.11.2020



al., 2010; Brimacombe, Fales, Gottesman, Hall & Handley, 2012). It has been found that derivatives of the 5-fluoroisatin ring with methylene/ethylene bridges with fluoroquinolone derivatives such as gatifloxacin, balofloxacin and 8-methoxyciprofloxacin have significant antituberculous activity (Feng et al., 2010; Banerjee et al., 2011). 5-Nitro/ 5-methyl/5-trifluoromethoxyisatin 3-thiosemicarbazone derivatives showed antituberculous activity (Karalı et al., 2007; Güzel, Karalı & Salman, 2008).

In this study, *in vitro* the anticancer and antituberculosis activities of 5-fluoro-1-methyl/ethyl-1*H*-indole-2,3-dione 3-[4-(4-substituted phenyl)thiosemicarbazones] derivatives, which were previously synthesized by our research, were screened. The structures of all the synthesized compounds were determined by analytical and spectral methods (Sevinçli, Duran, Özbil & Karalı, 2020). The molecular and isomeric structures of **6h** and **6j** were determined by X-ray single crystal diffraction analysis (Atioğlu, Sevinçli, Karalı, Akkurt & Ersanlı, 2017a; Atioğlu, Sevinçli, Karalı, Akkurt & Ersanlı, 2017b). In the study where A549 (human lung adenocarcinoma cells) and U-87 MG (human glioblastoma cells) cell lines were used to determine the anticancer activities of the compounds, CCD-19Lu (human normal lung fibroblast cells) cell line were used to determine cytotoxic effects. Cisplatin was used as a positive control. While *Mycobacterium tuberculosis* (MTB) H37Rv (ATCC 27294) cell line was used to determine antituberculosis activities, a BJ (human healthy fibroblast cell line) cell line was used to determine the cytotoxic effects of some compounds on healthy cells. Rifampicin was used as a standard to evaluate antituberculosis activities.

## MATERIAL AND METHODS

### Anticancer activity studies

U-87 MG (ATCC number HTB-14™), A549 (ATCC number CCL-185™) and CCD-19Lu (ATCC number CCL-210™) cell lines were obtained from the American Type Culture Collection. All the cell lines were grown in EMEM (Eagle's Minimum Essential Medium) supplemented with 2 mM L-glutamine, 10% fetal bovine serum and 1% penicillin/streptomycin at 37°C in a humidified incubator with a 5% CO<sub>2</sub> atmosphere. Cisplatin was used as positive control. Substances and positive control were dissolved in dimethyl sulfoxide (DMSO) and diluted to working concentrations with fresh medium. The control group (solvent control) was prepared with medium containing 0.1% DMSO like as working concentrations.

The viability of the cells were assessed by [3-(4,5-dimethylthiazol-2-yl)-2,5-diphenyltetrazolium bromide] (MTT) assay, which is based on the reduction of MTT by the mitochondrial dehydrogenase of intact cells to a purple formazan product. Yellow MTT is reduced to purple formazan in the mitochondria of living cells. This reduction takes place only when mitochondrial reductase enzymes are active, and therefore, the conversion can be directly related to the number of viable (living) cells (Mosmann, 1983; Dikmen, Öztürk & Öztürk, 2011).

In order to obtain IC<sub>50</sub> concentrations of the samples, the cell viability was determined by a MTT assay. In short, cells were grown in 96-well plates at a density of 5×10<sup>3</sup> cells per well. A

total of 70–80% confluent cells (after 24 h) were treated with concentrations (400, 200, 100 and 50 μM) of substances for 24 h in the growth medium. After 24 h incubation, a MTT solution was added to wells to reach a final concentration of 0.5 mg/mL. The cells were incubated for another 4 h and then the current medium was removed and 100 μL of DMSO solution was added. The absorbance values were measured at 540 nm using a Cytation 3 Cell Imaging Multi-Mode Reader (BioTek). The measured absorbance directly correlates with the number of viable cells. The cell viability rates were expressed as the percentage of the DMSO (0.1%) solvent control and then IC<sub>50</sub> concentrations were calculated according to the analysis result. In the experiment, each group was performed in 8 wells of three independent experiments.

### Antituberculosis activity studies

MTB H37Rv (ATCC 27294) was purchased from the American Type Culture Collection (ATCC) cell bank. BD BACTEC™ MGIT™ (mycobacterial growth indicator tubes) were reconstituted in tubes in seven days. Later on, a special medium, ATCC® Medium 1395: Middlebrook 7H9, was prepared for anti-tuberculous activity test, ADC (albumin-dextrose-catalase) and oleic acid were added to enrich the medium. The developed microorganisms were adjusted to McFarland Standard No. 1 and prepared for experiments. The test substances were prepared at concentrations of 0.97-500 μg/mL. Rifampicin (Sigma, R3501) was used as a positive control. Materials in 96-well plates and MTB H37Rv were incubated for 7 days at 37°C. Then, 20 μL MTT was added vigorously and left to incubate for 24 h under the same conditions. At the end of the 24<sup>th</sup> h, the vitality conditions were compared (Foongladda et al., 2002; Raut, Narang, Mendiratta, Narang & Deotale, 2008).

A BJ cell line (ATCC® CRL-2522™) was obtained from the American Type Culture Collection. The cells were grown in RPMI 1640 medium supplemented with 2 mM L-glutamine and 10% foetal bovine serum, 1% penicillin/streptomycin at a temperature of 37°C in a humidified incubator with a 5% CO<sub>2</sub> atmosphere. Compounds were dissolved in DMSO solution and the concentration-dependent cytotoxic effect was studied (0.97- 500 μg/mL). The BJ cells were inoculated into 96-well culture plates at a density of 5×10<sup>3</sup> cells per well. Then, after 24 h of incubation, 10 μL of MTT solution (5 mg/mL) was added to each well and the plates were incubated for a further 4 h (Mosmann 1983). The formazan crystals produced, which are converted with dye, are solubilized with DMSO. The culture plates were inserted in Cytation 3 Cell Imaging Multi-Mode Reader (BioTek) and the absorbance was measured at 540 nm. The percent values of cell proliferations were calculated relative to controls, whose cell proliferations were accepted as 100%.

## RESULTS AND DISCUSSION

### Chemistry

The structures of **6a-n** and **7a-n** were confirmed by analytical and spectral (IR, <sup>1</sup>H NMR, <sup>13</sup>C-NMR, HSQC-2D, HMBC-2D, HRMS-ESI+ and LCMS-ESI+) data (Sevinçli, Duran, Özbil & Karalı, 2020).



The molecular and isomeric structures of **6h** and **6j** were determined by X-ray single crystal diffraction analysis and the stable isomer was found to be in Z configuration (Figures 1 and 2) (Atioğlu, Sevinçli, Karalı, Akkurt & Ersanlı, 2017a; Atioğlu, Sevinçli, Karalı, Akkurt & Ersanlı, 2017b).

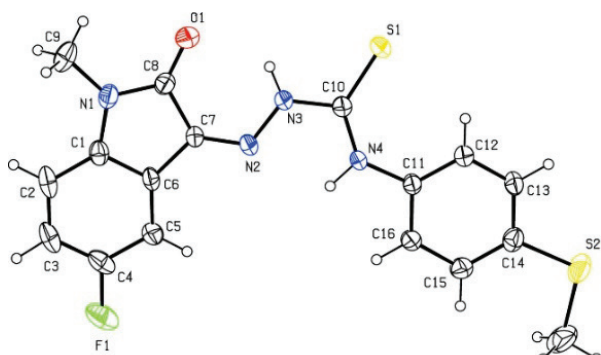


**Figure 1.** View of the molecular structure of **6h**, with the atom labelling

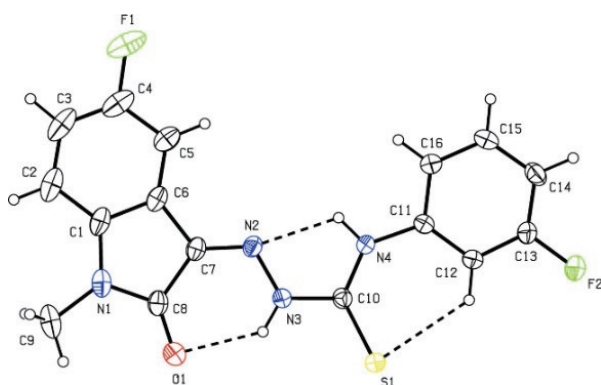


**Figure 2.** View of the molecular structure of **6j**, with the atom labelling.

### Biological activity

A549 and U-87 MG cell lines were used for the anticancer effects of the compounds, while CCD-19Lu cell line was used to determine their cytotoxic effects. Cisplatin was used as positive control. **6a**, **6b**, **6g**, **6h**, **6l**, **6n**, **7c**, **7k** and **7l** ( $IC_{50}$ = 10.6-58.8 mM) were found to be highly effective against A549 cell line compared to cisplatin ( $IC_{50}$ = 70.3 mM). It was determined that **6a**, **6b**, **6g**, **7c** and **7k** were highly effective against A549 cell line compared to cisplatin at 51.2, 26.8, 16.4, 35.8 and 10.6  $\mu$ M, respectively. The  $R_2$  methyl substituted derivatives **6a-n** are generally more effective than the  $R_2$  ethyl substituted derivatives **7a-n** against the A549 cells. Whereas, among the  $R_2$  ethyl substituted derivatives,  $R_1$  4-methyl substituted **7c** and  $R_1$  4-fluoro substituted **7k** have higher efficiency than the corresponding  $R_2$  methyl substituted derivatives **6c** and **6k**, but these compounds have higher cytotoxicity.  $R_1$  3-chloro substituted **6l** and **7l** were found to be effective against A549 cell line compared to cisplatin at 20.6 and 58.8  $\mu$ M, respectively. This result indicates that the chlorine atom in position 3 of the phenyl ring plays an important role in the activity. While **7l** had a selective and nontoxic effect, the selectivity decreased and toxicity increased at **6l**. It was also determined that  $R_1$  non-

substituted **6a**,  $R_1$  3-methyl substituted **6b** and 3-chloro substituted **7l** showed selective effects on the A549 cell line while not showing cytotoxic effects ( $IC_{50}$ = >400 mM) on CCD-19Lu cell line. **6b** was found to be the most effective, selective and nontoxic compound against A549 cell line. It was also determined that **6a**, **6b** and **7l** did not show cytotoxic effects on CCD-19Lu cell lines. **6d**, **6h**, **6l**, **6n**, **7d** and **7f** ( $IC_{50}$ = 34.9-93.9 mM) were found to be effective against U-87 MG cell line compared to cisplatin ( $IC_{50}$ = 96.7 mM). The results showed that  $R_1$  4-trifluoromethyl substituted **6d** ( $IC_{50}$ = 46.6 mM) and **7d** ( $IC_{50}$ = 34.9 mM) are more effective than cisplatin against U-87 MG. These results showed that the trifluoromethyl group at the 4 position of the phenyl ring and the  $R_2$  ethyl substitution contributed to the activity. The efficiency and selectivity of **7d** was higher than **6d**, and its toxicity was lower than **6d**.  $R_1$  3-methoxy substituted **7f** ( $IC_{50}$ = 91.1 mM) were found to be effective against U-87 MG whereas  $R_1$  4-methylthio substituted **6h** ( $IC_{50}$ = 93.9 mM),  $R_1$  3-chloro substituted **6l** ( $IC_{50}$ = 84.7 mM) and  $R_1$  4-bromo substituted **6n** ( $IC_{50}$ = 61.4 mM) were found to be more effective than cisplatin against both A549 and U87-MG cell lines (Table 1).

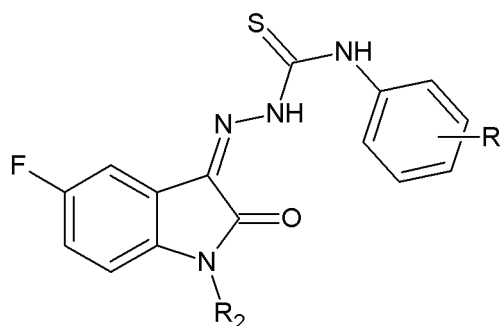


**Figure 3.** General structures of **6a-n** and **7a-n**.

The antituberculosis effects of the compounds were investigated on the MTB H37Rv (ATCC 27294) cell group using rifampicin ( $IC_{50}$ = 25.00  $\mu$ g/mL) as standard. **6b**, **6c**, **6g**, **6h**, **6i**, **6j**, **6k**, **6n**, **7b**, **7j** and **7l** were found effective with  $IC_{50}$  value of 31.25  $\mu$ g/mL.  $R_1$  3-methyl substituted **6b** and **7b** and  $R_1$  3-fluoro substituted **6j** and **7j** were found to be effective at 31.25  $\mu$ g/mL. In this way it was determined that these groups played an important role in the activity. Also  $R_1$  4-methyl substituted **6c**,  $R_1$  4-methoxy substituted **6g**,  $R_1$  3-thiomethyl substituted **6h**,  $R_1$  4-trifluoromethoxy substituted **6i**,  $R_1$  4-fluoro substituted **6k**,  $R_1$  4-bromo substituted **6n** and  $R_1$  3-chloro substituted **7l** were found effective at 31.25  $\mu$ g/mL. Whereas,  $R_1$  4-trifluoromethyl substituted **6d** and **7d**,  $R_1$  4-ethyl substituted **6e** and **7e**,  $R_1$  nonsubstituted **7a**,  $R_1$  4-methyl substituted **7c**,  $R_1$  3-methoxy substituted **7f**, 4-trifluoromethoxy substituted **7i**,  $R_1$  4-fluoro substituted **7k** and  $R_1$  4-chloro substituted **7m** showed the activity at 62.5  $\mu$ g/mL (Table 2). It was also determined that  $R_1$  3-methyl substituted **6b** and **7b** and  $R_1$  3-chloro substituted **7l** selected as a prototype did not show cytotoxic effects with  $IC_{50}$  value of >500  $\mu$ g/mL on BJ cell line (Table 3).

**Table 1. Anticancer activities of 6a-n and 7a-n against A549/ U-87 MG cell lines and cytotoxic effect for CCD-19Lu cell line.**

Compounds	R <sub>1</sub>	R <sub>2</sub>	IC <sub>50</sub> (μM)		
			A549	U-87 MG	CCD-19Lu
6a	H	CH <sub>3</sub>	51.2	>400	>400
6b	3-CH <sub>3</sub>	CH <sub>3</sub>	26.8	>400	>400
6c	4-CH <sub>3</sub>	CH <sub>3</sub>	91.2	165.4	302.0
6d	4-CF <sub>3</sub>	CH <sub>3</sub>	76.0	46.6	155.0
6e	4-C <sub>2</sub> H <sub>5</sub>	CH <sub>3</sub>	172.8	>400	>400
6f	3-OCH <sub>3</sub>	CH <sub>3</sub>	94.9	354.8	73.2
6g	4-OCH <sub>3</sub>	CH <sub>3</sub>	16.4	182.2	267.8
6h	4-SCH <sub>3</sub>	CH <sub>3</sub>	50.1	93.9	160.9
6i	4-OCF <sub>3</sub>	CH <sub>3</sub>	187.0	150.9	176.5
6j	3-F	CH <sub>3</sub>	97.4	384.1	205.1
6k	4-F	CH <sub>3</sub>	>400	>400	303.0
6l	3-Cl	CH <sub>3</sub>	20.6	84.7	98.3
6m	4-Cl	CH <sub>3</sub>	136.9	244.6	359.6
6n	4-Br	CH <sub>3</sub>	35.5	61.4	91.8
7a	H	C <sub>2</sub> H <sub>5</sub>	144.2	>400	>400
7b	3-CH <sub>3</sub>	C <sub>2</sub> H <sub>5</sub>	211.2	285.8	>400
7c	4-CH <sub>3</sub>	C <sub>2</sub> H <sub>5</sub>	35.8	>400	170.0
7d	4-CF <sub>3</sub>	C <sub>2</sub> H <sub>5</sub>	316.0	34.9	198.1
7e	4-C <sub>2</sub> H <sub>5</sub>	C <sub>2</sub> H <sub>5</sub>	>400	>400	>400
7f	3-OCH <sub>3</sub>	C <sub>2</sub> H <sub>5</sub>	247.2	91.1	250.6
7g	4-OCH <sub>3</sub>	C <sub>2</sub> H <sub>5</sub>	>400	>400	>400
7h	4-SCH <sub>3</sub>	C <sub>2</sub> H <sub>5</sub>	365.0	>400	>400
7i	4-OCF <sub>3</sub>	C <sub>2</sub> H <sub>5</sub>	118.1	>400	268.8
7j	3-F	C <sub>2</sub> H <sub>5</sub>	90.7	>400	260.2
7k	4-F	C <sub>2</sub> H <sub>5</sub>	10.6	196.9	93.3
7l	3-Cl	C <sub>2</sub> H <sub>5</sub>	58.8	>400	>400
7m	4-Cl	C <sub>2</sub> H <sub>5</sub>	>400	173.8	>400
7n	4-Br	C <sub>2</sub> H <sub>5</sub>	>400	>400	>400
Cisplatin			70.3	96.7	>400

**Table 2. Antituberculosis activities of 6a-n ve 7a-n against MTB H37Rv.**

Compounds	R <sub>1</sub>	R <sub>2</sub>	IC <sub>50</sub> (μg/mL)
			MTB H37Rv (ATCC 27294)
6a	H	CH <sub>3</sub>	500,00
6b	3-CH <sub>3</sub>	CH <sub>3</sub>	31,25
6c	4-CH <sub>3</sub>	CH <sub>3</sub>	31,25
6d	4-CF <sub>3</sub>	CH <sub>3</sub>	62,50
6e	4-C <sub>2</sub> H <sub>5</sub>	CH <sub>3</sub>	62,50
6f	3-OCH <sub>3</sub>	CH <sub>3</sub>	500
6g	4-OCH <sub>3</sub>	CH <sub>3</sub>	31,25
6h	4-SCH <sub>3</sub>	CH <sub>3</sub>	31,25
6i	4-OCF <sub>3</sub>	CH <sub>3</sub>	31,25
6j	3-F	CH <sub>3</sub>	31,25
6k	4-F	CH <sub>3</sub>	31,25
6l	3-Cl	CH <sub>3</sub>	500
6m	4-Cl	CH <sub>3</sub>	500
6n	4-Br	CH <sub>3</sub>	31,25
7a	H	C <sub>2</sub> H <sub>5</sub>	62,50
7b	3-CH <sub>3</sub>	C <sub>2</sub> H <sub>5</sub>	31,25
7c	4-CH <sub>3</sub>	C <sub>2</sub> H <sub>5</sub>	62,50
7d	4-CF <sub>3</sub>	C <sub>2</sub> H <sub>5</sub>	62,50
7e	4-C <sub>2</sub> H <sub>5</sub>	C <sub>2</sub> H <sub>5</sub>	62,50
7f	3-OCH <sub>3</sub>	C <sub>2</sub> H <sub>5</sub>	62,50
7g	4-OCH <sub>3</sub>	C <sub>2</sub> H <sub>5</sub>	500
7h	4-SCH <sub>3</sub>	C <sub>2</sub> H <sub>5</sub>	500
7i	4-OCF <sub>3</sub>	C <sub>2</sub> H <sub>5</sub>	62,5
7j	3-F	C <sub>2</sub> H <sub>5</sub>	31,25
7k	4-F	C <sub>2</sub> H <sub>5</sub>	62,50
7l	3-Cl	C <sub>2</sub> H <sub>5</sub>	31,25
7m	4-Cl	C <sub>2</sub> H <sub>5</sub>	62,50
7n	4-Br	C <sub>2</sub> H <sub>5</sub>	500
Rifampicin			25

**Table 3. Cytotoxic effect of 6b, 7b and 7l on BJ cell line.**

Compounds	R <sub>1</sub>	R <sub>2</sub>	IC <sub>50</sub> (μg/mL)
			BJ (ATCC® CRL-2522™)
6b	3-CH <sub>3</sub>	CH <sub>3</sub>	>500
7b	3-CH <sub>3</sub>	C <sub>2</sub> H <sub>5</sub>	>500
7l	3-Cl	C <sub>2</sub> H <sub>5</sub>	>500

## CONCLUSIONS

In summary, the anticancer and antituberculosis activities of 5-fluoro-1-methyl/ethyl-1*H*-indole-2,3-dione 3-[4-(4-substituted phenyl)thiosemicarbazones] derivatives previously synthesized by our research group have been performed and promising results have been obtained. The R<sub>2</sub> methyl substituted derivatives **6a-n** are generally more effective than the R<sub>2</sub> ethyl substituted derivatives **7a-n** against the A549 and U-87 MG cell lines. However, antituberculosis activity is generally increased with R<sub>2</sub> ethyl substitution. It is one of the most important findings that the R<sub>1</sub> unsubstituted **6a**, R<sub>1</sub> 3-methyl substituted **6b** and R<sub>1</sub> 3-chloro substituted **7l** compounds are selective and nontoxic effects on the A549 cell line. In addition, the prototype

selected antituberculosis effective R<sub>1</sub> 3-methyl substituted **6b** and **7b** and R<sub>1</sub> 3-chloro substituted **7i** compounds were found to be nontoxic on BJ cell line. These results show the importance of R<sub>1</sub> 3-methyl and 3-chlorine substitution.

**Peer-review:** Externally peer-reviewed.

**Author Contributions:** Conception/Design of Study- Z.Ş.S., N.K., Z.C., M.D.; Data Acquisition- Z.C., M.D.; Data Analysis/Interpretation- Z.Ş.S., N.K., Z.C., M.D.; Drafting Manuscript- Z.Ş.S., N.K.; Critical Revision of Manuscript- Z.Ş.S., N.K., Z.C., M.D.; Final Approval and Accountability- Z.Ş.S., N.K., Z.C., M.D.; Technical or Material Support- Z.Ş.S., N.K., Z.C., M.D.; Supervision- Z.Ş.S., N.K.

**Conflict of Interest:** The authors have no conflict of interest to declare.

**Financial Disclosure:** This study was financially supported by Scientific and Technological Research Council of Turkey (TÜBİTAK). (Grant number: 1003-2155011)

## REFERENCES

- Atioğlu, Z., Sevinçli, Z. Ş., Karalı, N., Akkurt, M., & Ersanlı C. C. (2017a). 2-(5-Fluoro-1-methyl-2-oxoindolin-3-ylidene)-N-[4-(methylsulfanyl)phenyl]hydrazine-1-carbothioamide. *IUCrData*, 2(5), x170671.
- Atioğlu, Z., Sevinçli, Z. Ş., Karalı, N., Akkurt, M., & Ersanlı C. C. (2017b). (2Z)-2-(5-Fluoro-1-methyl-2-oxoindolin-3-ylidene)-N-(3-fluorophenyl)hydrazine-1-carbothioamide. *IUCrData*, 2(6), x170900.
- Banerjee, D., Yogeewari, P., Bhat, P., Thomas, A., Srividya, M., & Sriram, D. (2011). Novel isatinyl thiosemicarbazones derivatives as potential molecule to combat HIV-TB co-infection. *European Journal of Medicinal Chemistry*, 46(1), 106–121.
- Brimacombe K., Fales H. M., Gottesman M. M., Hall, M. D., & Handley, M. (2012). *W.O. Patent No. 2012033601 A1*.
- Dikmen, M., Öztürk, N., & Öztürk, Y. The antioxidant potency of Punica granatum L. Fruit peel reduces cell proliferation and induces apoptosis on breast cancer. *Journal of Medicinal Food*, 14(12), 1638–1646.
- Feng, L. S., Liu, M. L., Wang, B., Chai, Y., Hao, X. Q., Meng, S., & Guo, H. Y. (2010). Synthesis and *in vitro* antimycobacterial activity of balofloxacin ethylene isatin derivatives. *European Journal of Medicinal Chemistry*, 45, 3407–3412.
- Foongladda, S., Roengsanthia, D., Arjattanakool, W., Chuchotaworn, C., Chairprasert, A., & Franzblau, S. G. (2002). Rapid and simple MTT method for rifampicin and isoniazid susceptibility testing of *Mycobacterium tuberculosis*. *The International Journal of Tuberculosis and Lung Disease*, 6(12), 1118–1122.
- Güzel, Ö., Karalı, N., & Salman, A. (2008). Synthesis and antituberculosis activity of 5-methyl/ trifluoromethoxy-1H-indole-2,3-dione 3-thiosemicarbazone derivatives. *Bioorganic & Medicinal Chemistry*, 16(19), 8976–8987.
- Hall, M. D., Salam, N. K., Hellawell, J. L., Fales, H. M., Kensler, C. B., Ludwig, J. A. ... Gottesman, M. M. (2009). Synthesis, activity, and pharmacophore development for isatin-β-thiosemicarbazones with selective activity toward multidrug-resistant cells. *Journal of Medicinal Chemistry*, 52(10), 3191–3204.
- Hall, M. D., Gottesman, M. M., Hellawell, J. L., Ludwig, J. A., Fales, H. M., Salam, N. K., & Szakács, G. (2010). *U.S. Patent Application No. 12/867,206*.
- Hall, M. D., Brimacombe, K. R., Varonka, M. S., Pluchino, K. M., Monda, J. K., Li, J. ... Gottesman, M. M. (2011). Synthesis and structure-activity evaluation of isatin-β-thiosemicarbazones with improved selective activity toward multidrug-resistant cells expressing P-glycoprotein. *Journal of Medicinal Chemistry*, 54, 5878–5889.
- Karalı, N. (2002). Synthesis and primary cytotoxicity evaluation of new 5-nitroindole-2,3-dione derivatives. *European Journal of Medicinal Chemistry*, 37(11), 909–918.
- Karalı, N., Gürsoy, A., Kandemirli, F., Shvets, N., Kaynak, F. B., Özbeş, S. ... Dimoglo, A. (2007). Synthesis and structure-antituberculosis activity relationship of 1H-indole-2,3-dione derivatives. *Bioorganic & Medicinal Chemistry*, 15(17), 5888–5904.
- Karalı, N., Akdemir, A., Göktaş, F., Eraslan-Elma, P., Angeli, A., Kızılırmak, M. & Supuran, C. T. (2017). Novel sulfonamide-containing 2-indolinones that selectively inhibit tumor-associated alpha carbonic anhydrases. *Bioorganic & Medicinal Chemistry*, 25(14), 3714–3718.
- Lin, H. H., Wu, W. Y., Cao, S. L., Liao, J., Ma, L., Gao, M. ... Xu, X. (2013). Synthesis and antiproliferative evaluation of piperazine-1-carbothiohydrazide derivatives of indolin-2-one. *Bioorganic & Medicinal Chemistry Letters*, 23(11), 3304–3307.
- Matesic, L., Locke, J. M., Bremner, J. B., Pyne, S. G., Skropeta, D., & Ranson, M. (2008). N-phenethyl and N-naphthylmethyl isatins and analogues as *in vitro* cytotoxic agents. *Bioorganic & Medicinal Chemistry*, 16, 3118–3124.
- Mosmann, T. (1983). Rapid colorimetric assay for cellular growth and survival: application to proliferation and cytotoxicity assays. *Journal of Immunological Methods*, 65, 55–63.
- Pape, V. F. S., Tóth, S., Füredi, A., Szebényi, K., Lovrics, A., Szabó, P. ... Szakács, G. (2016). Design, synthesis and biological evaluation of thiosemicarbazones, hydrazinobenzothiazoles and arylhydrazones as anticancer agents with a potential to overcome multidrug resistance. *European Journal of Medicinal Chemistry*, 117, 335–354.
- Pervez, H., Saira, N., Iqbal, M. S., Yaqub, M., & Khan, K. M. (2011). Synthesis and toxicity evaluation of some N4-aryl substituted 5-trifluoromethoxyisatin-3-thiosemicarbazones. *Molecules*, 16(8), 6408–6421.
- Pervez, H., Saira, N., Iqbal, M. S., Yaqub, M., & Khan, K. M. (2013). Synthesis and biological evaluation of some N 4-aryl-substituted 5-fluoroisatin-3-thiosemicarbazones. *Medicinal Chemistry Research*, 22(12), 5878–5889.
- Priyanka, K. B., Manasa, C., & Sammaiah, G. (2014). Synthesis and evaluation of new isatin derivatives for cytotoxic activity. *World Journal of Pharmacy and Pharmaceutical Sciences*, 3, 2393–2402.
- Raut, U., Narang, P., Mendiratta, D. K., Narang, R., & Deotale, V. (2008). Evaluation of rapid MTT tube method for detection of drug susceptibility of *Mycobacterium tuberculosis* to rifampicin and isoniazid. *Indian Journal of Medical Microbiology*, 26, 222–227.
- Sabet, R., Mohammadpour, M., Sadeghi, A. & Fassihi, A. (2010). QSAR study of isatin analogues as *in vitro* anti-cancer agents. *European Journal of Medicinal Chemistry*, 45, 1113–1118.
- Sevinçli, Z. Ş., Duran, G., Özbil, M., & Karalı, N. (2020). Synthesis, molecular modeling and antiviral activity of novel 5-fluoro-1H-indole-2,3-dione 3-thiosemicarbazones. *Bioorganic Chemistry*, In press, <https://doi.org/10.1016/j.bioorg.2020.104202>
- Vine, K. L., Locke, J. M., Ranson, M., Pyne, S. G., & Bremner, J. B. (2007). An investigation into the cytotoxicity and mode of action of some novel N-alkyl-substituted isatins. *Journal of Medicinal Chemistry*, 50, 5109–5117.

# Cytochrome P450 2A13 3375C>T gene polymorphism in a Turkish population

Zuhal Uçkun Şahinoğulları<sup>1</sup> 

<sup>1</sup>Mersin University, Faculty of Pharmacy, Department of Pharmaceutical Toxicology, Mersin, Turkey

ORCID IDs of the authors: Z.U.Ş. 0000-0002-3244-4103

Cite this article as: Uckun Sahinogullari, Z. (2020). Cytochrome P450 2A13 3375C>T gene polymorphism in a Turkish population. *Istanbul Journal of Pharmacy*, 50 (3), 181-187.

## ABSTRACT

**Background and Aims:** The polymorphisms in genes encoding xenobiotic-metabolizing enzymes may change the metabolic activation of various xenobiotics and therefore may affect individuals' susceptibility to xenobiotics-induced toxic effects. Cytochrome P450 2A13 (CYP2A13) is an important CYP enzyme predominantly expressed in the human respiratory tract. CYP2A13 metabolizes the xenobiotics and bioactivation of several carcinogens. The present study aimed to determine the allele and genotype frequencies of CYP2A13 3375C>T polymorphism in a Turkish population and also to compare the obtained results with those of various populations.

**Methods:** CYP2A13 3375C>T polymorphism was determined in 93 healthy Turkish individuals using the polymerase chain reaction-restriction fragment length method.

**Results:** The frequencies of CC, CT and TT genotypes were 89.2%, 9.7% and 1.1%, respectively. The frequencies of C and T alleles were 94.1% and 5.9%, respectively. The genotype frequencies did not deviate from the Hardy-Weinberg equilibrium. Significant differences were observed when comparing the results found with those of various populations, especially those of populations with black ancestry (excluding Tunisian).

**Conclusion:** This study can provide valuable data for further studies investigating the role of this polymorphism concerning the susceptibility to xenobiotics-induced toxic effects, including cancer, and may be used as a control group for such studies and also may contribute to toxicogenetic and epidemiological studies.

**Keywords:** CYP2A13 3375C>T, genetic polymorphism, Arg257Cys, Turkish population

## INTRODUCTION

Human cytochrome P450s (CYPs) account for the metabolism of therapeutic agents and bioactivation of numerous carcinogens (Kim et al., 2018). CYP2A is a subfamily of CYPs that play an important role in the bioactivation of chemicals. The CYP2A gene subfamily contains two functional genes, CYP2A13 and CYP2A6, and a nonfunctional gene, CYP2A7 (Fukami, Nakajima, Sakai, Kato, & Yokoi, 2007). CYP2A13 and CYP2A6 consist of 494 amino acids (Fukami, Nakajima, Matsumoto, Zen, Oda, & Yokoi, 2010) and the protein and nucleotide sequences of CYP2A13 are quite similar to CYP2A6 with 93.5% and 95.3% identity, respectively (Zhou, Liu, & Chowbay, 2009). CYP2A6 is chiefly expressed in the human liver, while CYP2A13 is mostly expressed in the human respiratory tract, at the highest level in the nasal mucosa, followed by the trachea and lungs (Fukami et al., 2007; Tamaki et al., 2011a). In addition, CYP2A13 is expressed in a range of human tissues that include the uterus, testis, prostate, mammary gland and brain (Zhou et al., 2009).

CYP2A13 plays a significant role in the metabolic activation of many procarcinogens (Zhou et al., 2009). The most effective enzyme in the metabolic activation of 4-(methylnitrosamino)-1-(3-pyridyl)-1-butanone (NNK) that is the main tobacco-specific procarcinogen is

### Address for Correspondence:

Zuhal Uçkun ŞAHİNOĞULLARI, e-mail: uckunzuhal@gmail.com

Submitted: 16.05.2020

Revision Requested: 26.06.2020

Last Revision Received: 07.07.2020

Accepted: 30.07.2020

This work is licensed under a Creative Commons Attribution 4.0 International License.



CYP2A13 (Cheng, Chen, Zhang, Zhou, Wang, & Zhou, 2004; Zhou et al., 2009). Furthermore, CYP2A13 metabolizes nicotine, cotinine, coumarin, aflatoxin B<sub>1</sub>, mycotoxin (Zhou et al., 2009), hexamethylphosphoramide (HMPA), N,N-dimethylaniline (DMA), N-nitrosomethylphenylamine (NMPhA) (Sharma, Ahuja, Panda, & Khullar, 2010), 3-N-nitrosoguvacoline, 3-methylindole (skatole), 3-(N-nitrosomethylamino)propionaldehyde, N-nitrosomorpholine (NNN), bergapten (5-methoxypsoralen), N-nitrosopyrrolidine (Alzahrani, & Rajendran, 2020), N-nitrosodiethylamine, methyl *tert*-butyl ether, 2,6-dichlorobenzonitrile, 2-methoxyacetophenone (2'-MAP) (Su, Bao, Zhang, Smith, Hong, & Ding, 2000; Zhou et al., 2009), 4-aminobiphenyl, toluene styrene, naphthalene (Fukami et al., 2010). In addition, CYP2A13 is responsible for the metabolism of theophylline and phenacetin, which are two typical CYP1A2 substrates (Zhou et al., 2009).

The CYP2A13 enzyme is encoded by the *CYP2A13* gene located in a CYP gene cluster on chromosome 19 (Tamaki et al., 2011a). Hitherto, nine allelic variants and many single nucleotide polymorphisms (SNPs) have been described in the *CYP2A13* gene (<http://www.pharmvar.org/gene/CYP2A13>). One of the important SNPs in the *CYP2A13* gene is non-synonymous 3375C>T polymorphism (rs8192789) (Cheng et al., 2004), which is a transition from C to T at nucleotide 3375 in exon 5 (Sharma et al., 2010). This polymorphism is in linkage with functional substitution in the exon 1 of *CYP2A13* gene, Arg25Gln (rs8192784) (Timofeeva et al., 2009), and the *CYP2A13*\*2 allele represents either one or both variations of 3375C>T leading to Arg257Cys and 74G>A leading to Arg25Gln (Wang, He, Shen, Wang, & Hong, 2006; Zhou et al., 2009). The Arg257Cys variant has been reported to be approximately 50% less active compared to the Arg-257 enzyme (Timofeeva et al., 2009). This decline may be elucidated by the location of the Arg at the 257 position, which is conservative in the CYP2As and which is located near the carboxyl end of the G-helix (Cauffiez et al., 2005; Zhou et al., 2009). The Arg257Cys polymorphism is functionally important, and it has been reported that this polymorphism could ensure some prevention against xenobiotic toxicity to carriers with homozygous for the Cys257 allele (Zhang et al., 2002). However, this association is controversial and this polymorphism should be studied in several ethnic groups.

Genetic variations in CYP enzymes may have the greatest effect on the fate of carcinogenic chemicals and therapeutic drugs (Kim et al., 2018). These variations in CYP enzymes may lead to susceptibility to diseases as well as protection from disease or reduced risk of illness (Elfaki, Mir, Almutairi, & Duhier, 2018). Genetic variations that affect the CYP2A13 enzyme function may give rise to inter-individual variability in susceptibility to a variety of diseases, including lung cancer (Tamaki et al., 2011a). The CYP2A13 enzyme plays a significant role in the metabolism of numerous carcinogens, drug, and other xenobiotics. Due to differentiation of enzyme activity in variant CYP2A13 alleles, inter- and intra-population diversity may be an important clinical problem in toxicity and response to xenobiotics metabolized by the CYP2A13 enzyme.

It is known that gene polymorphisms of CYPs indicate significant distinctions in frequency among different racial and

ethnic groups (Korytina, Kochetova, Akhmadishina, Viktorova, & Victorova, 2012; Uckun Sahinogullari, 2020). Thus, the objective of the current study was to detect the allele and genotype frequencies of 3375C>T SNP in *CYP2A13* gene (rs8192789) encoding CYP2A13 enzyme in a healthy Turkish population and to compare the obtained findings with the results of previously reported populations, and thus to provide useful data for toxicogenetic and epidemiological studies.

## MATERIALS AND METHODS

### Samples

The DNA samples isolated from the previous study (22/10/2015, protocol no: 2015/317) were included in the current survey. The present study was also approved by the Ethics Committee of Mersin University (19/02/2020, protocol no: 2020/169). This investigation was performed on the DNA samples of 93 healthy and unrelated Turkish individuals aged between 18-65 years. The study was executed according to Good Clinical Practices and the Helsinki Declaration.

### Genotyping

*CYP2A13* 3375 C>T polymorphism was conducted as per the method defined by Chen et al. (2004) with minor modifications. Polymerase chain reaction (PCR) amplification for *CYP2A13* was performed using the forward and reverse primers: 5'- CCTGGACAGATGCCTTTAACTCCG-3' and 5'- TGGCTTTG-CACCTGCCTGCACT-3', respectively. PCR was done in a 20- $\mu$ L reaction mixture which contained 300 to 500 ng of genomic DNA, 10 pmol of each primer, 10 x PCR buffer, 1.5 mM MgCl<sub>2</sub>, 0.2 mM each deoxynucleotide triphosphate and 1.20 unit of Taq polymerase (Fermentase) on MiniAmp Plus Thermal Cycler (Thermo Fisher, USA). The PCR process was as follows: 95°C for 3 min for initial denaturation and then 35 cycles of 95°C for 30 sec, 63°C for 45 sec, 72°C for 30 sec, followed by a final elongation at 72°C for 5 min. A negative control containing no DNA was included in each PCR analysis to ensure that the reagents used did not contain contaminating DNA. The PCR products (332 bp) were electrophoresed on a 1% agarose gel including ethidium bromide (0.5  $\mu$ g/mL) which made the products visible and then the 10  $\mu$ L PCR product was cut in 15 minutes at 37°C using 10 U of Fast Digest HhaI restriction enzyme with the proper buffer in total volume of 20  $\mu$ L. The variant genotype (TT) was digested to 332 bp fragment while the wild type genotype (CC) was digested to 233 and 99 bp fragments (Figure 1). 1.5% agarose gel with ethidium bromide was used to evaluate the digested fragments. 10% of the samples were re-analyzed at random for quality assurance and which provided 100% concordance.

### Statistical analysis

The allelic and genotypic frequencies were calculated using the genotype counting method. The expected and observed frequencies of *CYP2A13* were compared using the chi-square ( $\chi^2$ ) test based on the Hardy-Weinberg equilibrium. A comparison of the frequencies of this study with the results of previously reported populations was made using the chi-square test. The baseline properties between genotypes were compared using chi-square test and Mann-Whitney U test, where appropriate. Statistical analyses were carried out with IBM SPSS



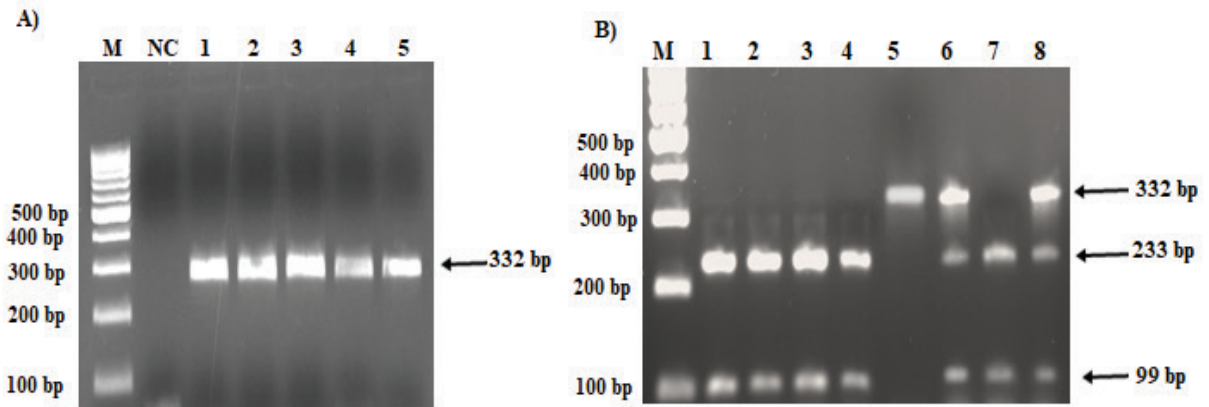


**Figure 1.** Agarose gel images of *CYP2A13 3375C>T* polymorphism using polymerase chain reaction (PCR) (A) and restriction fragment length polymorphism (RFLP) (B). Lane M: Marker (100 bp). For A (PCR) part; NC: Negative control, Lane 1-5: PCR product (332 bp). For B (RFLP) part; Lane 1-4,7: wild type genotype (233, 99 bp), Lane 5: mutant genotype (332 bp), Lane 6,8: heterozygous genotype (332, 233, 99 bp).

25.0 computer software for Windows.  $p < 0.05$ ,  $p < 0.001$  and  $p < 0.0001$  were considered statistically significant.

**RESULTS**

*CYP2A13 3375C>T* polymorphism was conducted in 93 healthy unrelated individuals. Of the 93 individuals, 40 (43% of all participants) were male and 53 (57%) were female. The mean age with standard deviation (SD) of the participants was  $28.34 \pm 10.14$  years, the mean body weight with SD was  $69.64 \pm 13.52$  kg, the mean height with SD was  $169.25 \pm 8.62$  cm and the mean body mass index (BMI) with SD was  $24.22 \pm 3.77$  kg/m<sup>2</sup>. No significant difference was noted between the genotypes and baseline properties ( $p > 0.05$ ) (Table 1).

As shown in Table 2, the frequencies of *CC*, *CT* and *TT* genotypes were 89.2%, 9.7% and 1.1%, respectively. The *C* and *T* allele frequencies were obtained as 94.1% and 5.9%, respectively. The genotype frequencies were consistent with Hardy-Weinberg equilibrium ( $\chi^2 = 1.58$ ,  $p > 0.05$ ).

**Table 1. Baseline properties of the individuals included in the study.**

Baseline properties	Total	CC	CT+TT	p value
<b>n (%)</b>				
Gender				
Male	40 (43)	37 (92.5)	3 (7.5)	0.379 <sup>a</sup>
Female	53 (57)	46 (86.8)	7 (13.2)	
Age range (years)				
< 40	77	70	7	0.256 <sup>a</sup>
≥ 40	16	13	3	
<b>mean±SD</b>				
Body weight (kg)	69.64±13.52	70.39±13.93	62.75±5.78	0.194 <sup>b</sup>
Height (cm)	169.25±8.62	169.45±8.23	167.50±12.16	0.627 <sup>b</sup>
BMI (kg/m <sup>2</sup> )	24.22±3.77	24.42±3.86	22.49±2.43	0.164 <sup>b</sup>

Data expressed as mean ± standard deviation (mean ± SD). BMI: Body mass index; <sup>a</sup>: Chi-square test; <sup>b</sup>: Mann-Whitney U test.

**Table 2. Distribution of *CYP2A13 3375 C>T* gene polymorphism in a healthy Turkish population.**

Genotype	n (Observed)	Genotype frequencies, %	n (Expected)	Allele frequencies, %
CC	83	89.2	82.3	C: 94.1
CT	9	9.7	10.4	T: 5.9
TT	1	1.1	0.3	$\chi^2: 1.58$
<b>Total</b>	<b>93</b>	<b>100</b>	<b>93</b>	$df = 1;$ $p > 0.05$

**DISCUSSION**

In the current study, the genotype and allele frequencies of *CYP2A13 3375C>T* polymorphism in a healthy Turkish population were investigated and compared with various populations. The *CC*, *CT* and *TT* genotype frequencies of *CYP2A13* polymorphism were 89.2%, 9.7% and 1.1%, respectively and thus the frequencies of *C* and *T* allele were 94.1% and 5.9%, respectively.

The findings of this study were compared with the results of the 1000 Genomes Project (<http://www.internationalgenome.org/1000-genomes-browsers/>) and previously reported populations as shown in Table 3 (Cauffiez et al., 2005; Cheng et al., 2004; Fujieda et al., 2003; Herr, Bettendorf, Denschlag, Keck, & Pietrowski, 2006; Song, Xing, Zhang, Li, Liu, & Qiao, 2009; Wang et al., 2003; Zhang et al., 2002). The allele frequencies of *CYP2A13 3375C>T* polymorphism were dominant in Black ancestry, including Black, Yoruba in Ibadan, Nigeria (YRI), Esan in Nigeria (ESN), Luhya in Webuye, Kenya (LWK), African Caribbeans in Barbados (ACB) populations, ranging from



**Table 3. Distribution of genotype and allele frequencies of CYP2A13 3375C >T polymorphism in different ethnic populations.**

Ethnicity	Population	Sample size n	Genotype frequencies n (%)			Allele frequencies n (%)		References
			CC	CT	TT	C	T	
<b>White</b>								
European	Whites	52	50 (96.2)	2 (3.8)	0 (0.0)	102 (98.1)	2 (1.9)	Zhang et al., 2002
	Turkish	93	83 (89.2)	9 (9.7)	1 (1.1)	175 (94.1)	11 (5.9)	The present study
	French*	52	52 (100)	0 (0.0)	0 (0.0)	52 (100)	0 (0.0)	Cauffiez et al., 2005
	British in England and Scotland (GBR)*	91	90 (98.9)	1 (1.1)	0 (0.0)	181 (99.5)	1 (0.5)	1000 Genomes Project <sup>a</sup>
	Iberian populations in Spain (IBS)*	107	105 (98.1)	2 (1.9)	0 (0.0)	212 (99.1)	2 (0.9)	1000 Genomes Project <sup>a</sup>
	Germany*	243	237 (97.5)	6 (2.5)	0 (0.0)	480 (98.8)	6 (1.2)	Herr et al., 2006
	Finnish in Finland (FIN)	99	96 (97.0)	3 (3.0)	0 (0.0)	195 (98.5)	3 (1.5)	1000 Genomes Project <sup>a</sup>
	Toscani in Italy (TSI)	106	102 (95.3)	5 (4.7)	0 (0.0)	209 (97.7)	5 (2.3)	1000 Genomes Project <sup>a</sup>
	Hispanic	52	46 (88.5)	6 (11.5)	0 (0.0)	98 (94.2)	6 (5.8)	Zhang et al., 2002
American	Mexican Ancestry in Los Angeles, California (MXL)*	64	64 (100)	0 (0.0)	0 (0.0)	128 (100)	0 (0.0)	1000 Genomes Project <sup>a</sup>
	Peruvian in Lima, Peru (PEL)*	85	84 (98.8)	1 (1.2)	0 (0.0)	169 (99.4)	1 (0.6)	1000 Genomes Project <sup>a</sup>
	Colombian in Medellin, Colombia (CLM)	94	88 (93.6)	6 (6.4)	0 (0.0)	182 (96.8)	6 (3.2)	1000 Genomes Project <sup>a</sup>
	Puerto Rican in Puerto Rico (PUR)	104	92 (88.5)	11 (10.6)	1 (0.9)	195 (93.8)	13 (6.2)	1000 Genomes Project <sup>a</sup>
<b>Asians</b>								
East Asian	Asians	52	44 (84.6)	8 (15.4)	0 (0.0)	96 (92.3)	8 (7.7)	Zhang et al., 2002
	Japanese**	192	192 (100)	0 (0.0)	0 (0.0)	384 (100)	0 (0.0)	Fujieda et al., 2003
	Japanese in Tokyo, Japan (JPT)	104	95 (91.3)	8 (7.7)	1 (1.0)	198 (95.2)	10 (4.8)	1000 Genomes Project <sup>a</sup>
	Southern Han Chinese, China (CHS)	105	94 (89.5)	11 (10.5)	0 (0.0)	199 (94.8)	11 (5.2)	1000 Genomes Project <sup>a</sup>
	Chinese	258	230 (89.1)	27 (10.5)	1 (0.4)	487 (94.4)	29 (5.6)	Cheng et al., 2004
	Kinh in Ho Chi Minh City, Vietnam (KHV)	99	87 (87.9)	11 (11.1)	1 (1.0)	185 (93.4)	13 (6.6)	1000 Genomes Project <sup>a</sup>
	Han Chinese in Beijing, China (CHB)	103	88 (85.4)	15 (14.6)	0 (0.0)	191 (92.7)	15 (7.3)	1000 Genomes Project <sup>a</sup>
	Chinese Dai in Xishuangbanna, China (CDX)	93	79 (84.9)	14 (15.1)	0 (0.0)	172 (92.5)	14 (7.5)	1000 Genomes Project <sup>a</sup>
	Chinese	212	180 (84.9)	31 (14.6)	1 (0.5)	391 (92.2)	33 (7.8)	Song et al., 2009
	Chinese	791	652 (82.4)	130 (16.4)	9 (1.2)	1434 (90.6)	148 (9.4)	Wang et al., 2003

**Table 3. Continued.**

South Asian	Indian Telugu in the UK (ITU)	102	96 (94.1)	6 (5.9)	0 (0.0)	198 (97.1)	6 (2.9)	1000 Genomes Project <sup>a</sup>
	Sri Lankan Tamil in the UK (STU)	102	95 (93.1)	7 (6.9)	0 (0.0)	197 (96.6)	7 (3.4)	1000 Genomes Project <sup>a</sup>
	Punjabi in Lahore, Pakistan (PJL)	96	80 (83.3)	15 (15.6)	1 (1.1)	175 (91.1)	17 (8.9)	1000 Genomes Project <sup>a</sup>
<b>Black</b>								
African	Black*	52	38 (73.1)	13 (25.0)	1 (1.9)	89 (85.6)	15 (14.4)	Zhang et al., 2002
	Tunisian	48	44 (91.7)	4 (8.3)	0 (0.0)	92 (95.8)	4 (4.2)	Cauffiez et al., 2005
	African Caribbeans in Barbados (ACB)***	96	64 (66.7)	27 (28.1)	5 (5.2)	155 (80.7)	37 (19.3)	1000 Genomes Project <sup>a</sup>
	Yoruba in Ibadan, Nigeria (YRI)***	108	70 (64.8)	33 (30.6)	5 (4.6)	173 (80.1)	43 (19.9)	1000 Genomes Project <sup>a</sup>
	Esan in Nigeria (ESN)**	99	61 (61.6)	32 (32.3)	6 (6.1)	154 (77.8)	44 (22.2)	1000 Genomes Project <sup>a</sup>
	Luhya in Webuye, Kenya (LWK)**	99	61 (61.6)	32 (32.3)	6 (6.1)	154 (77.8)	44 (22.2)	1000 Genomes Project <sup>a</sup>
Differences in the frequencies were examined using $\chi^2$ test. n total number of subjects; Significant at * $p < 0.05$ , ** $p < 0.0001$ and *** $p < 0.001$ when compared to the current study; <sup>a</sup> : <a href="http://www.internationalgenome.org/1000-genomes-browsers/">http-2: https://www.internationalgenome.org/1000-genomes-browsers/</a> .								

14.4 to 22.2%. The allele frequencies of these populations were predominantly determined to be higher compared to the Turkish population. Contrarily, the allele frequency of the Turkish population was similar to the Tunisian population with an allele frequency of 4.2%.

The frequencies in European ancestry, including French, British in England and Scotland (GBR), Iberian populations in Spain (IBS) and Germany populations with a range of 0.0 to 1.2% were determined to be significantly lower compared to the frequencies in the Turkish population ( $p < 0.05$ ), but no significant difference was observed between the results of this study and those of Whites, Finnish in Finland (FIN), Toscani in Italy (TSI) and Hispanic populations with a range from 1.5 to 5.8% ( $p > 0.05$ ). In addition, there were no significant differences between the allele frequencies of the Turkish population and those of American ancestry, including Colombian in Medellin, Colombia (CLM) with 3.2% allelic frequency and Puerto Rican in Puerto Rico (PUR) with 6.2% allelic frequency ( $p > 0.05$ ). However, the results of the present study were significantly higher compared to those of other American ancestry, including Mexican Ancestry in Los Angeles, California (MXL) with 0.0 % allelic frequency and Peruvian in Lima, Peru (PEL) with 0.6% allelic frequency ( $p < 0.05$ ).

Furthermore, there were significant differences between the allele frequency of 0.0% in the Japanese population and that of the Turkish population ( $p < 0.0001$ ). However, no significant differences were noted between the obtained results and those of populations with Asian ancestry, including, Asians, Japanese in Tokyo, Japan (JPT), Southern Han Chinese, China (CHS), Chinese, Kinh in Ho Chi Minh City, Vietnam (KHV), Han Chinese in Beijing, China (CHB), Chinese Dai in Xishuangbanna, China (CDX), Indian

Telugu in the UK (ITU), Sri Lankan Tamil in the UK (STU) and Punjabi in Lahore, Pakistan (PJL), ranging from 2.9 to 9.4%.

As mentioned above, the allele frequency of *CYP2A13* 3375C>T is variable among different populations. Therefore, this polymorphism may cause intra- and inter- population variations in drugs, other xenobiotics toxicity and predisposition to various diseases.

Wang et al. (2003) investigated 724 patients with lung cancer and 791 healthy controls in the Chinese population for contribution of *CYP2A13* Arg257Cys polymorphism to lung cancer risks with regard to tobacco smoking. The variant *CYP2A13* genotypes (CT or TT) were reported to have a decreased risk of lung adenocarcinoma in relation to light tobacco smoking compared to the *CYP2A13* CC genotype (odds ratio [OR]=0.23; 95% confidence interval [CI]=0.08-0.68;  $p=0.008$ ). However, Arg257Cys polymorphism had no protection against lung squamous cell carcinoma. Herr et al. (2006) investigated the relationship between *CYP2A13* 3375C>T polymorphism and the development of uterine leiomyoma in a case-control study consisting of 126 women with uterine leiomyoma and 243 controls and reported that this polymorphism had a significant association with uterine leiomyoma in a Caucasian population. In another case-control study consisting of 163 patients with bladder cancer and 161 healthy controls, Kumondai et al. (2016) examined the association between bladder cancer occurrence and *CYP2A13* genetic polymorphisms in Japanese smokers and it was reported that the adjusted odds ratio for the *CYP2A13*\*1/\*2 genotype was 0.34 (95% CI=0.17–0.69) and the presence of *CYP2A13*\*2 had a relationship with a decline in the risk of bladder cancer. D'Agostino et al. (2008) examined whether the *CYP2A13.2* protein has reduced expression levels and/or enzyme activity in the lung in comparison to *CY-*

P2A13.1. It was reported that the CYP2A13.2 protein was 20 to 40% lower active compared to CYP2A13.1 with the substrates studied; which were NNK, HMPA, 2'-MPA, DMA and NMPhA. Additionally, the CYP2A13\*2 allele was associated with an approximately 40% lower level of allelic expression than the CYP2A13\*1 allele. Zhang et al. (2002) reported that the Arg-257Cys variant had a 37 to 56% lower catalytic activity compared to the wild-type Arg-257 protein toward the substrates examined; NMPhA, DMA, 2'-MAP and HMPA and that Cys-257 had a >2-fold reduction in catalytic efficiency compared to Arg-257 for NNK. Furthermore, for CYP2A13\*2 (Arg257Cys) and CYP2A13\*8 (Asp158Glu), a decrease of 30 to 42% in coumarin 7-hydroxylation catalytic efficiency has been reported (Schlicht, Michno, Smith, Scott, & Murphy, 2007).

Contrary to the studies mentioned above, Song et al. (2009) reported that in a case-control survey of 208 cases and 212 controls, no significant relationship was found between the CYP2A13 variant alleles (CT or TT) and bladder cancer risk in central China (OR=1.07; 95% CI: 0.63-1.81; p=0.725). Timofeeva et al. (2009) found no significant relationship between the CYP2A13 rs8192789 polymorphism and the risk of lung cancer in Caucasian patients (OR=1.04; 95% CI=0.55-1.96; p=0.9019). Furthermore, no significant relationship between CYP2A13 (\*1-\*10) genetic polymorphisms and lung cancer was reported in a Japanese population of 192 lung cancer patients and 203 controls (for CYP2A13\*2 allele, crude OR=0.75; 95% CI=0.40-1.40; p<0.05) (Tamaki et al. 2011b). Jiang et al. (2004) examined the association between CYP2A13 genetic polymorphisms and the risk of developing nasopharyngeal cancer in the Cantonese population of southern China and found no association of the variant alleles containing 3375 C>T with nasopharyngeal cancer risk (for 3375 C>T, OR=0.85; 95% CI=0.59-1.22). In addition, CYP2A13 3375C>T variant has been reported to not be associated with head and neck cancer susceptibility in a North Indian population (OR=0.61; 95% CI=0.29-1.28; p=0.189) (Sharma et al., 2010).

Genetic polymorphisms can affect the activities of enzymes that play a role in the metabolism of carcinogens, drugs and other xenobiotics, and can cause inter- and intra-population differences in susceptibility to various diseases, drug safety and efficacy, toxicities of xenobiotics.

## CONCLUSION

The present study performs the frequencies of the CYP2A13 3375C>T polymorphism in a healthy Turkish population and a comparison of the obtained findings with those of other populations. Significant differences were observed in comparing the results found with those of some previously reported populations, especially those with black ancestry (excluding Tunisian). The results of this study can provide valuable data for further studies investigating the role of this polymorphism concerning susceptibility to xenobiotics-induced toxic effects, including cancer, and may even be used as a control group for such studies. Furthermore, the data of this study may improve toxicogenetic studies and contribute to epidemiological studies.

**Peer-review:** Externally peer-reviewed.

**Author Contributions:** Conception/Design of Study- Z.U.Ş.; Data Acquisition- Z.U.Ş.; Data Analysis/Interpretation- Z.U.Ş.; Drafting Manuscript- Z.U.Ş.; Critical Revision of Manuscript- Z.U.Ş.; Final Approval and Accountability- Z.U.Ş.

**Ethics Committee Approval:** This study was approved by the Ethics Committee of Mersin University. (date: 19/02/2020, number: 2020/169)

**Informed Consent:** The DNA samples used were obtained during the previous study, which was approved by Mersin University Ethics Committee (22/10/2015, protocol no: 2015/317). Informed consent form had been obtained while blood samples were taken from volunteers.

**Conflict of Interest:** The authors have no conflict of interest to declare.

**Financial Disclosure:** Authors declared no financial support.

## REFERENCES

- Alzahrani, A. M., & Rajendran, P. (2020). The multifarious link between cytochrome P450s and cancer. *Oxidative Medicine and Cellular Longevity*, 2020:3028387.
- Cauffiez, C., Pottier, N., Tournel, G., Lo-Guidice, J. M., Allorge, D., Chevalier, D., Migot-Nabias, F., Kenani, A., & Broly, F. (2005). CYP2A13 genetic polymorphism in French Caucasian, Gabonese and Tunisian populations. *Xenobiotica*, 35(7), 661–669.
- Cheng, X. Y., Chen, G. L., Zhang, W. X., Zhou, G., Wang, D., & Zhou, H. H. (2004). Arg257Cys polymorphism of CYP2A13 in a Chinese population. *Clinica Chimica Acta*, 343(1-2), 213–216.
- D'Agostino, J., Zhang, X., Wu, H., Ling, G., Wang, S., Zhang, Q.Y., Liu, F., & Ding, X. (2008). Characterization of CYP2A13\*2, a variant cytochrome P450 allele previously found to be associated with decreased incidences of lung adenocarcinoma in smokers. *Drug Metabolism and Disposition*, 36(11), 2316–2323.
- Elfaki, I., Mir, R., Almutairi, F. M., & Duhier, F. M. A. (2018). Cytochrome P450: Polymorphisms and Roles in Cancer, Diabetes and Atherosclerosis. *Asian Pacific Journal of Cancer Prevention*, 19(8), 2057–2070.
- Fujieda, M., Yamazaki, H., Kiyotani, K., Muroi, A., Kunitoh, H., Dosaka-Akita, H., Sawamura, Y., & Kamataki, T. (2003). Eighteen novel polymorphisms of the CYP2A13 gene in Japanese. *Drug Metabolism and Pharmacokinetics*, 18(1), 86–90.
- Fukami, T., Nakajima, M., Matsumoto, I., Zen, Y., Oda, M., & Yokoi, T. (2010). Immunohistochemical analysis of CYP2A13 in various types of human lung cancers. *Cancer Science*, 101(4), 1024–1028.
- Fukami, T., Nakajima, M., Sakai, H., Katoh, M., & Yokoi, T. (2007). CYP2A13 metabolizes the substrates of human CYP1A2, phenacetin, and theophylline. *Drug Metabolism and Disposition*, 35(3), 335–339.
- Herr, D., Bettendorf, H., Denschlag, D., Keck, C., & Pietrowski, D. (2006). Cytochrome P2A13 and P1A1 gene polymorphisms are associated with the occurrence of uterine leiomyoma. *Archives of Gynecology and Obstetrics*, 274(6), 367–371.
- http-1: <https://www.pharmvar.org/gene/CYP2A13>. Accessed 10.04.2020.
- http-2: <https://www.internationalgenome.org/1000-genomes-browsers/>. Accessed 03.04.2020.
- Jiang, J. H., Jia, W. H., Chen, H. K., Feng, B. J., Qin, H. D., Pan, Z. G., Shen, G. P., Huang, L. X., Feng, Q. S., Chen, L. Z., Lin, D. X., & Zeng, Y. X. (2004). Genetic polymorphisms of CYP2A13 and its relationship to nasopharyngeal carcinoma in the Cantonese population. *Journal of Translational Medicine*, 2(1), 24.

- Kim, V., Yeom, S., Lee, Y., Park, H. G., Cho, M. A., Kim, H., & Kim, D. (2018). In vitro functional analysis of human cytochrome P450 2A13 genetic variants: P450 2A13\*2, \*3, \*4, and \*10. *Journal of Toxicology and Environmental Health. Part A*, 81(12), 493–501.
- Korytina, G., Kochetova, O., Akhmadishina, L., Viktorova, E., & Viktorova, T. (2012). Polymorphisms of cytochrome p450 genes in three ethnic groups from Russia. *Balkan Medical Journal*, 29(3), 252–260.
- Kumondai, M., Hosono, H., Orikasa, K., Arai, Y., Arai, T., Sugimura, H., Ozono, S., Sugiyama, T., Takayama, T., Sasaki, T., Hirasawa, N., & Hiratsuka, M. (2016). CYP2A13 Genetic Polymorphisms in Relation to the Risk of Bladder Cancer in Japanese Smokers. *Biological & Pharmaceutical Bulletin*, 39(10), 1683–1686.
- Schlicht, K. E., Michno, N., Smith, B. D., Scott, E. E., & Murphy, S. E. (2007). Functional characterization of CYP2A13 polymorphisms. *Xenobiotica*, 37(12), 1439–1449.
- Sharma, R., Ahuja, M., Panda, N., & Khullar, M. (2010). Polymorphisms in CYP2A13 and UGT1A7 genes and head and neck cancer susceptibility in North Indians. *Oral Diseases*, 16(8), 760–768.
- Song, D. K., Xing, D. L., Zhang, L. R., Li, Z. X., Liu, J., & Qiao, B. P. (2009). Association of NAT2, GSTM1, GSTT1, CYP2A6, and CYP2A13 gene polymorphisms with susceptibility and clinicopathologic characteristics of bladder cancer in Central China. *Cancer Detection and Prevention*, 32(5-6), 416–423.
- Su, T., Bao, Z., Zhang, Q. Y., Smith, T. J., Hong, J. Y., & Ding, X. (2000). Human cytochrome P450 CYP2A13: predominant expression in the respiratory tract and its high efficiency metabolic activation of a tobacco-specific carcinogen, 4-(methylnitrosamino)-1-(3-pyridyl)-1-butanone. *Cancer Research*, 60(18), 5074–5079.
- Tamaki, Y., Honda, M., Muroi, Y., Arai, T., Sugimura, H., Matsubara, Y., Kanno, S., Ishikawa, M., Hirasawa, N., & Hiratsuka, M. (2011a). Novel single nucleotide polymorphism of the CYP2A13 gene in Japanese individuals. *Drug Metabolism and Pharmacokinetics*, 26(5), 544–547.
- Tamaki, Y., Arai, T., Sugimura, H., Sasaki, T., Honda, M., Muroi, Y., Matsubara, Y., Kanno, S., Ishikawa, M., Hirasawa, N., & Hiratsuka, M. (2011b). Association between cancer risk and drug-metabolizing enzyme gene (CYP2A6, CYP2A13, CYP4B1, SULT1A1, GSTM1, and GSTT1) polymorphisms in cases of lung cancer in Japan. *Drug Metabolism and Pharmacokinetics*, 26(5), 516–522.
- Timofeeva, M. N., Kropp, S., Sauter, W., Beckmann, L., Rosenberger, A., Illig, T., Jäger, B., Mittelstrass, K., Dienemann, H.; LUCY-Consortium, Bartsch, H., Bickeböller, H., Chang-Claude, J. C., Risch, A., & Wichmann, H. E. (2009). CYP450 polymorphisms as risk factors for early-onset lung cancer: gender-specific differences. *Carcinogenesis*, 30(7), 1161–1169.
- Uckun Sahinoğulları, Z. (2020). Genetic polymorphism of CYP2C8\*4 in a healthy Turkish population. *Medicine Science*, 9(2), 314–319.
- Wang, S. L., He, X. Y., Shen, J., Wang, J. S., & Hong, J. Y. (2006). The missense genetic polymorphisms of human CYP2A13: functional significance in carcinogen activation and identification of a null allelic variant. *Toxicological Sciences*, 94(1), 38–45.
- Wang, H., Tan, W., Hao, B., Miao, X., Zhou, G., He, F., & Lin, D. (2003). Substantial reduction in risk of lung adenocarcinoma associated with genetic polymorphism in CYP2A13, the most active cytochrome P450 for the metabolic activation of tobacco-specific carcinogen NNK. *Cancer Research*, 63(22), 8057–8061.
- Zhang, X., Su, T., Zhang, Q. Y., Gu, J., Caggana, M., Li, H., & Ding, X. (2002). Genetic polymorphisms of the human CYP2A13 gene: identification of single-nucleotide polymorphisms and functional characterization of an Arg257Cys variant. *Journal of Pharmacology and Experimental Therapeutics*, 302(2), 416–423.
- Zhou, S. F., Liu, J. P., & Chowbay, B. (2009). Polymorphism of human cytochrome P450 enzymes and its clinical impact. *Drug Metabolism Reviews*, 41(2), 89–295.

# Evaluation of the hepatotoxic potential of citalopram in rats

Sinem Ilgin<sup>1</sup> , Fulya Dağışan<sup>1</sup> , Dilek Burukoğlu Dönmez<sup>2</sup> , Merve Baysal<sup>1</sup> , Özlem Atlı Eklioğlu<sup>1</sup> 

<sup>1</sup>Anadolu University, Faculty of Pharmacy, Department of Pharmaceutical Toxicology, Eskisehir, Turkey

<sup>2</sup>Eskisehir Osmangazi University, Faculty of Medicine, Department of Histology, Eskisehir, Turkey

**ORCID IDs of the authors:** S.I. 0000-0001-7331-1975; F.D. 0000-0002-2136-0844; D.B.D. 0000-0002-6454-4424; M.B. 0000-0001-8387-435X; Ö.A.E. 0000-0002-6131-3399

**Cite this article as:** İlgin, S., Dağışan, F., Burukoglu Donmez, D., Baysal, M., & Atli Eklioglu, O. (2020). Evaluation of the hepatotoxic potential of citalopram in rats. *Istanbul Journal of Pharmacy*, 50 (3), 188-194.

## ABSTRACT

**Background and Aims:** Citalopram is a selective serotonin reuptake inhibitor with a high potency which is occasionally prescribed and used to treat major depression associated with mood disorders as a first-line drug. According to the results of previous studies, evidence of hepatotoxicity related to citalopram treatment were limited and conflicting. Therefore, we aimed to evaluate the hepatotoxicity potential of sub-chronic citalopram administration.

**Methods:** Citalopram was administered to female rats orally in 5 and 10 mg/kg for 30 days. After the exposure period, serum aspartate aminotransferase (AST), alanine aminotransferase (ALT), total and direct bilirubin levels as biomarkers of hepatotoxicity were measured and histopathological examination of liver tissues was performed. Additionally, GSH levels of liver tissues were determined.

**Results:** The risk of hepatotoxicity related to citalopram was shown by significant increases of serum hepatic biomarkers, AST, ALT, and total bilirubin in citalopram-administered groups. According to the histopathological findings, hepatocellular necrosis, hepatic nuclear asymmetry, and disarrangement of hepatic cord cells (hepatocytes) were prominent in the 10 mg/kg citalopram-administered group. On the other hand, there was no significant difference among the groups in terms of GSH levels.

**Conclusion:** The results suggested that the administration of citalopram might cause hepatotoxic effects, depending on the dose.

**Keywords:** Citalopram, hepatotoxicity, hepatic biomarker, liver histology, oxidative status

## INTRODUCTION

Selective serotonin reuptake inhibitors (SSRIs) are widely used in the treatment of major depressive disorders, such as obsessive-compulsive disorders, anxiety disorders, panic disorders, and post-traumatic stress disorder (Anderson & Edwards 2001; Locher et al., 2017). Citalopram (CTL), paroxetine, fluoxetine, and sertraline are recommended drugs in the treatment of depression (Ferguson, 2001; Sanchez, Reines, & Montgomery, 2014). While fluoxetine is considered the first-line drug in patients under 18 years and with poor medication compliance, sertraline and CTL are chosen as the first-line drugs in patients who are elderly or have chronic diseases due to their lowest potential for drug-drug interactions (Whittington et al., 2004; Wiese, 2011; NICE, 2019; NICE, 2020). Even though CTL treatment is considered safe and tolerable for patients, the case reports indicated that severe adverse effects rarely occurred, including suicidal behavior, prolonged QTc intervals, hemorrhage, and serotonin syndrome related to CTL treatment, at therapeutic and subtherapeutic doses (Sharbaf-Shoar & Padhy 2020).

The liver is the target for the adverse effects of many drugs because it has the largest blood supply and metabolizing enzymes (Sturgill & Lambert 1997; Jaeschke et al., 2002). CTL is metabolized to S/R desmethylcitalopram in the liver by

**Address for Correspondence:**  
Sinem ILGIN, e-mail: silgin@anadolu.edu.tr

This work is licensed under a Creative Commons Attribution 4.0 International License.



Submitted: 14.01.2020  
Revision Requested: 10.03.2020  
Last Revision Received: 19.06.2020  
Accepted: 26.06.2020

the isoenzymes CYP2C19, CYP2D6 and CYP3A4. The subsequent N-demethylation to R/S-didesmethylcitalopram is mediated by CYP2D6 (Herrlin et al., 2003; Sangkuhl, Klein, & Altman, 2011). Escitalopram or CTL treatment at therapeutic and subtherapeutic doses have been associated with acute liver injury (López-Torres, Lucena, Seoane, Verge, & Andrade, 2004; Solomons, Gooch, & Wong, 2005; Neumann, Csepregi, Evert, & Malfertheiner, 2008; Hunfeld, ten Berge, LeBrun, Smith, & Melief, 2010; Gessel & Alcorn 2016). CTL seems to have the least potential for liver injury according to some studies (Voican, Corruble, Naveau, & Perlemuter, 2014; Friedrich et al., 2016). Additionally, there have been no experimental studies related to CTL-induced hepatic adverse effects independent of other risk factors associated with hepatotoxicity. Therefore, we aimed to evaluate the hepatotoxic effects of CTL administration to rats at pharmacological doses in this study. For this purpose, levels of serum aspartate aminotransferase (AST), alanine aminotransferase (ALT), and direct and total bilirubin levels in rats were determined following oral CTL administration for 30 days. Furthermore, liver tissues of the rats were evaluated histopathologically as a biomarker of liver injury. Additionally, glutathione (GSH) levels were measured in liver homogenates to evaluate oxidative status in CTL-administered rats.

## MATERIALS AND METHODS

### Materials

CTL was a kind gift from IE Ulagay-Menarini Group, Turkey. The chemicals used for anesthesia were obtained from the following source: Ketamine (Ketalar®) (Pfizer, Turkey); Xylazine (Sigma, US). Serum AST, ALT, and total and direct bilirubin levels were determined by colorimetric kits from Biolabo S.A. (France). GSH levels were measured by using the ELISA kit from Cayman Chemical Company (USA).

### Animals

Female Sprague-Dawley rats (12 weeks-old) weighing 300-350 g were used. The animals were housed under controlled temperature (22°C) and lighting (12-h light/12-h dark cycle) with free access to food and water and used in accordance with ethical recommendations of the Local Ethics Committee on Animal Experimentation of Anadolu University, Eskisehir, Turkey (File Number: 2013-14). Three experimental groups were used in the present study:

Control group: animals received distilled water via gavage for 30 days (n=8).

CTL-5 group: animals received 5 mg/kg dose of CTL via gavage for 30 days (n=8).

CTL-10 group: animals received 10 mg/kg dose of CTL via gavage for 30 days (n=8).

The doses were determined according to the previous studies (Sekar et al., 2011; Vermoesen, Massie, Smolders, & Clinckers, 2012; Flores-Serrano et al., 2013; Karlsson et al., 2013; Zhang et al., 2013; Vega-Rivera, Gallardo-Tenorio, Fernández-Guasti, & Estrada-Camarena, 2016). Furthermore, clinical doses of CTL

were between 10 and 60 mg/day (Bech, Tanghøj, Andersen, & Overø 2002). The doses we have chosen were also included animal doses extrapolated from human doses by the guideline (CDER 2005). All drugs were administered at a volume of 1 mL/100 g by dissolving in distilled water.

At the end of 30 days, the animals were anesthetized by an intraperitoneal injection of 60 mg/kg ketamine and 5 mg/kg xylazine (IACUC Guidelines, 2017). Blood samples were collected from the right ventricle of the rats via syringe for the analysis of hepatic biomarkers (AST, ALT, total and direct bilirubin).

The rats were euthanized via withdrawal of large amounts of blood from the heart.

Livers were removed after euthanasia and cleaned from blood by using a phosphate buffer solution (PBS) (8 g/L NaCl, 0.2 g/L KCl, 0.2 g/L KH<sub>2</sub>PO<sub>4</sub>, 1.14 g/L Na<sub>2</sub>HPO<sub>4</sub>, pH 7.4). The left lateral lobe of the liver was used to determine the levels of GSH. The liver's right superior lobe was cleared of blood and other contaminants in PBS and then fixed for histological examination.

### Determination of serum hepatic enzymes in rats

After 30 minutes of allowing the blood for clotting, blood samples were centrifuged at 1,000 g for 15 min at 4°C to separate the serum. The enzyme analyses were performed using the commercially available kits according to the manufacturer's instructions.

### Histological analysis of liver tissue

The right superior lobe of the liver was used for histological examination. The tissues were sliced into small pieces (5 mm<sup>3</sup>) and then fixed in a 10% buffered formalin solution for 48 hours. They were dehydrated in a graded series of alcohols. Samples were then stained with hematoxylin and eosin and examined by light microscopy. All sections were observed under an Olympus BH-2 (Olympus Corp., Tokyo, Japan) microscope. Additionally, analyses of pathological changes were based on presence of hepatocellular necrosis, hepatic nuclear asymmetry, and disarrangement of hepatic cord cells (hepatocytes) and the changes were scored according to these criteria.

### Determination of GSH levels in liver tissues

The left lateral lobe of the liver was used to determine the levels of GSH. The tissue was homogenized in a proportion of 1:20 (w/v) in cold PBS containing 50 mm 2-(N-morpholino) ethanesulfonic acid (MES) and 1 mm EDTA, pH 6-7. The samples were centrifuged at 10,000 g for 15 min at 4°C and the supernatant aliquots were used for the GSH assay. The analysis was performed using the commercially available kits according to the manufacturer's instructions.

### Statistical analysis

Data are presented as mean ± standard deviation. Statistical analyses were performed using one-way variance analysis (ANOVA) with the Tukey test as a post hoc test on the SPSS program (version 15) with the significance level p<0.05.



## RESULTS

### The serum hepatic enzymes levels of control and CTL-administered rats

When the groups were compared in terms of serum AST levels, dose-related increases were observed in the CTL-administered groups compared to the control group. AST levels increased in CTL-5 and CTL-10 groups 41.11% and 47.74%, respectively, when compared to the control group. No significant differences were observed among the CTL-administered groups in terms of serum AST levels.

A statistically significant increase was found in the serum ALT levels of 5 and 10 mg/kg CTL-administered groups compared to the control group. Additionally, ALT levels increased in CTL-5 and CTL-10 groups 25.62% and 28.27%, respectively, when compared to the control group. No significant differences were observed among the CTL-administered groups in terms of serum ALT levels.

When the groups were compared in terms of serum total bilirubin level, statistically significant increases were found in 5 and 10 mg/kg CTL-administered groups when compared to the control group. Additionally, total bilirubin levels increased in CTL-5 and CTL-10 groups 26.23% and 22.95%, respectively, when compared to the control group. No significant differences were observed among the CTL-administered groups in terms of serum direct bilirubin levels. Among the CTL-administered groups, the serum total bilirubin and direct bilirubin levels did not show any statistical differences (Table 1).

**Table 1. The serum hepatic enzymes levels of control and CTL-administered rats.**

	C	CTL-5	CTL-10
<b>ALT (U/L)</b>	41.64±5.27	52.31±7.24*	53.41±7.26*
<b>AST (U/L)</b>	83.59±7.05	117.95±24.78*	123.5±30.79*
<b>BILD (mg/dL)</b>	0.034±0.013	0.036±0.016	0.036±0.016
<b>BILT (mg/dL)</b>	0.061±0.003	0.077±0.006*	0.075±0.007*

Definition of abbreviations: ALT: Alanine aminotransferase, AST: Aspartate aminotransferase, BILD: Direct bilirubin, BILT: Total bilirubin. C: Control group; CTL-5: 5 mg/kg CTL administered rats for 30 days group; CTL-10: 10 mg/kg CTL administered rats for 30 days group; All data were expressed as mean ± standard deviation; \* Significant differences when compared with control group (p<0.05).

### The liver histology of control and CTL-administered rats

In liver tissue obtained from the control rats, normal structural characteristics of hepatocytes and hepatic sinusoidal cells were observed histologically (Figure 1. A1 – A2).

Similar to control rats, normal hepatic structure was observed in the 5 mg/kg CTL-administered group. However, mild necrosis and disarrangement of hepatic cords were also seen in this group (Figure 1. B1 – B2).

In liver tissue of the 10 mg/kg CTL-administered rats, necrotic areas of hepatic parenchyma were identified and hepatic nuclear asymmetry was observed (Table 2). Additionally, disarrangement of hepatic cords in the portal area was more prominent than in the 5 mg/kg CTL-administered rats (Figure 1. C1 – C2).

### The liver GSH levels of control and CTL-administered rats

The GSH levels of liver tissue did not show any significant difference among the groups (Table 3).

**Table 2. Histopathological scoring of the tissue obtained from control and CTL-administered rats.**

	C	CTL-5	CTL-10
<b>Hepato-cellular necrosis</b>	-	+	+++
<b>Hepatic nuclear asymmetry</b>	-	-	++
<b>Disarrangement of hepatic cords</b>	-	+	++

Definition of abbreviations: C: Control group; CTL-5: 5 mg/kg CTL administered rats for 30 days group; CTL-10: 10 mg/kg CTL administered rats for 30 days group. The severity of various features of hepatic injury was evaluated based on those following scoring schemes: – normal, + mild, ++ moderate, and +++ severe.

**Table 3. The liver GSH levels of control and CTL-administered rats.**

	C	CTL-5	CTL-10
<b>GSH (ug/g Tissue)</b>	23.57±0.48	24.75±1.34	24.09±1.82

Definition of abbreviations: GSH: glutathione; C: Control group; CTL-5: 5 mg/kg CTL administered rats for 30 days group; CTL-10: 10 mg/kg CTL administered rats for 30 days group; All data were expressed as mean ± standard deviation.

## DISCUSSION

The increases of AST, ALT, and total bilirubin levels accompanied by observed morphological abnormalities in liver tissue were evaluated as indicators of hepatotoxicity following CTL administration in rats. According to our study results, independent from other risk factors associated with hepatotoxicity, it is found that CTL administration at repeated pharmacological doses may cause adverse effects in the liver, depending on the dose.

Although *in vitro* cell culture systems and animal studies for predicting drug-induced hepatotoxicity in humans were performed, these preclinical studies may not be sufficient for predicting the potential of hepatotoxicity in humans (Kim & Nam,

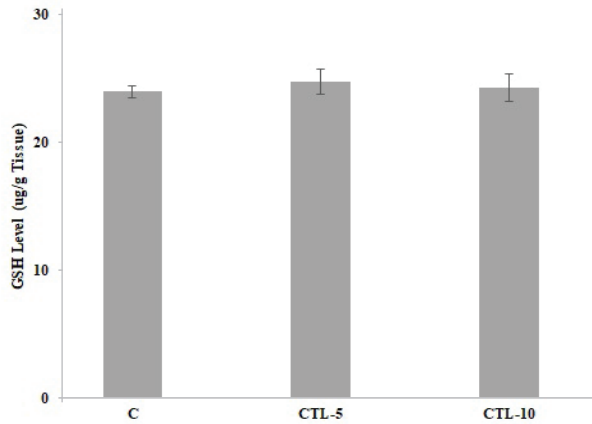
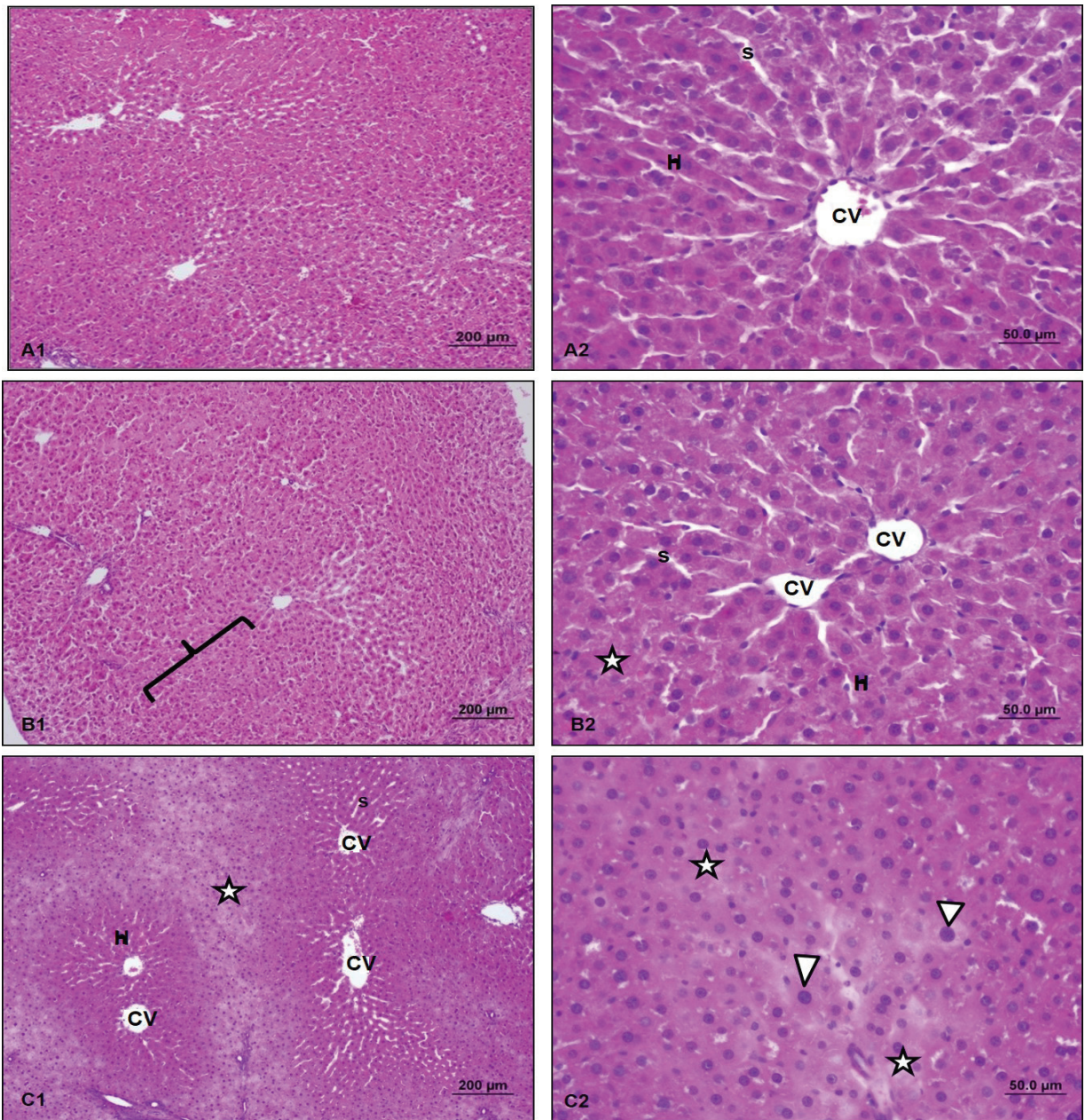


**Figure 1.** The liver histology of rats. **A1-A2:** C group showing normal hepatocytes and sinusoidal structures. (H&E, Scale bars=200 μm, 50 μm). **B1-B2:** CTL-5 group showing almost normal hepatocyte structure along with necrotic areas (⚡) and disarrangement of hepatic cords (⌋). (H&E, Scale bars=200 μm, 50 μm). **C1-C2:** CTL-10 group showing necrotic areas (⚡) and hepatic nuclear asymmetry (s). (H&E, Scale bars=200 μm, 50 μm). C: Control group; CTL-5: 5 mg/kg CTL administered rats for 30 days group; CTL-10: 10 mg/kg CTL administered rats for 30 days group; CV: Central vein; H: Hepatocytes; S: Sinusoids



2017; Babai, Auclert, & Le-Louët, 2018). Drug-induced liver injury (DILI) has been approved as an important reason for the withdrawal of drugs from the market (Chen, Suzuki, Borlak, Andrade, & Lucena, 2015; Alempijevic, Zec, & Milosavljevic, 2017). The risk factors of DILI are classified as host-, environmental-, and drug-related factors (Campion et al., 2013; Ortega-Alonso, Stephens, Lucena, & Andrade, 2016; Alempijevic et al., 2017). Although host-related risk factors are accepted as non-modifiable for DILI, particularly age and gender are the important factors for hepatic injury. Information about environmental risk factors such as coffee and alcohol consumption and dietary intake are limited. High daily dose, high lipophilicity, and extensive hepatic metabolism are specified as the risk factors related to DILI (Raschi & De Ponti, 2015; Alempijevic et al., 2017). While there is a lack of specific biomarkers, traditional liver biomarkers such as AST, ALT, alkaline phosphatase (ALP), and total bilirubin are used for the diagnosis of DILI (Singh, Bhat, & Sharma, 2011; Robles-Díaz, Medina-Caliz, Stephens, Andrade, & Lucena, 2016; Church & Watkins, 2017). However, increased levels of AST, ALT, and ALP following hepatocyte injury are also observed in the extrahepatic conditions (Gowda et al., 2009; Robles-Díaz et al., 2016). ALT is considered to be a more specific enzyme for liver injury than AST and ALP (Singh et al., 2011; Campion et al., 2013; Robles-Díaz et al., 2016). Increased ALT levels accompanied by increased total bilirubin levels are specifically accepted as important biomarkers for diagnosing the hepatocellular injury (Singh et al., 2011; Campion et al., 2013; Gwaltney-Brant, 2016). Additionally, in acute hepatic injury, total bilirubin can be a better indicator of disease severity compared to ALT (Dufour et al., 2000; Singh et al., 2011). In our study, increased AST, ALT, and total bilirubin levels were observed in CTL-administered groups. In addition to the case reports related to CTL-induced liver injury, the results of *in vitro* and *in vivo* studies performed by Ahmadian et al. showed hepatotoxicity findings related to CTL administration, depending on the dose (Ahmadian et al., 2017). While CTL has been expressed as one of the SSRIs with the least hepatotoxic potential in previous studies (Voican et al., 2014; Friedrich et al., 2016). However, our study highlighted the hepatotoxicity potential of CTL with clinical biochemical parameters. At this point, it could be emphasized that histopathological observations are needed to confirm the hepatotoxicity in addition to clinical biochemical parameters. Liver histology serves as an important biomarker for identifying and characterizing liver injury (Singh et al., 2011; Kullak-Ublick et al., 2017). In low dose CTL-administered rats, mild pathological findings were observed, whereas in high dose CTL-administered rats, moderate to severe morphological anomalies in liver tissue were observed. According to these results, we concluded that low-dose CTL administration induced biochemical effects without morphological changes and high-dose CTL administration caused both biochemical and morphological adverse effects in the liver.

The mechanism of CTL-induced liver injury cannot be defined, but it has been specified that cytochrome P450 enzymes-mediated CTL transformation into toxic metabolite may lead to liver injury (Fredricson-Overo & Svendsen, 1978; Ahmadian et al., 2017). At this point, it can be emphasized that GSH is

responsible for detoxification of toxic metabolites. But, in our study, GSH levels of the liver did not change after CTL administration. But, GSH conjugates of CTL were not detected in other studies using human liver-derived *in vitro* systems (Lassila, Mattila, Turpeinen, & Tolonen, 2015; Lassila et al., 2015). Conversely, GSH depletion have been observed in experimental models of liver injury induced with CTL (Ahmadian et al., 2017). So, it can be said that the findings indicating hepatic injury after CTL administration is not reflected by GSH levels according to our results.

## CONCLUSION

In our study which was performed independently of other risk factors, we obtained findings indicating hepatic injury after CTL administration. According to our findings, clinicians should be aware of hepatotoxicity in patients under CTL treatment, and biomarkers related to hepatic injury in patients should be monitored. Particularly, CTL should be cautiously used and the minimum effective dose of CTL should be recommended in elderly patients and in patients with liver failure. Additionally, formation of toxic metabolites is considered as one of the mechanisms of CTL-induced hepatotoxicity. As it is known that the metabolic pathway of CTL includes CYP2C19, CYP3A4 and CYP2D6, dose adjustments in CYP2C19 and CYP2D6 poor metabolizer patients under the CTL treatment could be needed for the drug safety in respect to hepatotoxicity.

**Ethics Committee Approval:** This study was approved by the Local Ethics Committee on Animal Experimentation of Anadolu University, Eskisehir, Turkey (Number: 2013-14)

**Informed Consent:** Written consent was obtained from the participants.

**Peer-review:** Externally peer-reviewed.

**Author Contributions:** Conception/Design of Study- S.I., Ö.A.E.; Data Acquisition- S.I., Ö.A.E., F.D., D.B.D.; Data Analysis/Interpretation- S.I., Ö.A.E, D.B.D.; Drafting Manuscript- S.I., Ö.A.E.; Critical Revision of Manuscript- S.I., Ö.A.E.; Final Approval and Accountability- S.I., F.D., D.B.D., M.B., Ö.A.E.

**Conflict of Interest:** The authors have no conflict of interest to declare.

**Financial Disclosure:** Authors declared no financial support.

## REFERENCES

- Ahmadian, E., Eftekhari, A., Fard, J. K., Babaei, H., Nayebi, A. M., Mohammadnejad, D., & Eghbal, M. A. (2017). *In vitro* and *in vivo* evaluation of the mechanisms of citalopram-induced hepatotoxicity. *Archives of Pharmacological Research*, 40(11), 1296–1313.
- Alempijevic, T., Zec, S., & Milosavljevic, T. (2017). Drug-induced liver injury: Do we know everything? *World Journal of Hepatology*, 9(10), 491–502.
- Anderson, I. M., & Edwards, J. G. (2001). Guidelines for choice of selective serotonin reuptake inhibitor in depressive illness. *Advances in Psychiatric Treatment*, 7, 170–180.
- Babai, S., Auclert, L., & Le-Louët, H. (2018). Safety data and withdrawal of hepatotoxic drugs. *Therapie*. [Epub ahead of print] <https://doi.org/10.1016/j.therap.2018.02.004>

- Bech, P., Tanghøj, P., Andersen, H. F., & Overø, K. (2002). Citalopram dose-response revisited using an alternative psychometric approach to evaluate clinical effects of four fixed citalopram doses compared to placebo in patients with major depression. *Psychopharmacology (Berl)*, 163(1), 20–25.
- Champion, S., Aubrecht, J., Boekelheide, K., Brewster, D. W., Vaidya, V. S., Anderson, L., Burt, D., Dere, E., Hwang, K., Pacheco, S., Saikumar, J., Schomaker, S., Sigman, M., & Goodsaid, F. (2013). The current status of biomarkers for predicting toxicity. *Expert Opinion on Drug Metabolism & Toxicology*, 9(11), 1391–408.
- Chen, M., Suzuki, A., Borlak, J., Andrade, R. J., & Lucena, M. I. (2015). Drug-induced liver injury: Interactions between drug properties and host factors. *Journal of Hepatology*, 63(2), 503–514.
- Church, R. J., & Watkins, P. B. (2017). The transformation in biomarker detection and management of drug-induced liver injury. *Liver International*, 37(11), 1582–1590.
- Dufour, D. R., Lott, J. A., Nolte, F. S., Gretch, D. R., Koff, R. S., & Seeff, L. B. (2000). Diagnosis and monitoring of hepatic injury. II. Recommendations for use of laboratory tests in screening, diagnosis, and monitoring. *Clinical Chemistry*, 46(12), 2050–2068.
- Ferguson, J. M. (2001). SSRI Antidepressant Medications: Adverse Effects and Tolerability. *Primary Care Companion to the Journal of Clinical Psychiatry*, 3(1), 22–27.
- Flores-Serrano, A., Vila-Luna, M., Álvarez-Cervera, F., Heredia-López, F., Góngora-Alfaro, J., & Pineda, J. C. (2013). Clinical doses of citalopram or reboxetine differentially modulate passive and active behaviors of female Wistar rats with high or low immobility time in the forced swimming test. *Pharmacology Biochemistry & Behavior*, 110, 89–97.
- Fredricson-Overo, K., & Svendsen, O. (1978). Hepatotoxicity of citalopram in rats and first-pass metabolism. *Archives of Toxicology*, 1, 177–180.
- Friedrich, M. E., Akimova, E., Huf, W., Konstantinidis, A., Papageorgiou, K., Winkler, D., Toto, S., Greil, W., Grohmann, R., & Kasper, S. (2016). Drug-Induced Liver Injury during Antidepressant Treatment: Results of AMSP, a Drug Surveillance Program. *International Journal of Neuropsychopharmacology*, 19(4).
- Gessel, L., & Alcorn, J. (2016). When Good Medications Go Bad, Don't DILI Dally. *Digestive Diseases and Sciences*, 61(6), 1491–1494.
- Gowda, S., Desai, P. B., Hull, V. V., Math, A. A., Vernekar, S. N., & Kulkarni, S. S. (2009). A review on laboratory liver function tests. *Pan African Medical Journal*, 3, 17.
- Gwaltney-Brant, S. M. (2016). Nutraceuticals in Hepatic Diseases. In R.C. Gupta (Eds.), *Nutraceuticals: Efficacy, Safety and Toxicity* (pp. 7-99). London, UK: Academic Press.
- Herrlin, K., Yasui-Furukori, N., Tybring, G., Widén, J., Gustafsson, L. L., & Bertilsson, L. (2003). Metabolism of citalopram enantiomers in CYP2C19/CYP2D6 phenotyped panel of healthy Swedes. *British Journal of Clinical Pharmacology*, 56(4), 415–421.
- Hunfeld, N. G. M., ten Berge, R. L., LeBrun, P. P. H., Smith, S. J., & Melief, P. H. G. J. (2010). Hepatotoxicity related to citalopram intake: a case report. *International Journal of Risk & Safety in Medicine*, 22, 1–5.
- Institutional Animal Care and Use Committee (IACUC) (2017). Anesthesia (Guideline). Retrieved from <https://animal.research.uiowa.edu/iacuc-guidelines-anesthesia>
- Jaeschke, H., Gores, G.J., Cederbaum, A. I., Hinson, J. A., Pessayre, D., & Lemasters J.J. (2002). Mechanisms of hepatotoxicity. *Toxicological Sciences*, 65(2), 166–176.
- Karlsson, L., Carlsson, B., Hiemke, C., Ahlner, J., Bengtsson, F., Schmitt, U., & Kugelberg, F. C. (2013). Altered brain concentrations of citalopram and escitalopram in P-glycoprotein deficient mice after acute and chronic treatment. *European Neuropsychopharmacology*, 23(11), 1636–1644.
- Kim, E., & Nam, H. (2017). Prediction models for drug-induced hepatotoxicity by using weighted molecular fingerprints. *BMC Bioinformatics*, 18(7), 227.
- Kullak-Ublick, G. A., Andrade, R. J., Merz, M., End, P., Benesic, A., Gerbes, A. L., & Aithal, G. P. (2017). Drug-induced liver injury: recent advances in diagnosis and risk assessment. *Gut*, 66(6), 1154–1164.
- Lassila, T., Mattila, S., Turpeinen, M., & Tolonen, A. (2015). Glutathione trapping of reactive drug metabolites produced by biomimetic metalloporphyrin catalysts. *Rapid Communications in Mass Spectrometry*, 29(6), 521–532.
- Lassila, T., Rousu, T., Mattila, S., Chesné, C., Pelkonen, O., Turpeinen, M., & Tolonen, A. (2015). Formation of GSH-trapped reactive metabolites in human liver microsomes, S9 fraction, HepaRG-cells, and human hepatocytes. *Journal of Pharmaceutical and Biomedical Analysis*, 115, 345–351.
- Locher, C., Koechlin, H., Zion, S. R., Werner, C., Pine, D. S., Kirsch, I., Kessler, R. C., & Kossowsky, J. (2017). Efficacy and Safety of Selective Serotonin Reuptake Inhibitors, Serotonin-Norepinephrine Reuptake Inhibitors, and Placebo for Common Psychiatric Disorders Among Children and Adolescents: A Systematic Review and Meta-analysis. *JAMA Psychiatry*, 74(10), 1011–1020.
- López-Torres, E., Lucena, M. I., Seoane, J., Verge, C., & Andrade, R. J. (2004). Hepatotoxicity related to citalopram (letter). *American Journal of Psychiatry*, 161(5), 923–924.
- Neumann, H., Csepregi, A., Evert, M., & Malfertheiner, P. (2008). Drug-induced liver disease related to citalopram (letter). *Journal of Clinical Psychopharmacology*, 28(2), 254–255.
- Ortega-Alonso, A., Stephens, C., Lucena, M. I., & Andrade, R. J. (2016). Case Characterization, Clinical Features and Risk Factors in Drug-Induced Liver Injury. *International Journal of Molecular Sciences*, 17(5).
- Raschi, E., & De Ponti, F. (2015). Drug- and herb-induced liver injury: Progress, current challenges and emerging signals of post-marketing risk. *World Journal of Hepatology*, 7(13), 1761–1771.
- Robles-Díaz, M., Medina-Caliz, I., Stephens, C., Andrade, R. J., & Lucena, M. I. (2016). Biomarkers in DILI: One More Step Forward. *Frontiers in Pharmacology*, 7, 267.
- Sanchez, C., Reines, E. H., & Montgomery, S. A. (2014). A comparative review of escitalopram, paroxetine, and sertraline: Are they all alike? *International Clinical Psychopharmacology*, 29(4), 185–196.
- Sangkuhl, K., Klein, T. E., & Altman, R. B. (2011). PharmGKB summary: citalopram pharmacokinetics pathway. *Pharmacogenetics and Genomics*, 21(11), 769–772.
- Sekar, S., Verhoye, M., Van Audekerke, J., Vanhoutte, G., Lowe, A. S., Blamire, A. M., Steckler, T., Van der Linden, A., & Shoab, M. (2011). Neuroadaptive responses to citalopram in rats using pharmacological magnetic resonance imaging. *Psychopharmacology*, 213(2-3), 521–531.
- Sharbaf-Shoar, N., & Padhy, R. K. (Updated 20 January 2020). Citalopram. In: StatPearls [Internet]. Retrieved from <https://www.ncbi.nlm.nih.gov/books/NBK482222/>
- Singh, A., Bhat, T. K., & Sharma, O. P. (2011). Clinical Biochemistry of Hepatotoxicity. *Journal of Clinical Toxicology*, S:4.
- Solomons, K., Gooch, S., & Wong, A. (2005). Toxicity with selective serotonin reuptake inhibitors (letter). *American Journal of Psychiatry*, 162(6), 1225.
- Sturgill, M. G., & Lambert, G. H. (1997). Xenobiotic-induced hepatotoxicity: mechanisms of liver injury and methods of monitoring hepatic function. *Clinical Chemistry*, 43(8 Pt 2), 1512–1526.
- The National Institute for Health and Care Excellence (NICE) Pathways. (Updated 1 January, 2019). Depression in children and young people: identification and management. Retrieved from <https://www.nice.org.uk/guidance/ng134/documents/draft-guideline>

- The National Institute for Health and Care Excellence (NICE) Pathways. (Updated 10 September, 2020). Antidepressant treatment in adults. Retrieved from <https://pathways.nice.org.uk/pathways/depression/antidepressant-treatment-in-adults>
- U.S. Department of Health and Human Services Food and Drug Administration Center for Drug Evaluation and Research (CDER). (July 2005). Estimating the Maximum Safe Starting Dose in Initial Clinical Trials for Therapeutics in Adult Healthy Volunteers. Retrieved from <https://www.fda.gov/regulatory-information/search-fda-guidance-documents/estimating-maximum-safe-starting-dose-initial-clinical-trials-therapeutics-adult-healthy-volunteers>
- Vega-Rivera, N. M., Gallardo-Tenorio, A., Fernández-Guasti, A., & Estrada-Camarena, E. (2016). The Post-Ovariectomy Interval Affects the Antidepressant-Like Action of Citalopram Combined with Ethynyl-Estradiol in the Forced Swim Test in Middle Aged Rats. *Pharmaceuticals (Basel)*, 9(2).
- Vermoesen, K., Massie, A., Smolders, I., & Clinckers, R. (2012). The antidepressants citalopram and reboxetine reduce seizure frequency in rats with chronic epilepsy. *Epilepsia*, 53(5), 870–878.
- Voican, C. S., Corruble, E., Naveau, S., & Perlemuter, G. (2014). Antidepressant-induced liver injury: a review for clinicians. *American Journal of Psychiatry*, 171(4), 404–415.
- Whittington, C. J., Kendall, T., Fonagy, P., Cottrell, D., Cotgrove, A., & Boddington, E. (2004). Selective serotonin reuptake inhibitors in childhood depression: systematic review of published versus unpublished data. *Lancet*, 363(9418), 1341–1345.
- Wiese, B. (2011). Geriatric Depression: The Use of Antidepressants in The Elderly. *British Columbia Medical Journal*, 53(47), 341–347.
- Zhang, J., Dennis, K. A., Darling, R. D., Alzghoul, L., Paul, I. A., Simpson, K. L., & Lin, R. C. (2013). Neonatal citalopram exposure decreases serotonergic fiber density in the olfactory bulb of male but not female adult rats. *Frontiers in Cellular Neuroscience*, 7, 67.

# Liquid chromatographic determination of citrinin residues in various meat products: A pioneer survey in Turkey

Fatih Mehmet Sari<sup>1</sup> , Ezgi Öztaş<sup>1</sup> , Sibel Özden<sup>1</sup> , Gül Özhan<sup>1</sup> 

<sup>1</sup>Istanbul University, Faculty of Pharmacy, Department of Pharmaceutical Toxicology, Istanbul, Turkey

**ORCID IDs of the authors:** F.M.S. 0000-0002-8552-4676; E.Ö. 0000-0002-0718-2359; S.Ö. 0000-0002-1662-2504; G.Ö. 0000-0002-6926-5723

**Cite this article as:** Sari, F. M., Oztas, S., Ozden, S., & Ozhan G. (2020). Liquid chromatographic determination of citrinin residues in various meat products: A pioneer survey in Turkey. (Fabaceae). *Istanbul Journal of Pharmacy*, 50 (3), 195-201.

## ABSTRACT

**Background and Aims:** Occurrence of the mycotoxin citrinin could increase during *Monascus purpureus* fermentation in red yeast rice resulting in contamination of meat products when the red yeast rice is used as food additive. The aim of this study was to investigate extraction of citrinin from meat products by different extraction methods including LLE, QuEChERS and IAC methods.

**Methods:** Because of high sensitivity IAC method was selected for the extraction of citrinin in 33 meat products (salami, sausage and minced meat), then citrinin was analysed by HPLC- FLD.

**Results:** IAC method was linear in the range of 0.25-100 ng/g ( $r^2 \geq 0.999$ ) in meat products. Citrinin was found at 0.28 to 1.79 ng/g in 6 of the 19 samples (36.84%); and in one sausage sample contained citrinin at LOD level. However, citrinin was not detected in the salami and minced meat samples.

**Conclusion:** Our results indicated that citrinin in meat products could be an important health concern. Since no limits were set in food products, regulations should be developed concerning the presence of citrinin in other products as well as meat products, in Turkey.

**Keywords:** Citrinin, HPLC-FLD, Meat products

## INTRODUCTION

Mycotoxins are secondary metabolites produced by fungi due to inappropriate temperature and humidity conditions during poor cultivation and storage conditions. Until now, about 400 mycotoxins, mainly produced by *Aspergillus*, *Penicillium*, *Fusarium*, *Alternaria*, *Cladosporium* and *Rhizopus* species, have been identified (Pohland, 1993; Moss, 2002; Pal, Gizaw, Abera, Shukla, & Hazarika, 2015). Since mycotoxins cause serious harmful effects on human health and the environment, the detection of mycotoxin residues has emerged in various raw and processed food products. Even if the studies have especially focused on aflatoxins, the interest in mycotoxins including ochratoxin A, patulin, citrinin and zearalenone has increased considerably. Also, mycotoxins can cause industrial and financial losses due to color change and unwanted odor in food products (Rawat, 2015). To minimize mycotoxin-mediated diseases, it is necessary to set the maximum values and the regulations on the mycotoxin content of food products.

### Address for Correspondence:

Gül ÖZHAN, e-mail: gulozhan@istanbul.edu.tr

This work is licensed under a Creative Commons Attribution 4.0 International License.



Submitted: 11.04.2020  
Revision Requested: 03.06.2020  
Last Revision Received: 09.06.2020  
Accepted: 06.08.2020



Citrinin, a pyran derivative, is predominantly produced by *Penicillium*, *Aspergillus* and *Monascus* species, and most commonly found in corn, rice, wheat, rye, barley, peanut, bread, fruits, oil-seeds (Shu & Lin, 2002; Chia-Hao, Feng-Yili, Li-Ting, Yi-Shen, & Bing-Hui, 2009). Because of the positive effects of the traditional Chinese food, red yeast rice on the digestive system and blood circulation, it is considered a valuable dietary supplement worldwide (Li, Xu, Li, Chen, & Ji, 2012; Srianta et al., 2014; Woo et al., 2014). Additionally, red yeast rice is widely used as a preservative, flavoring and food colorant, especially, in meat, fish and soybean products (Ma et al., 2000). Occurrence of citrinin could increase during *Monascus purpureus* fermentation in red yeast rice. Therefore, food processing for increasing the yield and attractiveness of the product is an important source of citrinin exposure as well as natural occurrence during agriculture.

The major adverse effects of citrinin on human health are nephrotoxicity and neurotoxicity, which can result in life-threatening consequences (Xu, Jia, Gu, & Sung, 2006). Moreover, citrinin usually occurs simultaneously with ochratoxin A, which have both hepatotoxic, immunotoxic, embryotoxic/teratogenic and carcinogenic effects, synergistically (Speijers & Speijers, 2014; Gupta, Srivastava, & Lall, 2018). Citrinin caused lipid peroxidation, mitochondrial respiratory dysfunction, and inhibition of several antioxidant enzymes, and induced micronuclei formation, aneuploidy, and chromosomal abnormalities; while it did not lead to DNA strand breaks, it did lead to oxidative DNA damage and sister chromatid exchange (EFSA, 2012).

It is well established that mycotoxin-contaminated food/feed could have substantial impacts on the economy, human health and environment. It has to be mentioned that the contamination of several foods with citrinin has been observed all over the world. Citrinin has been detected in many stored and dry foods such as cereal (Molinié, Faucet, Castegnaro, & Pfohl-Leszkowicz, 2005; Polinska et al., 2010; EFSA, 2012), cereal-based foods (Vrabcheva, Usleber, Dietrich, & Märtlbauer, 2000; Duarte, Pena, & Lino, 2010; Zaid, Zouaoui, Bacha, & Abid, 2012; EFSA, 2012), fruit juices, medical plants, nuts (EFSA, 2012), olives and olive oil (El Adlouni, Tozlovanu, Naman, Faid, & Pfohl-Leszkowicz, 2006; Tokusoglu & Bozoglu, 2010; EFSA, 2012), tomatoes (Tölgysli, Stroka, Tamosiunas, & Zwickel, 2015); cheese (Franco et al., 1996; EFSA, 2012), corn (Jackson, & Ciegler, 1978; Janardhana, Raveesha, & Shetty, 1999; Warth et al., 2012), beans (Petkova-Bocharova Castegnaro, Michelon, & Maru, 1991; EFSA, 2012), flour (Nishijima, 1984; Dick, Baumann, & Zimmerli, 1988), several spices (Saxena & Mehrotra, 1989; El-Kady, El-Maraghy, & Mostafa, 1995), soy (Kononenko & Burkin, 2008), rice (Hackbart, Pritetto, Primel, Garda-Buffer, & Badiale-Furlong, 2012; Nguyen, Tozlovanu, Tran, & Pfohl-Leszkowicz, 2007), red mold rice (Li, Xu, Li, Chen, & Ji, 2005; Li, Zhou, Yang, & Ou-Yang, 2012; Childress, Gay, Zargar, & Ito, 2013; Ostry, Malir, & Ruprich, 2013; Liao, Chen, Lin, Chiueh, & Shih, 2014; Ji et al., 2015), fermented meat products (Markov et al., 2013) and feed (Talmaciu Sandu, & Banu, 2008).

There is a regulation for citrinin regarding the maximum levels in food supplements based on *Monascus purpureus* fermented rice within the European Commission Regulation (EC) 212/2014 (EU, 212/2014); however, there is no regulation in Turkey. Hence,

there seems to be an urgent need to detect citrinin residues and set maximum limits. EC regulation has set the limit of 2 ng/g for citrinin in only red yeast rice (EU, 212/2014). Therefore, we aimed to detect citrinin residues in various meat products. For this purpose, three different extraction methods were used; LLE (Liquid-Liquid Extraction), QuEChERS (Quick, Easy, Cheap, Effective, Robust and Safe) multi-residue and IAC (Immuno-Affinity Column) for the extraction of citrinin in salami, sausage, and minced meat samples. Because of its high sensitivity, the IAC method was selected for the extraction of citrinin in meat products. Then, the samples were analysed by high-performance liquid chromatography (HPLC)-fluorescence detection (FLD). The study will contribute to further investigations regarding the residue levels for citrinin in food products and the results could be considered by the regulatory affairs for the risk assessment process for citrinin.

## MATERIALS AND METHODS

### Chemicals

Citrinin was obtained from Sigma-Aldrich (Bellefonte, PA, USA, Cat. No: C1017) at the purity of  $\geq 98\%$ . A standard stock solution was prepared at a concentration of 50  $\mu\text{g}/\text{mL}$  in methanol, and kept at 4 °C. Then, the HPLC standard solutions were prepared by serial dilutions at the concentration range of 0.25-100 ng/mL in the mobile phase. The mobile phase was freshly prepared by mixing water:acetonitrile: 2-propanol (65:30:5, v:v:v), and pH was adjusted to 2.95 with ortho-phosphoric acid. HPLC-grade methanol, acetonitrile, and other analytical grade reagents were purchased from Riedel-de Haën (Seelze, Germany) and Merck (Darmstadt, Germany).

### Samples

A total of 33 meat products, including 19 branded sausages, 7 branded salami and 5 branded minced meat samples and 2 unlicensed open ground meat samples made from beef, lamb and turkey, was purchased from various supermarkets, delicatessens and butchers in Istanbul, Turkey during 2016-2018. Samples were collected as a minimum 1 kg in weight and immediately brought to the laboratory. After homogenization with IKA Ultra-Turrax disperser homogenizer (Bender&Hobein GMBH, Maaßstr, Germany) at high speed, 10 g of each sample was aliquoted and stored in a polyethylene bag and kept at  $-20^{\circ}\text{C}$  until the day of analysis was conducted.

### Extraction of Citrinin

#### LLE (Liquid-liquid extraction)

Briefly, 1 g of the sample was extracted with 5 mL methanol:water (80:20, v:v) using the disperser homogenizer for 5 min. After centrifuging at 4000 rpm for 15 min, the sample extract was filtered through 0.45  $\mu\text{m}$  nylon syringe filter. Then, 100  $\mu\text{L}$  of the aliquot was injected into high-performance liquid chromatography HPLC-FLD.

#### 2.3.2. QuEChERS (Quick, Easy, Cheap, Effective, Robust and Safe) multi-residue

The QuEChERS multi-residue kit was obtained from Restek Corp. (Bellefonte, PA, USA, Cat. No: 26221), and the extraction was done by manufacturer's instructions. Briefly, 1 g of the sample was extracted with 10 mL methanol with 0.1% acetic

acid:water (80:20, v:v) using the disperser homogenizer for 1 min. The homogenized sample was added into the magnesium sulfate:sodium acetate (4:1) cleaning solution, shaken for 1 min, then centrifuged at 4000 rpm for 5 min. The supernatant was added into the magnesium sulfate:primary secondary amine (3:1, v:v) mixture, and shaken for 5 min, then centrifuged at 4000 rpm for 5 min. 10 mL of the supernatant was filtered through a 0.45 µm nylon syringe filter, and 40 µL of the aliquot was injected into HPLC-FLD.

#### IAC (Immuno-affinity column)

CitriTest™ immunoaffinity columns were purchased from VITCAM (Watertown, MA, USA), and the extraction was done according to manufacturer's instructions. Briefly, 1 g of the sample was extracted with 20 mL of methanol:water (70:30, v:v) on a shaker at 65 °C for 15 min. The supernatant was filtered through a black ribbon filter paper (Whatman, Sigma-Aldrich, Munich, Germany); and then, 1 mL of the filtrate was filtered through a 0.45 µm nylon syringe filter. The second filtrate was completed into the final volume of 40 mL with phosphate buffer, and mixed well. Ten mL of filtrate (=0.04 g sample equivalent) was passed through a CitriTest™ immunoaffinity column attached to a vacuum manifold (VacElut 20 Manifold, Agilent Biotechnologies, Santa Clara, CA, USA) at a flow rate of 1 drop/second until air came through the column. The column was washed with 10 mL of 0.1% tween20 / phosphate-buffered saline and 10 mL of water, then dried under a vacuum. Citrinin was eluted with 1 mL of methanol:10 mM phosphoric acid (70:30, v:v) into a glass syringe barrel at a rate of slower than 1 drop/second. For HPLC-FLD analysis, 40 µL of the aliquot was injected.

#### HPLC-FLD conditions

The chromatographic analysis was conducted using an LC-20A Shimadzu (Kyoto, Japan) high-performance liquid chromatographic system coupled to an RF-10A XL fluorescence detector. The chromatographic separation was performed using a reversed-phase Phenomenex HPLC column (C<sub>18</sub>, 250 mm x 4.6 mm, 5 µm, 100 A, Phenomenex, Torrance, CA, USA) with a mobile phase of acetonitrile:water:2-propanol (30:65:5, v/v/v, pH 2.95) at a flow rate of 1 mL min<sup>-1</sup>. The column temperature was kept at 25 °C. The fluorescence detection condition was at 330 nm for excitation and 500 nm for emission in the citrinin analysis. The retention time was about 11.5-12.5 min.

#### Method validation

The linearity of the method was assessed using the calibration curve, established with nine levels of citrinin in the final concentrations of 0.25, 0.5, 1, 2.5, 5, 10, 25, 50 and 100 ng/g in the meat samples. The method selectivity was validated by analysing the extracts of citrinin-free blank and the same spiked samples at 5 ng/g citrinin. The recovery experiments were performed on citrinin-free meat samples by spiking with the citrinin standard solutions to obtain the final concentrations of 1-100 ng/g for LLE, 2.5-100 ng/g for QuEChERS, and 0.25-100 ng/g for IAC. For the linearity and recovery studies, the four experiments were repeated, and each injected three times.

The method precision for the intra-day assay was assessed by analysing four independent spiked samples at five concentrations (0.25-100 ng/g) in three-replicated injections on the same day. The inter-day analysis was performed by analysing spiked samples at five concentrations (0.25-100 ng/g) in three-replicated injections on four consecutive days. The relative standard deviation of replicate results (RSD<sub>r</sub>) was used to evaluate intra- and inter-day precision. The method sensitivity was assessed by using the limit of detection (LOD; signal-to-noise ratio= 3) and the limit of quantification (LOQ; signal-to-noise ratio= 10) for citrinin. The method stability was determined with 5 ng/g citrinin-spiked samples at 25°C, 4°C and -20°C on the analysis day of 1, 3 and 10.

## RESULTS AND DISCUSSION

#### Method performance

No interfering peak was observed at the retention time of citrinin in the meat products after LLE, QuEChERS multi-residue and IAC methods. The calibration curve was linear at 0.25-100 ng/g in the meat products with a correlation coefficient  $r^2 > 0.9975$  (Table 1). The LOD levels were calculated to be 0.17-0.33 ng/g for LLE, 0.33 -1.67ng/g for QuEChERS multi-residue and 0.083 ng/g for IAC; and the LOQ levels were 1 ng/g for LLE, 2.5 ng/g for QuEChERS multi-residue and 0.25 ng/g for IAC.

The mean recoveries from the meat products were 64.71-87.58% for LLE (at 1-100 ng/g), 62.74-78.54% for QuEChERS multi-residue (at 2.5-100 ng/g), and 87.26-95.02% for IAC (at 0.25-100 ng/g) with a relative standard deviation (RSD<sub>r</sub>) less than 7.13% (Table 2). The inter-day repeatability recoveries

**Table 1. Linearity of citrinin in the meat products.**

		Range (ng/g)	Calibration equation	r <sup>2</sup>	LOD (ng/g)
LLE	<i>Salami</i>	1-100	$y = 5.7094x + 0.2787$	0.9997	0.167
	<i>Sausage</i>	1-100	$y = 6.1928x + 1.0844$	0.9997	0.330
	<i>Mince meat</i>	1-100	$y = 6.445x + 2.4693$	0.9986	0.167
QuEChERS multi-residue	<i>Salami</i>	2.5-100	$y = 5.3166x + 0.281$	0.9996	1.670
	<i>Sausage</i>	2.5-100	$y = 6.4089x + 5.3636$	0.9987	0.830
	<i>Mince meat</i>	2.5-100	$y = 5.0567x + 3.231$	0.9975	0.330
IAC	<i>Salami</i>	0.25-100	$y = 7.1135x + 4.4583$	0.9995	0.083
	<i>Sausage</i>	0.25-100	$y = 6.9218x + 3.729$	0.9990	0.083
	<i>Mince meat</i>	0.25-100	$y = 7.206x + 1.928$	0.9990	0.083

were mean  $\geq 62.40\%$ ,  $\geq 61.60\%$ , and  $\geq 86.60\%$ , and the intra-day repeatability recoveries were mean  $\geq 66.50\%$ ,  $\geq 64.30\%$ , and  $\geq 87.20\%$  for LLE (at 1-100 ng/g), QuEChERS multi-residue (at 2.5-100 ng/g), and IAC (at 0.25-100 ng/g), respectively (Table 3). EC Regulation No 519/2014 stated that for all levels of citrinin recoveries are acceptable in the range of 70-120% and the RSDr should be  $<22\%$  (EU, 519/2014). According to our study, we observed good precision using the IAC method; hence, we performed the IAC method for analysing the meat samples.

For the method stability studies, 5 ng/g citrinin-spiked samples were analysed at 25 °C, 4 °C and -20 °C. No change in recovery was observed after 1-3 days whereas the recovery decreased to  $12 \pm 3.4\%$  after 10 days.

Consistent with our results, Markov et al. (2013) showed that the citrinin recovery was 93.5% with a good precision of RSD 9.39% in the meat products after IAC-extraction following HPLC-FLD determination. They also observed the LOD level as 0.5 ng/g, the LOQ level as 1 ng/g (Markov et al., 2013). There are limited studies the reporting the presence of citrinin in meat products. Marley et al. (Marley, Brown, Leeman, & Donnelly, 2016) showed that LOQ for citrinin in red yeast rice was 10 ng/g, with an LOD of 3 ng/g and recoveries ranged from 80 to 110% after IAC cleanup and HPLC-FLD. In a study from Jiménez-López et al. (Jiménez-López, Llorent-Martínez, Ortega-Barrales, & Ruiz-Medina, 2014), developed a fluorometric flow-through optosensor using Sephadex SPC-25 as solid support for citrinin analysis in dietary supplements containing red yeast rice and

obtained an LOD value of 10.5 ng/mL with RSDs lower than 3%. Application of fluorescent immunochromatographic test strips to detect citrinin in *Monascus* fermented food demonstrated high recoveries (86.8–113.0%) and low RSDs (1.8–15.3%) (Chen, Xu, Ma, Cui, Sun, & Zhang, 2019). In red fermented rice samples, the limit of detection was obtained as 1.0 ng/g for LC-MS/MS and 250 ng/g for HPLC-FLD (Ji et al., 2015).

Data obtained in the present study indicated that the IAC extraction method was the most effective method for citrinin extraction from the meat products and had good precision. Therefore, citrinin residue analysis in various meat products was conducted with IAC method, then analysed using HPLC-FLD.

### Citrinin in meat products

The citrinin residue analysis was conducted for over a decade, and the surveys are still in progress worldwide. The physical conditions, such as climate change, affect the mycotoxin levels in food products and lead to concerns about food safety (Paterson & Lima, 2010; Tirado, Clarke, Jaykus, McQuatters-Gollop, & Frank, 2010); thus, annual monitoring all over the world is crucial to detect the residue levels and limit the possible health risks. Red yeast rice is widely used as a preservative and food colorant, especially, in meat products. American and European countries restrict the use of red yeast rice, but it has been still very common in Asian cuisine. *Monascus purpureus* fermented red yeast rice could be contaminated by citrinin, then, citrinin can be found in food products such as meat products which contain red yeast rice as a food colorant (EFSA, 2012).

**Table 2. The recoveries from different meat products for LLE, QuEChERS multi-residue and IAC methods (n=4).**

	LLE			QuEChERS multi-residue			IAC		
	Spiking level (ng/g)	Mean recovery (%) $\pm$ SD	RSDr (%)	Spiking level (ng/g)	Mean recovery (%) $\pm$ SD	RSDr (%)	Spiking level (ng/g)	Mean recovery (%) $\pm$ SD	RSDr (%)
<b>Salami</b>	1	66.07 $\pm$ 0.04	5.63	2.5 5 10 25	66.06 $\pm$ 0.12	7.13 4.94 3.27 3.91	0.25	91.98 $\pm$ 0.01	2.56
	2.5	72.65 $\pm$ 0.07	6.86		0.5		91.51 $\pm$ 0.02	3.25	
	5	79.01 $\pm$ 0.08	1.96		1		94.45 $\pm$ 0.03	1.92	
	10	86.34 $\pm$ 0.39	3.52		2.5		92.55 $\pm$ 0.11	4.17	
	25	86.93 $\pm$ 0.67	1.84		5		92.62 $\pm$ 0.06	2.73	
<b>Sausage</b>	1	64.71 $\pm$ 0.03	4.27	2.5 5 10 25	62.74 $\pm$ 0.10	6.57 4.78 3.36 3.97	0.25	89.06 $\pm$ 0.02	5.22
	2.5	69.50 $\pm$ 0.06	3.29		0.5		88.77 $\pm$ 0.01	2.24	
	5	77.96 $\pm$ 0.15	3.78		1		85.62 $\pm$ 0.06	5.56	
	10	75.91 $\pm$ 0.40	2.01		2.5		90.41 $\pm$ 0.03	2.18	
	25	83.84 $\pm$ 0.71	4.57		5		88.96 $\pm$ 0.17	3.47	
<b>Mince</b>	1	75.10 $\pm$ 0.04	5.21	2.5 5 10 25	66.12 $\pm$ 0.10	6.14 6.48 2.48 5.40	0.25	90.41 $\pm$ 0.01	3.91
	2.5	76.41 $\pm$ 0.11	5.77		0.5		92.18 $\pm$ 0.01	2.73	
	5	83.56 $\pm$ 0.38	4.24		1		90.66 $\pm$ 0.03	2.24	
	10	85.04 $\pm$ 0.35	2.29		2.5		89.63 $\pm$ 0.11	2.86	
	25	87.58 $\pm$ 0.76	3.49		5		87.26 $\pm$ 0.07	1.93	
							10	90.38 $\pm$ 0.15	1.73
							25	91.46 $\pm$ 0.46	1.35

SD: standard deviation; RSDr: Relative standard deviation of replicate results.

**Table 3. Inter- and intra-day repeatability of the method for different meat products for LLE, QuEChERS and IAC methods (n=4).**

		Inter-day Repeatability														
		LLE					QuEChERS multi-residue					IAC				
	Spiked (ng/g)	Found (mean)	Mean recovery (%) ±SD	RSDr (%)	Spiked (ng/g)	Found (mean)	Mean recovery (%) ±SD	RSDr (%)	Spiked (ng/g)	Found (mean)	Mean recovery (%) ±SD	RSDr (%)	Spiked (ng/g)	Found (mean)	Mean recovery (%) ±SD	RSDr (%)
<i>Salami</i>	1	0.656	65.60±0.03	4.73	2.5	1.69	67.60±0.13	7.74	0.5	0.47	94.2±0.02	4.09	0.5	0.47	94.2±0.02	4.09
	5	3.951	79.02±0.07	1.87	5	3.54	70.80±0.23	6.61	2.5	2.35	94.1±0.08	3.12	2.5	2.35	94.1±0.08	3.12
	10	84.98	84.98±0.35	4.07	10	6.98	69.80±0.33	4.76	5	4.70	94.3±0.11	2.34	5	4.70	94.3±0.11	2.34
	25	22.03	88.12±0.31	1.39	25	19.45	77.80±0.87	4.45	10	9.53	95.3±0.15	1.62	10	9.53	95.3±0.15	1.62
<i>Sausage</i>	1	0.624	62.40±0.01	1.76	2.5	1.54	61.60±0.08	5.21	0.5	0.45	90.2±0.01	1.77	0.5	0.45	90.2±0.01	1.77
	5	3.876	77.52±0.20	5.03	5	3.22	64.40±0.11	3.51	2.5	2.29	91.6±0.03	1.65	2.5	2.29	91.6±0.03	1.65
	10	7.807	78.07±0.29	4.13	10	7.23	72.30±0.22	3.04	5	4.43	88.6±0.16	4.55	5	4.43	88.6±0.16	4.55
	25	21.29	85.16±1.11	5.23	25	20.28	81.12±0.71	3.51	10	8.84	88.4±0.22	2.39	10	8.84	88.4±0.22	2.39
<i>Mince meat</i>	1	0.747	74.70±0.04	4.69	2.5	1.62	64.80±0.14	8.75	0.5	0.46	92.2±0.01	3.15	0.5	0.46	92.2±0.01	3.15
	5	4.18	83.60±0.23	5.54	5	3.09	61.70±0.13	4.04	2.5	2.26	90.4±0.10	1.43	2.5	2.26	90.4±0.10	1.43
	10	8.75	87.50±0.19	2.21	10	7.14	71.40±0.21	2.94	5	4.33	86.6±0.08	2.25	5	4.33	86.6±0.08	2.25
	25	22.51	90.04±0.57	2.55	25	18.18	72.71±1.05	5.78	10	8.99	89.9±0.10	1.13	10	8.99	89.9±0.10	1.13
		Intra-day Repeatability														
		LLE					QuEChERS multi-residue					IAC				
	Spiked (ng/g)	Found (mean)	Mean recovery (%) ±SD	RSDr (%)	Spiked (ng/g)	Found (mean)	Mean recovery (%) ±SD	RSDr (%)	Spiked (ng/g)	Found (mean)	Mean recovery (%) ±SD	RSDr (%)	Spiked (ng/g)	Found (mean)	Mean recovery (%) ±SD	RSDr (%)
<i>Salami</i>	1	0.665	66.5±0.04	6.52	2.5	1.61	64.4±0.11	6.52	0.5	0.44	88.2±0.01	2.41	0.5	0.44	88.2±0.01	2.41
	5	3.952	79.1±0.08	2.04	5	3.27	65.4±0.07	3.26	2.5	2.28	91.2±0.10	5.22	2.5	2.28	91.2±0.10	5.22
	10	8.54	85.4±0.38	4.43	10	6.78	67.8±0.42	1.77	5	4.56	91.3±0.14	3.11	5	4.56	91.3±0.14	3.11
	25	21.44	85.8±0.49	2.29	25	18.78	75.1±0.63	3.35	10	9.46	94.6±0.18	1.94	10	9.46	94.6±0.18	1.94
<i>Sausage</i>	1	0.673	67.3±0.05	6.77	2.5	1.64	64.3±0.13	7.94	0.5	0.44	88.0±0.01	2.71	0.5	0.44	88.0±0.01	2.71
	5	3.919	78.4±0.10	2.52	5	3.38	67.6±0.26	3.67	2.5	2.24	89.6±0.06	2.72	2.5	2.24	89.6±0.06	2.72
	10	7.374	73.7±0.50	6.83	10	7.19	71.9±0.27	3.39	5	4.48	89.6±0.11	2.38	5	4.48	89.6±0.11	2.38
	25	21.12	84.5±0.89	4.23	25	19.01	76.1±0.84	4.43	10	9.04	90.4±0.09	0.92	10	9.04	90.4±0.09	0.92
<i>Mince meat</i>	1	0.754	75.4±0.04	5.73	2.5	1.75	70.0±0.06	3.52	0.5	0.45	90.0±0.02	4.30	0.5	0.45	90.0±0.02	4.30
	5	4.17	83.4±0.12	2.93	5	3.43	68.6±0.31	8.93	2.5	2.19	87.6±0.15	6.80	2.5	2.19	87.6±0.15	6.80
	10	8.22	82.2±0.20	2.36	10	7.25	72.5±0.15	2.01	5	4.36	87.2±0.08	1.76	5	4.36	87.2±0.08	1.76
	25	21.27	85.1±0.94	4.43	25	18.20	72.8±0.91	5.01	10	9.08	90.8±0.21	2.33	10	9.08	90.8±0.21	2.33

SD: standard deviation, RSDr: Relative standard deviation of replicate results.

**Table 4. Citrinin occurrence in total of 32 meat products as determined by IAC-HPLC-FLD.**

	No. of samples	Positive (%)	LOD-LOQ (%)	Range (ng/g)	Mean $\pm$ SD
<i>Salami</i>	7	-	-	-	-
<i>Sausage</i>	19	6 (36.84)	1 (5.26)	0.28-1.79	0.867 $\pm$ 0.54
<i>Mince meat</i>	7	-	-	-	-
<b>Total</b>	33	7 (21.87)	1 (3.12)	0.083-1.79	0.867 $\pm$ 0.54

The analytical results in a total of 33 meat products (31 branded and 2 unlicensed), collected randomly from supermarkets, delicatessens and butchers in Istanbul, were shown in Table 4. Only, 6 out of the 19 (36.84%) sausage samples contained citrinin at the concentration range of 0.28-1.79 ng/g and in one sample citrinin level was found at LOD level (0.083 ng/g), whereas citrinin was not detected in seven of salami and six of mince samples. Markov et al. (2013) analysed fermented meat products (n=90) by IAC-HPLC-FLD and reported that 5.55% of the products were contaminated with citrinin at the level of LOQ (1 ng/g). There is a lack of data on citrinin levels in meat products. Therefore, when we considered the studies in red yeast rice products, Marley et al. (2016) showed that five of the nine samples containing citrinin levels exceeded the EU limit in food supplements based on rice fermented with the red yeast *M. purpureus* obtained from different parts of China. Accordingly, survey results from Taiwan showed that mean levels of citrinin contamination were 13.3, and 0.1  $\mu$ g/g for red yeast rice (raw material), and red yeast rice processed products, respectively (Liao et al., 2014). Ji et al. (2015) observed that citrinin was found in the range of 0.14-44.24  $\mu$ g/g in 10 of 12 commercial red fermented rice products.

In 2014, the citrinin concentration in red yeast rice was set at a limit of 2 ng/g by European Commission Regulation (EC) 212/2014 (EU, 212/2014). No limit was set for the other food products. Indeed, in Turkey, no limit was set even for red yeast rice regarding the citrinin residues in food products. According to our results, three of six citrinin positive meat samples contained citrinin levels of more than 1 ng/g which is 50% of the maximum limit for red yeast rice in the EU. Regarding the high consumption of fermented meat products containing red yeast rice which is the source of citrinin, the need for continuous monitoring of meat products, particularly, unbranded and produced in uncontrolled facilities is urged. Therefore, the citrinin levels of meat products as well as in other food products especially in red yeast rice products should be carefully considered. Furthermore, there is a need to set the limit of citrinin in various food products in the EU and Turkey.

**Peer-review:** Externally peer-reviewed.

**Author Contributions:** Conception/Design of Study- G.Ö., F.M.S., S.Ö.; Data Acquisition- G.Ö., F.M.S.; Data Analysis/Interpretation- G.Ö., F.M.S., S.Ö.; Drafting Manuscript- G.Ö., S.Ö., E.Ö.; Critical Revision of Manuscript- G.Ö., S.Ö., E.Ö.; Final Approval and Accountability- F.M.S., E.Ö., S.Ö., G.Ö.; Technical or Material Support- G.Ö.; Supervision- G.Ö., S.Ö.

**Conflict of Interest:** The authors have no conflict of interest to declare.

**Financial Disclosure:** This study was supported by the Research Fund of Istanbul University (Project No: 47083).

## REFERENCES

- Chen, E., Xu, Y., Ma, B., Cui, H., Sun, C., & Zhang, M. (2019). Carboxyl-Functionalized, Europium Nanoparticle-Based Fluorescent Immunochromatographic Assay for Sensitive Detection of Citrinin in *Monascus Fermented Food*. *Toxins*, 11(10), 605.
- Chia-Hao, C., Feng-Yili, Y., Li-Ting, W., Yi-Shen, L., & Biing-Hui, L. (2009). Activation of ERK and JNK signaling pathways by mycotoxin citrinin in humans cells. *Toxicology and Applied Pharmacology*, 237, 281–287.
- Childress, L., Gay, A., Zargar, A., & Ito, M. K. (2013). Review of red yeast rice content and current Food and Drug Administration oversight. *Journal of Clinical Lipidology*, 7(2), 117–122.
- Dick, R., Baumann, U., & Zimmerli, B. (1988). Occurrence of citrinin in cereal grains. *Mitteilungen aus dem Gebiete der Lebensmitteluntersuchung und Hygiene*, 79, 159–164.
- Duarte, S. C., Pena, A., & Lino, C. M. (2010). A review on ochratoxin A occurrence and effects of processing of cereal and cereal derived food products. *Food Microbiology*, 27(2), 187–198.
- EFSA, Panel on Contaminants in the Food Chain (CONTAM). (2012). Scientific Opinion on the risks for public and animal health related to the presence of citrinin in food and feed. *EFSA Journal*, 10(3), 2605.
- El Adlouni, C., Tozlovanu, M., Naman, F., Faid, M., & Pfohl-Leszkwicz, A. (2006). Preliminary data on the presence of mycotoxins (ochratoxin A, citrinin and aflatoxin B1) in black table olives "Greek style" of Moroccan origin. *Molecular Nutrition & Food Research*, 50(6), 507–512.
- El-Kady, I. A., El-Maraghy, S. S. M., & Mostafa, M. E. (1995). Natural occurrence of mycotoxins in different spices in Egypt. *Folia Microbiologica*, 40(3), 297–300.
- European Union Commission Regulation (EU) No 212/2014 of 6 March 2014 amending Regulation (EC) No 1881/2006 as regards maximum levels of the contaminant citrinin in food supplements based on rice fermented with red yeast *Monascus purpureus*. <https://publications.europa.eu/en/publication-detail/-/publication/26b34f77-a5d1-11e3-8438-01aa75ed71a1> (Accessed: 26 Jul 2019).
- European Union Commission Regulation (EU) No 519/2014 of 16 May 2014 amending Regulation (EC) No 401/2006 as regards methods of sampling of large lots, spices and food supplements, performance criteria for T-2, HT-2 toxin and citrinin and screening methods of analysis. [https://www.fsai.ie/uploadedFiles/Reg519\\_2014.pdf](https://www.fsai.ie/uploadedFiles/Reg519_2014.pdf) (Accessed: 31 Jun 2019).
- Franco, C. M., Fente, C. A., Vazquez, B., Cepeda, A., Lallaoui, L., Prognon, P., & Mahuzier, G. (1996). Simple and sensitive high-performance liquid chromatography-fluorescence method for the determination of citrinin application to the analysis of fungal cultures and cheese extracts. *Journal of Chromatography A*, 723(1), 69–75.
- Gupta, R. C., Srivastava, A., & Lall, R. (2018). Ochratoxins and citrinin. In *Veterinary Toxicology (Third Edition)* (pp. 1019–1027).
- Hackbart, H., Prietto, L., Primel, E. G., Garda-Bufferon, J., & Badiale-Furlong, E. (2012). Simultaneous extraction and detection of ochratoxin A and citrinin in rice. *Journal of the Brazilian Chemical Society*, 23(1), 103–109.



- Jackson, L. K., & Ciegler, A. (1978). Production and analysis of citrinin in corn. *Applied and Environmental Microbiology*, 36(3), 408–411.
- Janardhana, G. R., Raveesha, K. A., & Shetty, H. S. (1999). Mycotoxin contamination of maize grains grown in Karnataka (India). *Food and Chemical Toxicology*, 37(8), 863–868.
- Ji, X., Xu, J., Wang, X., Qi, P., Wei, W., Chen, X., ... & Zhou, Y. (2015). Citrinin determination in red fermented rice products by optimized extraction method coupled to liquid chromatography tandem mass spectrometry (LC-MS/MS). *Journal of Food Science*, 80(6), T1438-T1444.
- Jiménez-López, J., Llorent-Martínez, E. J., Ortega-Barrales, P., & Ruiz-Medina, A. (2014). Multi-commutated fluorometric optosensor for the determination of citrinin in rice and red yeast rice supplements. *Food Additives & Contaminants: Part A*, 31(10), 1744–1750.
- Kononenko, G. P., & Burkin, A. A. (2008). A survey on the occurrence of citrinin in feeds and their ingredients in Russia. *Mycotoxin Research*, 24(1), 3–6.
- Li, F. Q., Xu, G. R., Li, Y. W., Chen, Y., & Ji, R. (2005). Natural occurrence of citrinin in *Monascus* products. *Wei sheng yan jiu=Journal of Hygiene Research*, 34(4), 451–454.
- Li, Y., Zhou, Y. C., Yang, M. H., & Ou-Yang, Z. (2012). Natural occurrence of citrinin in widely consumed traditional Chinese food red yeast rice, medicinal plants and their related products. *Food Chemistry*, 132(2), 1040–1045.
- Liao, C. D., Chen, Y. C., Lin, H. Y., Chiueh, L. C., & Shih, D. Y. C. (2014). Incidence of citrinin in red yeast rice and various commercial *Monascus* products in Taiwan from 2009 to 2012. *Food Control*, 38, 178–183.
- Ma, J., Li, Y., Ye, Q., Li, J., Hua, Y., Ju, D. ... Chang, M. (2000). Constituents of red yeast rice, a traditional Chinese food and medicine. *Journal of Agricultural and Food Chemistry*, 48(11), 5220–5225.
- Markov, K., Pleadin, J., Bevardi, M., Vahčić, N., Sokolić-Mihalak, D., & Frece, J. (2013). Natural occurrence of aflatoxin B1, ochratoxin A and citrinin in Croatian fermented meat products. *Food Control*, 34(2), 312–317.
- Marley, E., Brown, P., Leeman, D., & Donnelly, C. (2016). Analysis of citrinin in cereals, red yeast rice dietary supplement, and animal feed by immunoaffinity column cleanup and LC with fluorescence detection. *Journal of AOAC International*, 99(4), 1025–1031.
- Molinié, A., Faucet, V., Castegnaro, M., & Pfohl-Leszkowicz, A. (2005). Analysis of some breakfast cereals on the French market for their contents of ochratoxin A, citrinin and fumonisin B1: development of a method for simultaneous extraction of ochratoxin A and citrinin. *Food Chemistry*, 92(3), 391–400.
- Moss, M. O. (2002). Mycotoxin review-1. *aspergillus and penicillium*. *Mycologist*, 16(3), 116–119.
- Nguyen, M. T., Tozlovanu, M., Tran, T. L., & Pfohl-Leszkowicz, A. (2007). Occurrence of aflatoxin B1, citrinin and ochratoxin A in rice in five provinces of the central region of Vietnam. *Food Chemistry*, 105(1), 42–47.
- Nishijima, M. (1984). Tokyo Metropolitan Research Laboratory of Public Health, Hyakunincho, Shinjuku-ku, Tokyo 160, Japan. In *Toxigenic Fungi: Their Toxins and Health Hazard: Proceedings of the Mycotoxin Symposia Held in the Third International Mycological Congress, Tokyo, August 30-September 3, 1983* (Vol. 7, p. 172). Elsevier Science Limited.
- Ostry, V., Malir, F., & Ruprich, J. (2013). Producers and important dietary sources of ochratoxin A and citrinin. *Toxins*, 5(9), 1574–1586.
- Pal, M., Gizaw, F., Abera, F., Shukla, P. K., & Hazarika, R. A. (2015). Mycotoxins: A growing concern to human and animal health. *Beverage Food World*, 42(5), 42–50.
- Paterson, R. R. M., & Lima, N. (2010). How will climate change affect mycotoxins in food?. *Food Research International*, 43(7), 1902–1914.
- Petkova-Bocharova, T., Castegnaro, M., Michelon, J., & Maru, V. (1991). Ochratoxin A and other mycotoxins in cereals from an area of Balkan endemic nephropathy and urinary tract tumours in Bulgaria. IARC scientific publications, (115), 83.
- Pohland, A. E. (1993). Mycotoxins in review. *Food Additives and Contaminants*, 10(1), 17–28.
- Polisenska, I., Pfohl-Leszkowicz, A., Hadjeba, K., Dohnal, V., Jirsa, O., Denesova, O., ... & Macharackova, P. (2010). Occurrence of ochratoxin A and citrinin in Czech cereals and comparison of two HPLC methods for ochratoxin A detection. *Food Additives and Contaminants*, 27(11), 1545–1557.
- Rawat, S. (2015). Food Spoilage: Microorganisms and their prevention. *Asian Journal of Plant Science and Research*, 5(4), 47–56.
- Saxena, J., & Mehrotra, B. S. (1989). Screening of spices commonly marketed in India for natural occurrence of mycotoxins. *Journal of Food Composition and Analysis*, 2(3), 286–292.
- Shu, P. Y., & Lin, C. H. (2002). Simple and sensitive determination of citrinin in *Monascus* by GC-selected ion monitoring mass spectrometry. *Analytical Sciences*, 18(3), 283–287.
- Speijers, G. J. A., & Speijers, M. H. M. (2004). Combined toxic effects of mycotoxins. *Toxicology Letters*, 153(1), 91–98.
- Srianta, I., Ristiarini, S., Nugrahani, I., Sen, S. K., Zhang, B. B., Xu, G. R., & Blanc, P. J. (2014). Recent research and development of *Monascus* fermentation products. *International Food Research Journal*, 21(1), 1–12.
- Talmaciu, E., Sandu, I., & Banu, T. (2008). Researches regarding the fungal contamination and the presence of citrinin in feed. *Fungi & Mycotoxins*, 2, 212–217.
- Tirado, M. C., Clarke, R., Jaykus, L. A., McQuatters-Gollop, A., & Frank, J. M. (2010). Climate change and food safety: A review. *Food Research International*, 43(7), 1745–1765.
- Tokusoglu, Ö., & Bozoglu, F. (2010). Citrinin risk in black and green table olives: Simultaneous determination with ochratoxin-a by optimized extraction and IAC-HPLC-FD. *Italian Journal of Food Science*, 22(3), 284.
- Tölgyesi, Á., Stroka, J., Tamosiunas, V., & Zwickel, T. (2015). Simultaneous analysis of *Alternaria* toxins and citrinin in tomato: an optimised method using liquid chromatography-tandem mass spectrometry. *Food Additives and Contaminants: Part A*, 32(9), 1512–1522.
- Vrabcheva, T., Usleber, E., Dietrich, R., & Märtlbauer, E. (2000). Co-occurrence of ochratoxin A and citrinin in cereals from Bulgarian villages with a history of Balkan endemic nephropathy. *Journal of Agricultural and Food Chemistry*, 48(6), 2483–2488.
- Warth, B., Parich, A., Atehnkeng, J., Bandyopadhyay, R., Schuhmacher, R., Sulyok, M., & Krska, R. (2012). Quantitation of mycotoxins in food and feed from Burkina Faso and Mozambique using a modern LC-MS/MS multitoxin method. *Journal of agricultural and food chemistry*, 60(36), 9352–9363.
- Woo, P. C., Lam, C. W., Tam, E. W., Lee, K. C., Yung, K. K., Leung, C. K., ... & Yuen, K. Y. (2014). The biosynthetic pathway for a thousand-year-old natural food colorant and citrinin in *Penicillium marneffei*. *Scientific Reports*, 4, 6728.
- Xu, B. J., Jia, X. Q., Gu, L. J., & Sung, C. K. (2006). Review on the qualitative and quantitative analysis of the mycotoxin citrinin. *Food Control*, 17(4), 271–285.
- Zaied, C., Zouaoui, N., Bacha, H., & Abid, S. (2012). Natural occurrence of citrinin in Tunisian wheat grains. *Food Control*, 28(1), 106–109.



# Interaction of curcumin on cisplatin cytotoxicity in HeLa and HepG2 carcinoma cells

Merve Becit<sup>1</sup> , Sevtap Aydın Dilsiz<sup>2</sup> , Nurşen Başaran<sup>2</sup> 

<sup>1</sup>Atatürk University, Faculty of Pharmacy, Department of Pharmacology, Erzurum, Turkey

<sup>2</sup>Hacettepe University, Faculty of Pharmacy, Department of Pharmaceutical Toxicology, Ankara, Turkey

**ORCID IDs of the authors:** M.B. 0000-0002-8084-4419; S.A.D. 0000-0002-6368-2745; N.B. 0000-0001-8581-8933

**Cite this article as:** Becit, M., Aydın Dilsiz, A., & Başaran, N. (2020). Interaction of curcumin on cisplatin cytotoxicity in HeLa and HepG2 carcinoma cells. *Istanbul Journal of Pharmacy*, 50 (3), 202-210.

## ABSTRACT

**Background and Aims:** Our study aimed to evaluate how curcumin affect cisplatin cytotoxicity in human cervical carcinoma (HeLa), human hepatocellular carcinoma (HepG2), and Chinese hamster lung fibroblast (V79) cells.

**Methods:** The cytotoxicity was evaluated by MTT assay.

**Results:** The IC<sub>50</sub> values of curcumin were 404 µM and 320 µM in HeLa cells; 236 µM and 98.3 µM in HepG2 cells; 877 µM and 119 µM in V79 cells; for 24 h and 48 h, respectively. The IC<sub>50</sub> values of cisplatin were 22.4 µM and 12.3 µM in HeLa cells; 25.5 µM and 7.7 µM in HepG2 cells; 15.4 µM and 4.9 µM in V79 cells; for 24 h and 48 h, respectively. Curcumin significantly decreased cisplatin cytotoxicity at 500 µM in HeLa cells and above 250 µM and 125 µM in HepG2 cells, for 24 h and 48 h, respectively. In V79 cells, curcumin significantly decreased the IC<sub>50</sub> values of cisplatin above 500 µM and 125 µM for 24 h and 48 h.

**Conclusion:** The results might contribute to the anticancer effect of the curcumin-cisplatin combination in cervical and hepatocellular carcinoma, but in order to support this result and determine its interactions with antineoplastic drugs, further studies are needed.

**Keywords:** Curcumin, cisplatin, cytotoxicity, HeLa cells, HepG2 cells

## INTRODUCTION

Multidisciplinary treatments, including surgical treatment, radiotherapy and chemotherapy are applied to patients with cancer. Recently, new and improved therapies have been investigated to improve the survival and quality of life of patients with various types of cancer (Falzone, Salomone, & Libra, 2018). Combination of antineoplastic drugs with antioxidant agents has become a promising method for cancer treatment; however, knowing how to improve the effect of the combination therapy is of great significance. Therefore, nowadays the combination therapies have been investigated with the aim of increasing anticancer effects and decreasing cytotoxicity (Chen, Xu, & Chen, 2015; Adahoun, Al-Akhras, Jaafar, & Bououdina, 2017; Perrone, et al., 2015; Taner, et al., 2014; Yang, Shin, & Cho, 2014).

Cisplatin, one of the chemotherapeutic agents, is often used in the treatment of solid tumors such as testis, over, bladder, prostate, cervix, and lung cancer (Rosenberg, 1985). It has severely dose-limiting toxicity including ototoxicity, neurotoxicity, nephrotoxicity and cardiotoxicity. One of the mechanisms responsible for the adverse effects of cisplatin is the stimulation of oxidative stress (Florea, & Busselberg, 2011; Dugbartey, Peppone, & de Graaf, 2016). Many researchers have shown that it is useful to combine cisplatin with antioxidant agents in order to increase the effectiveness of cancer chemotherapy, decrease resistance development and reduce cytotoxicity. However, supporting studies on this issue are still insufficient. (Florea, & Busselberg, 2011).

## Address for Correspondence:

Sevtap AYDIN DILSIZ, e-mail: sevtapay@hacettepe.edu.tr

Submitted: 29.04.2020

Revision Requested: 05.06.2020

Last Revision Received: 02.07.2020

Accepted: 18.07.2020

This work is licensed under a Creative Commons Attribution 4.0 International License.



Curcumin, (1,7-bis(4-hydroxy-3-methoxyphenyl)-1,6-heptadiene-3,5-dione), is a yellow-orange polyphenol derived from the plant *Curcuma longa* L. (*C. longa*), which is commonly called “turmeric, saffron root and jellyfish”. Extensive research has indicated that curcumin offer a lot of benefits including antioxidant, anti-inflammatory, anticarcinogenic, antimutagenic, antidiabetic, antibacterial, and antiviral properties (Menon & Sudheer, 2007; Koohpar, Entezari, Movafagh & Hashemi, 2015; Bulboacă, et al. 2009; Çikrikçi, Mezioğlu, Yılmaz, 2008). Nowadays, it is consumed as a food supplement in many countries owing to its strong antioxidant activity (Kunnumakara, Bordoloi, Padmavathi, Monisha, Roy, Prasad, & Aggarwal, 2017b; Guzman, 2019). Despite its reported benefits via inflammatory and antioxidant mechanisms, one of the major problems with ingesting curcumin by itself is its poor bio-availability, which appears to be primarily due to poor absorption, rapid metabolism, and rapid elimination. Curcuminoids have been approved by the United States Food and Drug Administration (FDA) as “Generally Recognized As Safe” (GRAS), and good tolerability and safety profiles have been reported even at doses between 4 and 8 g/day (Hewlings, & Kalman, 2017; Gupta, Patchva, & Aggarwal, 2013; Anand, Kunnumakara, Newman, & Aggarwal, 2007). Studies conducted in both animals and humans have suggested that this polyphenol is effective and safe for the prevention and treatment of many diseases. Curcumin-induced sensitization to cisplatin have been observed in many cancer cell models (Florea, & Busselberg, 2011; Guzman, 2019) such as breast cancer (Zou et al., 2018), cervical cancer (Roy & Mukherjee, 2014), bladder cancer (Zhang, Yong, Wu & Liu., 2014), human neuroblastoma cells (Sukumari-Ramesh et al., 2011), laryngeal carcinoma (Zhang, Tianyu, Lianji, Hui, Dan & Chunshun, 2013), human colorectal cancer (Wang, Liu & Su, 2014) and lymphoma cells (Zhang et al., 2014).

Curcumin has been suggested to exhibit chemopreventive and therapeutic effects through multiple mechanisms, as shown by several preclinical and clinical studies (Aggarwal, Prasad, Sung, Krishnan, & Guha, 2013; Shehzad, Lee, & Lee, 2013; Kunnumakara, Bordoloi, Harsha, Banik, Gupta, & Aggarwal, 2017a). However, whether or not the use of curcumin during chemotherapy cause interactions with efficacy of anti-neoplastic drugs is not well known. The underlying cellular and molecular processes are not clear, particularly on cancer; thus, new and advanced studies are needed to clarify the effects of curcumin in cancer cells (Çikrikçi, Mezioğlu, Yılmaz, 2008; Nagpal, & Sood, 2013; Bansal, Goel, Aqil, Vadhanam, & Gupta, 2011). More in vitro studies with other cancer cells as well as in vivo studies are suggested at different doses.

In this study, the cytotoxic effects of anticancer drug cisplatin were investigated in combination with curcumin which is known to be significant biological effects and of which the importance has been increasingly in recent studies, in different cell lines including human cervical carcinoma (HeLa) cells, human hepatocellular carcinoma (HepG2) cells, and Chinese hamster lung noncancer fibroblast (V79) cells using 3-(4,5-dimethylthiazol-2-yl)-2,5-diphenyltetrazolium bromide (MTT) assay. HeLa and HepG2 carcinoma cells were selected in our

study, since cisplatin is mainly used for the treatment of malignant tumors including cervical and liver carcinomas. V79 cells, non-tumor cell lines, has been widely used to study the toxicity of a wide variety of cytotoxic agents. It has been preferred as a healthy cell line in terms of revealing its difference with non-cancerous cells compared to cancerous cells including HeLa and HepG2 cells.

## MATERIALS AND METHODS

### Chemicals

The chemicals used in the experiments were purchased from the following suppliers: cisplatin (Koçak Farma, Turkey); curcumin, dimethyl sulfoxide (DMSO), Dublecco's modified Eagle's medium (DMEM), ethanol, fetal bovine serum (FBS), MTT, penicillin-streptomycin, trypan blue, trypsin-EDTA, RPMI 1640 medium, Dulbecco's phosphate buffered saline (PBS) from Sigma (St. Louis, MO, USA); millipore filters from Millipore (Billerica, MA, USA), all other plastic materials from Cornings (Corning Inc., NY, USA). The purity of curcumin is  $\geq 80\%$ .

### Cell culture

HeLa, HepG2 and V79 cells were obtained from the American Type Culture Collection (ATCC; Rockville, MD, USA). V79 cells were grown in RPMI-1640 medium with 10% heat-inactivated FBS, and 1% penicillin-streptomycin solution (10000 units of penicillin and 10 mg of streptomycin in 0.9% NaCl), and 2mM L-glutamine at 37°C in a humidified atmosphere of 5% CO<sub>2</sub>. HeLa and HepG2 cells were cultured in in Dulbecco's Modified Eagle Medium (DMEM) containing low glucose (1 g/L) and sodium pyruvate and supplemented with 10% heat-inactivated fetal bovine serum (FBS), 2mM L-glutamine and 1% penicillin-streptomycin solution (10000 units of penicillin and 10 mg of streptomycin in 0.9% NaCl) in a humidified atmosphere of 5% CO<sub>2</sub> and 95% air at 37°C. The cells were subcultured in 75 cm<sup>2</sup> cell culture flasks. The medium was changed every 3 days. The passage numbers used in our study for all cell lines were between passage 10 and passage 12.

### Determination of cytotoxicity

The cytotoxicity of curcumin and cisplatin were measured in HeLa, HepG2, and V79 cells using 3-(4,5-dimethylthiazol-2-yl)-2,5-diphenyltetrazolium bromide (MTT) assay, which is a colorimetric assay that measures the reduction of yellow MTT by mitochondrial succinate dehydrogenase (Mosmann, 1983; Hansen, & Nielsen, 1989).

After growing for 2 weeks, the cells were plated at  $1 \times 10^4$  cells/well by adding 200  $\mu$ L of a  $5 \times 10^4$  cells/mL suspension to each well of a 96-well tissue culture plate and allowed to grow for 24 h before treatment. The number of cells was calculated by trypan blue dye exclusion.

The stock solution of curcumin was freshly prepared in DMSO as solvent control and filtered with millipore filters (0.20  $\mu$ m). DMSO concentration was not exceed 0.5% (v/v) in medium. The cells were treated alone with CUR in a wide range of concentrations (1.95-2000  $\mu$ M) or cisplatin (0.49-500  $\mu$ M) in the

related culture medium for 24 h and 48 h. Negative control experiments were carried out with the culture medium containing DMSO (0.5%) or PBS (1%), for curcumin and cisplatin, respectively. After the values of  $IC_{50}$  were determined, the effects of curcumin in a wide range of doses on the cytotoxicity of cisplatin were evaluated in all cells for 24 h and 48 h.

There is no reference value for the selected doses. The  $IC_{50}$  values determined in our experiment were taken into account in the dose selection, since cytotoxic doses vary greatly depending on the cell type and number of passages studied, the exposure time and the cytotoxicity method used in the literature. After the effects of curcumin on cell viability in the wide dose range were determined for one non-cancer cell and two different cancer cells at two different periods of 24 h and 48 h, the result was extended by studying the wide dose range including the cytotoxic dose.  $IC_{50}$  value, kills 50% of the living cell population, is a dose which shows cytotoxicity of substances. The dose of cisplatin, which is cytotoxic, is also the target dose in chemotherapy, because the aim is to prevent cancer cell proliferation. In order to show how curcumin taken in various forms, such as food supplements or nano-drug formulations, changes the cytotoxic effect of cisplatin, the combination of curcumin in a wide dose range with the  $IC_{50}$  value of cisplatin was preferred. The results are crucial in terms of revealing the synergistic or antagonistic effects in terms of cell viability between cisplatin and curcumin, and these results also contribute to predicting possible interactions. At the end of the treatment (24 h and 48 h), the cells were then incubated with 0.5 mg/mL MTT solution for another 4 h at 37°C. Then the medium was discarded and washed with PBS. DMSO (100  $\mu$ l) was added and the plates were shaken for 5 min gently. The formazan crystals were dissolved in DMSO and absorbance of each sample was measured at 570 nm using the microplate reader (SpectraMax M2, Molecular Devices Limited, Berkshire, UK). Results were expressed as the mean percentage of viable cells compared with non-treated controls.

The percentage of cell viability was calculated using the formula:

"Percentage of cell viability = (The absorbance of sample/ control) x 100"

The cytotoxic concentration that killed cells by 50% ( $IC_{50}$ ) was determined from absorbance versus concentration curve.

### Statistical analysis

All experiments were carried out in quadruplicate. The results were given as the mean  $\pm$  standard deviation. The statistical analysis was performed with software programs "SPSS 10.5" (Statistical Package for the Social Sciences, Chicago, IL, USA). The distribution of the data was checked for normality using the Kolmogorov-Smirnov test. The means of data were compared by the one-way variance analysis test and post hoc analysis of group differences was performed by least significant difference (LSD) test.  $P$  value of less than 0.05 was considered as statistically significant.

## RESULTS

### Effects of curcumin and cisplatin on the viabilities of HeLa, HepG2, and V79 cells

In HeLa cells, the results of curcumin cytotoxicity are given in Figure 1. Curcumin did not cause significant cytotoxic effect at the concentrations of 1.95-250  $\mu$ M and at the concentrations of 1.95-125  $\mu$ M when compared to the negative control for 24 h and 48 h incubation, respectively; however, the cell viabilities were significantly decreased above 500  $\mu$ M and 250  $\mu$ M concentrations of curcumin ( $p < 0.05$ ) for 24 h and 48 h incubation, respectively, in a dose-dependent manner. The  $IC_{50}$  value of curcumin 403.5  $\mu$ M and 320.2  $\mu$ M for 24 h and 48 h, respectively (Figure 1).

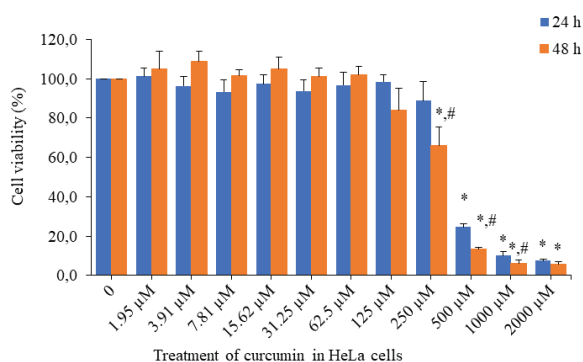


**Figure 1.** Cytotoxic effects of curcumin on HeLa cells viability for 24 h and 48 h. The values were given as the mean  $\pm$  standard deviation ( $n=4$ ). \* $p < 0.05$ , compared to negative control (untreated cells) (0.5% DMSO). # $p < 0.05$ , 24-hour cell viability was compared to 48-hour cell viability.

The results of cisplatin cytotoxicity in HeLa cells are given in Figure 2. Cisplatin did not cause significant cytotoxic effect at the concentrations of 0.49-7.81  $\mu$ M and at the concentrations of 0.49-3.91  $\mu$ M when compared to the negative control for 24 h and 48 h, respectively; however, the cell viabilities were significantly decreased above 15.63  $\mu$ M and 7.81  $\mu$ M of cisplatin for 24 h and 48 h incubation, respectively, in a dose-dependent manner ( $p < 0.05$ ). The  $IC_{50}$  values of cisplatin were 22.4  $\mu$ M and 12.3  $\mu$ M for 24 h and 48 h, respectively (Figure 2).

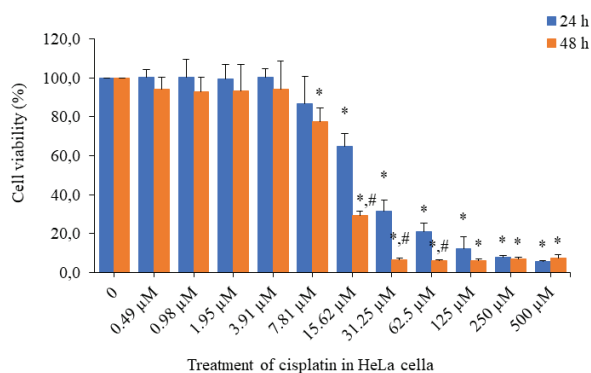


**Figure 2.** Cytotoxic effects of cisplatin on HeLa cells viability for 24 h and 48 h. The values were given as the mean  $\pm$  standard deviation ( $n=4$ ). \* $p < 0.05$ , compared to negative control (untreated cells) (PBS). # $p < 0.05$ , 24-hour cell viability was compared to 48-hour cell viability.

In HepG2 cells, the results of curcumin cytotoxicity are given in Figure 3. Curcumin did not cause significant cytotoxic effect at the concentrations of 1.95-125  $\mu\text{M}$  and at the concentrations of 1.95-31.25  $\mu\text{M}$  when compared to the negative control for 24 h and 48 h incubation, respectively; however, the cell viabilities were significantly decreased above 250  $\mu\text{M}$  and 62.5  $\mu\text{M}$  concentrations of curcumin ( $p < 0.05$ ) for 24 h and 48 h incubation, respectively, in a dose-dependent manner. The  $\text{IC}_{50}$  value of curcumin were 235.8  $\mu\text{M}$  and 98.3  $\mu\text{M}$  for 24 h and 48 h, respectively (Figure 3).

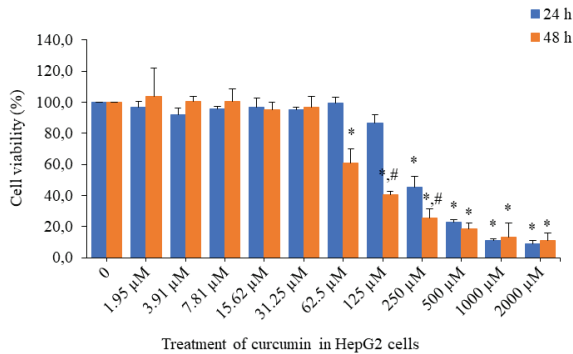


**Figure 3.** Cytotoxic effects of curcumin on HepG2 cells viability for 24 h and 48 h. The values were given as the mean  $\pm$  standard deviation (n=4). \* $p < 0.05$ , compared to negative control (untreated cells) (0.5% DMSO). # $p < 0.05$ , 24-hour cell viability was compared to 48-hour cell viability.

The results of cisplatin cytotoxicity in HepG2 cells are given in Figure 4. Cisplatin did not cause significant cytotoxic effect at the concentrations of 0.49-7.81  $\mu\text{M}$  and at the concentrations of 0.49-3.91  $\mu\text{M}$  when compared to the negative control for 24 h and 48 h, respectively; however, the cell viabilities were significantly decreased above 15.63  $\mu\text{M}$  and 7.81  $\mu\text{M}$  of cisplatin for 24 h and 48 h incubation, respectively, in a dose-dependent manner ( $p < 0.05$ ). The  $\text{IC}_{50}$  values of cisplatin were 25.5  $\mu\text{M}$  and 7.7  $\mu\text{M}$  for 24 h and 48 h, respectively (Figure 4).

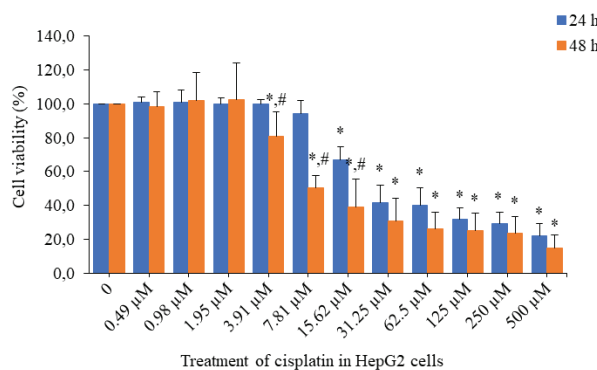


**Figure 4.** Cytotoxic effects of cisplatin on HepG2 cells viability for 24 h and 48 h. The values were given as the mean  $\pm$  standard deviation (n=4). \* $p < 0.05$ , compared to negative control (untreated cells) (PBS). # $p < 0.05$ , 24-hour cell viability was compared to 48-hour cell viability.

In V79 cells, the results of curcumin cytotoxicity are given in Figure 5. Curcumin did not cause significant cytotoxic effect at the concentrations of 1.95-250  $\mu\text{M}$  and at the concentrations

of 1.95-62.5  $\mu\text{M}$  when compared to the negative control for 24 h and 48 h incubation, respectively; however, the cell viabilities were significantly decreased above 500  $\mu\text{M}$  and 125  $\mu\text{M}$  concentrations of curcumin ( $p < 0.05$ ) for 24 h and 48 h incubation, respectively, in a dose-dependent manner. The  $\text{IC}_{50}$  value of curcumin were 876.7  $\mu\text{M}$  and 118.7  $\mu\text{M}$  for 24 h and 48 h, respectively (Figure 5).

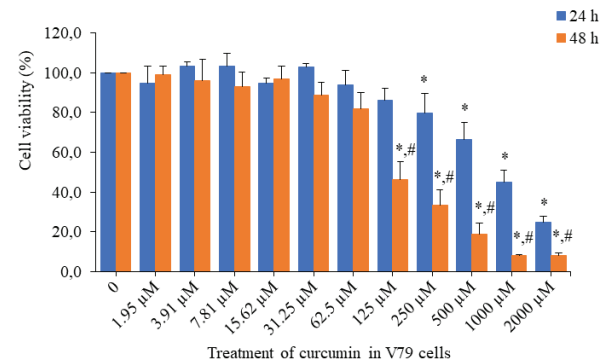


**Figure 5.** Cytotoxic effects of curcumin on V79 cells viability for 24 h and 48 h. The values were given as the mean  $\pm$  standard deviation (n=4). \* $p < 0.05$ , compared to negative control (untreated cells) (0.5% DMSO). # $p < 0.05$ , 24-hour cell viability was compared to 48-hour cell viability.

The results of cisplatin cytotoxicity in V79 cells are given in Figure 6. Cisplatin did not cause significant cytotoxic effect at the concentrations of 0.49-7.81  $\mu\text{M}$  and at the concentrations of 0.49-1.95  $\mu\text{M}$  when compared to the negative control for 24 h and 48 h, respectively; however, the cell viabilities were significantly decreased above 15.63  $\mu\text{M}$  and 3.91  $\mu\text{M}$  of cisplatin for 24 h and 48 h incubation, respectively, in a dose-dependent manner ( $p < 0.05$ ). The  $\text{IC}_{50}$  values of cisplatin were 15.4  $\mu\text{M}$  and 4.9  $\mu\text{M}$  for 24 h and 48 h, respectively (Figure 6).

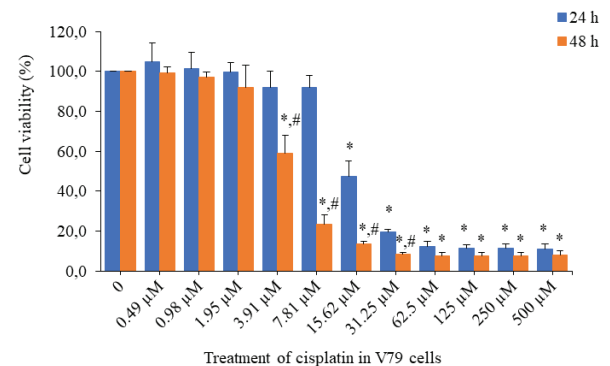


**Figure 6.** Cytotoxic effects of cisplatin on V79 cells viability for 24 h and 48 h. The values were given as the mean  $\pm$  standard deviation (n=4). \* $p < 0.05$ , compared to negative control (untreated cells) (PBS). # $p < 0.05$ , 24-hour cell viability was compared to 48-hour cell viability.

**Effects of curcumin on cisplatin cytotoxicity in HeLa, HepG2, and V79 cells**

In HeLa cells, the effects of curcumin at the concentrations of 15.6-500  $\mu\text{M}$  on cisplatin cytotoxicity are shown in Figure 7, for 24 h and 48 h incubation. As shown in Figure 7a, curcumin

did not change the IC<sub>50</sub> value of cisplatin (20 μM, approximately) at the concentrations of 15.6-250 μM for 24 h incubation; however, the IC<sub>50</sub> value of cisplatin was significantly reduced at the concentration of 500 μM of curcumin (1.83 fold, vs. IC<sub>50</sub> of cisplatin) when compared to the negative control for 24 h incubation (*p*<0.05). As shown in Figure 7b, when compared to the negative control, curcumin did not change the IC<sub>50</sub> value of cisplatin (10 μM, approximately) at the concentrations of 15.6-250 μM for 48 h incubation; however, the IC<sub>50</sub> value of cisplatin was significantly reduced at concentrations of 500 μM of curcumin (1.41 fold for 500 μM, vs. IC<sub>50</sub> of cisplatin) (*p*<0.05). As a result, curcumin reduced the cytotoxicity of cisplatin at highest doses (500 μM).

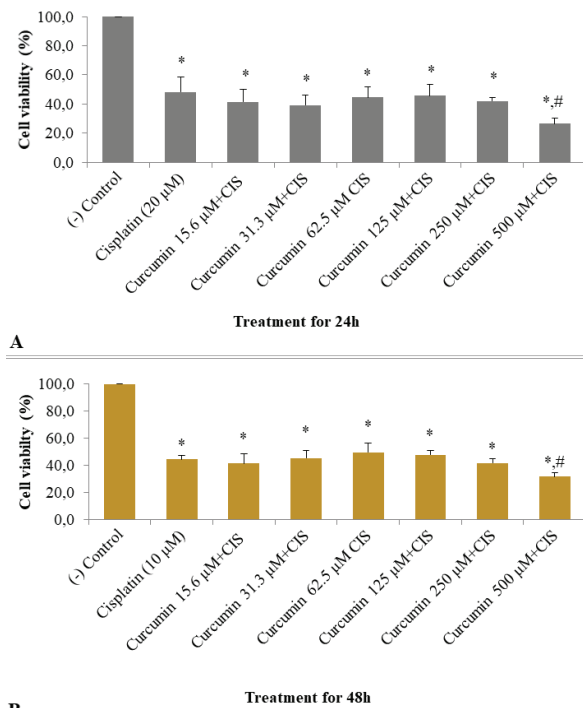


**Figure 7.** Effects of curcumin on the cisplatin cytotoxicity in HeLa cells for 24 h (A) and 48 h (B). The values were given as mean ± standard deviation (n=4). \**p*<0.05, compared to negative control (untreated cells) (0.5% DMSO); #*p*<0.05, compared to cisplatin as positive control (20 μM for 24 h treatment and 10 μM for 48 h treatment). CIS, cisplatin.

In HepG2, the effects of curcumin at the concentrations of 15.6-500 μM on cisplatin cytotoxicity cells are shown in Figure 6, for 24 h and 48 h incubation. As shown in Figure 8a, curcumin did not change the IC<sub>50</sub> value of cisplatin (25 μM, approximately) at the concentrations of 15.6-125 μM for 24 h incubation; however, the IC<sub>50</sub> value of cisplatin was significantly reduced at concentrations of 250 and 500 μM of curcumin (1.81 and 3.48 fold, vs. IC<sub>50</sub> of cisplatin) when compared to the negative control for 24 h incubation (*p*<0.05). As shown in Figure 8b, when compared to the negative control, curcumin did not change the IC<sub>50</sub> value of cisplatin (10 μM, approximately) at the concentrations of 15.6-62.5 μM for 48 h incubation; however, the IC<sub>50</sub> value of cisplatin was significantly reduced at concentrations of 125, 250 and 500 μM of curcumin (1.71, 4.09 and 19.04 fold vs. IC<sub>50</sub> of cisplatin) (*p*<0.05). As a result, curcumin reduced the cytotoxicity of cisplatin at the high doses (125-500 μM).

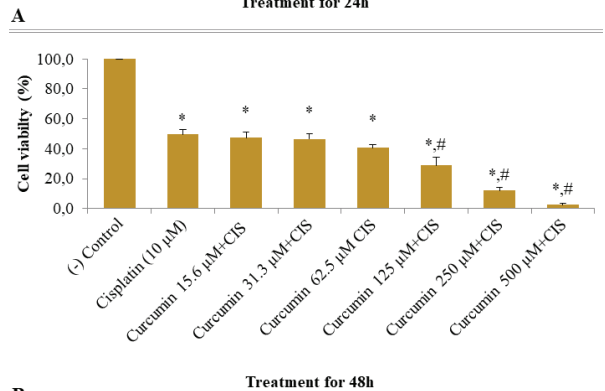
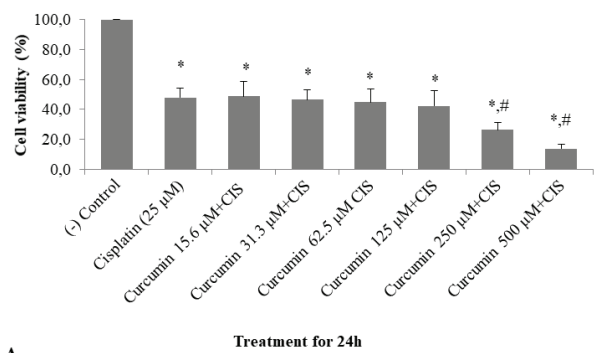


**Figure 8.** Effects of curcumin on the cisplatin cytotoxicity in HepG2 cells for 24 h (A) and 48 h (B). The values were given as mean ± standard deviation (n=4). \**p*<0.05, compared to negative control (untreated cells) (0.5% DMSO); #*p*<0.05, compared to cisplatin as positive control (25 μM for 24 h treatment and 10 μM for 48 h treatment). CIS, cisplatin.

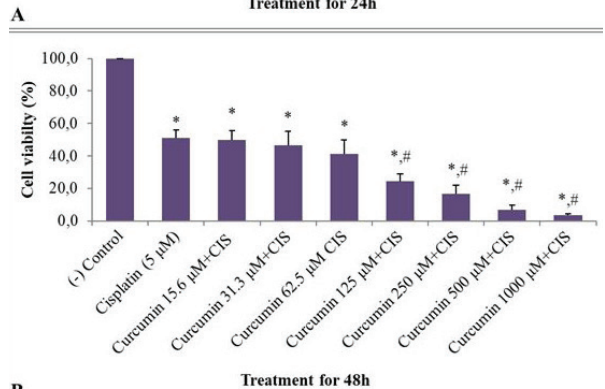
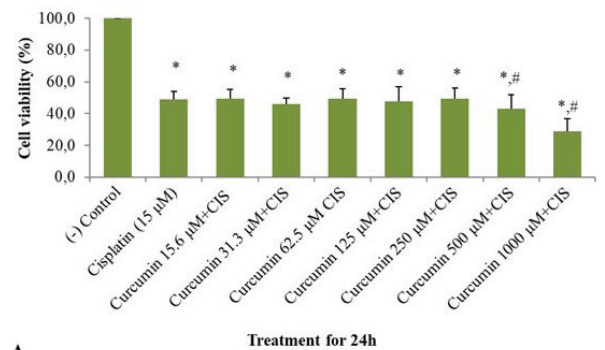


**Figure 9.** Effects of curcumin on the cisplatin cytotoxicity in V79 cells for 24 h (A) and 48 h (B). The values were given as mean ± standard deviation (n=4). \**p*<0.05, compared to negative control (untreated cells) (0.5% DMSO); #*p*<0.05, compared to cisplatin as positive control (15 μM for 24 h treatment and 5 μM for 48 h treatment). CIS, cisplatin.



In V79 cells, the effects of curcumin in a wide range of concentrations (15.6-1000  $\mu\text{M}$ ) on cisplatin cytotoxicity are shown in Figure 9, for 24 h and 48 h incubation. As shown in Figure 9a, curcumin did not change the  $\text{IC}_{50}$  value of *cisplatin* (15  $\mu\text{M}$ , approximately) at the concentrations of 15.6-500  $\mu\text{M}$  for 24 h incubation; however, the  $\text{IC}_{50}$  value of *cisplatin* was significantly reduced at concentrations of 1000  $\mu\text{M}$  of curcumin (1.71 fold, vs.  $\text{IC}_{50}$  of cisplatin) when compared to the negative control for 24 h incubation ( $p < 0.05$ ). As shown in Figure 9b, when compared to the negative control, curcumin did not change the  $\text{IC}_{50}$  value of *cisplatin* (5  $\mu\text{M}$ , approximately) at the concentrations of 15.6-62.5  $\mu\text{M}$  for 48 h incubation; however, the  $\text{IC}_{50}$  value of cisplatin was significantly reduced at concentrations of 125, 250, 500 and 1000  $\mu\text{M}$  of curcumin (2.08, 3.07, 7.66 and 14.76 fold vs.  $\text{IC}_{50}$  of cisplatin) ( $p < 0.05$ ). As a result, curcumin reduced the cytotoxicity of cisplatin at high doses (125-1000  $\mu\text{M}$ ).

## DISCUSSION

Multidisciplinary treatments, including surgical treatment, radiotherapy and chemotherapy are applied for patients with cancer. Recently, new and improved therapies have been investigated to improve the survival and quality of life of cancer patients with various types of cancer (Falzone, Salomone, & Libra, 2018). Combination of antioxidant agents and antineoplastic drugs has become promising method for cancer therapy; however, knowing how to improve the effect of the combination therapy is of great importance. Therefore, nowadays the combination therapies have been investigated with the aim of increasing anticancer effect and decreasing cytotoxicity (Perone, et al., 2015; Guzman, 2019).

As is well known, cisplatin is often used in the treatment of many types of cancer (Rosenberg, 1985). It has severely dose-limiting toxicity including ototoxicity, neurotoxicity, nephrotoxicity and cardiotoxicity. One of the mechanisms responsible for the adverse effects of cisplatin is the stimulation of oxidative stress (Florea, & Busselberg, 2011; Dugbartey, Peppone, & de Graaf, 2016). Many researchers have shown that it is useful to combine cisplatin with antioxidant agents in order to increase the effectiveness of cancer chemotherapy, decrease resistance development, and also reduce cytotoxicity. However, studies are insufficient to support this (Florea, & Busselberg, 2011).

Curcumin is considered as a supportive alternative in the treatment in terms of safe, effective and low cost in the prevention and treatment of many diseases due to primarily its antioxidant and anti-inflammatory properties. However, whether the use of curcumin during chemotherapy cause interactions with the efficacy of antineoplastic drugs is not well known. The cellular and molecular processes should be clarified in cancer cells, with advanced studies (Aggarwal, Kumar, & Bharti, 2003; Moron, Montano, Salvador, Robles, & Lazaro, 2010).

Present study aimed to explain the potential synergistic cytotoxic activity of the well-known herbal origin secondary metabolite, curcumin and the clinically used drug, cisplatin. We investigated the cytotoxicity of HeLa, HepG2 and V79 cells treated with curcumin and cisplatin alone or in combination for 24 h and 48 h using MTT, a colorimetric analysis that evaluates cell metabolic

activity. It seems that the cytotoxicity profiles of curcumin and cisplatin alone were different depending on the dose and time. The effects of curcumin on cell viability measured after 24 h and 48 h incubation in HeLa, HepG2, and V79 cells in a wide range of doses (1.95-2000  $\mu\text{M}$ ) were evaluated. In our study,  $\text{IC}_{50}$  values of curcumin were determined as 404  $\mu\text{M}$ , 236  $\mu\text{M}$ , and 877  $\mu\text{M}$  in HeLa, HepG2 and V79 cells, respectively, for 24 h incubation. Curcumin cytotoxicity in HepG2 cells was  $\sim 1.7$  times higher compared to HeLa cell and  $\sim 3.7$  times higher compared to V79 cell, for 24 h. For 48 h incubation,  $\text{IC}_{50}$  values of curcumin were determined as 320  $\mu\text{M}$ , 98.3  $\mu\text{M}$ , and 119  $\mu\text{M}$  in HeLa, HepG2 and V79 cells, respectively. Curcumin cytotoxicity in HepG2 cells was  $\sim 3.2$  times higher compared to HeLa cell and  $\sim 1.2$  times higher compared to V79 cell, for 48 h. When 48 h incubation is compared to 24 h incubation, the cytotoxicity of curcumin was determined as  $\sim 1.3$  times higher in HeLa cells,  $\sim 2.4$  times higher in the HepG2 cells and  $\sim 7.4$  times higher in the V79 cells. The effects of cisplatin on cell viability measured after 24 h and 48 h in V79, HeLa, and HepG2 cells were evaluated at the concentrations of 0.49-500  $\mu\text{M}$ .  $\text{IC}_{50}$  values of cisplatin were determined as 22.4  $\mu\text{M}$ , 25.5  $\mu\text{M}$ , and 15.4  $\mu\text{M}$  at 24 h exposure and 12.3  $\mu\text{M}$ , 7.7  $\mu\text{M}$ , and 4.9  $\mu\text{M}$  at 48 h exposure, for HeLa, HepG2 and V79 cells, respectively. When 48 h incubation is compared to 24 h incubation, the cytotoxicity of cisplatin was determined as  $\sim 1.8$  times higher for HeLa cells,  $\sim 3.3$  times higher for the HepG2 cells and  $\sim 3.1$  times higher for the V79 cells. In our study, it was determined whether or not the combination of curcumin with cisplatin increased cytotoxicity when compared to positive control (cisplatin treatment at  $\text{IC}_{50}$  doses) in the selected cancer (HeLa and HepG2) and normal (V79) cell lines. In HeLa cells, curcumin significantly reduced the  $\text{IC}_{50}$  value of cisplatin (20  $\mu\text{M}$  (24 h) and 10  $\mu\text{M}$  (48 h), approximately) at the concentration of 500  $\mu\text{M}$  for 24 h, at the concentrations of 250-500  $\mu\text{M}$  for 48 h incubation, respectively. In HepG2 cells, curcumin significantly reduced the  $\text{IC}_{50}$  value of cisplatin (25  $\mu\text{M}$  (24 h) and 10  $\mu\text{M}$  (48 h), approximately) at the concentrations of 250-500  $\mu\text{M}$  for 24 h, at the concentration of 125-500  $\mu\text{M}$  for 48 h incubation, respectively. In V79 cells, curcumin significantly reduced the  $\text{IC}_{50}$  value of cisplatin (15  $\mu\text{M}$  (24 h) and 5  $\mu\text{M}$  (48 h), approximately) at the concentration of 500  $\mu\text{M}$  for 24 h, at the concentrations of 125  $\mu\text{M}$  and 500  $\mu\text{M}$  for 48 h incubation, respectively.

As shown in our findings, the combination of cisplatin with curcumin inhibited cell viability and significantly showed an agonist effect in selected cancer cells in time and dose dependent manner. Our results suggest that a curcumin-cisplatin combination could be useful as a therapeutic agent for human cervical and hepatocellular carcinoma and add a new perspective to anticancer treatment.

Consistent with our findings, it has been reported that curcumin could inhibit cell proliferation in the various cancer cell lines in many studies. There are many studies in which the possible mechanism underlying the cytotoxic effect of curcumin is associated with apoptosis. In a study investigating the effect and possible mechanism of curcumin, cisplatin and their synergistic effect, both curcumin and cisplatin have been shown to enhance the growth inhibition and apoptosis of human lung adenocarcinoma A549 cells in a concentration-depen-

dent pattern, using MTT (Cao, Diao, & Xia, 2008). In another study, it was investigated the role of curcumin in lung cancer (A549) cell proliferation and apoptosis in regulating the signaling pathway which plays an important role in tumor occurrence. CCK-8 assay and EdU staining for cell proliferation and Real-time quantitative PCR for mRNA expressions and Western blot for protein levels were carry out. It was reported that curcumin (10  $\mu$ M) treatment markedly inhibited A549 cell proliferation and induced apoptosis in a dose dependent manner. It was also reported that curcumin could inhibit lung cancer cell proliferation and promote apoptosis by downregulating DJ-1 to regulate the activity of PTEN/PI3K/AKT pathway (Li, Qin, & Li, 2019). It is thought that new and advanced studies should be carried in order to illuminate the underlying mechanisms of these effects of curcumin in a better way.

Some research has reported IC<sub>50</sub> values of curcumin in different cells using different methods. In a study, in human breast cancer MCF-7 cells, using MTT assay, IC<sub>50</sub> values of curcumin were determined as 79.58  $\mu$ g/ml (~216  $\mu$ M) and 53.18  $\mu$ g/ml (~144  $\mu$ M) and 30.78  $\mu$ g/ml (~83.5  $\mu$ M) in 24, 48 h and 72 h incubation, respectively (Koochpar, Entezari, Movafagh, & Hashemi, 2015). In another study, in human hepatocellular carcinoma HepG2 cells, using the neutral red uptake (NRU) assay, IC<sub>50</sub> value of curcumin was reported as 41.5  $\mu$ g/ml (~ 113  $\mu$ M) in 72 h incubation (Abdel-Lateef et al., 2016). In another also study, IC<sub>50</sub> value of curcumin were reported as 9.40  $\mu$ g/ml (~25.5  $\mu$ M) and 17.67  $\mu$ g/ml (~47.9  $\mu$ M), and 22.88  $\mu$ g/ml (~62.1  $\mu$ M), in MCF-7, HeLa, and HepG2 cell, respectively (Ding, Ma, Lou, Sun, & Ji, 2015). The IC<sub>50</sub> values of CIS was reported to be 54.07  $\mu$ M and 96.38  $\mu$ M in cervical cancer cells (HeLa and Caco-2), respectively; 97.20  $\mu$ M and 85.66  $\mu$ M in pancreatic cancer cells (MIA PaCa-2 and BxPC-3), respectively; 14.87  $\mu$ M and 77.89  $\mu$ M in hepatocellular carcinoma cells (Hep-G2 and SK-HEP-1), respectively, for 24 h incubation, using MTT method (Nurcahyanti, & Wink, 2016).

Baharuddin et al., (2016) have reported that curcumin increased cisplatin-induced apoptosis and metastasis inhibition in non-small lung cancer A549 and H2170 cells. In this study, it has been concluded that curcumin (10-40  $\mu$ M) is able to increase the efficacy of low dose cisplatin (3  $\mu$ M) in both cells. Nowadays the combination therapies with the aim of increasing anticancer effects and decreasing toxicity have been focus of great interest. Many researchers have revealed that cisplatin has positive effects in combination with antioxidants (Mosalam, Zidan, Mehanna, Mesbah, & Abo-Elmatty, 2020; Toric, Markovic, Brala, Barbaric, 2019). Curcumin has various pharmacological properties and exhibits the ability to interact with multiple molecular targets and intracellular signaling pathways. It has antiproliferative and chemopreventive efficacy through the various pathways such as NF- $\kappa$ B pathway (a proinflammatory transcription factor, has a role in tumorigenesis and inflammation), STAT3 pathway (a proinflammatory transcription factor that plays a major role in the pathogenesis of various cancers), PI3K/AKT/mTOR pathway, EGFR pathway (a family of receptor tyrosine kinases, is a complex signal transduction cascade that is involved in the modulation of cell proliferation, survival, adhesion, migration, and differentiation), Nrf2 pathway (a key regulator of a variety of genes that are involved in the detoxi-

fication of electrophiles and ROS and the repair or removal of some of their damage products), Wnt/ $\beta$ -catenin pathway (plays a pivotal role in the regulation of cell proliferation, survival, and apoptosis), EGR-1 pathway (plays vital role in regulating growth, differentiation, and apoptosis in many cell types via the regulation of over 30 genes). Curcumin has a poor bio-availability which limits its therapeutic efficacy, and extensive research is needed to deal with the factors that cause poor bio-availability of curcumin. Besides, various analogs of curcumin and different formulations such as adjuvants, nanoparticles, and liposomes, must be be searched extensively in order to obtain its maximum efficacy and facilitate the successful prevention and treatment of cancer (Kunnumakkara, Bordoloi, Harsha, Banik, Gupta, & Aggarwal, 2017a).

There are some reports on the cytotoxic and the synergistic effects of cisplatin and curcumin either as solution or their nanosome/liposome forms on both HepG2 and HeLa cells. Ma et al., (2015) evaluated the efficacy of electrospun nanofibers co-loaded with cisplatin and curcumin to prevent local recurrence of cervical cancer after surgery. The combination of cisplatin with curcumin showed a synergetic effect on growth inhibition and apoptosis induction in HeLa cells and nanofiber-based local combination chemotherapy was more effective and less toxic than systemic combination chemotherapy for the prevention of U14 cervical cancer recurrence in mice, which may indicate its great clinical potential in the future. Chang et al., (2018) showed a combination strategy using co-loaded liposomes with cisplatin and curcumin to have the higher anti-tumor activity in vitro against HepG2 cells. They suggested that this combinational application might effectively deliver and release cisplatin and curcumin to HepG2 cells to overcome the unsatisfactory clinical outcome of cisplatin monotherapy.

## CONCLUSION

In conclusion, our study shows that there are no negative interactions between curcumin and cisplatin in terms of cell viability and curcumin-cisplatin combination could be useful therapeutic agent for human cervical and hepatocellular carcinoma and add a new perspective to anticancer treatment. These findings suggest that curcumin may become as promising therapeutic candidate to increase the anticancer effects and to decrease toxicity of cisplatin in chemotherapy. However, due to curcumin having poor solubility and low bioavailability, new formulations such as nano-particles and nano-emulsion should be integrated into treatment. Our studies may thus be extended to reveal the effects of phenolic compounds including curcumin on cancer and combined with antineoplastic drugs in different doses.

**Peer-review:** Externally peer-reviewed.

**Author Contributions:** Conception/Design of Study- M.B., S.A.D., N.B.; Data Acquisition- M.B., S.A.D.; Data Analysis/Interpretation- M.B., S.A.D.; Drafting Manuscript- M.B., S.A.D.; Critical Revision of Manuscript- S.A.D., N.B.; Final Approval and Accountability- M.B., S.A.D., N.B.; Technical or Material Support- M.B., S.A.D., N.B.; Supervision- S.A.D.

**Conflict of Interest:** The authors have no conflict of interest to declare.

**Financial Disclosure:** Authors declared no financial support.

## REFERENCES

- Abdel-Lateef, E., Mahmoud, F., Hammam, O., El-Ahwany, E., El-Wakil, E., Kandil, S. ... Hassenein H. (2016). Bioactive chemical constituents of *Curcuma longa* L. rhizomes extract inhibit the growth of human hepatoma cell line (HepG2). *Acta pharmaceutica (Zagreb, Croatia)*, 66, 387–398.
- Adahoun, M. A., Al-Akhras, M. H., Jaafar, M. S., & Bououdina, M. (2017). Enhanced anti-cancer and antimicrobial activities of curcumin nanoparticles. *Artificial Cells, Nanomedicine and Biotechnology*, 45(1), 98–107.
- Aggarwal, B., Prasad, S., Sung, B., Krishnan, S., & Guha, S. (2013). Prevention and treatment of colorectal cancer by agents from mother nature. *Current Colorectal Cancer Reports*, 9(1), 37–56.
- Aggarwal, B. B., Kumar, A., & Bharti, A. C. (2003). Anticancer potential of curcumin: Preclinical and clinical studies. *Anticancer Research*, 23, 363–398.
- Anand, P., Kunnumakkara, A. B., Newman, R. A. & Aggarwal, B. B. (2007). Bioavailability of curcumin: problems and promises. *Molecular pharmaceutics*, 4, 807–818.
- Baharuddin, P., Satar, N., Fakiruddin, K. S., Zakaria, N., Lim, M. N., Yusoff, N. M. ... Yahaya, B.H. (2016). Curcumin improves the efficacy of cisplatin by targeting cancer stem-like cells through p21 and cyclin D1-mediated tumour cell inhibition in non-small cell lung cancer cell lines. *Oncology Reports*, 35, 13–25.
- Bansal, S. S., Goel, M., Aqil, F., Vadhanam, M. V. & Gupta, R. C. (2011). Advanced drug-delivery systems of curcumin for cancer chemoprevention. *Cancer Prevention Research*, 4(8), 1158–1171.
- Bulboacă, A. E., Porfire, A. S., Tefas, L. R., Boarescu, P. M., Bolboacă, S. D., Stănescu, I. C., Bulboacă, A. C., Dogaru G. (2009). Liposomal curcumin is better than curcumin to alleviate complications in experimental diabetic mellitus. *Molecules*, 24(5), 846.
- Cao, H., Diao, L. M., & Xia, D. (2008). Effects of curcumin combined with cisplatin on the proliferation and apoptosis of human lung cancer cell line A549 in vitro. *Medical Journal of Wuhan University*, 29, 213–217.
- Chen, J., Xu, T., & Chen, C. (2015). The critical roles of miR-21 in anti-cancer effects of curcumin. *Annals of Translational Medicine*, 3(21), 330–337.
- Cheng, Y., Zhao P., Wu, S., Yang, T., Chen, Y., Zhang, X. ... Xiang, G. (2018). Cisplatin and curcumin co-loaded nano-liposomes for the treatment of hepatocellular carcinoma. *International Journal of Pharmaceutics*, 545(1–2), 261–273.
- Çikrikçi, S., Mozioglu, E., & Yılmaz, H. (2008). Biological activity of curcuminoids isolated from *Curcuma longa*. *Records of Natural Products*, 2(1), 19–24.
- Ding, L., Ma, S., Lou, H., Sun, L., & Ji, M. (2015). Synthesis and biological evaluation of curcumin derivatives with water-soluble groups as potential antitumor agents: An in vitro investigation using tumor cell lines. *Molecules*, 20, 21501–21512.
- Dugbartey, G. J., Peppone, L. J., & de Graaf, I. A. (2016). An integrative view of cisplatin-induced renal and cardiac toxicities: Molecular mechanisms, current treatment challenges and potential protective measures. *Toxicology*, 371, 58–66.
- Falzone, L., Salomone, S., & Libra, M. (2018). Evolution of cancer pharmacological treatments at the turn of the third millennium. *Frontiers in Pharmacology*, 9, 1300–1326.
- Florea, A. M., & Busselberg, D. (2011). Cisplatin as an anti-tumor drug: Cellular mechanisms of activity, drug resistance and induced side effects. *Cancers (Basel)*, 3(1), 1351–1371.
- Gupta, S. C., Patchva, S., & Aggarwal, B. B. (2013). Therapeutic roles of curcumin: Lessons learned from clinical trials. *American Association of Pharmaceutical Scientists journal*, 15, 195–218.
- Guzman, M. N. (2019). Combinations of the antioxidants sulforaphane or curcumin and the conventional antineoplastics cisplatin or doxorubicin as prospects for anticancer chemotherapy. *European Journal of Pharmacology*, 859, 172513.
- Hansen, S. E., & Nielsen, K. B. (1989). Re-examination and further development of a precise and rapid dye method for measuring cell growth/cell kill. *Journal of Immunological Methods*, 119, 203–210.
- Hewlings, S. J., & Kalman, D. S. (2017). Curcumin: A review of its effects on human health. *Foods*, 6(10), 92–103.
- Koohpar, Z. K., Entezari, M., Movafagh, A., & Hashemi, M. (2015). Anticancer activity of curcumin on human breast adenocarcinoma: role of Mcl-1 gene. *Iranian Journal of Cancer Prevention*, 8(3), 2331–2335.
- Kunnumakkara, A. B., Bordoloi, D., Harsha, C., Banik, K., Gupta, S. C., & Aggarwal, B.B. (2017a). Curcumin mediates anticancer effects by modulating multiple cell signaling pathways. *Clinical science (London, England : 1979)*, 131(15), 1781–1799.
- Kunnumakkara, A. B., Bordoloi, D., Padmavathi, G., Monisha, J., Roy, N. K., Prasad, S., & Aggarwal, B. B. (2017b). Curcumin, the golden nutraceutical: Multitargeting for multiple chronic diseases. *British Journal of Pharmacology*, 174, 1325–1348.
- Li, P., Qin, H., & Li, X-J. (2019). The effect of curcumin on the apoptosis of lung cancer cells by regulating DJ-1-PTEN/PI3K/AKT signaling. *International journal of Clinical and Experimental Medicine*, 12(7), 8739–8745.
- Ma, Y., Wang, X., Zong, S., Zhang, Z., Xi.e Z., Huang, Y. ... Jing, X. (2015). Local, combination chemotherapy in prevention of cervical cancer recurrence after surgery by using nanofibers co-loaded with cisplatin and curcumin. *RSC Advances*, 5, 106325–106332.
- Menon, V. P., & Sudheer, A. R. (2007). Antioxidant and anti-inflammatory properties of curcumin. *Advances in Experimental Medicine and Biology*, 595, 105–125.
- Moron, B. E., Montano, J. M. C., Salvador, J., Robles, A., & Lazaro, M. L. (2010). The dark side of curcumin. *International Journal of Cancer*, 126, 1771–1775.
- Mosalam, E. M., Zidan, A. A. A., Mehanna, E. T., Mesbah, N. M., & Abo-Elmatty, D. M. (2020). Thymoquinone and pentoxifylline enhance the chemotherapeutic effect of cisplatin by targeting Notch signaling pathway in mice. *Life Sciences*, 244, 117299.
- Mosmann, T. (1983). Rapid colorimetric assay for cellular growth and survival: Application to proliferation and cytotoxicity assays. *Journal of Immunological Methods*, 65, 55–63.
- Nagpal, M., & Sood, D. (2013). Role of curcumin in systemic and oral health: An overview. *Journal of Natural Science, Biology and Medicine*, 4(1), 3–7.
- Nurcahyanti, A. D. R., & Wink, M. (2016). L-Canavanine potentiates the cytotoxicity of doxorubicin and cisplatin in arginine deprived human cancer cells. *PeerJ*, 4, 1542–1560.
- Perrone, D., Ardito, F., Giannatempo, G., Dioguardi, M., Troiano, G., Russo, L. L. ... Lo Muzio L. (2015). Biological and therapeutic activities and anticancer properties of curcumin. *Experimental and Therapeutic Medicine*, 10(5), 1615–1623.
- Rosenberg, B. (1985). Fundamental studies with cisplatin. *Cancer*, 55, 2303–2316.
- Roy, M., & Mukherjee, S. (2014). Reversal of resistance towards cisplatin by curcumin in cervical cancer cells. *Asian Pacific Journal of Cancer Prevention (APJCP)*, 15, 1403–1410.
- Shehzad, A., Lee, J., & Lee, Y.S. (2013). Curcumin in various cancers. *Biofactors*, 39(1), 56–68.
- Sukumari-Ramesh, S., Bentley, J. N., Laird, M. D., Singh, N., Vender, J. R., Dhandapani, K. M. (2011). Dietary phytochemicals induce p53- and caspase-independent cell death in human neuroblastoma cells. *International Journal of Developmental Neuroscience*, 29, 701–710.

- Taner, G., Aydin, S., Bacanli, M., Sarigol, Z., Sahin, T., Basaran, A. A., & Basaran, N. (2014). Modulating effects of pycnogenol(R) on oxidative stress and DNA damage induced by sepsis in rats. *Phytotherapy Research*, 28(11), 1692–1700.
- Toric, J., Markovic, A. K., Brala, C. J., & Barbaric, M. (2019). Anticancer effects of olive oil polyphenols and their combinations with anti-cancer drugs. *Acta pharmaceutica (Zagreb, Croatia)*, 69, 461–482.
- Wang, Y.-T., Liu, H.-S., & Su, C.-L. (2014). Curcumin-enhanced chemosensitivity of FDA-approved platinum (II)-based anti-cancer drugs involves downregulation of nuclear endonuclease G and NF- $\kappa$ B as well as induction of apoptosis and G2/M arrest. *International Journal of Food Sciences and Nutrition*, 65, 368–374.
- Yang, I. H., Shin, J. A., & Cho, S. D. (2014). Pycnogenol induces nuclear translocation of apoptosis-inducing factor and caspase-independent apoptosis in MC-3 human mucoepidermoid carcinoma cell line. *Journal of Cancer Prevention*, 19(4), 265–272.
- Zhang, H., Tianyu, Y., Lianji, W., Hui, W., Dan, F., & Chunshun, J. (2013). Curcumin enhances the effectiveness of cisplatin by suppressing CD133+cancer stem cells in laryngeal carcinoma treatment. *Experimental and Therapeutic Medicine*, 6, 1317–1321.
- Zhang, J. R., Lu, F., Lu, T., Dong, W. H., Li, P., Liu, N. ... Ji, C. Y. (2014). Inactivation of FoxM1 transcription factor contributes to curcumin-induced inhibition of survival, angiogenesis, and chemosensitivity in acute myeloid leukaemia cells. *Journal of Molecular Medicine*, 92, 1319–1330.
- Zhang, S., Yong, Q., Wu, X., & Liu, X. (2014). [Synergism inhibition of curcumin combined with cisplatin on T24 bladder carcinoma cells and its related mechanism]. *Zhong Yao Cai*, 37, 2043–2046.
- Zou, J., Zhu, L., Jiang, X., Wang, Yang, Wang, Yue, Wang, X., & Chen, B. (2018). Curcumin increases breast cancer cell sensitivity to cisplatin by decreasing FEN1 expression. *Oncotarget*, 9, 11268–11278.

# Study of the beneficial effect of vanadium sulfate on the liver of experimental diabetic rats

Sevim Tunalı<sup>1</sup> , Ayşegül Peksel<sup>2</sup> , İnci Arisan<sup>2</sup> , Refiye Yanardağ<sup>1</sup> 

<sup>1</sup>Istanbul University-Cerrahpaşa, Faculty of Engineering, Department of Chemistry, Istanbul, Turkey

<sup>2</sup>Yıldız Technical University, Arts and Science Faculty, Department of Chemistry, Istanbul, Turkey

**ORCID IDs of the authors:** S.T. 0000-0003-3363-1290; A.P. 0000-0003-3881-8513; İ.A. 0000-0001-8706-0097; R.Y. 0000-0003-4185-4363

**Cite this article as:** Tunalı, S., Peksel, A., Arisan, İ., & Yanardağ, R. (2020). Study of the beneficial effect of vanadium sulfate on the liver of experimental diabetic rats. *Istanbul Journal of Pharmacy*, 50 (3), 211-215.

## ABSTRACT

**Background and Aims:** Liver is a tissue that is negatively affected by diabetes mellitus (DM). This is due to its central function in the regulation of carbohydrate metabolism. Vanadium salts, which have insulinomimetic effects, have been found to stimulate glycogenesis and glycolysis, as well as to inhibit glycogenolysis and lipolysis. The aim of this study is to evaluate the effect of vanadium sulfate (VS) on biochemical changes in liver tissue of diabetic rats.

**Methods:** Randomly selected 6.0 - 6.5 months Swiss Albino rats were separated into two diabetic and two control groups. Group I: non treated animals. Group II: non treated animals orally administered VS (100mg/kg/day for 60 days), group III: STZ-induced diabetic animals (65 mg/kg with intraperitoneally) and group IV: STZ-induced diabetic animals administered VS (at same dose and time). Antioxidant enzymes such as catalase, superoxide dismutase, glutathione peroxidase, glutathione reductase, glutathione-S-transferase, as well as alkaline phosphatase, glucose-6-phosphate dehydrogenase, carbonic anhydrase, myeloperoxidase, paraoxonase and lactate dehydrogenase were estimated in liver tissue homogenates of the groups.

**Results:** Liver catalase, superoxide dismutase, glutathione peroxidase, glutathione reductase, glutathione-S-transferase, lactate dehydrogenase, carbonic anhydrase and paraoxonase activities were decrease, but alkaline phosphatase, glucose-6-phosphate dehydrogenase and myeloperoxidase activities were increase in diabetic rats when compared to normal rats.

**Conclusion:** Results show that VS restored altered parameters in the liver tissue and prevented oxidative stress in diabetic rats.

**Keywords:** Liver, vanadium sulfate, diabetes mellitus, hyperglycaemia, antioxidant enzymes, streptozotocin, oxidative stress

## INTRODUCTION

Hyperglycaemia is the primary clinical indication of diabetic manifestation and is responsible for the development of many chronic diabetic complications. It is associated with long-term microvascular and macrovascular damage, with the dysfunction and failure of various organs, leading to atherosclerosis, blindness, renal failure and neuropathy (Hussain, Claussen, Ramachandran, & Williams, 2007). Diabetic complications induced by hyperglycaemia are due to free radical generation, thus perturb cellular antioxidant defence systems and damage cells. In a typical diabetic profile, the formation of free radicals is disproportionate. Oxidation of glucose, non-enzymatic gly-

cation of proteins, increased transcription factors and oxidative degradation of glycosylated proteins are the main responsible factors for this occurrence (Pari, & Saravanan, 2007). Particularly high free radical development and weakening of the antioxidant defence mechanism can cause damage to cell organelles and enzymes, as well as lipid peroxidation and increased insulin resistance (Maritim, Sanders, & Watkins, 2003).

The liver has a central function in regulating carbohydrate metabolism by maintaining blood sugar level and the continuous supply of glucose to meet the needs of other organs. A significant part of liver damage is caused by reactive oxygen species (ROS) and  $\beta$  cell dysfunction, which in turn is damaged by

## Address for Correspondence:

Sevim TUNALI, e-mail: stunalı@istanbul.edu.tr

Submitted: 30.06.2020

Accepted: 18.07.2020

Published Online: 09.12.2020

This work is licensed under a Creative Commons Attribution 4.0 International License.





autoimmune and inflammatory reactions (Molehin, & Oloyede, 2018).

Different types of insulin arrangements and synthetic medical remedies are available for clinical use in diabetic patients. Unfortunately, none of the available treatment strategies restores the release of physiological insulin, or has an effect in healing the cellular lesions caused by diabetes. As current treatments produce undesirable side effects and contraindications, the necessity of new approaches to DM treatment has arisen (Wagenaar, Kuck, & Hoekstra, 1999; Luft, Schmülling, & Eggstein, 1978). A variety of vanadium compounds have been shown to have insulinomimetic properties in animal model and cell culture systems. They exhibit great potential for the pharmacotherapy of diabetes (Yanardag, et al., & Bolkent, 2009; Zhang, Yang, Wang, & Crans, 2006).

Vanadium is an essential element which is responsible of regulation in biological systems. Just like other essential micronutrients, this ultra-trace element is required in small quantities for the cells to maintain their normal functions and growth and development of healthy organisms. It affects the activity of enzymes, adjust the second messengers actions, some signal transduction cascades and carbohydrate metabolism, mimics insulin and growth factor activities, induce protein tyrosine kinase activity, decrease phosphotyrosine phosphatases and regulate expression of genes (Chakraborty et al., 2007). Vanadium ions and its complexes exert various insulinomimetic and anti-diabetic properties, for instance increasing glucose transport in the liver tissue and skeletal muscle, stimulating the glycogen synthesis and lipogenesis as well as adipocyte metabolism, and inhibiting lipolysis and protein catabolism (Gao et al., 2006). Previous investigations indicate that vanadium compounds inhibit protein tyrosine phosphatase activity (an enzyme involved in the direct phosphorylation of insulin receptor substrate 1, stimulation of insulin receptor and cytosolic non-receptor tyrosine kinase activity, as well as the activation of phosphatidylinositol 3 kinase) leading to glucose transporter 4 (GLUT4) translocation (Kawabe, Yoshikawa, Adachi, & Sakurai, 2006).

The present study was carried out to evaluate the effect of vanadium sulfate (VS) on biochemical changes in liver tissue of diabetic rats. Our aim is to focus on the beneficial effect of VS on the oxidatively damaged liver tissue of streptozotocin (STZ)-induced diabetic rats.

## MATERIALS AND METHODS

### Experimental rats

In this study, 6.0-6.5 month old male rats were used. All animals were kept in cages at standard conditions.

### Induction of diabetes

The rats were made diabetic with a single dose of streptozotocin (STZ). STZ were (65 mg/kg) dissolved in a freshly solution (citrate buffer 0.01 M pH=4.5) intraperitoneally (Junod, Lambert, Stauffacher, & Renold, 1969). The data related with blood glucose concentrations were are presented in our previous study (Koyuturk, Tunali, Bolkent, & Yanardag, 2005).

### Experimental design

The experiments were examined and confirmed by the Local Institute's Animal Care and Use Committees of Istanbul University. Four groups were randomly created; group I untreated, nondiabetic controls (n=13); group II nondiabetic control animals administered VS (n=5); group III diabetes induced animals with STZ (n=11); group IV STZ-induced diabetic animals administered with VS (n=11). VS was given (100 mg/kg/day) for 60 days without interruption by gavage technique. Blood glucose concentrations were determined according to the o-toluidine method (Relander, & Rähä, 1963).

### Preparation of liver tissue homogenates

At 60 days all fasted animals were sacrificed under anesthesia. Liver tissues were taken, washed with cold solution (0.9% saline) and frozen until needed for study at -76 °C. After made 10% (w/v) homogenate with glass equipment, clear supernatants were obtained by centrifugation and used for analysis of enzymatic antioxidants, tissue enzyme activities and protein level estimation.

### Assay of liver enzymes activities and protein level

Freshly prepared homogenates were used to assay for enzyme activities as follows: catalase (CAT) (Aebi, 1984), superoxide dismutase (SOD) (Mylorie, Collins, Umbles, & Kyle, 1986), glutathione peroxidase (GPx) (Paglia, & Valentine, 1967), glutathione reductase (GR) (Beutler, 1971), glutathione-S-transferase (GST) (Habig, 1981), alkaline phosphatase (ALP) (Walter, & Schult, 1974), glucose-6-phosphate dehydrogenase (G6PD) (Betke et al., 1967), lactate dehydrogenase (LDH) (Wroblewski, 1957), carbonic anhydrase (CA) (Verpoorte, 1967), myeloperoxidase (MPO) (Wei, & Frenkel, 1991) and paraoxonase (PON) (Furlong, Richter, Seidel, & Motulsky, 1988). Liver protein level was measured by the method of Lowry using bovine serum albumin as standard (Lowry, Rosebrough, Farr, & Randall, 1951).

### Statistical data

The unpaired Student's t-test and analysis of variance (ANOVA) were used to analyse biochemical results calculated with statistical computer package (NCSS). Mann-Whitney test was used for comparison between control and experimental animals. The results were performed as mean  $\pm$  SD.  $p < 0.05$  values were accepted as significant.

## RESULTS

Table 1 shows the activities of antioxidant enzymes in all groups. A significant decrease in CAT, SOD, GPx, GR and GST activities in liver tissue of STZ-diabetic group compared to control group ( $^aP < 0.0001$ ) was observed. The activities of the enzymes were increased in diabetic group given VS compared to non-treated diabetic group ( $^bP < 0.0001$ ). A significant difference was observed between all groups ( $P_{ANOVA} = 0.0001$ ; Table 1).

Liver tissue ALP, G6PDH and LDH activities were significantly increased ( $^aP < 0.0001$ ) in diabetic rats as compared to the control group. Orally given VS was meaningfully reduced liver ALP, G6PDH and LDH activities ( $^bP < 0.0001$ ,  $^cP < 0.001$ ) when compared to diabetic rats. All enzymatic activities were observed to have significant difference between the groups ( $P_{ANOVA} = 0.0001$ ; Table 2).

**Table 1. Liver CAT, SOD, GPx, GR and GST activities of control and diabetic rats.\***

Groups	CAT (U/mg protein)	SOD (U/mg protein)	GPx (U/gprotein)	GR (U/mg protein)	GST (U/mg protein)
Control	2733.25±65.34	2.91±0.39	3632.18±69.5	0.0232±0.0008	3.85±0.04
Control + VS	3080.93±118.86	1.82±0.32	3351.84±31.62	0.0188±0.0006	4.37±0.06
Diabetic	1526.74±50.31 <sup>a</sup>	1.92±0.14 <sup>a</sup>	2187.58±65.79 <sup>a</sup>	0.0130±0.0003 <sup>a</sup>	2.29±0.06 <sup>a</sup>
Diabetic + VS	2722.35±107.18 <sup>b</sup>	3.20±0.15 <sup>b</sup>	3890.72±45.92 <sup>b</sup>	0.0250±0.0003 <sup>b</sup>	3.80±0.06 <sup>b</sup>
P <sub>ANOVA</sub>	0.0001	0.0001	0.0001	0.0001	0.0001

\*Mean ± SD, <sup>a</sup>P < 0.0001 compared to control rats, <sup>b</sup>P < 0.0001 compared to diabetic rats.

**Table 2. Liver ALP, G6PDH and LDH activities of control and diabetic rats\*.**

Groups	ALP (U/mg protein)	G6PDH (U/g protein)	LDH (U/mg protein)
Control	4.40±0.88	5.10±0.40	38.36±3.71
Control + VS	7.53±1.32	6.25±0.12	26.68±7.32
Diabetic	8.24±0.80 <sup>a</sup>	7.90±0.28 <sup>a</sup>	119.57±7.99 <sup>a</sup>
Diabetic + VS	4.94±0.48 <sup>b</sup>	5.68±0.18 <sup>b</sup>	87.61±13.64 <sup>c</sup>
P <sub>ANOVA</sub>	0.0001	0.0001	0.0001

\*Mean ± SD, <sup>a</sup>P < 0.0001 compared to control rats, <sup>b</sup>P < 0.0001 compared to diabetic rats, <sup>c</sup>P < 0.001 compared to diabetic rats.

Liver CA, MPO and PON activities of control and diabetic rats are presented in Table 3. The liver CA and PON activities at 60 days of diabetes induction showed a significant decrease when compared to control rats (<sup>a</sup>P < 0.0001). Treatment with VS significantly reversed the altered activities of CA and PON of the diabetic rats in comparison to non-treated diabetic animals (<sup>b</sup>P < 0.0001). On the other hand, experimentally-induced diabetes caused a mean increase in liver MPO activity (<sup>a</sup>P < 0.0001) in comparison to control animals. Orally vanadyl treated diabetic group demonstrated significant decrease in MPO activity when compared with STZ-induced diabetic group (<sup>b</sup>P < 0.0001). A significant difference was observed between treated and non-treated animals (P<sub>ANOVA</sub> = 0.0001; Table 3).

**Table 3. Liver CA, MPO and PON activities of control and diabetic rats.\***

Groups	CA (U/mg protein)	MPO (U/g protein)	PON (U/g protein)
Control	7.58±1.42	0.41±0.09	21.22±2.44
Control + VS	4.00±0.94	0.57±0.01	20.38±1.06
Diabetic	3.98±0.50 <sup>a</sup>	0.60±0.01 <sup>a</sup>	15.93±0.55 <sup>a</sup>
Diabetic + VS	6.96±0.86 <sup>b</sup>	0.26±0.03 <sup>b</sup>	19.12±1.50 <sup>b</sup>
P <sub>ANOVA</sub>	0.0001	0.0001	0.0001

\*Mean ± SD, <sup>a</sup>P < 0.0001 compared to control rats, <sup>b</sup>P < 0.0001 compared to diabetic rats.

## DISCUSSION

Oxidative stress, resulting from the production of uncontrolled reactive oxygen species (ROS) is a condition that is attributed and accepted in the aetiology of diabetes. Alterations in the antioxidant enzymes activities makes tissues defenceless to oxidative stress and this leads to the onset and progression of diabetes complications (Pandey & Rizvi, 2009; Lipinski, 2001).

Increased ROS production due to persistent hyperglycaemia may lead to a decrease in hepatic antioxidant enzyme activities and depletion of hepatic antioxidants. Treatment with VS significantly improved CAT, SOD and GSH related enzymatic activities (GPx, GR and GST) in hepatic system. The observed results may be attributable to the antioxidant activity of VS.

It was found in our previous work that VS treatment alleviated some liver tissue alterations such as decreased level of reduced glutathione (GSH) that are associated with diabetic state (Koyuturk et al., 2005). This could indicate an increase in activities of antioxidant enzymes of the liver tissue, suggests the normal functioning and protective activity of vanadium and supports the hepatoprotective efficacy of VS.

ALP is an enzyme indicator of hepatic lesion and a biomarker for acute hepatotoxicity in type 1 DM (Rodríguez, Plavnik, & Tolosa de Talamoni, 2018; Kanikarla-Marie & Jain, 2015; Liang et al., 2015). The increased activity of liver ALP activity suggest defective utilization of glucose. The administration of VS in our study normalized the ALP activity in the diabetic liver tissue.

The fate of glucose through the pentose phosphate pathway has not been well characterized, more so there is conflicting evidence about the activity of G6PDH in DM. Gupte et al., (2009) demonstrated that the expression of protein level and activity of G6PDH is much higher in the liver in the type 2 DM Zucker obese rats (Gupte et al., 2009). Accordingly, in the present study, we observed an increased G6PDH activity in diabetic liver tissue. The higher G6PDH activities drive NADPH - a fuel of NADPH oxidase, and O<sub>2</sub><sup>-</sup> production. The studies suggest that this is one of the reasons of increased oxidative stress in multi-organ dysfunction and damage in experimental diabetic rats (Gupte et al., 2009; Gupte et al., 2005; Matsui et al., 2005). In our study, oral vanadium supplementation decreased significantly the activity of this enzyme in hepatic tissue, thus highlighting another possible mechanism of anti diabetogenic activity.

The lactic acid formation from pyruvate is catalysed by LDH, a cytosolic enzyme in anaerobic glycolysis pathway. In hyperglycemic state, a significant increase in LDH activity was found due to impaired glucose-induced insulin secretion in diabetes (Ainscow, Zhao & Rutter, 2000). The LDH system reflects NAD<sup>+</sup>/NADH ratio indicated by the lactate/pyruvate ratio of the hepatocyte cytosol (Sekar, Sivagnanam & Subramanian, 2005). Similarly, in the present study, a significant increase in LDH activity of was observed in the diabetic group. A significant reduction in the LDH activity was observed due to the regulation of the ratio of NAD<sup>+</sup>/NADH by oxidation of blood glucose, in VS given diabetic rats.

CA is involved in many important physiological and pathological conditions, and provides HCO<sub>3</sub><sup>-</sup> as a substrate for pyruvate carboxylase (Ismail, 2018). It is reported that the concentration of CA-III is reduced in the liver and serum of STZ-induced DM adult male rats (Nishita, Igarashi, & Asari, 1995). In our study, oral VS treatment increased the CA activity in diabetic rats. This increase may lead to increased hepatic glucose production by the presence of these substrates.

Increased MPO production in neutrophilic granulocytes can produce strong oxidants (such as HOCl, HOBr), provoke oxidation of nitric oxide and nitration of tyrosine. This MPO-derived reactive species could eventually mediate the development of oxidative damages in liver tissue. Wiersma et al., (2008) suggested that type 2 DM is associated with mildly increased plasma levels of MPO. In our research, we observed a significant increase in MPO activity in the diabetic tissue. Antioxidant effect of vanadium decreased MPO activity and this suggest a reduction in oxidative stress and subsequent neutrophil production.

PON1 plays an important role in the regulation of glucose metabolism. In the muscles, GLUT4 expression is upregulated by PON1 in an insulin receptor-independent manner (Koren-Gluzer, Aviram & Hayek, 2013). Besides that, PON1 regulates directly some important enzymes of glycolytic pathway, (Meneses, Silvestre, Sousa-Lima, & Macedo, 2019; Koren-Gluzer et al., 2013; Khersonsky & Tawfik, 2006). Our data showed that VS significantly increased the activity of PON, an enzyme mainly synthesized in the liver tissue.

## CONCLUSION

In conclusion, the findings of the current study demonstrate that VS may provide effective protection against oxidative damage in liver tissue of STZ-induced diabetic rats. This suggests that vanadium is able to ameliorate the enzymatic antioxidant defence systems and prevent peroxidation in tissue. VS significantly improved metabolic alterations, oxidative and inflammatory status in liver tissue through its antidiabetic, anti-oxidative and anti-inflammatory effects. Therefore, VS could be an ideal auxiliary treatment option for DM.

**Peer-review:** Externally peer-reviewed.

**Author Contributions:** Conception/Design of Study- S.T., A.P., İ.A., R.Y.; Data Acquisition- S.T., A.P.; Data Analysis/Interpretation- S.T., A.P., İ.A., R.Y.; Drafting Manuscript- S.T., A.P., R.Y.; Critical Revision of Manuscript-

S.T., R.Y.; Final Approval and Accountability- S.T., A.P., İ.A., R.Y.; Technical or Material Support- S.T., A.P.; Supervision- R.Y.

**Conflict of Interest:** The authors have no conflict of interest to declare.








**Financial Disclosure:** Authors declared no financial support.

## REFERENCES

- Aebi, H. (1984). Catalase in vitro. In: Methods of enzymatic analysis, 2nd Edition, Vol.2, Bergmeyer H.U. (Ed.), pp. 121–126.
- Ainscow, E. K., Zhao, C., & Rutter, G. A. (2000). Acute overexpression of lactate dehydrogenase-A perturbs beta-cell mitochondrial metabolism and insulin secretion. *Diabetes*, 49, 1149–1155. <https://doi.org/10.2337/diabetes.49.7.1149>
- Betke, K., Beutler, E., Brewer, G. J., Kirkman, H. N., Luzzatto, L., Motulsky, A. G., Ramot, B., Siniscalco, M. (1967). Standardization of procedures for the study of glucose-6-phosphate dehydrogenase. Report of a WHO Scientific Group. *World Health Organization Technical Report Series*, 366, 1–53.
- Beutler, E. (1971). Red cell metabolism. A manual of biochemical methods, vol. 12. London: Academic Press.
- Chakraborty, T., Chatterjee, A., Rana, A., Dhachinamoorthi, D., Kumar P, A., & Chatterjee, M. (2007). Carcinogen-induced early molecular events and its implication in the initiation of chemical hepatocarcinogenesis in rats: chemopreventive role of vanadium on this process. *Biochimica et Biophysica Acta*, 1772, 48–59. <https://doi.org/10.1016/j.bbadis.2006.10.019>
- Furlong, C. E., Richter, R. J., Seidel, S. L., & Motulsky, A. G. (1988). Role of genetic polymorphism of human plasma paraoxonase/arylesterase in hydrolysis of the insecticide metabolites chlorpyrifos oxon and paraoxon. *American Journal of Human Genetics*, 43, 230–238.
- Gao, L. H., Liu, W. P., Wang, B. L., Li, L., Xie, M. J., Li, Y. R., Chen, Z. H., & Chen, X. Z. (2006). Effects of bis(alpha-furancarboxylato) oxovanadium(IV) on non-diabetic and streptozotocin-diabetic rats. *Clinica Chimica Acta; International Journal of Clinical Chemistry*, 368, 173–178. <https://doi.org/10.1016/j.cca.2005.12.028>
- Gupte, R. S., Floyd, B. C., Kozicky, M., George, S., Ungvari, Z. I., Neito, V., Wolin, M. S., & Gupte, S. A. (2009). Synergistic activation of glucose-6-phosphate dehydrogenase and NAD(P)H oxidase by Src kinase elevates superoxide in type 2 diabetic, Zucker fa/fa, rat liver. *Free Radical Biology & Medicine*, 47, 219–228. <https://doi.org/10.1016/j.freeradbiomed.2009.01.028>
- Gupte, S. A., Kaminski, P. M., Floyd, B., Agarwal, R., Ali, N., Ahmad, M., Edwards, J., & Wolin, M. S. (2005). Cytosolic NADPH may regulate differences in basal Nox oxidase-derived superoxide generation in bovine coronary and pulmonary arteries. *American Journal of Physiology. Heart and Circulatory Physiology*, 288, H13–H21. <https://doi.org/10.1152/ajpheart.00629.2004>
- Habig, W. H., & Jakoby, W. B. (1981). Assays for differentiation of glutathione S-transferases. *Methods in Enzymology*, 77, 398–405. [https://doi.org/10.1016/s0076-6879\(81\)77053-8](https://doi.org/10.1016/s0076-6879(81)77053-8)
- Hussain, A., Claussen, B., Ramachandran, A., & Williams, R. (2007). Prevention of type 2 diabetes: a review. *Diabetes Research and Clinical Practice*, 76, 317–326. <https://doi.org/10.1016/j.diabres.2006.09.020>
- Ismail I. S. (2018). The role of carbonic anhydrase in hepatic glucose production. *Current Diabetes Reviews*, 14, 108–112. <https://doi.org/10.2174/1573399812666161214122351>
- Junod, A., Lambert, A. E., Stauffacher, W., & Renold, A. E. (1969). Diabetogenic action of streptozotocin: relationship of dose to metabolic response. *The Journal of Clinical Investigation*, 48, 2129–2139. <https://doi.org/10.1172/JCI106180>

- Kanikarla-Marie, P., & Jain, S. K. (2015). Role of hyperketonemia in inducing oxidative stress and cellular damage in cultured hepatocytes and type 1 diabetic rat liver. *Cellular Physiology and Biochemistry: International Journal of Experimental Cellular Physiology, Biochemistry, and Pharmacology*, 37, 2160–2170. <https://doi.org/10.1159/000438573>
- Kawabe, K., Yoshikawa, Y., Adachi, Y., & Sakurai, H. (2006). Possible mode of action for insulinomimetic activity of vanadyl(IV) compounds in adipocytes. *Life Sciences*, 78, 2860–2866. <https://doi.org/10.1016/j.lfs.2005.11.008>
- Khersonsky, O., & Tawfik, D. S. (2006). The histidine 115-histidine 134 dyad mediates the lactonase activity of mammalian serum paraoxonases. *The Journal of Biological Chemistry*, 281, 7649–7656. <https://doi.org/10.1074/jbc.M512594200>
- Koren-Gluzer, M., Aviram, M., & Hayek, T. (2013). Paraoxonase1 (PON1) reduces insulin resistance in mice fed a high-fat diet, and promotes GLUT4 overexpression in myocytes, via the IRS-1/Akt pathway. *Atherosclerosis*, 229, 71–78. <https://doi.org/10.1016/j.atherosclerosis.2013.03.028>
- Koyuturk, M., Tunali, S., Bolkent, S., & Yanardag, R. (2005). Effects of vanadyl sulfate on liver of streptozotocin-induced diabetic rats. *Biological Trace Element Research*, 104, 233–247. <https://doi.org/10.1385/BTER:104:3:233>
- Liang, T., Zhang, Q., Sun, W., Xin, Y., Zhang, Z., Tan, Y., Zhou, S., Zhang, C., Cai, L., Lu, X., & Cheng, M. (2015). Zinc treatment prevents type 1 diabetes-induced hepatic oxidative damage, endoplasmic reticulum stress, and cell death, and even prevents possible steatohepatitis in the OVE26 mouse model: Important role of metallothionein. *Toxicology Letters*, 233, 114–124. <https://doi.org/10.1016/j.toxlet.2015.01.010>
- Lipinski, B. (2001). Pathophysiology of oxidative stress in diabetes mellitus. *Journal of Diabetes and its Complications*, 15, 203–210. [https://doi.org/10.1016/s1056-8727\(01\)00143-x](https://doi.org/10.1016/s1056-8727(01)00143-x)
- Lowry, O. H., Rosebrough, N. J., Farr, A. L., & Randall, R. J. (1951). Protein measurement with the Folin phenol reagent. *The Journal of Biological Chemistry*, 193, 265–275.
- Luft, D., Schmölling, R. M., & Eggstein, M. (1978). Lactic acidosis in biguanide-treated diabetics: a review of 330 cases. *Diabetologia*, 14, 75–87. <https://doi.org/10.1007/BF01263444>
- Maritim, A. C., Sanders, R. A., & Watkins, J. B., 3rd (2003). Diabetes, oxidative stress, and antioxidants: a review. *Journal of Biochemical and Molecular Toxicology*, 17, 24–38. <https://doi.org/10.1002/jbt.10058>
- Matsui, R., Xu, S., Maitland, K. A., Hayes, A., Leopold, J. A., Handy, D. E., Loscalzo, J., & Cohen, R. A. (2005). Glucose-6 phosphate dehydrogenase deficiency decreases the vascular response to angiotensin II. *Circulation*, 112, 257–263. <https://doi.org/10.1161/CIRCULATIONAHA.104.499095>
- Meneses, M. J., Silvestre, R., Sousa-Lima, I., & Macedo, M. P. (2019). Paraoxonase-1 as a regulator of glucose and lipid homeostasis: Impact on the onset and progression of metabolic disorders. *International Journal of Molecular Sciences*, 20, 4049. <https://doi.org/10.3390/ijms20164049>
- Molehin, O. R., & Oloyede, O. I. (2018). Attenuation of oxidative stress and hepatic damage by white butterfly (*Clerodendrum volubile*) leaves in streptozotocin-induced diabetes in rats. *Journal of Basic and Clinical Physiology and Pharmacology*, 30, 81–89. <https://doi.org/10.1515/jbcpp-2018-0083>
- Mylorie, A. A., Collins, H., Umbles, C., Kyle, J. (1986). Erythrocyte superoxide dismutase activity and other parameters of copper status in rats ingesting lead acetate. *Toxicology and Applied Pharmacology*, 82, 512–520
- Nishita, T., Igarashi, S., & Asari, M. (1995). Determination of carbonic anhydrase-III by enzyme-immunoassay in liver, muscle and serum of male rats with streptozotocin-induced diabetes mellitus. *The International Journal of Biochemistry & Cell Biology*, 27, 359–364. [https://doi.org/10.1016/1357-2725\(94\)00090-x](https://doi.org/10.1016/1357-2725(94)00090-x)
- Paglia, D. E., & Valentine, W. N. (1967). Studies on the quantitative and qualitative characterization of erythrocyte glutathione peroxidase. *The Journal of Laboratory and Clinical Medicine*, 70, 158–169.
- Pandey, K. B., & Rizvi, S. I. (2009). Plant polyphenols as dietary antioxidants in human health and disease. *Oxidative Medicine and Cellular Longevity*, 2, 270–278. <https://doi.org/10.4161/oxim.2.5.9498>
- Pari, L., & Saravanan, R. (2007). Beneficial effect of succinic acid monoethyl ester on erythrocyte membrane bound enzymes and antioxidant status in streptozotocin-nicotinamide induced type 2 diabetes. *Chemico-Biological Interactions*, 169, 15–24. <https://doi.org/10.1016/j.cbi.2007.04.010>
- Rains, J. L., & Jain, S. K. (2011). Oxidative stress, insulin signaling, and diabetes. *Free Radical Biology & Medicine*, 50, 567–575. <https://doi.org/10.1016/j.freeradbiomed.2010.12.006>
- Relander, A., & Riih a C. E. (1963) Differences between the enzymatic and o-toluidine methods of blood glucose determination. *Scandinavian Journal of Clinical and Laboratory* 15, 221-224
- Rodr guez, V., Plavnik, L., & Tolosa de Talamoni, N. (2018). Naringin attenuates liver damage in streptozotocin-induced diabetic rats. *Biomedicine & Pharmacotherapy = Biomedecine & Pharmacotherapie*, 105, 95–102. <https://doi.org/10.1016/j.biopha.2018.05.120>
- Sekar, D. S., Sivagnanam, K., & Subramanian, S. (2005). Antidiabetic activity of Momordica charantia seeds on streptozotocin induced diabetic rats. *Die Pharmazie*, 60, 383–387.
- Verpoorte, J. A., Mehta, S., & Edsall, J. T. (1967). Esterase activities of human carbonic anhydrases B and C. *The Journal of Biological Chemistry*, 242, 4221–4229.
- Wagenaar, L. J., Kuck, E. M., & Hoekstra, J. B. (1999). Troglitazone. Is it all over?. *The Netherlands Journal of Medicine*, 55, 4–12. [https://doi.org/10.1016/s0300-2977\(99\)00021-2](https://doi.org/10.1016/s0300-2977(99)00021-2)
- Walter, W., & Schult, C. (1974). In: *Methods of Enzymatic Analysis*, Vol.2, Bergmeyer H.U., pp. 856-886.
- Wei, H., & Frenkel, K. (1991). In vivo formation of oxidized DNA bases in tumor promoter-treated mouse skin. *Cancer Research*, 51, 4443–4449.
- Wiersma, J. J., Meuwese, M. C., van Miert, J. N., Kastelein, A., Tijssen, J. G., Piek, J. J., & Trip, M. D. (2008). Diabetes mellitus type 2 is associated with higher levels of myeloperoxidase. *Medical Science Monitor : International Medical Journal of Experimental and Clinical Research*, 14, CR406–CR410.
- Wroblewski F. (1957). Clinical significance of serum enzyme alterations associated with myocardial infarction. *American Heart Journal*, 54, 219–224. [https://doi.org/10.1016/0002-8703\(57\)90149-7](https://doi.org/10.1016/0002-8703(57)90149-7)
- Yanardag, R., Demirci, T. B., Ulk seven, B., Bolkent, S., Tunali, S., & Bolkent, S. (2009). Synthesis, characterization and antidiabetic properties of N(1)-2,4-dihydroxybenzylidene-N(4)-2-hydroxybenzylidene-S-methyl-thiosemicarbazidato-oxovanadium (IV). *European Journal of Medicinal Chemistry*, 44, 818–826. <https://doi.org/10.1016/j.ejmech.2008.04.023>
- Zhang, Y., Yang, X. D., Wang, K., & Crans, D. C. (2006). The permeability and cytotoxicity of insulin-mimetic vanadium (III,IV,V)-dipicolinate complexes. *Journal of Inorganic Biochemistry*, 100, 80–87. <https://doi.org/10.1016/j.jinorgbio.2005.10.006>

# Effect of gel formulation obtained from *Fomes fomentarius* on bleeding and clotting time: A pilot study

Gülşah Gedik<sup>1</sup> , Hülya Asan<sup>2</sup> , Anıl Özyurt<sup>2</sup> , Hakan Allı<sup>3</sup> , Ahmet Asan<sup>4</sup> , Hakan Nazlı<sup>5</sup> ,  
Önder Sarp<sup>5</sup> 

<sup>1</sup>Trakya University, Faculty of Pharmacy, Department of Pharmaceutical Technology, Edirne, Turkey

<sup>2</sup>Trakya University, Faculty of Dentistry, Edirne, Turkey

<sup>3</sup>Mugla Sitki Kocman University, Faculty of Arts and Science, Department of Biology, Mugla, Turkey

<sup>4</sup>Trakya University, Faculty of Science, Department of Biology, Edirne, Turkey,

<sup>5</sup>Trakya University, Faculty of Pharmacy, Department of Pharmaceutical Technology, Edirne, Turkey

**ORCID IDs of the authors:** G.G. 0000-0003-4147-6729; H.A. 0000-0002-9650-9498; A.Ö. 0000-0002-3243-3156; H.A. 0000-0002-1238-3227; A.A. 0000-0002-4132-3848; H.N. 0000-0001-5763-1450; Ö.S. 0000-0003-1127-9273

**Cite this article as:** Gedik, G., Asan, H., Ozyurt, A., Allı, H., Asan, M., Nazlı, H., & Sarp, O. (2020). Effect of gel formulation obtained from *Fomes fomentarius* on bleeding and clotting time: A pilot study. *Istanbul Journal of Pharmacy*, 50 (3), 216-223.

## ABSTRACT

**Background and Aims:** *Fomes fomentarius* (L.) Fr. (jar fungus) has been used extensively in the past by surgeons, barbers, dentists, and is therefore called surgeon's fungus. The hemostatic properties of *F. fomentarius* extracts are important in medicine. The aim of this study was to investigate the effect of the gel formulation obtained from *Fomes Fomentarius* on bleeding and clotting time in rat models.

**Methods:** The gel was made for this purpose and a cross-linked polymer of acrylic acid was used as a gelling agent.

**Results:** The outcomes of the characterization analysis indicate the development of a successful gel formulation with optimum characteristics. Data from the antimicrobial study showed a good inhibition zone, with the strongest values against *Klebsiella pneumoniae*, *Candida krusei*, *C. tropicalis*, *C. guilliermondii*. The gel administration shortened the hemostasis time after bleeding from skin incisions by 63.9% and tail incisions by 55.63% from the original time. For coagulation time, these results are determined as 71.56% from the original time. The gel administration shortened the coagulation time after bleeding from the tail incisions by 69.9% from the original time.

**Conclusion:** Our preliminary study showed that the gel formulation obtained from *F. fomentarius* is a potent hemostatic agent in a rat-bleeding model.

**Keywords:** *Fomes fomentarius*, bleeding time, coagulation time

## INTRODUCTION

*Fomes fomentarius*, beech tree (*Fagus sylvatica* L.) and other deciduous species are developing as parasites or saprophytes, large wide variety of woody, perennial fungus with various sizes (Vetrovsky, Vorísková, & Snajdr, 2011). *F. fomentarius* is a white root fungus. Fruit body of between 5 and 50 cm across, 3 and 25 cm wide and 2 and 25 cm thick, which attaches broadly to the tree on which the fungus is growing. While typically shaped like a horse's hoof, it can also be more bracket-like with an umbonate attachment to the substrate. The species typically has broad, concentric ridges, with a blunt and rounded margin. The flesh is hard and fibrous, and a cinnamon brown colour. The pores are circular, and there are 2–3 per millimeter. Odor pleasantly fungoid, taste

### Address for Correspondence:

Gülşah GEDİK, e-mail: gulsahgedik@trakya.edu.tr

This work is licensed under a Creative Commons Attribution 4.0 International License.



Submitted: 03.02.2020  
Revision Requested: 18.05.2020  
Last Revision Received: 19.07.2020  
Accepted: 22.07.2020



rather bitter. A saprophyte or weak parasite on *Fagus* (beech), also on other hardwoods and rarely on conifers (Pacioni, 1985; Ellis & Ellis, 1990). Spores is oblong-ellipsoid, smooth, hyaline, 18-19x5-6  $\mu$ . It is known as "kav mantarı" in Turkey. The inside was a fungus used to light fire (Allı, Işiloğlu, & Solak, 2007).

*F. fomentarius* has been used extensively in the past by surgeons, barbers and dentists, and is therefore called surgeon's fungus. People used it as a medicine in Germany. In addition, *F. fomentarius* extract has been used in Europe, West Siberia and Indian folk medicine for dressing with iodine for external wounds and burns. Mushrooms are called "Wundschwamm" or "Chirurgenschwamm" in the alpine region of Switzerland. This preparation was sold in pharmacies in bandage form as an anti-bleeding agent and was used by Austrian farmers until the 19<sup>th</sup> century. Fomitin, the active ingredient of the *F. fomentarius*, is also used against dysmenorrhea, hemorrhoids and bladder diseases. There is information about the use of *F. fomentarius* for esophagus, stomach and uterine cancer in the literature (Grienke, Zöll, & Peintner, 2014). Also *F. fomentarius* has been used in traditional Chinese medicine for the treatment of oral ulcers, gastroenteritis, inflammations and various cancers (Chen, Zhao, & Li, 2011). In some studies, *F. fomentarius* has been reported to have hypoglycemic, anti-nociceptive, anti-inflammatory, anti-infective and anti-tumor activities (Seniuk et al., 2011; Park et al., 2004). A study demonstrated that *F. fomentarius* ethanol extract inhibits cell motility and growth and induces apoptosis by inhibiting the phosphoinositide 3-kinase /AKT pathway and caspase activation (Seon-Ok, Min-Ho, & Kyung-Ran, 2019).

Several classes of metabolites were identified: Primary metabolites polysaccharides (glucans), polysaccharide-protein complexes, and secondary metabolites such as triterpene glycosides, esters and lactones (fungisterollinoleate, betulin 28-O-acetate), alcohols (7 ergosterol, sitosterol), aldehydes and ketones (protocatechualdehyde), organic acids, benzofurans (paulownin), coumarins (daphnetin), and volatile components (Grienke et al., 2014). The most important compounds with clinically beneficial activity are glucans. In vitro studies have suggested that large molecular weight or particular glucans can directly activate leukocytes, stimulating their phagocytic, cytotoxic and antimicrobial activities, including the production of reactive oxygen and nitrogen intermediates (Akramiene, Kondrotas, & Didziapetriene, 2007). The presence of polysaccharides in the polar extracts was considered to be very important because a previous study had shown that a water-soluble melanin-glucan complex (containing 80% melanins and 20%  $\beta$ -glucans) completely inhibited the growth of *C. albicans* (Seniuk et al., 2011). The antifungal activities of *F. fomentarius* against *Aspergillus flavus*, *A. fumigatus*, *Absidia orchidis* and *Candida krusei* were shown in a study (Dresh et al., 2015). Hemorrhagic properties of *F. fomentarius* extracts are important in medicine and dentistry. This feature of *F. fomentarius*, we wanted to make human life safe by using these extracts to save lives of patients in traffic accidents, injuries, allergies and respiratory diseases, genetic disorders, hemophilia and bleeding and clotting disorders and to improve the quality of life.

The characteristics of an ideal topical hemostat should include various properties such as, stopping arterial and venous bleeding in 2 minutes, no need special storage conditions, durable and light insensitive, long shelf live (>2 years), no need special training for its use, easy to use in difficult whether and war conditions, easy to be self applicable, effective on complex, tourniquetless and hypothermic wounds, effective in patients using antiaggregants or anticoagulants, do not delay wound healing, easily cleaned and bioabsorbed from the application area and provide an antimicrobial environment, no local or systemic side effects and cost effective (Kheirabadi, 2011; Pusateri et al., 2003).

Some hemostat agents types, mechanism of action, studies and disadvantages are given in Table 1. Although very important studies have been carried out over the last years, a product with all the characteristics of the ideal topical hemostat, even with clinical trials and animal experiments, has not yet been developed. Our study was planned to demonstrate the bleeding-inhibiting properties of *F. fomentarius*.

## MATERIALS AND METHODS

### Reagents and chemicals

Carbomer 940 powder (Lubrizol) and Triethanolamine (Sigma-Aldrich) was chosen for the gel formulation. Double-distilled water was used throughout the study.

### Mushroom material

The aerial parts (fruit bodies) of *F. fomentarius* were collected by Hakan Allı on March 25, 2014, on *Liquidambar orientalis* Mill. in Köycegiz in the Toparlar region of Mugla, Turkey. A sample of the fungus was authenticated and a voucher specimen (No: 5379) was deposited in the herbarium of the Mugla University Faculty of Sciences. The fungus parts were ground to a powder using a porcelain mortar and pestle.

### Preparation of gel formulation

The aqueous extract for formulation was obtained via extraction of 5 g fungus powder with 100 mL distilled water at 80°C for 30 min using a water bath (Daihan Scientific, WB-22, Korea). The extract was filtered through Grade 1 Whatman paper. Carbomer 940 powder (2%) was added to the filtrate. Triethanolamine was then added and mixed with it enough to gel. The formulation was kept at 25±1°C for 48 hours to see a possible phase separation.

### Characterization of gel formulation

Gel was evaluated as for its clarity, pH and viscosity. The experiments were repeated four times.

### Clarity of formulation

The clarity of gels was determined by optical check under dark color background, and it was scaled as follows: turbid, +; clear, ++; and very clear, +++ (Okur, Yoltaş, & Yozgatli, 2016).

### Measurement of pH

The pH of the formulation was detected by a digital pH-meter (Mettler Toledo S 220, Switzerland). Measurements were performed four times and an average of these measurements was accepted as the pH of the in-situ gels.

**Table 1. Type, content, brand name, mechanism of action, studies and disadvantages of some hemostatic agents.**

Type	Content	Brand Name(s)	Mechanism of Action	Studies and Disadvantages: Drawbacks of Materials
Absorbable Agents	Oxidized Regenerated Cellulose	Surgicel® Original® NuKnit® Fibrillar™	Creates scaffold for platelet aggregation, Bactericidal properties.	Infection, abscess, foreign body reaction (Voormolen et al. 1987; Güven, 2019).
Absorbable Agents	Microfibrillar Collagen	Avitene® Ultrafoam Helitene®	Creates scaffold for platelet aggregation.	Granuloma formation Ereth-Market al., 2008).
Absorbable Agents	Microporous Polysaccharide	Arista™	Absorbs water and other low molecular weight compounds from the blood and concentrates these components to form platelet plug.	Expensive, no disadvantages reported (Güven, 2019).
Absorbable Agents	Gelatin	Gelfoam® Surgifoam®	Gelatin matrix: Absorbs surrounding blood, increasing the agent's size and weight.	Infection, abscess (Lindstrom, 1956).
Biologic Agents	Topical Thrombin Gelatin	Thrombi-Gel®	Topical thrombin: Converts fibrinogen to fibrin, activates platelets, aiding in formation of platelet plug Gelatin matrix: Absorbs surrounding blood, increasing the agent's size and weight.	Intravascular implementation: coagulopathies due to thrombosis, expensive (Güven, 2019).
Biologic Agents	Fibrin Sealant*	Tisseel® TachoSil® Evicel®	Comprised of two components: Sealer protein solution: Contains aprotinin, factor XIII and fibrinogen Thrombin solution: Converts fibrinogen in protein solution to fibrin.	Risk of bloodborne virus, expensive (Güven, 2019). Preparation requirements make it an impractical choice in the emergency setting (Schreiber & Neveleff, 2011).
Chemical Agents	<i>Thymus vulgaris, Glycyrrhiza glabra, Vitis vinifera, Alpinia officinarum, Urtica dioica</i> extract	Ankaferd Bloodstopper®	Ankaferd Bloodstopper® has hemostatic effects on vascular dynamics and mediators.	Application difficulty in narrow areas due to low viscosity. The agent led to increased acute and chronic inflammatory changes in the lungs and serosal surfaces of the intestines with minor architectural changes in the liver (Cömert et al., 2010).
Chemical Agents	Epinephrine Chloride	Adrenalin® Auvi-Q® Epipen® Epipen Jr®	Epinephrine chloride works as a vasoconstrictor and reduces the amount of blood that accumulates in the wound area by narrowing the capillaries.	Vasoconstriction occurs with the use of adrenaline, but then vasodilation is seen (Tanaka, Key & Levy, 2009).
Chemical Agents	Tranexamic acid	Transamine®	The binding of plasminogen to fibrin is blocked, activation of plasminogen is also prevented.	When taken in the first three hours, it was found to have a tremendous effect (Napolitano, Cohen, Cotton, Schreiber & Moore, 2013).
Chemical Agents	Vitamin K	Konakion®	Adequate amounts of Vitamin K are used in the prevention of clotting problems in newborns and in the treatment of bleeding induced by medicines.	It can be used to reverse the effect of warfarin used in excessive amounts to prevent blood clotting. Taking vitamin K1 orally or by injection may counteract anticoagulation caused by warfarin. However, it is thought that injecting vitamin K1 under the skin is not effective (Pathak et al. Hamm, Eyal, Walter, Rijhsinghanie & Bohlman, 1990).
Chemical Agents	Protamine	Promin® Pamintu®	Protamine is used in cardiac surgery, vascular surgeries and interventional radiology procedures to neutralize the anticoagulant effects of heparin.	Side effects include increased pulmonary artery pressure and peripheral blood pressure, decreased myocardial oxygen consumption, decreased heart output and heart rate (Carr & Silverman, 1999).

**Table 1. Continued.**

Type	Content	Brand Name(s)	Mechanism of Action	Studies and Disadvantages: Drawbacks of Materials
Chemical Agents	Aminocaproic Acid	Amicar®	It has also been approved by the FDA to prevent recurrent bleeding in patients with traumatic hyphema.	Control of perioperative bleeding associated with cardiac surgery is also used to prevent excessive bleeding in patients under anticoagulation therapy and to reduce the risk of bleeding in acute promyelocytic leukemia patients (Lu et al., 2015).
Chemical Agents	Granular clay made out of smectite	WoundStat®	It swells and thus can conform to any wound.	Removing can be difficult and requires debridement (Schreiber et al., 2011).
Chemical Agents	Granular zeolite and kaolin	QuikClot Combat Gauze®	QuikClot works by absorbing water and concentrating coagulation factors.	It should not be touched by the clinician without the use of gloves. This substance has the potential to produce burns (Schreiber et al., 2011).
Chemical Agents	Chitosan	HemCon®	Chitosan has mucoadhesive properties that enable the HemCon bandage to stick to the wound.	These dressings are stiff and nonconformable and thus can be difficult to apply (Wedmore, McManus, Pusateri & Holcomb, 2006).

### Determination of viscosity

The viscosity of the in-situ gel formulations was performed with a vibro viscometer (AND, SV-10, Japan). The formulations were performed with 50 Hz at 32±2°C.

### Spreadability studies of formulation

The spreadability of the gel was measured by spreading of 0.5 g of the gel on a circle of 2 cm diameter premarked on a glass plate and then a second glass plate was employed. Half kilogram of weight was permitted to rest on the upper glass plate for 5 min. The diameter of the circle after spreading of the gel was determined (Shinde, Pokharkar, & Modani, 2012).

### Screening antimicrobial activity

All test microorganisms, including *Klebsiella pneumoniae*, *Acinetobacter baumannii*, *Staphylococcus aureus*, vancomycin-resistant *enterococci* (VRE)+, *Escherichia coli*, *Candida albicans* (C.P. Robin) *C. tropicalis* (Castell.) *C. krusei* (Kudryavtsev), *C. guilliermondii* (Kurtzman and Suzuki) and *C. glabrata* (H.W. Anderson) were obtained from the Duzce University Research Hospital (Duzce, Turkey). The microorganisms were stored in a refrigerator at 4°C prior to the study.

The disk diffusion method for antimicrobial susceptibility testing was carried out according to the Clinical and Laboratory Standards Institute (CLSI) technique to assess the antimicrobial activities of the gel formulation. The formulation was performed under sterile conditions in duplicate and repeated three times (Gedik et al., 2019).

### In-vivo experimental design

Three healthy female rats were supplied by Trakya University's Experimental Research Center Animal Laboratory for bleeding and clotting time tests. The study was approved by the Animal Experiments Local Ethics Committee of Trakya University (TU-HADYEK-2016/36). Experimental animals were maintained in

the same room in a clean environment with adequate ventilation under the following conditions: 1 atm pressure, 25°C temperature, and 12-hour light-and-dark cycle. During the study, the rats were fed dry pellets and water *ad libitum*.

### Bleeding assay

One of the rats was used as a control for determining normal bleeding and clotting time. The others were for testing 5% *F. fomentarius* gel formulation effect on bleeding and clotting time. On behalf of bleeding, two wound models were created in two different area of the rat body:

- 1) 5 mm diameter biopsy punch wound on nape,
- 2) 5 mm diameter tail cut wound

5% formula dose was prepared as separated 0.1 g sufficient applicable packages to fully-cover wound surface areas. All surgical procedures were performed under sterile conditions. The animals were anesthetized by an intramuscular injection of ketamine hydrochloride 50 mg/kg and xylazine hydrochloride 10 mg/kg. All test procedures were performed according to Duke's Method and Slide Method (Nilsson, Magnusson & Borchgrevink 1963; Waghmare & Muniyappanavar, 2018).

Before creating a skin wound on the nape, the neck hair was shaved then cleaned with 70% alcohol. A 5 mm diameter skin was incised using a biopsy punch with a 2 mm depth. Bleeding time was counted with a stopwatch (refers to incision to end of bleeding). Three drops of blood were carried on a glass plate to observe the clotting time with another stopwatch simultaneously.

A 5 mm diameter tail cut wound was created using a scalpel after the skin test. The cut tail was left on the ground at the same level as the heart. The same measurement procedures for bleeding and clotting time were conducted. All wounds

were sutured and cleaned with iodized antiseptic after the procedure was completed. The rats were placed in their cages and allowed to wake up.

### Statistical analysis

Statistical analyses were conducted using SPSS, version 20.0 (SPSS, Inc., Chicago, IL). The mean and standard deviation were calculated for each group. All data were expressed as means and 95% confidence intervals (CIs)  $p < 0.05$  was considered statistically significant.

## RESULTS

### Preparation and characterization of gel formulations

The physicochemical characterization parameters of gels are reported in Table 2. The clarity, viscosity and spreadability of all the formulations were found to be satisfactory. The pH of the developed gel ranged between 5.49 and 5.55. The pH of the gels was appropriate for the dermal application. The spreadability of the gel was considered high by having, only two seconds. The therapeutic efficacy of gels depends on their spread.

**Table 2. Clarity, pH, viscosity, spreadability of gel formulation.**

Clarity	++
pH	5.52 ± 0.01
Viscosity (P)	34.1P ± 0.22 (29,4°C)
Spreadability (cm)	1.72 ± 0.17 (≤ 2 seconds)
The data are presented as the mean ± standard deviation (SD).	

### Screening antimicrobial activity

The antimicrobial activity of gel formulation was performed against *Klebsiella pneumoniae*, *Acinetobacter baumannii*, *Staphylococcus aureus*, vancomycin-resistant *enterococci* (VRE)+,

*Escherichia coli*, *Candida albicans*, *C. tropicalis*, *C. krusei*, *C. guilliermondii* and *C. glabrata*. The antimicrobial results of formulations are reported in Table 3. Agar well diffusion test results revealed that gel formulation showed a good inhibition zone with the strongest value against *Klebsiella pneumoniae* (10.3±0.79 mm), *Candida krusei* (11±0.26 mm), *C. tropicalis* (9±0.17 mm), *C. guilliermondii* (10.2 ±0.4 mm) (Gedik et al., 2019)

### Bleeding assay

5 mm diameter biopsy punch wound on nape:

Results obtained from the experiments were summarized in the Table 4. After confirming continuous bleeding from the full-thickness skin wound, the application of the gel resulted in rapid hemostasis. The gel administration shortened the hemostasis time after bleeding from the skin incisions by 3:32:57 minutes or 63.9% from the original time of 9:48:39. For coagulation time these results are determined as follows: 2:31:20 minutes or 71.56 % from the original time of 8:51:50.

**Table 4. Bleeding Assay with Biopsy Punch Wound on Nape.**

Control		Gel Application	
Bleeding Time	Coagulation Time	Bleeding Time	Coagulation Time
9:48:39 (588sn) (n=1)	8:51:50±0.07 (531sn) (n=3)	3:32:57±0.09 (212sn) (n=2)	2:31:20±0.06 (151sn) (n=6)
(p=0.002)			

5 mm diameter tail cut wound:

Results obtained from the experiments were summarized in the Table 5. After confirming continuous bleeding from the tail wound, the application of the gel resulted in rapid hemostasis. The gel administration shortened the hemostasis time after bleeding from the tail incisions by 5:27:05 minutes or 55.63%

**Table 3. Antibacterial and antifungal activity of gel formulation.**

Test Microorganisms	Inhibition zones (mm)*						
	Gel Formulation	E	GN	AM	AMB	FLU	KTC
<i>Klebsiella pneumoniae</i>	10.3 ± 0.79	NT	-	7	NT	NT	NT
<i>Acinetobacter baumannii</i>	-	NT	9	10	NT	NT	NT
<i>Staphylococcus aureus</i>	10.5 ± 0.43	14	NT	11	NT	NT	NT
**VRE+	-	10	12	9	NT	NT	NT
<i>Escherichia coli</i>	7.0 ± 0.01	11	NT	-	NT	NT	NT
<i>Candida krusei</i>	11 ± 0.26	NT	NT	NT	9	-	-
<i>C. albicans</i>	7 ± 0.45	NT	NT	NT	9	8	9
<i>C. tropicalis</i>	9 ± 0.17	NT	NT	NT	-	-	-
<i>C. guilliermondii</i>	10.2 ± 0.4	NT	NT	NT	8	-	-
<i>C. glabrata</i>	10 ± 0.62	NT	NT	NT	-	-	15
*GN: Gentamicin 30 µg; AM: Ampicillin 10 µg; AMB: Amphotericin B 100 µg; FLU: Fluconazole 25 µg; KTC: Ketoconazole 10 µg; NT: Not tried.							
**Vancomycin Resistant <i>Enterococci</i> .							

from the original time of 12:17:06. For coagulation time these results are determined as follows: 2:01:69 minutes or 69.9% from the original time of 6:42:48.

Control		Gel Application	
Bleeding Time	Coagulation Time	Bleeding Time	Coagulation Time
12:17:06 (737sn) (n=1)	6:42:48±0.11 (402sn) (n=3)	5:27:05±0.07 (327sn) (n=2)	2:01:69±0.02 (121sn) (n=6)
(p=0.006)			

## DISCUSSION

This study evaluated the hemostatic effects of 5% *F. fomentarius* gel formulation in vivo in rat skin-tail bleeding models. Today, in addition to conventional anti-bleeding methods, the use of extracts from various plants and marine organisms has become popular. The aim of this study was to investigate the effect of the *F. fomentarius* which is a common fungal species on bleeding time and clotting time. Gel formulation provides better application property and stability in comparison to cream and ointment. Topical gel drug administration is a localized drug delivery system anywhere in the body (Kaur & Guleri, 2013). The gel was made for this purpose and cross-linked polymer of acrylic acid was used as a gelling agent. Carbomer 940 polymer is a white powder, crosslinked polyacrylic acid polymer. Its short flow, non-drip properties are ideal for applications such as clear gels, hydroalcoholic gels, and creams. This gels are optimum viscosity at 25°C and physiological temperature, making them optimum gelling agent for dermal applications (<https://www.lubrizol.com/en/Personal-Care/Products/Product-Finder/Products-Data/Carbopol-940-polymer>).

The gel formulation characterized based on its pH, clarity, and viscosity. Physicochemical characterization of in situ gel formulations is an important subject to be considered in the formulation part, especially those intended for dermal application. The gel has a clear appearance on visual inspection. The pH of the developed gel ranged between 5.49 and 5.55. Ideally, dermal formulations should possess pH in the range of 5-6, for minimizing the discomfort of patient or skin irritation due to acidic pH and microbial growth on the skin because of basic pH (Okur, Çağlar, & Arpa, 2017). The outcomes of the characterization analysis indicate the development of successful gel formulation with optimum characteristics.

The spreadability of the gel was considered high by having a low spread of time. The gel spreading helps in the uniform application of the gel to the skin, so the prepared gels must have a good spreadability and satisfy the ideal quality in topical application. Furthermore, this is considered an important factor in patient compliance with treatment. This gels viscosity properties with possible pseudoplastic behavior observed in the formulation, confirms the characteristic of high spreadability due to the decrease in viscosity when applying certain force,

and at the same time has the property of remaining at the application site without drain (Carvalho et al., 2010).

Data from the antimicrobial study showed a good inhibition zone with the strongest value against *Klebsiella pneumoniae*, *Candida krusei*, *C. tropicalis*, *C. guilliermondii*. Similar to the our study, Kolundžić et al. (2016) tested the antimicrobial activity of *F. fomentarius* extracts of different polarity, especially against Gram-negative and Gram-positive bacteria that are commonly related to dermal and hospital infections (*Staphylococcus aureus* Rosenbach, *S. epidermidis* (Winslow and Winslow), *Micrococcus luteus* (Schroeter), *Bacillus subtilis* (Ehrenberg), *Enterococcus faecalis* (Andrewes and Horder), *Escherichia coli* (Migula) Castellani and Chalmers, *Klebsiella pneumoniae* (Schroeter) Trevisan and *Pseudomonas aeruginosa* (Schröter). They indicated that their *F. fomentarius* extracts (C-cyclohexane, D-dichloromethane, M-methanol and A-aqueous) displayed strong antimicrobial activity. Hereby, it can be concluded that the antimicrobial efficiency of the fungi gel formulation could provide a convenient surrounding for hemostatic efficacy by preventing wound infections caused by bleeding.

Pyranose is a collective term for saccharides that have a chemical structure that includes a six-membered ring consisting of five carbon atoms and one oxygen atom. This saccharide's pKa is also 11.8 in strong acid character. These electrolyte structures are biological environments force them to load cationic. (<http://foodb.ca/compounds/FDB015634>).

It has an anti-hemorrhagic effect by positively charged polysaccharide and polysaccharide-protein complex structure by binding chemical and mechanical effects with negatively charged erythrocytes, activating platelets and forming an adhesive structure in the tissue and forming a physical barrier around the injured vessel.

In our study, the gel administration shortened the hemostasis time after bleeding from the skin incisions by 63.9% and the tail incisions by 55.63% from the original time. For coagulation time these results are determined as follows 71.56% from the original time in skin incisions model and 69.9% from the original time in the tail incisions model.

## CONCLUSION

Our preliminary study showed that the gel formulation obtained from *F. fomentarius* is a potent hemostatic agent for cutaneous bleeding resulting from surgical skin defects in a rat-bleeding model. The use of the gel in especially in patients with hemostatic abnormalities, those undergoing anticoagulant or antiaggregant therapy, pregnant patients, or people with cancer may be an alternative to other hemostatic agents for achieving effective bleeding control. Future controlled clinical trials are needed to evaluate the efficacy of the plant extract in the control of hemorrhaging during surgery.

In particular, the search for hemostatic agent of natural origin is progressing rapidly, which points to the need for further studies exploring the utilization of the therapeutic agents from *F. fomentarius*.



**Ethics Committee Approval:** The study were approved by animal experiments local ethics committee of Trakya University (TUHADY-EK-2016/36) and indicated in the method section.

**Peer-review:** Externally peer-reviewed.

**Author Contributions:** Conception/Design of Study- G.G., A.Ö., H.A.; Data Acquisition- G.G., A.Ö.; Data Analysis/Interpretation- G.G., H.N., Ö.S.; Drafting Manuscript- G.G., A.Ö., H.A., H.A., A.A.; Critical Revision of Manuscript- A.A., G.G.; Final Approval and Accountability- G.G., H.A., A.Ö., H.A., A.A., H.N., Ö.S.; Technical or Material Support- H.A., G.G.; Supervision- A.A., G.G.

**Conflict of Interest:** The authors have no conflict of interest to declare.

**Financial Disclosure:** Authors declared no financial support.

## REFERENCES

- Akramiene, D., Kondrotas, A., Didziapetriene, J. & Kevelaitis, E. (2007). Effects of beta-glucans on the immune system. *Medicina*, 43(8), 597–606. <https://doi.org/10.3390/medicina43080076>
- Alli, H., Işiloğlu, M. & Solak, M. H. (2007). Macrofungi of Aydın Province. *Mycotaxon*, 99(1), 163–165. Retrieved from [https://www.researchgate.net/publication/282726082\\_Macrofungi\\_of\\_Aydin\\_Province\\_Turkey\\_65/link/5c8966b5a6fdcc3817526251](https://www.researchgate.net/publication/282726082_Macrofungi_of_Aydin_Province_Turkey_65/link/5c8966b5a6fdcc3817526251).
- Carr, J. A., Silverman, N. (1999). The heparin-protamine interaction: A review. *The Journal of Cardiovascular Surgery*, 40(5), 659–666. Retrieved from <https://europepmc.org/article/med/10596998>.
- Carvalho, F. C., Barb, M. S., Sarmento, V. H. V., Chiavacci, L. A., Netto, F. M. & Gremiao, M. P. D. (2010). Surfactant systems for nasal zidovudine delivery structural, rheological and mucoadhesive properties. *Journal of Pharmacy Pharmacology*, 62(4), 430–439. <https://doi.org/10.1211/jpp.62.04.0004>.
- Chen, W, Zhao Z, Li Y. (2011). Simultaneous increase of mycelial biomass and intracellular polysaccharide from *Fomes fomentarius* and its biological function of gastric cancer intervention. *Carbohydrate Polymers*, 85(2), 369–375. <https://doi.org/10.1016/j.carbpol.2011.02.035>.
- Cömert, M., Karakaya, K, Barut, F., Çakmak, K. G., Uçan, H. B., Gültekin, F. A., Emre, A. U., Taşçılar, Ö., İrkörücü, O., Ankaralı, H. (2010). Does intraabdominal use of Ankaferd Blood Stopper cause increased intraperitoneal adhesions. *National Trauma and Emergency of Surgery Journal*, 16(5), 383–389. Retrieved from <https://pubmed.ncbi.nlm.nih.gov/21038113>.
- Dresch, P., D'Aguzzo, M. N., Rosam, K., Grienke, U., Rollinger, J. M., Ursula Peintner, U. (2015). Fungal strain matters: colony growth and bioactivity of the European medicinal polypores *Fomes fomentarius*, *Fomitopsis pinicola* and *Piptoporus betulinus*. *AMB Express*, 5(4). <https://doi.org/10.1186/s13568-014-0093-0>.
- Ellis, M. B. & Ellis, J. P. (1990). *Fungi without gills (Hymenomycetes and Gasteromycetes)*. An Identification Handbook. XI, 329 S., 543 Abb. Chapman and Hall, London, New York, Tokyo, Melbourne, Madras, 1990. ISBN 0-412-36970-2
- Ereth-Mark, H., Schaft, M., Ericson, E., Wetgen, N., Nuttal, G., Oliver, W. C. (2008). Comparative safety and efficacy of topical hemostatic agents in a rat neurosurgical model. *Neurosurgery*, 63, 369–372. <https://doi.org/10.1227/01.neu.0000327031.98098.dd>.
- Gedik, G., Dülger, G., Asan, H., Özyurt, A., Alli, H. & Asan A. (2019). The antimicrobial effect of various formulations obtained from *Fomes fomentarius* against hospital isolates. *Mantar Dergisi- The Journal of Fungus*, 10(2), 103–109. <https://doi.org/10.30708/mantar.535994>.
- Grienke, U., Zöll, M., Peintner, U. & Rollinger, J. M. (2014). European medicinal polypores—A modern view on traditional uses. *Journal of Ethnopharmacology*, 154(3), 564–583. <https://doi.org/10.1016/j.jep.2014.04.030>.
- Güven, R. (2019). An experimental study investigating the effect of local hemostatic agents on hemostatic, histopathological, anti-mullerian hormone and postoperative intraabdominal adhesion in a laceration model of complicated ovarian hyperstimulation (Expertise thesis in medicine). Available from [tez.yok.gov.tr](http://tez.yok.gov.tr). (No. 535721).
- Kaur, L. P., Guleri, T. K. (2013). Topical Gel: A Recent Approach for Novel Drug delivery. *Asian Journal of Biomedical and Pharmaceutical Sciences*, 3(17), 1–5. <https://doi.org/10.15272/AJBPS.V3I17.183>.
- Kheirabadi, B. S. (2011). Evaluation of topical hemostatic agents for combat wound treatment. *The United States Army Medical Department Journal*, 2, 25–38. Retrieved from <https://pubmed.ncbi.nlm.nih.gov/21607904>.
- Kolundžić, M., Grozdanić, N. D., Dodevska, M., Milenković, M., Sisto, F., Miani, A. & Kundaković, T. (2016). Antibacterial and cytotoxic activities of wild mushroom *Fomes fomentarius* (L.) Fr. *Polyporaceae*. *Industrial Crops and Products*, 79, 110–115. <https://doi.org/10.1016/j.indcrop.2015.10.030>.
- Lindstrom, P. A. (1956). Complications from the use of absorbable hemostatic sponges. *American Medical Association Archive of Surgery*, 73(1), 133–141. <https://doi.org/10.1001/arch-surg.1956.01280010135018>.
- Lu, J., Meng, H., Meng, Z., Sun, Y., Pribis, J. P., Zhu, C., Li, Q. (2015). Epsilon aminocaproic acid reduces blood transfusion and improves the coagulation test after pediatric open-heart surgery: A meta-analysis of 5 clinical trials. *International Journal of Clinical and Experimental Pathology*, 8(7), 7978–7987. Retrieved from <https://pubmed.ncbi.nlm.nih.gov/26339364>.
- Napolitano, L. M., Cohen, M. J., Cotton, B. A., Schreiber, M. A., Moore, E. E. (2013). Tranexamic acid in trauma: how should we use it? *Journal of Trauma and Acute Care Surgery*, 74(6), 1575–86. <https://doi.org/10.1097/ta.0b013e318292cc54>.
- Nilsson, I. M., Magnusson, S., Borchgrevink, C. (1963). The Duke and Ivy methods for determination of the bleeding time. *Thrombosis et Diathesis Haemorrhagica* 10.02: 223–234. Retrieved from <https://europepmc.org/article/med/14081283>
- Okur, N. Ü., Çağlar, E. Ş., Arpa, M. D. & Karasulu, H. Y. (2017). Preparation and evaluation of novel microemulsion-based hydrogels for dermal delivery of benzocaine. *Pharmaceutical Development and Technology*, 22(4), 500–510. <https://doi.org/10.3109/10837450.2015.1131716>.
- Okur, N. Ü., Yoltaş, A. & Yozgatlı, V. (2016). Development and characterization of voriconazole loaded in situ gel formulations for ophthalmic application. *Turkish Journal of Pharmaceutical Sciences*, 13(3): 311–317. <https://doi.org/10.4274/tjps.2016.05>
- Pacioni, G. (1985). *Mac Ency Mushrooms Toadstools* (Macdonald encyclopedias). London.
- Park, Y. M., Kim, I. T., Park, H. J., Choi, J. W., Park, K. Y., Lee, J. D., Nam, B. H., Kim, D. G., Lee, J. Y. & Lee, K. T. (2004). Anti-inflammatory and anti-nociceptive effects of the methanol extract of *Fomes fomentarius*. *Biological & Pharmaceutical Bulletin*, 27(10), 1588–1593. <https://doi.org/10.1248/bpb.27.1588>.
- Pathak, A., Hamm, C. R., Eyal, F. G., Walter, K., Rijhsinghani, A., Bohlman, M. (1990). Maternal Vitamin K administration for prevention of intraventricular hemorrhage in preterm infants. *Pediatric Research*, 27, 219. Retrieved from <https://www.ncbi.nlm.nih.gov/pmc/articles/PMC7043360>.
- Pusateri, A. E., McCarthy, S. J., Gregory, K. W., Harris, R. A., Cardenas, L., McManus, A. T., & Goodwin Jr, C. W. (2003). Effect of a chitosan-based hemostatic dressing on blood loss and survival in a model of severe venous hemorrhage and hepatic injury in swine. *Journal of Trauma and Acute Care Surgery*, 54(1), 177–182. <https://doi.org/10.1097/00005373-200301000-00023>.

- Schreiber, M. A, Neveleff J. D. (2011). Achieving hemostasis with topical hemostats: Making clinically and economically appropriate decisions in the surgical and trauma settings. *The Association of Perioperative Registered Nurses Journal*, 94(5), 1–20. <https://doi.org/10.1016/j.aorn.2011.09.018>.
- Seniuk, O. F., Gorovoj, L. F., Beketova, G. V., Savichuk, N. O., Rytik, P. G., Kucherov, I. & Prilutsky A. (2011). Anti-infective properties of the melanin-glucan complex obtained from medicinal tinder bracket mushroom, *Fomes fomentarius* (L.: Fr.) Fr. (*Aphyllorphoromycetideae*). *International Journal of Medicinal Mushrooms*, 13(1), 7–18. <https://doi.org/10.1615/intjmedmushr.v13.i1.20>.
- Seon-OK, L., Min-Ho, L., Kyung-Ran, L., Eun-Ok, L., Hyo-Jeong, L. (2019). *Fomes fomentarius* Ethanol Extract Exerts Inhibition of Cell Growth and Motility Induction of Apoptosis via Targeting AKT in Human Breast Cancer MDA-MB-231 Cells. *International Journal of Molecular Science*, 20(5), 1147. <https://doi.org/10.3390/ijms20051147>.
- Shinde, U., Pokharkar, S. & Modani, S. (2012). Design and evaluation of microemulsion gel system of nadifloxacin. *Indian Journal of Pharmaceutical Sciences*, 74(3), 237–247. <https://dx.doi.org/10.4103%2F0250-474X.106066>.
- Tanaka, A. K., Key, N. S., Levy, J. H. (2009). Blood coagulation: Hemostasis and thrombin regulation. *Anesthesia & Analgesia*, 108(5), 1433–1446. <http://doi.org/10.1213/ane.0b013e31819bcc9c>.
- Vetrovsky, T., Vorísková, J., Snajdr, J., Gabriel, J. & Baldrian, P. (2011). Ecology of coarse wood decomposition by the saprotrophic fungus *Fomes fomentarius*. *Biodegradation*, 22(4), 709–718. <https://doi.org/10.1007/s10532-010-9390-8>.
- Voormolen, J. H. C., Ringers, J., Bots, G. A. M., Van Der Heide, A., Hermans, J. (1987). Hemostatic agents: Brain tissue reaction and effectiveness. *Neurosurgery*, 20(5), 702–709. <https://doi.org/10.1227/00006123-198705000-00005>.
- Waghmare, R.V., Muniyappanavar, N. S. (2018). Influence of blood groups on bleeding and clotting time. *International Physiology* 6(3), 200–204. <https://dx.doi.org/10.21088/ip.2347.1506.6318.6>.
- Wedmore, I., McManus, J. G., Pusateri, A. E., Holcomb, J. B. (2006). A special report on the chitosan-based hemostatic dressing: experience in current combat operations. *Journal of Trauma*, 60(3), 655–658. <https://doi.org/10.1097/01.ta.0000199392.91772.44>.
- FOODB. (2019, November 19) Retrieved from <http://foodb.ca/compounds/FDB01563>.
- Lubrizol. (2019, December 28) Retrieved from <https://www.lubrizol.com/en/Personal-Care/Products/Product-Finder/Products-Data/Carbopol-940-polymer>.

# Development of inhalable cubosome nanoparticles of nystatin for effective management of invasive pulmonary aspergillosis

Marzuka Kazi<sup>1</sup> , Mohamed Hassan Dehghan<sup>1</sup> <sup>1</sup>Y.B. Chavan College of Pharmacy, Department of Pharmaceutics, Aurangabad, India**ORCID IDs of the authors:** M.K. 0000-0002-6103-7806; M.H.D. 0000-0002-8082-9454**Cite this article as:** Kazi, M., & Dehghan M. H. (2020). Development of inhalable cubosome nanoparticles of nystatin for effective management of invasive pulmonary aspergillosis. *Istanbul Journal of Pharmacy*, 50 (3), 224-237.

## ABSTRACT

**Background and Aims:** Invasive pulmonary aspergillosis (IPA) is an imperative concern in the present era due to its high occurrence and mortality rate in severely immunocompromised patients. The present study was designed to develop, optimize and characterize encapsulated nystatin (NYS) cubosome nanoparticles as an inhalable system, a viable alternative for effective management of IPA.

**Methods:** A dry lipidic film comprising glycerol monooleate (GMO), Span 83, Poloxamer (P-407) and dispersed NYS was subjected to ultrasound sonication to produce colloidal dispersion of cubosomes. The process and formulation variables were screened using Plackett Burman design and further optimized by Box Behnken design by evaluating its effect on particle size, polydispersity index (PDI), zeta potential and entrapment efficiency.

**Results:** The optimized NYS cubosomes were nearly spherical with some irregular polyangular symmetry as visualized by transmission electron microscopy (TEM). Further, small angle X-ray scattering (SAXS) affirmed Pn3m cubic mesophasic structure. The optimized nanoparticles had particle size 263.5 nm, zeta potential -14.4 mV, PDI 0.283 and entrapment efficiency 82%. The *in-vitro* cytotoxicity assay indicated that NYS cubosomes reduced cell cytotoxicity in contrast to pure drug post 48h. *In-vitro* haemolytic assay denoted lower toxicity of formulation as compared to free drug. *In-vitro* drug release studies highlighted, slow but continuous release from NYS cubosomes until 48h and showcased Higuchi release kinetics. Likewise, NYS cubosome demonstrated higher antifungal activity compared to drug suspended in phosphate buffer.

**Conclusion:** Thus, non-invasive feature and contemplated target specificity of nystatin loaded cubosome nanoparticles pave a mode for its prospect as pulmonary delivery to combat IPA.

**Keywords:** Nystatin, cubosome nanoparticles, aspergillosis, drug design, pulmonary

## INTRODUCTION

Lipidic, polymeric and polyelectrolyte complex based nanoparticulate drug delivery lately has been widely studied as potential carriers for delivery of numerous drug candidates such as anti-cancer (Chishti, Jagwani, Dhamecha, Jalalpure, & Dehghan, 2019), peptide (on Halling Laier et al., 2018; Poddar & Sawant, 2017), antifungals (Furedi et al., 2017), antivirals (Mandal, Prathipati, Belshan, & Destache, 2019) and antibacterials (Carneiro et al., 2019; Rani et

al., 2018). The prevalence rate of invasive pulmonary aspergillosis (IPA) is high in severely immunocompromised patients suffering from HIV, cancer, critically ill patients, organ transplant patients and in individuals with known history of chronic obstructive pulmonary disease (Szalewski, Hinrichs, Zinniel, & Barletta, 2018). The management of IPA still remains a challenge as most of the antifungal used in its treatment present resistance or pose a high toxicity profiles (Kosmidis & Muldoon, 2017). Nystatin (NYS) a broad

**Address for Correspondence:**  
Marzuka KAZI, e-mail: marzi345@gmail.com

Submitted: 02.02.2020  
Revision Requested: 06.04.2020  
Last Revision Received: 30.06.2020  
Accepted: 18.07.2020

This work is licensed under a Creative Commons Attribution 4.0 International License.



spectrum is effective against azole resistant and amphotericin B resistant strains of *Candida albicans* (Offner et al., 2004). Concentration dependent activity of NYS is key-in factor to rapid onset of action for successful treatment. Additionally, NYS is known to showcase long post-antifungal effect, thus justifies the rational for reduction in its frequency of administration (Marin-Quintero et al., 2013; Ryder, 1999). The formulation challenge revealed by NYS as a result of low solubility and low permeability, is the prime reason that makes it complicated to design a controlled release delivery for this drug (Fernandez Campos, Calpena Campmany, Rodríguez Delgado, Lopez Serrano, & Clares Naveros, 2012). Researchers have tried formulating NYS in various delivery systems such as lipid intravenous emulsion (Ryder, 1999), nanoemulsions (Fernandez Campos et al., 2012), micellar gels (Maqsood et al., 2015), mucoadhesives for topical use (Sakeer, Al-Zein, Hassan, Desai, & Nokhodchi, 2010), liposomes (Khan, Faisal, & Mohamad, 2006), niosomes (El-Ridy, Abdelbary, Essam, El-Salam, & Kassem, 2011), microparticles (Kim, Son, & Kwon, 2018), pastilles (Silva et al., 2017), pellets and drug particulates system in toothpaste (Pinto Reis, Vasques Roque, Baptista, & Rijo, 2016) to solve drug related problems.

Nano-particulate formulations as new frontiers are being developed to improve treatment outcomes in IPA patients. Cubosomes, a dispersion of the bicontinuous cubic mesophase have contorted lipid bilayer as their basic unit and two extremely tortuous non-intersecting water channels (Esposito et al., 2005). The high lipidic content and large surface area posed by these structures makes them desirable carriers for efficient encapsulation of hydrophilic, hydrophobic, or amphiphilic drug molecules (Shi et al., 2017). Biocompatibility, biodegradability, bioadhesion and prolonged drug release ability interpret cubosomes to be an effective carrier for IPA drug therapy (Madheswaran, Kandasamy, Bose, & Karuppagounder, 2019). Moreover, the nanoparticle size range of these structures facilitates passive targeting to pulmonary route, and leads to deposition of the drug to the most sorted areas of the lower respiratory tract or into the deep regions of lungs (Newman, 2017). In case of pulmonary infection, delivering the drug to the target site of action is beneficial in reducing drug level in the systemic circulation although the desired therapeutic index at the site of infection is maintained (Islam & Ferro, 2016). This route of administration helps to reduce the drug related toxicity in comparison to the parenteral route (Das et al., 2015).

On the basis of these considerations, the research objective was to overcome formulation challenges presented by the drug and in conception of a site-specific delivery system, so as to achieve enhanced effectiveness. The present study was designed to develop, optimize and characterize encapsulated Nystatin cubosome nanoparticles for effective management of IPA, to be targeted through inhalable pulmonary route.

## MATERIALS AND METHODS

Nystatin (NYS), Polaxamer 407 (P-407) was a kind gift sample from Glenmark Pharmaceuticals, (Mumbai, India). Dimodan HPM-90 (solid grade GMO) and Cithrol GMO-HP-SO-LK was sorted as a gift sample obtained from Dupont (Gurgaon, India) and Croda, (Mumbai, India) respectively. Span 80 and Span 83

was a generously donated by Cipla Pvt. Ltd., (Mumbai, India). Organic solvents like dimethyl sulfoxide, methanol, dimethyl formamide, chloroform were purchased from Loba chemie, Mumbai whereas dextrose, peptone and agar were procured from Fisher scientific, India. *Aspergillus fumigatus* (NCIM 902) was procured from National chemical laboratory, Pune. Dialysis bag with a molecular weight cut-off (MWCO) of 3,500 Da was purchased from Merck Millipore, India, Pvt. Ltd. (Bengaluru).

## Ishikawa Fishbone diagram and risk assessment by failure mode and effects analysis (FMEA)

Risk assessment for the material attributes and process variables was carried out after analyzing the available literature, in order to estimate its effect on critical quality attributes (CQAs) viz., particle size (prediction of inhalation through nasopulmonary route and its absorption potential in lungs), drug loading and entrapment efficiency (to predict available drug for absorption, release kinetics of drug). Ishikawa or Fishbone presentation is a cause and effect type of diagram that was established in order to find all the possible variables that could have an impact on CQAs of the drug product i.e. NYS loaded cubosomes shown on the primary arrow (central horizontal arrow i.e. the studied effect is "the fish head"). The secondary arrows (vertical slanting arrows i.e. the potential causes and sub-causes define the "fish bone structure") represent the process and formulation variables e.g. materials, people, cubosome formation process and instrument. The tertiary arrows represent the factors in-return impacting these process and formulation variables e.g. sonication, lyophilizer, surfactant, organic solvent, drug etc. Thus, the use of the Ishikawa diagram helps illustrate, identify and analyze all the factors connected to the main aim of the study. The factors marked in the red text have been studied in the present work. The quality target product profile (QTPP) was identified as dosage form, its shape, its type, strength, route of administration.

## Plackett Burman experimental design

Based on preliminary trial results and literature survey potential factors which could impact the critical attributes of the final product was identified. Screening of process variables and formulation components was essentially studied using Plackett Burman design (Table 1) to understand its effect on critical qual-

**Table 1. Factors and their levels in Plackett Burman Experimental design.**

Factors	Levels	
	Low	High
X <sub>1</sub> : NYS concentration	1.23%	2.23%
X <sub>2</sub> : Type of GMO	HPM-90	HP-SO-LK
X <sub>3</sub> : Type of high HLB surfactant	Span 80	Span 83
X <sub>4</sub> : Type of low HLB surfactant	P 188	P 407
X <sub>5</sub> : Concentration of high HLB surfactant (mg)	150	300
X <sub>6</sub> : Concentration of low HLB surfactant (mg)	100	200
X <sub>7</sub> : Sonication time (min)	15	30
X <sub>8</sub> : pulse rate	3/7 sec	9/18 sec

ity attributes (CQAs). Accordingly, the study was undertaken for 8 factors at 2 levels and 12 experimental runs were conducted.

NYS-loaded cubosomes were prepared through a modified coarse method (Ali, Noguchi, Iwao, Oka, & Itai, 2016; Bei, Marszalek, & Youan, 2009). Briefly, for each batch, different concentration of GMO (600 mg), Poloxamer and Span as in Table 2 was placed in a 100 ml round bottom flask. Further chloroform (5 ml) was added to aid complete solubilization of lipids and surfactant so as to establish a one-phase system. Subsequently, a second phase comprising of Nystatin dissolved in DMSO (0.5-1ml), was added to the above lipidic surfactant system. Chloroform was allowed to evaporate in a rotatory evaporator (IKA RV 10 Digital V) under reduced pressure at  $60\pm 2$  rpm and a temperature of  $60\pm 2^\circ\text{C}$ , leading to the formation of a thin film at the bottom of the flask. A volume of 50 ml of PBS buffer saline (pH=7.4) was added to the dry lipidic drug film to form coarse dispersions by the aid of a probe sonicator (Ali et al., 2016) (Sonics Vibra cell VCX 500) at  $25^\circ\text{C}$ , 70 % amplitude with varying the sonication time and pulse rate as indicated in Table 2. The resulting cubosome colloidal dispersions were micro-centrifuge (Remi motors, RM 12-C) at 12000 rpm for 30 mins with repeated washings to remove the untrapped drug, and were stored in a vial at R.T ( $25^\circ\text{C}$ ) until further evaluation.

The implications of the model and factor coefficients were analyzed by undertaking multi-linear regression analysis and analysis of variance. Experimental checks were taken in triplicate. The dependent variables (CQAs) were identified as average particle size ( $Y_1$ ), zeta potential ( $Y_2$ ), entrapment efficiency ( $Y_3$ ) and polydispersity index ( $Y_4$ ) and in-vitro antifungal activity ( $Y_5$ ).

#### Optimization of NYS cubosomes using Box Behnken (BB) design

After studying Plackett Burman design for 8 factors at 2 levels, the cubosomes were optimized for process and formulation variables using Box Behnken design. Factors that were fixed are as follows GMO grade was selected as HP-SO-LK, low HLB surfactant was preferred to be Span 83 whereas high HLB surfactant was chosen to be poloxamer 407, the pulse rate was set to be 3/7sec. The concentration of drug and GMO was fixed to 1.23% w/w and 600 mg. The factors such as the concentration

of high HLB surfactant, low HLB surfactant and probe sonication time were rigidly studied at 3 levels in BB design (Table 3) for further optimization of NYS cubosomes. The randomized experimental designed batches were formulated (Table 4) as per the above-mentioned procedure and statistically analyzed by Design expert®7 software.

**Table 3. Factors and their levels set in Box Behnken Experimental design.**

Factors	Levels		
	-	0	+
X <sub>1</sub> : concentration of Low HLB surfactant	150	225	300
X <sub>2</sub> : concentration of High HLB surfactant	50	100	150
X <sub>3</sub> : sonication time	10	15	20

**Table 4. Box Behnken Design of Experiment.**

Formulation	X <sub>1</sub> (mg)	X <sub>2</sub> (mg)	X <sub>3</sub> (mins)
B1	225	100	15
B2	225	150	10
B3	225	50	10
B4	150	100	20
B5	225	100	15
B6	225	50	20
B7	225	100	15
B8	150	150	15
B9	225	150	20
B10	300	150	15
B11	150	150	15
B12	300	100	20
B13	225	100	15
B14	225	100	15
B15	300	100	10
B16	300	50	15
B17	150	100	10

**Table 2. Plackett Burman Design of Experiment.**

Formulation	X <sub>1</sub> (%)	X <sub>2</sub>	X <sub>3</sub> (%)	X <sub>4</sub>	X <sub>5</sub> (mg)	X <sub>6</sub> (mg)	X <sub>7</sub> (min)	X <sub>8</sub> (rpm)
D1	1.23	HPM-90	Span 80	P-188	150	100	15	3/7
D2	1.23	HP-SO-LK	Span 83	P-188	300	200	30	3/7
D3	2.23	HPM-90	Span 83	P-407	300	100	15	3/7
D4	1.23	HP-SO-LK	Span 83	P-407	150	100	15	9/18
D5	1.23	HPM-90	Span 83	P-188	300	200	15	9/18
D6	2.23	HPM-90	Span 80	P-188	300	100	30	9/18
D7	2.23	HPM-90	Span 83	P-407	150	200	30	9/18
D8	1.23	HP-SO-LK	Span 80	P-407	300	100	30	9/18
D9	2.23	HP-SO-LK	Span 80	P-188	150	200	15	9/18
D10	1.23	HPM-90	Span 80	P-407	150	200	30	3/7
D11	2.23	HP-SO-LK	Span 83	P-188	150	100	30	3/7
D12	2.23	HP-SO-LK	Span 80	P-407	300	200	15	3/7



## Characterization

### Particle size, zeta potential and poly dispersibility index

The mean size and size distribution of colloidal particles is measured using Malvern Zetasizer Nano Series (Malvern Instruments, Malvern, India). Prior to the examination, samples were diluted with purified water to a scattering intensity of about 150–300 kcps and the dispersant viscosity was set to 0.8872 cP at 25°C. The size (z-average), polydispersity index (PDI) and zeta potential was determined in triplicate.

### Polarized light microscopy (PLM)

PLM (Carl Zeiss, Jena, Germany) imaging was performed so as to ascertain the gross morphology of the formed nanoparticle at 25°C i.e. cubosome or hexosome.

### Encapsulation efficiency

Samples from each batch were centrifuged using microcentrifuge (Remi motors, RM 12-LC) at 12,000 rpm for 30 min. Aliquots from the supernatant of each batch were diluted using 5% Triton-X solution in PBS (pH 7.4) to disrupt any lipidic fragment (Rizwan et al., 2011). The entrapped drug amount was calculated after analysis of the drug concentration in the diluted supernatant using UV spectrophotometer (UV 1800, Shimadzu Japan) at max 306 nm.

EE was calculated using the following equation:

$$EE\% = \frac{C(\text{total drug concentration}) - C(\text{free drug})}{C(\text{total drug concentration})} \times 100 \text{ (Eq. 1)}$$

### In vitro antifungal activity

The *in vitro* antifungal activity of the optimized colloidal dispersion was evaluated against *Aspergillus fumigatus* (NCIM 902). Inoculum suspensions of *Aspergillus fumigatus* were prepared from fresh, mature (3-5 day old) cultures grown on Sabouraud dextrose agar slants. The colonies were covered with 5 ml of distilled sterile water. Tween 20 (1%) was added to facilitate the preparation of *Aspergillus* inocula. The inocula were achieved by carefully rubbing the colonies with a sterile loop; the isolates were then shaken vigorously for 15 s with a vortex mixer and then transferred to a sterile tube. The optical density of the suspensions was measured by UV spectrophotometer (Shimadzu UV-1600) was set as 0.13 at 530 nm (Petrikou et al., 2001). Agar well diffusion method was used to evaluate antifungal activity, 1 ml of microbial inoculum was seeded into SDA medium and poured into petri plates, a sterile cork borer of diameter 6 mm were punched aseptically to create a well and colloidal dispersion (0.1 ml) is added into the well. The plates were incubated for 48 hrs, 27°C (*Aspergillus fumigatus*).

### In-vitro drug release

The *in-vitro* release profiles of NYS-loaded cubosomes were evaluated using a membrane dialysis method (Yang et al., 2012). Optimized cubosome formulation (2 ml) was dispersed in 1 ml of release medium (phosphate buffer pH 7.4) consisting of 0.25% w/v of sodium lauryl sulphate. The resulting dispersion was added to the dialysis bag (MWCO 3,500 Da) and sealed. The dialysis bag was immersed in beaker containing

10 ml of release medium placed over a magnetic stirrer (Remi Equipment, Mumbai, India), maintained at 37°C and set at 100 rpm. At specified time intervals of 1, 2, 4, 6, 8, 12 and 24 h on the first day followed by 24 h interval for the subsequent day's samples were withdrawn and replaced with same volume of release medium. NYS content in the release medium was assayed using the UV spectroscopy method as used in encapsulation efficiency determination.

### Cytotoxicity assays

The MTT (3-(4,5-dimethylthiazolyl-2-yl)-2,5-diphenyl-tetrazoliumbromide) colorimetric assay was employed to assess the cytotoxicity of NYS and optimized NYS cubosome formulation on A549 cell lines (Adhikari, 2017; Lestner et al., 2010). Cells were seeded in 96-wellplates at a density of  $1 \times 10^5$  cells/well suspended in 100  $\mu$ l of Dulbecco's modified Eagle's medium (DMEM, HiMedia, Nashik, India). Following incubation for 24 h, the medium was aspirated from all wells and replaced with 100  $\mu$ l/well culture medium with NYS or NYS cubosome formulation (3.125, 6.125, 12.25, 25, 50, 100, 150, 200  $\mu$ g/ml) and incubated for further 24 h. Cell viability was found by adding 200  $\mu$ l of a 1.25 mg/ml MTT (Invitrogen, USA) to all well, trail by 4 h of incubation. Post incubation, MTT and medium were aspirated; formazan product was solubilized in 200  $\mu$ l DMSO. Multi-detection microplate reader (Biohit BP 800, Helsinki, Finland) was used to measure absorbance at 570 nm. IC<sub>50</sub> values were determined for both NYS and optimized NYS cubosomes.

### In-vitro hemolysis assay

Fresh sheep red blood cells (SRBC) obtained from local slaughter house were suspended in sterile saline 5% v/v and washed twice with saline by centrifugation at 1,800g for 10 min (Chuealee, Aramwit, Noipha, & Srichana, 2011). 0.5 ml of serially diluted NYS or optimized NYS cubosomes having concentrations in the range of 10-500  $\mu$ g/ml were suspended in 4.5 ml of the washed SRBC having a final hematocrit of 1%. Subsequent to incubation (37°C for 1 h), the tube was centrifuged (1,800g, 10 min), the unlysed cells were removed and hemolysis in the supernatant was estimated by measuring absorbance at 540 nm. No lysis was observed in sterile saline used as negative control whereas 100% lysis was seen in positive control (1% Triton X-100). HC<sub>50</sub> value was found for both NYS and optimized formulation.

$$\text{Hemolysis \%} = \frac{(\text{OD of sample} - \text{OD of negative control})}{(\text{OD of positive control} - \text{OD of negative control})} \times 100 \text{ (Eq. 2)}$$

### Small angle X-ray scattering (SAXS)

The SAXS measurements were carried out using Xeuss 2 (Xenocs SAS, France), which consisted of an Eiger R 1M as the detector, GeniX3D Cu 30 Watts Cu tube with 50 KV 0.6 mA current, 1.54 Å as the radiation wavelength, and the scattering angle ranged as 0.2° to 2.8°. The measurements were taken in a vacuum (25±0.1°C). The diffraction patterns acquired were converted to plots of intensity vs. q-value, which facilitated the identifications of the peak point, and its conversion to Miller Indices to recognize the phase structure using SAXS processing software [Scatter developed by S. Förster (University of Hamburg), and L. Apostol (DUBBLE/ESRF)].

**Differential scanning calorimeter (DSC)**

The physical state of NYS encapsulated in cubic nanoparticles was characterized by DSC thermal analyzer (DSC 60 plus, Shimadzu, Japan). Approximately 5–10 mg of samples including pure NYS, P-407, GMO and optimized NYS cubosomes were placed in a standard aluminum pan and an empty hermetic pan was used as a reference. After purging with pure nitrogen at a flow rate of 10 mL/min, the samples were analyzed at a heating rate of 10°C/min from 40°C to 300°C.

**Fourier transformer infrared spectroscopy (FTIR)**

The physical state of NYS encapsulated in cubic nanoparticles was also characterized by FTIR (IRAffinity-1S, Shimadzu, Japan). Approximately 10-20 mg of samples were compressed to prepare circular KBr disc of GMO, P-407, Span 83, NYS, optimized cubosome formulation were screened in the range of 400 to 4000 cm<sup>-1</sup>.

**X-ray diffractometer**

XRD experiments were carried out on a PW3040/60 X'pert PRO (PANalytical, Netherlands). Cu X-ray tube operating at 45 kV and 40 mA produced incident X-radiation. Diffraction images were obtained on an X'Pert data collector. Samples such as NYS and optimized NYS cubosome formulation were analysed at 25°C over the 2θ range 2-80° with a step size of 0.05° (60 s).

**Field emission gun transmission electron microscope (FEG TEM)**

The samples were prepared by negatively staining in 1% (w/v) phosphotungstic acid for 3–5 min. A 5-μl droplet of the cubo-

some suspension was placed onto a 300 mesh carbon coated copper grid, and was allowed to settle for 3–5 min. Next, the excess fluid was removed by absorbent paper. Thereafter visualized on a FEI Model Tecnai G2, F30 300KV (FEI-USA) and snapped on a Gatan axis-mount 2kx2k digital camera.

**RESULTS AND DISCUSSION**

**Risk estimation: Ishikawa diagram**

The fishbone diagram was used to estimate the potential cause and effect correlation of process and formulation variable for development of inhalable cubosomes. CQAs such as particle size, PDI, zeta potential and entrapment efficiency were identified to critically effect the QTPPs (Figure 1). Prior knowledge gained through literature review and preliminary studies enabled to identify eight potential factors for evaluating experimental design as shown in Table 1.

**Screening by Plackett Burman design**

Plackett Burman design was applied for screening the most significant process and formulation factors to elucidate its effect on achieving the QTPP. The outline of the response on the dependent variable is shown in Table 4. The statistical evaluation with context to independent variable and its effect on the selected response is indicated in Table 5.

Particle size a very critical factor in design of inhalable nanoparticles, was seen to be affected by independent variables namely concentration of drug (X<sub>1</sub>), type of GMO (X<sub>2</sub>), type of high HLB surfactant (X<sub>4</sub>), concentration of low HLB surfactant (X<sub>5</sub>),

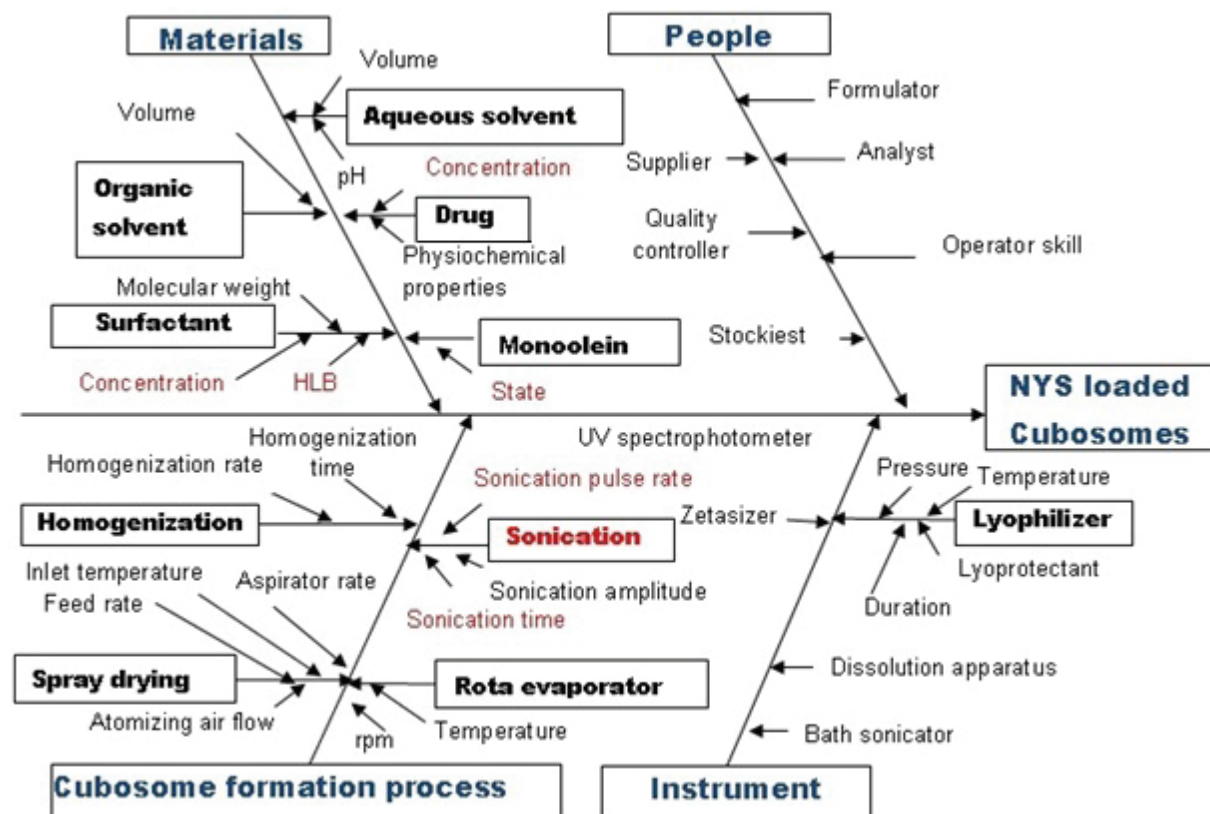


**Figure 1.** Ishikawa diagram representing process and formulation variables that may affect the CQAs of Cubosomes. The studied effect is "the fish head" and the potential causes and sub-causes define the "fish bone structure".

**Table 5. Outline of the response on the dependent variable obtained using Plackett Burman Design.**

Formulation	Y <sub>1</sub> : Average particle size (nm)	Y <sub>2</sub> : Polydispersity index (PDI)	Y <sub>3</sub> : Zeta potential (mV)	Y <sub>4</sub> : Drug Entrapment (%)
D1	1638	0.376	-13.4	82
D2	505.5	0.568	-25.4	84
D3	2588	1	-32	76
D4	253	0.614	-28.6	86
D5	2687	1	-18.6	79
D6	3147	1	-17.6	77
D7	1328	0.376	-27.9	76
D8	347.7	0.446	-27.3	83
D9	878.6	0.833	-30.9	78
D10	1601	0.866	-27.3	74
D11	1069	0.697	-14.1	76
D12	817	0.62	-33.5	82

concentration of high HLB surfactant ( $X_6$ ), sonication time ( $X_7$ ) and pulse rate ( $X_8$ ). In a way  $X_2$ ,  $X_4$ ,  $X_6$  and  $X_7$  had a negative effect and decreased particle, while  $X_1$ ,  $X_5$ ,  $X_8$  effected particle size positively by increasing particle size. Moreover literature reports have previously identified poloxamer to be 'gold standard surfactants as a stabilizer' for reducing particle size and for better stability profiling (Rizwan & Boyd, 2015). We found that incorporation of higher grade of poloxamer (P-407) significantly reduced particle size. It was noted that, solid grade of GMO increased particle size in contrast to liquid grade of GMO. Although with increasing low HLB surfactant concentration particle size increased as it favored more structural binding with lipidic GMO (Dong, Chang, Qian, Tong, & Zhou, 2016). Increase in sonication time lead to decrease in particle size and is credited to the high energy regions of cavitations and compression that grounds coarse dispersion into nanosize, the same has been reported elsewhere (Sugita, Ambarsari, & Lidiniyah, 2015).

PDI of the colloidal dispersion was chosen to be CQA in order to obtain knowledge regarding the homogeneity of the particle size. The type of GMO ( $X_2$ ), type of high HLB surfactant ( $X_4$ ) and sonication time ( $X_7$ ) produced a decrease in  $Y_2$  (PDI), whilst there is an increase in PDI observed with increase in concentration of drug ( $X_1$ ), and concentration of low HLB surfactant ( $X_5$ ).

Zeta potential ( $Y_3$ ) of the system was also identified as CQA, to indicate physical stability of nanoparticle suspensions.  $Y_3$ , notably depended on type of GMO ( $X_2$ ), type of high HLB surfactant ( $X_4$ ) and concentration of high HLB surfactant ( $X_6$ ) had a desirable effect whereas and sonication time ( $X_7$ ) had a negative effect.

Encapsulation efficiency was assigned to be CQA, since it is a paramount dependent variable that governs the delivery system, it manipulates the effectiveness of the nanoparticle to target site by increasing drug loading. Input factors such as concentration of drug ( $X_1$ ), concentration of high HLB surfac-

tant ( $X_6$ ) and sonication time ( $X_7$ ) exhibited negative effects and increasing these input parameters lead to decline in drug entrapment efficiency, on the other hand factors such as type of GMO ( $X_2$ ), concentration of low HLB surfactant ( $X_5$ ), show-cased a positive effect and improved encapsulation efficiency. Our findings are very well in concurrence with earlier reported outcomes, as the concentration of low HLB lipidic surfactant increases the payload also increases owing to addition of more solubilizing groups with expansion of the core radius (Hao et al., 2011). Increase in drug concentration lead to decrease in entrapment efficiency and could be as a result of insufficient quantity of lipidic polymers needed to effectively encapsulate the drug (Pawar, Gholap, Kuchekar, Bothiraja, & Mali, 2015). Electrostatic repulsion in between surfactant and drug could be the possible reason for decline in EE% with increase in concentration of high HLB surfactant. Plausible cause of decrease in EE% with increase in sonication time is as a result of reduction in particle size during sonication cycle leading to loss of drug (Sugita et al., 2015). Thus, it becomes very essential to either fix certain independent variables or to optimize them to achieve the desired goal.

#### Optimization using Box Beknkh design

Optimization of cubosomes was undertaken by fixing some of the independent variables. The concentration of drug was fixed to 1.23% w/w since our goal was to obtain particle size in the range 200-400 nm and maximize % EE. Pulse rate was defined at 3/7 sec to achieve particle size in the desired range. Liquid grade of GMO, P-407 displayed better response for studied dependent variables, hence were fixed as type of GMO and type of high HLB surfactant respectively for BB design. Type of low HLB surfactant had insignificant effect on the selected responses, thus Span 83 was chosen. Input factors such as  $X_5$ ,  $X_6$  and  $X_7$  were critically studied at three levels to optimize cubosomes, Table 6 depicts the observed responses. The coefficient of correlation and p values is presented in Table 7.

**Table 6. Statistical Evaluation of the observed responses –Plackett Burman Design.**

Response	Y <sub>1</sub> : Particle size		Y <sub>2</sub> : PDI		Y <sub>3</sub> : Zeta potential		Y <sub>4</sub> : Entrapment efficiency	
	Coefficient	p-value	Coefficient	p-value	Coefficient	p-value	Coefficient	p-value
α <sub>0</sub>	1404.98	0.0003	0.6997	0.0179	-24.72	0.0181	79.42	0.0046
X <sub>1</sub>	232.95	0.0003	0.0547	0.0330	-1.28	0.0507	-1.92	0.0019
X <sub>2</sub>	-759.85	<0.0001	-0.0700	0.0205	-1.92	0.0237	2.08	0.0016
X <sub>3</sub>	e	e	e	e	e	e	e	e
X <sub>4</sub>	-249.20	0.0003	-0.0460	0.0457	-4.72	0.0040	e	e
X <sub>5</sub>	277.05	0.0002	0.0727	0.0191	-1.02	0.0773	0.7500	0.0121
X <sub>6</sub>	-102.13	0.0006	e	e	-2.55	0.0136	-0.5833	0.0198
X <sub>7</sub>	-71.95	0.0009	-0.0408	0.0570	1.45	0.0404	-1.08	0.0059
X <sub>8</sub>	35.23	0.0018	0.0118	0.3653	-0.4333	0.2860	0.3167	0.0507

<sup>a</sup>α<sub>0</sub> - constant; e - not modeled by software; X<sub>1</sub> - concentration of drug; X<sub>2</sub> - type of GMO, X<sub>3</sub> - type of high HLB surfactant; X<sub>4</sub> - type of low HLB surfactant; X<sub>5</sub> - concentration of low HLB surfactant; X<sub>6</sub> - concentration of high HLB surfactant; X<sub>7</sub> - sonication time; X<sub>8</sub> - pulse rate

**Table 7. Outline of the response on the dependent variable obtained using Box Behnken Design.**

Formulation	Y <sub>1</sub> : Particle size (nm)	Y <sub>2</sub> : Zeta potential (mV)	Y <sub>3</sub> : Polydispersity	Y <sub>4</sub> : Drug entrapment (%)
B1	197.7	-10	0.459	76
B2	209.5	-18.5	0.360	78
B3	263.5	-14.4	0.283	82
B4	383	-26.02	0.149	86
B5	191.7	-9.98	0.387	78
B6	338.7	-27.5	0.222	88
B7	188.6	-8.81	0.525	76
B8	175.7	-6.33	0.410	81
B9	233.5	-18.1	0.154	87
B10	171.8	-4.77	0.217	86
B11	229.8	-14	0.245	88
B12	310	-31.3	0.320	90
B13	188.6	-8.34	0.568	77
B14	185.7	-8.43	0.462	78
B15	320.4	-29.2	0.317	90
B16	420.8	-27.3	0.362	92
B17	169.3	-4.11	0.333	70

R<sup>2</sup> value for particle size (Y<sub>1</sub>), zeta potential (Y<sub>2</sub>), polydispersibility index (Y<sub>3</sub>), entrapment efficiency (Y<sub>4</sub>) is as 0.9457, 0.8714, 0.8775 and 0.9432 respectively. The p values for all the model responses (Table 8) was less than 0.05 indicating that the concerning responses can be forecasted with exactness using the mathematical model.

The factors that impacted particle size significantly were concentration of low HLB surfactant (X<sub>1</sub>), concentration of high HLB surfactant (X<sub>2</sub>), sonication time (X<sub>3</sub>). Interaction of X<sub>1</sub>X<sub>2</sub> and X<sub>1</sub>X<sub>3</sub>, quadratic effect of X<sub>1</sub><sup>2</sup> and X<sub>3</sub><sup>2</sup> significantly affected particle size. Increase in the concentration of low HLB surfactant

and sonication time caused increase in particle size whereas increasing concentration of high HLB surfactant decreased particle size. Increase in the sonication time and concentration of low HLB surfactant exhibited synergistic action by promoting ionic interaction between drug and Span 83 leading to agglomerates of large particle size (Poddar & Sawant, 2017). The polynomial equation of the second order to estimate mean particle size is as obtained:

$$Y = 190.46 + 33.15X_1 - 57.79X_2 + 37.81X_3 - 48.72X_1X_2 - 56.03X_1X_3 - 12.80X_2X_3 + 46.72X_1^2 + 12.34X_2^2 + 58.50X_3^2 \quad (\text{Eq.3})$$

**Table 8. Statistical Evaluation of the observed responses – Box Behnken Design.**

Response	Y <sub>1</sub> particle size (nm)		Y <sub>2</sub> zeta potential (mV)		Y <sub>3</sub> PDI		Y <sub>4</sub> Entrapment efficiency	
	Coefficient	p-value	Coefficient	p-value	Coefficient	p-value	Coefficient	p-value
β <sub>0</sub>	190.46	0.0012	-9.11	0.0091	0.48	0.0145	77.40	0.0015
X <sub>1</sub>	33.15	0.0124	4.44	0.0125	0.0098	0.6716	4.25	0.0011
X <sub>2</sub>	-57.79	0.0006	-5.26	0.0261	0.0011	0.9608	-2.00	0.0407
X <sub>3</sub>	37.81	0.0066	4.59	0.0228	-0.058	0.0333	4.00	0.0015
X <sub>1</sub> X <sub>2</sub>	-48.72	0.0104	3.71	0.1401	-0.078	0.0422	0.0000	1
X <sub>1</sub> X <sub>3</sub>	-56.03	0.0052	4.95	0.0620	0.047	0.1800	-4.00	0.0094
X <sub>2</sub> X <sub>3</sub>	-12.80	0.3919	3.37	0.1744	-0.031	0.3507	1.0000	0.4052
X <sub>1</sub> <sup>2</sup>	46.72	0.0112	3.51	0.1508	-0.076	0.0418	4.55	0.0044
X <sub>2</sub> <sup>2</sup>	12.34	0.3967	-0.48	0.8325	-0.096	0.0162	4.55	0.0044
X <sub>3</sub> <sup>2</sup>	58.50	0.0037	10.04	0.0025	-0.12	0.0046	2.05	0.1048

<sup>a</sup>β<sub>0</sub> –constant; X<sub>1</sub>–concentration of low HLB surfactant; X<sub>2</sub> –concentration of high HLB surfactant; X<sub>3</sub>–sonication time

**Table 9. The observed and predicted values of the optimized NYS cubosome formulation with respect to desirability**

Response	Observed	Predicted
Particle size (nm)	263.5	247.99
Zeta potential (mV)	-14.4	-14
PDI	0.283	0.278
Entrapment efficiency (%)	82	81.81

Zeta potential (Y<sub>2</sub>) of the colloidal dispersion dependent on individual factors X<sub>1</sub>, X<sub>2</sub>, X<sub>3</sub> in addition to quadratic effect of X<sub>3</sub><sup>2</sup> and had a significant on Y<sub>2</sub>. The increase in concentration of P-407 and increase in sonication time affected zeta potential positively thus increased its magnitude while increase in concentration of Span 83 had negative impact on zeta potential by decreasing its magnitude. Similar outcomes have been portrayed previously (Sugita et al., 2015). The polynomial equation of the second order to estimate zeta potential is as obtained:

$$Y = -9.11 + 4.44X_1 - 5.26X_2 - 4.59X_3 + 3.71X_1X_2 + 4.95X_2X_3 + 3.37X_2X_3 + 3.51X_1^2 - 0.48X_2^2 - 10.04 \quad (\text{Eq.4})$$

PDI (Y<sub>3</sub>) was significantly affected by sonication time (X<sub>3</sub>), the interaction of X<sub>1</sub>X<sub>2</sub> and the quadratic effect of individual inputs X<sub>1</sub><sup>2</sup>, X<sub>2</sub><sup>2</sup> and X<sub>3</sub><sup>2</sup>. Increasing the sonication time lead to decline in PDI values, similar findings of sonication time effecting PDI has been reported (Pawar et al., 2015). The polynomial equation of the second order to estimate PDI is as obtained:

$$Y = 0.48 + 0.0098X_1 + 0.0011X_2 - 0.058X_3 - 0.078X_1X_2 + 0.047X_1X_3 - 0.031X_2X_3 - 0.076X_1^2 - 0.096X_2^2 - 0.12X_3^2 \quad (\text{Eq.5})$$

Entrapment efficiency (%EE) was influenced by X<sub>1</sub>, X<sub>2</sub>, X<sub>3</sub>, X<sub>1</sub>X<sub>3</sub> interaction, quadratic effect of X<sub>1</sub><sup>2</sup> and X<sub>2</sub><sup>2</sup>, these terms showed significant effect. In case of % EE concentration of low HLB surfactant was critical variable and as the concentration increased

entrapment also increased, similar findings have been reported (Gabr, Mortada, & Sallam, 2017). However, concentration of Span 83 should be optimal so that the size of the nanoparticles is also beneath the defined dimensions. The polynomial equation of the second order to estimate % EE is as obtained:

$$Y = 77.40 + 4.25X_1 - 2X_2 + 4X_3 - 4X_1X_2 + 0XX_1X_2 + 1X_2X_3 + 4.55X_1^2 + 4.55X_2^2 + 2.05X_3^2 \quad (\text{Eq.6})$$

To carefully estimate the effect of various factors on selected responses, contour plots depicting the effect of two independent variables simultaneously (interactions) on the third variable (dependant variable) are presented in Figure 2.

The desirability function was obtained to acquire the optimized formulation. The optimum formulation was set on goal of achieving particle size less than 350 nm, entrapment efficiency greater than 75%, PDI less than 0.3 and zeta potential of upper limit -14 mV. Accordingly, cubosome nanoparticle with the projected levels of formulation factors was prepared to bear out the validity of the optimization method. Table 8 displays the optimum and predicted response of formulated optimized cubosome and Figure 3 is the representation of the overlaid contour plots.

**Polarised light microscopy (PLM)**

Crossed PLM image are presented in Figure 4. The PLM studies were undertaken for finding out whether the particles formed were cubosomes or hexosomes. The image appeared completely black under the cross polarizers indicating the presence of cubic phase, thus confirming formation of Cubosomes (Gabr et al., 2017).

**In-vitro antifungal activity**

In-vitro antifungal activity was estimated to confirm the efficacy of drug loaded cubosome against fungi of the genus Aspergillus fumigatus, the causative agent for IPA in immunocompromised patients. NYS solution and NYS suspension were considered as reference standards. The zone of inhibi-



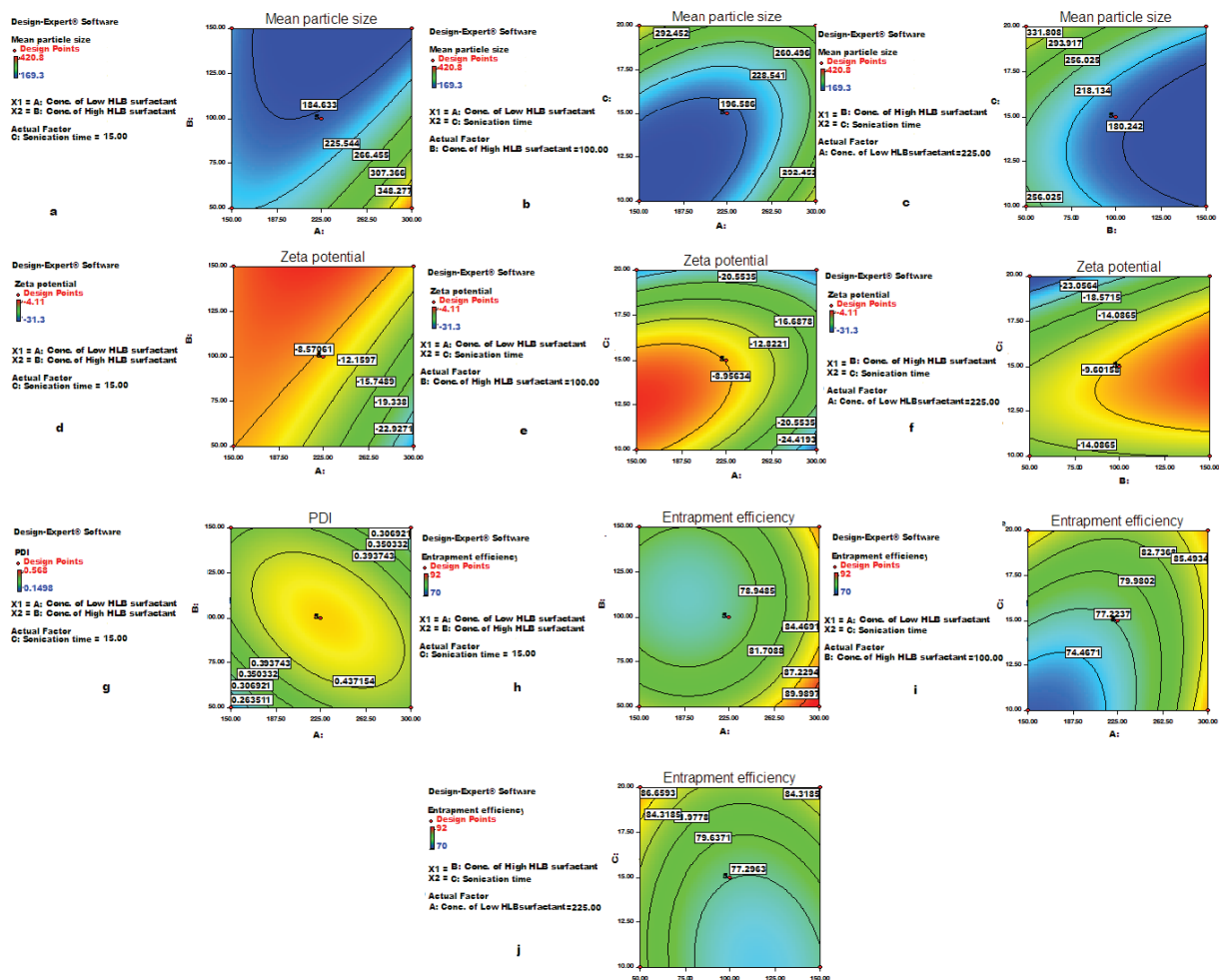


**Figure 2.** Contour plots presenting impact of (a) Concentration of low HLB surfactant and concentration of high HLB surfactant on mean particle size, (b) Concentration of low HLB surfactant and sonication time on mean particle size (c) Concentration of high HLB and sonication time on mean particle size (d) Concentration of low HLB surfactant and concentration of high HLB surfactant on zeta potential (e) Concentration of low HLB surfactant and sonication time on zeta potential (f) Concentration of high HLB and sonication time on zeta potential (g) Concentration of low HLB surfactant and concentration of high HLB surfactant on PDI (h) Concentration of low HLB surfactant and concentration of high HLB surfactant on entrapment efficiency (i) Concentration of low HLB surfactant and sonication time on entrapment efficiency (j) Concentration of high HLB and sonication time on entrapment efficiency.

tion of NYS from optimized cubosome (B3) was compared with NYS suspended in phosphate buffer and nystatin solution (Figure 5). It was notably seen that optimized NYS cubosomes displayed significantly higher zone of inhibition in comparison to NYS suspended in phosphate buffer ( $p < 0.05$ ), whereas with pure drug solution no significant difference was found ( $p > 0.05$ ).

**In-vitro drug release**

Release profile was investigated to assess the successful development and release of the encapsulated drug from cubosome nanoparticles. The study aimed to demonstrate the developed formulations superiority over drug suspension and drug solution. It was observed that complete drug release was achieved within 3 hours from NYS solution. The faster release of drug from pure solution is due to the fact that the drug particles are in molecular state. The release rate of NYS from optimized cubosome (B3) was further compared with NYS suspended in phosphate buffer (NYS suspension)

(Figure 6). Release profile points out to NYS release to be significantly higher from cubosome formulations compared to NYS suspension after 96 h. Faster drug release from cubosome as compared to suspension can be attributed to the fact that the drug was in the solubilized state and moreover molecularly dispersed in amorphous form (Kassem, Mohsen, Samir Ahmed, & Mohamed Essam, 2016; Prajapati, Jain, Jain, Sahu, & Kohli, 2014). Although, in case of cubosome formulation a bi-phasic release pattern was seen, an initial burst release is due to adsorbed drug placed at or just below the surface of the nanoparticles followed by subsequent slower drug release rate up to 48 hrs. The results corroborate to earlier finding (Shi et al., 2017). The release kinetics from cubosome was studied using PCP DISSO V3 and was found to follow Higuchi release pattern ( $R^2 = 0.941$ ). Hence the release from these cubosome structures is controlled by the microstructure formed, number of water channels and the location of the drug moiety (Prajapati et al., 2014; Shi et al., 2017).

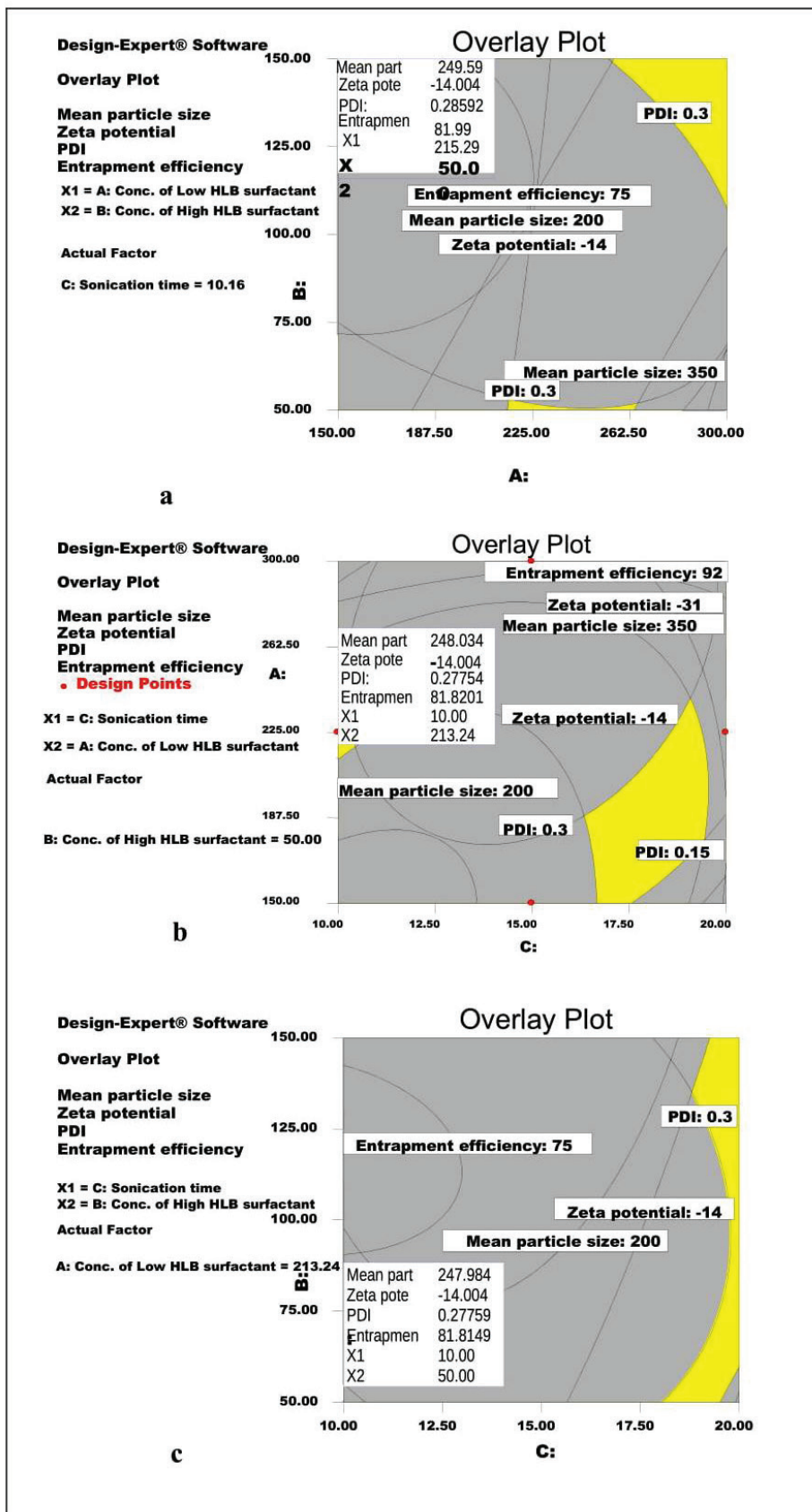


**Figure 3.** Design space for NYS cubosomes. Yellow regions depicts the likely permutations to achieve predictable results for average nanoparticle size (200–350 nm), zeta potential (<-14), encapsulation efficiency (>75%) and polydispersity index (0.15–0.3). (a) Overlay plot of concentration of low HLB surfactant and concentration of high HLB surfactant, (b) overlay plot of concentration of low HLB surfactant and sonication time (c) overlay plot of concentration of high HLB surfactant and sonication time.

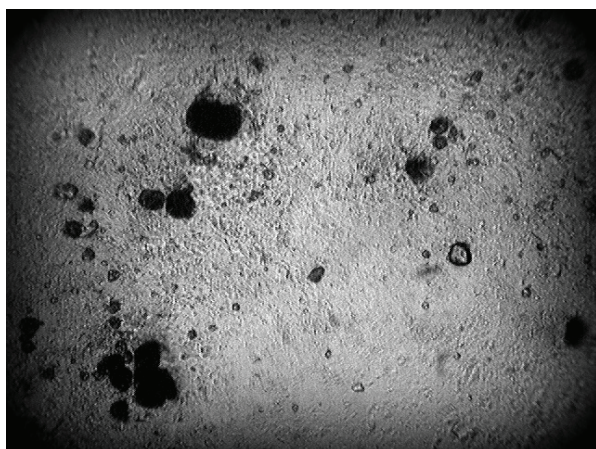


**Figure 4.** Polarised light microscopy image of optimized NYS cubosomes under cross polarizers.

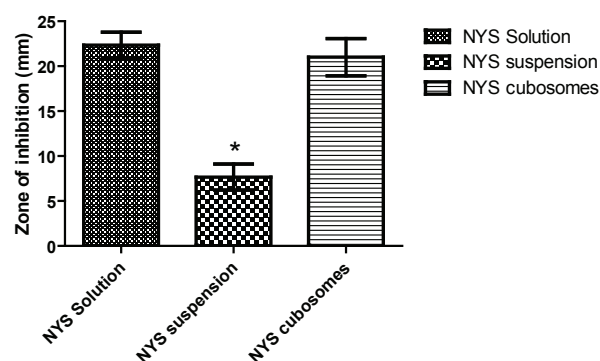


**Figure 5.** *In-vitro* antifungal activity of NYS solution, NYS Cubosomes and NYS suspension against *Aspergillus fumigatus*.

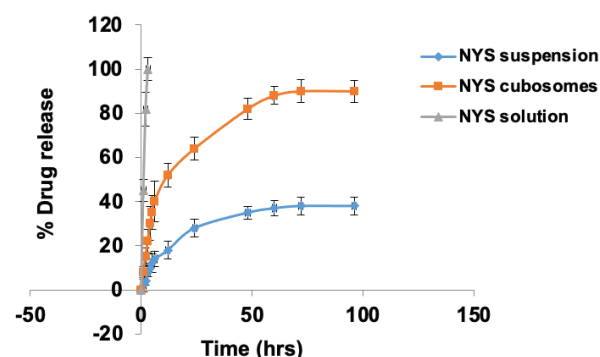


**Figure 6.** *In-vitro* drug release profile of NYS Cubosomes, NYS suspension and NYS solution.

**Cytotoxicity assays**

Cytotoxicity assay of NYS and optimized NYS cubosomes (B3) performed on A549 cell line after 72 hours of treatment is represented in Figure 7. The cytotoxicity is expected to be maximum in solution since the drug is in its molecular state. The % cell viability on A549 cell line at concentration 100 µg/ml for these samples was found to be 22% and 70% respectively. IC<sub>50</sub> values were calculated to be 60.178 µg/ml and 151.35 µg/ml respectively. Thus the cubosome formulation exhibits reduced cell cytotoxicity as compared to pure drug solution, similar

findings for nanocomposites have been reported elsewhere (Hussein-Al-Ali et al., 2014).

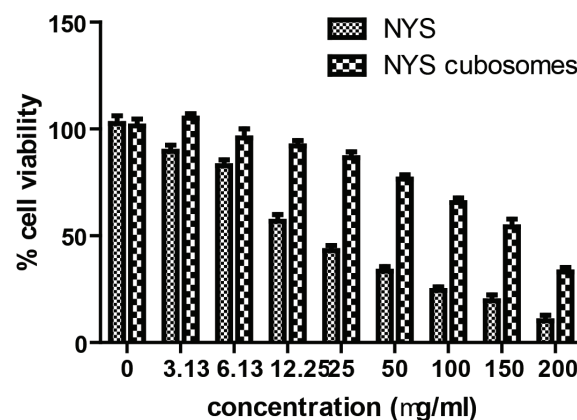


**Figure 7.** Cytotoxicity assay of NYS and NYS Cubosomes on A549 cell lines.

***In-vitro* haemolytic assay**

To determine the toxic potential of the formulated cubosomes, *in-vitro* haemolytic assay was performed on various concentrations of both NYS and optimized formulation (B3). Figure 8 indicates that the HC<sub>50</sub> for NYS cubosome was 400 µg/ml, while for NYS it was seen at 40 µg/ml, similar findings have been reported (Kim et al., 2017). Thus, the results signify lower toxicity of the formulation as compared to NYS. This is observed as nystatin is well binded to the lipidic surfactant in the cubical structure, thus low release of free form is accessible to form dimer and induce haemolysis.

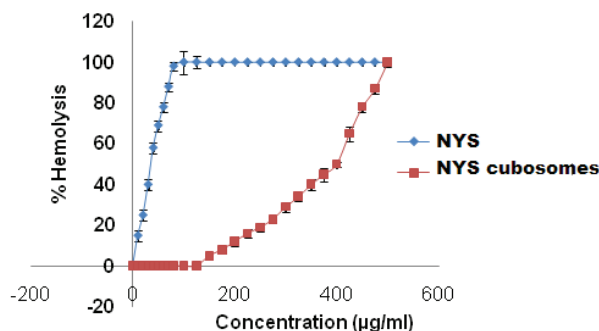


**Figure 8.** Hemolytic assay of NYS and NYS cubosomes.

**Small angle X-ray scattering**

Scattering profile for the optimized formulation is presented in Figure 9. SAXS studies was undertaken to identify the cubic mesophasic structure, measure lattice parameters and also to confirm particle size of the formed nanoparticles. The scattering peaks ratios were indicative of Pn3m bicontinuous cubic phase ( $\sqrt{2}:\sqrt{3}:\sqrt{4}$ ) (Deshpande & Singh, 2017). The lattice parameter was found to be 78.88 nm and the particle size was 245.77nm.

**Differential scanning calorimeter**

DSC thermograms of NYS, GMO, P-407 and NYS cubosomes are presented in Figure10. The thermogram of NYS exhibits

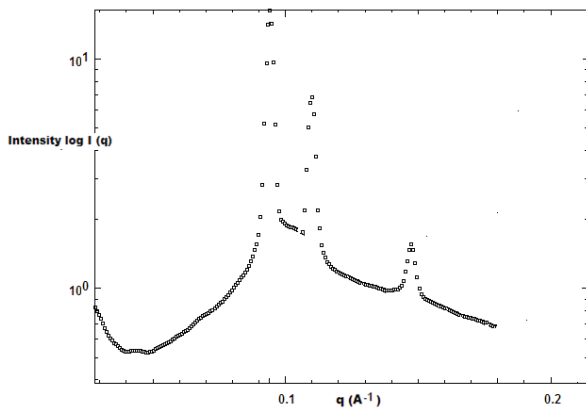


Figure 9. SAX scattering profile of optimized NYS Cubosomes.

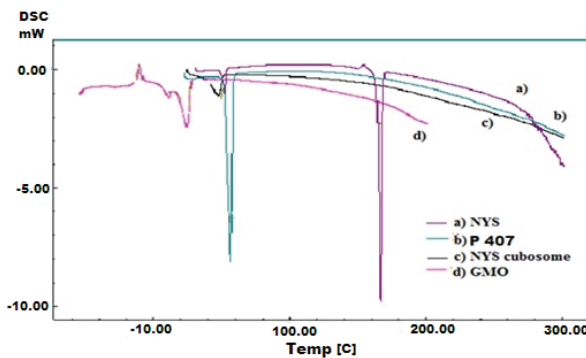


Figure 10. DSC thermogram of a) NYS b) P-407 c) NYS cubosome d) GMO.

a sharp endothermic melting peak at 166°C which is in conformity to literature reports (Michel, 1977). Nevertheless, NYS melting peak completely vanished in thermogram of NYS cubosomes. Thus, this justifies the incorporation of drug in the cubosomes to be a non-crystalline form.

### FTIR spectroscopy

FTIR studies were undertaken to examine any interaction between NYS and excipients in the optimized cubosome formulation. Figure 11 illustrates the FTIR spectra of these samples. The spectra of NYS (Michel, 1977) distinctly shows a NH stretching peak at 3012  $\text{cm}^{-1}$ , OH stretching at 3351  $\text{cm}^{-1}$ , peak at 1701  $\text{cm}^{-1}$  corresponds to unstrained lactone group, carboxylate ion

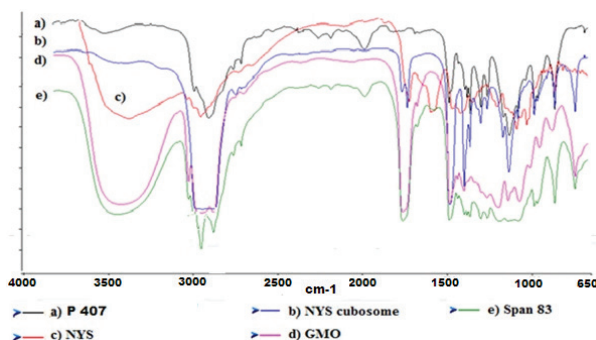


Figure 11. FTIR spectra of a) P-407 b) NYS cubosome c) NYS d) GMO e) Span 83.

at 1574  $\text{cm}^{-1}$ ,  $\text{CH}_3$  deformation (asym) and  $\text{CH}_2$  deformation at 1448  $\text{cm}^{-1}$ ,  $\text{CH}_3$  deformation (sym) at 1399  $\text{cm}^{-1}$ , C-OH stretching at 1069  $\text{cm}^{-1}$  and CH deformation (out of plane) in  $-\text{CH}=\text{CH}-$  (trans) at 946  $\text{cm}^{-1}$ . The IR spectra of GMO demonstrated OH stretching peak at 3400.80  $\text{cm}^{-1}$ . The  $\text{CH}_2$  stretching and ester bond was definite by peaks at 2960  $\text{cm}^{-1}$  and 1740  $\text{cm}^{-1}$  respectively. IR spectra of P-407 highlighted peaks at 2970.65, 1343.17, and 1061.21  $\text{cm}^{-1}$  related to C-H aliphatic stretch, in plane O-H bond, and C-O stretch, respectively. Span 83 spectra showed characteristic peaks at 1630  $\text{cm}^{-1}$ , 3430  $\text{cm}^{-1}$ , are assigned OH group. It is to be noted, peaks at 1720  $\text{cm}^{-1}$ , 1562  $\text{cm}^{-1}$ , 1357  $\text{cm}^{-1}$  are attributed to the C=O, C-H bending in  $\text{CH}_3$  and  $\text{CH}_2$ . FTIR spectra for the drug loaded cubosome proves retention of characteristic functional groups, thus explicatory of no signs of interaction and assuring encapsulation of drug moiety in the nanostructure.

### X-ray diffraction

XRD pattern of pure drug and optimized formulation is depicted in Figure 12. Typical sharp peaks for free NYS  $2\theta$  values 4.33°, 13.95°, 15.60°, 16.72° and 21.51° (Michel, 1977) affirm to its crystalline nature. Though these peaks were not observed in the diffractogram of NYS cubosome formulation, thereby confirm to amorphous form of drug. DSC findings are in agreement to the above results and are suggestive of the drug encapsulated in the cubical nanostructure. However, the diffraction spectra of the optimized formulation did show some peaks at  $2\theta$  values 18.5° and 22.37°, which may correspond to mannitol, the same has been reported (Sugita et al., 2015).

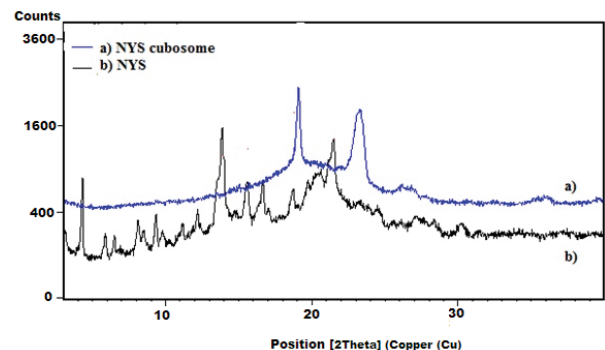


Figure 12. X-ray diffractogram of a) NYS cubosome b) NYS.

### FEG Transmission electron microscopy

The structure of cubosomes is validated by both SAXS and TEM analysis. Figure 13 images denote outer shape and inner microstructure of the cubosomes. Outer virtually spherical structure with some irregular polyangular symmetry and extensive internal water channels clearly explains Pn3m mesophasic structure as interpreted through SAXS data and reported elsewhere (Shi et al., 2017). Particle size obtained by TEM (200 nm) is in good agreement to the zetasizer findings.

### CONCLUSIONS

Nystatin loaded cubosome nanoparticles were formulated by dispersing the dry drug loaded lipidic film in phosphate buffer pH 7.4 by the aid of ultrasound probe sonicator. The effects of



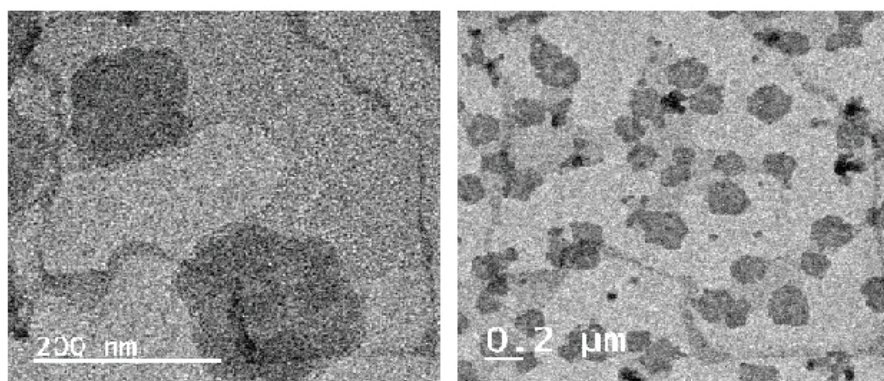


**Figure 13.** TEM images of optimized NYS cubosomes.

formulation and process parameters on CQAs of cubosome was screened and optimized with the help of experimental designs Plackett–Burman followed by Box–Behnken. Design space was constructed following optimization of formulation. PLM, TEM images and SAXS profiles confirmed the formation of cubosome nanoparticles. XRD spectra, FTIR spectra and DSC thermogram indicated successful encapsulation of the drug. The *in-vitro* cell toxicity and *in-vitro* hemolytic assay revealed lower toxicity of NYS cubosomes as compared to free drug.

Although the *in-vitro* release profiles and *in-vitro* antifungal studies point out sustained effect, the conceptualization of target specificity can be assured only by evaluating the *in-vivo* deposition and fate of NYS-cubosomes in lungs which is essential for pulmonary administration of drugs. Thus, non-invasive feature and contemplated target specificity of nystatin loaded cubosome nanoparticles pave a way for its prospect as pulmonary delivery to combat IPA.

**Peer-review:** Externally peer-reviewed.

**Author Contributions:** Conception/Design of Study- M.K., M.H.D.; Data Acquisition- M.K.; Data Analysis/Interpretation- M.K., M.H.D.; Drafting Manuscript- M.K.; Critical Revision of Manuscript- M.K., M.H.D.; Final Approval and Accountability- M.K., M.H.D.; Technical or Material Support- M.K.; Supervision- M.H.D.

**Conflict of Interest:** The authors have no conflict of interest to declare.

**Financial Disclosure:** Authors declared no financial support.

**Acknowledgments:** The authors are thankful to Glenmark Pharmaceuticals (Mumbai, India) for providing Nystatin and Poloxamer P407, Dupont (Gurgaon, India) and Croda, (Mumbai, India) for generous supply of Dimodan HPM-90 and Cithrol GMO-HP-SO-LK respectively. We would also like to thank Cipla Limited (Mumbai, India) for providing Span 80 and Span 83. The authors thank SAIF, IIT-Bombay (Maharashtra, India) and Wockhardt Ltd. (Aurangabad, India) for rendering provisions to use SAXS facility and XRD, FTIR respectively.

## REFERENCES

- Adhikari, K. (2017). In vitro Toxicity Study of Reconstituted Amphotericin B - Lipid Derivatives Dry Powder for Nebulization. *Dhaka University Journal of Pharmaceutical Sciences*, 15, 127.
- Ali, M. A., Noguchi, S., Iwao, Y., Oka, T., & Itai, S. (2016). Preparation and Characterization of SN-38-Encapsulated Phytantriol Cubosomes Containing alpha-Monoglyceride Additives. *Chemical & Pharmaceutical Bulletin*, 64(6), 577–584.
- Bei, D., Marszalek, J., & Youan, B.-B. C. (2009). Formulation of dacarbazine-loaded cubosomes-part I: influence of formulation variables. *AAPS PharmSciTech*, 10(3), 1032–1039.
- Carneiro, S. P., Carvalho, K. V., de Oliveira Aguiar Soares, R. D., Carneiro, C. M., de Andrade, M. H. G., Duarte, R. S., & Dos Santos, O. D. H. (2019). Functionalized rifampicin-loaded nanostructured lipid carriers enhance macrophages uptake and antimycobacterial activity. *Colloids and Surfaces. B, Biointerfaces*, 175, 306–313.
- Chishti, N., Jagwani, S., Dhamecha, D., Jalalpure, S., & Dehghan, M. H. (2019). Preparation, Optimization, and In Vivo Evaluation of Nanoparticle-Based Formulation for Pulmonary Delivery of Anti-cancer Drug. *Medicina (Kaunas, Lithuania)*, 55(6).
- Chuealee, R., Aramwit, P., Noipha, K., & Srichana, T. (2011). Bioactivity and toxicity studies of amphotericin B incorporated in liquid crystals. *European Journal of Pharmaceutical Sciences: Official Journal of the European Federation for Pharmaceutical Sciences*, 43(4), 308–317.
- Das, P. J., Paul, P., Mukherjee, B., Mazumder, B., Mondal, L., Baishya, R., Debnath, M. C., & Dey, K. S. (2015). Pulmonary Delivery of Voriconazole Loaded Nanoparticles Providing a Prolonged Drug Level in Lungs: A Promise for Treating Fungal Infection. *Molecular Pharmaceutics*, 12(8), 2651–2664.
- Deshpande, S., & Singh, N. (2017). Influence of Cubosome Surface Architecture on Its Cellular Uptake Mechanism. *Langmuir*, 33(14), 3509–3516.
- Dong, Y., Chang, Y., Qian, W., Tong, J., & Zhou, J. (2016). Effects of surfactants on size and structure of amylose nanoparticles prepared by precipitation. *Bulletin of Materials Science*, 39.
- El-Ridy, M. S., Abdelbary, A., Essam, T., El-Salam, R. M. A., & Kassem, A. A. A. (2011). Niosomes as a potential drug delivery system for increasing the efficacy and safety of nystatin. *Drug Development and Industrial Pharmacy*, 37(12), 1491–1508.
- Esposito, E., Cortesi, R., Drechsler, M., Paccamiccio, L., Mariani, P., Contado, C., Stellin, E., Menegatti, E., Bonina, F., & Puglia, C. (2005). Cubosome dispersions as delivery systems for percutaneous administration of indomethacin. *Pharmaceutical Research*, 22(12), 2163–2173.
- Kim, E. S., Han, K. B., Lin, S., Kong, D., Bai, L., Deng, Z., ... & Lee, M. J. (2017). Polyene compound, method for preparing the same, and antifungal drug comprising novel polyene compound as active ingredient U.S. Patent No. 9,605,015. Washington, DC: U.S. Patent and Trademark Office.
- Fernandez Campos, F., Calpena Campmany, A. C., Rodriguez Delgado, G., Lopez Serrano, O., & Clares Naveros, B. (2012). Development and characterization of a novel nystatin-loaded nanoemulsion for the buccal treatment of candidosis: ultrastructural effects and release studies. *Journal of Pharmaceutical Sciences*, 101(10), 3739–3752.



- Furedi, P., Papay, Z. E., Kovacs, K., Kiss, B. D., Ludanyi, K., Antal, I., & Klebovich, I. (2017). Development and characterization of the voriconazole loaded lipid-based nanoparticles. *Journal of Pharmaceutical and Biomedical Analysis*, 132, 184–189.
- Gabr, M. M., Mortada, S. M., & Sallam, M. A. (2017). Hexagonal Liquid Crystalline Nanodispersions Proven Superiority for Enhanced Oral Delivery of Rosuvastatin: In Vitro Characterization and In Vivo Pharmacokinetic Study. *Journal of Pharmaceutical Sciences*, 106(10), 3103–3112.
- Hao, J., Fang, X., Zhou, Y., Wang, J., Guo, F., Li, F., & Peng, X. (2011). Development and optimization of solid lipid nanoparticle formulation for ophthalmic delivery of chloramphenicol using a Box-Behnken design. *International Journal of Nanomedicine*, 6, 683–692.
- Hussein-Al-Ali, S. H., El Zowalaty, M. E., Kura, A. U., Geilich, B., Fakurazi, S., Webster, T. J., & Hussein, M. Z. (2014). Antimicrobial and controlled release studies of a novel nystatin conjugated iron oxide nanocomposite. *BioMed Research International*, 2014, 651831.
- Islam, N., & Ferro, V. (2016). Recent advances in chitosan-based nanoparticulate pulmonary drug delivery. *Nanoscale*, 8(30), 14341–14358.
- Kassem, A., Mohsen, A., Samir Ahmed, R., & Mohamed Essam, T. (2016). Self-nanoemulsifying drug delivery system (SNEDDS) with enhanced solubilization of nystatin for treatment of oral candidiasis: Design, optimization, in vitro and in vivo evaluation. *Journal of Molecular Liquids*, 218, 219–232.
- Khan, M. A., Faisal, S. M., & Mohammad, O. (2006). Safety, efficacy and pharmacokinetics of tuftsin-loaded nystatin liposomes in murine model. *Journal of Drug Targeting*, 14(4), 233–241.
- Kim, H.-J., Son, J. S., & Kwon, T.-Y. (2018). Antifungal Effect of a Dental Tissue Conditioner Containing Nystatin-Loaded Alginate Microparticles. *Journal of Nanoscience and Nanotechnology*, 18(2), 848–852.
- Kosmidis, C., & Muldoon, E. G. (2017). Challenges in the management of chronic pulmonary aspergillosis. *Medical Mycology*, 55(1), 63–68.
- Lestner, J. M., Howard, S. J., Goodwin, J., Gregson, L., Majithiya, J., Walsh, T. J., Jensen, G. M., & Hope, W. W. (2010). Pharmacokinetics and pharmacodynamics of amphotericin B deoxycholate, liposomal amphotericin B, and amphotericin B lipid complex in an in vitro model of invasive pulmonary aspergillosis. *Antimicrobial Agents and Chemotherapy*, 54(8), 3432–3441.
- Madheswaran, T., Kandasamy, M., Bose, R. J., & Karuppagounder, V. (2019). Current potential and challenges in the advances of liquid crystalline nanoparticles as drug delivery systems. *Drug Discovery Today*, 24(7), 1405–1412.
- Mandal, S., Prathipati, P. K., Belshan, M., & Destache, C. J. (2019). A potential long-acting bicitegravir loaded nano-drug delivery system for HIV-1 infection: A proof-of-concept study. *Antiviral Research*, 167, 83–88.
- Maqsood, I., Masood, M. I., Bashir, S., Nawaz, H. M. A., Anjum, A. A., Shahzadi, I., Ahmad, M., & Imran Masood, I. M. (2015). Preparation and in vitro evaluation of Nystatin micro emulsion based gel. *Pakistan Journal of Pharmaceutical Sciences*, 28(5), 1587–1593.
- Marin-Quintero, D., Fernandez-Campos, F., Calpena-Campmany, A. C., Montes-Lopez, M. J., Clares-Naveros, B., & Del Pozo-Carrasco, A. (2013). Formulation design and optimization for the improvement of nystatin-loaded lipid intravenous emulsion. *Journal of Pharmaceutical Sciences*, 102(11), 4015–4023.
- Michel, G. W. (1977). *Nystatin* (K. Florey (ed.); Vol. 6, pp. 341–421). Academic Press.
- Newman, S. P. (2017). Drug delivery to the lungs: challenges and opportunities. *Therapeutic Delivery*, 8(8), 647–661.
- Offner, F., Krcmery, V., Boogaerts, M., Doyen, C., Engelhard, D., Ribaud, P., Cordonnier, C., de Pauw, B., Durrant, S., Marie, J.-P., Moreau, P., Guiot, H., Samonis, G., Sylvester, R., & Herbrecht, R. (2004). Liposomal nystatin in patients with invasive aspergillosis refractory to or intolerant of amphotericin B. *Antimicrobial Agents and Chemotherapy*, 48(12), 4808–4812.
- Pawar, A. P., Gholap, A. P., Kuchekar, A. B., Bothiraja, C., & Mali, A. J. (2015). Formulation and evaluation of optimized oxybenzone micro-sponge gel for topical delivery. *Journal of Drug Delivery*, 2015, 261068.
- Petrikkou, E., Rodriguez-Tudela, J. L., Cuenca-Estrella, M., Gomez, A., Molleja, A., & Mellado, E. (2001). Inoculum standardization for antifungal susceptibility testing of filamentous fungi pathogenic for humans. *Journal of Clinical Microbiology*, 39(4), 1345–1347.
- Pinto Reis, C., Vasques Roque, L., Baptista, M., & Rijo, P. (2016). Innovative formulation of nystatin particulate systems in toothpaste for candidiasis treatment. *Pharmaceutical Development and Technology*, 21(3), 282–287.
- Poddar, A., & Sawant, K. (2017). Optimization of Galantamine Loaded Bovine Serum Albumin Nanoparticles by Quality by Design and Its Preliminary Characterizations. *J Nanomed Nanotechnol*, 8(5), 1–10.
- Prajapati, V., Jain, A., Jain, R., Sahu, S., & Kohli, D. V. (2014). Treatment of cutaneous candidiasis through fluconazole encapsulated cubosomes. *Drug Delivery and Translational Research*, 4(5–6), 400–408.
- Rani, S., Gothwal, A., Pandey, P. K., Chauhan, D. S., Pachouri, P. K., Gupta, U. D., & Gupta, U. (2018). HPMA-PLGA Based Nanoparticles for Effective In Vitro Delivery of Rifampicin. *Pharmaceutical Research*, 36(1), 19.
- Rizwan, S. B., Assmus, D., Boehnke, A., Hanley, T., Boyd, B. J., Rades, T., & Hook, S. (2011). Preparation of phytantriol cubosomes by solvent precursor dilution for the delivery of protein vaccines. *European Journal of Pharmaceutics and Biopharmaceutics: Official Journal of Arbeitsgemeinschaft Fur Pharmazeutische Verfahrenstechnik eV*, 79(1), 15–22.
- Rizwan, S.?, & Boyd, B. (2015). *Cubosomes: Structure, Preparation and Use as an Antigen Delivery System* (pp. 125–140).
- Ryder, N. S. (1999). Antifungal agents. *IDrugs: The Investigational Drugs Journal*, 2(12), 1253–1255.
- Sakeer, K., Al-Zein, H., Hassan, I., Desai, S., & Nokhodchi, A. (2010). Enhancement of dissolution of nystatin from buccoadhesive tablets containing various surfactants and a solid dispersion formulation. *Archives of Pharmacol Research*, 33(11), 1771–1779.
- Shi, X., Peng, T., Huang, Y., Mei, L., Gu, Y., Huang, J., Han, K., Li, G., Hu, C., Pan, X., & Wu, C. (2017). Comparative studies on glycerol monooleate- and phytantriol-based cubosomes containing oridonin in vitro and in vivo. *Pharmaceutical Development and Technology*, 22(3), 322–329.
- Silva, F. C., Marto, J. M., Salgado, A., Machado, P., Silva, A. N., & Almeida, A. J. (2017). Nystatin and lidocaine pastilles for the local treatment of oral mucositis. *Pharmaceutical Development and Technology*, 22(2), 266–274.
- Sugita, P., Ambarsari, L., & Lidiniyah. (2015). Optimization of Ketoprofen-loaded Chitosan Nanoparticle Ultrasonication Process. *Procedia Chemistry*, 16, 673–680.
- Szalewski, D. A., Hinrichs, V. S., Zinniel, D. K., & Barletta, R. G. (2018). The pathogenicity of *Aspergillus fumigatus*, drug resistance, and nanoparticle delivery. *Canadian Journal of Microbiology*, 64(7), 439–453.
- von Halling Laier, C., Gibson, B., van de Weert, M., Boyd, B. J., Rades, T., Boisen, A., Hook, S., & Nielsen, L. H. (2018). Spray dried cubosomes with ovalbumin and Quil-A as a nanoparticulate dry powder vaccine formulation. *International Journal of Pharmaceutics*, 550(1–2), 35–44.
- Yang, Z., Tan, Y., Chen, M., Dian, L., Shan, Z., Peng, X., & Wu, C. (2012). Development of amphotericin B-loaded cubosomes through the SolEmuls technology for enhancing the oral bioavailability. *AAPS PharmSciTech*, 13(4), 1483–1491.

# Chitosan films and chitosan/pectin polyelectrolyte complexes encapsulating silver sulfadiazine for wound healing

Gökçen Yaşayan<sup>1</sup> 

<sup>1</sup>Marmara University, Faculty of Pharmacy, Department of Pharmaceutical Technology, Haydarpaşa, İstanbul, Turkey

**ORCID IDs of the authors:** G.Y. 0000-0002-5299-2924

**Cite this article as:** Yasayan, G. (2020). Chitosan films and chitosan/pectin polyelectrolyte complexes encapsulating silver sulfadiazine for wound healing. *Istanbul Journal of Pharmacy*, 50 (3), 238-244.

## ABSTRACT

**Background and Aims:** The use of natural polymers as wound dressings is attracting more interest due to their favoured properties such as biodegradability and biocompatibility. With this background, chitosan films and chitosan/pectin polyelectrolyte complex films encapsulating silver sulfadiazine were fabricated as novel wound dressings.

**Methods:** Films were fabricated, and the surface topography and the surface roughness of the films were characterised by atomic force microscopy. Swelling and hydrolytic degradation behaviours of the films were monitored, and surface chemistry analysis was carried out. Following drug release studies, release kinetics were studied to evaluate the films for drug delivery.

**Results:** Results suggest that the characteristic crystalline structure of chitosan films disappears after complexation with pectin. Polyelectrolyte complex films were found to be more durable than chitosan films due to their improved resistance to hydrolytic degradation. No incompatibilities amongst formulation components were detected. *In vitro* drug release studies indicated a rapid release of the drug from chitosan films compared to polyelectrolyte complex films.

**Conclusion:** The overall results suggest that chitosan/pectin polyelectrolyte complex films have improved properties in terms of durability compared to chitosan films. Both films could be a promising candidate for wound healing applications considering the specific needs of different types of wounds.

**Keywords:** Chitosan, silver sulfadiazine, polyelectrolyte

## INTRODUCTION

Wound care is an important topic in the worldwide health care systems for both clinical and economic reasons. Wounds, especially chronic non-healing types, may affect living standards of the patients significantly, and treatment costs of wound therapies cause an economic burden (Gottrup, 2004; Olsson et al., 2019). It has been foreseen that number of people facing wounds will increase as a result of increases in ageing populations, as well as in the incidence rates of patients with chronic diseases such as diabetes and circulatory abnormalities (Lai et al., 2014).

Coping efficiently with wounds involves three main strategies: prevention, diagnosis and treatment. For wound treatment, the type of wound and the function of the wound dressing should be considered in order to facilitate wound healing. Dressings should be selected based on the specific needs of the wound to provide the optimum conditions for healing. These conditions could be adjusting moisture and temperature, enabling gas exchange, promoting new tissue regeneration, protecting against pathogens and other external contaminations. Also being non-toxic, non-allergic, and non-adherent to newly formed granu-

### Address for Correspondence:

Gökçen YAŞAYAN, e-mail: gokcen.yasayan@marmara.edu.tr

Submitted: 31.03.2020

Revision Requested: 04.05.2020

Last Revision Received: 09.05.2020

Accepted: 26.05.2020

Published Online: 04.11.2020

This work is licensed under a Creative Commons Attribution 4.0 International License.



lation tissue are favoured (Dhivya, Padma & Santhini, 2015; Vowden & Vowden, 2017; Han & Ceilley, 2017).

Traditional wound dressings such as gauze and cotton wool and modern ones including film, foam, hydrogel, hydrocolloid, alginate, and membrane dressings are used for treatment. Traditional dressings could keep the wound dry and clean, while modern ones have additional functionalities to support wound healing, such as hydrating/dehydrating wound, controlling exudate accumulation and avoiding bacterial contamination. More recent modern dressings include dressings fabricated using biopolymers; most commonly chitosan, pectin, elastin, collagen and hyaluronic acid (Ehterami et al., 2018; Singh & Han, 2016; Dhivya et al., 2015). These biopolymers are either the main structural elements of the extracellular matrix, or support wound healing due to their characteristic properties (Saghazadeh et al., 2018).

Chitosan is a natural polysaccharide that is commonly used in wound dressings. It uses many mechanisms to promote wound healing; by enhancing granulation, supporting organisation, and accelerating the production of biological mediators, macrophages, and fibroblasts (Ueno, Mori & Fujinaga, 2001). In addition, this biocompatible and biodegradable polymer has haemostatic, fungistatic, anti-inflammatory, and antimicrobial properties (Jayakumar, Prabakaran, Kumar, Nair, & Tamura, 2011; Dai, Tanaka, Huang & Hamblin, 2011). In literature, the use of chitosan alone or in combination with other polymers as polyelectrolyte complexes or blends has been reported (Berger, Reist, Mayer, Felt & Gurny, 2004).

Pectin is also a polysaccharide that has a low toxicity. They are commonly obtained from the cell walls of plants, such as apple pomace and citrus (Coimbra et al., 2011). It is a natural polymer with anti-inflammatory and anti-carcinogenic properties and it has been demonstrated that modified citrus pectin is effective in many cancer types and stages (Glinsky & Raz, 2009; Coimbra et al., 2011; Martins, Camargo, Bishop, Papat, Kipper, & Martins, 2018).

Considering the advantages of chitosan and pectin in wound healing, in this study, we have fabricated a novel wound dressing with the use of chitosan and chitosan/pectin polyelectrolyte complexes encapsulating silver sulfadiazine. Chitosan/pectin polyelectrolyte complexes (PEC) are formed mainly due to strong electrostatic interactions of cationic chitosan and anionic pectin, between the ionized amino groups of chitosan and the ionized carboxyl acid groups of pectin (Maciel, Yoshida, & Franco, 2015; Rashidova et al., 2004; Coimbra et al., 2011).

These PEC films have many advantages such as the use of natural polymers, easy fabrication, biocompatibility and biodegradability, and improved mechanical properties (Maciel et al., 2015). Studies with chitosan/pectin PECs are carried for drug delivery applications and as wound dressings in literature (Coimbra et al., 2011; Martins et al., 2018; Bigucci et al., 2008). However, silver sulfadiazine has not encapsulated within these complexes previously.

Silver sulfadiazine is an effective antimicrobial agent, and consists of two agents: silver and sulphonamide. It is remarkably

safe, and used mainly in wound dressings, most commonly for the treatment of burns. More recently, silver sulfadiazine has been used to coat medical devices such as catheters to avoid infections in the wound area (Klasen 2000; Kleinbeck, Bader, & Kao, 2009; White & Cooper, 2005).

Once the films were fabricated, they were characterised by atomic force microscopy (AFM) and fourier transform infrared (FT-IR) spectroscopy. The swelling behaviour of the films was evaluated, and hydrolytic degradation studies were carried out. Afterwards, the silver sulfadiazine was loaded to formulations and *in vitro* drug release studies were carried out.

## MATERIALS AND METHODS

### Materials

Silver sulfadiazine was a kind gift from Deva Pharmaceuticals (Turkey). Chitosan (molecular weight 100.000-300.000 Da) was purchased from Acros Organics (US). Pectin (citrus type USP/100) was purchased from Herbstreith and Fox KG. Glacial acetic acid and sodium hydroxide was purchased from Honeywell Riedel-de-Haën (Germany). PPP-NCLR AFM probes were purchased Nanosensors (Switzerland) and all the other reagents used were analytical grade and purchased from Sigma-Aldrich (Germany).

### Fabrication of chitosan films

Chitosan was dissolved in acetic acid (10 mg/mL) at room temperature, and afterwards neutralized to pH 6.0 (Llanos, de Oliveira Vercik, & Vercik, 2015; Tanabe, Okitsu, Tachibana, & Yamauchi, 2002). The solution was poured over moulds and dried in an oven at 30 °C (Memmert UM500), and the films were obtained. For preparation of the drug loaded films, silver sulfadiazine was dissolved in the polymer solution at 5 mg/ml, and the procedure described was followed (Yaşayan, Karaca, Akgüner, & Bal-Öztürk, 2020).

### Fabrication of chitosan/pectin polyelectrolyte complex films

The optimum complexation ratio for chitosan and pectin was selected as 1:4.3 (w:w) at pH 5.5 (Maciel et al., 2015). Briefly, chitosan was dissolved in aqueous acetic acid, while pectin was distilled water using a magnetic stirrer at room temperature. Once the polymers were dissolved, the pH values of each mixture was adjusted to 5.5. The chitosan suspension was then added to pectin suspension slowly by a micropipette under stirring, and mixed for 30 minutes using a magnetic stirrer to obtain PECs. The PECs were then centrifuged at 12000 rpm for 30 minutes at 4 °C (Beckman Coulter Allegra X-30R Centrifuge) to be separated from the unreacted chitosan and pectin remaining. Finally, the PEC precipitate was placed in petri dishes, and dried in a drying oven at 37 °C (Maciel et al., 2015), and the films were obtained. For preparation of the drug loaded films, silver sulfadiazine was added to chitosan solution (5 mg/ml) under magnetic stirring at room temperature, and the procedure described was followed (Yaşayan et al., 2020).

### Topographical investigations

Topography images of the films were obtained using an Ambient AFM™ (Nanomagnetics Instruments). The AFM study was

carried in air, operating in dynamic mode at scan rates between 0.5-1.5 Hz. PPP-NCLR AFM probes (nominal resonance frequency: 190 kHz, nominal force constant: 48 N/m) were used. Image data was analysed by a NMI Image Analyzer v1.5 (Nanomagnetics Instruments). Using the image data, surface roughness analyses were carried out.

### Swelling studies

Films were cut into square pieces. Accurately weighted dry films were immersed in phosphate buffer saline (PBS) at pH 7.4 at 37 °C. At predetermined time points, scaffolds were taken out of the buffer, and weighed immediately after the gentle removal of the water droplets on their surface. Swelling percentages were calculated using the following formula (Yaşayan et al., 2020):

$$\text{Swelling (\%)} = \frac{W_s - W_d}{W_d} \times 100$$

where  $W_s$  is the weight of swollen scaffold, and  $W_d$  is the weight of dried scaffold.

### Hydrolytic degradation studies

Accurately weighted dry films were immersed in PBS at pH 7.4 and placed in a shaking water bath at 37 °C. At predetermined time points, scaffolds were taken out of buffer, dried under a fume hood, and weighed. The weight remaining percentages of the films were calculated using the following formula given (Yaşayan et al., 2020):

$$\text{Weight remaining (\%)} = \frac{W_{\text{after}}}{W_{\text{before}}} \times 100$$

where  $W_{\text{before}}$  is the weight of a dried scaffolds before hydrolytic degradation, and  $W_{\text{after}}$  is the weight after hydrolytic degradation.

### Surface chemistry analysis

Fourier transform infrared spectroscopy (FT-IR) studies were carried out using a Shimadzu IR Prestige 21 spectrometer in the range of 4000–700  $\text{cm}^{-1}$ . The studies were carried out to detect any chemical incompatibilities between the formulation components.

### Encapsulation efficiency and in vitro drug release studies

Drug-loaded films were cut into pieces, and placed into glacial acetic acid and PBS containing capped glass vials using a shaking bath. Once the samples dissolved, the supernatant was centrifuged. Following a pH adjustment, the supernatant was diluted suitably, and quantified using a UV spectrophotometer (BioTek Epoch microplate reader, BioTek Instruments, Inc.) at 300 nm. Encapsulation efficiency was calculated using the equation given below:

$$\text{Encapsulation efficiency (\%)} = \frac{\text{Actual drug content}}{\text{Theoretical drug content}} \times 100$$

For *in vitro* drug release studies, films were immersed in screw capped vials filled with 20 ml of PBS medium at pH 7.4. Dissolution studies were carried out using a water bath shaker at 37 °C for 24 hours under sink conditions. At predetermined time points, samples were withdrawn for analysis, and the same vol-

ume of fresh PBS medium was added to vials to maintain the total dissolution volume after each withdrawal. The amount of released drug was measured spectroscopically at 300 nm using a UV spectrophotometer (BioTek Epoch microplate reader, BioTek Instruments, Inc.). The results were calculated cumulatively (Kleinbeck et al., 2009).

The drug release mechanisms were determined by applying kinetic models. The cumulative drug release data were fitted to zero-order, first-order, Higuchi, Korsmeyer-Peppas, and Hixson-Crowell models. The determination coefficient ( $R^2$ ) value was calculated by fitting 60% of the linear regression data of release profiles, and the best fit model was determined by evaluation of  $R^2$  value proximity to 1 (England, Miller, Kuttan, Trent, & Frieboes, 2015).

### Statistical analysis

Statistical analyses of the data were performed by a t-test.  $P < 0.05$  was considered statistically significant.

## RESULTS AND DISCUSSION

In this study, chitosan films and chitosan/pectin PEC films were fabricated by casting and solvent evaporation methods. In literature, the optimum complexation ratio for chitosan and pectin is given as 1:4.3 (w:w) at pH 5.5 to obtain the highest product yield (Maciel et al., 2015). The pKa value of pectin is in the range of 3.5-4.5, and the pKa value of chitosan is around 6.2-7.0 (Maciel et al., 2015). Considering the pKa values of polymers, PECs of chitosan and pectin are prepared at pH 5.5, in between the pKa values of these two polymers where both polymers have a high ratio of ionised groups for ionic interaction (Coimbra et al., 2011; Rashidova et al., 2004; Bigucci et al., 2008). Therefore, the complexation of PEC films was conducted using these parameters. After fabrication, silver sulfadiazine was loaded to films to further support wound healing.

AFM topography images of films before and after drug loading is given in Figure 1. For the chitosan films (Figure 1a), characteristic crystalline structure of the chitosan could be observed from image data (Lewandowska, Sionkowska, & Grabska, 2015;

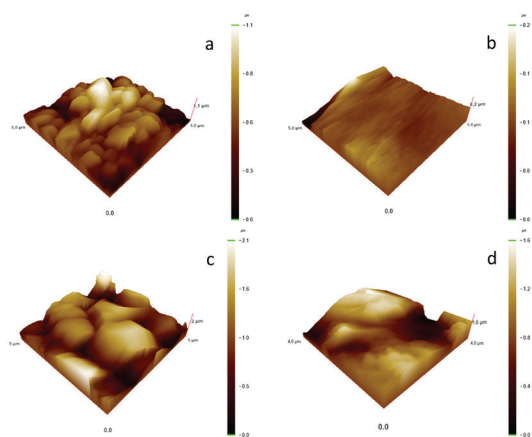


**Figure 1.** AFM topography images of films before and after drug loading. Chitosan films (a), chitosan-pectin PEC films (b), silver sulfadiazine loaded chitosan films (c), silver sulfadiazine loaded chitosan-pectin PEC films (d).

Rinaudo, 2006). After formation of the PECs with pectin (Figure 1b), the chitosan's characteristic structure disappeared, and relatively flat surfaces were observed. In literature, flat, smooth and homogeneous surface morphology is reported for chitosan/pectin PEC films as the indicator of complex formation with a strong interaction (Maciel et al., 2015). Surface roughness values were calculated from AFM image data, and the results were given in Table 1. Indeed, the surface roughness of the crystalline chitosan films was found to be relatively high compared to smooth PEC films. The average roughness value for the chitosan films was found to be 177.58 nm, whereas for the chitosan-pectin PEC films it was 10.73 nm.

The surface roughness values calculated from the image data for drug loaded surfaces was found to be 344.20 nm for chitosan films and 300.56 nm for PEC films (Table 1). It was observed that the roughness values increased after the addition of the drug.

**Table 1. Average roughness values of chitosan films and chitosan-pectin polyelectrolyte complex (PEC) films before and after drug loading.**

Sample	Average Roughness (Ra) (nm)
<i>Films</i>	
Chitosan films	177.58
Chitosan-pectin PEC films	10.73
<i>Silver sulfadiazine loaded films</i>	
Chitosan films	344.20
Chitosan-pectin PEC films	300.56

The roughness values were calculated using AFM image data from Figure 1.

After drug loading, the morphology of surfaces changed dramatically, and characteristic morphologies of the chitosan films and the PEC films disappeared (Figure 1c-d). Silver sulfadiazine loaded chitosan films were observed to have large microdomains probably due to molecular interactions between the chitosan and the drug. For PEC films, the smooth structure disappeared after drug loading, and the drug loaded surface was characterized with holes and microdomains.

After morphological investigations, the films were characterised by swelling and hydrolytic degradation studies. Wound dressings should provide a moist environment to enhance wound healing. Thus swelling, and gel formation over the wound is desired for wound dressings. This gel provides occlusive conditions due to gel formation, where the gel acts as a barrier. Also an ideal wound dressing should absorb the exudate of the wound (Boateng, Matthews, Stevens, & Eccleston, 2008).

Swelling studies were performed by accurately weighting the dry films, and immersing them into PBS buffer at pH 7.4 at 37 °C, and the results are given in Figure 2a. According to the results, after 30 minutes, both films were attained an equilibrium state. After the 30<sup>th</sup> minute, it was observed that the swelling ratio of the chitosan films was higher compared to the PEC films. The swelling ratio was in the range of 650-700% for the chitosan films, and in the range of 230-260% for the PEC films.

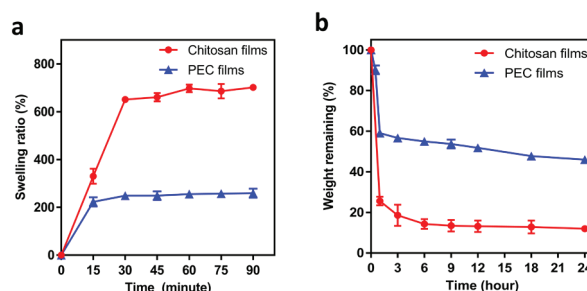


**Figure 2.** Swelling studies (a) and hydrolytic degradation studies (b) of chitosan films and chitosan-pectin PEC films.

The hydrolytic degradation results are given in Figure 2b. According to the results, it was observed that the hydrolytic degradation rates of films were reduced by complexation of chitosan with pectin. For the chitosan films, the remaining weight percentage was 26% after the 1<sup>st</sup> hour, and reduced to 12% by the 24<sup>th</sup> hour. For the PEC films, the reduction of weight loss was not as fast as the chitosan films; the remaining weight percentage was 60% after the 1<sup>st</sup> hour, and reduced to 46% by the 24<sup>th</sup> hour. The results indicate that polyelectrolyte complex formation between the polymers has improved the mechanical stability and durability of the films significantly; and by PEC formation, rapid degradation of chitosan is eliminated.

Comparative FT-IR spectra of the components in the chitosan film formulation are given in Figure 3. Chitosan has typical bands for polysaccharides in the range of 3400-2800  $\text{cm}^{-1}$ . Characteristic peaks of chitosan are observed at 3351  $\text{cm}^{-1}$ , 2940  $\text{cm}^{-1}$ , 2879  $\text{cm}^{-1}$  that corresponds to the stretching vibrations of -NH and -OH groups, aliphatic -CH<sub>2</sub> groups, and aliphatic -CH<sub>3</sub> groups respectively. At 1656  $\text{cm}^{-1}$  peak of amide I (C=O band), and at 1586  $\text{cm}^{-1}$  amide II band, N-H bending vibrations are observed

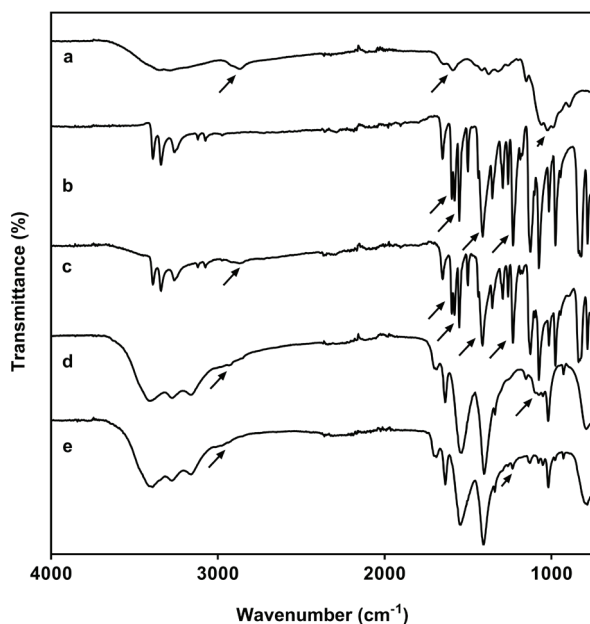


**Figure 3.** Comparative FT-IR spectra of the components in the chitosan film formulation. Chitosan (a), silver sulfadiazine (b), physical mixture of chitosan and silver sulfadiazine (c), chitosan films before drug loading (d), chitosan films after drug loading (e).



(Yaşayan et al., 2020) (Figure 3a). For silver sulfadiazine, silver ion is in coordination with various functional groups within the molecule; these groups are deprotonated amine nitrogen, sulfonyl oxygen, the pyrimidine nitrogen in the same chain. It is also in coordination with the further pyrimidine nitrogen. The characteristic bands are at 1596 and at 1583  $\text{cm}^{-1}$  for phenyl skeletal vibrations conjugated to the  $\text{NH}_2$  group and the aromatic ring's C–C stretching vibrations. The bands at 1556, 1503 and 1412  $\text{cm}^{-1}$  correspond to pyrimidine skeletal vibrations (Szegeci et al., 2014). The bands at 3340 and 3389  $\text{cm}^{-1}$  correspond to  $-\text{NH}_2$  stretching vibrations (Shao et al., 2017). The peak at 1233  $\text{cm}^{-1}$  was attributed to the asymmetrical S=O stretching vibration (Shao et al., 2017) (Figure 3b). For the data of physical mixture of chitosan and silver sulfadiazine, characteristic bands of silver sulfadiazine are observed clearly from the data (Figure 3c). For the chitosan films, it was observed that characteristic peaks of pure chitosan were shifted due to use of acetic acid to prepare films, and then the neutralization of chitosan solution by NaOH. In literature it is reported that deprotonation of amine groups results in peak shifts (Takara, Marchese, & Ochoa, 2015). The band at 1645 is attributed to the asymmetric and symmetric bending vibrations of the  $\text{NH}_3^+$  (Coimbra et al., 2011) (Figure 3d). For the drug loaded chitosan films, the characteristic peaks of the drug were detected in lower intensities, however the presence of the drug is evident at 1233  $\text{cm}^{-1}$ . It was observed that the characteristic band of the silver sulfadiazine at 1597  $\text{cm}^{-1}$  was shifted to 1645  $\text{cm}^{-1}$ . This is probably as a result of the formation of hydrogen bonds among the amino groups of chitosan and silver sulfadiazine, which resulted in shift of the band to a higher wavenumber, and a reduction in the band intensities (Fajardo et al, 2013). When characteristic bands of silver sulfadiazine are considered, the data suggests that no undesired interactions are observed between the drug and the polymers (Figure 3e).

FTIR spectra of chitosan and silver sulfadiazine were again inserted to Figure 4 in order to better evaluate any possible interactions amongst the formulation components (Figure 4a, c). Pectin has characteristic bands in the range of 3400-2800  $\text{cm}^{-1}$  that correspond to polysaccharides. The peak in the range of at 1727  $\text{cm}^{-1}$  corresponds to the C=O stretching vibrations of the methyl ester group and the un-dissociated carboxyl group, and at 1606  $\text{cm}^{-1}$  to the C=O asymmetric stretching vibrations and the carboxylate group (Bigucci et al., 2008; Maciel et al., 2015) (Figure 4b). For the data of physical mixture of the polymers and silver sulfadiazine, characteristic bands of silver sulfadiazine are observed clearly at 1233  $\text{cm}^{-1}$  and at 1596  $\text{cm}^{-1}$  (Figure 4d). For PEC films, shifts in amine group of chitosan to 1559  $\text{cm}^{-1}$  could be related with the formation of complexes. When the characteristic bands of chitosan and pectin are considered, the characteristic bands of PEC films are changed due to an ionic interaction of protonated amino groups of chitosan and the carboxyl groups of pectin. Also other groups in the polymers may interact, such as  $-\text{OH}$  groups (Figure 4e). For drug loaded PEC films, the characteristic peaks of the drug were detected in lower intensities; probably due to lower amounts of the drug compared to polymer amounts. Similar to chitosan films, the presence of the drug is evident at 1233  $\text{cm}^{-1}$  It was observed that the characteristic band of the silver sulfadiazine at 1597  $\text{cm}^{-1}$  was shifted to 1645  $\text{cm}^{-1}$ , probably

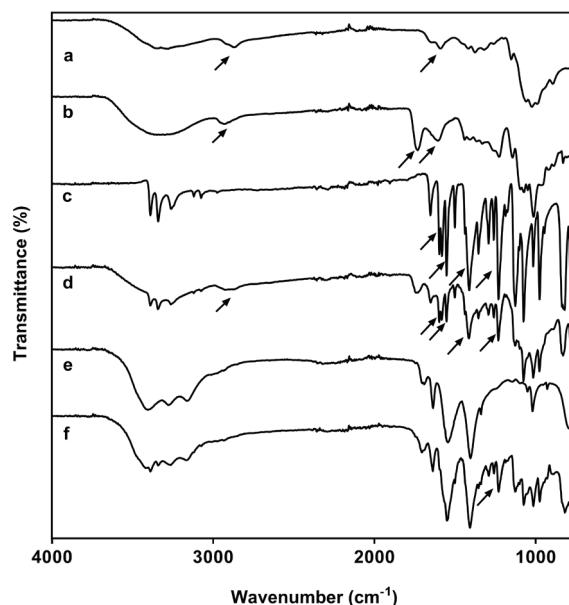


**Figure 4.** Comparative FT-IR spectra of the components in the PEC film formulation. Chitosan (a), pectin (b), silver sulfadiazine (c), physical mixture of chitosan, pectin, and silver sulfadiazine (d), PEC films before drug loading (e), PEC films after drug loading (f).

as a result of a hydrogen bond formation among the amino groups of chitosan and silver sulfadiazine (Fajardo et al, 2013). (Figure 4f). From the overall FT-IR data, undesired interactions were not detected between the formulation components.

When FT-IR data is evaluated together with AFM data, change in surface topography and the formation of microdomains in drug loaded films could be a result of hydrogen bonds among silver sulfadiazine and chitosan.

Encapsulation efficiencies of the films were studied briefly by cutting the films into small pieces, dissolving them using acetic acid, and quantifying the drug amount in the supernatant. According to the results, encapsulation efficiencies of the drug were  $\sim >95\%$  for the chitosan films and  $\sim >90\%$  for the PEC films.

*In vitro* drug release studies were performed in PBS at 37 °C, pH 7.4, and the results are given in Figure 5. According to the re-

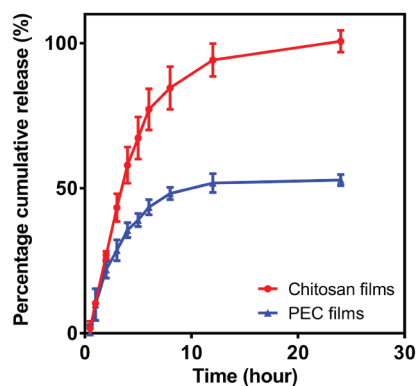


**Figure 5.** *In vitro* drug release studies of chitosan films and chitosan-pectin PEC films.

**Table 2. Drug release kinetics of the chitosan (CS) films and polyelectrolyte complex (PEC) films.**

Films	Zero order		First order		Higuchi		Korsmeyer Peppas			Hixson-Crowell	
	R <sup>2</sup>	K <sub>0</sub> (h <sup>-1</sup> )	R <sup>2</sup>	K <sub>1</sub> (h <sup>-1</sup> )	R <sup>2</sup>	K <sub>H</sub> (h <sup>-1/2</sup> )	R <sup>2</sup>	n	K <sub>KP</sub> (h <sup>-n</sup> )	R <sup>2</sup>	K <sub>HC</sub> (h <sup>-1/3</sup> )
CS	0.999	16.12	0.992	-0.105	0.988	43.642	0.966	1.639	7.333	0.997	0.324
PEC	0.566	1.529	0.631	-0.011	0.763	10.726	0.833	0.517	14.598	0.61	0.033

Zero order, first-order, Higuchi, Korsmeyer Peppas, and Hixson-Crowell models were applied to evaluate drug release kinetics. The R<sup>2</sup> values, release rate constants (K), and for Korsmeyer Peppas model, release exponent (n) values were calculated.

sults, it was observed that polyelectrolyte complex formation between the polymers affect the cumulative release of the drugs from the films. From the data, the chitosan films released all of the drug at the end of 24 hours, while the PEC films released 52% of the drug loaded within 24 hours. This drug release at a slower rate with the PEC films could have advantages especially for slow-healing wounds.

After the *in vitro* drug release studies, mathematical models were applied to drug release profiles to study drug release mechanisms. The R<sup>2</sup> values were calculated by fitting the first 60% of the linear regression data of the cumulative drug release profiles (England et al., 2015). During the studies, zero order, first-order, Higuchi, Korsmeyer Peppas, and Hixson-Crowell models were applied to evaluate drug release kinetics. The best-fit model was selected by a proximity of R<sup>2</sup> value to 1. The R<sup>2</sup> values and release rate constants (K), and the release exponent (n) values for the Korsmeyer Peppas model are given in Table 2. The results indicated that chitosan films best fit into the zero order model, whereas PEC films fit into the Korsmeyer Peppas model. Zero order kinetics indicates a constant drug release from the chitosan films. For Korsmeyer Peppas model, the n value is calculated to evaluate the release mechanism. It is well known that the drug transport mechanism is Fickian diffusion when the n value is 0.5, non-Fickian transport when 0.45 < n < 0.89, Case II transport when the n value is 0.89, super case II transport when the n value is higher than 0.89 (Gouda et al., 2017). In our results, the n value was found to be 0.517, which indicates the drug release mechanism is non-Fickian transport (Gouda, Raishya, & Qing, 2017).

## CONCLUSION

In this study, chitosan films and chitosan/pectin PEC wound dressings were fabricated encapsulating silver sulfadiazine by casting and solvent evaporation methods. The ease of fabrication, having favoured properties of polymers in wound healing, and additional benefits of these polymers that promote wound healing are the aims of our choice. These films are designed to improve wound healing, and for this purpose silver sulfadiazine is loaded in the films to further support wound healing by antimicrobial properties of the drug. We found that by formation of polyelectrolyte complexes, mechanical properties and durability of the films could be improved, and drug release could be extended compared to chitosan films. Future studies should be conducted to fully evaluate the films in terms of wound healing properties and antimicrobial properties including *in-vivo* studies. We hope these wound dressings

may have a potential application as wound dressings, and this study could be useful for the fabrication of novel dressings that replace conventional dressings.

**Acknowledgement:** We would like to thank to Deva Pharmaceuticals (Turkey) for providing silver sulfadiazine as a gift.

**Peer-review:** Externally peer-reviewed.

**Author Contributions:** Conception/Design of Study- G.Y.; Data Acquisition- G.Y.; Data Analysis/Interpretation- G.Y.; Drafting Manuscript- G.Y.; Critical Revision of Manuscript- G.Y.; Final Approval and Accountability- G.Y.; Technical or Material Support- G.Y.; Supervision- G.Y.

**Conflict of Interest:** The authors have no conflict of interest to declare.

**Financial Disclosure:** Authors declared no financial support.

## REFERENCES

- Berger, J., Reist, M., Mayer, J. M., Felt, O., & Gurny, R. (2004). Structure and interactions in chitosan hydrogels formed by complexation or aggregation for biomedical applications. *European Journal of Pharmaceutics and Biopharmaceutics*, 57(1), 35–52.
- Bigucci, F., Luppi, B., Cerchiara, T., Sorrenti, M., Bettinetti, G., Rodriguez, L., & Zecchi, V. (2008). Chitosan/pectin polyelectrolyte complexes: selection of suitable preparative conditions for colon-specific delivery of vancomycin. *European Journal of Pharmaceutical Sciences*, 35(5), 435–441.
- Boateng, J. S., Matthews, K. H., Stevens, H. N. E., & Eccleston, G. M. (2008). Wound healing dressings and drug delivery systems: A review. *Journal of Pharmaceutical Sciences*, 97(8), 2892–2923. <http://dx.doi.org/10.1002/jps.21210>
- Coimbra, P., Ferreira, P., De Sousa, H., Batista, P., Rodrigues, M., Correia, I., & Gil, M. (2011). Preparation and chemical and biological characterization of a pectin/chitosan polyelectrolyte complex scaffold for possible bone tissue engineering applications. *International Journal of Biological Macromolecules*, 48(1), 112–118.
- Dai, T., Tanaka, M., Huang, Y. Y., & Hamblin, M. R. (2011). Chitosan preparations for wounds and burns: antimicrobial and wound-healing effects. *Expert Review of Anti-infective Therapy*, 9(7), 857–879. <http://dx.doi.org/10.1586/eri.11.59>
- Dhivya, S., Padma, V. V., & Santhini, E. (2015). Wound dressings - a review. *BioMedicine*, 5(4), 22–22. <http://dx.doi.org/10.7603/s40681-015-0022-9>
- Ehterami, A., Salehi, M., Farzamfar, S., Vaez, A., Samadian, H., Sahrapeyma, H. ... Goodarzi, A. (2018). In vitro and in vivo study of PCL/COLL wound dressing loaded with insulin-chitosan nanoparticles on cutaneous wound healing in rats model. *International Journal of Biological Macromolecules*, 117, 601–609. <http://dx.doi.org/10.1016/j.ijbiomac.2018.05.184>

- England, C. G., Miller, M. C., Kuttan, A., Trent, J. O., & Frieboes, H. B. (2015). Release kinetics of paclitaxel and cisplatin from two and three layered gold nanoparticles. *European Journal of Pharmaceutical and Biopharmaceutics*, 92, 120–129. <http://dx.doi.org/10.1016/j.ejpb.2015.02.017>
- Fajardo, A. R., Lopes, L. C., Caleare, A. O., Britta, E. A., Nakamura, C. V., Rubira, A. F., & Muniz, E. C. (2013). Silver sulfadiazine loaded chitosan/chondroitin sulfate films for a potential wound dressing application. *Materials Science and Engineering: C*, 33(2), 588–595. <https://doi.org/10.1016/j.msec.2012.09.025>
- Glinsky, V. V., & Raz, A. (2009). Modified citrus pectin anti-metastatic properties: one bullet, multiple targets. *Carbohydrate Research*, 344(14), 1788–1791. <http://dx.doi.org/10.1016/j.carres.2008.08.038>
- Gottrup, F. (2004). A specialized wound-healing center concept: importance of a multidisciplinary department structure and surgical treatment facilities in the treatment of chronic wounds. *The American Journal of Surgery*, 187(5, Supplement 1), S38–S43. [http://dx.doi.org/10.1016/S0002-9610\(03\)00303-9](http://dx.doi.org/10.1016/S0002-9610(03)00303-9)
- Gouda, R., Baishya, H., & Qing, Z. (2017). Application of mathematical models in drug release kinetics of carbidopa and levodopa ER tablets. *Journal of Developing Drugs*, 6(02).
- Han, G., & Ceilley, R. (2017). Chronic Wound Healing: A Review of Current Management and Treatments. *Advances in therapy*, 34(3), 599–610. <http://dx.doi.org/10.1007/s12325-017-0478-y>
- Llanos, J. H. R., de Oliveira Vercik, L. C., & Vercik, A. (2015). Physical properties of chitosan films obtained after neutralization of polycation by slow drip method. *Journal of Biomaterials and Nanobiotechnology*, 6(04), 276.
- Jayakumar, R., Prabakaran, M., Kumar, P. T. S., Nair, S. V., & Tamura, H. (2011). Biomaterials based on chitin and chitosan in wound dressing applications. *Biotechnology Advances*, 29(3), 322–337. <http://dx.doi.org/10.1016/j.biotechadv.2011.01.005>
- Klasen, H. J. (2000). A historical review of the use of silver in the treatment of burns. II. Renewed interest for silver. *Burns*, 26(2), 131–138. [http://dx.doi.org/10.1016/S0305-4179\(99\)00116-3](http://dx.doi.org/10.1016/S0305-4179(99)00116-3)
- Kleinbeck, K. R., Bader, R. A., & Kao, W. J. (2009). Concurrent in vitro release of silver sulfadiazine and bupivacaine from semi-interpenetrating networks for wound management. *Journal of burn care & research: Official publication of the American Burn Association*, 30(1), 98–104. <http://dx.doi.org/10.1097/BCR.0b013e3181921ed9>
- Lai, H. J., Kuan, C. H., Wu, H. C., Tsai, J. C., Chen, T. M., Hsieh, D. J., & Wang, T. W. (2014). Tailored design of electrospun composite nanofibers with staged release of multiple angiogenic growth factors for chronic wound healing. *Acta Biomaterialia*, 10(10), 4156–4166.
- Lewandowska, K., Sionkowska, A., & Grabska, S. (2015). Chitosan blends containing hyaluronic acid and collagen. Compatibility behaviour. *Journal of Molecular Liquids*, 212, 879–884. <http://dx.doi.org/10.1016/j.molliq.2015.10.047>
- Maciel, V. B. V., Yoshida, C. M., & Franco, T. T. (2015). Chitosan/pectin polyelectrolyte complex as a pH indicator. *Carbohydrate Polymers*, 132, 537–545.
- Martins, J. G., Camargo, S. E., Bishop, T. T., Popat, K. C., Kipper, M. J., & Martins, A. F. (2018). Pectin-chitosan membrane scaffold imparts controlled stem cell adhesion and proliferation. *Carbohydrate Polymers*, 197, 47–56.
- Olsson, M., Järbrink, K., Divakar, U., Bajpai, R., Upton, Z., Schmidtchen, A., & Car, J. (2019). The humanistic and economic burden of chronic wounds: A systematic review. *Wound Repair and Regeneration*, 27(1), 114–125. <http://dx.doi.org/10.1111/wrr.12683>
- Rashidova, S. S., Milusheva, R. Y., Semenova, L., Mukhamedjanova, M. Y., Voropaeva, N., Vasilyeva, S., ... Ruban, I. (2004). Characteristics of interactions in the pectin–chitosan system. *Chromatographia*, 59(11–12), 779–782.
- Rinaudo, M. (2006). Chitin and chitosan: Properties and applications. *Progress in Polymer Science (Oxford)*, 31(7), 603–632. <http://dx.doi.org/10.1016/j.progpolymsci.2006.06.001>
- Saghazadeh, S., Rinaldi, C., Schot, M., Kashaf, S. S., Sharifi, F., Jalilian, E., ... Khademhosseini, A. (2018). Drug delivery systems and materials for wound healing applications. *Advanced Drug Delivery Reviews*, 127, 138–166. <http://dx.doi.org/10.1016/j.addr.2018.04.008>
- Shao, W., Wu, J., Wang, S., Huang, M., Liu, X., & Zhang, R. (2017). Construction of silver sulfadiazine loaded chitosan composite sponges as potential wound dressings. *Carbohydrate Polymers*, 157, 1963–1970. <http://dx.doi.org/10.1016/j.carbpol.2016.11.087>
- Singh, D., & Han, S. S. (2016). 3D Printing of Scaffold for Cells Delivery: Advances in Skin Tissue Engineering. *Polymers*, 8(1). <http://dx.doi.org/10.3390/polym8010019>
- Szegedi, Á., Popova, M., Yoncheva, K., Makk, J., Mihály, J., & Shestakova, P. (2014). Silver- and sulfadiazine-loaded nanostructured silica materials as potential replacement of silver sulfadiazine. *Journal of Materials Chemistry B*, 2(37), 6283–6292. <http://dx.doi.org/10.1039/C4TB00619D>
- Takara, E. A., Marchese, J., & Ochoa, N. A. (2015). NaOH treatment of chitosan films: Impact on macromolecular structure and film properties. *Carbohydrate Polymers*, 132, 25–30. <http://dx.doi.org/10.1016/j.carbpol.2015.05.077>
- Tanabe, T., Okitsu, N., Tachibana, A., & Yamauchi, K. (2002). Preparation and characterization of keratin – chitosan composite film. *Biomaterials*, 23(May 2001), 817–825.
- Ueno, H., Mori, T., & Fujinaga, T. (2001). Topical formulations and wound healing applications of chitosan. *Advanced Drug Delivery Reviews*, 52(2), 105–115. [http://dx.doi.org/10.1016/S0169-409X\(01\)00189-2](http://dx.doi.org/10.1016/S0169-409X(01)00189-2)
- Vowden, K., & Vowden, P. (2017). Wound dressings: principles and practice. *Surgery (Oxford)*, 35(9), 489–494.
- White, R., & Cooper, R. (2005). Silver sulphadiazine: a review of the evidence. *Wounds UK*, 1(2), 51.
- Yaşayan, G., Karaca, G., Akgüner, Z. P., & Bal-Öztürk, A. (2020). Chitosan/collagen composite films as wound dressings encapsulating allantoin and lidocaine hydrochloride. *International Journal of Polymeric Materials and Polymeric Biomaterials*. Advance online publication. <https://doi.org/10.1080/00914037.2020.1740993>

# Enhancing the antibacterial activity of the biosynthesized silver nanoparticles by "püse"

Arzu Özgen<sup>1</sup> , Sinem Gürkan Aydın<sup>1</sup> , Erdi Bilgiç<sup>1</sup> 

<sup>1</sup>Istanbul Gelişim University, Vocational School of Health Sciences, Department of Medical Services and Techniques, Istanbul, Turkey

**ORCID IDs of the authors:** A.Ö. 0000-0003-2104-6019; S.G.A. 0000-0002-5146-8936; E.B. 0000-0002-2892-274X

**Cite this article as:** Ozgen, A., Gurkan Aydin, S., & Bilgic, E. (2020). Enhancing the antibacterial activity of the biosynthesized silver nanoparticles by "püse". *Istanbul Journal of Pharmacy*, 50 (3), 245-250.

## ABSTRACT

**Background and Aims:** The silver nanoparticles (Ag NPs) synthesized by green synthesis have antimicrobial properties and their potential to be used in the medical field is quite high. Püse, also called "black doctor", is widely used as a treatment for the health problems of animals and in folk medicine in Turkish nomad culture. It has been reported that Ag NPs biosynthesized with *Juglans regia* L. leaf extracts have antibacterial activity. The aim and importance of this study is the preparation of a mixture of "püse" and Ag NPs for the first time and the investigation of its antibacterial activity.

**Methods:** In this paper, Ag NPs were synthesized by using *J. regia* leaves and morphological characteristics of the NPs obtained were determined using TEM. The formation of NPs was identified using an UV-Vis spectrophotometer. The antibacterial activity was investigated by combining the obtained and characterized Ag NPs with the "püse". The antibacterial activity of the mixture was tested on Gram (+) bacteria and Gram (-) bacter.

**Results:** The mixture that was prepared with püse and Ag NPs showed higher antibacterial activity than antibiotics.

**Conclusion:** The positive results showed that this mixture has the potential to be used as a preparation especially in the treatment of animal wounds and the skin infections caused by bacteria.

**Keywords:** Biosynthesized, silver nanoparticles, antibacterial activity, *Juglans regia*, püse

## INTRODUCTION

It is a well-known fact that nanosilvers, which are obtained from silver particles with a size of 1-100 nm, have antibacterial, antiviral, and antifungal properties and the potential to be used in common areas such as food packaging, textile, electronic devices, cosmetics, medical devices, and materials. (McShan, Ray, & Yu, 2014; Luther, Schmidt, Diendorf, Epple, & Dringen, 2012; You et al., 2012). The antimicrobial properties of nanosilvers are described via the release of Ag<sup>+</sup> ions and inhibition of the transcription which means survival for the living (Wang et al., 2013). The release of Ag<sup>+</sup> ions from AgNPs into cells is called the "Trojan horse" effect and the smaller the nanosilver particles are, the higher the surface area to volume ratio and the more Ag<sup>+</sup> ions that are released (Cameron, Hosseinian, & Willmore, 2018).

Humankind have used plants as a source of medicine and treatment since ancient times and the methods found through trial and error were transferred from generation to generation (Gurib-Fakim, 2006). Ethnobotany was defined by Schultes in 1967 as the relationship between man and his ambient vegetation (Gurib-Fakim, 2006). In other words, ethnobotany is a discipline that takes place in the natural and social sciences and deals with relationships between humans and plants (Garnatje, Peñuelas, & Val-lès, 2017). There are numerous studies conducted with plants for human health and well-being. Drugs of plant origin are based

**Address for Correspondence:**  
Arzu ÖZGEN, e-mail: aozgen@gelisim.edu.tr

Submitted: 30.10.2019  
Revision Requested: 01.04.2020  
Last Revision Received: 24.04.2020  
Accepted: 04.05.2020  
Published Online: 04.11.2020

This work is licensed under a Creative Commons Attribution 4.0 International License.



on ethnobotany information. In fact, ethnobotany-oriented approaches have become more powerful than random tests for the detection and identification of bioactive molecules from plants (Garnatje et al., 2017). Ethnobotany helps to find the when, where, and how of plants with different medicinal properties (de la Parra & Quave, 2017).

*Pinus nigra* J.F. Arnold is a species that grows in Southern Europe and Anatolia, especially in the Mediterranean Basin. It can grow from anywhere between 100-1800 meters above sea level, but mostly from 500-1600 meters. It is considered one of the most important coniferous species (Topacoglu, 2013). The various parts of the *Pinus* species derived from resin, cones, tar, and pine have ethnobotany and ethnomedical uses for skin problems, asthma, bronchitis, colds, coughs, and wounds (Kızıllarslan & Sevgi, 2013).

In nomadic culture (Turks having nomadic life in Anatolia and Rumelia), "püse" which is an important drug in every situation and obtained from pine, cedar and juniper, also known as the "black doctor", is used for the treatment of health problems such as abdominal pain, diarrhea, nausea, gas pains, bullet wounds, scabies, fissures in mumps, hands, and feet (Ak, 2017).

*J. regia*, a member of the Juglandaceae family, more commonly known as walnut, is a forest tree grown in temperate regions (Faraz, Islam, & Rehman, 2012; Alam, Islam, Kamal, & Gan, 2018). Walnut leaves are used as a source of health materials and bioactive molecules (Santos et al., 2013). Antibacterial and biofilm-inhibiting effects of walnuts on *Pseudomonas aeruginosa* have been shown by Dolatabadi, Moghadam, & Mahdavi-Ourtakand in 2018. The green husks, bark, leaves, and fruit of walnut are used in pharmacology for a variety of purposes and studies have shown that products of walnut and special compounds of juglone have antimicrobial properties (Dolatabadi et al., 2018; Zhao, Jiang, Liu, & Li, 2014; Shah, Ganesh, & Akthar, 2013; Moravej et al., 2016; Kaur, Michael, Arora, Härkönen, & Kumar, 2003).

The aim of this study was to investigate the antibacterial activity of the mixture obtained by combining püse, used as ethnomedical in the nomadic culture, with synthesized NPs. For this purpose, synthesized AgNPs from the *J. regia* leaf was used. The morphological characteristics of the obtained mixture were determined using a Transmission Electron Microscopy (TEM) and particular size analyzer. The formation of kinetics from the mixture was identified using a UV-Vis spectrophotometer. The antibacterial activity of synthesized AgNPs from the *J. regia* leaf and "püse" mixture was tested on various Gram (+) and Gram (-) bacteria strains.

## MATERIALS AND METHODS

### Preparation of "Püse"

The resinous parts of *P. nigra* wood was divided into thin pieces of 30-40 cm, placed on top of a smooth and curved surface, and covered with soil so that there was no hole. A fire was lit on the soil and a small exit path opened on the side of the slope of the device. The resin that melted with the temperature of the burning fire was isolated from the wood flow into the pit and collected from there as "püse".

### AgNPs synthesis

One g of *J. regia* leaves, purchased from an herbal store, were mixed with 100 ml of distilled water (pH= 6.9), then boiled using a magnetic stirrer for 30 minutes, and the resulting plant extract was cooled at room temperature. The mixture brought to room temperature (25 °C) was filtered with Whatman No 1 filter paper, then 50 ml of the prepared leaf extract was taken, and 2 mM 50 ml AgNO<sub>3</sub> solution was added. The final solution was incubated for about 24 hours under room conditions to reduce the colloidal NPs.

### Characterization of Ag NPs

The UV-vis absorbance spectrum of the final concentration was recorded in the wavelength range of 300-700 nm by the Eon™ Microplate Spectrophotometer operating at a resolution of 10 nm. On the spectra, the *J. regia* leaves extract diluted at a ratio of 1:1 with distilled water was taken as the reference solution, and the extract-AgNO<sub>3</sub> mixture was examined in the presence of this reference solution. A 96 well plate was used in the spectrophotometer. The morphological characteristics of the Ag NPs were determined by the ZEIS-LEO 906E Brand-Model Transmission Electron Microscopy (TEM).

### Preparation of Ag NPs and püse mixture

Water molecules were completely removed by an evaporation method from the Ag NPs which were biosynthesized by *J. regia* leaves in an aqueous solution. Then the extract of püse was added to the Ag NPs. The mixture was kept in an ultrasonic bath for 30 minutes to prevent agglomeration.

### Antibacterial activity

The antibacterial activity of the synthesized Ag NPs using an extract of *J. regia* leaves and "püse" (local name) was carried out in Gram (+) bacteria (*S. aureus* ATCC 29213,) and Gram (-) bacteria (*E. coli* ATCC 25922,) by a disc diffusion method on solid media (Russell & Furr, 1977; Irobi, Moo-Young, Anderson, & Daramola, 1994). The bacterial strains were grown for 12 hours at 37 °C in Müller Hinton Agar (MHA, pH= 7.3). The density of the bacterial suspensions were adjusted to 0.5 McFarland turbidity standard (1.5 x 10<sup>8</sup> CFU/mL) by diluted 1:100 with MHA. Subsequently, 100 µl of bacteria cells were spread onto MHA Petri dishes using a sterile spreader. Then, sterile Whatman filter papers (6-mm-diameters) were placed over the medium using sterile forceps and impregnated with 50 µl (8.5 µg/ disc) of the Ag NPs and *J. regia* leaves extract and pure püse as the mixture. The *J. regia* leaves extract was used as the negative control and doxycycline 30 µg/disc and amoxicillin + clavulanic acid 20 µg/disc were used as the positive control. The plates were placed for 24 hours at 37°C in an incubator. The growth inhibition zones of each disc were measured in millimeters. All experiments were duplicated.

## RESULTS AND DISCUSSION

Nowadays, nanoparticles synthesized using silver, gold, zinc, copper and hybrid Ag / ZnO draw interest especially in the biomedical field as antibacterial, antifungal, antiviral, anti-inflammatory, anti-angiogenic, and anti-cancer agents (Chaloupka, Malam, & Seifalian, 2010; Strayer, Ocoy, Tan, Jones, & Paret, 2016). The physical and chemical methods used to produce nanoparticles



have major disadvantages, as they contain expensive, raw, toxic, and dangerous chemicals (Some et al., 2019). To overcome these problems, studies have focused on the production of nanoparticles by biosynthesis. For this purpose, various organisms including plants, algae, and microorganisms are used as biosynthesis agents in the synthesis of NPs (Shah, Fawcett, Sharma, Tripathy, & Poinern, 2015; Roy, Bulut, Some, Mandal, & Yilmaz, 2019). In addition, biomolecules including DNA, enzymes, peptides, proteins, and plant extracts are also used in NP synthesis (Duman, Ocsoy, & Kup, 2016). Especially because plant extracts are very cheap, scalable, easily available, stable, and require no special storage conditions compared to other biomolecules (Ocsoy et al., 2013; Demirbas, Welt, & Ocsoy, 2016).

In this study, the *J. regia* aqueous extract was mixed with an  $\text{AgNO}_3$  solution, and the color of the initially transparent mixture changed to brown within about 30 minutes by reducing the silver ions (Figures 1A and 1B). Color change is an indication that Ag NPs are formed, and this change is due to the superficial plasmon vibrations of nanoparticles (Forough & Farhadi, 2010). The reduction of pure  $\text{Ag}^+$  ions to  $\text{Ag}^0$  was monitored by measuring the UV-vis spectrum of the reaction. The absorbance of the mixtures whose color turned brown showed SPR (Surface Plasmon Resonance) peaks at 420 nm after 24 hours (Figure 2). The morphological properties of the NPs were determined by TEM. As shown in Figure 3, the sizes of the NPs are between 8 and 35 nm and the shape of the NPs is spherical.

The mechanism of how Ag NPs biosynthesized using plant extracts has not been fully clarified (Okaiyeto, Ojemaye, Hoppe,



**Figure 1.** A-B The images of synthesized Ag NPs, (A) *J. regia* extract, (B) Ag NPs and *J. regia* leaf mixture.

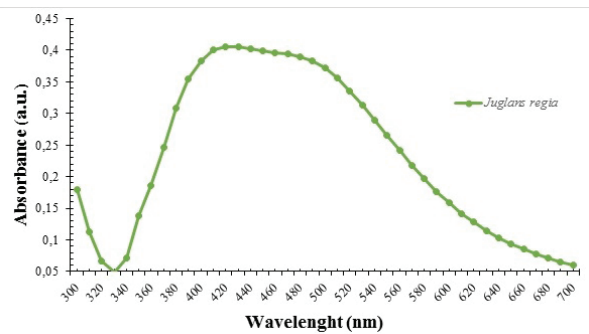


**Figure 2.** UV-Vis absorbance spectrums of Ag NPs and *J. regia* leaf mixture.

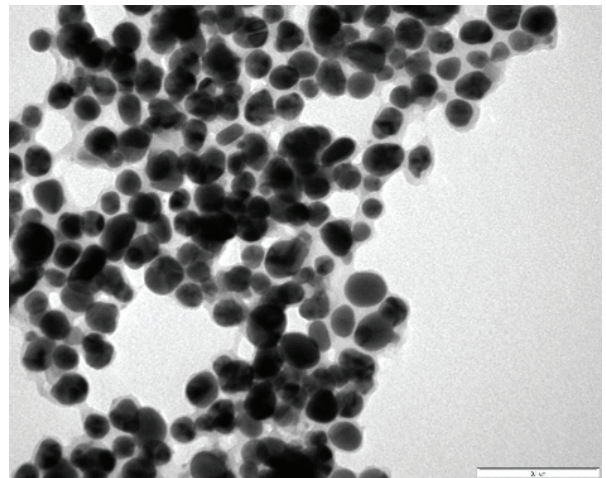


**Figure 3.** Transmission Electron Microscopy (TEM) imaging of Ag NPs.

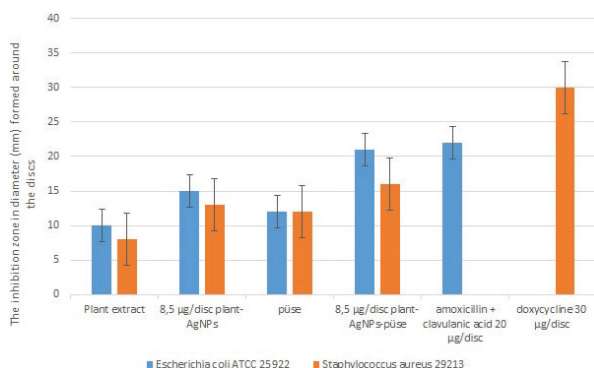
Mabinya, & Okoh, 2019). However, studies have shown that phytochemical compounds such as phenolic, flavonoids, carbohydrates, terpenoids, and proteins are responsible for the reduction and capping/stabilization of Ag NPs (Al-Sheddi et al., 2018; Ramesh, Devi, Battu, & Basavaiah, 2018; Karatoprak et al., 2017; Ocsoy et al., 2017). In other words, these compounds contain active oxygen that has the potential to donate electrons for the reduction of silver precursor into Ag NPs. Triterpenoic acid, a terpenoid type, present in plant extract has a  $-\text{COO}-$  group which acts as a chelating group for capping of the synthesized Ag NPs (Ramesh et al., 2018).

Studies have shown that *J. regia* leaf extracts are rich in phenolic acids, tannins, essential fatty acids, ascorbic acid, flavonoids, caffeic acid, 26 terpenoid substances, and paracomaric acid (Mohammadi, Mirzaei, Azizi, Rouzbehi, & Delaviz, 2012; Nahrstedt, Vetter, & Hammerschmidt, 1981; Paudel, Satyal, Dosoky, Maharjan, & Setzer, 2013). Therefore, it can be said that the biomolecules responsible for the formation of NPs synthesized with *J. regia* leaf extract may be phenolic acids, flavonoids, and terpenoids.

The antibacterial activity of the synthesized Ag NPs using extracts of *J. regia* leaves and "püse" was carried out in Gram (+) bacteria (*S. aureus* ATCC 29213,) and Gram (-) bacteria (*E. coli* ATCC 25922.). The results are reported in Table 1 and Figure 4.

**Table 1. The inhibition zone in diameter (mm) formed around the discs impregnated with mixtures in various volume.**

Bacterial species	The inhibition zone in diameter (mm) formed around the discs impregnated with mixtures in various volume					
	Plant extract	8,5 µg/disc plant-AgNPs	püse	8,5 µg/disc AgNPs-püse	amoxicillin + Clavulanic acid 20 µg/disc	Doxycycline 30 µg/disc
<i>E. coli</i>	10	15	12	21	22	
<i>S. aureus</i>	8	13	12	16		30

**Figure 4.** The antibacterial activity of the synthesized Ag NPs using extracts of *J. regia* leaves and "püse".

Antibacterial activities of the walnut leaf extract, which was used as the control group, on *E. coli* and *S. aureus* bacteria were investigated. According to the obtained data, the walnut leaf extract produced an inhibition zone of 8-and10-mm diameter on both bacterial species, respectively. These results are consistent with the results of Pereira et al. Flavonoids, phenolic, and other compounds contained in natural products have antibacterial effects. For example, quercetin in *J. regia* has been at least partially attributed to inhibition of DNA gyrase (Pereira et al., 2007). The antibacterial activity of the walnut-Ag NPs, which was another control group, formed inhibition zones of 15-and 13-mm diameters on both bacterial species, respectively.

*P. nigra* is an important plant used in the production of folk medicine in the Turkish nomadic culture. They used the resin of the pine tree produced by a special method in the treatment of various diseases that occur in both people and the animals they raised (Alptekin, 2019).

In this study, antibacterial activities of püse on *E. coli* and *S. aureus* bacteria were investigated as another control group. The results showed that there was a 12 mm diameter inhibition zone on two bacterial species.

Silver NPs were synthesized by using walnut leaves as described in the method section and a mixture was obtained with the synthesized product. The antibacterial activity of this mixture on *E. coli* and *S. aureus* bacterial species were compared to the effect of antibiotics. The mixture produced a 21 mm diameter inhibition zone in *E. coli* at a concentration of 8.5 µg / disc, while amoxicillin + clavulanic acid produced 22 mm diameter at a concentration of 20 µg / disc. Here, the

concentration of antibiotic is 2.35 times the concentration of the mixture. Thus, the mixture showed a more effective antibacterial activity than the antibiotic. Likewise, when the antibacterial activity of the mixture on *S. aureus* was investigated, Doxycycline with a concentration of 30 µg / disc produced an inhibition zone of 30 mm diameter while the mixture with a concentration of 8.5 µg / disc produced an inhibition zone of 16 mm diameter. Compared to antibiotics, the mixture with a concentration of 3.5 times less was highly effective. This is a clear result of the synergistic effects of püse and silver ions whose NPs were synthesized by using a walnut extract.

Bacteria have a genetic flexibility that can manipulate threats from the environment that is dangerous to them, including antibiotics. Bacteria that develop resistance to antibiotics usually use two genetic strategies. These are mutations in the genes related to the mechanisms that the molecule will affect and a horizontal gene transfer of DNA containing resistance determinants against these molecules from one bacterium to another (Munita & Arias, 2016).

Antibiotic resistance has become a global crisis threatening human and animal health all over the world due to its increasing and unlimited use (Qiao, Ying, Singer, & Zhu, 2018). Unconscious consumption, as well as overuse of antibiotics, accelerated the emergence of antibiotic-resistant bacterial strains and antibiotic resistant genes, thereby reducing the therapeutic effect of these molecules on bacteria that cause infection in humans and animals (Qiao et al., 2018; Wright, 2010). In general, antibiotics are poorly metabolised by humans and animals and are therefore excreted as active main chemicals with urine and feces and released into the environment through wastewater and fertilizer (Qiao et al., 2018). This means that more bacteria in our environment gain resistance.

Infections associated with health care are defined as infection of patients by infectious agents while receiving health care (Haque, Sartelli, McKimm, & Bakar, 2018; Collins, 2008). Most of these infections are surgical site infections (SSIs), pneumonia, and gastrointestinal infections (Magill et al., 2014). Around 12-17 microorganisms, including *E. coli* and *S. aureus*, cause 80-87% of hospital infections (HCAs) (Sievert et al., 2013; Hidron et al., 2008; Weiner et al., 2016). This major problem, which we will have to face in the very near future, has made it necessary to find alternative solutions to antibiotics or rather to take precautions to prevent infection.

According to the results obtained in this study, this product has the potential to be converted into a commercial product

in the field of health that can be used as a disinfectant to prevent cross-contamination and also as an antibacterial product especially in animal hospitals for the treatment of various diseases.

**Peer-review:** Externally peer-reviewed.

**Author Contributions:** Conception/Design of Study- A.Ö., S.G.A., E.B.; Data Acquisition- A.Ö., S.G.A., E.B.; Data Analysis/Interpretation- A.Ö., S.G.A., E.B.; Drafting Manuscript- A.Ö., S.G.A., E.B.; Critical Revision of Manuscript-A.Ö.; Final Approval and Accountability- A.Ö., S.G.A., E.B.; Technical or Material Support- A.Ö., S.G.A., E.B.; Supervision- A.Ö.

**Conflict of Interest:** The authors have no conflict of interest to declare.

**Financial Disclosure:** Authors declared no financial support.




## REFERENCES

- Ak, M. (2017). Folk Medicine In The Yoruks. *International Journal of Social Science*, 57, 395–405.
- Alam, F., Islam, M. A., Kamal, M. A., & Gan, S. H. (2018). Updates on managing type 2 diabetes mellitus with natural products: towards antidiabetic drug development. *Current Medicinal Chemistry*, 25(39), 5395–5431.
- Alptekin, M. (2019). Mersin Folklorunda Püse (Kara Hekim) İle İlgili Tespitler. *Karabük Üniversitesi Sosyal Bilimler Enstitüsü Dergisi*, 9(1), 323–336.
- Al-Sheddi, E. S., Farshori, N. N., Al-Oqail, M. M., Al-Massarani, S. M., Saquib, Q., Wahab, R., ... Siddiqui, M. A. (2018). Anticancer potential of green synthesized silver nanoparticles using extract of *Nepeta deflersiana* against human cervical cancer cells (HeLa). *Bioinorganic Chemistry and Applications*, 2018, 9390784.
- Cameron, S. J., Hosseini, F., & Willmore, W. G. (2018). A current overview of the biological and cellular effects of nanosilver. *International Journal of Molecular Sciences*, 19(7), 2030.
- Chaloupka, K., Malam, Y., & Seifalian, A. M. (2010). Nanosilver as a new generation of nanoparticle in biomedical applications. *Trends In Biotechnology*, 28(11), 580–588.
- Collins, A. S. (2008). Preventing Health Care–Associated Infections. In R. G. Hughes (Ed.), *Patient Safety and Quality: An Evidence-Based Handbook for Nurses*. Agency for Healthcare Research and Quality (US).
- de la Parra, J., & Quave, C. L. (2017). Ethnophytotechnology: Harnessing the power of ethnobotany with biotechnology. *Trends In Biotechnology*, 35(9), 802–806.
- Demirbas, A., Welt, B. A., & Ocsoy, I. (2016). Biosynthesis of red cabbage extract directed Ag NPs and their effect on the loss of antioxidant activity. *Materials Letters*, 179, 20–23. <https://doi.org/10.1016/j.matlet.2016.05.056>
- Dolatabadi, S., Moghadam, H. N., & Mahdavi-Ourtakand, M. (2018). Evaluating the anti-biofilm and antibacterial effects of *Juglans regia* L. extracts against clinical isolates of *Pseudomonas aeruginosa*. *Microbial Pathogenesis*, 118, 285–289.
- Duman, F., Ocsoy, I., & Kup, F. O. (2016). Chamomile flower extract-directed CuO nanoparticle formation for its antioxidant and DNA cleavage properties. *Materials Science and Engineering: C*, 60, 333–338.
- Faraz, N., Islam, Z., & Rehman, R. (2012). Sehrish Antibiofilm forming activity of naturally occurring compound. *Biomedica*, 28(2), 171–175.
- Forough, M., & Fahadi, K. (2010). Biological and green synthesis of silver nanoparticles. *Turkish Journal of Engineering and Environmental Sciences*, 34(4), 281–287.
- Garnatje, T., Peñuelas, J., & Vallès, J. (2017). Ethnobotany, phylogeny, and 'omics' for human health and food security. *Trends In Plant Science*, 22(3), 187–191.
- Gurib-Fakim, A. (2006). Medicinal plants: traditions of yesterday and drugs of tomorrow. *Molecular Aspects of Medicine*, 27(1), 1–93.
- Haque, M., Sartelli, M., McKimm, J., & Bakar, M. A. (2018). Health care-associated infections—an overview. *Infection and Drug Resistance*, 11, 2321–2333.
- Hidron, A. I., Edwards, J. R., Patel, J., Horan, T. C., Sievert, D. M., Pollock, D. A., & Fridkin, S. K. (2008). Antimicrobial-resistant pathogens associated with healthcare-associated infections: annual summary of data reported to the National Healthcare Safety Network at the Centers for Disease Control and Prevention, 2006–2007. *Infection Control & Hospital Epidemiology*, 29(11), 996–1011.
- Irobi, O. N., Moo-Young, M., Anderson, W. A., & Daramola, S. O. (1994). Antimicrobial activity of bark extracts of *Bridelia ferruginea* (Euphorbiaceae). *Journal of Ethnopharmacology*, 43(3), 185–190.
- Karatoprak, G. Ş., Aydin, G., Altinsoy, B., Altinkaynak, C., Koşar, M., & Ocsoy, I. (2017). The Effect of *Pelargonium endlicherianum* Fenzl. root extracts on formation of nanoparticles and their antimicrobial activities. *Enzyme and Microbial Technology*, 97, 21–26.
- Kaur, K., Michael, H., Arora, S., Harkonen, P. L., & Kumar, S. (2003). Studies on correlation of antimutagenic and antiproliferative activities of *Juglans regia* L. *Journal of environmental pathology, Toxicology and Oncology*, 22(1), 59–67.
- Kızırlarlan, Ç., & Sevgi, E. (2013). Ethnobotanical uses of genus *Pinus* L. (Pinaceae) in Turkey. *Indian Journal of Traditional Knowledge*, 12, 209–220.
- Luther, E. M., Schmidt, M. M., Diendorf, J., Epple, M., & Dringen, R. (2012). Upregulation of metallothioneins after exposure of cultured primary astrocytes to silver nanoparticles. *Neurochemical Research*, 37(8), 1639–1648.
- Magill, S. S., Edwards, J. R., Bamberg, W., Beldavs, Z. G., Dumayati, G., Kainer, M. A., ... Ray, S. M. (2014). Multistate point-prevalence survey of health care–associated infections. *New England Journal of Medicine*, 370(13), 1198–1208.
- McShan, D., Ray, P. C., & Yu, H. (2014). Molecular toxicity mechanism of nanosilver. *Journal of Food and Drug Analysis*, 22(1), 116–127.
- Moravej, H., Salehi, A., Razavi, Z., Moein, M. R., Etemadfard, H., Karami, F., & Ghahremani, F. (2016). Chemical composition and the effect of walnut hydrosol on glycemic control of patients with type 1 diabetes. *International Journal of Endocrinology and Metabolism*, 14(1).
- Mohammadi, J., Mirzaie, A., Azizi, A., Roozbeh, A., & Delaviz, H. (2012). The effects of hydroalcoholic extract of *Juglans regia* leaf on histological changes of Langerhans islet in diabetic rats model. *ISMJ*, 15(4), 293–302.
- Munita, J. M., & Arias, C. A. (2016). Mechanisms of antibiotic resistance. *Virulence Mechanisms of Bacterial Pathogens*, 4(2), 481–511.
- Nahrstedt, A., Vetter, U., & Hammerschmidt, F. J. (1981). Composition of the steam distillation product from the leaves of *Juglans regia* (author's transl). *Planta Medica*, 42(4), 313.
- Ocsoy, I., Gulbakan, B., Chen, T., Zhu, G., Chen, Z., Sari, M. M., ... Tan, W. (2013). DNA-guided metal-nanoparticle formation on graphene oxide surface. *Advanced Materials*, 25(16), 2319–2325.
- Ocsoy, I., Temiz, M., Celik, C., Altinsoy, B., Yilmaz, V., & Duman, F. (2017). A green approach for formation of silver nanoparticles on magnetic graphene oxide and highly effective antimicrobial activity and reusability. *Journal of Molecular Liquids*, 227, 147–152.
- Okaiyeto, K., Ojemaye, M. O., Hoppe, H., Mabinya, L. V., & Okoh, A. I. (2019). Phytofabrication of Silver/Silver Chloride Nanoparticles Using Aqueous Leaf Extract of *Oedera genistifolia*: Characterization and Antibacterial Potential. *Molecules*, 24(23), 4382.

- Paudel, P., Satyal, P., Dosoky, N. S., Maharjan, S., & Setzer, W. N. (2013). Juglans regia and J. nigra, two trees important in traditional medicine: A comparison of leaf essential oil compositions and biological activities. *Natural Product Communications*, 8(10), 1934578X1300801038.
- Pereira, J. A., Oliveira, I., Sousa, A., Valentão, P., Andrade, P. B., Ferreira, I. C., ... Estevinho, L. (2007). Walnut (*Juglans regia* L.) leaves: phenolic compounds, antibacterial activity and antioxidant potential of different cultivars. *Food and Chemical Toxicology*, 45(11), 2287–2295.
- Ramesh, A. V., Devi, D. R., Battu, G., & Basavaiah, K. (2018). A facile plant mediated synthesis of silver nanoparticles using an aqueous leaf extract of *Ficus hispida* Linn. f. for catalytic, antioxidant and antibacterial applications. *South African Journal of Chemical Engineering*, 26, 25–34.
- Qiao, M., Ying, G. G., Singer, A. C., & Zhu, Y. G. (2018). Review of antibiotic resistance in China and its environment. *Environment International*, 110, 160–172.
- Roy, A., Bulut, O., Some, S., Mandal, A. K., & Yilmaz, M. D. (2019). Green synthesis of silver nanoparticles: biomolecule-nanoparticle organizations targeting antimicrobial activity. *RSC Advances*, 9(5), 2673–2702.
- Russell, A. D., & Furr, J. R. (1977). The antibacterial activity of a new chloroxylenol preparation containing ethylenediamine tetraacetic acid. *Journal of Applied Bacteriology*, 43(2), 253–260.
- Santos, A., Barros, L., Calheta, R. C., Dueñas, M., Carvalho, A. M., Santos-Buelga, C., & Ferreira, I. C. (2013). Leaves and decoction of *Juglans regia* L.: Different performances regarding bioactive compounds and in vitro antioxidant and antitumor effects. *Industrial Crops and Products*, 51, 430–436.
- Shah, T. I., Ganesh, N., & Akthar, S. (2013). Preliminary phytochemical evaluation and antibacterial potential of different leaf extracts of *Juglans Regia*: A ubiquitous dry fruit from Kashmir-India. *Pharm Sci Rev Res*, 19, 93–96.
- Shah, M., Fawcett, D., Sharma, S., Tripathy, S. K., & Poinern, G. E. J. (2015). Green synthesis of metallic nanoparticles via biological entities. *Materials*, 8(11), 7278–7308.
- Sievert, D. M., Ricks, P., Edwards, J. R., Schneider, A., Patel, J., Srinivasan, A., ... Fridkin, S. (2013). Antimicrobial-resistant pathogens associated with healthcare-associated infections summary of data reported to the National Healthcare Safety Network at the Centers for Disease Control and Prevention, 2009–2010. *Infection Control & Hospital Epidemiology*, 34(1), 1–14.
- Some, S., Bulut, O., Biswas, K., Kumar, A., Roy, A., Sen, I. K., ... Das, S. (2019). Effect of feed supplementation with biosynthesized silver nanoparticles using leaf extract of *Morus indica* L. V1 on *Bombyx mori* L. (Lepidoptera: Bombycidae). *Scientific Reports*, 9(1), 1–13.
- Strayer, A., Ocsoy, I., Tan, W., Jones, J. B., & Paret, M. L. (2016). Low concentrations of a silver-based nanocomposite to manage bacterial spot of tomato in the greenhouse. *Plant Disease*, 100(7), 1460–1465.
- Topacoglu, O. (2013). Genetic diversity among populations in Black Pine (*Pinus nigra* Arnold. subsp. *pallasiana* (Lamb.) Holmboe) seed stands in Turkey. *Bulgarian Journal of Agricultural Science*, 19(6), 1459–1464.
- Wang, Z., Liu, S., Ma, J., Qu, G., Wang, X., Yu, S., ... Jiang, G. B. (2013). Silver nanoparticles induced RNA polymerase-silver binding and RNA transcription inhibition in erythroid progenitor cells. *ACS Nano*, 7(5), 4171–4186.
- Weiner, L. M., Webb, A. K., Limbago, B., Dudeck, M. A., Patel, J., Kallen, A. J., ... Sievert, D. M. (2016). Antimicrobial-resistant pathogens associated with healthcare-associated infections: summary of data reported to the National Healthcare Safety Network at the Centers for Disease Control and Prevention, 2011–2014. *Infection Control & Hospital Epidemiology*, 37(11), 1288–1301.
- Wright, G. D. (2010). Antibiotic resistance in the environment: a link to the clinic?. *Current Opinion in Microbiology*, 13(5), 589–594.
- You, C., Han, C., Wang, X., Zheng, Y., Li, Q., Hu, X., Sun, H. (2012). The progress of silver nanoparticles in the antibacterial mechanism, clinical application and cytotoxicity. *Molecular Biology Reports*, 39(9), 9193–9201.
- Zhao, M. H., Jiang, Z. T., Liu, T., & Li, R. (2014). Flavonoids in *Juglans regia* L. leaves and evaluation of in vitro antioxidant activity via intracellular and chemical methods. *The Scientific World Journal*, 2014, 1–6.



# Evaluation of Caco-2 cell permeability of ritonavir nanosuspensions

Alptuğ Karaküçük<sup>1</sup> , Naile Öztürk<sup>2</sup> , Nevin Çelebi<sup>1,3</sup> 

<sup>1</sup>Gazi University, Faculty of Pharmacy, Department of Pharmaceutical Technology, Ankara, Turkey

<sup>2</sup>Inonu University, Faculty of Pharmacy, Department of Pharmaceutical Technology, Malatya, Turkey

<sup>3</sup>Baskent University, Faculty of Pharmacy, Department of Pharmaceutical Technology, Ankara, Turkey

**ORCID IDs of the authors:** A.K. 0000-0002-9061-2427; N.Ö. 0000-0002-7617-8433; N.Ç. 0000-0002-6402-5042

**Cite this article as:** Karakucuk, A., Ozturk, N., & Celebi, N. (2020). Evaluation of Caco-2 cell permeability of ritonavir nanosuspensions. *Istanbul Journal of Pharmacy*, 50 (3), 251-255.

## ABSTRACT

**Background and Aims:** Poor aqueous solubility limits drug absorption through intestinal mucosa. Nanosuspensions with nanometer range particle size provides enhanced aqueous solubility and hence permeability. The objective of this study was to investigate the cytotoxicity and *in vitro* cell permeability through human adenocarcinoma (Caco-2) cells of ritonavir (RTV) nanosuspensions.

**Methods:** The Microfluidization method was used to prepare nanosuspensions. Particle size (PS), polydispersity index (PI) and zeta potential (ZP) values were measured as characterization. MTT test was applied to evaluate the cytotoxic effect. Caco-2 cell lines were used for transport studies with RTV coarse powder, physical mixtures and nanosuspension.

**Results:** Approximately 600 nm PS, 0.4 PDI and 22 mV ZP values were observed for nanosuspensions. The sample groups showed no cytotoxicity on the cell lines in any RTV concentration. However, significant cytotoxic effect was determined in groups with high amounts of sodium dodecyl sulfate. The transported RTV in nanosuspension formulation enhanced by 5.3-fold and 1.5-fold in comparison with RTV coarse powder and physical mixture, respectively. Rate of the transportation and also the amount of the transported RTV were improved with nanosuspension formulation.

**Conclusion:** Particle size reduction of RTV into nanometer size and preparing nanosuspension system was found effective to obtain enhanced cell permeability.

**Keywords:** Ritonavir, nanosuspension, Caco-2, permeability

## INTRODUCTION

The solubility in intestinal fluids and permeability from intestinal membrane effect the drug absorption efficiency. Poor drug solubility limits dissolution and hence lower concentration gradient occurs across the intestinal mucosa (Lenhardt, Vergnault, Grenier, Scherer, & Langguth, 2008). Nanosuspensions are colloidal systems with a particle size below 1 µm. The increased surface area of particles by reducing their particle size under nano meter range improves the saturation solubility and dissolution velocity (Xie, Luo, Liu, Ma, Yue, & Yang, 2019). Hence, the poorly soluble drug may have sufficient therapeutic effects with reduced side effects and better transportation to cells of the drug molecules Karakucuk, Alptug, Teksin, Ero-

glu, & Celebi, 2019). The conventional precipitation method or top-down methods are used to prepare nanosuspensions. More preferred approaches are the top-down methods such as media milling or high pressure homogenization, which downsize the particles by high energy creating cavitation and shear forces (Tashan, Karakucuk, & Celebi, 2019). Nanosuspensions are thermodynamically unstable system and stabilization process by using surfactant or polymer is mandatory. Steric or electrostatic stabilization can be achieved in the system with surfactant and/or polymers.

Cell and tissue culture studies are used to investigate the transport of drug from delivery system into specific cells and across specific barriers. Caco-2 cell lines demonstrate the morpho-

**Address for Correspondence:**  
Nevin ÇELEBI, e-mail: ncelebi51@gmail.com

This work is licensed under a Creative Commons Attribution 4.0 International License.



Submitted: 13.04.2020  
Revision Requested: 03.06.2020  
Last Revision Received: 07.06.2020  
Accepted: 07.07.2020  
Published Online: 09.12.2020



logical and biochemical features of adult differentiated enterocytes and goblet cells, which bring benefit to study intestinal epithelial differentiation and function (Wilson, 1990). The well-established Caco-2 cell monolayer system allows direct measurement of the drug fluxes across an epithelium (Lenhardt et al., 2008). They also, indicate P-gp and metabolizing enzymes to predict the absorption of orally administrated compounds (Matsumoto, Kaifuchi, Mizuhara, Warabi, & Watanabe, 2018).

The *in vitro* (Karakucuk, Celebi, & Teksin, 2016) and *in vivo* studies (Karakucuk et al., 2019) were evaluated in previous studies. Therefore, this study mainly focused on the investigation of cytotoxicity and Caco-2 cell permeability of RTV nanosuspensions. Possible P-gp effect of the formulation was also examined.

## MATERIALS AND METHODS

### Materials

Ritonavir (RTV) was kindly gifted by Mylan Pharmaceuticals (India) and hydroxypropyl methyl cellulose (HPMC) (3 cps) was donated by Colorcon Limited (Istanbul, Turkey). Sodium dodecyl sulfate (SDS) was purchased from Merck (Darmstadt, Germany). Human epithelial colorectal adenocarcinoma cell (Caco-2, ATCC HTB 37) was obtained from ATCC. Methyl-thiazolyl tetrazolium (MTT), Hank's balanced salt solution (HBSS), and Dulbecco's modified eagle medium (DMEM) were purchased from Sigma-Aldrich (St. Louis, Missouri, USA). Other chemicals were HPLC or analytical grade.

### Preparation of ritonavir nanosuspensions

RTV nanosuspensions were prepared according to previous study (Karakucuk et al., 2016). Briefly, the stabilizer solution, which was consisted of 4% HPMC 3 cps and 0.8% SDS was prepared. 2% w/w of RTV was dispersed this solution and pre-homogenized for 10 minutes at 10 000 rpm using ultraturrax. The pre-treatment step allowed to reduce particle size below 84  $\mu\text{m}$  in regard to  $d_{99}$ . It is because 84  $\mu\text{m}$  Z-type chamber was used to perform interaction of particles on microfluidization. Then, the coarse suspension was processed by jet stream homogenizer (Microfluidizer® Processors, Westwood, Massachusetts, USA) under high pressure (30 000 psi). After 20 cycles of homogenization nanosuspensions were obtained. The process continued with lyophilization, and nanosuspensions were freeze-dried to fill in the capsules as dosage form and also improve physical stability. For the lyophilization process approximately 2 mL of the nanosuspensions were frozen at  $-80\text{ }^{\circ}\text{C}$  for 2 h. Freeze-dry process was performed at  $-50\text{ }^{\circ}\text{C}$ , 0.021 mbar for 40 h using Christ Alpha 1-2 LD Freeze Dryer.

### Cell culture studies

The Caco-2 cells were used to investigate permeability of coarse RTV and compare permeability values with nanosuspensions. The Caco-2 cells were cultured using DMEM with L-glutamine, supplemented with fetal bovine serum (10%, v/v) and penicillin/ streptomycin (50 IU/mL and 50  $\mu\text{g}/\text{mL}$ , respectively) in a humidified incubator at  $37^{\circ}\text{C}$  in air containing 5%  $\text{CO}_2$ .

### *In vitro* cytotoxicity

Before performing permeability studies, the effect of the formulations on cell viability of Caco-2 cells was investigated by

MTT assay. Cells were seeded at a density of  $5 \times 10^3$  cells per well to 96-well plate and incubated overnight and then the drug solution and formulations (RTV coarse powder, physical mixtures, stabilizer mixtures and nanosuspension) were added to the wells at different concentrations and incubated for 4 hours. DMSO was used to solubilize the drug; therefore, DMSO solution (0.25-4 %) was also applied as control. After incubation period, 25  $\mu\text{L}$  MTT solution was added to wells and incubated for 4 hours. Then the medium was removed and 200  $\mu\text{L}$  of DMSO was added to wells to solubilize the formazan crystals and optical density of wells was measured at 570 nm.

### *In vitro* permeability studies

For permeability studies, cell monolayers were prepared by seeding harvested cells onto inserts (12 mm Snapwell Insert with 0.4  $\mu\text{m}$  pore) at a density of  $7 \times 10^4$  cells per well. After 21 days of culturing (changing the medium every other day), TEER values were measured to determine monolayer integrity. Apical to basolateral transport studies were conducted after the application of formulations in Hank's Balanced Salt Solution (HBSS pH 7.4) to the donor compartment (0.5 mL). RTV bulk powder, nanosuspension, and physical mixtures of stabilizers with or without RTV were used as samples (RTV concentration was 50 mg/mL in all RTV containing samples, n=6). At predetermined time intervals (30, 60, 90, 120 and 240 mins), 0.5 mL sample was withdrawn from basolateral compartment and then fresh medium (HBSS) was added to the wells. Samples were isolated from the receiver compartment (1.5 mL) 4 hours after the incubation. The apparent permeability coefficients ( $P_{app}$ , cm/sn) were calculated according to equation below (Eq. 1):

$$P_{app} = \frac{dQ/dt}{A \cdot 60 \cdot C_0} \quad (\text{Eq. 1})$$

Where  $dQ/dt$  ( $\mu\text{mol}/\text{L} \cdot \text{min}$ ) is the cumulative amount of RTV which has been transported over the membrane, A (1.12  $\text{cm}^2$ ) is the surface area of the inserts and  $C_0$  ( $\mu\text{mol}/\text{L}$ ) is the initial concentration of the RTV on the donor site.

The HPLC method was used to analyze of the samples at 239 nm, which was validated according to accuracy, precision, repeatability, specificity, detection limit, quantitation limit, linearity, and range. The HPLC instrument was HP 1050 series and the C18 RP column (250 mm x 4.6 mm, 5  $\mu\text{m}$ ) was equipped as an analytical column. The mobile phase was consisted of acetonitrile: 0.05 M phosphoric acid (55:45 v/v). Injection volume was 25  $\mu\text{L}$  and flow rate was 1 mL/min. Retention time of RTV was 11-12 minutes.

### Statistical analysis

Statistical evaluation was performed with one-way ANOVA followed Tukey HSD Post hoc test at the significance level of 0.05. Mean  $\pm$  standard deviation was provided for all data.

## RESULTS AND DISCUSSION

### Preparation of ritonavir nanosuspensions

The main process factors for the microfluidization method that effect quality of final nanosuspensions are the chamber type and size, temperature, homogenization cycle, and pressure

(Salazar, Heinzerling, Müller, & Möschwitzer, 2011). Additionally, formulation parameters such as physicochemical properties of the drug, amount of the drug, type and amount of the stabilizers should be considered and optimized (Van Eerdenbrugh, Van den Mooter, & Augustijns, 2008). In this study, 84  $\mu\text{m}$  Z-type chamber was used to obtain nanosuspensions, which is the appropriate size and type for microfluidization. Temperature was controlled during the study. 20 homogenization cycles were applied. The well-known stabilizers, which were HPMC and SDS were used to stabilize the nanosuspensions. 2% of RTV was added in the formulations considering the final oral dose for capsule dosage form. The nanosuspensions were obtained approximately 600 nm PS, 0.4 PDI and -22 mV ZP values. The final RTV nanosuspensions were found physically stable for 30 days of storage time at room temperature. Also, physicochemical properties of RTV were preserved according to differential calorimetry and X-ray diffraction results which is shown in previous study (Karakucuk et al., 2016).

### Caco-2 cell viability and permeability

Monolayer integrity of Caco-2 cell was shown with TEER values of 500-1000  $\text{ohm}\cdot\text{cm}^2$ . MTT assay was conducted to understand the in vitro toxicity of the RTV in different formulations. Cell viability (%) was observed after the interaction between Caco-2 cells and RTV formulations for 4 hours. Cytotoxicity was not observed by using RTV coarse powder even in the highest dose which was 400  $\mu\text{g}$ . The cytotoxicity was resulted from the formulations with SDS either in the existence of RTV or not. In the findings from different concentrations, the increased use of SDS caused toxicity on Caco-2 cells. Nanosuspension and the other formulations had no cytotoxic effect at the 50  $\mu\text{g}$  dose used in the permeability study (Figure 1). Cell viability results were above 100% for some treatment groups, especially for coarse RTV powder. MTT is converted to formazan by viable cells with active metabolism so MTT reduction indicates viable cell metabolism rather than cell proliferation (Riss et al., 2016). Thus our results suggest that increasing RTV concentration, increases cellular metabolic activity of Caco-2 cells.

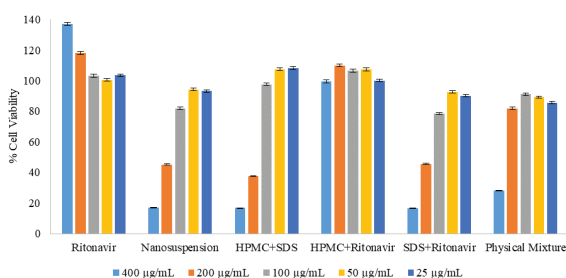


Figure 1. Cell viabilities (%) for the sample groups (n=6).

The Permeability value of coarse RTV and physical mixture were determined  $1.57 \times 10^{-5}$   $\text{cm/s}$  and  $5.75 \times 10^{-5}$   $\text{cm/s}$ , respectively (Figure 2). The permeability value of coarse RTV was found similar to the literature which is at about  $2 \times 10^{-5}$   $\text{cm/s}$  (Alsenz, Steffen, & Alex, 1998; Holmstock, Annaert, & Augustijns, 2012). As the permeability value of RTV was found above  $1 \times 10^{-5}$   $\text{cm/s}$ , it was concluded that the RTV has high permeability property which means RTV belongs to BCS Class II drug with this per-

meability value. The literature data have also proven this result (Chowdary, Annamma Devi, & Dhanalakshmi, 2012; Sinha, Ali, Baboota, Ahuja, Kumar, & Ali, 2010).

The permeability value of nanosuspension was increased and was found  $8.38 \times 10^{-5}$   $\text{cm/s}$  (Figure 2). The permeability value of nanosuspension was higher than the other physical mixtures ( $p < 0.05$ ). The increment of the permeability value of nanosuspension can be resulted from decreasing particle size under micrometer scale. Beside the nanometer particle size values, nanosuspension was prepared by SDS and it is known that SDS can inhibit P-glycoprotein (P-gp) which can result in permeability enhancement (Koga, Ohyashiki, Murakami, & Kawashima, 2000; Miller, Batrakova, & Kabanov, 1999; Rege, Yu Lawrence, Hussain, & Polli, 2001). It is also known that RTV is p-gp substrate by itself (Schmitt, Kaeser, Riek, Bech, & Kreuzer, 2010) and studies showed that RTV induced protein expression of p-gp and increased cellular drug exclusion (Perloff, Von Moltke, Marchand, & Greenblatt, 2001). Using RTV as drug efflux transporter is a strategy to improve intracellular concentration of drug molecules (Janneh, Jones, Chandler, Owen, & Khoo, 2007).

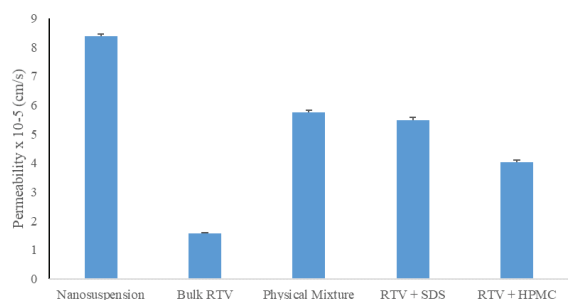


Figure 2. Permeability values of different groups (n=6).

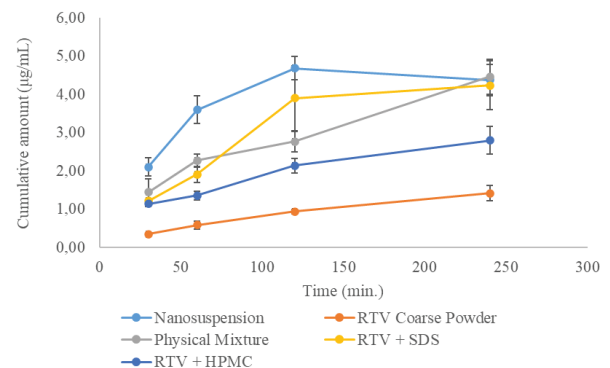


Figure 3. Cumulative amount of RTV in basolateral membrane (n=6).

Cumulative transported RTV amount to the basolateral membrane is given in Figure 3. No further drug transportation was observed after 120 minutes by nanosuspension exposure.

Even the nanosuspension showed faster drug transport, the cumulative drug transported at the end of the assay was similar among nanosuspension, physical mixture, and RTV with SDS formulations. SDS was provided P-gp inhibition which was resulted in an increase in RTV amount in basolateral

membrane. However, RTV coarse powder showed slower and lower drug transport to the basolateral membrane even in comparison with RTV and HPMC mixture. As a polymer, HPMC possessing p-gp inhibiting activity (Rehman et al., 2017), this could also explain that HPMC might be caused P-gp inhibition. It is known that inhibition or induction of functionality of P-gp can affect the pharmacokinetics, efficacy, safety, or tissue levels (Matsumoto et al., 2018).

## CONCLUSION

The microfluidization method was found an effective method to develop nanosuspension formulation regarding to fewer process parameters and easy for scale-up. Neither nanometer range RSV nor using stabilizer combination did not show cytotoxic effect on Caco-2 cells at desired concentration. The nanosuspensions with particle size below 1000 nm showed enhanced permeability through Caco-2 cells due to increased saturation solubility. It could also be said that stabilizers showed P-gp effect, which resulted in improved cumulative drug transport. It is concluded that beside nanosuspensions being beneficial to improve saturation solubility, dissolution and bioavailability, they also increase the cell permeability of poorly soluble drugs.

**Peer-review:** Externally peer-reviewed.

**Informed Consent:** Written consent was obtained from the participants.

**Author Contributions:** Conception/Design of Study- A.K., N.Ö., N.Ç.; Data Acquisition- A.K., N.Ö., N.Ç.; Data Analysis/Interpretation- A.K., N.Ö., N.Ç.; Drafting Manuscript- A.K., N.Ö., N.Ç.; Critical Revision of Manuscript- A.K., N.Ö., N.Ç.; Final Approval and Accountability- A.K., N.Ö., N.Ç.; Technical or Material Support- A.K., N.Ö., N.Ç.; Supervision- A.K., N.Ö., N.Ç.

**Conflict of Interest:** The authors have no conflict of interest to declare.

**Financial Disclosure:** This study was supported by a grant from The Scientific and Technological Research Council of Turkey. (Project No: 113S842, TUBITAK)

## REFERENCES

- Alsenz, J., Steffen, H., & Alex, R. (1998). Active apical secretory efflux of the HIV protease inhibitors saquinavir and ritonavir in Caco-2 cell monolayers. *Pharmaceutical Research*, 15(3), 423–428. <https://doi.org/10.1023/A:1011924314899>
- Chowdary, K. P. R., Annamma Devi, D. G., & Dhanalakshmi, K. (2012). A factorial study on enhancement of solubility and dissolution rate of ibuprofen by hydroxy propyl  $\beta$  cyclodextrin and solutol hs15. *International Journal of Pharmaceutical Sciences Review and Research*, 2(4), 1–7.
- Holmstock, N., Annaert, P., & Augustijns, P. (2012). Boosting of HIV protease inhibitors by ritonavir in the intestine: The relative role of cytochrome P450 and P-glycoprotein inhibition based on Caco-2 monolayers versus in situ intestinal perfusion in mice. *Drug Metabolism and Disposition*, 40(8), 1473–1477. <https://doi.org/10.1124/dmd.112.044677>
- Janneh, O., Jones, E., Chandler, B., Owen, A., & Khoo, S. H. (2007). Inhibition of P-glycoprotein and multidrug resistance-associated proteins modulates the intracellular concentration of lopinavir in cultured CD4 T cells and primary human lymphocytes. *Journal of Antimicrobial Chemotherapy*, 60(5), 987–993. <https://doi.org/10.1093/jac/dkm353>
- Karakucuk, A., Celebi, N., & Teksin, Z. S. (2016). Preparation of ritonavir nanosuspensions by microfluidization using polymeric stabilizers: I. A Design of Experiment approach. *European Journal of Pharmaceutical Sciences*, 95, 111–121. <https://doi.org/10.1016/j.ejps.2016.05.010>
- Karakucuk, Alptug, Teksin, Z. S., Eroglu, H., & Celebi, N. (2019). Evaluation of improved oral bioavailability of ritonavir nanosuspension. *European Journal of Pharmaceutical Sciences*, 131(February), 153–158. <https://doi.org/10.1016/j.ejps.2019.02.028>
- Koga, K., Ohyashiki, T., Murakami, M., & Kawashima, S. (2000). Modification of ceftibuten transport by the addition of non-ionic surfactants. *European Journal of Pharmaceutics and Biopharmaceutics*, 49(1), 17–25. [https://doi.org/10.1016/S0939-6411\(99\)00059-4](https://doi.org/10.1016/S0939-6411(99)00059-4)
- Lenhardt, T., Vergnault, G., Grenier, P., Scherer, D., & Langguth, P. (2008). Evaluation of nanosuspensions for absorption enhancement of poorly soluble drugs: In vitro transport studies across intestinal epithelial monolayers. *AAPS Journal*, 10(3), 435–438. <https://doi.org/10.1208/s12248-008-9050-7>
- Matsumoto, T., Kaifuchi, N., Mizuhara, Y., Warabi, E., & Watanabe, J. (2018). Use of a Caco-2 permeability assay to evaluate the effects of several Kampo medicines on the drug transporter P-glycoprotein. *Journal of Natural Medicines*, 72(4), 897–904. <https://doi.org/10.1007/s11418-018-1222-x>
- Miller, D. W., Batrakova, E. V., & Kabanov, A. V. (1999). Inhibition of multidrug resistance-associated protein (MRP) functional activity with pluronic block copolymers. *Pharmaceutical Research*, 16(3), 396–401. <https://doi.org/10.1023/A:1018873702411>
- Perloff, M. D., Von Moltke, L. L., Marchand, J. E., & Greenblatt, D. J. (2001). Ritonavir induces P-glycoprotein expression, multidrug resistance-associated protein (MRP1) expression, and drug transporter-mediated activity in a human intestinal cell line. *Journal of Pharmaceutical Sciences*, 90(11), 1829–1837. <https://doi.org/10.1002/jps.1133>
- Rege, B. D., Yu Lawrence, X., Hussain, A. S., & Polli, J. E. (2001). Effect of common excipients on Caco-2 transport of low-permeability drugs. *Journal of Pharmaceutical Sciences*, 90(11), 1776–1786. <https://doi.org/10.1002/jps.1127>
- Rehman, S., Nabi, B., Fazil, M., Khan, S., Bari, N. K., Singh, R., Ahmad, S., Kumar, V., Baboota, S., & Ali, J. (2017). Role of P-Glycoprotein Inhibitors in the Bioavailability Enhancement of Solid Dispersion of Darunavir. *BioMed Research International*, 2017, 1–17. <https://doi.org/10.1155/2017/8274927>
- Riss, T. L., Moravec, R. A., Niles, A. L., Duellman, S., Benink, H. A., Worzella, T. J., & Minor, L. (2016). Cell viability assays. In *Assay Guidance Manual [Internet]*. Eli Lilly & Company and the National Center for Advancing Translational Sciences.
- Salazar, J., Heinzerling, O., Müller, R. H., & Möschwitzer, J. P. (2011). Process optimization of a novel production method for nanosuspensions using design of experiments (DoE). *International Journal of Pharmaceutics*, 420(2), 395–403. <https://doi.org/10.1016/j.ijpharm.2011.09.003>
- Schmitt, C., Kaeser, B., Riek, M., Bech, N., & Kreuzer, C. (2010). Effect of saquinavir/ritonavir on P-glycoprotein activity in healthy volunteers using digoxin as a probe. *International Journal of Clinical Pharmacology and Therapeutics*, 48(3), 192–199. <https://doi.org/10.5414/CPP48192>
- Sinha, S., Ali, M., Baboota, S., Ahuja, A., Kumar, A., & Ali, J. (2010). Solid dispersion as an approach for bioavailability enhancement of poorly water-soluble drug ritonavir. *AAPS PharmSciTech*, 11(2), 518–527. <https://doi.org/10.1208/s12249-010-9404-1>
- Tashan, E., Karakucuk, A., & Celebi, N. (2019). Optimization and in vitro evaluation of ziprasidone nanosuspensions produced by a top-down approach. *Journal of Drug Delivery Science and Technology*, 52(March), 37–45. <https://doi.org/10.1016/j.jddst.2019.04.024>

- Van Eerdenbrugh, B., Van den Mooter, G., & Augustijns, P. (2008). Top-down production of drug nanocrystals: Nanosuspension stabilization, miniaturization and transformation into solid products. *International Journal of Pharmaceutics*, 364(1), 64–75. <https://doi.org/10.1016/j.ijpharm.2008.07.023>
- Wilson, G. (1990). Cell culture techniques for the study of drug transport. *European Journal of Drug Metabolism and Pharmacokinetics*, 15(2), 159–163. <https://doi.org/10.1007/BF03190199>
- Xie, J., Luo, Y., Liu, Y., Ma, Y., Yue, P., & Yang, M. (2019). Novel re-dispersible nanosuspensions stabilized by co-processed nanocrystalline cellulose–Sodium carboxymethyl starch for enhancing dissolution and oral bioavailability of baicalin. *International Journal of Nanomedicine*, 14, 353–369. <https://doi.org/10.2147/IJN.S184374>

# Natural pigment of red-fleshed pitaya (*Hylocereus polyrhizus*) as dental plaque disclosing agent: A preliminary study

Amaliya Amaliya<sup>1</sup> , Regi Taufik Firdaus<sup>2</sup> , Nunung Rusminah<sup>1</sup> 

<sup>1</sup>Universitas Padjadjaran, Dental Faculty, Department of Periodontology, Bandung, Indonesia

<sup>2</sup>Universitas Padjadjaran, Dental Faculty, Undergraduate Programme, Bandung, Indonesia

**ORCID IDs of the authors:** A.A. 0000-0002-9164-0542; R.T.F. 0000-0001-7076-7272; N.R. 0000-0002-3709-8625

**Cite this article as:** Amaliya, A., Firdaus, R. T., & Rusminah, N. (2020). Natural pigment of red-fleshed Pitaya (*Hylocereus polyrhizus*) as dental plaque disclosing agent: A preliminary study. *Istanbul Journal of Pharmacy*, 50 (3), 256-261.

## ABSTRACT

**Background and Aims:** Dental plaque as the main etiological factor for caries and periodontal disease is transparent, colorless and not easily visible. Visualized dental plaque can be an aid for patients to develop an efficient system of plaque removal. Several disclosing agents have been developed and applied to clinical and home-care use, yet people are still searching for a natural coloring agent which could be considered safe for long term use.

**Methods:** In this study, various concentrations of Pitaya flesh extract were tested to stain dental plaque taken from 30 volunteers. A disclosing agent of basic-fuchsin already marketed was used as a positive control. The dental plaque specimens were divided into 5 groups and each group was randomly stained either with 0.05 mL of basic fuchsin as a positive control, or 25%, 50%, 75%, or 100% Pitaya flesh extract. The specimens were then analyzed using a spectrophotometer.

**Results:** The results showed that Pitaya flesh extract exhibited dental plaque staining ability. The concentration of 75% Pitaya was similar to the staining ability of basic-fuchsin, while 100% was superior to that of basic-fuchsin.

**Conclusion:** Under the limitations of this study, 75% and 100% extract of pitaya flesh exhibited dental plaque staining in vitro as assessed by a spectrophotometer.

**Keywords:** Natural pigment, Pitaya, dental plaque

## INTRODUCTION

Dental plaque is the etiological agent for major dental diseases such as caries and periodontal disease. Plaque accumulation may increase under certain conditions, such as poor oral hygiene and inappropriate dietary behavior. When left uncontrolled, following adhesion to the tooth surface, dental plaque grows and reaches maturation and leads to these potential consequences; inflammatory changes on the periodontium resulting in destruction of tissues and loss of attachment or irreversible solubilization of tooth mineral by acid produced by certain bacteria in dental plaque (Seneviratne, Zhang, & Samaranayake, 2011; Broadbent, Thomson, Boyens, & Poulton, 2011).

Dental plaque is a biofilm, formed over the hard surfaces in the oral cavity, including calculus and restorations or prosthetic appliances placed in the oral cavity. It comprises living bacterial communities, embedded in a matrix of polymers of host and bacterial origins (Marsh 2010). Mechanical plaque control procedures such as brushing and flossing are effective in reducing plaque, but plaque is rarely removed completely using these measures (Flemmig & Beikler 2011). Since dental plaque is transparent, colorless, and not easily visible, an individual is not generally aware of the amount or the location of dental plaque in his oral cavity. Therefore, it is necessary

### Address for Correspondence:

Amaliya AMALIYA, e-mail: amaliya@fkg.unpad.ac.id

Submitted: 19.11.2019

Revision Requested: 17.01.2020

Last Revision Received: 29.01.2020

Accepted: 10.03.2020

Published Online: 20.11.2020

This work is licensed under a Creative Commons Attribution 4.0 International License.





to detect plaque-covered areas in the oral cavity by using disclosing solutions. Clearly seen plaque can help patients develop an efficient system of plaque removal (Chetrus & Ion, 2013).

Disclosing solutions work by changing the color of dental plaque so that it contrasts with the tooth surface. Several agents have been incorporated in dentistry, from iodine and erythrosine dye, to a fluorescence and three tone dye that are able to disclose and differentiate between early plaque formation and matured ones (Jayanthi, Shilpapiya, Reddy, Elangovan, Sakthivel, & Vijayakumar, 2015; Datta, Kumar, Narayanan, Selvamary, & Sujatha, 2017). However, in the majority of cases, these colorants have disadvantages such as an unpleasant flavor causing subjects to strongly dislike it. In this sense, natural colorants have been suggested as alternatives to the use of synthetic colorants to promote dental hygiene and a patient's motivation. In addition, some artificial colorants caused allergic reactions, or acute toxicity and genetic potential in experimental animals (Miyachi & Tsutsui, 2005; Sania, Aggarwal, & Chaubey, 2016). These disadvantages have driven the replacement of synthetic colorants with natural-derived alternatives.

Pitaya or Pitahaya, a fruit native to Mesoamerica, or also called Dragon Fruit or *Buah Naga* in Indonesia, gathered much interest due to its attractive appearance and taste, as well as nutritional contents (Ortiz-Hernández & Carrillo-Salazar, 2012; Suh et al., 2014). It is classified under the Cactaceae family with the genus name of *Hylocereus*. *Hylocereus polyrhizus* or red-fleshed Pitaya rich in betacyanin pigment is largely cultivated in Indonesia. As people become more interested in natural food, herbal medicines, and traditional practices for a healthy life, the betacyanin pigment from red Pitaya may be utilized as an alternative for dental plaque disclosing agents, while as a food colorant, it has showed promising application in dairy products such as milk and yogurt (Gengatharan, Dykes, & Choo, 2016; Gengatharan, Dykes, & Choo 2017).

The objective of this present study was to explore the potential use of extracted red-fleshed Pitaya in various concentrations as a dental plaque disclosing agent in samples taken from volunteers' teeth. A disclosing agent of basic-fuchsin already marketed was used as a positive control.

## MATERIALS AND METHODS

The experimental design and protocols were reviewed and approved by the Ethics Committee in Hasan Sadikin Hospital Bandung, West Java-Indonesia (89/UN6.KEP/EC/2018). All of the subjects gave their informed consent.

### Plant material and extract preparation

*Hylocereus polyrhizus* fruit were collected in February 2018 from a plantation located in Manglayang, Parongpong, West Bandung Regency, West Java, Indonesia. The fruit was harvested for analysis when it reached the full ripening stage, i.e. 30-35 days after pollination (Figure 1). It was authenticated with collection number 558/HB/02/2018 and deposited in the Herbarium of Plant Taxonomy Laboratory, Department of Biology, Faculty of Math and Nature Sciences, Universitas Padjadjaran Jatinangor, West Java, Indonesia.



Figure 1. Red-fleshed Pitaya (*Hylocereus polyrhizus*).

### Preparation of *Hylocereus polyrhizus* flesh extract

The fruit was washed and wiped dry. Using a stainless-steel knife, the peel was separated from the flesh, and the flesh was cut into portions. The flesh was extracted using distilled water at a fresh weight to solvent ratio (w/v) of 1:1, performed by a maceration process for 72 hours. The extract was then filtrated using filter paper number 41. The solvent was evaporated using a rotary evaporator. The filtrate was diluted into 4 concentrations; 25%, 50%, 75% and 100%, respectively, subsequently placed in dark glass vials, and stored in a refrigerator until further analysis within 2 days.

### Dental plaque samples

Supragingival dental plaque was harvested from 30 dental students with healthy periodontium and free of caries using a sterile curette. Before plaque sampling, volunteers were given dental prophylaxis and asked to refrain from any dental hygiene measures for 48 hours. To remove the food debris from the tooth surfaces, the volunteers were instructed to rinse with water for 30 seconds before the plaque collection. From each volunteer, one sampling site was chosen from buccal/labial surface, either from molars or incisors representing the 4 regions of the mouth.

Dental plaque was weighted at 1 g and placed on a sterile glass slide. The specimens were divided into 5 groups and each group was randomly stained either with 0.05 mL of basic fuchsin (Eviplac, Biodinamica, Brazil) as a positive control, or 25%, 50%, 75%, or 100% Pitaya flesh extract. The pigments were absorbed for 60 seconds before being covered and fixed by air-drying and passing through the flame of a Bunsen burner 3 times, with smear side facing up.

**Spectrophotometer analysis**

The specimens were then analyzed using CM 3600D Spectrophotometer (Minolta, Osaka, Japan).

**RESULTS**

Thirty samples stained with Pitaya extract were tested to compare color intensity. Color intensity of different concentrations was descriptively presented as mean wavelengths (Table 1).

Table 1. Mean of Color Wavelength assessed by Spectrophotometer	
Agent of Plaque Staining	Wavelength (λ)
Basic-fuchsin (Eviplac)	5.9613
Pitaya flesh extract 100%	6.4962
Pitaya flesh extract 75%	5.3134
Pitaya flesh extract 50%	3.3105
Pitaya flesh extract 25%	1.8194

Figure 2 presents the comparison of a spectrophotometer curve of positive control from basic-fuchsin staining (green line) with Pitaya extract 25% (blue line). From the curve, it shows that at 500 λ, basic-fuchsin gives the highest color intensity. From this cut-off point, the color intensity of Pitaya extract 25% is inferior compared to basic-fuchsin.

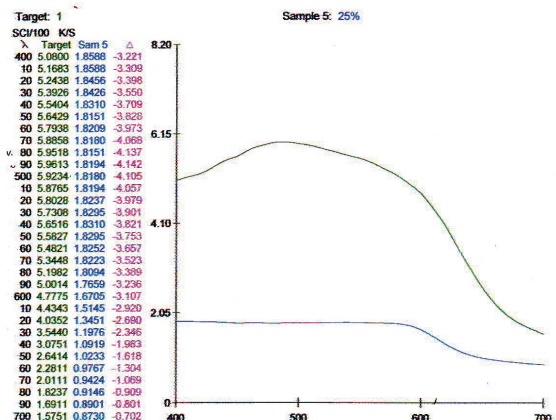


Figure 2. Color wavelength of Pitaya 25% (blue line) and basic-fuchsin (green line).

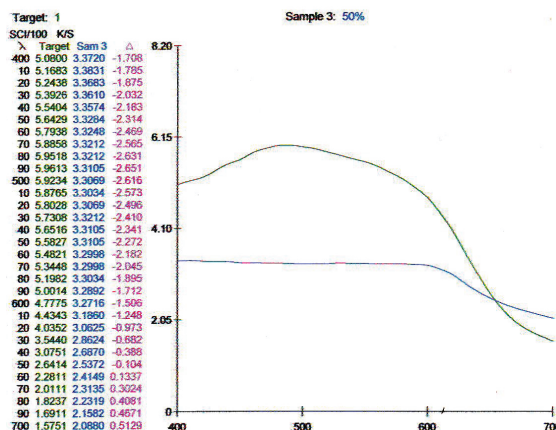


Figure 3. Color wavelength of Pitaya 50% (blue line) and basic-fuchsin (green line).

Figure 3 is the comparison between positive control (green line) and Pitaya extract 50% staining (blue line). It shows that Pitaya extract at 50% color intensity is lower than basic-fuchsin color intensity at 500 λ.

Figure 4 compares positive control (green line) and Pitaya extract at 75% color intensity (blue line). The color intensity of Pitaya extract is almost the same as basic-fuchsin.

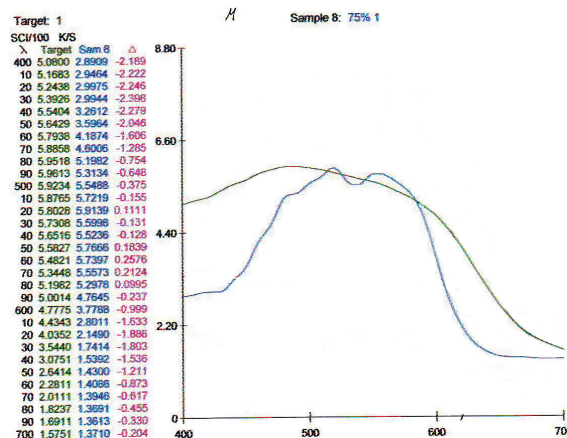


Figure 4. Color wavelength of Pitaya 75% (blue line) and basic-fuchsin (green line).

Figure 5 exhibits that Pitaya extract at 100% color intensity is superior to that of basic-fuchsin at 500 λ.

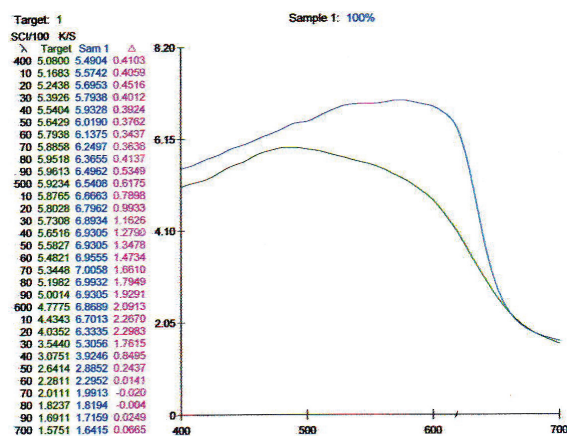


Figure 5. Color wavelength of Pitaya 100% (blue line) and basic-fuchsin (green line).

Figure 6 shows a stained plaque specimen image



Figure 6. Specimen of dental plaque stained with 75% Pitaya extract.

Figure 7 exhibits patient intraoral images of 48-hour old dental plaque without staining



**Figure 7.** Intra-oral image of dental plaque without staining.

Figure 8 indicates patient intraoral images of 48-hour old dental plaque with staining



**Figure 8.** Intra-oral image of dental plaque with staining.

## DISCUSSION

The present study was undertaken to evaluate the potential of using a natural pigment derived from red-fleshed Pitaya fruit extract with different concentrations as a dental plaque disclosing solution.

A disclosing solution is used to reveal plaque to the patient and the clinician to reinforce instruction in oral hygiene. Daily removal of bacterial dental plaque by the patient is paramount to the maintenance of oral health in order to prevent periodontal diseases and tooth decay. Following therapy, these oral hygiene measures play a role in lifelong supportive care (Strömberg, Hagman-Gustafsson, Holmén, Wårdh, & Gabre, 2012).

Dental plaque has the ability to retain a large number of dye substances because of the polarity difference between the components of the plaque and dyes. The particles are bound to the surface by electrostatic interaction (proteins) and hydrogen bonds (polysaccharides) (Chetrus & Ion, 2013). Clean tooth surfaces cannot absorb the coloring agent. When pellicle and bacterial plaque are present, they absorb the agent and are revealed. Pellicle stains as a thin relatively clear covering, whereas bacterial plaque appears darker, thicker and more opaque (Sharma, 2010).

In adults with gingivitis, the quality of self-performed mechanical plaque removal is not sufficiently effective and should be improved. Oral hygiene instruction has a significant, albeit small, positive effect on the reduction of gingivitis (Hioe & van der Weijden, 2005). The existing problem is that total removal of plaque in tooth cleaning measures is difficult to obtain because plaque cannot be seen. Demonstrating the amount of the plaque to patients would improve the standard of oral hygiene. This has been addressed by several research groups. The

effect of using plaque disclosing tablets on plaque removal was investigated in subjects refraining from any tooth cleaning for 24 hours; it was shown that significantly more plaque was removed when using the toothbrush together with the disclosing tablet compared to brushing with the toothbrush alone (Sandeep, Vinay, Madhuri, Rao, Uloopi, & Sekhar, 2014; Peng et al., 2014). In a cross-over study, children without any tooth brushing instruction improved their tooth brushing ability with the use of a disclosing solution staining the amount of dental plaque, as compared with tooth brushing alone (Chouchaisithi, Santiwong, Sutthavong, & Asvanit, 2014). Moreover, the improved removal of biofilm during periodontal surgery could be accomplished by a clinician, when plaque was revealed by a disclosing solution (Montevicchi, Checchi, Gatto, Klein, & Checchi, 2012).

The results of the present study showed that Pitaya was able to stain dental plaque with a concentration of 75% and 100%, which were comparable to the standard disclosing solutions already available on the market. Pitaya fruit produces a colorant of the betacyanin type that belongs to hydro-soluble pigments that presents as deep red–purple, with their stable appearance in a broad pH range. Pitaya fruit have a great potential as natural coloring agents for a wide array of food and are considered to be the third richest betacyanin source for food-coloring agents after *Beta vulgaris* and *Amaranthus* species. (Wybraniec & Mizrahi, 2002). Moreover, betacyanin pigment is also a potent antibacterial agent (Tenore, Novellino, & Basile, 2012). A disclosing solution is required to have an antibacterial agent; hence Pitaya extract could be a good candidate. It has been proposed that if a disclosing solution has antibacterial properties, then it may be able to protect an open wound in the oral mucosa from unnecessary contamination during a procedure.

Studies of dental plaque staining in vitro with Pitaya extract were scarce, one published study written in Indonesian, observed the penetration strength of staining of flesh extract in potato blocks. The result showed that a concentration of 75% Pitaya extract had the highest penetration (Hakim, Prharani, & Purwanto, 2018). Nevertheless, this study was done using visually assessed caliper gauge, that maybe high in risk of bias, despite a calibration performed with 3 examiners. In the present study, a spectrophotometer was employed to analyze the color intensity of plaque staining, eliminating the risk of bias.

Several natural plaque colorants derived from plants have been proposed as plaque disclosing agents. *Beta vulgaris* (sugar beet), *Euterpe oleracea* (acai berry) and *Bixa orellana* (urucum) extracts has been used to stain dental plaque (de Nazaré, Emmi, Barroso, & da Rocha, 2007). In general, the colorants were prepared by extracting the fruits or the part of a plant by maceration and extracted with a solvent followed by filtration and recuperation of the liquid phase until extracts were obtained.

Betacyanin retention and stability during storage is a crucial factor for the application of a plaque disclosing solution. This present study did not evaluate the degradation of betacyanin of Pitaya extract during the course of the trial. Since light was



reported previously to accelerate betalain degradation (Herbach, Maier, Stintzing, & Carle, 2007), the extract was stored in dark storage. Another study showed that refrigeration storage at 4°C condition without light exposure managed to preserve the color of the fruit juice up to 3 weeks (Woo, Ngou, Ngo, Soong, & Tang, 2011). Supplementation with ascorbic acid has been recently reported to delay betacyanin degradation during thermal treatment of purple pitaya juice. The addition of 0.25% (w/w) ascorbic acid showed a stabilizing effect on betacyanin of concentrate samples that were stored in light. Supplementation with the antioxidant was found to inhibit light damage, thus allowing storage in transparent packaging materials (Wong & Siow, 2015).

Under the limitation of this study, we concluded that both a 75% and 100% extract of pitaya flesh exhibited good dental plaque staining in vitro as assessed by a spectrophotometer. This ability was similar to a benchmark disclosing solution product. This finding merits further study to clarify the optimal concentration and physical stability before its clinical application.

**Peer-review:** Externally peer-reviewed.

**Author Contributions:** Conception/Design of Study- A.A., N.R.; Data Acquisition- A.A., R.T.F., N.R.; Data Analysis/Interpretation- A.A., R.T.F.; Drafting Manuscript- A.A.; Critical Revision of Manuscript- A.A.; Final Approval and Accountability- A.A., R.T.F., N.R.; Technical or Material Support- A.A., R.T.F.; Supervision- A.A., N.R.

**Conflict of Interest:** The authors have no conflict of interest to declare.

**Financial Disclosure:** Authors declared no financial support.

**Acknowledgements:** We thank to Textiel Inrichting Bandoeng (Sekolah Tinggi Teknologi Tekstil Bandung) for their assistance in performing spectrophotometry assessment.

## REFERENCES

- Broadbent, J. M., Thomson, W. M., Boyens, J. V., & Poulton, R. (2011). Dental plaque and oral health during the first 32 years of life. *The Journal of the American Dental Association*, 142(4), 415–426. <https://doi.org/10.14219/jada.archive.2011.0197>
- Chetrus, V., & Ion, I. R. (2013). Dental plaque-classification, formation, and identification. *International Journal of Medical Dentistry*, 3(2), 139–143.
- Chouchaisithi, N., Santiwong, B., Sutthavong, S., & Asvanit, P. (2014). Use of a disclosed plaque visualization technique improved the self-performed, tooth brushing ability of primary schoolchildren. *Journal of Medical Association Thailand*, 97(2), 88–95. Retrieved from <https://pdfs.semanticscholar.org/6e3f/924e04cade2ae3bdd022a6dc64fab415900a.pdf>
- Datta, D., Kumar, S. R., Narayanan, M. A., Selvamary, A. L., & Sujatha, A. (2017). Disclosing solutions used in dentistry. *World Journal of Pharmaceutical Research*, 6(6), 1648–1656.
- de Nazaré, R. F. R., Emmi, D. T., Barroso, R. F. F., & da Rocha, P. O. (2007). U.S. Patent No. 7,182,935. Washington, DC: U.S. Patent and Trademark Office. Retrieved from [https://www.lens.org/lens/patent/US\\_7182935\\_B2](https://www.lens.org/lens/patent/US_7182935_B2)
- Flemmig, T. F., & Beikler, T. (2011). Control of oral biofilms. *Periodontology 2000*, 55(1), 9–15. <https://doi.org/10.1111/j.1600-0757.2010.00383.x>
- Gengatharan, A., Dykes, G. A., & Choo, W. S. (2016). Stability of betacyanin from red pitahaya (*Hylocereus polyrhizus*) and its potential application as a natural colourant in milk. *International Journal of Food Science & Technology*, 51(2), 427–434. <https://doi.org/10.1111/ijfs.12999>
- Gengatharan, A., Dykes, G. A., & Choo, W. S. (2017). The effect of pH treatment and refrigerated storage on natural colourant preparations (betacyanins) from red pitahaya and their potential application in yoghurt. *LWT-Food Science and Technology*, 80, 437–445. <https://doi.org/10.1016/j.lwt.2017.03.014>
- Hakim, A., Praharani, D., & Purwanto, P. (2018). Comparison of Color Penetration between Disclosing Solution and Red Dragon Fruit Extract. (in Indonesian). Proceeding of Seminar : Great Dentist for Achieving Excellent Service, Universitas Jember – East Java, Indonesia. Retrieved from <https://repository.unej.ac.id/handle/123456789/89454>
- Herbach, K. M., Maier, C., Stintzing, F. C., & Carle, R. (2007). Effects of processing and storage on juice colour and betacyanin stability of purple pitaya (*Hylocereus polyrhizus*) juice. *European Food Research and Technology*, 224(5), 649–658. <https://doi.org/10.1007/s00217-006-0354-5>
- Hioe, K. P. K. J., & Van der Weijden, G. A. (2005). The effectiveness of self-performed mechanical plaque control with triclosan containing dentifrices. *International Journal of Dental Hygiene*, 3(4), 192–204. <https://doi.org/10.1111/j.1601-5037.2005.00150.x>
- Jayanthi, M., Shilpapiya, M., Reddy, V. N., Elangovan, A., Sakthivel, R., & Vijayakumar, P. (2015). Efficacy of three-tone disclosing agent as an adjunct in caries risk assessment. *Contemporary Clinical Dentistry*, 6(3), 358. <https://dx.doi.org/10.4103%2F0976-237X.161887>
- Marsh, P. D. (2010). Microbiology of dental plaque biofilms and their role in oral health and caries. *Dental Clinics*, 54(3), 441–454. <https://doi.org/10.1016/j.cden.2010.03.002>
- Miyachi, T., & Tsutsui, T. (2005). Ability of 13 chemical agents used in dental practice to induce sister-chromatid exchanges in Syrian hamster embryo cells. *Odontology*, 93(1), 24–29. <https://doi.org/10.1007/s10266-005-0055-8>
- Montevecchi, M., Checchi, V., Gatto, M. R., Klein, S., & Checchi, L. (2012). The use of a disclosing agent during resective periodontal surgery for improved removal of biofilm. *The Open Dentistry Journal*, 6, 46–50. <https://dx.doi.org/10.2174%2F1874210601206010046>
- Ortiz-Hernández, Y. D., & Carrillo-Salazar, J. A. (2012). Pitahaya (*Hylocereus* spp.): a short review. *Comunicata Scientiae*, 3(4), 220-237. <https://doi.org/10.14295/cs.v3i4.334>
- Peng, Y., Wu, R., Qu, W., Wu, W., Chen, J., Fang, J. ... & Mei, L. (2014). Effect of visual method vs plaque disclosure in enhancing oral hygiene in adolescents and young adults: A single-blind randomized controlled trial. *American Journal of Orthodontics and Dentofacial Orthopedics*, 145(3), 280–286. <https://doi.org/10.1016/j.ajodo.2013.10.021>
- Sandeep, V., Vinay, C., Madhuri, V., Rao, V. V., Uloopi, K. S., & Sekhar, R. C. (2014). Impact of visual instruction on oral hygiene status of children with hearing impairment. *Journal of Indian Society of Pedodontics and Preventive Dentistry*, 32(1), 39–43. <https://doi.org/10.4103/0970-4388.127053>
- Sania, M. S., Aggarwal, M. C., & Chaubey, K. K. (2016) An overreaction to plaque disclosing agent: an unusual case. *Journal of Periodontal Medicine and Clinical Practice*, 3, 51–55.
- Seneviratne, C. J., Zhang, C. F., & Samaranayake, L. P. (2011). Dental plaque biofilm in oral health and disease. *Chinese Journal of Dental Research*, 14(2), 87–94.
- Sharma, S. (2010). Plaque disclosing agent a review. *Journal of Advanced Dental Research*, 2(1). Available from: <http://www.ispcd.org/~cmsdev/userfiles/rishabh/plaque%20final%20new.pdf>

- Strömberg, E., Hagman-Gustafsson, M. L., Holmén, A., Wårdh, I., & Gabre, P. (2012). Oral status, oral hygiene habits and caries risk factors in home-dwelling elderly dependent on moderate or substantial supportive care for daily living. *Community Dentistry and Oral Epidemiology*, *40*(3), 221–229. <https://doi.org/10.1111/j.1600-0528.2011.00653.x>
- Suh, D. H., Lee, S., Heo, D. Y., Kim, Y. S., Cho, S. K., Lee, S., & Lee, C. H. (2014). Metabolite profiling of red and white pitayas (*Hylocereus polyrhizus* and *Hylocereus undatus*) for comparing betalain biosynthesis and antioxidant activity. *Journal of Agricultural and Food Chemistry*, *62*(34), 8764–8771. <https://doi.org/10.1021/jf5020704>
- Tenore, G. C., Novellino, E., & Basile, A. (2012). Nutraceutical potential and antioxidant benefits of red pitaya (*Hylocereus polyrhizus*) extracts. *Journal of Functional Foods*, *4*(1), 129–136. <https://doi.org/10.1016/j.jff.2011.09.003>
- Wong, Y. M., & Siow, L. F. (2015). Effects of heat, pH, antioxidant, agitation and light on betacyanin stability using red-fleshed dragon fruit (*Hylocereus polyrhizus*) juice and concentrate as models. *Journal of Food Science and Technology*, *52*(5), 3086–3092. <https://doi.org/10.1007/s13197-014-1362-2>
- Woo, K. K., Ngou, F. H., Ngo, L. S., Soong, W. K., & Tang, P. Y. (2011). Stability of betalain pigment from red dragon fruit (*Hylocereus polyrhizus*). *American Journal of Food Technology*, *6*(2), 140–148. Retrieved from <http://docsdrive.com/pdfs/academicjournals/ajft/2011/140-148.pdf>
- Wybraniec, S., & Mizrahi, Y. (2002). Fruit flesh betacyanin pigments in *Hylocereus cacti*. *Journal of Agricultural and Food Chemistry*, *50*(21), 6086–6089. <https://doi.org/10.1021/jf020145k>



# Investigation of the effect of some plant aqueous extracts on calcium phosphate precipitation as a simulation of initial dental calculus formation *in vitro*

Büşra Selmi Çepiş<sup>1</sup> , Serap Akyüz<sup>2</sup> , Özlem Saçan<sup>3</sup> , Refiye Yanardağ<sup>3</sup> , Aysen Yarat<sup>4</sup> 

<sup>1</sup>Marmara University, Faculty of Pharmacy, Health Sciences Institutes, Department of Biochemistry, Istanbul, Turkey

<sup>2</sup>Marmara University, Faculty of Dentistry, Department of Clinical Sciences (Pedodontics), Istanbul, Turkey

<sup>3</sup>Istanbul University-Cerrahpasa, Faculty of Engineering, Department of Chemistry (Biochemistry), Istanbul, Turkey

<sup>4</sup>Marmara University, Faculty of Dentistry, Department of Basic Medical Sciences (Biochemistry), Istanbul, Turkey

**ORCID IDs of the authors:** B.S.Ç. 0000-0002-6198-2218; S.A. 0000-0002-1358-0150; Ö.S. 0000-0001-6503-4613; R.Y. 0000-0003-4185-4363; A.Y. 0000-0002-8258-6118

**Cite this article as:** Selmi Cepis, B., Akyuz, S., Sacan, O., Yanardag, R., & Yarat, A. (2020). Investigation of the effect of some plant aqueous extracts on calcium phosphate precipitation as a simulation of initial dental calculus formation *in vitro*. *Istanbul Journal of Pharmacy*, 50 (3), 262-267.

## ABSTRACT

**Background and Aims:** Calcium phosphate is most of the inorganic content of dental calculus. Therefore, knowing or controlling the precipitation mechanism of calcium phosphate is very important for the inhibition of dental calculus formation at the beginning. Plants have been known to be excellent sources of many nutritional and phytochemical content. The aim of this study is to investigate the effects of *Petroselinum crispum* (Mill.) Fuss, *Eruca vesicaria* subsp. *sativa* (Mill.) Thell., *Beta vulgaris* var. *cicla* L., *Rumex crispatus* DC. and *Cotinus coggygria* Scop. aqueous extracts on calcium phosphate precipitation, which is thought to reflect the onset of dental calculus formation *in vitro*.

**Methods:** The optical density (OD) increases first with the calcium phosphate nucleation and when the balance is reached, the optical density decreases gradually when the nuclei begin to aggregate and precipitate. The OD change was monitored by recording the absorbance at 620 nm.

**Results:** The effect on the calcium phosphate precipitation varied differently among the 5 types of aqueous extracts. The smoke tree (*Cotinus coggygria*) extract activated calcium phosphate precipitation while all others inhibited precipitation.

**Conclusion:** These results suggest that some types of plant aqueous extracts may have protective potential against dental calculus initially and, therefore they may be used in toothpastes or in mouthwashes.

**Keywords:** Dental calculus, calcium phosphate precipitation, plant aqueous extract

## INTRODUCTION

Among oral and dental health problems, dental calculus has an increasing prevalence due to changes in the diet and nutritional habits of societies (Akar, 2014) and causes many oral problems, such as noneaesthetic appearance and bad breath. Although dental calculus is not directly responsible for the occurrence of health problems such as diabetes, urinary stone formation, and cardiovascular disease, it is a secondary factor in disease progression (Batool et al., 2018, Clarke, 2015).

Dental calculus is a mineralized bacterial plaque which is a hard and calcified deposit with a bacterial plaque layer clustered on natural teeth and restorations (Moolya et al., 2010). It is composed of various inorganic components, mainly calcium phosphate

## Address for Correspondence:

Ayşen YARAT, e-mail: ayaratster@gmail.com; ayarat@marmara.edu.tr

This work is licensed under a Creative Commons Attribution 4.0 International License.



Submitted: 16.05.2020  
Revision Requested: 11.08.2020  
Last Revision Received: 17.08.2020  
Accepted: 02.09.2020

compound, and organic matrix (Jin & Yip, 2002; White, 1997). Many factors such as diet, especially alkaline foods and sugars, saliva pH, composition and bacterial load, age, sex, race, gender, tobacco use, presence of systemic diseases, drugs used, oral hygiene practices and socioeconomic status affect dental calculus formation (Akçalı & Lang, 2018). Bacterial endotoxins damage the gum and periodontal tissue (Hidaka, Nishimura, Nakajima, & Liu, 1996). Knowing and controlling the factors affecting calcium phosphate precipitation is very important for the inhibition of initial dental calculus formation (Tarasevich, Chusuei, & Alloro, 2003). The use of plants has also become widespread in dental and oral health, with secondary metabolites and a wide range of biological activities (Gulfraz, Sadiq, Tariq, Imran, & Qureshi, 2011).

*Petroselinum crispum* (parsley, Apiaceae) has an antihistaminic, antiseptic, hepatogenic, hypotensive, and plasma calcium-enhancing effect (Hazim, Al-Daraji, Al-Mashadani, Al-Hassani, & Mirza, 2012). It contains high amounts of apigenin, ascorbic acid, eugenol, carotenoids, flavonoids, coumarins, phenylpropanoids, phthalates, furano coumarins and tocopherol components (Ajmera, Kalani, & Sharma, 2019; Pápáy, Kállai-Szabó, Ludányi, Klebovich, & Antal, 2016; Tunali et al., 1999). *Eruca vesicaria ssp. sativa* (garden rocket) belongs to the cabbage *Brassicaceae* family. It is known as a diuretic, antiulcer, antithrombotic, antioxidant, anticancer, antiplatelet and anti-inflammatory (Taviano et al., 2018 and 2017; Gulfraz et al., 2011; Sacan, Orak, & Yanardag, 2008). It contains important secondary metabolites such as flavonoids, alkaloids, tannins, phenols, saponins and ascorbic acid. Its essential oils contain high concentrations of an especially antibacterially effective erucic acid (Sarwar Alam, Kaur, Jabbar, Javed, & Athar, 2007). *Beta vulgaris var. cicla* (chard) is from the family *Chenopodiaceae* and is a vegetable rich in vitamins A, B, C, calcium, iron, and phosphorus. In its structure, it contains fatty acids such as palmitic acid, citric acid, oleic acid, linoleic acid, and phospholipids, glycolipids, polysaccharides, saponin, pectin, and flavonoids (Tunali, 2020; Mzoughi et al., 2019). It has antidiabetic, antioxidant, antitumor, antimicrobial, hepatoprotective, antiseptic, and anti-acetylcholinesterase activity (Sacan & Yanardag, 2010; Bolkent, Yanardağ, Tabakoğlu-Oğuz, & Özsoy-Saçan, 2000; Mzoughi et al., 2019). *Rumex crispus* (curled dock) *Polygonaceae* is a plant rich in anthracene derivatives from the blackgrain family. It also contains tannins, flavonoids, and naphthalene derivatives. It has antioxidant and antimicrobial effects (Idris, Wintola, & Afolayan, 2019; Demir, Bozkurt, Onur, Kay, & Somer, 2017; Coruh, Gormez, Ercisli, & Sengul, 2008). *Cotinus coggygria* (smoke tree) is a plant belonging to the Anacardiaceae family, generally known as "smoke tree". It has been shown by *in vivo* and *in vitro* studies that it has many activities such as antioxidant, antibacterial, antifungal, antiviral, hepatoprotective, and anti-inflammatory (Matić, Stanić, Mihailović, & Bogojević, 2016). It has been reported that the *Cotinus coggygria*, which has a high flavonoid content, has cytotoxic effects on bacteria and shows inhibitory properties against the common components of the dental plaque, *S. mutans* and *S. sanguinis* (Ferrazzano et al., 2013; Wang, Wang, Du, Fei, & To, 2016).

In this study, the effects of five plant aqueous extracts (*Petroselinum crispum*, *Eruca vesicaria ssp. sativa*, *Beta vulgaris var. cicla*, *Rumex cristatus DC.* and *Cotinus coggygria Scop.*) on the mechanism of nucleation and aggregation of calcium phosphate precipitation which is thought to reflect initial dental calculus formation *in vitro*, was evaluated.

## MATERIALS AND METHODS

### Preparation of plant aqueous extracts

Plant extracts were prepared at the Department of Chemistry, Faculty of Engineering, Istanbul University-Cerrahpasa. *Petroselinum crispum*, *Beta vulgaris var. cicla* were identified by Prof. Dr. Neriman Ozhatay. *Rumex cristatus*, and *Eruca sativa* were identified by Prof. Dr. Kerim Alpınar. *Cotinus coggygria* was identified by Prof. Dr. Sukran Kultur, Faculty of Pharmacy, Istanbul University. The plant materials were washed with water and dried at room temperature. The dried plants were stored at -20°C until used. Dried leaves (50 g) were extracted by adding 500 mL of distilled water and boiling for 8 hours. The extracts were then filtered and lyophilized. Then, were kept at -20°C. When used, the extracts were dissolved in distilled water to obtain a saturated solution.

### Screening of calcium phosphate precipitation

To obtain the standard curve for nucleation and aggregation of calcium phosphate precipitates were obtained by recording the change in optical density at 620 nm at two-minute intervals for approximately 30 minutes using the RT-9000 Semi-auto Chemistry Analyzer instrument, after mixing equal volumes of calcium chloride dihydrate (4 mM) and trisodium phosphate (10 mM) solutions at 37°C. Final concentrations of calcium and phosphate ions were about 2mM and 5 mM respectively. They are between physiological salivary concentrations. The optical density increases first with the calcium phosphate nucleation, when the balance is reached, the optical density decreases gradually when the nuclei begin to aggregate and precipitate (Selmi Cepic, Akyuz, & Yarat, 2020).

The effects of plant aqueous extract on calcium phosphate precipitation were examined by the addition of 50 µL of an aqueous extract into the mixture of calcium and phosphate ions. Each sample was studied five times. At the end of the experiment, charts drawn between time and optical density (absorbance) and the effects of each aqueous extract on calcium phosphate precipitation were evaluated statistically.

### Statistics

The Statistical Program for the Social Sciences (SPSS) (16.0, Windows) was used in the statistical evaluation of the data obtained as a result of the study and  $p < 0.05$  was considered statistically significant. The consistency of continuous variables to normal distribution was investigated using the Kolmogorov-Smirnov test. Student's t test was used in two independent group comparisons for normally distributed variables. Mann Whitney U test was used in comparison of two independent groups for non-normally distributed variables. Values are given as mean  $\pm$  standard deviation (SD).

**RESULTS**

**The standard curve for precipitation of calcium phosphate:**

Time-course measurements of optic density obtained by 2 mM of calcium and 5 mM of phosphate solutions at 620 nm were illustrated in Figure 1 (Selmi Cepis, Akyuz, & Yarat, 2020).

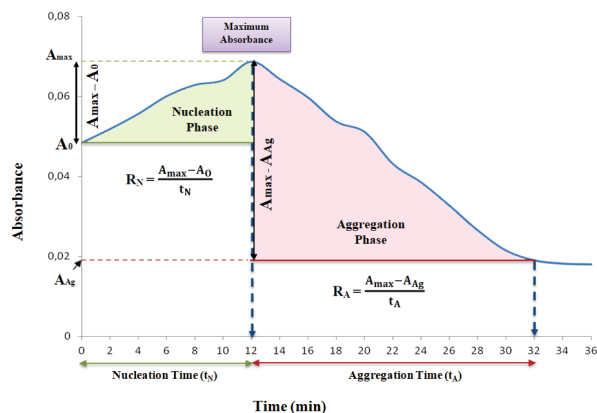


**Figure 1.** The standard curve for nucleation and aggregation phases of the formation of calcium phosphate precipitate (Selmi Cepis, Akyuz, & Yarat, 2020). After mixing the calcium and phosphate solutions, the increase in optical density over time reflects the rate of formation of new nuclei and the increase in the number of calcium phosphate nuclei. When the optical density reaches the maximum value, the formation of calcium phosphate nuclei is complete. This phase is called the nucleation phase. Nucleation rate ( $R_N$ ) is the ratio of the difference between the maximum absorbance value and the original absorbance value to the time taken to reach the maximum absorbance value ( $t_N$ ). Optical density decreases gradually over time. The decrease in the optical density reflects the reduction of the number of nuclei dispersed in the solution due to the aggregation of calcium phosphate nuclei. This is called the aggregation phase.  $R_A$  is the ratio of difference between the maximum absorbance value and the absorbance value where the optical density no longer decreases to the time taken to decrease the maximum absorbance ( $t_A$ ).

**Effects of plants aqueous extracts in calcium phosphate precipitation:**

The effects of *Petroselinum crispum*, *Eruca vesicaria ssp. sativa*, *Beta vulgaris var.cicla*, *Rumex cristatus* and *Cotinus coggygria* aqueous extracts are shown in the Figure 2. Compared to a standard curve, all extracts except *Cotinus coggygria* prolonged nucleation time, decarsed the nucleation rate significantly. *Cotinus coggygria* and *Rumex crispus* shortened aggregation time significantly. All extracts increased aggregation rate significantly compared to a standard curve. The increase in the aggregation rate for *Cotinus coggygria* was significantly more than those of other extracts (Table 1 and Figure 2).

**DISCUSSION**

Physiologically, normal  $Ca^{2+}$  ion concentration in saliva has been reported to be 1.03–3.6 mM and  $PO_4^{3-}$  ion concentration 4.5–6 mM. Any imbalance in these concentrations bring various problems in terms of dental and oral health. The most important of these is dental calculus formation. Calcium phosphate supersaturation, which is realized by increasing the concentration of  $Ca^{2+}$  and  $PO_4^{3-}$  ions in saliva, is a thermodynamic driving factor for dental calculus formation (Morta, Mante, Rasa, & Gintaras, 2018). Therefore, to obtain a standard curve, which nucleation and aggregation phases of calcium phosphate precipitation can be monitored in a short time interval and in a good manner, preliminary experiments were carried out with different concentrations of these two ions. As a result, for final concentration in the mixture, 2 mM calcium and 5 mM phosphate ion concentrations, which are in the interval of salivary physiologic concentration, were found suitable to obtain a standard curve of calcium phosphate precipitation. To examine the effect of plant aqueous extracts, this standard curve was used for comparison in the present study.

In their study, Hidaka & Oishi (2007), examined the effect of nutritional components on dental calculus formation, and used both calcium and phosphate ion final concentrations of 3 mM,

**Table 1. The effects of plant aqueous extracts on the nucleation and aggregation phases of calcium phosphate precipitation.**

	Standard (Calsium phosphathe without extracts)	<i>Petroselinum crispum</i>	<i>Eruca vesicaria ssp. sativa</i>	<i>Beta vulgaris var. cicla</i>	<i>Rumex cristatus</i>	<i>Cotinus coggygria</i>
Nucleation rate ( $R_N$ ) ( $\times 10^{-3}/\text{min}$ )	1.66±0.69	1.42±0.29	1.04±0.11	1.36±0.61	1,10±0,71	3,14±0,89 <sup>***b</sup>
Aggregation rate (RA) ( $\times 10^{-3}/\text{min}$ )	2.68±0.35	3.36±0.38 <sup>a</sup>	3.90±0.83 <sup>a</sup>	0.72±0,25 <sup>**b</sup>	3,92±0,29 <sup>**b</sup>	5,46±1,34 <sup>***#b</sup>
Nucleation time ( $t_N$ ) (min)	12.80±1.78	40.0±4.24 <sup>**b</sup>	60.0±3.16 <sup>**#b</sup>	17,20±3,03 <sup>a</sup>	37,6±0,89 <sup>**b</sup>	12,40±1,67
Aggregation time ( $t_A$ ) (min)	21.20±2.04	22.40±3.20	20.40±2.94	25,60±3,44	14,4±0,80 <sup>**b</sup>	17,60±1,49 <sup>a</sup>

Values were given as mean ± standard deviation; \*p<0.05, \*\*p<0.01: Significantly different from standard; \*\*p<0.01: Significantly different from *Petroselinum crispum*, *Eruca vesicaria ssp. sativa*, *Beta vulgaris L. var.cicla*, *Rumex crispus*; <sup>#</sup>p<0.01: Significantly different from *Petroselinum crispum*, *Beta vulgaris L. var.cicla*, *Rumex crispus*; *Cotinus coggygria* <sup>a</sup>Student t test, <sup>b</sup>Mann Whitney U test

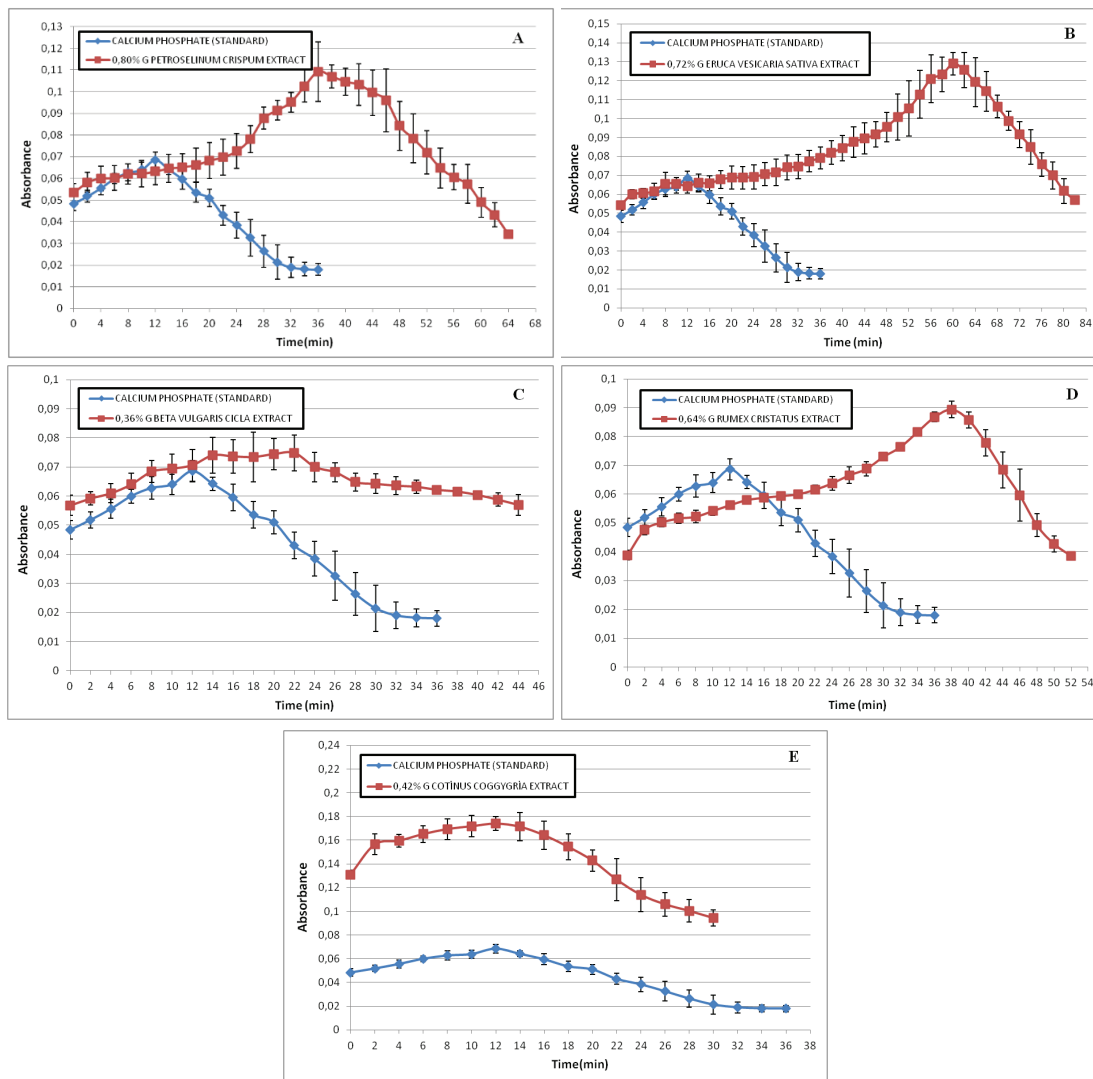


**Figure 2.** The effect of (A) *Petroselinum crispum*, (B) *Eruca vesicaria ssp. sativa*, (C) *Beta vulgaris L. var.cicla*, (D) *Rumex crispus*, (E) *Cotinus coggyria*, aqueous extracts on calcium phosphate precipitation.

unlike our study. However, the concentrations they used did not fully reflect saliva conditions.

Plant extracts have an important place in modern medicine due to their chemical and medicinal ingredients. As their metabolites have a wide range of biological activities, the use of plants has also become widespread in dental and oral health (Sener & Kilic, 2019; Chandra Shekar et al., 2015; Gulfranz et al., 2011). It has been suggested that some plant extracts can be effective in the formation of calculus in different rates because of their phenolic components such as flavonoids, tannins, and coumarins (Ohtani & Nishimura 2020; Ben Lagha, Dudonné, Desjardins, & Grenier, 2015; Weber, Hannig, Pötschke, Höhne, & Hannig, 2015; Ferrazzano et al., 2011). In studies conducted with high polyphenol content, plants have an inhibitory effect on calcium phosphate precipitation. Hidaka, Okamoto, Ishiyama, & Hashimoto (2008) reported that propolis and honey varieties known to contain flavonoids have an inhibitory effect on calcium phosphate precipitation, and that their inhibitory effects increase with increasing flavonoid content. Similar results were obtained in studies with

green tea, *R. rhizoma* plant, and various Kampo plants with high polyphenol content (Torki et al., 2018; Anushya & Freeda, 2017; Hidaka et al., 1996). In the present study, *Petroselinum crispum*, *Eruca vesicaria ssp. sativa*, *Beta vulgaris var.cicla* and *Rumex crispus* were shown to inhibit calcium phosphate precipitation.

However, the *Cotinus coggyria* aqueous extract showed an activator effect on calcium phosphate precipitation. It has been reported that *Cotinus coggyria* with a high flavonoid content has cytotoxic effects on bacteria, and shows inhibitory properties against the common components of dental plaque such as *S. mutans* and *S. sanguinis* (Ferrazzano et al., 2013; Wang et al., 2016). The contrasting effect of *Cotinus coggyria*, rich in polyphenols and expected to prevent calcium phosphate precipitation, may have arisen from its antibacterial effects and dye components.

Moreover, polyphenols in plants have been reported to inhibit the glucosyl transferase activity of *Streptococcus mutans* (Velo et al., 2016; Guven & Erkan, 2015; Smullen, Finney, Storey, & Foster, 2012). For this reason, polyphenols are considered as

important substances for oral hygiene in terms of dental caries and dental calculus formations (Dash, Singh, Gupta, Panwar, & Ramisetty, 2014). Its mechanisms of action is based on their affinity for proteins. When approached from this perspective, they bind to amylase and glycosyl transferase enzymes and they inactivate those enzymes.

## CONCLUSION

The results of our study showed that *Petroselinum crispum*, *Rumex cristatus*, *Beta vulgaris* var. *cicla*, and *Eruca sativa* aqueous extracts can be effective at the beginning on the calcium phosphate precipitation which may reflect on dental calculus formation. In the limitations of our study, any effect of *Cotinus coggygria* was found on precipitation. Nevertheless, more study needs to be done. Our study is the first attempt to apply the plant aqueous extracts to the area of oral health, such as their potential effects on calcium phosphate precipitation at the beginning of dental calculus formation. Furthermore our study also highlights that more plants can be examined in this way.

In our study, we examined the effects of plant extracts separately. Our aim was to determine the impact of each separately. Further studies may be done to see what kind of result can be obtained by mixing two or more of the plant extracts having synergic effects. This may be especially important in the process of producing more effective products to prevent dental calculus precipitation.

**Ethics Committee Approval:** Not necessary for this study.

**Informed Consent:** Written consent was obtained from the participants.

**Peer-review:** Externally peer-reviewed.

**Author Contributions:** Conception/Design of Study: A.Y., S.A.; Data Acquisition: B.S.Ç., A.Y.; Data Analysis/Interpretation: A.Y., B.S.Ç., S.A., Ö.S., R.Y.; Drafting Manuscript: B.S.Ç., A.Y.; Critical Revision of Manuscript: S.A., Ö.S., R.Y.; Final Approval and Accountability: A.Y., B.S.Ç., S.A., Ö.S., R.Y.

**Conflict of Interest:** The authors have no conflict of interest to declare.

**Financial Disclosure:** This study was supported by Marmara University Scientific Research and Project Commission (Project No: SAG-C-YLP-120619-0219).

## REFERENCES

- Ajmera, P., Kalani, S., & Sharma, L. (2019). Parsley-benefits and side effects on health. *International Journal of Physiology, Nutrition and Physical Education* 4(1), 1236–1242. <http://www.journalofsports.com/pdf/2019/vol4issue1/PartAA/4-1-308-629.pdf>
- Akar, C. (2014). Türkiye’de ağız-diş sağlığı hizmetlerinin strateji değerlendirilmesi. *Türk Diş Hekimleri Birliği Yayınları Araştırma Dizisi*, 9(11), 1–12. <https://dergipark.org.tr/tr/download/article-file/620472>
- Akcalı, A., & Lang, N. P. (2018). Dental calculus: the calcified biofilm and its role in disease development. *Periodontology* 2000, 76(1), 109–115. <https://doi.org/10.1111/prd.12151>
- Anushya, G., & Freeda, T. H. (2017). Effect of green tea on the growth of brushite crystals. *International Journal of Latest Trends in Engineering and Technology*, (Special issue), 139–143.
- Batool, H., Nadeem, A., Kashif, M., Shahzad, F., Tahir, R., & Afzal, N. (2018). Salivary levels of IL-6 and IL-17 could be an indicator of disease severity in patients with calculus associated chronic periodontitis. *BioMed Research International*, 8531961. <https://doi.org/10.1155/2018/8531961>
- Ben Lagha, A., Dudonné, S., Desjardins, Y., & Grenier, D. (2015). Wild blueberry (*Vaccinium angustifolium* Ait.) polyphenols target fusobacterium nucleatum and the host inflammatory response: Potential innovative molecules for treating periodontal diseases. *Journal of Agricultural Food Chemistry*, 63(31), 6999–7008. doi:10.1021/acs.jafc.5b01525
- Bolkent, S., Yanardağ, R., Tabakoğlu-Oğuz, A., & Ozsoy-Saçan, O. (2000). Effects of chard (*Beta vulgaris* L. var. *cicla*) extract on pancreatic B cells in streptozotocin-diabetic rats: a morphological and biochemical study. *Journal of Ethnopharmacology*, 73(1-2), 251–259. [https://doi.org/10.1016/s0378-8741\(00\)00328-7](https://doi.org/10.1016/s0378-8741(00)00328-7)
- Chandra Shekar, B. R., Nagarajappa, R., Suma, S., & Thakur, R. (2015). Herbal extracts in oral health care - A review of the current scenario and its future needs. *Pharmacognosy Reviews*, 9(18), 87–92. <https://doi.org/10.4103/0973-7847.162101>
- Clarke, M. R. (2015). Dental calculus: Combining current methods in the study of diet and mouth use activities among neolithic and early bronze age hunter-gatherers of the Cis-Baikal, Siberia. University of Saskatchewan. Department of Archaeology and Anthropology, Thesis Submitted to the College of Graduate Studies and Research, Saskatoon.
- Coruh, I., Gormez, A., Ercisli, S., & Sengul, M. (2008). Total phenolic content, antioxidant and antibacterial activity of *Rumex crispus* grown wild in Turkey. *Pharmaceutical Biology*, 46, 634–638. <https://doi.org/10.1080/13880200802182240>
- Dash, T. R., Singh, N., Gupta, D., Panwar, E., & Ramisetty, S. (2014). Role of medicinal herbs in oral health management. *International Journal of Dental and Medical Research*, 1(2), 113–119. <http://www.ijohmr.com/upload/20.pdf>
- Demir, S., Bozkurt, B., Onur, M. A., Kay, I. G., & Somer, N. U. (2017). Determination of antioxidant properties of *Rumex crispus* and *Scrophularia canina* subsp. *bicolor*. *International Journal of Secondary Metabolite*, 4(3), 55–57. doi.org/10.21448/ijsm.356275
- Ferrazzano, G. F., Amato, I., Ingenito, A., Zarelli, A., Pinto, G., & Pollio, A. (2011). Plant polyphenols and their anti-cariogenic properties: A review. *Molecules*, 16, 1486–1507. doi:10.3390/molecules16021486
- Ferrazzano, G. F., Roberto, L., Catania, M. R., Chiaviello, A., De Natale, A., Roscetto, E., Pinto, G., Pollio, A., Ingenito, A., & Palumbo, G. (2013). Screening and scoring of antimicrobial and biological activities of Italian vulnerary plants against major oral pathogenic bacteria. *Evidence-Based Complementary and Alternative Medicine: eCAM*, 2013, 316280. <https://doi.org/10.1155/2013/316280>
- Gulfraz, M., Sadiq, A., Tariq, H., Imran, M., & Qureshi, R. (2011). Phytochemical analysis and antibacterial activity of *Eruca sativa* seed. *Pakistan Journal of Botany*. 43(2), 1351–1359. <http://www.pakbs.org/pjbot/PDFs>
- Guven, A., & Erkan, E. (2015). Fare karaciğer dokusunda yeşil çay (*Camellia sinensis* L.) ve maydanozun (*Petroselinum crispum*) MDA ve GSH düzeyleri üzerine etkilerinin araştırılması. *Caucasian Journal of Science*, 6, 65–72. <https://dergipark.org.tr/tr/pub/cjo/issue/33907/382470>
- Hazim, J., Al-Daraji, H. A., Al-Mashadani A. S., Al-Hassani, H. A., & Mirza, W. K. (2012). The influence of parsley (*Petroselinum crispum*) as feed additive on hematological traits of local Iraqi Geese. *Advances in Nutritional Research*, 1(1), 1–5. <https://www.iasj.net/iasj?func=fulltext&ald=120570>
- Hidaka, S., Nishimura, H., Nakajima, K., & Liu, S. Y. (1996). Effects of a rhubarb (*Rhei rhizoma*) solution and its fractions on the formation of calcium phosphate precipitates. *Journal of Periodontal Research*, 31(6), 408–413. <https://doi.org/10.1111/j.1600-0765.1996.tb00509.x>



- Hidaka, S., & Oishi, A. (2007). An *in vitro* study of the effect of some dietary components on calculus formation: regulation of calcium phosphate precipitation. *Oral Diseases*, 13(3), 296–302. <https://doi.org/10.1111/j.1601-0825.2006.01283.x>
- Hidaka, S., Okamoto, Y., Ishiyama, K., & Hashimoto, K. (2008). Inhibition of the formation of oral calcium phosphate precipitates: the possible effects of certain honeybee products. *Journal of Periodontal Research*, 43(4), 450–458. <https://doi.org/10.1111/j.1600-0765.2008.01088.x>
- Idris, O. A., Wintola, O. A., & Afolayan, A. J. (2019). Evaluation of the bioactivities of *Rumex crispus* L. leaves and root extracts using toxicity, antimicrobial, and antiparasitic assays. *Evidence-Based Complementary and Alternative Medicine: eCAM*, 2019, 6825297. <https://doi.org/10.1155/2019/6825297>
- Jin, Y., & Yip, H. K. (2002). Supragingival calculus: formation and control. *Critical Reviews in Oral Biology and Medicine: an official publication of the American Association of Oral Biologists*, 13(5), 426–441. <https://doi.org/10.1177/154411130201300506>
- Matić, S., Stanić, S., Mihailović, M., & Bogojević, D. (2016). *Cotinus coggygria* Scop.: An overview of its chemical constituents, pharmacological and toxicological potential. *Saudi Journal of Biological Sciences*, 23(4), 452–461. <https://doi.org/10.1016/j.sjbs.2015.05.012>
- Moolya, N. N., Thakur, S., Ravindra, S., Setty, S. B., Kulkarni, R., & Hallikeri, K. (2010). Viability of bacteria in dental calculus - A microbiological study. *Journal of Indian Society of Periodontology*, 14(4), 222–226. <https://doi.org/10.4103/0972-124X.76921>
- Morta, S., Mante, K., Rasa, B., & Gintaras, J. (2018). The influence of salivary pH and calcium/phosphate ions concentration on salivary gland stones' formation. *Journal of International Medicine and Dentistry*, 5(1), 30–38. <https://www.lsmuni.lt/cris/handle/20.500.12512/20296>
- Mzoughi, Z., Chahdoura, H., Chakroun, Y., Cámara, M., Fernández-Ruiz, V., Morales, P., Mosbah, H., Flamini, G., Snoussi, M., & Majdoub, H. (2019). Wild edible Swiss chard leaves (*Beta vulgaris* L. var. *cicla*): Nutritional, phytochemical composition and biological activities. *Food Research International (Ottawa, Ont.)*, 119, 612–621. <https://doi.org/10.1016/j.foodres.2018.10.039>
- Ohtani, M., & Nishimura, T. (2020). The preventive and therapeutic application of garlic and other plant ingredients in the treatment of periodontal diseases. *Experimental and Therapeutic Medicine*, 19(2), 1507–1510. <https://doi.org/10.3892/etm.2019.8382>
- Pápay, Z. E., Kállai-Szabó, N., Ludányi, K., Klebovich, I., & Antal, I. (2016). Development of oral site-specific pellets containing flavonoid extract with antioxidant activity. *European Journal of Pharmaceutical Sciences*, 95, 161–169. <https://doi.org/10.1016/j.ejps.2016.10.029>
- Sacan, O., Orak, H., & Yanardag, R. (2008). Antioxidant activity of water extract of *Eruca sativa* Mill. *Asian Journal of Chemistry*, 20, 3462–3474. <https://www.researchgate.net/publication/286940034>
- Sacan, O., & Yanardag, R. (2010). Antioxidant and anticholinesterase activities of chard (*Beta vulgaris* L. var. *cicla*). *Food and Chemical Toxicology*, 48(5), 1275–1280. <https://doi.org/10.1016/j.fct.2010.02.022>
- Sarwar Alam, M., Kaur, G., Jabbar, Z., Javed, K., & Athar, M. (2007). *Eruca sativa* seeds possess antioxidant activity and exert a protective effect on mercuric chloride induced renal toxicity. *Food and Chemical Toxicology*, 45(6), 910–920. <https://doi.org/10.1016/j.fct.2006.11.013>
- Selmi Cepis, B., Akyuz, S., & Yarat, A. (2020). Evaluation of the effect of coffee and carbonated beverages on calcium phosphate precipitation, in the point of formation of calculus. Proceeding 3rd International Eurasian Conference on Biological and Chemical Sciences (EurasianBioChem 2020), (pp. 567–573). Ankara: Turkey [www.EurasianBioChem.org](http://www.EurasianBioChem.org). Book.
- Sener, B., & Kilic, M. (2019). Herbal extracts used in dental disorders. *Biomedical Journal of Scientific and Thecnical Research*, 19(1) [https://www.researchgate.net/publication/334397321\\_Herbal\\_Extracts\\_Used\\_in\\_Dental\\_Disorders](https://www.researchgate.net/publication/334397321_Herbal_Extracts_Used_in_Dental_Disorders)
- Smullen, J., Finney, M., Storey, D. M., & Foster, H. A. (2012). Prevention of artificial dental plaque formation *in vitro* by plant extracts. *Journal of Applied Microbiology*, 113(4), 964–973. <https://doi.org/10.1111/j.1365-2672.2012.05380.x>
- Tarasevich, B. J., Chusuei, C. C., & Alloro, D. L. (2003). Nucleation and growth of calcium phosphate from physiological solutions onto self-assembled templates by a solution formed nucleus mechanism. *The Journal of Physical Chemistry B*, 107 (38), 10367–10377. <https://doi.org/10.1021/jp027445p>
- Taviano, M. F., Melchini, A., Filocamo, A., Costa, C., Catania, S., Raciti, R., Saha, S., Needs, P., Bisignano, G. G., & Miceli, N. (2017). Contribution of the glucosinolate fraction to the overall antioxidant potential, cytoprotection against oxidative insult and antimicrobial activity of *Eruca sativa* Mill. leaves extract. *Pharmacognosy Magazine*, 13(52), 738–743. [https://doi.org/10.4103/pm.pm\\_245\\_16](https://doi.org/10.4103/pm.pm_245_16)
- Taviano, M. F., Filocamo, A., Ragusac, S., Cacciola, F., Dugo, P., Mondello, L., Paterniti Mastrazza, G., De Rosec, R. F., Celano, M., Lombardo, G. E., Melchinie, A., & Miceli, N. (2018). Phenolic profile, antioxidant and cytotoxic properties of polar extracts from leaves and flowers of *Isatis tinctoria* L. (*Brassicaceae*) growing in Sicily. *Plant Biosystems*, 152, 795–803. <https://doi.org/10.1080/11263504.2017.1338629>
- Torki, A., Hosseinabadi, T., Fasihzadeh, S., Sadeghimanesh, A., Wibowo, J. P., & Lorigooini, Z. (2018). Solubility of calcium oxalate and calcium phosphate crystallization in the presence of crude extract and fractions from *Kelussia odoratissima* Mozaff. *Pharmacognosy Research*, 10(4), 379–384.
- Tunali, T., Yarat, A., Yanardağ, R., Özçelik, F., Özsoy, O., Ergenekon, G., & Emekli, N. (1999). Effect of parsley (*Petroselinum crispum*) on the skin of STZ induced diabetic rats. *Phytotherapy Research: PTR*, 13(2), 138–141. [https://doi.org/10.1002/\(SICI\)1099-1573\(199903\)13:2<138::AID-PTR390>3.0.CO;2-X](https://doi.org/10.1002/(SICI)1099-1573(199903)13:2<138::AID-PTR390>3.0.CO;2-X)
- Tunali, S., Cimen, E. S., & Yanardag, R. (2020). The effects of chard on brain damage in valproic acid induced toxicity. *Journal of Food Biochemistry*, 44(10), XX–XX <https://doi.org/10.1111/jfbc.13382>
- Veloz, J. J., Saavedra, N., Alvear, M., Zambrano, T., Barrientos, L., & Salazar, L. A. (2016). Polyphenol-rich extract from propolis reduces the expression and activity of *Streptococcus mutans* glucosyltransferases at subinhibitory concentrations. *BioMed Research International*, 4302706. <https://doi.org/10.1155/2016/4302706>
- Wang, G., Wang, J. J., Du, L., Fei, L., & To, S. T. (2016). Inhibitory kinetics and mechanism of flavonoids extracted from *Cotinus coggygria* Scop. against glioblastoma cancer. *Nutrition and Cancer*, 68(8), 1357–1368. <https://doi.org/10.1080/01635581.2016.1225105>
- Weber, M. T., Hannig, M., Pötschke, S., Höhne, F., & Hannig, C. (2015). Application of plant extracts for the prevention of dental erosion: An *in situ/in vitro* study. *Caries Research*, 49(5), 477–487. <https://doi.org/10.1159/000431294>
- White D. J. (1997). Dental calculus: recent insights into occurrence, formation, prevention, removal and oral health effects of supragingival and subgingival deposits. *European Journal of Oral Sciences*, 105, 508–522. <https://doi.org/10.1111/j.1600-0722.1997.tb00238.x>

# Tyrosinase and cholinesterase inhibitory activities and molecular docking studies on apigenin and vitexin

Esen Sezen Karaoğlan<sup>1</sup> , Mehmet Koca<sup>2</sup> 

<sup>1</sup>Ataturk University, Faculty of Pharmacy, Department of Pharmaceutical Botany, Erzurum, Turkey

<sup>2</sup>Ataturk University, Faculty of Pharmacy, Department of Pharmaceutical Chemistry, Erzurum, Turkey

**ORCID IDs of the authors:** E.S.K. 0000-0002-9098-9021; M.K. 0000-0002-1517-5925

**Cite this article as:** Karaoğlan, E. S., & Koca, M. (2020). Tyrosinase and cholinesterase inhibitory activities and molecular docking studies on apigenin and vitexin. *Istanbul Journal of Pharmacy*, 50 (3), 268-271.

## ABSTRACT

**Background and Aims:** Apigenin and vitexin are two phytochemical compounds in flavone structure. In this study, tyrosinase and cholinesterase inhibitory effects of apigenin and vitexin were tested. Then, molecular docking studies were conducted on these molecules.

**Methods:** Cholinesterase inhibition was evaluated by minor modifications of Ellman's method and tyrosinase inhibition was evaluated by minor modifications of Masuda's method. Docking simulations were performed using the Schrödinger software suite.

**Results:** When apigenin and vitexin were compared, apigenin showed higher inhibitory effect against butyrylcholinesterase ( $54 \pm 1.7\%$ ) and tyrosinase ( $49.36 \pm 0.24\%$ ), vitexin showed a higher inhibitory effect against acetylcholinesterase ( $66 \pm 1.6\%$ ).

**Conclusion:** When molecular interactions between tested compounds and inhibited enzymes were examined, it was observed that there were interactions especially between enzyme structures and benzopyran rings of these compounds and hydroxyl groups bound to these rings.

**Keywords:** Apigenin, vitexin, enzyme inhibitory activity, molecular simulation

## INTRODUCTION

Tyrosinase (TYR) is a copper-containing enzyme that plays a role in melanin formation, especially in microorganisms, animals, and plants. TYR accumulates in the skin and causes hyperpigmentation diseases in mammals. It also creates undesirable browning in fruits and vegetables. In recent years, compounds that inhibit TYR from both natural and synthetic sources are being investigated (Erdogan Orhan, 2014; Seo, Sharma, & Sharma, 2003). The previous studies have shown that phenolic compounds and their derivatives and several compounds, including terpenoid, phenyl, pyridine, piperidine, pyridinone, hydroxypyridinone, thiosemicarbazone, thiosemicarbazide,azole, thiazolidine, kojic acid, benzaldehyde and xanthate derivatives, have tyrosinase inhibitory effects. Tyrosinase inhibitors are very important in the food, cosmetics, and medicinal industries (Zolghadri et al., 2019). Therefore, tyrosinase inhibitors have become extremely important in the past few decades (Chang, 2009).

Alzheimer's is a common age-related neurodegenerative disease. It is a disease that develops due to deficiency in the cholinergic systems and is characterized by the accumulation of beta amyloid (A $\beta$ ) as neurofibrillary tangles and amyloid plaques. The cholinergic system is very important in the steps of learning and memory. Acetylcholinesterase (AChE) and butyrylcholinesterase (BuChE) are enzymes that catalyze the hydrolysis of acetylcholine. Both enzymes play an important role in A $\beta$ -aggregation. Cholinesterase (ChE) inhibitors are recently one of the most preferred treatment strategies for Alzheimer's disease. ChE inhibitors are also used to increase muscle strength in patients with *Myasthenia gravis* (Komloova et al., 2011). ChE inhibitors such as

### Address for Correspondence:

Esen Sezen KARAOĞLAN, e-mail: esen.karaoglan@atauni.edu.tr

This work is licensed under a Creative Commons Attribution 4.0 International License.



Submitted: 16.01.2020  
Revision Requested: 31.03.2020  
Last Revision Received: 02.06.2020  
Accepted: 29.06.2020  
Published Online: 13.11.2020

donepezil and rivastigmin are used in symptomatic treatment. The drugs have various side effects and drug interactions. The development of novel ChE inhibitors with optimal efficacy and tolerability is important (Anand & Sigh, 2013; Grutzendler & Morris, 2001; Nordberg & Svensson, 1998).

Molecular docking is a valuable method in molecular structure and drug design. The aim of ligand-protein docking is to prognosticate the prepotent binding mode(s) of a ligand with a protein of well-known three-dimensional structure. Accomplished docking methods investigate high-dimensional areas effectively and utilize a scoring function that correctly ranks nominee dockings (Morris & Lim-Wilby, 2008). Molecular docking has become an progressively important vehicle for drug discovery (Meng et al., 2011).

Apigenin is a medically used compound known to have low toxicity. Vitexin is a C-glycosylated derivative of apigenin and is known to have potent anti-diabetic, anti-Alzheimer's disease, and anti-inflammatory activities (Choi et al., 2014).

In this study, AChE, BuChE, and TYR inhibitory effects of apigenin and vitexin were comparatively investigated. In addition, molecular docking studies have been conducted on effective molecules.

## MATERIALS AND METHODS

### Test materials

Apigenin was isolated from *Alyssum murale* Waldst. & Kit. and vitexin was purchased from Sigma-Aldrich.

### Tyrosinase inhibitory activity

Mushroom tyrosinase inhibition activity was determined as described by Masuda's colorimetric method with some modification (Masuda Yamashita, Takeda, & Yonemori 2005). 3,4-Dihydroxyl- L-phenylalanin (L-DOPA) was used as a substrate while kojic acid (KA) was used as positive control. 40 µl sample solution was mixed with 40 µl TYR solution (46 U/ml) and 80 µl phosphate buffer (pH=6.8) in a 96 well microplate and incubated for 10 min at 23°C and 40 µl of L-DOPA (2.5 mM) were put into each well. After incubation at 23 °C for 10 minutes, the absorbance values at 490 nm for each well was measured by a microplate reader (Bio Tek ELx800). All test materials were tested at different concentrations (25, 50, 100, 200 µl/ml). Experiments were performed in 3 replicates. The percentage of TYR inhibition (%) was calculated as follows:  $\% = [(A-B)-(C-D)/A-B] \times 100$ , where A is the absorbance of the control (buffer and TYR), B is the absorbance of the blank (buffer), C is the absorbance of the reaction mixture (buffer, TYR and sample), and D is the absorbance of the blank of C (buffer and sample).

### Cholinesterase inhibitory activity

Cholinesterase (ChE) inhibition activities of the compounds were evaluated by slight modification of the cholometric Ellman method (Elmann et al., 1961). Donepezil hydrochloride (DH) was used as the reference compound. In conducting the experiment, the reference compound and test compounds were dissolved in dimethyl sulfoxide (DMSO) and diluted with Tris buffer solution (50 µM, pH 8.0) to different concentrations (25, 50, 100, 200 µl/ml). 125 µl of 3 mM 5,5-dithiobis-(2-nitrobenzoic acid) (DTNB) and 25 µl (0.2 U/ml) of enzyme (AChE or

BuChE) were added and incubated at 37°C for 15 minutes. Followed by the addition of the corresponding substrate (acetylthiocholine iodide (ATCI) or butyrylthiocholine iodide (BTCI)), the absorbance of the reaction mixture was measured three times at wavelength of 412 nm every 45 s using a microplate reader (Bio-Tek ELx800, Winooski, VT). The percentage inhibitions (%) were calculated. Results were enounced as mean ± SD, and all experiments were enforced in triplicate.

### In-silico molecular docking and simulation studies

Docking simulations were performed using the Schrödinger software suite (Maestro 11.8) The crystal structures of enzymes (PDB ID for AChE: 1-EVE; PDB ID for BuChE: 1P0I; PDB ID TYR: 2Y9X) were downloaded from the RSCB PDB. Related ligands were used for grid box generation for docking (In 1EVE: binding position of donepezil, centers of grid box: X = 2.8, Y = 64.5, Z = 67.9; In 1P0I: binding position of butanoic acid, centers of grid box: X = 139.4, Y = 113, Z = 41.71; In 2Y9X: binding site of tropolone, centers of grid box: X = -9.9, Y = -28.8, Z = -43.64 ). The enzyme structures were formulated by the PROPKA software, in which water molecules present were eliminated from the structure part, hydrogen atoms were added to the PDB structures, and pH was set at 7. Eventually, restrained minimization was applied with optimized potentials for liquid simulations (OPLS3e) force field.

The structures of the ligands (vitexin and apigenin) were constructed using the MacroModel module in Schrödinger software suite (Maestro 11.8). Later, the structures of the compounds were minimized via Ploak-Ribiere conjugates gradient (PRCG) minimization method. All compounds were docked to the target enzymes by Glide/XP docking protocols. Glide score was utilized as higher criteria for the best-docked ligands.

## RESULTS AND DISCUSSION

### Enzyme inhibitory, in-silico molecular docking and simulation studies

In this study, AChE, BuChE, and TYR inhibitory activities of different concentrations of apigenin and vitexin were tested. % Inhibition effects of vitexin, apigenin, and positive controls against AChE, BuChE, and TYR at 100 µg/ml concentration are shown in Table 1. As a result of the experiments, the molecular interactions of molecules with effective percent inhibition with the relevant enzyme were investigated.

**Table 1. Percentage inhibitory effects of apigenin and vitexin.**

Test material (100 µg/ml)	Acetylcholinesterase Inhibition %	Butyrylcholinesterase Inhibition %	Tyrosinase Inhibition %
Apigenin	2±0.4	54±1.7	49.36±0.24
Vitexin	66±1.6	41±2.5	23.85±0.22
KA	-	-	93.62±1.4
DH	100±2	100±3	-

KA: Kojic acid (Positive control), DH: Donepezil hydrochloride (Positive control), n=3

According to the results, the molecular interaction of vitexin with AChE was investigated. In addition, the interactions of apigenin with both BuChE and TYR were examined. The molecular interactions of vitexin with AChE, apigenin with BuChE and TYR are shown in Figure 1,2,3, respectively.

Docking score of vitexin was determined as kcal/mol -4.98 for AChE (1-EVE). In AChE and vitexin complex, two hydrogen bonds were formed. One of the hydrogen bonds was between phenolic hydroxyl group (HO-Ph) of the molecule and carbonyl group (C=O) of SER286 (1.82 Å<sup>0</sup>). The other hydrogen bond was between hydroxyl (HO-CH<sub>2</sub>) group of the molecule and carbonyl group (C=O) of ASP276 (1.82 Å<sup>0</sup>). Hydrophobic interaction occurred with residues of ILE287, PHE288, PHE290, LEU282, TRP279, TYR70, VAL277, ILE275. The polar interactions were realized by ASN280, SER296. In addition negative load interaction was observed between ASP276 residue and vitexin.

Docking score of apigenin was determined as kcal/mol -5.91 for BuChE (1-P0I). In BuChE and apigenin complex, two hydrogen bonds were formed. One of the hydrogen bonds was between phenolic hydroxyl group of the molecule and carbonyl group of SER198 (1.83 Å<sup>0</sup>). The other hydrogen bond was between hydroxyl (7-OH) of benzopyran ring in molecule and carbonyl group (C=O) of ASP70 (1.5 Å<sup>0</sup>).  $\pi$ - $\pi$  stacking interaction was observed between benzopyran benzene ring and phenyl group of TYR332 (4.96 Å<sup>0</sup>). Hydrophobic interaction occurred with residues of ALA199, TRP231, PRO285, LEU286, VAL288, PHE329, TYR332, PHE398. The polar interactions were realized by SER198, SER287. In addition negative load interaction was detected between ASP70 residue and apigenin.

Docking score of apigenin was determined as kcal/mol -5.7 for TYR (PDB ID: 2Y9X). In TYR and apigenin complex, a hydrogen bond was formed between hydroxyl (7-OH) of benzopyran ring in molecule and carbonyl group (C=O) of MET280 (1.85 Å<sup>0</sup>).  $\pi$ - $\pi$  stacking interactions were observed between benzene ring of benzopyran and the phenyl ring of HIS263 (4.0 Å<sup>0</sup>) and HIS259 (5.37 Å<sup>0</sup>), respectively. Hydrophobic interaction occurred with residues of VAL248, PHE264, MET280, VAL283, ALA286, PHE292. The polar interactions were realized by HIS61, HID85, SER282, HIS263, ASN260, HIS259. In addition negative load interaction was detected between GLU256

residue and apigenin. The docking study results are summarized in Table 2.

According to our results, it was observed that there was a tendency in terms of  $\pi$ - $\pi$  interaction between electronic rich benzopyran rings of tested compounds and enzyme structures. In addition, it was determined that -OH groups bound to benzopyran ring tend to form hydrogen bonds with enzymes.

Apigenin identified as 4',5,7-trihydroxyflavone is present in a various medicinal plants, in which it is responsible for various biological activities (Zhou, Wang, Zhou, Song, & Xie, et al., 2017). Katalinic et al. defined the BuChE inhibitory activities of some flavonoids such as galangin, kaempferol, quercetin, myricetin, fisetin, apigenin, luteolin and rutin. They predicated the inhibition potentials of flavonoids to their chemical structures, the number of OH groups, and their side on the phenyl ring (Katalinic et al., 2010). In addition, Ye et al indicated that apigenin has a potent melanogenic activity in B16 cells (Ye et al., 2010). Flavonoids have been reported to have promising tyrosinase inhibitory effects (Erdogan Orhan, 2014). In this context, the BuChE and TYR effects of apigenin observed in our results have been found compatible with these literature findings. Vitexin is a flavone glycoside of apigenin with various pharmacological activities, which is contained in some medicinal plants (He et al., 2016; Jung, Karki, Kim, & Choi 2015; Sheeja Malar, Shafreen, Karutha Pandian, & Devi, 2017; Spandana, Bhaskaran, Karri & Natarajan 2020). It is thought that vitexin is very important for neurodegenerative diseases (Lima et al., 2018). In our study, the AChE inhibition effect of vitexin has been consistent with literatures. However, although *in vivo* studies have demonstrated that flavonoids are beneficial for brain health, informations about their transport from the blood brain barrier and brain bioavailability are inadequate and inconsistent (Faria, Mateus & Calhau, 2012). In central nervous system diseases, it is important that drug molecules cross the blood brain barrier. Transmembrane diffusion and membrane transporter systems are important mechanisms in crossing the blood brain barrier (Banks, 2009). Although the mechanisms of action of flavonoids in the human brain are not fully explained, it is possible that they are precursors to the development of the new generation of molecules (Dajas et al. 2003).

**Table 2. The interactions of ligands with enzymes.**

Ligand-Enzyme	Enzyme Residues	Ligand Interaction Site	Distance (Å <sup>0</sup> )	Interaction	RMSD (Å <sup>0</sup> )
Vitexin-1EVE	SER286 (C=O)	Ph-OH	1.82	H-bond	0.8
Vitexin-1EVE	ASP276 (C=O)	CH <sub>2</sub> OH	1.82	H-bond	0.8
Apigenin-1P0I	SER198 (C=O)	Ph-OH	1.83	H-bond	0.6
Apigenin-1P0I	ASP70 (C=O)	7-OH of benzopyran	1.50	H-bond	0.6
Apigenin-1P0I	TYR332 (Ph)	benzene of benzopyran	4.96	$\pi$ - $\pi$ stacking	0.6
Apigenin-2Y9X	MET280 (C=O)	7-OH of benzopyran	1.85	H-bond	0.6
Apigenin-2Y9X	HIS263 (Ph)	benzene of benzopyran	4.00	$\pi$ - $\pi$ stacking	0.6
Apigenin-2Y9X	HIS259 (Ph)	benzene of benzopyran	5.37	$\pi$ - $\pi$ stacking	0.6

## CONCLUSION

As a conclusion, it was observed that electronic rich benzopyran ring tends to interfere with  $\pi$ - $\pi$  interaction with enzyme structures and -OH groups bound to benzopyran ring have potential to form hydrogen bonds with enzyme.

**Peer-review:** Externally peer-reviewed.

**Author Contributions:** Conception/Design of Study- E.S.K.; Data Acquisition-E.S.K., M.K.; Data Analysis/Interpretation- E.S.K., M.K.; Drafting Manuscript- E.S.K., M.K.; Critical Revision of Manuscript- E.S.K., M.K.; Final Approval and Accountability- E.S.K., M.K.; Technical or Material Support- E.S.K., M.K.; Supervision- E.S.K., M.K.

**Conflict of Interest:** The authors have no conflict of interest to declare.



**Financial Disclosure:** Authors declared no financial support.

## REFERENCES

- Anand, P., & Singh, B. (2013). Cite as a review on cholinesterase inhibitors for Alzheimer's disease. *Archives of Pharmacol Research*, 36 (4), 375–399.
- Banks, W.A. (2009). Characteristics of compounds that cross the blood-brain barrier. *BMC Neurology*, 9 (1), 1–5.
- Chang, T.S. (2009). An updated review of tyrosinase inhibitors. *International Journal of Molecular Sciences*, 10, 2440–2475.
- Choi, J.S., Islam, M.N., Ali, M.Y., Kim, E.J., Kim, Y.M., & Jung, H.A. (2014). Effects of C-glycosylation on anti-diabetic, anti-Alzheimer's disease and anti-inflammatory potential of apigenin. *Food and Chemical Toxicology*, 64, 27–33.
- Dajas, F., Rivera-Megret, F., Blasina, F., Arredondo, F., Abin-Carriquiry, J.A., Costa, G., Echeverry, C., Lafon, L., Heizen, H., Ferreira, M., & Morquio, A. (2003). Neuroprotection by flavonoids. *Brazilian Journal of Medical and Biological Research*, 36, 1613–1620.
- Ellman, G. L., Courtney, K. D., Andres, V., & Feather-Stone, R. M. (1961). A new and rapid colorimetric determination of acetylcholinesterase activity. *Biochemical Pharmacology*, 7, 88–95.
- Erdogan Orhan, I., Khan, M.T.H. (2014). Flavonoid derivatives as potent tyrosinase inhibitors - a survey of recent findings between 2008-2013. *Current Topics in Medicinal Chemistry*, 14(12), 1486–1493.
- Faria, A., Mateus, N., & Calhau, C. (2012). Flavonoid transport across blood-brain barrier: Implication for their direct neuroprotective actions. *Nutrition and Aging*, 1, 89–97.
- Grutzendler, J., & Morris, J. C. (2001). Cholinesterase inhibitors for Alzheimer's disease. *Drugs*, 61(1), 41–52.
- He, M., Min, J. W., Kong, W. L., He, X. H., Li, J. X., & Peng, B. W. (2016). A review on the pharmacological effects of vitexin and isovitexin. *Fitoterapia*, 115, 74–85.
- Jung, H. A., Karki, S., Kim, J. H., & Choi, J. S. (2015). BACE1 and cholinesterase inhibitory activities of *Nelumbo nucifera* embryos. *Archives of Pharmacol Research*, 38, 1178–1187.
- Katalinic, M., Rusak, G., Barovic, J. D., Sinko, G., Jelic, D., Antolovic, R., & Kovarik, Z. (2010). Structural aspects of flavonoids as inhibitors of human butyrylcholinesterase. *European Journal of Medicinal Chemistry*, 45, 186–192.
- Komloova, M., Musilek, K., Horova, A., Holas, O., Dohnal, V., Gunn-Moore, F., & Kuca, K. (2011). Preparation, in vitro screening and molecular modelling of symmetrical bis-quinolinium cholinesterase inhibitors-implications for early Myasthenia gravis treatment. *Bioorganic & Medicinal Chemistry Letters*, 21 (8), 2505–2509.
- Lima, L. K. F., Pereira, S. K. S., Junior, R. S. S., Santos, F. P. S., Nasciminto, A. S., Feitosa, C. M., Figuerêdo, J. S., Cavalcante, A. N., Araújo, E. C. C., & Rai, M. (2018). A brief review on the neuroprotective mechanisms of vitexin. *BioMed Research International*, 2018, 1–8. <https://doi.org/10.1155/2018/4785089>.
- Masuda, T., Yamashita, D., Takeda, Y., & Yonemori, S. (2005). Screening for tyrosinase inhibitors among extracts of seashore plants and identification of potent inhibitors from *Garcinia subelliptica*. *Bioscience, Biotechnology, and Biochemistry*, 69, 197–201.
- Meng, X.Y., Zhang, H.X., Mezei, M., & Cui, M. (2011). Molecular Docking: A powerful approach for structure-based drug discovery. *Current Computer-Aided Drug Design*, 7(2), 146–157.
- Morris, G. M., & Lim-Wilby, M. (2008). Molecular docking. *Methods in Molecular Biology*, 443, 365–382.
- Nordberg, A., & Svensson, A. L. (1998). Cholinesterase inhibitors in the treatment of Alzheimer's disease A comparison of tolerability and pharmacology. *Drug Safety*, 19(6), 465–480.
- Seo, S.Y., Sharma, V. K., & Sharma, N. (2003). Mushroom tyrosinase: Recent prospects. *Journal of Agricultural and Food Chemistry*, 51, 2837–2853.
- Sheeja Malar, D., Shafreen, R. B., Karutha Pandian, S. T., & Devi, K. P. (2017). Cholinesterase inhibitory, anti-amyloidogenic and neuroprotective effect of the medicinal plant *Grewia tiliaefolia* -An in vitro and in silico study. *Pharmaceutical Biology*, 55(1), 381–393.
- Spandana, K. M. A., Bhaskaran, M., Karri, V. S. N. R., & Natarajan, J. (2020). A comprehensive review of nano drug delivery system in the treatment of CNS disorders. *The Journal of Drug Delivery Science and Technology*. <https://doi.org/10.1016/j.jddst.2020.101628>.
- Ye, Y., Chou, G. X., Wang, H., Chu, J. H., & Yu, Z. L. (2010). Flavonoids, apigenin and icariin exert potent melanogenic activities in murine B16 melanoma cells. *Phytomedicine*, 18, 32–35.
- Zhou, X., Wang, F., Zhou, R., Song, X., & Xie, M. (2017). Apigenin: A current review on its beneficial biological activities. *Journal of Food Biochemistry*, 41, e12376.
- Zolghadri, S., Bahrami, A., Khan, M. T. H., Munoz-Munoz, J., Garcia-Molina, F., Garcia-Canovas, F., & Saboury, A. A. (2019). A comprehensive review on tyrosinase inhibitors. *Journal of Enzyme Inhibition and Medicinal Chemistry*, 34 (1), 279–309.



# Isolation and characterization of antimicrobial compounds from *Cotinus coggygia* Scop. ethyl acetate extract

Ali Şen<sup>1</sup> , Ayşe Seher Birteksöz Tan<sup>2</sup> , Şükran Kültür<sup>3</sup> , Leyla Bitiş<sup>1</sup> 

<sup>1</sup>Marmara University, Faculty of Pharmacy, Department of Pharmacognosy, İstanbul, Turkey

<sup>2</sup>İstanbul University, Faculty of Pharmacy, Department of Pharmaceutical Microbiology, İstanbul, Turkey

<sup>3</sup>İstanbul University, Faculty of Pharmacy, Department of Pharmaceutical Botany, İstanbul, Turkey

**ORCID IDs of the authors:** A.Ş. 0000-0002-2144-5741; A.S.B.T. 0000-0003-2123-1468; Ş.K. 0000-0001-9413-5210; L.B. 0000-0003-1167-6666

**Cite this article as:** Sen, A., Birteksöz Tan, A.S., Kültür, S., & Bitiş, L. (2020). Isolation and characterization of antimicrobial compounds from *Cotinus coggygia* Scop. ethyl acetate extract. *Istanbul Journal of Pharmacy*, 50 (3), 272-276.

## ABSTRACT

**Background and Aims:** *Cotinus coggygia* leaves are traditionally used in the treatment of various diseases, including their use for antifungal purposes. The aim of this study was to evaluate the antimicrobial activity of the extracts of *C. coggygia* and to discover compounds that may be responsible for the activity of the most active extract.

**Methods:** The antimicrobial activities of extracts and compounds were assessed by the microbroth dilution technique. Major compounds of active extract were isolated using chromatographic methods and identified by spectroscopic methods.

**Results:** Diethylether (CCD), ethyl acetate (CCEA), methanol (CCM), ethanol (CCE) and water (CCW) extracts of *C. coggygia* exhibited noticeable antifungal activities against *Candida albicans* with MIC values of 39, 4.9, 4.9, 4.9 and 9.8 µg/mL, respectively. Also, CCEA extract showed good antibacterial activity against *Proteus mirabilis* with an MIC value of 156 µg/mL. Two major compounds, gallic acid and methyl gallate, were isolated from CCEA, the most active extract. Gallic acid was found to be highly active against *C. albicans* and *C. tropicalis* with an MIC value of 9.8 µg/mL (for both fungi). In addition, gallic acid showed moderate antimicrobial activity against *Staphylococcus aureus*, *S. epidermidis* and *C. parapsilosis* with MIC values of 78, 156 and 156 µg/mL, respectively.

**Conclusion:** This study is the first study to reveal the compounds responsible for the activity of CCEA extract with antifungal activity. These results suggest that gallic acid, along with other phenolic compounds, is responsible for the antifungal activity of CCEA. Also, it confirms the ethnobotanical use of *C. coggygia* for antifungal purposes.

**Keywords:** Antimicrobial activity, *Candida* species, *Cotinus coggygia*, ethyl acetate extract, gallic acid, methyl gallate

## INTRODUCTION

Infectious diseases, especially in tropical and developing countries, are responsible for more than 50% of deaths worldwide, according to World Health Organization (WHO) reports (Zhang et al., 2013). At the same time, microbial contamination is one of the major concerns of the food and pharmaceutical industries, and the increasing tendency of microorganisms to develop resistance to existing antibiotics has led researchers to find new antimicrobial agents (Singh, Pandey, Agnihotri, Singh, & Pandey, 2017). Recent scientific studies have shown that there is a significant agreement between the traditional use of plants by the people in the treatment of specific symptoms and the experimental studies carried out in the laboratory such as anti-bacterial, anti-fungal, anti-cancer, and antiviral activities (Zhang et al., 2013). At the same time, the fact that *Cotinus coggygia*, which is used for wound-he-

### Address for Correspondence:

Ali ŞEN, e-mail: ali.sen@marmara.edu.tr; alisenbjk@gmail.com

Submitted: 26.02.2020

Revision Requested: 31.03.2020

Last Revision Received: 03.04.2020

Accepted: 04.05.2020

Published Online: 04.11.2020

This work is licensed under a Creative Commons Attribution 4.0 International License.



aling purposes, has shown an important wound-healing effect on normal and diabetic wounds in the previous pharmacological studies conducted by our team supports this idea (Aksoy et al., 2016a; Aksoy et al., 2016b). Various compounds with antimicrobial activity have been isolated from higher plants, and many of these compounds have shown promising potential to treat infectious diseases (Madikizela, Aderogba, Finnie, & Van Staden, 2014). Therefore, it is important to conduct research on plants to discover promising new and natural antimicrobial compounds or products.

The genus *Cotinus*, a member of the Anacardiaceae family, is represented by a single species in Turkey (Davis, 1967). This species is *C. coggygia* and the leaves of this species are used directly fresh, or in the form of an infusion or decoction. Leaves of *C. coggygia* have been used in the treatment of stomach pain, gastritis, ulcer, cuts, burns, wounds, eczema, fractures, diabetes, urinary diseases, cardiac diseases, kidney stones, nephritis, cancer, cough, abdominal pain, arm numbness, asthma, hemorrhoids, enteritis and anthrax in Turkey. It is also used as an antifungal, antihypertensive and a vasodilator (Kültür, 2007). Previous studies on phytochemical analysis of *C. coggygia* indicated the presence flavonoids (fisetin, fustin, sulfuretin, myricetin, quercetin, myricetin-3-O- $\alpha$ -rhamnoside, myricetin-3-O- $\beta$ -galactoside, 2,10-oxy-10-methoxysulfuretin, cotinignan A, sulfuretin, 2,3-trans-fustin, fisetin, butin, butein, taxifolin, eriodictyol, 3',5,5',7-tetrahydroxyflavanone, 3',4',7-trihydroxyflavone, 3-O-methyl-2,3-trans-fustin, 3-O-galloyl-2,3-trans-fustin); anthocyanins (leucodelphinidine, leucocyanidine, delphinidine 3-galactoside, cyanidine 3-galactoside, petunidine 3-glucoside, delphinidine 7-glucoside, cyanidine 3-glucoside-7-rhamnoside); essential oil (limonene, (Z)- $\beta$ -oximene, (E)- $\beta$ -oximene); gallic tannin (gallic acid), methyl gallate, galocatechin, pentagalloyl glucose, biazuron,  $\beta$ -resorcylic acid and 3-O- $\beta$ -sitosterol glucoside (Hegnauer, 1964; Tanchev & Timberlake, 1969; Westernburg et al., 2000; Demirci, Demirci, & Baser, 2003; Kultur & Bitis, 2007; Novakovic et al., 2007; Dulger, Hacioglu, & Bilen, 2009; Özbek et al., 2019; Novakovic et al., 2019).

There are studies in the literature showing that different extracts obtained from the leaves, stem and aerial parts of *C. coggygia* have antimicrobial and antifungal activity (Tunc, Hoş, & Güneş, 2013; Marcetić et al., 2013; Matic, Stanic, Solujic, Milosevic, & Niciforovic, 2011). However, a report on compounds that may be responsible for the antimicrobial activity of this plant has not been published so far. To the best of our knowledge, this study is the first to find compounds that may be responsible for the activity of the ethyl acetate extract, which has been found to have potent antifungal activity. Therefore, the aim of our current study is to evaluate antimicrobial activities of the various extracts obtained by Soxhlet and maceration from *C. coggygia* and to isolate the compounds that may be responsible for the activity of the extract that is showing the best activity.

## MATERIALS AND METHODS

### Plant material

*C. coggygia* leaves were collected in the flowering periods from the Kırklareli province of Turkey and identified by Dr. Sukran Kultur, a botanist of the Faculty of Pharmacy, University

of Istanbul. Voucher specimens were deposited in the Herbarium of the Faculty of Pharmacy, Istanbul University (ISTE No: 80926).

### Extraction

*C. coggygia* leaves were dried in the shade and powdered by a mechanical grinder. A total of 20 grams of powdered material was extracted with solvents of increased polarity such as petroleum ether, chloroform, diethylether, ethyl acetate, methanol using Soxhlet apparatus and extraction was continued until the solution became colorless. A total of 20 grams of powdered material was separately extracted with 96% ethanol and water using maceration method. Also, about 300 g of the plant was weighed for isolation and similar extraction procedures described above were carried out.

### Antimicrobial activity

In this study, the *in vitro* antimicrobial activities of the extracts and isolated compounds was determined using the microbroth dilution technique described by the Clinical and Laboratory Standards Institute (CLSI) (CLSI, 2006; CLSI, 2008). The minimum inhibitory concentrations (MICs) of the extracts were investigated against *Staphylococcus aureus* ATCC 6538, *S. epidermidis* ATCC 12228, *Escherichia coli* ATCC 25922, *Klebsiella pneumoniae* ATCC 4352, *Pseudomonas aeruginosa* ATCC 27853, *Proteus mirabilis* ATCC 14153, *Candida albicans* ATCC 10231, *C. parapsilosis*, ATCC 22019, *C. tropicalis* ATCC 750. Serial twofold dilutions ranging from 5000 to 4.8  $\mu$ g/mL were prepared in Mueller–Hinton broth (MHB) (Difco, Detroit, MI, USA) for the bacteria and RPMI-1640 medium buffered to pH 7.0 with MOPS for yeast strain were used as the test medium. (Sigma, St. Louis, MO, USA) medium for the yeast. DMSO was used as a solvent for the extracts. Each well was inoculated with 50  $\mu$ L of a 4–6 h broth culture to give a final concentration of  $5 \times 10^5$  cfu/mL for the bacteria and  $0.5 \times 10^3$  to  $2.5 \times 10^3$  cfu/mL for the yeast in the test trays. The trays were covered and placed in plastic bags to prevent evaporation. The trays containing MHB were incubated at 37°C for 24 h, while those containing the RPMI-1640 medium were incubated at 30°C for 48 h. The MIC of each extract and isolated compounds were defined as the lowest concentration of compound required for complete inhibition of visible growth. Ciprofloxacin and fluconazole were used as reference antimicrobials for bacteria and yeast, respectively. Also, as a control, the antimicrobial effects of the dimethyl sulfoxide were investigated against test microorganisms. According to the values of the controls, the results were evaluated. The MIC values of the ciprofloxacin and fluconazole were within the accuracy range in CLSI throughout the study (CLSI, 2014).

### Isolation of active compounds from CCEA extract

In the antimicrobial activity experiment, the CCEA showed the best antibacterial and antifungal activity among all extracts (Table 1). Therefore, CCEA was chosen for isolation. The CCEA (1.91 g) was fractionated by CC on polyamide, eluting with  $\text{CH}_3\text{OH}/\text{H}_2\text{O}$  mixture in increasing polarity to yield thirty fractions (Figure 1). Fractions showing similar TLC profiles were combined to give seven sub-fractions (F1-F7, F8-F10, F11-F14, F15-F17, F19-F21, F22-F23, F24-F30). When the fractions were examined on the TLC plate, isolation was continued with F11-

**Table 1. Antimicrobial activity of various extracts from *Cotinus coggygia* leaves.**

Microorganisms	CCP	CCC	CCD	CCEA	CCM	CCE	CCW	CPFX	FCZ
	MIC values ( $\mu\text{g/mL}$ )								
<i>Staphylococcus aureus</i>	-	-	-	-	-	-	-	-	-
<i>Staphylococcus epidermidis</i>	-	-	-	-	-	-	-	-	-
<i>Escherichia coli</i>	-	-	-	-	-	-	-	-	-
<i>Klebsiella pneumoniae</i>	-	-	-	-	-	-	-	-	-
<i>Pseudomonas aeruginosa</i>	-	-	-	-	-	-	-	-	-
<i>Proteus mirabilis</i>	-	-	-	156	-	-	-	0.31	-
<i>Candida albicans</i>	-	-	39	4.9	4.9	4.9	9.8	-	1

Abbreviations: CCP, CCC, CCD, CCEA, CCM, CCE and CCW show petroleum ether, chloroform, diethylether, ethyl acetate, methanol, ethanol and water extracts, respectively. CPFX: Ciprofloxacin, FCZ: Fluconazole, -: No activity

F14 fraction, where the major compounds appeared to be the most pure. F11-F14 was repeatedly chromatographed on a Sephadex LH-20 column, eluted with  $\text{CH}_3\text{OH}$  and then combined sub-fractions were re-chromatographed by preparative TLC with toluene: acetone: formic acid (5:5:1) to give gallic acid (25.7 mg) and methyl gallate (17.4 mg) (Figure 1).

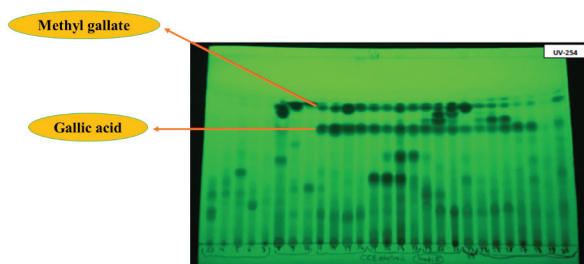


**Figure 1.** Thin layer chromatography (TLC) chromatogram of fractions of CCEA.

## RESULTS AND DISCUSSION

In this study, the antimicrobial activities of various extracts obtained by different extraction methods from *C. coggygia* as well as the major compounds isolated from the active extract were investigated. The antimicrobial activities of extracts were investigated against *S. aureus* ATCC 6538, *S. epidermidis* ATCC 12228, *E. coli* ATCC 25922, *K. pneumoniae* ATCC 4352, *P. aeruginosa* ATCC 27853, *P. mirabilis* ATCC 14153, *C. albicans* ATCC 10231. Saraiva et al. (2011) suggested that plant extracts with MIC values of  $< 100 \mu\text{g/mL}$  were considered to be highly active antimicrobial agents; those with MICs of 100 to  $500 \mu\text{g/mL}$  were defined as active; those with MICs of 500 to  $1000 \mu\text{g/mL}$  were defined as moderately active; those with MICs of 1000 to  $2000 \mu\text{g/mL}$  were considered to have low activity; and those with MICs of  $> 2000 \mu\text{g/mL}$  were defined as inactive. According to this view, CCD, CCEA, CCM, CCE and CCW extracts showed significant antifungal activity against *C. albicans* with MIC values of 39, 4.9, 4.9, 4.9 and  $9.8 \mu\text{g/mL}$ , respectively. In

particular, the effects of the last four extracts against this fungus were very strong. In addition, none of the extracts, except the CCEA extract, had any effect against the bacteria used in this study. The CCEA extract exhibited good antibacterial activity against *P. mirabilis* with a MIC value of  $156 \mu\text{g/mL}$  (Table 1). In a study conducted by Tunç et al. (2013), antibacterial effects of petroleum ether, chloroform, acetone, methanol, ethanol and distilled water extracts from the leaves of *C. coggygia* on *S. epidermidis*, *E. coli*, *Salmonella typhimurium*, *Enterococcus faecalis*, *P. aeruginosa*, *S. aureus*, and *Bacillus subtilis* were investigated and it was revealed that distilled water and methanol extracts showed good activity against *S. aureus*, *S. epidermidis*, and *E. faecalis*. In addition, it was found that distilled water extract had the highest activity with 22 mm inhibition zone against *E. faecalis* among these extracts (Tunç et al., 2013). In another study, Marcetic et al. (2013) tested antimicrobial activities of 70% acetone extract obtained from young shoots which included leaves and branches of *C. coggygia* and its chloroform, ethyl acetate and water fractions against *S. aureus*, *S. epidermidis*, *Micrococcus luteus*, *E. faecalis*, *B. subtilis*, *P. aeruginosa*, *E. coli*, *K. pneumoniae*, *C. albicans* (ATCC 10259 and ATCC 24433) and reported that the extracts showed antimicrobial activity with MIC values in the range of 3.1–200  $\mu\text{g/mL}$  (Marcetić et al., 2013). Additionally, Matic et al. (2011) examined antibacterial and antifungal effects of the methanol extract obtained by Soxhlet from the stem of *C. coggygia* against *B. subtilis*, *K. pneumoniae*, *E. coli*, *S. aureus*, *Micrococcus lysodeikticus*, *C. albicans* and found that the MIC values of extract were in the range of 125–250  $\mu\text{g/mL}$ . When compared with our current study, it was seen in previous studies that extracts from different parts of *C. coggygia* have antibacterial effects against various bacterial species. In the current study, it was observed that antibacterial activities of all the extracts were quite weak except for the activity shown by CCEA extract against *P. mirabilis*. However, the antifungal activity values of the extracts against *C. albicans* were close to or higher than previous studies. This may be due to the fact that collection time, growth place, extracted part of the plant as well as

the extraction method, seasonal changes, growth stage and climate conditions are different.

Two major compounds, gallic acid and methyl gallate, were isolated from the CCEA extract, which showed the best antimicrobial activity. All isolated compounds were analyzed by spectroscopic methods ( $^1\text{H}$  NMR,  $^{13}\text{C}$  NMR-APT, HMBC) and their data were compared with those reported in the literature (Xu et al., 2015; Banday et al., 2012). Also, gallic acid isolated in this study was compared on TLC with an authentic sample. The compounds were identified as follows:

**Gallic acid:** Colourless amorphous powder.  $^1\text{H}$  NMR (500 MHz,  $\text{CD}_3\text{OD}$ ,  $\delta$ , ppm, J/Hz): 7.04 (s, 2H, H-2/H-6) (Figure 2).

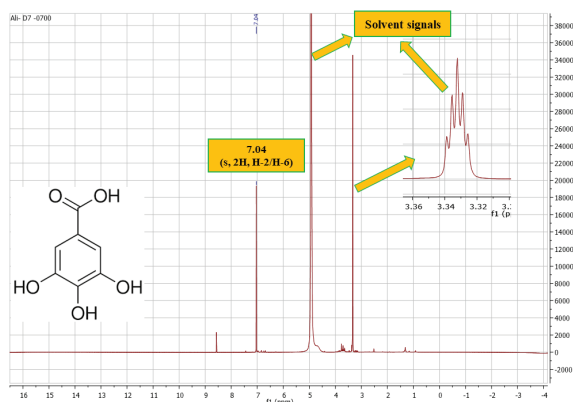


**Figure 2.**  $^1\text{H}$ -NMR (500 MHz,  $\text{CD}_3\text{OD}$ ) spectrum of gallic acid.

**Methyl gallate:** Colourless amorphous powder.  $^1\text{H}$  NMR (500 MHz,  $\text{CD}_3\text{OD}$ ,  $\delta$ , ppm, J/Hz): 6.95 (s, 2H, H-2/H-6), 3.71 (s, 3H,  $-\text{OCH}_3$ ).  $^{13}\text{C}$  NMR (125 MHz,  $\text{CD}_3\text{OD}$ ,  $\delta$ , ppm): 169.05 (C-7), 146.52 (C-3/C-5), 139.74 (C-4), 121.54 (C-1), 110.11 (C-2/C-6), 52.30 ( $\text{OCH}_3$ ) (Figure 3).

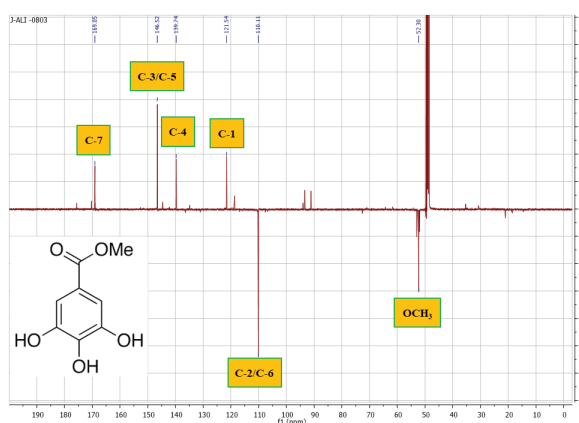


**Figure 3.**  $^{13}\text{C}$ -NMR (APT) (125 MHz,  $\text{CD}_3\text{OD}$ ) spectrum of methyl gallate.

The antimicrobial activities of major compounds were investigated against *S. aureus*, *S. epidermidis*, *E. coli*, *K. pneumoniae*, *P. aeruginosa*, *P. mirabilis*, *C. albicans*, *C. parapsilosis*, *C. tropicalis*. Gallic acid showed moderate antibacterial activity against *S. aureus* and *S. epidermidis* with MIC values of 78 and 156  $\mu\text{g}/\text{mL}$  while it showed weak antibacterial effect against *E. coli* and

*P. aeruginosa* with MIC value of 625  $\mu\text{g}/\text{mL}$  (for both bacteria), respectively. Methyl gallate did not show any antibacterial effect. Gallic acid exhibited strong antifungal activity against *C. albicans* and *C. tropicalis* with MIC value of 9.8  $\mu\text{g}/\text{mL}$  (for both fungi) while it possessed moderate activity 156  $\mu\text{g}/\text{mL}$  against *C. parapsilosis*. Methyl gallate showed moderate antifungal effect against *C. albicans*, *C. parapsilosis* and *C. tropicalis* with MIC values of 312 and 156  $\mu\text{g}/\text{mL}$  (for the last two fungi), respectively (Table 2). Especially considering the strong antifungal effect of gallic acid against different *C. species*, it suggests that this compound, with other phenolic compounds, may be highly responsible for the activity of CCEA, which exhibits strong antifungal effect against *C. albicans*. Also, previous studies showing that gallic acid has strong antifungal activity against *Candida* species support the results of our current study (Li et al., 2017; Alves et al., 2014).

**Table 2. Antimicrobial activity of major compounds isolated from CCEA.**

Microorganisms	Gallic acid	Methyl gallate	CPF	FCZ	
					MIC values ( $\mu\text{g}/\text{mL}$ )
<i>Staphylococcus aureus</i>	78	-	0.25		
<i>Staphylococcus epidermidis</i>	156	-			
<i>Escherichia coli</i>	625	-			
<i>Klebsiella pneumoniae</i>	-	-			
<i>Pseudomonas aeruginosa</i>	625	-			
<i>Proteus mirabilis</i>	-	-			
<i>Candida albicans</i>	9.8	312		1	
<i>Candida parapsilosis</i>	156	156			
<i>Candida tropicalis</i>	9.8	156			

CPF: Ciprofloxacin, FCZ: Fluconazole, -: No activity

## CONCLUSION

These results indicate that *C. coggygia* have strong antifungal activity confirming its ethnobotanical use for the treatment of fungal infections. It also shows that the compound that is significantly responsible for the activity of CCEA, one of the extracts with strong antifungal effect, is gallic acid together with other phenolic compounds.

**Peer-review:** Externally peer-reviewed.

**Author Contributions:** Conception/Design of Study- A.Ş., L.B.; Data Acquisition- A.Ş., A.S.B.T., Ş.K., L.B.; Data Analysis/Interpretation- A.Ş., A.S.B.T., Ş.K., L.B.; Drafting Manuscript- A.Ş., L.B.; Critical Revision of Manuscript- A.Ş., A.S.B.T., Ş.K., L.B.; Final Approval and Accountability- A.Ş., A.S.B.T., Ş.K., L.B.; Technical or Material Support- Ş.K.; Supervision- A.S.B.T., Ş.K., L.B.

**Conflict of Interest:** The authors have no conflict of interest to declare.







**Financial Disclosure:** Authors declared no financial support.

## REFERENCES

- Aksoy, H., Sancar, M., Sen, A., Okuyan, B., Bitis, L., Uras F. ... İzzettin, F.V. (2016a). The effect of topical ethanol extract of *Cotinus coggygia* Scop. on cutaneous wound healing in rats. *Natural Product Research*, 30(4), 452–455.
- Aksoy, H., Sen, A., Sancar, M., Sekerler, T., Akakin, D., Bitis, L. ... İzzettin F.V. (2016b). Ethanol extract of *Cotinus coggygia* leaves accelerates wound healing process in diabetic rats. *Pharmaceutical Biology*, 54(11), 2732–2736.
- Alves, C. T., Ferreira, I. C. F. R., Barros, L., Silva, S., Azeredo, J., & Henriques, M. (2014). Antifungal activity of phenolic compounds identified in flowers from North Eastern Portugal against *Candida* species. *Future Microbiology*, 9(2), 139–146.
- Banday, J. A., Mir, F. A., Farooq, S., Qurishi, M. A., Koul, S., & Razdan, T. K. (2012). Salicylic acid and methyl gallate from the roots of *Conyza canedensis*. *International Journal of Chemical and Analytical Science*, 3(2), 1305–1308.
- Clinical and Laboratory Standards Institute (2006). *Methods for dilution antimicrobial susceptibility tests for bacteria that grow aerobically: Approved Standard M7-A7*. Wayne, USA.
- Clinical and Laboratory Standards Institute (2008). *Reference Method for Broth Dilution Antifungal Susceptibility Testing of Yeasts; Approved Standard M27-A3*. Wayne, USA.
- Clinical and Laboratory Standards Institute (2014). Performance standards for antimicrobial susceptibility testing; 24th informational supplement. M 100-S24:CLSI. Wayne, USA.
- Davis P. H. (1967). *Flora of Turkey and the East Aegean Islands* (pp. 543). Edinburgh, UK: Edinburgh University Press.
- Demirci, B., Demirci, F., & Baser, K. H. C. (2003). Composition of the essential oil of *Cotinus coggygia* Scop. from Turkey. *Flavour and Fragrance Journal*, 18(1), 43–44.
- Dulger, B., Hacıoğlu, N., & Bilen, S. (2009). Antimicrobial activity of *Cotinus coggygia* from Turkey. *Asian Journal of Chemistry*, 21(5), 4139–4140.
- Hegnauer, R. (1964). *Chemotaxonomie der Pflanzen*. Basel und Stuttgart: Birkhauser Verlag.
- Kültür, S. (2007). Medicinal plants used in Kırklareli province (Turkey). *Journal of Ethnopharmacology*, 111(2), 341–364.
- Kultur, S., & Bitis, L. (2007). Anatomical and preliminary chemical studies on the leaves of *Cotinus coggygia* Scop. (Anacardiaceae). *Journal of Faculty of Pharmacy of Istanbul*, 39, 65–71.
- Li, Z.-J., Liu M., Dawuti G., Dou Q., Ma Y., Liu H.-G., & Aiba S. (2017). Antifungal activity of gallic acid *in vitro* and *in vivo*. *Phytotherapy Research*, 31(7), 1039–1045.
- Madikizela, B., Aderogba, M. A., Finnie, J. F., & Van Staden, J. (2014). Isolation and characterization of antimicrobial compounds from *Terminalia phanerophlebia* Engl. & Diels leaf extracts. *Journal of Ethnopharmacology*, 156, 228–234.
- Matic, S., Stanic, S., Solujic, S., Milosevic, T., & Niciforovic N. (2011). Biological properties of the *Cotinus coggygia* methanol extract. *Periodicum biologorum*, 113(1), 87–92.
- Marcetić M., Božić D., Milenković, M., Malesević, N., Radulović, S., & Kovacević N. (2013). Antimicrobial, antioxidant and anti-inflammatory activity of young shoots of the smoke tree, *Cotinus coggygia* Scop. *Phytotherapy Research*, 27(11), 1658–1663.
- Novakovic, M., Vuckovic, I., Janackovic, P., Sokovic, M., Filipovic, A., Tesevic, V., & Milosavljevic, S. 2007. Chemical composition, antibacterial and antifungal activity of the essential oils of *Cotinus coggygia* from Serbia. *Journal of the Serbian Chemical Society*, 72(11), 1045–1051.
- Novakovic, M., Djordjevic, I., Todorovic, N., Trifunovic, S., Andjelkovic, B., Mandic, B., Jadranić, M., Vuckovic, I., Vajs, V., Milosavljevic, S., & Tesevic, V. 2019. New aurone epoxide and auronolignan from the heartwood of *Cotinus coggygia* Scop. *Natural Product Research*, 33(19), 2837–2844.
- Özbek, H., Yuca, H., Gözcü, S., Dursunoğlu, B., Özener, N., Güvenalp Z., Kazaz C., Önal, M., & Demirezer L.Ö. 2019. Phenolic compounds from *Cotinus coggygia* Scop. with alpha glucosidase inhibition. *FABAD Journal of Pharmaceutical Sciences*, 44(2), 127–132.
- Saraiva, A. M., Castro, R. H. A., Cordeiro, R. P., Peixoto Sobrinho, T. J. S., Castro, V. T. N. A., Amorim, E. L. C., Xavier H. S., Pisciotano M. N. C. 2011. *In vitro* evaluation of antioxidant, antimicrobial and toxicity properties of extracts of *Schinopsis brasiliensis* Engl. (Anacardiaceae). *African Journal of Pharmacy and Pharmacology*, 5(14), 1724–1731.
- Singh, M., Pandey, N., Agnihotri, V., Singh, K. K., & Pandey A. (2017). Antioxidant, antimicrobial activity and bioactive compounds of *Bergenia ciliata* Sternb.: A valuable medicinal herb of Sikkim Himalaya. *Journal of Traditional and Complementary Medicine*, 7(2), 152–157.
- Tanchev, S. S., & Timberlake, C. F. (1969). Anthocyanins in leaves of *Cotinus coggygia*. *Pytochemistry*, 8(12), 2367–2369.
- Tunç, K., Hoş, A., & Güneş, B. (2013). Investigation of antibacterial properties of *Cotinus coggygia* from Turkey. *Polish Journal of Environmental Studies*, 22(5), 1559–1561.
- Xu, J., Zhao, Q., Wei, L., Yang, Y., Xu, R., Yu, N., & Zhao, Y. (2015). Phytochemical composition and antinociceptive activity of *Bauhinia glauca* subsp. hupehana in rats. *PLoS one*, 10(2), e0117801.
- Westernburg, H. E., Lee, K. J., Lee, S. K., Fong, H. H. S., Bremen, R. B. V., Pezutto, J. M., & Kinghorn, A. D. 2000. Activity-guided isolation of antioxidative constituents of *Cotinus coggygia*. *Journal of Natural Products*, 63(12), 1696–1698.
- Zhang, L., Ravipati, A. S., Koyyalamudi, S.R., Jeong, S. C., Reddy N., Bartlett J. ... Vicente F. (2013). Anti-fungal and anti-bacterial activities of ethanol extracts of selected traditional Chinese medicinal herbs. *Asian Pacific Journal of Tropical Medicine*, 6(9), 673–681.



# Antispasmodic activities of the methanolic extract from aerial parts of *Origanum* species on excised rat ileum

Muhammet Emin Çam<sup>1,2,3</sup> , Ayse Nur Hazar Yavuz<sup>1</sup> , Levent Kabasakal<sup>1</sup> , Turgut Taşkın<sup>4</sup> ,  
Leyla Bitiş<sup>4</sup> , Hatice Kübra Elçioğlu<sup>1</sup> 

<sup>1</sup>Marmara University, Faculty of Pharmacy, Department of Pharmacology, Istanbul, Turkey

<sup>2</sup>University College London, Torrington Place, Department of Mechanical Engineering, London, UK

<sup>3</sup>Marmara University, Center for Nanotechnology and Biomaterials Research, Turkey

<sup>4</sup>Marmara University, Faculty of Pharmacy, Department of Pharmacognosy, Istanbul, Turkey

**ORCID IDs of the authors:** M.E.Ç. 0000-0001-5398-6801; A.N.H.Y. 0000-0003-0784-8779; L.K. 0000-0002-5474-6436; T.T. 0000-0001-8475-6478; L.B. 0000-0003-1167-6666; H.K.E. 0000-0001-6386-1711

**Cite this article as:** Cam, M. E., Hazar Yavuz, A. N., Kabasakal, L., Taskin, T., Bitis, L., & Elcioglu, H. K. (2020). Antispasmodic activities of the methanolic extract from aerial parts of *Origanum* species on excised rat ileum. *Istanbul Journal of Pharmacy*, 50 (3), 277-282.

## ABSTRACT

**Background and Aims:** *Origanum hypericifolium*, *Origanum minutiflorum*, *Origanum saccatum*, and *Origanum haussknechtii* are some of the endemic *Origanum* species in Turkey. In the literature, besides the known effects of these *Origanum* species, no antispasmodic activity was determined. Therefore, we investigated *Origanum* species for possible antispasmodic effects to rationalize its traditional medicinal use. The present study aimed to investigate the antispasmodic activity of *Origanum* species with the organ bath.

**Methods:** Rats were divided into 5 groups. While no treatment was given to the control group, plant extracts were given to other groups. Ileal tissues taken by rats were used for evaluating the contraction responses elicited with potassium chloride (KCl) and acetylcholine (ACh). Thereafter, the extracts of *Origanum* species were applied and cumulative concentration-response curves of these species were constructed in each experiment.

**Results:** All treatments with *Origanum* species have a relaxation effect on rat ileum as compared with the control group. According to the results of the isolated organ bath study, KCl and ACh-induced ileum contractions were significantly decreased by all *Origanum* species.

**Conclusion:** *Origanum* species that were used in the present study can prevent smooth muscle contraction of ileum, and therefore they can be used to reduce intestinal spasms.

**Keywords:** *Origanum hypericifolium*, *Origanum minutiflorum*, *Origanum saccatum*, *Origanum haussknechtii*, Organ bath, Antispasmodic effect

## Address for Correspondence:

Muhammet Emin ÇAM, e-mail: m.cam@ucl.ac.uk

Submitted: 21.01.2020  
Revision Requested: 16.03.2020  
Last Revision Received: 30.05.2020  
Accepted: 06.07.2020  
Published Online: 30.10.2020

This work is licensed under a Creative Commons Attribution 4.0 International License.



## INTRODUCTION

Turkey, an important gene center for the Lamiaceae family, is represented by 45 genera, 546 species, and 730 taxa (Celik, Herken, Arslan, Ozel, & Mercan, 2010). The endemism rate of the Lamiaceae family in Turkey is 53% (Cam et al., 2019). Lamiaceae members are mainly common in the mountainous areas of the Mediterranean region of Turkey (Taskin, Cam, Taskin, & Rayaman, 2019).

Oregano is a term that refers to members of Lamiaceae with many common characteristics, all of which contain carvacrol as the major component in their essential oils. Oregano includes *Origanum*, *Thymus*, *Thymbra*, *Satureja*, and *Coridothymus* of the Lamiaceae family. *Origanum*, one of these, is among important aromatic plants common in the world and comprises the largest portion of oregano used in trade (Baser, 2008). Hippocrates (500 BC) was aware of the antiseptic properties of oregano, and it is used for respiratory diseases and stomach pain. Dioscorides (1<sup>st</sup> century AD), the author of the famous for *Materia Medica*, has proposed oregano tea for snakebites. Paracelsus (16<sup>th</sup> century AD) suggested using oregano for the treatment of diarrhea, psoriasis, and fungal diseases (Baser, 2008).

Some of the endemic *Origanum* species in Turkey are *Origanum hypericifolium* Schwarz et Davis, *Origanum minutiflorum* Schwarz et Davis, *Origanum saccatum* Davis, and *Origanum haussknechtii* Boiss.. The first of these is *O. hypericifolium*, which is used in traditional medicine for the treatment of some diseases, especially diabetes (Ocak, Çelik, Özel, Korcan, & Konuk, 2012). It mainly contains p-cymene,  $\gamma$ -terpinene, thymol, and carvacrol (Keskin, Ili, & Sahin, 2012). Previous studies have shown that *O. hypericifolium* has antimicrobial (Celik et al., 2010) and antifungal (Ocak et al., 2012) activities. The second *Origanum* species is *O. minutiflorum* that has  $\alpha$ -pinene, camphene,  $\alpha$ -terpinene, p-cymene, carvacrol-methyl-ether, and carvacrol (Dadalioglu & Evrendilek, 2004). According to the literature data, *O. minutiflorum* has antibacterial (Dadalioglu & Evrendilek, 2004) and antifungal activity (Bayramoglu, Gülümser, & Karaboz, 2006). The third *Origanum* species is *O. saccatum* which has  $\alpha$ -pinene, camphene, p-cymene, thymol, and carvacrol (Tumen, Baser, Kirimer, & Ozek, 1995). Previous studies have shown that *O. saccatum* has antimicrobial activity (Ozcan & Chalchat, 2009). In addition to this, the fourth plant *O. haussknechtii* contains camphene,  $\alpha$ -terpinene, and carvacrol (Baser, Kürkçüoglu, & Tumen, 1998), and it is reported that it has antioxidant activity (Koseoglu, Taskin, Sadikoglu, & Bitis, 2016).

In the literature, besides these known effects of the *Origanum* species mentioned above, none of them have been determined for their antispasmodic activities. Unlike these *Origanum* species, the antispasmodic effect was determined in some other *Origanum* species such as *Origanum acutidens* Handz.-Mazz. (Goze et al., 2010), *Origanum compactum* Benth (Van Den Broucke & Lemli, 1980), *Origanum vulgare* L (Khan, Bashir, Khan, & Gilani, 2011), and *Origanum majorana* L (Makrane et al., 2019).

Plants and their products are used worldwide as traditional medicines, and these are all potential reservoirs for new drugs. Traditional medicinal plants have become very important

in novel drug discovery due to their bioactive components (Taskin et al., 2018). Additionally, in recent years, increased interest has been shown in herbal products due to their strong effects and cheaper costs. Although new agents are developing, adverse effects are still a problem (Cam et al., 2017). At present, many people have consulted the use of natural remedies for the treatment of intestinal diseases due to their antispasmodic effects. One of the natural remedies used in the treatment of intestinal disease is the *Origanum* species with antispasmodic effects. Therefore, we investigated *O. hypericifolium*, *O. minutiflorum*, *O. saccatum*, and *O. haussknechtii* for possible antispasmodic effect and rationalization of their traditional medicinal use. The present study aimed to investigate antispasmodic activity of these *Origanum* species which have been used in folk medicine, in the organ bath system. Additionally, no acute or chronic toxicity related to these *Origanum* species were found in the literature.

## MATERIALS AND METHODS

### Materials

All chemicals used in the organ bath were purchased from Sigma (St. Louis, Missouri, USA).

### Collection of plant material

*O. hypericifolium*, *O. minutiflorum*, *O. saccatum*, and *O. haussknechtii* were collected from Burdur, Isparta-Çandır, Antalya-Alanya, and Erzincan-Kemaliye provinces, respectively. The plant materials were identified by Dr. Narin Sadikoglu. Voucher specimens are deposited in the herbarium of the Faculty of Pharmacy, Inonu University, and herbarium voucher numbers: *Origanum* 2009/016, *Origanum* 2009/013, *Origanum* 2009/033, *Origanum* 2009/002, respectively.

### Methods

#### Preparation of the extracts

The aerial parts of four dried *Origanum* species (20 g) were extracted with 100 ml portions of methanol by maceration at room temperature (25 °C) for 7 days stirring several times until the extracts remained colorless. The extracts were filtered and evaporated to dryness under reduced pressure at 45 °C in a rotary evaporator. The crude extracts were then transferred to vials and kept at +4 °C. The crude extract was administered by diluting with distilled water at different concentrations before being used in the organ bath.

### Animals

All animal experiments were carried out with the approval of the Marmara University Animal Experiments Local Ethics Committee (permission number: 51.2013.mar). Adult female Sprague-Dawley rats (250-350 g) (n=8 in each experiment) were obtained from Marmara University The Experimental Animal Implementation and Research Center (Istanbul, Turkey). The rats were housed under controlled temperature (20-23 °C), in humidity (40-60%), and light (12 h light/dark regime)-regulated rooms. The animals were kept on a standard rodent pellet diet, with tap water available ad libitum. Before starting to the experiments, all necessary precautions were taken, and the factors that would adversely affect the parameters during the study were minimized.

### Organ bath studies

Healthy animals were divided into 5 groups. In the organ bath system, the control group was given methanol as a vehicle, while the other groups were given plant extracts. Ileum was removed from the rats after the rats were sacrificed by guillotine. 2 cm-long part of ileum were sliced from all ileum; subsequently, the surrounding mesentery and fat tissues were carefully removed from ileum, and ileum was mounted vertically in an organ bath containing 20 ml Tyrode buffer [composition (mM): NaCl, 139.9; KCl, 2.68; CaCl<sub>2</sub>, 1.8; MgCl<sub>2</sub>, 1.05; NaHCO<sub>3</sub>, 11.9; NaH<sub>2</sub>PO<sub>4</sub>, 0.42; and glucose 5.55] at pH 7.40. The temperature of the organ bath was maintained at 37 °C, and carbogen (95% O<sub>2</sub> and 5% CO<sub>2</sub> gas mixture) was perfused through the bath. After mounting, ileum was equilibrated for approximately 60 min before the experiments were started with a buffer change every 15 min. The initial tension of the preparation was set to about 1 g. The tension of ileum was measured with an isometric force transducer (PowerLab, ADInstruments, Australia) and recorded on-line on a computer via a four-channel transducer data acquisition system using appropriate software (LabChart, ADInstruments, Australia).

### Contractility studies

In the isolated ileum, rhythmic and tonic contractions were elicited with 80 mM KCl and 10<sup>-6</sup> M acetylcholine (ACh). Firstly, contraction with KCl was measured, this measurement was used for % of KCl maximum and then KCl was removed by changing the water bath three times. The contraction responses of ACh were determined 15 minutes after removing KCl and *Origanum* species were cumulatively (0.025, 0.05, 0.1, 0.25, 0.5, 1 mg/ml) administered at the highest point of contraction with ACh. The relaxation response of ileal tissues were evaluated by adding cumulative concentrations of *Origanum* species on ACh induced precontractions. ACh induced contraction values were calculated according to KCl. Following the addition of each concentration of *Origanum* species, the recording was performed for 120 s. KCl induced contractions before the administration of *Origanum* species on rat ileum was obtained to investigate the viability of the tissues. Similar responses to KCl were observed for tissues among the groups. Concentration-response curves were fitted and areas under curves (AUC) were evaluated and analyzed statistically with Prism 6.05 (GraphPad Software Inc. San Diego, CA, USA). The AUC values and the maximal inhibitory effect of *Origanum* species (E<sub>max</sub>) values were calculated according to % relaxation response of tissues to ACh contraction.

### Statistical analysis

All values are presented as mean ± standard error of the mean (SEM). Differences in the contractile effect of KCl and ACh were analyzed using analysis of variance (ANOVA) tests with the Tukey multiple comparison test. Concentration-response curves were fitted, AUC determined, and E<sub>max</sub> (%) calculated with the Prism 6.05 software. The value of p<0.05 was considered statistically significant.

## RESULTS

The main focus of our study is to clarify and compare the effects of some endemic species of *Origanum* in Turkey on rat ileum relaxations and contractions in the organ bath experi-

ments. Therefore, the effect of these plants used in folk medicine was verified, and hence, the relaxation effect of *Origanum* species in various diseases can be utilized. The results obtained from the *in vitro* organ bath are given below according to responses to KCl and ACh contractions on rat ileum.

### Contraction responses of KCl on rat ileum

The results of isolated organ bath experiments studied on rat ileum demonstrated that there are no significant differences between groups on contraction responses of the ileum tissues to 80 mM KCl which acts via voltage-gated calcium channels on all groups. It is clearly seen that the contraction responses of the ileum tissues to 80 mM KCl was similar before the administration of *Origanum* species.

### Relaxation responses of cumulative concentrations of *Origanum* species on rat ileum

The relaxation response of *Origanum* species at the concentration range of 0.025 to 1 mg/ml on ACh induced contraction on rat ileum was demonstrated in Figure 1. In the previous studies, some other *Origanum* species (*O. acutidens*, *O. compactum*, *O. vulgare*, and *O. majorana*) was found to display a relaxation response. Similar to the results of the previous studies, all treatments with *Origanum* species at the concentration range of 0.025-1 mg/ml have a relaxation response on rat ileum as compared with the control group. In comparison with the control group, the highest ileum relaxing effect of *Origanum* species belong to *O. saccatum* (p<0.05), *O. haussknechtii* (p<0.05), *O. hypericifolium* (p<0.01), and *O. minutiflorum* (p<0.001), respectively. Relaxation responses was augmented with the increase in concentration of *Origanum* species in all groups. Thus, concentration-dependent relaxations were observed and these relaxation effects were completely recovered during washout period.

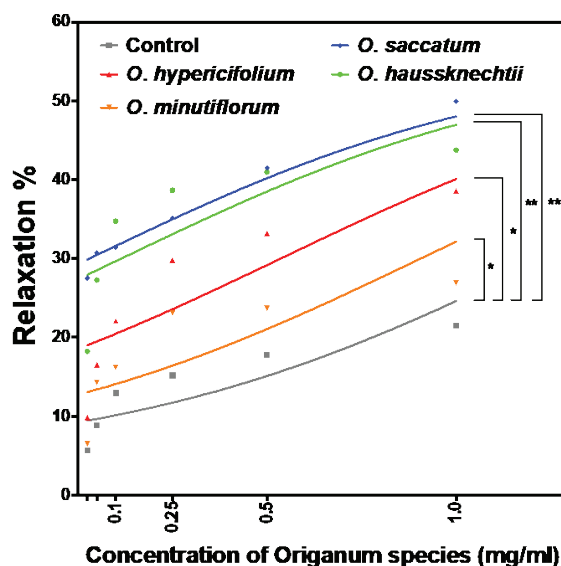


**Figure 1.** Changes in the relaxation responses of the cumulative *Origanum* species after contraction with ACh. Concentration of *Origanum* species: 0.025, 0.05, 0.1, 0.25, 0.5, and 1 mg/ml. Each group (n=8) represents Mean ± SEM. The statistical analyses were carried out with ANOVA tests with the Tukey multiple comparison test. \*p<0.05, \*\*p<0.01, \*\*\*p<0.001 vs control group.

Besides,  $E_{max}$  and AUC values for *Origanum* species were listed in Table 1. *O. hypericifolium* ( $p<0.05$ ), *O. saccatum* ( $p<0.01$ ), and *O. haussknechtii* ( $p<0.05$ ) treatments increased the  $E_{max}$  values compared to the control group.

**Table 1: Changes ( $E_{max}$  and AUC values) in the relaxation response of *Origanum* species on ACh induced contractions in the rat ileum.**

	$E_{max}$ (%)	AUC (%)
Control	21.470±3.561	16.77
<i>O. hypericifolium</i>	38.570±4.301*	30.99
<i>O. minutiflorum</i>	26.870±2.704	22.46
<i>O. saccatum</i>	49.950±5.405**	39.72
<i>O. haussknechtii</i>	43.750±5.211*	38.75

\* $p<0.05$ , \*\* $p<0.01$  vs control (vehicle) group (Mean ± SEM). AUC: Area under the curve.  $E_{max}$  (%): the maximum relaxing effect of *Origanum* species.

**Changes in ACh induced contraction with the presence of *Origanum* species**

The effects of different concentrations (0.025-1 mg/ml) of *Origanum* species on ACh induced contractions in the rat ileum were given in Figure 2. *O. hypericifolium*, *O. minutiflorum*, *O. saccatum*, and *O. haussknechtii* reduced contractility induced by ACh on rat ileum as compared with control group ( $p<0.05$ ,  $p<0.05$ ,  $p<0.05$  and  $p<0.01$ , respectively). *Origanum* species showed concentration-dependent inhibition on ACh induced contractions in rat ileum.

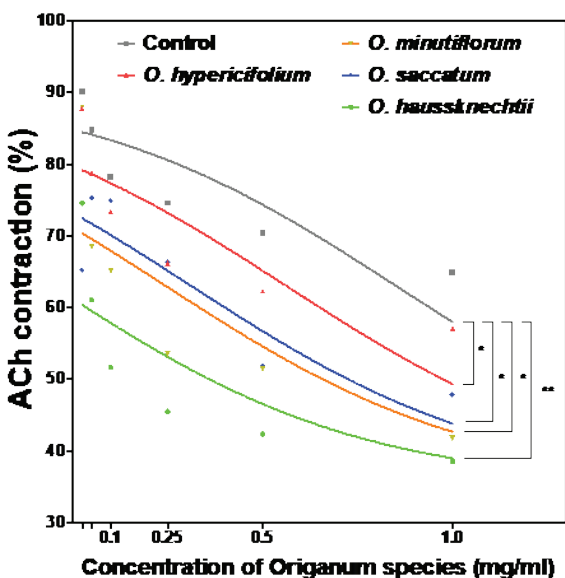


**Figure 2.** Changes in the ACh induced contraction responses after administration of cumulative *Origanum* species. Concentrations of *Origanum* species: 0.025, 0.05, 0.1, 0.25, 0.5, and 1 mg/ml. Each group (n=8) represents Mean ± SEM. The statistical analyses were carried out with ANOVA tests with the Tukey multiple comparison test. \* $p<0.05$ , \*\* $p<0.01$ .

Besides,  $E_{max}$  and AUC values for *Origanum* species were listed in Table 2. *O. saccatum* ( $p<0.01$ ) and *O. haussknechtii* ( $p<0.05$ ) treatments reduced  $E_{max}$  values compared to control group.

**Table 2: Changes ( $E_{max}$  and AUC values) in the ACh induced contractions in the presence of *Origanum* species on the rat ileum.**

	$E_{max}$ (%)	AUC (%)
Control	90.110±3.310	72.10
<i>O. hypericifolium</i>	87.780±2.528	64.64
<i>O. minutiflorum</i>	87.980±5.301	52.96
<i>O. saccatum</i>	65.220±13.980**	57.88
<i>O. haussknechtii</i>	74.550±5.172*	45.17

\* $p<0.05$ , \*\* $p<0.01$  vs control group (Mean ± SEM). AUC: Area under the curve.  $E_{max}$  (%): the maximum contraction of ACh.

**DISCUSSION**

In literature, the antispasmodic activity of *O. acutidens* essential oil in rat ileum was investigated by organ bath study. In that study, the essential oil of *O. acutidens* was applied in cumulative doses (0.1, 0.5, and 1 mg) and decreased ileal tissue contraction. According to their results, the antispasmodic effect of that essential oil is strong, concentration-independently and fully reversible (Goze et al., 2010). In another study, which investigated the antispasmodic activity of *O. compactum*, an organ bath study with the guinea-pig ileum and duodenum, and the rat fundus strip and duodenum were performed. According to their results, *O. compactum* showed antispasmodic activity on smooth muscles. In that study, it was suggested that the effects of *O. compactum* on muscle relaxation were caused by a decrease in the presence of the calcium for contraction of muscle due to inhibition of intracellular  $Ca^{+2}$  release and extracellular  $Ca^{+2}$  influx in the smooth muscle cells (Van Den Broucke & Lemli, 1980). In another study, the antispasmodic activity of *O. vulgare* was investigated with an organ bath study in the strips of rabbit urinary bladder. *O. vulgare* inhibited carbachol and  $K^{+}$ -induced contractions in concentration-dependent manner (Khan et al., 2011). The antispasmodic activity of the essential oil from the aerial part of *O. majorana* on muscle relaxation was investigated on rabbit and rat intestinal smooth muscle. According to these results, *O. majorana* essential oil inhibited the carbachol and KCl-induced contraction of tissue (Makrane et al., 2019). We investigated the antispasmodic effect of *Origanum* species and examined their relaxation response in ACh ( $10^{-6}M$ ) induced contractions on rat ileum. As obtained from our results, *Origanum* species reduced contractions on rat ileum.

The membrane of smooth muscle includes more voltage-dependent  $Ca^{+2}$  channels than skeletal muscle, but on the contrary, it contains much less voltage-dependent sodium channels. For this reason, calcium ions are responsible for contracting as they flow from the slow calcium-sodium channels to the fiber by the action of KCl (Ratz, Berg, Urban, & Miner, 2005). It is known that KCl at high concentrations causes the

contraction of smooth muscle by the opening of the voltage-induced L-type calcium channels, thus resulting in the contraction of the smooth muscles because of the influx of extracellular  $\text{Ca}^{2+}$  (Khan et al., 2011).

ACh, due to its effect on muscarinic  $M_4$  receptors, leads to contraction by decreasing cyclic adenosine monophosphate (cAMP) levels, increasing the amount of intracellular calcium or affecting nicotinic receptor and opening ion channels, and thus produce depolarization (Nausch, Heppner, & Nelson, 2010). It is also well known that contraction induced by  $\text{K}^+$  in smooth muscles is caused by an increase in  $\text{Ca}^{2+}$  flow through voltage-gated  $\text{Ca}^{2+}$  channels, and therefore, any substance that inhibits high  $\text{K}^+$  mediated contractions of smooth muscles is claimed to be an inhibitor of  $\text{Ca}^{2+}$  flux (Chiwororo & Ojewole, 2009). KCl induced contraction on ileum smooth muscle is mainly caused by calcium influx through voltage-sensitive calcium channels (Ponce-Monter et al., 2006). The present findings show that the *Origanum* species inhibit ACh induced ileum contractions acting on the stress-sensitive calcium channels. These *Origanum* species led to concentration-dependent and reversible inhibition of the isolated rat ileum contractions. The contraction caused by ACh was inhibited by *Origanum* species in a concentration-dependent manner.

Additionally, according to our results, the inhibitory effects of *Origanum* species induced by ACh is not reversible. These effects are only reduced and eliminated by washing tissues. The relative decrease in the effects of the extract after tissue washing can be related to the removal of the extract from the surface of receptors. Moreover, prolonged ileum contractions without a reduction in contractile force with ACh in control tissues showed that the decrease in contractile strength was due to the performance of the extract rather than muscle fatigue.

Phytochemical studies reveal the presence of various substances in plants. The activities observed in the extracts of the *Origanum* species that we tested are probably due to the presence of these phytochemicals. For example, it is known that flavonoids exhibit antispasmodic activity. However, other phytochemicals in the extracts also contribute to the effects found (Tumen et al., 1995). Considering the phytochemical studies on these *Origanum* species, these plants contain tannins, flavonoids, sitosterols, phenolic glycosides, phenolic terpenoids, arbutin, and numerous essential oil molecules.

Carvacrol ( $\text{C}_{10}\text{H}_{14}\text{O}$ , a monoterpenoid phenol), one of the major components of *Origanum* species, is investigated in the *Origanum* species extract and it is known to have antispasmodic activity. Thus, the antispasmodic activity observed in the present study can be attributed to the carvacrol of *Origanum* (Baser, 2008). It is reported that carvacrol content of the *O. hypericifolium*, *O. minutiflorum*, *O. saccatum*, *O. haussknechtii* are 42-82% (Baser, Ermin, Kurkcuoglu, & Tumen, 1994), 34-64% (Baser, Tumen, & Sezik, 1991), 6.36-7.18% (Tumen et al., 1995), and 4.34% (Koseoglu et al., 2016), respectively. In addition to carvacrol, it is reported that thymol, another component of *Origanum* species, has antispasmodic effect; however, p-cymene has no antispasmodic effect. According to the study, which is a continuation of the same study, the basic fact emerging from the results

is that pharmacological inhibition of smooth muscle activity plays a major role in the non-specific and non-competitive antagonism of thymol and carvacrol. Changes in the degree of effect of the *Origanum* species whose effects were investigated in our study are likely to vary according to the presence of carvacrol, thymol, and other components at different rates. However, further investigations are needed on that subject. Additionally, an edible plant with a long history of medical use is considered to be relatively safe, but detailed studies of the safety profile are needed before being recommended for clinical use.

Any report of antispasmodic properties of these *Origanum* species on the literature was not mentioned before. According to our results, the extracts of *Origanum* species reduced smooth muscle contraction on rat ileum. The effects of the extract were concentration-dependent and completely reversed during washing. The exact mechanism of *Origanum* species may be related to  $\text{Ca}^{2+}$  level changes in the ileum smooth muscle in the presence of extract. The antispasmodic effect of the extract observed in this study supports the clinical efficacy and use of the extracts of *Origanum* species in the treatment of spasmodic disorders. Further studies are needed to explain the underlying mechanism of action of *Origanum* species and evaluate its use in folk medicine. Due to the antispasmodic activity of *Origanum* species, these plants can be considered as a natural source and freely used in the food and pharmaceutical industry.

## CONCLUSION

The antispasmodic effects of some *Origanum* species, such as *Origanum hypericifolium*, *Origanum minutiflorum*, *Origanum saccatum*, and *Origanum haussknechtii*, were investigated. The *Origanum* species have shown significant antispasmodic activity by acting on various pharmacological pathways. The contraction caused by ACh was inhibited by *Origanum* species in a concentration-dependent manner. Consequently, *Origanum* species can cause concentration-dependent and reversible inhibition of spontaneous contractions on isolated rat ileum, and they can inhibit contraction of the smooth muscle of ileum on rats. Thus, it can be used to decrease intestinal spasms. Further studies are needed to determine the mechanism of action and major effective compounds.

**Peer-review:** Externally peer-reviewed.

**Ethics Committee Approval:** All animal experiments were carried out with the approval of the Marmara University Animal Experiments Ethics Committee (number 51.2013.mar).

**Author Contributions:** Conception/Design of Study- H.K.E., M.E.Ç., A.N.H.Y., L.K.; Data Acquisition- M.E.Ç., A.N.H.Y.; Data Analysis/Interpretation- M.E.Ç., L.K.; Drafting Manuscript- M.E.Ç., A.N.H.Y.; Critical Revision of Manuscript- L.K., H.K.E.; Final Approval and Accountability- M.E.Ç., A.N.H.Y., L.K., T.T., L.B., H.K.E.; Technical or Material Support-T.T.; Supervision- L.B.

**Conflict of Interest:** The authors have no conflict of interest to declare.

**Financial Disclosure:** This study was supported by Marmara University, Scientific Research Projects Committee (MU-BAPKO; Project number: SAG-B-131113-0419).



## REFERENCES

- Baser, K.H.C. (2008). Biological and pharmacological activities of carvacrol and carvacrol bearing essential oils. *Current Pharmacological Design*, 14, 3106-3019. <https://dx.doi.org/10.2174/138161208786404227>
- Baser, K.H.C., Ermin, N., Kurkcuoglu, M., & Tümen, G. (1994). Essential Oil of *Origanum hypericifolium* O. Schwarz et P. H. Davis. *The Journal of Essential Oil Research*, 6(6), 631-633. <https://dx.doi.org/10.1080/10412905.1994.9699355>
- Baser, K.H.C., Kürkçüoğlu, M., & Tumen, G. (1998). Composition of the Essential Oil of *Origanum haussknechtii* Boiss. *The Journal of Essential Oil Research*, 10, 227-228. <https://dx.doi.org/10.1080/10412905.1998.9700888>
- Baser, K.H.C., Tümen, G., & Sezik, E. (1991). The Essential Oil of *Origanum minutiflorum* O. Schwarz and P. H. Davis. *The Journal of Essential Oil Research*, 3(6), 445-446. <https://dx.doi.org/10.1080/10412905.1991.9697982>
- Bayramoglu, E., Gülümser, G., & Karaboz, I. (2006). Ecological and innovative fungicide for the leather industry: Essential oil of *Origanum minutiflorum*. *Journal of American Leather Chemists Association*, 101, 96-104.
- Cam, M.E., Yildiz, S., Ertas, B., Acar, A.E., Taskin, T., & Kabasakal, L. (2017). Antidiabetic effects of *Salvia triloba* and *Thymus praecox* subsp. *skorpilii* var. *skorpilii* in a rat model of streptozotocin/nicotinamide-induced diabetes. *Marmara Pharmaceutical Journal*, 21(4), 818-827. <https://dx.doi.org/10.12991/mpj.2017.8>
- Cam, M.E., Hazar-Yavuz, A.N., Yildiz, S., Ertas, B., Ayaz Adakul, B., Taskin, T., Alan, S., & Kabasakal, L. (2019). The methanolic extract of *Thymus praecox* subsp. *skorpilii* var. *skorpilii* restores glucose homeostasis, ameliorates insulin resistance and improves pancreatic beta-cell function on streptozotocin/nicotinamide-induced type 2 diabetic rats. *Journal of Ethnopharmacology*, 231, 29-38. <https://dx.doi.org/10.1016/j.jep.2018.10.028>
- Celik, A., Herken, E.N., Arslan, I., Ozel, M.Z., & Mercan, N. (2010). Screening of the constituents, antimicrobial and antioxidant activity of endemic *Origanum hypericifolium* O. Schwarz & P.H. Davis. *Natural Product Research*, 24, 1568-1577. <https://dx.doi.org/10.1080/14786419.2010.496366>
- Chiwororo, D.H.W., & Ojewole, A.O.J. (2009). Spasmolytic effect of *Psidium guajava* Linn. (Myrtaceae) leaf aqueous extract on rat isolated uterine horns. *Journal of Smooth Muscle Research*, 45, 31-38. <https://dx.doi.org/10.1540/jsmr.45.31>
- Dadalioglu, I., & Evrendilek, G.A. (2004). Chemical compositions and antibacterial effects of essential oils of Turkish oregano (*Origanum minutiflorum*), bay laurel (*Laurus nobilis*), Spanish lavender (*Lavandula stoechas* L.), and fennel (*Foeniculum vulgare*) on common foodborne pathogens. *Journal of Agricultural and Food Chemistry*, 52, 8255-8260. <https://dx.doi.org/10.1021/jf049033e>
- Goze, I., Alim, A., Cetinus, S.A., Cetin, A., Durmus, N., Atas, A.T., & Vural, S. (2010). *In vitro* antimicrobial, antioxidant, and antispasmodic activities and the composition of the essential oil of *Origanum acutidens* (Hand.-Mazz.) letswaart. *Journal of Medicinal Food*, 13, 705-709. <https://dx.doi.org/10.1089/jmf.2009.0094>
- Keskin, N., Ili, P., & Sahin, B. (2012). Histochemical demonstration of mucosubstances in the mouse gastrointestinal tract treated with *Origanum hypericifolium* O. Schwarz and P.H. Davis extract. *African Journal of Biotechnology*, 11, 2436-2444. <https://dx.doi.org/10.5897/AJB11.1930>
- Khan, A., Bashir, S., Khan S.R., & Gilani, A.H. (2011). Antiurolithic activity of *Origanum vulgare* is mediated through multiple pathways. *BMC Complementary and Alternative Medicine*, 11(1):96. <https://dx.doi.org/10.1186/1472-6882-11-96>
- Koseoglu, A., Taskin, T., Sadikoglu, N., & Bitis, L. (2016). Antioxidant Capacity of Methanol Extract of Turkish Endemic Species *Origanum haussknechtii*. *Chemistry*, 23, 289-292.
- Makrane, H., Aziz, M., Berrabah, M., Mekhfi, H., Ziyat, A., Bnouham, M., Legssyer, A., Elombo, F.K., Gressier, B., & Eto, B. (2019). Myorelaxant Activity of essential oil from *Origanum majorana* L. on rat and rabbit. *Journal of Ethnopharmacology*, 228, 40-49. <https://dx.doi.org/10.1016/j.jep.2018.08.036>
- Nausch, B., Heppner, T., & Nelson, T.M. (2010). Nerve-released acetylcholine contracts urinary bladder smooth muscle by inducing action potentials independently of IP3-mediated calcium release. *American Journal of Physiology-Regulatory, Integrative and Comparative Physiology*, 299, 878-888. <https://dx.doi.org/10.1152/ajp-regu.00180.2010>
- Ocak, I., Çelik, A., Özel, M.Z., Korcan, E., & Konuk, M. (2012). Antifungal Activity and Chemical Composition of Essential Oil of *Origanum Hypericifolium*. *International Journal of Food Properties*, 15, 38-48. <https://dx.doi.org/10.1080/10942911003687249>
- Ozcan, M., & Chalchat, J.C. (2009). Chemical composition and antimicrobial properties of the essential oil of *Origanum saccatum* L. *Journal of Food Safety*, 29, 617-628. <https://dx.doi.org/10.1111/j.1745-4565.2009.00181.x>
- Ponce-Monter, H., Pérez, S., Zavala, M., Pérez-González, C., Meckes, M., Macias, A., & Campos, M. (2006). Relaxant Effect of Xanthomicrol and 3 $\alpha$ -Angeloyloxy-2 $\alpha$ -hydroxy-13,14Z-dehydrocativic Acid from *Brickellia paniculata* on Rat Uterus. *Biological and Pharmaceutical Bulletin*, 29, 1501-1503. <https://dx.doi.org/10.1248/bpb.29.1501>
- Ratz, P., Berg, M.K., Urban, H.N., & Miner, A. (2005). Regulation of smooth muscle calcium sensitivity: KCl as calcium-sensitizing stimulus. *The American Journal of Physiology: Cell Physiology*, 288, 769-783. <https://dx.doi.org/10.1152/ajpcell.00529.2004>
- Taskin, T., Cam, M.E., Bulut, G., Hazar-Yavuz, A.N., Kabasakal, L., & Bitis, L. (2018). Antioxidant and anti-inflammatory activities of *Phlomis pungens* and *Coridothymus capitatus*. *Marmara Pharmaceutical Journal*, 22, 80-85. <https://dx.doi.org/10.12991/mpj.2018.44>
- Taskin, T., Cam, M.E., Taskin, D., & Rayaman, E.. (2019). *In vitro* and *In vivo* biological activities and phenolic characterization of *Thymus praecox* subsp. *skorpilii* var. *skorpilii*. *Journal of Food Measurement and Characterization*, 13, 536-544. <https://dx.doi.org/10.1007/s11694-018-9967-1>
- Tumen, G., Baser, K., Kirimer, N., & Ozek, T. (1995). Essential oil of *Origanum saccatum* PH Davis. *The Journal of Essential Oil Res*, 7, 175-176. <https://dx.doi.org/10.1080/10412905.1995.9698493>
- Van Den Broucke, C., Lemli, J. (1980). Antispasmodic activity of *Origanum compactum*. *Planta Medica*, 38, 317-331. <https://dx.doi.org/10.1055/s-2008-1074884>

# *In vitro* adenosine deaminase inhibitory activity of some selected plant extracts and chemical compounds

Aris Tercan<sup>1</sup> , Özlem Saçan<sup>1</sup> 

<sup>1</sup>Istanbul University-Cerrahpasa, Faculty of Engineering, Department of Chemistry, Avcilar, Istanbul, Turkey

**ORCID IDs of the authors:** A.T. 0000-0003-4805-5337; Ö.S. 0000-0001-6503-4613

**Cite this article as:** Tercan, A., & Saçan, O. (2020). *In vitro* adenosine deaminase inhibitory activity of some selected plant extracts and chemical compounds. *Istanbul Journal of Pharmacy*, 50 (3), 283-288.

## ABSTRACT

**Background and Aims:** Adenosine deaminase (EC 3.5.4.4, ADA) is distributed in all human tissues. It catalyses the deamination of adenosine (deoxyadenosine) to inosine (deoxyinosine) via removal of an amino group. The determination of ADA-inhibition is of extreme significance in the field of fundamental research and clinical diagnosis. In our study, the effects of various plant extracts and chemicals on ADA activity were investigated.

**Methods:** Adenosine deaminase activity was determined spectrophotometrically at 625 nm.

**Results:** The inhibitory activities of the extracts and chemical compounds increased in a dose-dependent manner. Among the plant extracts used, lemon extract was observed to exhibit the highest ADA inhibition activity with an  $IC_{50}$  value of  $0.05 \pm 0.001$  mg/mL, while quercetin had the highest ADA inhibition ( $IC_{50}$  value of  $0.004 \pm 0.0005$  mg/mL) among the chemical compounds. All plant extracts and chemical compounds showed ADA inhibition activities.

**Conclusion:** The obtained results indicate that plant extracts and some chemical compounds examined in this study can be a potential source of novel ADA-inhibitors for therapeutics.

**Keywords:** Adenosine deaminase, enzyme inhibition, plant extracts, chemical compounds

## INTRODUCTION

Cancer is a complicated disease that varies from one patient to another in terms of manifestation, development and outcomes. It is a multi-step process whereby cells undergo metabolic and behavioural changes leading to extreme and timeless proliferation, which escapes from the observation of the immune system, and which consequently leads to the invasion of distant tissues to form metastases (Markman & Shiao, 2015). Due to the increasing frequency of cancer and cancer related deaths, in addition to complications in cancer treatment, the presence of cancer-causing factors, and the need for social and psychological support, cancer is regarded as a major public health problem worldwide and its significance is increasing day by day.

The most important factors in the development of cancer include the use of tobacco and tobacco products, alcohol consumption, malnutrition, obesity, viruses, exposure to ionizing radiation, occupational diseases and environmental pollution (Soerjomataram et al., 2018). Different treatment modalities such as chemotherapy, radiotherapy, surgical methods, hormone therapy and biological methods have been the main methods of cancer treatment. (Zaigham & Sakina, 2018). Adenosine deaminase (EC 3.5.4.4, ADA), is distributed in all human tissues. It is a vital enzyme in intracellular and extracellular purine metabolism, and

### Address for Correspondence:

Özlem SAÇAN, e-mail: osacan@istanbul.edu.tr

Submitted: 14.01.2020  
Revision Requested: 26.02.2020  
Last Revision Received: 30.04.2020  
Accepted: 04.05.2020  
Published Online: 29.09.2020

This work is licensed under a Creative Commons Attribution 4.0 International License.



its primary function is the deamination of deoxyadenosine into deoxyinosine by removing an amino group (Dolezelova, Zurovec, Dolezal, Simek, & Bryant, 2005). It also plays an essential role in the maturation, function and maintenance of immunology response (Van der Weyden & Kelley, 1976; Fleischman et al., 1998). Accumulating evidences have proven that ADA deregulation or altered expression is closely related to many malignant diseases. For example, about 20% of severe combined immunodeficiency disease (SCID) cases are linked to ADA deficiency (Aiuti et al., 2009; Aldrich, Blackburn, & Kellems, 2000). By contrast, over-expression of ADA is a great potential cause of liver cancer, acute leukaemia, oesophagus tumors and so on (Hoffbrand & Janossy, 1981; Ibiş et al., 2007). Moreover, increased serum ADA activity is reported in laryngeal cancer (Canbolat, Akyol, Kavutcu, Isik, & Durak, 1994), head and neck cancer (Lal, Munjal, Wig, & Saini, 1987), breast cancer (Walia, Mahajan, & Singh, 1995) and lung cancer (Nishihara, Akedo, Okada, & Hattori, 1970). Plants have been used for therapeutic purposes for centuries. Their extracts exhibit protective effects due to abundance of secondary metabolites, therefore are potential sources of novel compounds for treatment of various diseases. As a consequence, the determination of ADA-inhibition potentials of plant extract is of extreme significance in fundamental research and clinical cancer therapy (Wang, Chen, Su, Wang, & Su, 2019).

In this study, we investigated adenosine deaminase activity of some selected plant extracts and chemical compounds.

## MATERIALS AND METHODS

### Preparation of aqueous extracts

Plants were collected from local markets in Istanbul. The plant materials were washed with distilled water and dried at room temperature. In the study, aqueous extracts of edible parts of plants were prepared. Dried plants (5 g) were extracted by adding distilled water and then they were boiled for 7 hours. The extracts were filtered and the filtrates were evaporated under reduced pressure using a rotary evaporator. These extracts were used in the experiment.

### Preparation of ADA homogenate

Mature male bovine liver was used as the source of ADA in the study. The collected liver was homogenized in phosphate buffer (pH=8.8) to make up a 10% (w/v) homogenate. The homogenate was employed in the ADA inhibitory assay.

### Adenosine deaminase inhibitory activity assay

Adenosine deaminase inhibition was performed according to the method of Blum and Schwedt (Blum & Schwedt, 1998). 1 mL of acetate buffer (pH=5.6) was added to each tube. Then 0.5 mL of inhibitor's solutions was added to the respective tube, followed by 0.1 mL of homogenate, and incubation at 25°C for 60 min. A 0.1 mL of adenosine as substrate was thereafter added to each tube, incubated for 30 min at 25°C, before addition of 1 mL of 1 M sodium hydroxide solution, 1 mL of phenol solution and 50 µL of hypochloric acid (HOCl). After incubation for 45 minutes at room temperature, absorbance was taken spectrophotometrically at 625 nm. In the control solution, distilled water was added in place of the inhibitor. *Erythro-*

9-(2-Hydroxy-3-nonyl)adenine hydrochloride EHNA was used as a standard compound. The inhibition ADA was calculated according to the following formula

$$\text{Inhibition (\%)} = \left[ \frac{A_c - A_n}{A_c} \right] \times 100$$

Where:  $A_c$  = Absorbance of control and  $A_n$  = Absorbance of test.

For ADA inhibitor activities, the results are given as half maximal inhibitory concentrations (IC<sub>50</sub> values) calculated regression prepared from the concentrations of samples.

## RESULTS

The ADA inhibitor activities of plant extracts and chemical compounds were found to increase in a dose dependent manner. A higher ADA inhibitor activity is associated with a lower IC<sub>50</sub> value. The IC<sub>50</sub> values of plant extracts and chemical compounds used in the ADA inhibition studies are presented in Table 1 and 2 respectively. For ADA, plant extract showed IC<sub>50</sub> values between 0.05±0.001 mg/mL 0.05±0.001 mg/mL and 22.02±0.40 mg/mL.

Among the plant extracts, lemon had the highest ADA inhibition activity resulting from its lowest IC<sub>50</sub> value of 0.05±0.001 mg/mL, followed by black grape (3.55±0.03 mg/mL), pomegranate (4.43±0.55 mg/mL), kiwi (5.11±0.02 mg/mL) and quince (6.37±0.17 mg/mL) respectively. The lowest ADA inhibition was observed in extract of grapefruit and red apple with an IC<sub>50</sub> of 22.02±0.40 mg/mL and 16.84±0.57 mg/mL respectively.

Among the chemical compounds used, quercetin exhibited the highest ADA inhibitor effect, with the lowest IC<sub>50</sub> value of 0.004±0.0005 mg/mL. This is followed by kaempferol, myristine and xanthine with IC<sub>50</sub> values of 0.06±0.003 mg/mL, 0.081±0.002 mg/mL and 0.14±0.005 mg/mL respectively. EHNA which was employed as the standard inhibitor had an IC<sub>50</sub> value of 6.38±1.13 mg/mL. Adenosine deaminase inhibitor activities of chemical compounds and standard compounds decreased in following order: Quercetin > kaempferol > myristicin > xanthine > guanine > adenine > AgNO<sub>3</sub> > CuSO<sub>4</sub>·7H<sub>2</sub>O > EHNA > biotin > vitamin U > guanosine > cytosine > uracil > allopurinol > nicotinamide > VOSO<sub>4</sub>·H<sub>2</sub>O > ZnSO<sub>4</sub>·7H<sub>2</sub>O.

## DISCUSSION

Inadequate physical activity, obesity, unbalanced nutrition, and alcohol and tobacco consumption are among the most common risk factors for cancer. These factors are considered to cause more than half of all cancers (Colditz & Wei, 2012). In addition, environment factors such as UV radiation, smoke and radon exposure increase the risk of cancer development. Some dietary foods may be protective, while others may increase the risk of cancer (Ozdemir, Serin, & Savas, 2018). Reports have shown that 70% of all cancers are linked or associated with nutritional habits, and an estimated 40% of cancer-related deaths (Willett, 2000). The leading methods in cancer treatment are chemotherapy,

**Table 1. Adenosine deaminase inhibitory activity of some selected aqueous plant extracts.**

Plant extract	Collected of plants	Concentration (mg/mL)	Inhibition (%)*	IC <sub>50</sub> (mg/mL)*
Black grape	Fruit	1	11.47±0.93	3.55±0.03
		1.5	21.64±2.32	
		2	28.17±0.70	
		2.5	33.58±0.09	
Black radish	Root	5	26.77±2.11	10.73±0.32
		10	43.94±1.62	
		15	70.72±0.38	
		20	88.63±0.75	
Cabbage	Vegetables	10	51.78±2.74	9.48±1.10
		12.5	56.49±3.42	
		15	65.81±1.01	
		20	79.56±1.55	
Grapefruit	Fruit	10	16.84±0.66	22.02±0.40
		15	25.22±0.80	
		20	42.89±4.81	
		25	60.87±1.41	
Green apple	Fruit	5	19.59±0.43	12.28±0.19
		10	37.93±1.56	
		15	54.10±1.26	
		20	92.71±0.43	
Kiwi	Fruit	1	19.46±1.47	5.11±0.02
		2	27.27±1.85	
		3	34.49±0.55	
		4	41.60±0.30	
Lemon	Fruit	0.0001	8.73±1.25	0.049±0.001
		0.001	18.20±1.47	
		0.01	36.04±4.33	
		0.5	47.60±0.34	
Pear	Fruit	5	12.65±2.16	14.66±0.51
		10	29.82±4.32	
		15	56.68±1.16	
		20	67.58±1.41	
Persimmon	Fruit	5	39.75±3.25	7.89±0.93
		10	56.28±4.07	
		15	77.18±1.59	
		20	89.54±0.61	
Pomegranate	Fruit	0.5	16.05±8.30	4.43±0.55
		1.5	24.47±3.20	
		2	33.95±4.95	
		5	53.64±4.35	
Quince	Fruit	2.5	17.28±0.71	6.37±0.17
		5	31.92±2.11	
		7.5	50.33±0.79	
		10	54.55±2.08	
Red apple	Fruit	5	18.98±0.38	16.84±0.57
		10	33.00±1.22	
		15	50.33±0.79	
		20	54.55±2.08	
Red radish	Root	5	5.80±1.76	12.50±0.36
		10	30.51±3.10	
		15	70.97±3.68	
		20	92.58±0.17	
White grape	Fruit	5	31.33±0.28	7.35±0.17
		7.5	53.36±2.69	
		10	71.67±0.37	
		15	90.77±0.25	

\*Mean ± SD

**Table 2. Adenosine deaminase inhibitory activities of some chemical compounds.**

Chemical compounds and standard	Concentration (mg/mL)	Inhibition (%)*	IC <sub>50</sub> (mg/mL)*
Allopurinol	12.5	19.86±1.75	42.14±2.25
	25	44.25±7.19	
	50	67.99±2.85	
	100	79.68±1.88	
Adenine	25	40.05±0.74	4.43±3.01
	50	56.86±1.68	
	75	64.33±1.44	
	100	70.11±3.39	
AgNO <sub>3</sub>	2	5.09±0.71	4.55±0.12
	3	21.73±1.41	
	4	40.70±4.44	
	5	57.86±0.90	
Biotin	1	9.85±1.22	7.75±0.24
	5	33.56±2.15	
	7.5	53.60±0.95	
	10	59.69±1.56	
CuSO <sub>4</sub> .7H <sub>2</sub> O	1	11.71±0.69	5.49±0.13
	2	25.17±1.44	
	3	36.63±1.77	
	6	51.30±0.90	
Cytosine	1	22.25±1.30	14.60±0.75
	5	30.28±2.78	
	10	44.33±1.06	
	25	69.20±1.22	
Guanine	0.1	8.23±2.18	4.29±0.28
	1	33.01±0.89	
	5	62.79±2.49	
	10	88.05±0.56	
Guanosine	0.1	10.50±1.59	11.08±0.99
	1	18.61±1.97	
	5	34.03±2.41	
	10	44.34±3.24	
Kaempferol	0.001	13.70±1.83	0.06±0.003
	0.01	32.99±2.65	
	0.05	52.87±0.81	
	0.1	60.49±1.30	
Myrisitine	0.001	5.23±1.72	0.081±0.002
	0.01	20.31±1.17	
	0.05	40.15±1.77	
	0.1	55.63±0.77	
Nicotinamide	2.5	4.92±1.47	92.45±4.43
	5	20.88±1.47	
	10	37.38±5.24	
	100	51.38±1.30	
Quercetin	0.05	57.71±1.07	0.004±0.0005
	0.1	65.84±0.94	
	0.5	74.38±1.88	
	1	85.90±0.47	
Uracil	5	31.95±3.18	16.17±2.17
	10	48.07±0.53	
	25	66.31±3.03	
	50	76.71±0.77	
Xanthine	0.001	4.04±0.64	0.14±0.005
	0.01	9.64±0.45	
	0.05	25.67±0.68	
	0.1	34.82±2.33	



**Table 2. Continued.**

<b>Vitamin U</b>	5	29.80±1.88	
	10	58.64±1.50	10.44±1.34
	25	77.04±0.80	
	50	88.00±1.71	
<b>VOSO<sub>4</sub>·H<sub>2</sub>O</b>	250	26.88±4.79	628.14±48.50
	500	49.34±3.61	
	750	58.67±0.84	
	1000	64.55±0.92	
<b>ZnSO<sub>4</sub>·7H<sub>2</sub>O</b>	500	12.39±1.15	5074.60±70.00
	1000	23.24±1.53	
	2000	27.78±0.47	
	3000	33.33±0.35	
<b>EHNA (Standard)</b>	0.01	9.33±0.59	6.38±1.13
	0.1	32.31±0.89	
	1	47.52±1.31	
	10	69.20±1.22	

\*Mean ± SD

radiotherapy and surgical operations (Arruebo et al., 2011). Nevertheless, hormone therapy as well as biological methods can be employed as a support to these main methods (Portenoy & Ahmed, 2018). Despite advances in cancer treatment and use of these methods, challenges still exist. These challenges are due to individual variations, existence of variant forms of a cancer, requirements for modified treatment protocols, and nonexistence of an established single clear-cut standard procedure for treatment of all cancers types (Russo & Sundaramurthi, 2019). For this reason, complementary and alternative treatment methods are necessary and significant besides main treatment methods. In this research, the effects of some plant extracts and chemical compounds on the activity of adenosine deaminase, which is found in virtually all the human tissues and plays a vital role in purine metabolism as well as development and maintenance of the immune system, were investigated.

Citruses are rich sources of vitamin C. In addition they are cheap sources of folic acid, potassium, pectin and a wide range of active phytochemical substances that can protect cells or tissues and improve wellbeing. Lemon has an important place among citrus fruits owing to its high content of vitamin C, its antioxidant activity and phenolic contents (Proteggente, Saija, De Pasquale, & Rice-Evans, 2003; Gorinstein et al., 2004; Anagnostopoulou, Kefalas, Papageorgiou, Assimopoulou, & Boskou, 2006; Guimarães et al., 2009). Citrus fruits are reported to exhibit a wide range of pharmacological properties including antiatherogenic, antiinflammatory, anti-tumor, antithrombotic as well as antioxidant activity (Alu'datt et al., 2017; Asencio et al., 2018; Musumeci et al., 2020). It is suggested that flavonoid compounds in citrus fruits (such as quercetin, myricetin and kaempferol and their derivatives) are responsible for an inhibitory effect on ADA activity, as well as *in vivo* modulation of hepatic lipid metabolism (Cha et al., 2001). A study by Arun et al., reported that hibifolin molecule (a flavonoid type substance) inhibited ADA activity (Arun et al., 2016). The high ADA inhibitory potential of lemon (IC<sub>50</sub> value

of 0.050±0.001 mg/mL) observed in this study may be attributed to the aforementioned flavonoids present in lemon fruit extract. On the other hand, quercetin followed by kaempferol (IC<sub>50</sub>=0.004±0.0005 mg/mL and 0.06±0.003 mg/mL respectively) which have been previously reported to be present in citrus extract had the highest inhibitory effect on ADA activity when compared to other chemical substances used in this study. Therefore, a strong correlation exists between these flavonoids and the high ADA inhibitory action of lemon extract.

## CONCLUSION

It can be concluded that the consumption of quercetin and kaempferol rich fruits/foods such as lemons may serve as a potential source of ADA inhibitor and ultimately affect purine metabolism as well as the maintenance of the immune system in cancer patients.

**Peer-review:** Externally peer-reviewed.

**Author Contributions:** Conception/Design of Study- Ö.S.; Data Acquisition- Ö.S., A.T.; Data Analysis/Interpretation- Ö.S., A.T.; Drafting Manuscript- Ö.S., A.T.; Critical Revision of Manuscript-Ö.S.; Final Approval and Accountability- Ö.S., A.T.

**Conflict of Interest:** The authors have no conflict of interest to declare.







**Financial Disclosure:** Authors declared no financial support.

## REFERENCES

- Aiuti, A., Cattaneo, F., Galimberti, S., Benninghoff, U., Cassani, B., Callegaro, L., ... Roncarolo, M. G. (2009). Gene therapy for immunodeficiency due to adenosine deaminase deficiency. *New England Journal of Medicine*, 360, 447–458. <https://www.nejm.org/doi/full/10.1056/NEJMoa0805817>
- Aldrich, M. B., Blackburn, M. R., & Kellems, R. E. (2000). The importance of adenosine deaminase for lymphocyte development and function. *Biochemical and Biophysical Research Communications*, 72, 311–315. <https://doi.org/10.1006/bbrc.2000.2773>

- Alu'datt, M. H., Rababah, T., Alhamad, M. N., Al-Mahasneh, M. A., Ereifej, K., Al-Karak, G., ... Ghozlana, K. A. (2017). Profiles of free and bound phenolics extracted from *Citrus* fruits and their roles in biological systems: content, and antioxidant, anti-diabetic and anti-hypertensive properties. *Food and Function*, 8, 3187–3197. <https://doi.org/10.1039/C7FO00212B>
- Anagnostopoulou, M. A., Kefalas, P., Papageorgiou, V. P., Assimopoulou, A. N., & Boskou, D. (2006). Radical scavenging activity of various extracts and fractions of sweet orange flavedo (*Citrus sinensis*). *Food Chemistry*, 94, 19–25. <https://doi.org/10.1016/j.foodchem.2004.09.047>
- Arruebo, M., Viláboa, N., Sáez-Gutierrez, B., Lambea, J., Tres, A., Val-ladares, M., & González-Fernández, A. (2011). Assessment of the evolution of cancer treatment therapies. *Cancers*, 3, 3279–3330. <http://dx.doi:10.3390/cancers3033279>
- Arun, K. G., Sharanyaa, C. S., Sandeepa, P. M., & Sadasivana, C. (2016). Inhibitory activity of hibifolin on adenosine deaminase-experimental and molecular modeling study. *Computational Biology and Chemistry*, 64, 353–358. <https://doi.org/10.1016/j.compbiolchem.2016.08.005>
- Asencio, A. D., Serrano, M., Garcia-Martinez, S., & Pretel, M. T. (2018). Organic acids, sugars, antioxidant activity, sensorial and other fruit characteristics of nine traditional Spanish *citrus* fruits. *European Food Research and Technology*, 244, 1497–1508. <https://doi.org/10.1007/s00217-018-3064-x>
- Blum, U., & Schwedt, G. (1998). Inhibition behavior of phosphatase, phosphodiesterase I and adenosine deaminase as tools for trace metal analysis and speciation. *Analytica Chimica Acta*, 360, 101–108. [https://doi.org/10.1016/S0003-2670\(97\)00717-4](https://doi.org/10.1016/S0003-2670(97)00717-4)
- Canbolat, O., Akyol, O., Kavutcu, M., Isik, A. Ü., & Durak, I. (1994). Serum adenosine deaminase and total superoxide dismutase activities before and after surgical removal of cancerous laryngeal tissue. *Journal of Laryngology and Otolaryngology*, 108, 849–851. <https://doi.org/10.1017/S0022215100128300>
- Colditz, G. A., & Wei, E. K. (2012). Preventability of cancer: The relative contributions of biologic and social and physical environmental determinants of cancer mortality. *Annual Review and Public Health*, 33, 137–156. <https://www.annualreviews.org/doi/abs/10.1146/annurev-publhealth-031811-124627>
- Cha, J. Y., Cho, Y. S., Kim, I., Anno, T., Rahman, S. M., & Yanagita, T. (2001). Effect of hesperitin, a citrus flavonoid, on the liver triacylglycerol content and phosphatidate phosphohydrolase activity in orotic acid-fed rats. *Plant Foods for Human Nutrition*, 56, 349–358. Retrieved from <https://www.ncbi.nlm.nih.gov/pubmed/11678440>
- Dolezelova, E., Zurovec, M., Dolezal, T., Simek, P., & Bryant, P. J. (2005). The emerging role of adenosine deaminases in insects. *Insect Biochemistry and Molecular Biology*, 35, 381–389. <https://doi.org/10.1016/j.ibmb.2004.12.009>
- Fleischman, A., Hershfield, M. S., Toutain, S., Lederman, H. M., Sullivan, K. E., Fasano, M. B., ... Winkelstein, J. A. (1998). Adenosine deaminase deficiency and purine nucleoside phosphorylase deficiency in common variable immunodeficiency. *Clinical and Diagnostic Laboratory Immunology*, 5, 399–400. Retrieved from <https://www.ncbi.nlm.nih.gov/pmc/articles/PMC104530>
- Gorinstein, S., Cvikrova, M., Machackova, I., Haruenkit, R., Park, Y. S., Jung, S. T., ... Trakhtenberg, S. (2004). Characterization of antioxidant compounds in Jaffa sweets and white grapefruits. *Food Chemistry*, 84, 503–510. [https://doi.org/10.1016/S0308-8146\(03\)00127-4](https://doi.org/10.1016/S0308-8146(03)00127-4)
- Guimarães, R., Barros, L., Barreira, J. C. M., Sousa, M. J., Carvalho, A. M., & Ferreira, I. C. F. R. (2009). Targeting excessive free radicals with peels and juices of citrus fruits: grapefruit, lemon, lime and orange. *Food and Chemical Toxicology*, 48, 99–106. <https://doi.org/10.1016/j.fct.2009.09.022>
- Hoffbrand, A. V., & Janossy, G. (1981). Enzyme and membrane markers in leukaemia: recent developments. *Journal of Clinical Pathology*, 34, 254–262. Retrieved from <https://jcp.bmj.com/content/34/3/254>
- İbiş, M., Koklu, S., Yilmaz, F. M., Basar, O., Yilmaz, G., Yuksel, O., ... Ozturk, Z. A. (2007). Serum adenosine deaminase levels in pancreatic diseases. *Pancreatology*, 7, 526–530. <https://doi.org/10.1159/000108970>
- Lal, H., Munjal, S. K., Wig, U., & Saini, A. S. (1987). Serum enzymes in head and neck cancer III. *Journal of Laryngology and Otolaryngology*, 101, 1062–1065. <https://doi.org/10.1017/S0022215100103226>
- Markman, J. L., & Shiao, S. L. (2015). Impact of the immune system and immunotherapy in colorectal cancer. *Journal of Gastrointestinal Oncology*, 6(2), 208–223. <https://doi.org/10.3978/j.issn.2078-6891.2014.077>
- Musumeci, L., Maugeri, A., Cirmi, S., Lombardo, G. E., Russo, C., Gangemi, S., ... Navarra, M. (2020). Citrus fruits and their flavonoids in inflammatory bowel disease: an overview. *Natural Product Research*, 34, 122-136. <https://doi.org/10.1080/14786419.2019.1601196>
- Nishihara, H., Akedo, H., Okada, H., & Hattori, S. (1970). Multienzyme patterns of serum adenosine deaminase by agar gel electrophoresis: an evaluation of the diagnostic value in lung cancer. *Clinica Chimica Acta*, 30, 251–258. [https://doi.org/10.1016/0009-8981\(70\)90110-5](https://doi.org/10.1016/0009-8981(70)90110-5)
- Ozdemir, A., Kaplan Serin, E., & Savas, M. (2018). Cancer risk factors and prevention in Turkey. *International Journal of Health Services Research and Policy*, 3, 143-150. <https://doi.org/10.23884/ijhsrp.2018.3.3.06>
- Portenoy, R. K., & Ahmed, E. (2018). Cancer pain syndromes. *Hematology / Oncology Clinics*, 32, 371–386. <https://doi.org/10.1016/j.hoc.2018.01.002>
- Proteggente, A. R., Saija, A., De Pasquale, A., & Rice-Evans, C. A. (2003). The compositional characterisation and antioxidant activity of fresh juices from Sicilian sweet orange (*Citrus sinensis* L. Osbeck) varieties. *Free Radical Research*, 37, 681–687. <https://doi.org/10.1080/1071576031000083198>
- Russo, M. M., & Sundaramurthi, T. (2019). An overview of cancer pain: Epidemiology and pathophysiology. *Seminars in Oncology Nursing*, 35, 223–228. <https://doi.org/10.1016/j.soncn.2019.04.002>
- Soerjomataram, I., Kevin Shield, K., Marant-Micallef, C., Vignat, J., Hill, C., Rogel, A., ... Bray, F. (2018). Cancers related to lifestyle and environmental factors in France in 2015. *European Journal of Cancer*, 105, 103–113. <https://doi.org/10.1016/j.ejca.2018.09.009>
- Van der Weyden, M. B., & Kelley, W. N. (1976). Human adenosine deaminase. *Journal of Biological Chemistry*, 251(18), 5448–5456. Retrieved from <https://www.jbc.org/content/251/18/5448>
- Walia, M., Mahajan, M., & Singh, K. (1995). Serum adenosine deaminase, 5'-nucleotidase & alkaline phosphatase in breast cancer patients. *The Indian Journal of Medical Research*, 101, 247–249. Retrieved from <https://europepmc.org/article/med/7672835>
- Willett W. C. (2000). Diet and cancer. *The Oncologist*, 5, 393–404. <https://doi.org/10.1634/theoncologist.5-5-393>
- Wang, M., Chen, J., Su, D., Wang, G., & Su, X. (2019). Split aptamer based sensing platform for adenosine deaminase detection by fluorescence resonance energy transfer. *Talanta*, 198, 1–7. <https://doi.org/10.1016/j.talanta.2019.01.041>
- Zaigham, A., & Sakina, R. (2018). An overview of cancer treatment modalities. In HN Shahzad (Ed.), *Neoplasm* (pp 139-157), London, UK: Intechopen Ebook Press.

# Investigation of *in vitro* anti-hyperpigmentation, antidiabetic, neuroprotective and antioxidant potential of *Medicago murex* Willd. (Fabaceae)

Damla Pamukcu<sup>1</sup> , Volkan Aylanc<sup>2</sup> , Bülent Eskin<sup>3</sup> , Gökhan Zengin<sup>4</sup> , Mehmet Dursun<sup>5</sup> ,  
Yavuz Selim Çakmak<sup>6</sup> 

<sup>1</sup>Aksaray University, Faculty of Science and Arts, Department of Biotechnology and Molecular, Aksaray, Turkey

<sup>2</sup>Centro de Investigação de Montanha (CIMO), Instituto Politécnico de Bragança, Bragança, Portugal

<sup>3</sup>Aksaray University, Faculty of Science and Arts, Department of Biotechnology and Molecular, Aksaray, Turkey

<sup>4</sup>Selçuk University, Faculty of Science, Department of Biology, Konya, Turkey

<sup>5</sup>Montana State University, Collage of Letter and Science, Department of Microbiology and Immunology, Bozeman Montana, USA

<sup>6</sup>Aksaray University, Faculty of Science and Arts, Department of Biotechnology and Molecular, Aksaray, Turkey

**ORCID IDs of the authors:** D.P. 0000-0001-5819-7449; V.A. 0000-0003-4060-766X; B.E. 0000-0002-7990-4138; G.Z. 0000-0001-6548-7823; M.D. 0000-0002-8214-4942; Y.S.Ç. 0000-0001-8954-5485

**Cite this article as:** Pamukcu, D., Aylanc, V., Eskin, B., Zengin, G., Dursun, M., & Çakmak, Y. S. (2020). Investigation of *in vitro* anti-hyperpigmentation, antidiabetic, neuroprotective and antioxidant potential of *Medicago murex* Willd. (Fabaceae). *Istanbul Journal of Pharmacy*, 50 (3), 289-293.

## ABSTRACT

**Background and Aims:** Most of the *Medicago* species are considered good quality forage crops due to their rich protein content. This study reports antioxidant properties, total phenolic and flavonoid content, enzyme (acetylcholinesterase (AChE), tyrosinase,  $\alpha$ -amylase and  $\alpha$ -glucosidase) inhibition activities of methanol (MeOH), ethyl acetate (EA) and, aqueous (AQ) extracts of *Medicago murex* (*M. murex*).

**Methods:** The antioxidant activity of the different extracts of *M. murex* were evaluated using FRAP and CUPRAC assays. The contents of total phenolic and flavonoid were determined by the Folin-Ciocalteu and the Aluminium chloride (AlCl<sub>3</sub>) colorimetric methods. Also, the enzyme inhibition activities were shown spectrophotometrically for AChE,  $\alpha$ -amylase,  $\alpha$ -glucosidase and tyrosinase enzymes.

**Results:** Total phenolic and flavonoid contents of different extracts were determined between 83.70-163.93 mg GAE/g extract and 24.48-26.05  $\mu$ g QE/g extract, respectively. AQ extracts were the most active extracts in FRAP while being the best inhibitor of the AChE enzyme. On the other hand, EA extracts were the most active extracts in CUPRAC methods and the best inhibitors for other enzymes.

**Conclusion:** Considering the findings, *M. murex* appears to be an important source of natural antioxidants and enzyme inhibitors, and it provides important baseline data for the food and pharmaceutical industries.

**Keywords:** *M. murex*, bioactive substances content, antioxidant potential, enzyme inhibition

## Address for Correspondence:

Yavuz Selim ÇAKMAK, e-mail: yavuzselimcakmak@gmail.com;  
cakmakys@aksaray.edu.tr

Submitted: 02.05.2020  
Revision Requested: 06.07.2020  
Last Revision Received: 15.07.2020  
Accepted: 30.07.2020

## INTRODUCTION

Plants have been used for therapeutic purposes throughout history. There has been an increasing interest in bioactive compounds from the plant kingdom recently because they have fewer side effects, are cheaper than general synthetic drugs, and influence the production of free radicals (Martins, Barros & Ferreira, 2016). Apart from these facts, bioactive compounds have been reported to have protecting effects against extensive dietary-related diseases, including cancer, obesity, cardiovascular diseases, diabetes and various inflammatory conditions (Quideau, Deffieux, Douat-Casassus, & Pouységu, 2011).

*Medicago* spp., a member of the family Fabaceae, is one of the important forage plants around the world with economic value and includes 87 flowering plant species, some of which are consumed by humans (Gholami, De Geyter, Pollier, Goormachtig & Goossens, 2014). *Medicago* species synthesize various natural bioactive products to maintain symbiotic interactions and at the same time to deter pathogens and herbivores (Ghimire, Ghimire, Yu, & Chung, 2019). These products are most of the time natural bioactive compounds with a functional nutrient source and promising pharmaceutical properties for humans. *Medicago* species are traditionally consumed as salads, sandwiches, soups and tisane (Takyi, Kido, Rikimaru, & Kennedy, 1992), and also its leaves are used to reduce cholesterol level (Mølgaard, von Schenck, & Olsson, 1987). Despite these uses, *Medicago* spp. has been practiced in health problems, including diabetes, gastric ulcer, cancer and menopause symptoms due to its different therapeutic effects (Mortensen et al., 2009).

*Medicago* spp. contain bioactive compounds like flavonoids, ligands, carotenoids and phenolic acids that have beneficial effects on health (Xu et al., 2017). Especially are a major group of phenolic compounds and there is a great interest in these compounds because of their strong antioxidant activity against oxidative stress. Recently, some studies have identified the relationship between these compounds and cancer risk (Sudhakaran, Sardesai, & Doseff, 2019).

*M. murex* is a member of the *Medicago* genus and is an annual legume of Mediterranean origin, usually grown in acidic soils. It is also an important grazing plant that is commonly seen in the pastures and is widely distributed from the Mediterranean to Central Asia (Francis & Gillespie, 1981). Studies on *Medicago* spp. generally focus on Alfalfa (*Medicago sativa* L.). Other *Medicago* species, including *M. murex* have been ignored. The studies on *M. murex* are generally limited to molecular cytogenetics, phylogenetics, morphology and geographical distribution (Gillespie & McComb, 1991). In this study, *M. murex* plant was chosen as a bioactive compound source for the following reasons; i) easy cultivation, ii) worldwide distribution, and iii) used as a functional food in different countries. This research is the first study to reveal the therapeutic properties of *M. murex* such as anti-hyperpigmentation, antidiabetic, neuroprotective and antioxidant. The aim of this study was to investigate the antioxidant properties, enzyme inhibition activities and phenolic composition of different extracts of *M. murex* and to evaluate the potential of this species for food and pharmacology industries.

## MATERIALS AND METHODS

### Plant material

Aerial parts of *M. murex* were collected from Kargin Village (Aksaray-Turkey) in the vegetation period in February 2015 and were identified by botanist experts, Assist. Prof. Dr. Bulent Eskin and Dr. Mustafa Keskin. A voucher specimen (No. (AKSU) BE-2226) has been deposited at Aksaray University Herbarium, Turkey.

### Preparation of extracts

For the extraction process of plant samples, the aerial parts of *M. murex* samples were dried at room temperature and weighed at 15 g each in order to make MeOH, EA and AQ extracts. MeOH and EA extracts were subjected to extraction using a Soxhlet apparatus for 6-8 h. AQ extract was carried out by steeping in boiling water for 30 min. After that, the extracts were filtered and evaporated. Total yields of dried samples were calculated and stored at -20 °C until analysis. Stock solutions were prepared from these extracts at a concentration of 2 mg/mL prior to analysis.

### Profile of bioactive compounds

The content of two major groups of bioactives; phenols (TPC) and flavonoids (TFC) in obtained extracts was determined by using spectrophotometric methods. Expression of obtained results was done by equivalents of standards - gallic acid (TPC) and quercetin (TFC) (Uysal et al., 2017).

### Determination of enzyme inhibition and antioxidant activity

The polarity and chemical properties of different solvents are known to affect the solubility of bioactive compounds. Therefore, solvents with different polarities (AQ (high polarity) > MeOH (less polar than AQ) > EA (moderately polar) were preferred. Potential biological activities of the obtained extracts with different solvents were performed: antioxidant, anti- $\alpha$ -amylase, anti- $\alpha$ -glucosidase, anti-AChE and anti-tyrosinase activity assays. Estimation of anti-enzymatic activity of the extracts was done by *in vitro* assays previously described by Uysal et al. (2017). The enzyme inhibitory actions of extracts were assessed as equivalents of kojic acid (KAE) for tyrosinase, galantamine for AChE and acarbose for  $\alpha$ -amylase and  $\alpha$ -glucosidase.

Antioxidant activity of different extracts was measured by ferric ion reducing antioxidant power (FRAP) and cupric ion reducing antioxidant capacity (CUPRAC) assays. Detailed description of applied assays were given previously (Uysal et al., 2017). The findings were given as standard compounds equivalent of Trolox (TE/g). The assay methods were given in our earlier work.

### Statistical analysis

All analyses were performed in triplicate and the obtained results were expressed as mean  $\pm$  standard deviation (SD). The obtained data was analysed using SPSS 26 software (Chicago, IL, USA). One-way analysis of variance was conducted to see whether there is a statistical significance.  $p < 0.05$  was considered as significant.

## RESULTS AND DISCUSSION

### Total phenolic and flavonoid content

Phenol or polyphenol substances can be defined as chemical plant components containing a phenolic ring in structure. Ac-

According to the results given in Table 1, the TPC of the extracts of the plant were found to vary between 83.70 and 163.93 mg GAE/g extract. The highest phenolic content was seen in AQ extract followed by MeOH and EA extract. In previous studies on *Medicago* species Kicel & Olszewska (2015) showed that the TPC of different fractions obtained from *M. lupulina* were between 6.6 and 162.4 mg GAE and, while Çakmak et al. (2017) found the TPC of *M. rigidula* as 79.61 mg GAE. Based on the studies reported in the literature, different or same *Medicago* species may have different rates of phenolic substance content depending on different factors such as geographical area, climate or genetics (Baiano, Terracone, Viggiani, & Del Nobile, 2013).

The TFC of three different extracts of *M. murex* was determined by using the  $AlCl_3$  colorimetric method. As stated in Table 1; the highest TFC was found in MeOH extract (26.05 µg QE/g) and also no flavonoid content was detected in EA extract. This may be due to the flavonoid compounds with different chemical properties and polarities that can be dissolved or insoluble in the *M. murex* plant in moderately polar solvents like EA. Besides, parameters such as the type of plant, the chemical nature of the extractable bioactive compounds and the solubilizing effect of solvents may affect the obtaining of phenolics from extracts (Adaramola & Onigbinde, 2016).

In a study on *M. rigidula*, the TFC of the plant was 27.38 µg QE/g extract (Çakmak et al., 2017). Rodrigues et al. (2013) investigated the TPC and TFC of some *Medicago* species and found that TFC ranged from 5.54 to 11.67 mg CEQ/g db. In the present study, considering the TFC being found in different extracts, one could conclude that *M. murex* contains a good amount of flavonoids. Besides that, no statistically significant correlation was found between TPC and TFC in the statistical analysis performed.

### Antioxidant activity

In the present study, the FRAP results of the different extracts obtained from *M. murex* are given in Table 1 as equivalent to Trolox. The iron-reducing antioxidant power of extracts was found quite close to each other, and for MeOH, EA and AQ were measured as 81.94, 85.81 and 91.41 mg TE/g, respectively. A previously reported study, FRAP test was applied to the MeOH extract of *M. lupulina*, and it was observed that MeOH extract had 0.2 mmol  $Fe^{+2}$ /g dry extract activity but when Trolox and quercetin used as a standard were found as 9.2 and 36.7 0.2 mmol  $Fe^{+2}$ /g dry extract activity (Kicel & Olszewska,

2015). In another study investigating different *Medicago* species, the highest FRAP activity (with 120.84 µmol TE/g) was determined in *M. segitalis*, while the lowest FRAP activity (with 58.05 µmol/g) was determined in *M. minima* (Rodrigues et al., 2013). Also, a correlation analysis was conducted between FRAP and TPC/TFC of *M. murex* extracts in this study. Based on the obtained results, there is a strong correlation between FRAP and TPC and TFC. In the previously reported studies, it was mentioned that there is a correlation between total phenolic and flavonoid substance and FRAP (Babbar, Oberoi, Upal, & Patil, 2011).

The results of the applied CUPRAC test to determine the reducing power of copper ions are given in Figure 1. Accordingly, at the highest concentration (400 µg/mL), the EA extract had an absorbance of 0.510 abs, followed by MeOH (0.358 abs) and AQ extract (0.313 abs). In a study on *M. rigidula*, it was found that the absorbance values vary between 0.058 to 0.733 in the same concentration range (50, 100, 200 and 400 µg/ml) (Çakmak et al., 2017). There was a correlation between TPC and CUPRAC in our study based on the statistical evaluation of obtained results, as some authors have previously stated (Fidriany, Budiana, & Ruslan, 2015). Besides, a strong correlation was determined between TFC and CUPRAC, and it was observed that the correlation coefficient decreased when copper ions concentration increases:  $r = 0.997$ ,  $r = 0,424$ ,  $r = 0,321$  and  $r = 0,218$  correlation coefficients were obtained for 50, 100, 200 and 400 of CUPRAC concentrations, respectively.

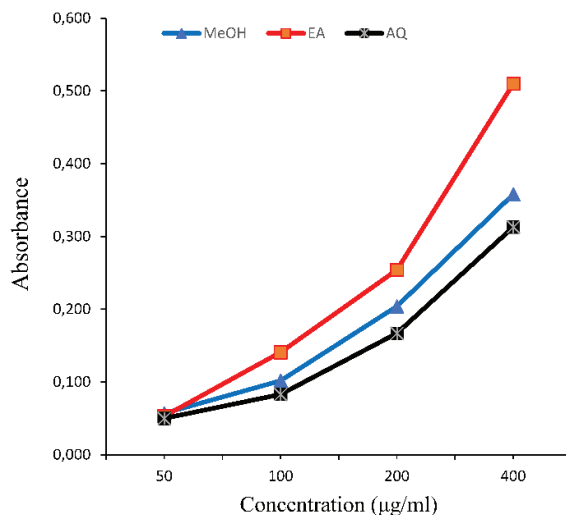


Figure 1. Cupric ion reducing power activity of *M. murex*.

**Table 1. The TPC, TFC and FRAP activity of different extracts obtained from *M. murex*.**

Extracts	Yield (%)	TPC <sup>a</sup> (mg GAE/g)	TFC <sup>b</sup> (µg QE/g)	FRAP <sup>c</sup> (mg TE/g)
MeOH	12.09	95.98±0.64*	26.05±2.16	81.94±1.74
EA	3.77	83.70±3.36	-	85.81±0.05
AQ	11.80	163.93±0.64	24.48±0.35	91.41±2.22

<sup>a</sup> TPC expressed as gallic acid equivalent (mg GAE g<sup>-1</sup> extract);  
<sup>b</sup> TFC expressed as quercetin equivalents (µg QE g<sup>-1</sup> extract);  
<sup>c</sup> FRAP expressed as trolox equivalents (mg TE g<sup>-1</sup> extract); \* Values expressed are means ± S.D. of three parallel measurements.

### Enzyme inhibitory effects

Metabolic diseases are among the most common diseases, especially diabetes, Alzheimer's disease (AD) or skin pigmentation disorders and enzyme inhibition studies are a novel and up-to-date alternative in the treatment of these diseases (Zengin et al., 2019). Therefore, potential enzyme inhibitor research of phytochemicals in plants is becoming more common. In this study, MeOH, EA and AQ extracts of *M. murex* were



**Table 2. Enzyme inhibitory potentials of *M. murex*.**

Extracts	AChE Inhibition (mg GALAE/g extract)	$\alpha$ -Amylase Inhibition (mmol ACAE/g extract)	$\alpha$ -Glucosidase Inhibition (mmol ACAE/g extract)	Tyrosinase Inhibition (mg KAE/g extract)
MeOH	1.84±0.06	0.82±0.03	4.28±0.31	17.92±0.18
EA	1.17±0.14	1.01±0.02	6.34±0.17	28.29±1.02
AQ	2.02±0.16	0.41±0.02	2.70±0.16	4.23±0.56

Values expressed are means  $\pm$  S.D. of three parallel measurements. GALAE: Galantamine equivalent; ACAE: Acarbose equivalent; KAE: Kojic acid equivalent.

investigated to evaluate for potential inhibitory activity against key enzymes related to diabetes, AD and hyperpigmentation problems and the obtained results are given in Table 2.

Control of AD is largely dependent on the inhibition of AChE. The AChE is the principal therapeutic target in the treatment of AD because of its ability to hydrolyse neurotransmitter acetylcholine. The elevation of AChE causes acetylcholine deficiency in the brain and hence, inhibition of AChE plays an important role in alleviating the symptoms of AD (Hassan, Raza, Abbasi, Moustafa, & Seo, 2019). Based on our findings, the highest activity in AChE enzyme inhibition was found in AQ extract (2.02 mg GALAE/g) and the lowest value was found in EA extract (1.17 mg GALAE/g). Also, all three extracts were found to be active against AChE.

The  $\alpha$ -amylase and  $\alpha$ -glucosidase enzymes, which are effective on glucose metabolism, showed inhibition activity as 1.01 mmol ACAE/g and 6.34 mmol ACAE/g extract, respectively, and the highest ratio was observed in EA extract for both enzymes.  $\alpha$ -amylase and  $\alpha$ -glucosidase are carbohydrate hydrolysing enzymes and inhibition of both enzymes has a considerable role in the regulation of hyperglycemia. Nowadays, hypoglycemic drugs have many side effects, including gastrointestinal disorders. Excessive  $\alpha$ -amylase inhibition has been found to disrupt the normal digestion process and cause different gastrointestinal problems such as bloating, diarrhea, and abdominal pain (Alam, Shafique, Amjad, & Bin Asad, 2019). While the tested extracts showed a weak activity on the  $\alpha$ -amylase enzyme, they showed a moderate activity on the  $\alpha$ -glucosidase enzyme. At the same time,  $\alpha$ -amylase enzyme inhibition activities were found to be statistically significant ( $p < 0.05$ ) with both TPC and TFC. In a study on the enzyme inhibition in MeOH extract of *M. rigidula*, AChE, amylase,  $\alpha$ -glucosidase and tyrosinase enzyme inhibitions were determined as 2.05 mg GALAE/g, 0.73 mmol ACAE/g, 1.30 mmol ACAE/g and 16.36 mg KAE/g extract, respectively (Çakmak et al., 2017).

Hyperpigmentation management in today's common diseases is largely dependent on the tyrosinase enzyme, an enzyme-containing copper, and the tyrosinase enzyme also plays an important role in melanin synthesis (Zengin et al., 2019). The use of tyrosinase inhibitors is increasing in the pharmaceutical and cosmetic industries, especially because of their skin whitening and anti-pigmentation effects after sunburn. In the present study, EA extract showed higher tyrosinase inhibitory activity than MeOH and AQ extracts (Table 2).

## CONCLUSION

In this study, besides antioxidant and enzyme inhibition activities of *M. murex*, total phenolic and flavonoid substance contents were also studied. According to the obtained results, the TPC was recorded highest in the AQ extract, while the TFC was recorded in the MeOH extract. In addition, the FRAP value was found the highest in AQ extract as well as maximum CUPRAC value was recorded in EA extract. All of the extracts of the *M. murex* plant showed inhibitory activity against all the studied enzymes. Especially  $\alpha$ -glucosidase enzyme inhibition has been found to be at high levels compared to the  $\alpha$ -amylase enzyme which works together with  $\alpha$ -glucosidase in glucose metabolism. High inhibition of  $\alpha$ -amylase and  $\alpha$ -glucosidase enzymes, especially in EA extract, may be considered as an indicator that the plant has an important potential in the treatment of type 2 diabetes. However, more research is needed to understand the mechanisms and effects of *M. murex* biological activity.

**Peer-review:** Externally peer-reviewed.

**Author Contributions:** Conception/Design of Study- D.P., B.E., Y.S.Ç.; Data Acquisition- D.P., V.A., G.Z., M.D., Y.S.Ç.; Data Analysis/Interpretation- D.P., V.A., G.Z., M.D., Y.S.Ç.; Drafting Manuscript- V.A., G.Z., M.D., Y.S.Ç.; Critical Revision of Manuscript- V.A., G.Z., M.D., Y.S.Ç.; Final Approval and Accountability- D.P., V.A., B.E., G.Z., M.D., Y.S.Ç.; Technical or Material Support- B.E., Y.S.Ç.; Supervision- G.Z., Y.S.Ç.

**Conflict of Interest:** The authors have no conflict of interest to declare.

**Financial Disclosure:** Authors declared no financial support.

**Acknowledgement:** We would like to thank botanist experts Dr Mustafa Keskin for identifying the plant.

## REFERENCES

- Adaramola, B., & Onigbinde, A. (2016). Effect of extraction solvent on the phenolic content, flavonoid content and antioxidant capacity of clove bud. *Article in IOSR Journal of Pharmacy and Biological Sciences*, 11(2), 33–38.
- Alam, F., Shafique, Z., Amjad, S. T., & Bin Asad, M. H. H. (2019). Enzymes inhibitors from natural sources with antidiabetic activity: A review. *Phytotherapy Research*, 33(1), 41–54.
- Babbar, N., Oberoi, H. S., Uppal, D. S., & Patil, R. T. (2011). Total phenolic content and antioxidant capacity of extracts obtained from six important fruit residues. *Food Research International*, 44(1), 391–396.

- Baiano, A., Terracone, C., Viggiani, I., & Del Nobile, M. A. (2013). Effects of cultivars and location on quality, phenolic content and antioxidant activity of extra-virgin olive oils. *JAOCS, Journal of the American Oil Chemists' Society*, 90(1), 103–111.
- Çakmak, Y. S., Zengin, G., Eskin, B., Yıldırım, K., Topal, M., Aydın, G. H. ... Erten, K. (2017). Investigation of Antioxidant and Enzyme Inhibition Activities and Phenolic Compound of *Medicago rigidula* (L.) All. *Marmara Pharmaceutical Journal*, 21(3), 522–529.
- Fidrianny, I., Budiana, W., & Ruslan, K. (2015). Antioxidant activities of various extracts from *ardisia* sp leaves using dpph and cuprac assays and correlation with total flavonoid, phenolic, carotenoid content. *International Journal of Pharmacognosy and Phytochemical Research*, 7, 859–865.
- Francis, C. M., & Gillespie, D. J. (1981). Ecology and distribution of subterranean clover and *Medicago* species in Sardinia. *Australian Plant Introduction Review*, 13, 15–25.
- Ghimire, B. K., Ghimire, B., Yu, C. Y., & Chung, I.-M. (2019). Allelopathic and Autotoxic Effects of *Medicago sativa*—Derived Allelochemicals. *Plants*, 8(7), 233.
- Gholami, A., De Geyter, N., Pollier, J., Goormachtig, S., & Goossens, A. (2014). Natural product biosynthesis in *Medicago* species. *Natural Product Reports*, 31(3), 356–380.
- Gillespie, D. J., & McComb, J. A. (1991). Morphology and distribution of species in the *Medicago murex* complex. *Canadian Journal of Botany*, 69(12), 2655–2662.
- Hassan, M., Raza, H., Abbasi, M. A., Moustafa, A. A., & Seo, S.-Y. (2019). The exploration of novel Alzheimer's therapeutic agents from the pool of FDA approved medicines using drug repositioning, enzyme inhibition and kinetic mechanism approaches. *Bio-medicine & Pharmacotherapy*, 109, 2513–2526.
- Kicel, A., & Olszewska, M. A. (2015). Evaluation of antioxidant activity, and quantitative estimation of flavonoids, saponins and phenols in crude extract and dry fractions of *Medicago lupulina* aerial parts. *Natural Product Communications*, 10(3), 483–486.
- Martins, N., Barros, L., & Ferreira, I. C. F. R. (2016). In vivo antioxidant activity of phenolic compounds: Facts and gaps. *Trends in Food Science & Technology*, 48, 1–12.
- Mølgaard, J., von Schenck, H., & Olsson, A. G. (1987). Alfalfa seeds lower low density lipoprotein cholesterol and apolipoprotein B concentrations in patients with type II hyperlipoproteinemia. *Atherosclerosis*, 65(1–2), 173–179.
- Mortensen, A., Kulling, S. E., Schwartz, H., Rowland, I., Ruefer, C. E., Rimbach, G., Cassidy, A., Magee, P., Millar, J., & Hall, W. L. (2009). Analytical and compositional aspects of isoflavones in food and their biological effects. *Molecular Nutrition & Food Research*, 53(S2), S266–S309.
- Quideau, S., Deffieux, D., Douat-Casassus, C., & Pouységu, L. (2011). Plant polyphenols: Chemical properties, biological activities, and synthesis. In *Angewandte Chemie - International Edition* (pp. 586–621).
- Rodrigues, F., Palmeira-de-Oliveira, A., das Neves, J., Sarmento, B., Amaral, M. H., & Oliveira, M. B. (2013). *Medicago* spp. extracts as promising ingredients for skin care products. *Industrial Crops and Products*, 49, 634–644.
- Sudhakaran, M., Sardesai, S., & Doseff, A. I. (2019). Flavonoids: new frontier for immuno-regulation and breast cancer control. *Antioxidants*, 8(4), 103.
- Takyi, E. E. K., Kido, Y., Rikimaru, T., & Kennedy, D. O. (1992). Possible use of alfalfa (*Medicago sativa*) as supplement in infant nutrition: Comparison of weight gained by rats fed on alfalfa and a popular weaning diet. *Journal of the Science of Food and Agriculture*, 59(1), 109–115.
- Uysal, S., Zengin, G., Locatelli, M., Bahadori, M. B., Mocan, A., Bel-lagamba, G. ... Aktumsek, A. (2017). Cytotoxic and enzyme inhibitory potential of two potentilla species (*P. speciosa* L. and *P. reptans* Willd.) and their chemical composition. *Frontiers in Pharmacology*, 8, 290.
- Xu, D.-P., Li, Y., Meng, X., Zhou, T., Zhou, Y., Zheng, J., Zhang, J.-J., & Li, H.-B. (2017). Natural antioxidants in foods and medicinal plants: Extraction, assessment and resources. *International Journal of Molecular Sciences*, 18(1), 96.
- Zengin, G., Sieniawska, E., Senkardes, I., Picot-Allain, M. C. N., Sinan, K. I., & Mahomoodally, M. F. (2019). Antioxidant abilities, key enzyme inhibitory potential and phytochemical profile of *Tanacetum poteriifolium* Grierson. *Industrial Crops and Products*, 140, 111629.

# Phenolic compounds and bioactivity of *Scorzonera pygmaea* Sibth. & Sm. aerial parts: *In vitro* antioxidant, anti-inflammatory and antimicrobial activities

Hasan Şahin<sup>1,2,3</sup> , Aynur Sarı<sup>1</sup> , Nurten Özsoy<sup>4</sup> , Berna Özbek Çelik<sup>5</sup> 

<sup>1</sup>Istanbul University, Faculty of Pharmacy, Department of Pharmacognosy, Istanbul, Turkey

<sup>2</sup>Istanbul University, Graduate School of Health Sciences, Istanbul, Turkey

<sup>3</sup>Dicle University, Faculty of Pharmacy, Department of Pharmacognosy Diyarbakır, Turkey

<sup>4</sup>Istanbul University, Faculty of Pharmacy, Department of Biochemistry, Istanbul, Turkey

<sup>5</sup>Istanbul University, Faculty of Pharmacy, Department of Pharmaceutical Microbiology, Istanbul, Turkey

**ORCID IDs of the authors:** H.Ş. 0000-0002-8325-8116; A.S. 0000-0001-8116-7053; N.Ö. 0000-0002-2419-9128; B.Ö.Ç. 0000-0001-8909-8398

**Cite this article as:** Sahin, H., Sari, A., Ozsoy, N., & Ozbek Celik, B. (2020). Phenolic compounds and bioactivity of *Scorzonera pygmaea* Sibth. & Sm. aerial parts: *In vitro* antioxidant, anti-inflammatory and antimicrobial activities. *Istanbul Journal of Pharmacy*, 50 (3), 294-299.

## ABSTRACT

**Background and Aims:** *Scorzonera* L. genus contains several medicinal and edible plants. Both roots and aerial parts of *Scorzonera* species are used. *S. pygmaea* is endemic to Turkey. In a previous study, nine phenolic compounds were reported from the roots of the plant alongside certain biological activities. The current study was designed to investigate the aerial parts of the plant in the same manner and compare the potentials of the two parts.

**Methods:** Chromatographic and spectroscopic methods were used to isolate and identify the phenolics. Total phenolic contents were determined by Folin-Ciocalteu method. FRAP assay, anti-LPO, scavenging DPPH, ABTS and superoxide radicals were employed to evaluate the antioxidant activity. COX inhibition test and micro broth dilution technique were used for anti-inflammatory and antimicrobial activities, respectively.

**Results:** Seven phenolic compounds; thunberginol C (1), protocatechuic acid (2), chlorogenic acid methyl ester (3), cudrabenzyl A (4), scorzocreticin (5), scorzocreticoside I (6) and II (7) were purified. All the compounds are new for the aerial parts of the plant and 2 is new for the genus. The aerial parts showed a high antioxidant capacity which correlated with its phenolic content. COX inhibitory activity was found to be lower compared to Indomethacin. Weak antimicrobial activity was determined against *Staphylococcus aureus* and *S. epidermidis*.

**Conclusion:** Aerial parts possess significant/infrequent phenolics and the ethyl acetate (EtOAc) fraction of the ethanol extract is the most promising fraction for isolating these compounds. Phenolic compositions of aerial parts and roots are very similar. However, aerial parts can be a better rich source of natural antioxidants with protocatechuic acid and higher antioxidant potential.

**Keywords:** *Scorzonera pygmaea*, phenolics, antioxidant, protocatechuic acid

## INTRODUCTION

There are about 160 *Scorzonera* (Asteraceae) species in the world. Turkey is currently host to 52 species and 31 of them are endemic (Coşkunçelebi, Makbul, Gültepe, Okur, & Güzel, 2015). Members of the genus are both medicinal and edible plants. *S. hispanica* L., a related species, is used in several countries' cuisines and commonly known as black salsify or viper's grass. Although

**Address for Correspondence:**  
Aynur SARI, e-mail: aynur@istanbul.edu.tr

This work is licensed under a Creative Commons Attribution 4.0 International License.



Submitted: 24.05.2020  
Revision Requested: 07.07.2020  
Last Revision Received: 10.07.2020  
Accepted: 30.07.2020

this species is cultivated as a vegetable in some regions of Europe, *Scorzonera* species are rather considered as forgotten vegetables in the world due to their disappearing culinary uses over time. Many records show the traditional usage of *Scorzonera* species for the treatment of gout, pain, rheumatism, injuries, diabetes, diarrhoea, infertility, gastric disorders, pulmonary oedema and hypertension (Baytop, 1999; Dalar, Mukemre, Unal, & Ozgokce, 2018; Polat, 2019; Tsevegsuren et al., 2007). There are several phytochemical investigations on the genus. Previously, flavonoids (Acikara, Ergene Öz, Bakar, Saltan Çitoğlu, & Nebioğlu, 2017), bibenzyl derivatives (Zidorn, Ellmerer-Müller, & Stuppner, 2000), benzyl phthalates (Sari, 2010), coumarins (Harkati, Akkal, Bayat, Laouer, & Franca, 2010), dihydroisocoumarins (Sari et al., 2007), phenolic acid derivatives (Sari, Şahin, Özsoy, & Özbek Çelik, 2019), lignans – neolignans (Bader, De Tommasi, Cotugno, & Braca, 2011), sesquiterpenes (Yong Jin Yang et al., 2016) and triterpenes (O. B. Acikara et al., 2012) were determined in the genus.

With regard to black salsify or other *Scorzonera* species; roots are more conceivable but it's known that the fresh leaves of these plants are eaten as a vegetable in Turkey and some other countries in Europe too (Baytop, 1999; Şenkardeş, Bulut, Doğan, & Tuzlacı, 2019; Tsevegsuren et al., 2007). Even more so, the aerial parts of the genus are used as ethnomedicines against liver disorders, diabetes, headache, hypertension and infertility (Dalar et al., 2018; Singh & Lal, 2008). *Scorzonera pygmaea* Sibth. & Sm. is a perennial herb. It's endemic to West Anatolia and measures only 1.5 – 11 cm in height as its name signifies (Koyuncu, Yaylacı, & Kuş, 2014). The roots of the plant were investigated in another study and nine phenolic compounds were reported along with certain biological activities (Şahin, Sari, Özsoy, Özbek Çelik, & Koyuncu, 2020). Thus, the aerial parts of *S. pygmaea* were subjected to this study in terms of phenolics and *in-vitro* bioactivity studies. Thereby, the evaluation of the significance of the aerial parts and comparison between potentials of the roots and aerial parts were aimed.

## MATERIALS AND METHODS

### Plant material

Flowered herba of *S. pygmaea* were collected from Eskişehir in July 2015 and identified by O. Koyuncu (Associate Prof.). A voucher specimen was deposited with the ESK 18397 number at Osmangazi University Herbarium (Eskişehir).

### Extraction, isolation and structure elucidation

The aerial parts of *S. pygmaea* were air-dried by protecting direct sunlight and powdered. 2 kg of this powder was extracted using the maceration technique with ethanol. The macerate was concentrated with a rotary evaporator at 45 °C. A methanol/water (1:2) mixture was used to dissolve this macerate. Then the macerate was successively extracted with petroleum ether (yielded 46.8 g), chloroform (yielded 4.1 g), ethyl acetate (yielded 9.8 g) and *n*-butanol (yielded 8.2 g) respectively. 9 g of the ethyl acetate fraction was subjected to column chromatography (CC) (CHCl<sub>3</sub>/MeOH 100:0, 98:2, 96:4, 94:6, 92:8, 88:12, 80:20, 70:30, 50:50, 0:100; silica gel) and 210 fractions (Fr) were obtained. Fr 8-16 was purified by CC (MeOH; Sephadex LH-20) and gave 47 further fractions (FFr). FFr 17-29 was subjected to

preparative thin layer chromatography (TLC) (toluene/EtOAc/HCOOH 7:4:1; silica gel) to afford **1** (7.1 mg). Fr 17-22 was purified by preparative TLC (toluene/EtOAc/HCOOH 5:4:1; silica gel) and gave **2** (15.0 mg). Fr 36-38 was further separated by preparative TLC (toluene/EtOAc/HCOOH 5:5:1; silica gel) to provide **3** (7.0 mg). Fr 56-68 was subjected to CC (MeOH; Sephadex LH-20) and gave 50 further fractions (FFr). FFr 27-43 was purified with preparative TLC (CHCl<sub>3</sub>/MeOH 75:25; silica gel) to afford pure compounds **4** (20 mg), **5** (20 mg) and **6** (10 mg). Fr 71-77 was purified by CC (MeOH; Sephadex LH-20) and gave 64 further fractions (FFr). FFr 10-15 was purified with preparative TLC (CHCl<sub>3</sub>/MeOH 70:20; silica gel) to yield pure **7** (8.3 mg).

### Chemicals, solvents and instrumental details

6-hydroxy-2,5,7,8-tetramethylchromane-2-carboxylic acid (Trolox), β-nicotinamide adenine dinucleotide reduced (β-NADH), Nitroblue tetrazolium (NBT), 2,2'-Azino-bis(3-ethylbenzothiazoline-6-sulfonic acid) diammonium salt (ABTS), butylated hydroxytoluene (BHT), and rutin were obtained from Fluka (Buchs, Switzerland). Phenazine methosulphate (PMS), 2,2-diphenyl-1-picryl-hydrazyl (DPPH), soybean L-α-phosphatidylcholine type IV-S, gallic acid and ascorbic acid were obtained from Sigma- Aldrich (St. Louis, MO, USA). Other chemicals were obtained from Merck (Darmstadt, Germany) including 2,4,6-tripyridyl-s-triazine (TPTZ), trichloroacetic acid (TCA), thiobarbituric acid (TBA) and ferric chloride. Remaining reagents and solvents were analytical grade. Shimadzu UV 1700 Pharmaspec UV-VIS, Bruker Avance III 500 MHz and Thermo Finnigan LCQ Advantage MAX (ESI) were employed for acquiring UV, NMR and ESI-MS spectrums.

### Total phenolic content determination

A method using the Folin-Ciocalteu reagent was chosen for determining the total phenolic contents of the fractions (Slinkard & Singleton, 1977). Gallic acid equivalents were calculated (GAE/g fraction) for expressing the results.

### Antioxidant activity assays

Five different methods were used to evaluate the antioxidant potential of the fractions. Rutin was used as standard for all assays. The EC<sub>50</sub> values are given where applicable. The scavenging activity of ABTS radical was expressed as both EC<sub>50</sub> and Trolox equivalent. The results are given as mM Trolox equivalents (Re et al., 1999). The DPPH scavenging activities of the fractions were measured by a procedure described by Brand-Williams et al. (Brand-Williams, Cuvelier, & Berset, 1995). The nitroblue tetrazolium reduction method was employed to evaluate the effect of the fractions on producing superoxide radicals (Nishikimi, Rao, & Yagi, 1972). The determination of inhibitory activities of the fractions on lipid peroxidation and the ferric reducing antioxidant power assay (FRAP) were conducted according to Duh et al. (Duh, Tu, & Yen, 1999) and Benzie and Strain (Benzie & Strain, 1996) respectively. The results are given as mM Fe<sup>2+</sup>/L and calculated with a standard curve of iron sulfate heptahydrate in FRAP assay.

### Antimicrobial activity

The antimicrobial potentials of the fractions were evaluated using the micro broth dilution technique (CLSI, 2000, 2006). *Escherichia coli* ATCC 8739, *Candida albicans* ATCC 10231, Pro-

*teus mirabilis* ATCC 14153, *Staphylococcus aureus* ATCC 6538, *Klebsiella pneumoniae* ATCC 4352, *Staphylococcus epidermidis* ATCC 12228, *Enterococcus faecalis* ATCC 29212 and *Pseudomonas aeruginosa* ATCC 1539 were used for testing the activity. All microorganisms were purchased from the American Type Culture Collection (ATCC, Manassas, VA, USA).

### Anti-inflammatory activity

An enzyme immunoassay kit (Cayman 560131) was employed for determination of COX inhibitory activity for the fractions. The assay was conducted according to the kit's protocol.

### Statistical analysis

The results are expressed as means of three replicates  $\pm$  standard deviation. GraphPad Prism version 7.00 was used to perform statistical comparisons with Student's *t*-test ( $p < 0.05$ ).

## RESULTS AND DISCUSSION

Isolation studies conducted on ethyl acetate fraction of *S. pygmaea* aerial parts yielded four dihydroisocoumarins [thunberginol C (**1**), scorzocreticin (**5**), scorzocreticoside I (**6**) and scorzocreticoside II (**7**)], two phenolic acid derivatives [protocatechuic acid (**2**), chlorogenic acid methyl ester (**3**)] and one bibenzyl derivative [cudrabibenzyl A (**4**)] (Figure 1). Structure elucidation of the compounds **1** (Toshikawa et al., 1992), **2** (Chang et al., 2009), **3** (Sari, 2012; Zhu, Dong, Wang, Peng, & Luo, 2005), **4** (Nguyen, Juvik, Øvstedal, & Fossen, 2014), **5**, **6** and **7** (Paraschos, Magiatis, Kalpoutzakis, Harvala, & Skaltsounis, 2001) was achieved by interpreting their spectroscopic data (UV, proton NMR, carbon NMR, HSQC, HMBC and ESI-MS) and comparing them with the relevant literature.

All reported compounds are new for the aerial parts of *S. pygmaea*. The phytochemical composition of the subaerial and aerial parts of the plant seems to be very similar in terms of phenolic compounds (Şahin et al., 2020). Apart from protocat-

echuic acid, the other compounds were previously identified in the root extract of the plant. Protocatechuic acid, which is shown to be a metabolite of some polyphenols and a significant contributor to the alleged benefits of anthocyanins, is very common in several food plants (Vitaglione et al., 2007). This study is the first report to show a *Scorzonera* species containing protocatechuic acid. This compound might be considered as rare in the family Asteraceae due to its limited distribution with a few genera like *Centaurea* L. and *Rhaponticum* Hill (Baykan-Erel, Bedir, Khan, & Karaalp, 2010; Kokoska & Janovska, 2009). A new compound (Cudrabibenzyl A) for the family Asteraceae and another (Thunberginol C) new for the genus *Scorzonera* are reported in this study excluding the report for the roots of the same plant. Scorzocreticin and scorzocreticoside II were found in only *S. cretica* Willd. (an endemic of Crete and South Aegean which is commonly used in meat dishes) and *S. pygmaea* by now (Paraschos et al., 2001; Şahin et al., 2020). However, scorzocreticoside I is a common compound in *S. cretica*, *T. porrifolius* L. (white salsify) and *S. pygmaea* (Zidorn et al., 2005). Phenolic acids, such as quinic acid, caffeic acid and ferulic acid esters have a high incidence in the genus *Scorzonera*. Chlorogenic acid methyl ester was previously isolated from *S. latifolia* and *S. veratrifolia* Fenzl (Sari, 2010, 2012). These esters comprise a large group of natural polyphenols in the human diet which are counted in the phytochemicals responsible for the beneficial effects of vegetables, fruits and beverages (Liang & Kitts, 2016).

The total phenolic contents of ethyl acetate, chloroform and *n*-butanol fractions obtained from the ethanol extract of the *S. pygmaea* aerial parts were determined. Values are gallic acid equivalents and  $124.3 \pm 4.09$ ;  $26.8 \pm 2.33$  and  $34.49 \pm 3.44$  mg/g fraction, respectively. The petroleum ether fraction failed to extract any phenolic compounds. These results indicate that the aerial parts have a higher amount of total phenolic content than the roots (Şahin et al., 2020).

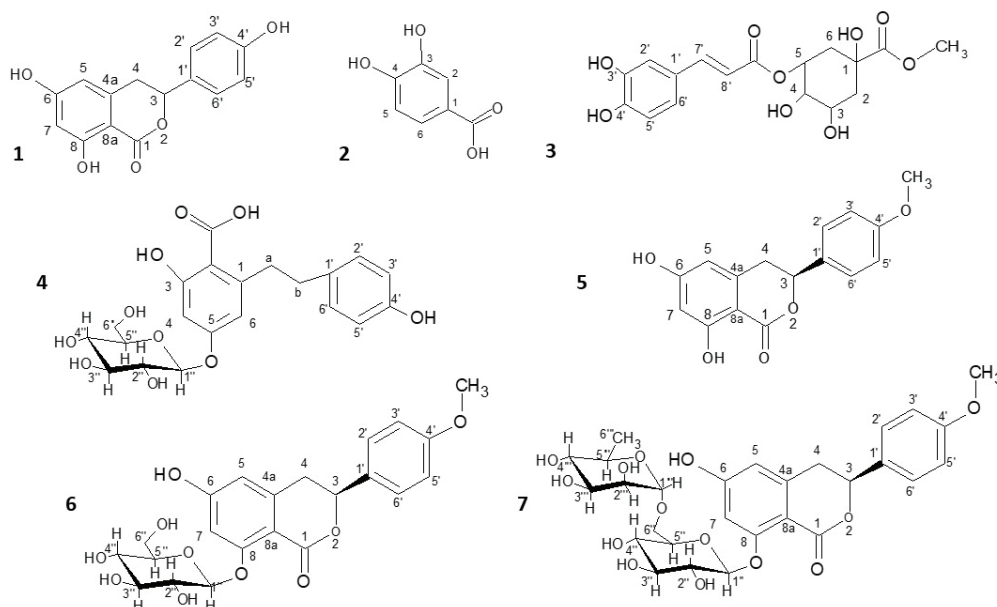


**Figure 1.** Structures of the compounds isolated from *S. pygmaea* aerial parts.



The antioxidant activity results are given in Table 1. The highest efficiency rates of extracting phenolic compounds and the highest antioxidant potential were observed in the EtOAc fraction. The most scavenged radical by all fractions was found to be superoxide, which might be explained by the relatively weak nature of this radical. However, scavenging activity of superoxide is much desired because it is a widespread precursor of several reactive oxygen species (Phaniendra, Jestadi, & Periyasamy, 2015). EtOAc fraction of the aerial parts showed better or nearly equal activities compared to rutin in LPO, SO and FRAP assays. Moreover, the EtOAc fraction of the aerial parts showed stronger antioxidant effect than the same fraction of the roots in all the methods apart from the scavenging activity of DPPH (this was almost equal). This might be due to its relatively high total phenolic content. Compared to the roots, it is observed that the aerial parts are more promising for antioxidant potential (Şahin et al., 2020). There have been a considerable number of antioxidant studies conducted on *Scorzonera* species (Acikara et al., 2017; Athmouni, Belghith, Bellassouad, Feki, & Ayadi, 2015; Milella, Bader, De Tommasi, Russo, & Braca, 2014; Nasser, Sharifi Bigy, Allahresani, & Malekaneh, 2015; Sari et al., 2019; Şahin et al., 2020; Tsevegsuren et al., 2007; Wang,

Wray, Tsevegsuren, Lin, & Proksch, 2012; Y. J. Yang et al., 2013). These studies are in accordance with the current results of *S. pygmaea* as they displayed potent antioxidant activity pointing to the phenolics as responsible substances.

Antimicrobial activity results of the fractions and standards are given in Table 2. No activity was observed against gram negative bacteria and yeast strain; however, a weak activity was determined against gram positive bacteria. These results are in accordance with the limited available data about antimicrobial activity of *Scorzonera* species (Sarı, Özbek, & Özgökçe, 2009; Şahin et al., 2020; Christian Zidorn et al., 2002).

The results of COX inhibition (a well-known anti-inflammatory mechanism) assay are given in Table 3. All fractions showed no anti COX-1/2 activity comparable with that of indomethacin. Considering the traditional anti-inflammatory usage of *Scorzonera* species and anti-inflammatory compounds of *S. pygmaea* (protocatechuic acid, chlorogenic acid methyl ester (Lende et al., 2011; Liang & Kitts, 2016)), different methods such as inhibition of pro-inflammatory cytokines or in-vivo models might be used for evaluating anti-inflammatory potential of the plant.

**Table 1. Antioxidant potential of *S. pygmaea* aerial parts.**

	EC <sub>50</sub> <sup>A</sup>				TEAC <sup>B*</sup>	FRAP <sup>C*</sup>
	Anti-LPO	SO	DPPH	ABTS		
PE	-	-	-	-	-	-
CHCl <sub>3</sub>	6.60 ± 0.46 <sup>a</sup>	0.48 ± 0.01 <sup>a</sup>	8.40 ± 0.22 <sup>a</sup>	6.66 ± 0.40 <sup>a</sup>	0.782 ± 0.04 <sup>a</sup>	0.957 ± 0.030 <sup>a</sup>
EtOAc	0.92 ± 0.02 <sup>b</sup>	0.46 ± 0.02 <sup>a</sup>	1.24 ± 0.02 <sup>b</sup>	1.09 ± 0.12 <sup>b</sup>	1.856 ± 0.06 <sup>b</sup>	2.774 ± 0.018 <sup>b</sup>
BuOH	7.79 ± 0.42 <sup>c</sup>	1.42 ± 0.01 <sup>b</sup>	5.21 ± 0.11 <sup>c</sup>	8.63 ± 0.14 <sup>c</sup>	0.484 ± 0.01 <sup>c</sup>	0.698 ± 0.037 <sup>c</sup>
Rutin	0.72 ± 0.02 <sup>d</sup>	0.53 ± 0.03 <sup>a</sup>	0.142 ± 0.02 <sup>d</sup>	0.61 ± 0.03 <sup>d</sup>	2.113 ± 0.04 <sup>d**</sup>	2.864 ± 0.04 <sup>d**</sup>

<sup>A</sup> mg/mL  
<sup>B</sup> Trolox equivalents as mmol/L (mM)  
<sup>C</sup> Ferrous ions equivalents as mmol Fe<sup>2+</sup>/L (mM)  
 PE (petroleum ether), CHCl<sub>3</sub> (chloroform), EtOAc (ethyl acetate), BuOH (n-butanol) fractions were obtained from ethanol macerate of *S. pygmaea* aerial parts  
 Values with different letters in the same column were significantly (p < 0.05) different.  
 \*Concentration of the fractions: 2.5 mg/mL, \*\* Concentration of rutin: 1.25 mg/mL

**Table 2. MIC values of the fractions obtained from ethanol extract of *S. pygmaea* aerial parts and of the standards (mg/L)**

Microorganisms	PE	CHCl <sub>3</sub>	AcOEt	BuOH	Standards
<i>Staphylococcus aureus</i>	-	-	1250	-	1.2 (Cefuroxime-sodium)
<i>Staphylococcus epidermidis</i>	-	-	78	1250	9.8 (Cefuroxime-sodium)
<i>Enterococcus faecalis</i>	-	-	-	-	8.0 (Ampicilin-sodium)
<i>Proteus mirabilis</i>	-	-	-	-	2.4 (Cefuroxime-sodium)
<i>Pseudomonas aeruginosa</i>	-	-	-	-	2.4 (Ceftazidime pentahydrate)
<i>Klebsiella pneumoniae</i>	-	-	-	-	4.9 (Cefuroxim-sodium)
<i>Escherichia coli</i>	-	-	-	-	4.9 (Cefuroxime-sodium)
<i>Candida albicans</i>	-	-	-	-	4.9 (Clotrimazole)

**Table 3. Results of anti-inflammatory studies**

Fractions (20mg/mL)	COX-1	COX-2
PE	69.76 ± 3.74 <sup>a</sup>	44.94 ± 4.80 <sup>a</sup>
CHCl <sub>3</sub>	84.65 ± 6.30 <sup>b</sup>	33.83 ± 2.11 <sup>b</sup>
EtOAc	67.05 ± 3.62 <sup>a</sup>	26.21 ± 3.49 <sup>c</sup>
BuOH	36.06 ± 3.08 <sup>c</sup>	26.21 ± 2.41 <sup>c</sup>
Indomethacin	87.56 ± 0.66 <sup>a*</sup>	93.42 ± 2.99 <sup>d**</sup>

PE (petroleum ether), CHCl<sub>3</sub> (chloroform), EtOAc (ethyl acetate), BuOH (n-butanol) fractions were obtained from ethanol macerate of *S. pygmaea* aerial parts  
 Values with different letters in the same column were significantly (p < 0.05) different.  
 \* The concentration was 12.5 µg/mL, \*\* The concentration was 50 µg/mL

## CONCLUSION

The aerial parts of *S. pygmaea* contain significant and infrequent phenolics. The EtOAc fraction of the ethanol extract is the most promising fraction for isolating these compounds. Some of these phenolics gain nutritional interest such as protocatechuic acid which is determined in the genus *Scorzonera* for the first time in the present study. The phenolic composition of the aerial parts is very similar to its roots. The aerial parts of *S. pygmaea* possess a potent and higher antioxidant capacity than its roots which might be derived from a higher amount of total phenolic content. Hence, the whole plant, especially the aerial parts, can be used as a source of natural antioxidants with a consequent impact on health benefits. No noteworthy result was observed for COX inhibition and antimicrobial potentials of the plant.

**Peer-review:** Externally peer-reviewed.

**Author Contributions:** Conception/Design of Study- A.S., H.Ş.; Data Acquisition- A.S., H.Ş., N.Ö., B.Ö.Ç.; Data Analysis/Interpretation- A.S., H.Ş., N.Ö., B.Ö.Ç.; Drafting Manuscript- H.Ş.; Critical Revision of Manuscript- A.S., H.Ş., N.Ö., B.Ö.Ç.; Final Approval and Accountability- A.S., H.Ş., N.Ö., B.Ö.Ç.; Technical or Material Support- A.S., H.Ş., N.Ö., B.Ö.Ç.; Supervision- A.S., H.Ş., N.Ö., B.Ö.Ç.

**Conflict of Interest:** The authors have no conflict of interest to declare.

**Financial Disclosure:** This study was financially supported by the Coordination Office of Lecturer Training Program of Istanbul University. (Grant number: 181.2015-DR-35/27-07)

**Acknowledgement:** The authors want to thank Onur Koyuncu for collecting and identifying the plant material.

## REFERENCES

Acikara, O. B., Çitoglu, G. S., Dall'Acqua, S., Smejkal, K., Cvacka, J., & Zemlicka, M. (2012). A new triterpene from *Scorzonera latifolia* (Fisch. and Mey.) DC. *Natural Product Research*, 26(20), 1892–1897. doi:10.1080/14786419.2011.625644

Acikara, Ö. B., Ergene Öz, B., Bakar, F., Saltan Çitoğlu, G., & Nebioğlu, S. (2017). Evaluation of Antioxidant Activities and Phenolic Compounds of *Scorzonera latifolia* (Fisch. & Mey.) DC. Collected from Different Geographic Origins in Turkey. *The Turkish Journal of Pharmaceutical Sciences*, 14(2), 179–184. doi:10.4274/tjps.57070

Athmouni, K., Belghith, T., Bellassouad, K., Feki, A. E., & Ayadi, H. (2015). Effect of extraction solvents on the biomolecules and antioxidant properties of *Scorzonera undulata* (Asteraceae): Application of factorial design optimization phenolic extraction. *Acta Scientiarum Polonorum, Technologia Alimentaria*, 14(4), 313–330. doi:10.17306/j.afs.2015.4.32

Bader, A., De Tommasi, N., Cotugno, R., & Braca, A. (2011). Phenolic compounds from the roots of Jordanian viper's grass, *Scorzonera judaica*. *Journal of Natural Products*, 74(6), 1421–1426. doi:10.1021/np200143s

Baykan-Erel, S., Bedir, E., Khan, I. A., & Karaalp, C. (2010). Secondary metabolites from *Centaurea ensiformis* P.H. Davis. *Biochemical Systematics and Ecology*, 38(5), 1056–1058. doi:https://doi.org/10.1016/j.bse.2010.09.004

Baytop, T. (1999). *Türkiye'de Bitkilerle Tedavi Geçmişte ve Bugün (Therapy with medicinal plants in Turkey)*. Istanbul: Nobel Tıp.

Benzie, I. F. F., & Strain, J. J. (1996). The Ferric Reducing Ability of Plasma (FRAP) as a Measure of "Antioxidant Power": The FRAP Assay. *Analytical Biochemistry*, 239(1), 70–76. doi:http://dx.doi.org/10.1006/abio.1996.0292

Brand-Williams, W., Cuvelier, M. E., & Berset, C. (1995). Use of a free radical method to evaluate antioxidant activity. *Food Science Technology (London)*, 28(1), 25–30. doi:10.1016/S0023-6438(95)80008-5

Chang, S. W., Kim, K. H., Lee, I. K., Choi, S. U., Ryu, S. Y., & Lee, K. R. (2009). Phytochemical constituents of *Bistorta manshuriensis*. *Natural Products Sciences*, 15(4), 234–240.

CLSI. (2000). Reference Method for Broth Dilution Antifungal Susceptibility Testing of Yeasts; Approved Standart M27-A NCCLS. Wayne, Pennsylvania: CLSI.

CLSI. (2006). Methods for dilution antimicrobial susceptibility tests for bacteria that grow aerobically: Approved Standard M7-A5. Wayne, PA: CLSI.

Coşkunçelebi, K., Makbul, S., Gültepe, M., Okur, S., & Güzel, M. E. (2015). A conspectus of *Scorzonera* s.l. in Turkey. *Turkish Journal of Botany*, 39, 76–87. doi:10.3906/bot-1401-10

Dalar, A., Mukemre, M., Unal, M., & Ozgokce, F. (2018). Traditional medicinal plants of Ağrı Province, Turkey. *Journal of Ethnopharmacology*, 226, 56–72. doi:https://doi.org/10.1016/j.jep.2018.08.004

Duh, P. D., Tu, Y. Y., & Yen, G. C. (1999). Antioxidant Activity of Water Extract of Harnng Jyur (*Chrysanthemum morifolium* Ramat). *LWT - Food Science Technology*, 32(5), 269–277. doi:http://dx.doi.org/10.1006/fstl.1999.0548

Harkati, B., Akkal, S., Bayat, C., Laouer, H., & Franca, M. G. D. (2010). Secondary metabolites from *Scorzonera undulata* ssp. *deliciosa* (Guss.) Maire (Asteraceae) and their antioxidant activities. *Records of Natural Products*, 4(3), 171–175.

Kokoska, L., & Janovska, D. (2009). Chemistry and pharmacology of *Rhaponticum carthamoides*: A review. *Phytochemistry*, 70(7), 842–855. doi:https://doi.org/10.1016/j.phytochem.2009.04.008

Koyuncu, O., Yaylacı, Ö. K., & Kuş, G. (2014). Taxonomical Studies on Endemic *Scorzonera pygmaea* var. *pygmaea* and var. *nutans* Stat. Nov. (Asteraceae) From Turkey. *Pakistan Journal of Botany*, 46(2), 555–563.

Lende, A. B., Kshirsagar, A. D., Deshpande, A. D., Muley, M. M., Patil, R. R., Bafna, P. A., & Naik, S. R. (2011). Anti-inflammatory and analgesic activity of protocatechuic acid in rats and mice. *Inflammopharmacology*, 19(5), 255. doi:10.1007/s10787-011-0086-4

- Liang, N., & Kitts, D. D. (2016). Role of Chlorogenic Acids in Controlling Oxidative and Inflammatory Stress Conditions. *Nutrients*, 8(1), 16. doi:10.3390/nu8010016
- Milella, L., Bader, A., De Tommasi, N., Russo, D., & Braca, A. (2014). Antioxidant and free radical-scavenging activity of constituents from two *Scorzonera* species. *Food Chemistry*, 160, 298–304. doi:http://dx.doi.org/10.1016/j.foodchem.2014.03.097
- Nasseri, M. A., Sharifi Bigy, S., Allahresani, A., & Malekaneh, M. (2015). Assessment of Antioxidant Activity, Chemical Characterization and Evaluation of Fatty Acid Compositions of *Scorzonera paradoxa* Fisch and C. A. Mey. *Jundishapur Journal of Natural Pharmaceutical Products*, 10(4), e19781. doi:10.17795/jjnpp-19781
- Nguyen, X. H. T., Juvik, O. J., Øvstedal, D. O., & Fossen, T. (2014). 6-Carboxydihydroresveratrol 3-O-β-glucopyranoside — A novel natural product from the Cretaceous relict *Metasequoia glyptostroboides*. *Fitoterapia*, 95, 109–114. doi:https://doi.org/10.1016/j.fitote.2014.03.001
- Nishikimi, M., Rao, N. A., & Yagi, K. (1972). Occurrence of superoxide anion in the reaction of reduced phenazine methosulfate and molecular oxygen. *Biochemical and Biophysical Research Communications*, 46(2), 849–854. doi:10.1016/S0006-291X(72)80218-3
- Paraschos, S., Magiatis, P., Kalpoutzakis, E., Harvala, C., & Skaltsounis, A. L. (2001). Three new dihydroisocoumarins from the Greek endemic species *Scorzonera cretica*. *Journal of Natural Products*, 64(12), 1585–1587. doi:10.1021/np0103665
- Phaniendra, A., Jestadi, D. B., & Periyasamy, L. (2015). Free radicals: properties, sources, targets, and their implication in various diseases. *Indian Journal of clinical biochemistry : IJCB*, 30(1), 11–26. doi:10.1007/s12291-014-0446-0
- Polat, R. (2019). Ethnobotanical study on medicinal plants in Bingöl (City center) (Turkey). *Journal of Herbal Medicine*, 16, 100211. doi:https://doi.org/10.1016/j.hermed.2018.01.007
- Re, R., Pellegrini, N., Proteggente, A., Pannala, A., Yang, M., & Rice-Evans, C. (1999). Antioxidant activity applying an improved ABTS radical cation decolorization assay. *Free Radical Biology and Medicine*, 26(9/10), 1231–1237. doi:10.1016/S0891-5849(98)00315-3
- Sarı, A. (2010). Two new 3-benzylphthalides from *Scorzonera veratrifolia* Fenzl. *Natural Product Research*, 24(1), 56–62. doi:10.1080/14786410902800699
- Sarı, A. (2012). Phenolic compounds from *Scorzonera latifolia* (Fisch. & Mey.) DC. *Natural Product Research*, 26(1), 50–55. doi:10.1080/14786419.2010.533666
- Sarı, A., Özbek, B., & Özgökçe, F. (2009). Antimicrobial activities of two *Scorzonera* species growing in Turkey. *Asian Journal of Chemistry*, 21(6), 4785–4788.
- Sarı, A., Şahin, H., Özsoy, N., & Özbek Çelik, B. (2019). Phenolic compounds and in vitro antioxidant, anti-inflammatory, antimicrobial activities of *Scorzonera hieraciifolia* Hayek roots. *South African Journal of Botany*, 125, 116–119. doi:https://doi.org/10.1016/j.sajb.2019.07.009
- Sarı, A., Zidorn, C., Ellmerer, E. P., Özgökçe, F., Ongania, K.-H., & Stuppner, H. (2007). Phenolic Compounds from *Scorzonera tomentosa* L. *Helvetica Chimica Acta*, 90, 311–317.
- Singh, K. N., & Lal, B. (2008). Ethnomedicines used against four common ailments by the tribal communities of Lahaul-Spiti in western Himalaya. *Journal of Ethnopharmacology*, 115(1), 147–159. doi:https://doi.org/10.1016/j.jep.2007.09.017
- Slinkard, K., & Singleton, V. L. (1977). Total phenol analysis: automation and comparison with manual methods. *American Journal of Enology and Viticulture*, 28(1), 49–55.
- Şahin, H., Sarı, A., Özsoy, N., Özbek Çelik, B., & Koyuncu, O. (2020). Two new phenolic compounds and some biological activities of *Scorzonera pygmaea* Sibth. & Sm. subaerial parts. *Natural Product Research*, 34(5), 621–628. doi:10.1080/14786419.2018.1493585
- Şenkardeş, İ., Bulut, G., Doğan, A., & Tuzlacı, E. (2019). An Ethnobotanical Analysis on Wild Edible Plants of the Turkish Asteraceae Taxa. *Agriculturae Conspectus Scientificus*, 84(1), 17–28.
- Toshikawa, M., Uchida, E., Chatani, N., Kobayashi, H., Naitoh, Y., Okuno, Y., . . . Murakami, N. (1992). Thunberginols C,D and E, New Antiallergic and Antimicrobial Dihydroisocoumarins and Thunberginol G 3'-O-Glucoside and (-)-Hydrangenol 4'-O-Glucoside, New Dihydroisocoumarin Glycosides from *Hydrangea dulcis* Folium. *Chemical and Pharmaceutical Bulletin*, 40(12), 3352–3354. doi:10.1248/cpb.40.3352
- Tsevegsuren, N., Edrada, R., Lin, W., Ebel, R., Torre, C., Ortlepp, S., . . . Proksch, P. (2007). Biologically active natural products from Mongolian medicinal plants *Scorzonera divaricata* and *Scorzonera pseudodivaricata*. *Journal of Natural Products*, 70, 962–967.
- Vitaglione, P., Donnarumma, G., Napolitano, A., Galvano, F., Gallo, A., Scalfi, L., & Fogliano, V. (2007). Protocatechuic Acid Is the Major Human Metabolite of Cyanidin-Glucosides. *The Journal of Nutrition*, 137(9), 2043–2048. doi:10.1093/jn/137.9.2043
- Wang, Y., Wray, V., Tsevegsuren, N., Lin, W. H., & Proksch, P. (2012). Phenolic Compounds from the Mongolian Medicinal Plant *Scorzonera radiata*. *Zeitschrift Fur Naturforschung Section C-a Journal of Biosciences*, 67(3-4), 135–143.
- Yang, Y. J., Liu, X., Wu, H. R., He, X. F., Bi, Y. R., Zhu, Y., & Liu, Z. L. (2013). Radical scavenging activity and cytotoxicity of active quinic acid derivatives from *Scorzonera divaricata* roots. *Food Chemistry*, 138(2-3), 2057–2063. doi:10.1016/j.foodchem.2012.10.122
- Yang, Y. J., Yao, J., Jin, X. J., Shi, Z. N., Shen, T. F., Fang, J. G., . . . Zhu, Y. (2016). Sesquiterpenoids and tirucallane triterpenoids from the roots of *Scorzonera divaricata*. *Phytochemistry*, 124, 86–98. doi:http://dx.doi.org/10.1016/j.phytochem.2016.01.015
- Zhu, X., Dong, X., Wang, Y., Peng, J., & Luo, S. (2005). Phenolic compounds from *Viburnum cylindricum*. *Helvetica Chimica Acta*, 88(2), 339–342. doi:10.1002/hlca.200590017
- Zidorn, C., Ellmerer-Müller, E. P., & Stuppner, H. (2000). Tyrolobibenzyls - Novel secondary metabolites from *Scorzonera humilis*. *Helvetica Chimica Acta*, 83, 2920–2925.
- Zidorn, C., Lohwasser, U., Pschorr, S., Salvenmoser, D., Ongania, K.-H., Ellmerer, E. P., . . . Stuppner, H. (2005). Bibenzyls and dihydroisocoumarins from white salsify (*Tragopogon porrifolius* subsp. *porrifolius*). *Phytochemistry*, 66(14), 1691–1697. doi:10.1016/j.phytochem.2005.05.004
- Zidorn, C., Spitaler, R., Ellmerer-Müller, E.-P., Perry, N. B., Gerhäuser, C., & Stuppner, H. (2002). Structure of Tyrolobibenzyl D and Biological Activity of Tyrolobibenzyls from *Scorzonera humilis*. *Zeitschrift für Naturforschung C*, 57(7-8), 614–619. doi:10.1515/znc-2002-7-811

# About the presence of *Pulmonaria angustifolia* L. (Boraginaceae) in Turkey

Bülent Olcay<sup>1</sup> , Hüseyin Onur Tuncay<sup>1</sup> 

<sup>1</sup>Istanbul University Faculty of Pharmacy Department of Pharmaceutical Botany, Istanbul, Turkey

**ORCID IDs of the authors:** B.O. 0000-0002-0521-488X; H.O.T. 0000-0003-1566-4806

**Cite this article as:** Olcay, B., & Tuncay H. O. (2020). About the presence of *Pulmonaria angustifolia* L. (Boraginaceae) in Turkey. *Istanbul Journal of Pharmacy*, 50 (3), 300-303.

## ABSTRACT

**Background and Aims:** Approximately 12,000 plant species grow naturally in Turkey. About 3500 of them are endemic. This number is increasing day by day with new floristic studies. The aim of this study; to confirm the existence of the *Pulmonaria angustifolia* L. species, whose record is suspicious.

**Methods:** This study is based on a herbarium sample collected by Bülent Olcay during the field study conducted in Western Anatolia (Bursa) in April 2019. As a result of the various relevant floras and literature studies, the specimen was identified as *P. angustifolia*. The *P. angustifolia* sample was confirmed by comparison with various herbarium samples. In this study, a description of the *Pulmonaria angustifolia* species was given. The species was examined in detail morphologically and compared with other herbarium samples.

**Results:** The presence of the *P. angustifolia* species, which has been mentioned as a doubtful record in the flora of Turkey, has been proven for the first time in Turkey. A new record has been added that the *Pulmonaria* species grow in Turkey. An identification key has been established for the *Pulmonaria* species found in Turkey, including the new record.

**Conclusion:** With this study, presence of *P. angustifolia*, which is mentioned as doubtful record is confirmed.

**Keywords:** *Pulmonaria*, Boraginaceae, new record, Turkey

## INTRODUCTION

Boraginaceae is one of the largest Angiosperm families, and includes approximately 151 genera in the world. The genus *Pulmonaria* L. belongs to the Boraginaceae family, and is composed of about 18 species according to The International Plant Names Index (<http://powo.science.kew.org>). It's native range is Europe and Asia-Temperate. The *Pulmonaria* genus is represented by 4 species in Turkey. According to Edmonson (1978), 2 of them are mentioned as doubtful records; *Pulmonaria angustifolia* L. and *Pulmonaria officinalis* L. *Pulmonaria officinalis* is cultivated in the European part of Turkey (Yıldırım, 2000). In the Royal Botanic Gardens, Kew, Herbarium the presence of a plant specimen labelled *Pulmonaria azurea* Besser, collected from "Mt. Olympus" in 1844, is mentioned (Edmonson, 1978). *Pulmonaria azurea* is the synonym of *Pulmonaria angustifolia* (Körüklü, 2012; Merxmüller and Sauer, 1972, Sauer, 1987). It is uncertain whether the location information refers to "Uludağ", and W.Sauer was unable to find any *Pulmonaria* species on Uludağ in 1977 (Edmonson, 1978). The presence of *Pangustifolia* in Turkey requires confirmation. In this paper, a new record for the Flora of Turkey is reported.

## MATERIALS AND METHODS

This study is based on a herbarium sample collected by Bülent Olcay during the field study conducted in Western Anatolia (Bursa) in April 2019. We tried to identify the plant with the diagnostic key in Flora of Turkey (Edmonson 1978), but it could not

### Address for Correspondence:

Bülent OLCAY, e-mail: [bulentolcay@istanbul.edu.tr](mailto:bulentolcay@istanbul.edu.tr)

Submitted: 27.02.2020

Revision Requested: 15.04.2020

Last Revision Received: 18.04.2020

Accepted: 04.05.2020

Published Online: 04.11.2020

This work is licensed under a Creative Commons Attribution 4.0 International License.



be identified. Subsequently, as a result of the various relevant floras (Mathew, 2000; Merxmüller & Sauer, 1972; Shiskin, 1953; Coste, 1937; Bonnier, 1926; Boissier, 1879) and literature studies, the specimen was identified as *P. angustifolia*. The *P. angustifolia* sample was compared with herbarium samples from B, BM, BR, GAP, GJO, KEW, L, MHA, O, P, TAA, TUL, US, WU herbaria with online access (JSTOR, 2020), as shown in Table 1.

A description was written with the aid of the The European Garden Flora (Mathew, 2000), Flora of Turkey (Edmonson, 1978), Flora Europaea (Merxmüller & Sauer, 1972) and Flora of

the U.S.S.R (Shiskin, 1953), Flore de la France (Coste, 1937), Flore complete illustree en couleurs de France (Bonnier, 1926), and Flora Orientalis (Boissier, 1879). Plant specimens were stored at the Istanbul University Faculty of Pharmacy Herbarium (ISTE). Current scientific names of *Pulmonaria* species have been checked on International Plant Names Index. (IPNI, 2020) Morphological photographs were taken with an iPhone X. The measurements were made with the ImageJ© program.

## RESULTS AND DISCUSSION

*Pulmonaria angustifolia* L. First published in Sp. Pl.: 135 (1753)

**Table 1: The examined herbarium samples and their herbarium numbers.**

Herbarium Number	Origin	Herbarium Code	Collector	Date
B 10 0741930	Germany.	B	R. Hand	2017
BM000657894	Netherlands.	BM	-	-
BR0000014441400	Belgium.	BR	J. Lambinon	1954
GAP001846	France.	GAP	-	-
GJO_0081816	Austria.	GJO	B. Ocepek	2009
K001085765	Switzerland.	KEW	S.Coll	1822
K001085767	Austria.	KEW	-	1828
K001085763	Italy.	KEW	-	1822
K001085764	Italy.	KEW	-	1828
K001085766	Italy.	KEW	-	1828
L2761522	Poland.	L	-	-
MHA 0 067 353	Russian Federation.	MHA	-	1948
MHA 0 067 347	Russian Federation.	MHA	V. Kuvaev - Danilov	1980
O 583039	Sweden.	O	-	-
O 583044	Sweden.	O	-	1880
O-V2242315	France.	O	-	-
O-V2242330	Czechia.	O	-	-
O 583032	Sweden.	O	-	1938
P00505801	Sweden.	P	-	1849
P00505792	Sweden.	P	-	-
P00505793	Sweden.	P	-	-
P00505781	Romania.	P	-	-
P00505791	Sweden.	P	-	1856
P00505730	Germany.	P	Woth	-
P00505739	Hungary.	P	J. Wiesbaur S. J.	1877
P00505740	Hungary.	P	C. Müller - W. Retzdorff	1877
P00505630	France.	P	Rabou	1873
TAA0128370	Russian Federation.	TAA	-	-
TAA0026605	Estonia.	TAA	H. Tamm	1962
TAA0026606	Estonia.	TAA	M. Kask - L. Viljasoo	1974
TUL 005 396	Russian Federation.	TUL	I.S. Sheremetyeva	1988
TUL 005 401	Russian Federation.	TUL	A.I. Alyushin	1976
TUL 005 397	Russian Federation.	TUL	-	1987
.02910630	France.	US	L. Corbiree	-
.078000	Austria.	WU	Hofbauer M. - Berger A. - Flatscher C. - Gilli & D. Reich	2014



Synonym: *Pulmonaria azurea* Besser, *Pulmonaria tuberosa* Schrank, *Pulmonaria angustifolia* subsp. *azurea* (Besser) Gams, *Pulmonaria angustifolia* subsp. *tuberosa* (Schrank) Gams.

**Description**

Perennial; rhizome short, black, with extension like cord. Stems low, hairy, 15-30 cm, radical leaves unmarked, narrow, up to 40 cm long, 5 cm wide, narrowly lanceolate, very gradually narrowed to the base, with setae, not or only very slightly glandular. Cauline leaves sessile, narrowly lanceolate-linear, acute, vaguely decurrent, both surfaces with coarse hair and bristles. Inflorescence bracteate cymes, at apex of stem with lateral branches, in shortly cluster, bristly-hairy and also vaguely glandular. Calyx cylindrical, toothed, 1.5-2.5 mm, densely pubescent, slightly glandular. Calyx in fruit very thin and short. Corolla campanulate, bright blue or violet blue, corolla tube hairless inside below the ring of hairs in throat. Nutlets ovoid, 4-3.5 mm high, subglabrous. The general view of *P. angustifolia*, the glandular hairs on the calyx, the corolla and the calyx are given in Figure 1.

**General distribution:** Europe, Central Asia, Turkey (as shown in Figure 2,3),

**Flowering time:** April.

**Examined specimen:** A2 Bursa: Mustafakemalpaşa district Suuçtu waterfall, near the walking path, 450m, 21 April 2019, B.Olcay, 117019 (ISTE).

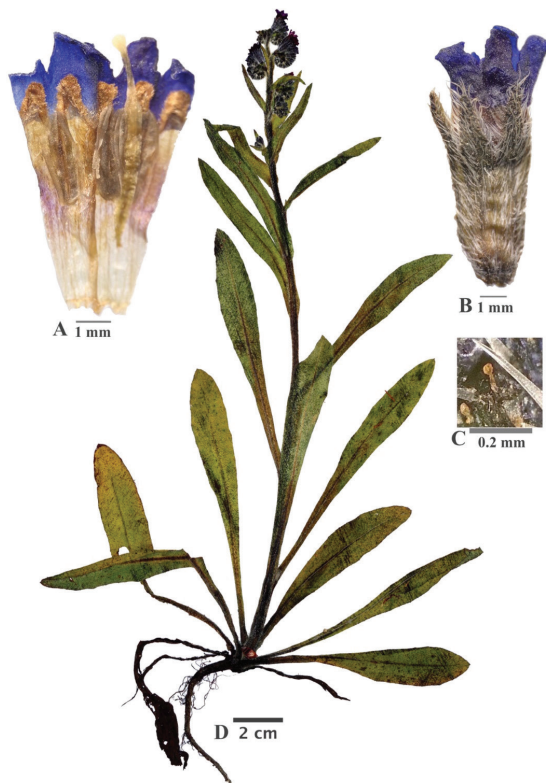


**Figure 1.** A: Corolla, B: Calyx, C: the glandular hairs on the calyx, D: general view of *P. angustifolia* L.

The *Pulmonaria* species are found in humus-rich soil, often in shade, but some also occur in sunny places, such as *Pulmonaria angustifolia*. The distribution area of *P. angustifolia* is considered to be quite small in Turkey. The fact that this specimen could not be found by anyone for many years supports this information. The *Pulmonaria* genus is represented by 4 species in Turkey (Edmonson 1978). But 2 of them are mentioned as doubtful records. With this study, the presence of *P. angustifolia*, is confirmed. The number of *Pulmonaria* species is increased with *P. angustifolia*, and updated, and as a result, it amounts to 3 species. According to Flora of Turkey, *P. officinalis* might have been cultivated in the vicinity of Istanbul, but confirmation is still needed regarding the presence of this species. The identification key to *P. angustifolia* is given below.

**Identification key to *Pulmonaria angustifolia* L.**

- 1. Basal leaves with cordate to truncate at base.....**2.**
  - 2. Summer leaves unspotted or with faint green spots; lamina shorter than petiole.....***P. obscura***
  - 2. Summer leaves white-spotted; lamina longer than petiole .....***P. officinalis***
- 1. Basal leaves attenuate into a petiole .....**3.**
  - 3. Stem 30-50 cm, corolla tubes pubescent within below the ring of hairs in throat. Cauline leaves rounded to subcordate at base.....***P. dacica***
  - 3. Stem 15-30 cm, corolla tube glabrous inside below the ring of hairs in throat.
    - Cauline leaves not rounded to subcordate at base.....***P. angustifolia***

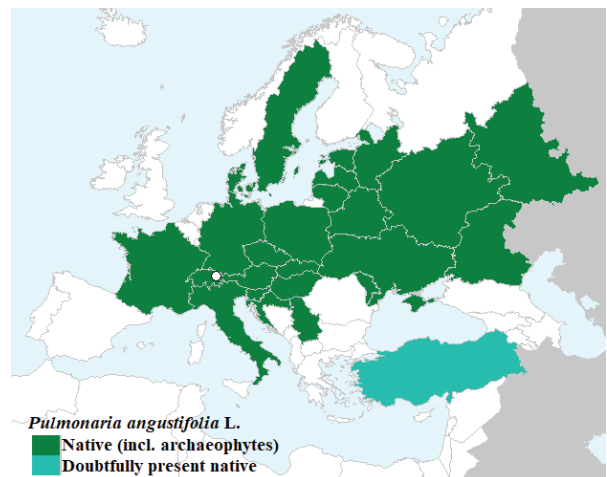


**Figure 2.** Distribution map of *P. angustifolia* in Europe, Central Asia (Valdes, 2011).

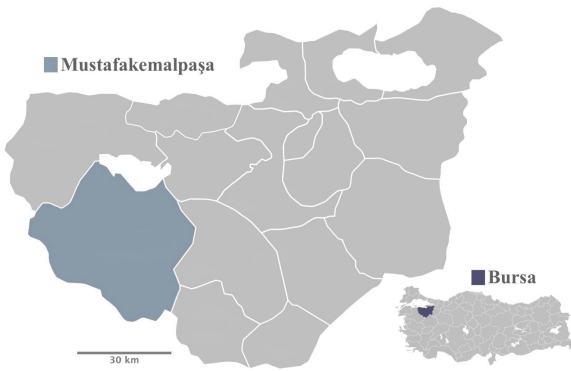


**Figure 3.** Distribution map of *P. angustifolia* in Turkey.

**Acknowledgement:** We would like to thank to Elif Nur Dilek and Fatma Selin Uzun for their contributions.

**Peer-review:** Externally peer-reviewed.

**Author Contributions:** Conception/Design of Study- B.O., H.O.T.; Data Acquisition- B.O., H.O.T.; Data Analysis/Interpretation- B.O., H.O.T.; Drafting Manuscript- B.O., H.O.T.; Critical Revision of Manuscript- B.O., H.O.T.; Final Approval and Accountability- B.O., H.O.T.

**Conflict of Interest:** The authors have no conflict of interest to declare.

**Financial Disclosure:** Authors declared no financial support.

## REFERENCES

- Boissier, E. (1879). *Flora Orientalis*, Vol. 4 (pp. 170–171). Genevae et Basileae: apud H. Georg, Bibliopolam Lugduni.
- Bonnier G. (1926). *Pulmonaria L.* In E. Orhac (Ed.), *Flore complete illustree en couleurs de France, Suisse et Belgique*, Vol. VIII (pp. 7–9). Paris, France: Librairie Generale de L'Enseignement.

- Coste H. (1937). *Flore descriptive et illustrée de la France, de la Corse et des contrées limitrophes*, Vol. 2 (pp. 594–596) Paris, France: Librairie des Sciences et des Arts.
- Edmonson, J.R. (1978). *Pulmonaria* In P.H. Davis (Ed.), *Flora of Turkey and the East Aegean Islands*, Vol. 6 (pp. 402–404). Edinburgh, UK: Edinburgh University Press.
- IPNI. (2020, February 26). *Pulmonaria L.: The International Plant Names Index*. Retrieved from <https://www.ipni.org/n/4771-1>
- JSTOR. (2020, February 26). *Pulmonaria angustifolia L.: Global Plants*. Retrieved from <https://plants.jstor.org/>
- Körüklü, S.T. (2012). *Pulmonaria L.* In A. Güner, S. Aslan, T. Ekim, M. Vural, & M.T. Babaç (Eds.), *Türkiye Bitkileri Listesi (Damarlı Bitkiler)* (pp. 242–243). İstanbul, Turkey: Nezahat Gökyiğit Botanik Bahçesi ve Flora Araştırmaları Derneği Yayını.
- Mathew, B. (2000). *Pulmonaria L.* In J. Cullen, J.C.M. Alexander, C.D. Brickell, J.R. Edmondson, & P.S. Green (Eds.), *The European garden flora*, Vol. 6 (pp. 135–137). Cambridge, UK: Cambridge University Press.
- Merxmüller, H., & Sauer, W. (1972). *Pulmonaria* In T. G. Tutin, V. H. Heywood, N. A. Burges, D. M. Moore, D. H. Valentine, S. M. Walters,... & A. O. Chater (Eds.), *Flora Europaea*, Vol. 3, *Diapensiaceae to Myoporaceae* (pp. 100–102). Cambridge, UK: Cambridge University Press.
- Shishkin, B.K. (1953). *Pulmonaria L.* In Popov, M.G. (Ed.), *Flora of the USSR*, Vol 19 (pp. 344 -352). Leningrad, USSR: Editio Academiae Scientiarum.
- Sauer, W. (1987). The *Pulmonaria dacica* Group: Its Affinities with Central and South-East European Allies and with the Genus *Paraskevia* (Boraginaceae). *Plant Systematics and Evolution*, 155(1–4), 257–76.
- Valdes, B. (2011). Boraginaceae.: Euro Med Plantbase. Retrieved from <http://ww2.bgbm.org/EuroPlusMed/>
- Yıldırım, Ş. (2000). The chorology of the Turkish species of Boraginaceae family. *Ot Sistematik Botanik Dergisi*, 7(2), 257–272.

# Reshaping cytoskeleton: different acts of modulatory compounds

Pelin Zobaroglu<sup>1</sup> , Gamze Bora<sup>1</sup> 

<sup>1</sup>Hacettepe University, Faculty of Medicine, Department of Medical Biology, Ankara, Turkey

**ORCID IDs of the authors:** P.Z. 0000-0003-1607-9481; G.B. 0000-0002-4206-8332

**Cite this article as:** Zobaroglu, P., & Bora, G. (2020). Reshaping cytoskeleton: Different acts of modulatory compounds. *Istanbul Journal of Pharmacy*, 50 (3), 304-311.

## ABSTRACT

The eukaryotic cytoskeleton is composed of filamentous structures, namely microfilaments, microtubules and intermediate filaments. The cytoskeleton is an essential component of cells due to its role in various cellular functions, such as intracellular transport, organelle positioning, chromosome segregation and cytokinesis. Abnormalities in cytoskeleton, as well as associated proteins and regulatory pathways, have been shown to contribute to disease pathomechanisms including cancer and neurodegenerative diseases. Therefore, cytoskeleton is an important therapeutic target and many compounds have been identified or developed to modulate the cytoskeleton. In this review, we focused on cytoskeleton modulatory compounds and summarized their mechanisms of action.

**Keywords:** Microtubule, actin, cytoskeleton modulatory compounds

## INTRODUCTION

The cytoskeleton is an intracellular network maintaining the internal organization of cells and also providing specific cell morphology and mechanical support. It plays a role in various cellular processes such as cell movement, division, contraction in muscle cells and axonal transport in neurons. It is made of different types of filaments, namely microfilaments, microtubules, and intermediate filaments. These filaments interact with each other with the help of associated proteins to establish and maintain the cytoskeletal network. Recent studies showed that defects in the cytoskeleton are involved in pathomechanisms of several diseases such as cancer, neurodegenerative disease, myopathies, cardiovascular disease, liver cirrhosis and pulmonary fibrosis. For this reason, many compounds have been investigated so far for therapeutic purposes. Additionally, such compounds are powerful tools in cell biology to understand the structural properties of filaments as well as functions of cytoskeleton related proteins. Therefore, a broad spectrum of cytoskeleton modulatory compounds has been extensively studied in *in vitro* and *in vivo* model systems as well as in clinical trials. Several synthetic and natural compounds obtained from minerals, microorganisms, and animals, have been studied mostly for altering microfilament and microtubule structures. These compounds generally alter the cytoskeleton by directly binding to monomer/filament or associated-proteins, targeting post-translational modifications and regulatory signaling pathways. In this review, we summarized different acts of cytoskeleton modulatory compounds considering their mechanisms of action.

### Microtubules and modulatory compounds

Microtubules are hollow cylindrical polymers and the thickest filaments (25 nm in diameter) of cytoskeleton. It is composed of two globular protein subunits, namely alpha ( $\alpha$ ) and beta ( $\beta$ ) tubulin. The  $\alpha$  and  $\beta$  tubulin proteins form a heterodimer, which is added sequentially in a certain direction to form protofilaments. Laterally interacting 13 protofilaments establish microtubule

**Address for Correspondence:**  
Gamze BORA, e-mail: gamzeb@hacettepe.edu.tr

Submitted: 05.03.2020  
Revision Requested: 30.07.2020  
Last Revision Received: 31.07.2020  
Accepted: 04.09.2020  
Published Online: 21.10.2020

This work is licensed under a Creative Commons Attribution 4.0 International License.



structure. The position of  $\alpha$  and  $\beta$  tubulin proteins within a filament gives a polar feature to microtubules and forms plus and minus ends. The polymerization of tubulin heterodimers primarily occurs at plus ends. Minus ends are generally attached to the “microtubule organization center” (MTOC), a region where microtubules are formed. Microtubules are dynamic structures that shorten with depolymerization and elongate with polymerization. This dynamic behavior is called dynamic instability and GTP hydrolysis plays an important role in the regulation of this behavior (Lodish et al., 2003; Bora, Koyunoğlu, Sunguroğlu, & Yurter, 2019) (Figure 1). The dynamic structure of microtubules is regulated by microtubule-binding proteins such as microtubule-associated proteins (MAPs), microtubule plus-end-tracking proteins (+TIPs) and also post-translational modifications of tubulin subunits. Microtubules are involved in diverse cellular processes in eukaryotic cells such as cell movement, division, polarization, intracellular

transport of macromolecules (protein, RNA, vesicle, etc) and organelle positions.

Microtubules are known as druggable targets and pharmacological alteration of microtubule structure has long been utilized for cancer treatment to arrest cell cycle by interfering mitotic spindle formation and also promote apoptotic cell death. Besides, dysregulations in microtubule dynamics contribute to the pathomechanisms of several neurodegenerative diseases (Bora, Sicularlı, Hensel, Claus, & Yurter, 2019). Reduced stability of neuronal microtubules has been reported in Alzheimer’s disease, Parkinson’s disease and Amyotrophic lateral sclerosis (Dubey, Ratnakaran, & Koushika, 2015), whereas microtubules are hyperstabilized in Hereditary spastic paraplegia (Hazan J.,1999; Evans K. J., 2005). Therefore, microtubules could also be promising targets for neurodegenerative diseases as well as for nervous system injuries. Microtubule

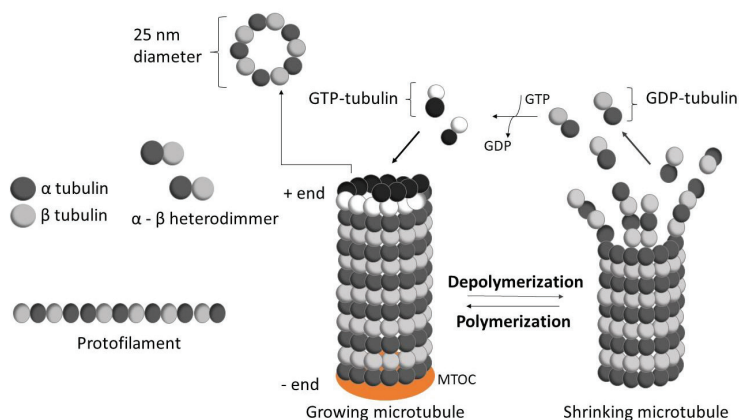


Figure 1. Microtubule structure and organization.

Table 1. Microtubule stabilizers, destabilizers and its binding sites.							
Compounds	Binding sites			Compounds	Binding sites		
	Between tubulin dimer	Within tubulin dimer	Microtubule luminal packet		Between tubulin dimer	Within tubulin dimer	Microtubule luminal packet
Stabilizers				Destabilizers			
Paclitaxel*			+	Maytansine*	+		
Epothilones**			+	Rotenone*		+	
Discodermolide***			+	Noscipine*		+	
Docetaxel			+	Vinorelbine		+	
Dictyostatin***		+		Colchicine*		+	
Zampanolide***			+	Halichondrin B***	+		
Rhizoxin****	+			Eribulin			+
Eleutherobin***			+	Nocodazole		+	
Laulimalide***		+		Combrestatins A4*	+		
Peloruside A***		+		Tivantinib		+	
Cyclostreptin**			+	Dolastatins-10***	+		
				Pironetin**	+		

Natural compounds originally derived from \* plants, \*\*bacteria, \*\*\*marine species and \*\*\*\* fungi

modifying compounds having different mechanisms of action are summarized below.

### Direct binding to tubulin or microtubule

Several compounds alter microtubule structure by directly binding to either tubulins or microtubule filament (Table 1). These compounds are collectively called as microtubule targeting agents (MTAs), tubulin-binding agents (TBA) or anti-mitotic drugs. (Figure 2A) Tubulin-binding agents can interact with  $\alpha$  and  $\beta$  tubulin proteins from six different binding sites. Mostly microtubule stabilizers bind to the taxane and/or laulimalide/peloruside sites in  $\beta$  tubulin, whereas microtubule depolymerizers bind to pironetin, colchicine, maytansine and vinca sites (Steinmetz & Prota, 2018). Microtubule stabilizers support tubulin polymerization and increase microtubule density, whereas destabilizers initiate microtubule depolymerization, disassembly and cause a reduction in microtubule density. Colchicine which is a natural compound derived from the *Colchicum autumnale*, is the first tubulin-targeting compound, in fact, it played a role in the discovery and characterization of tubulin proteins. It destabilizes microtubules by binding itself to  $\beta$  tubulin at the colchicine binding site. Colchicine binding leads to conformational changes of tubulin heterodimer, which can not further polymerize into microtubule thereby disrupting microtubule function (Niel & Scherrmann, 2006). Colchicine is an FDA approved drug for prophylaxis, gout and related inflammatory diseases such as Familial mediterranean fever (Zemer

D,1986;Dalbeth, Lauterio, & Wolfe, 2014). Additionally, recent studies have provided evidence that colchicine increases the expression of a heat shock protein thereby it may be repurposed for Amyotrophic lateral sclerosis with a different mechanism (clinical trial ID: NCT03693781). Conversely, epothilone D (EpoD), a member of epothilone family isolated from the myxobacterium *Sorangium cellulosum*, is a strong promoter of tubulin polymerization *in vitro* that binds to the luminal surface of  $\beta$ -tubulin and inhibits microtubule depolymerization. In this way, it inhibits spindle formation and induces mitotic arrest (Lee & Swain, 2008). It has significant antitumor activity in patients with breast cancer (Overmoyer et al., 2005), but failed to show any activity in patients with non-small cell lung cancer (Yee et al., 2005). Additionally, EpoD has been investigated in Alzheimer's disease and it has been reported that EpoD treatment both increased axonal microtubule density and reduced axonal dystrophy. Although promising preclinical studies, phase I trial of EpoD in Alzheimer's disease was discontinued because of the severe toxic side-effect (Brunden et al., 2011).

### Modulation of tubulin post-translational modifications

It is also possible to modify microtubules by altering post-translational modifications (PTMs) of tubulin proteins. PTMs occur at amino and carboxyl ends of  $\alpha$  and  $\beta$  tubulins and form tubulin code regulating microtubule functions. Most of the PTMs occur after the formation of the microtubule structure, therefore, stable microtubules have more modifications than the dynamic

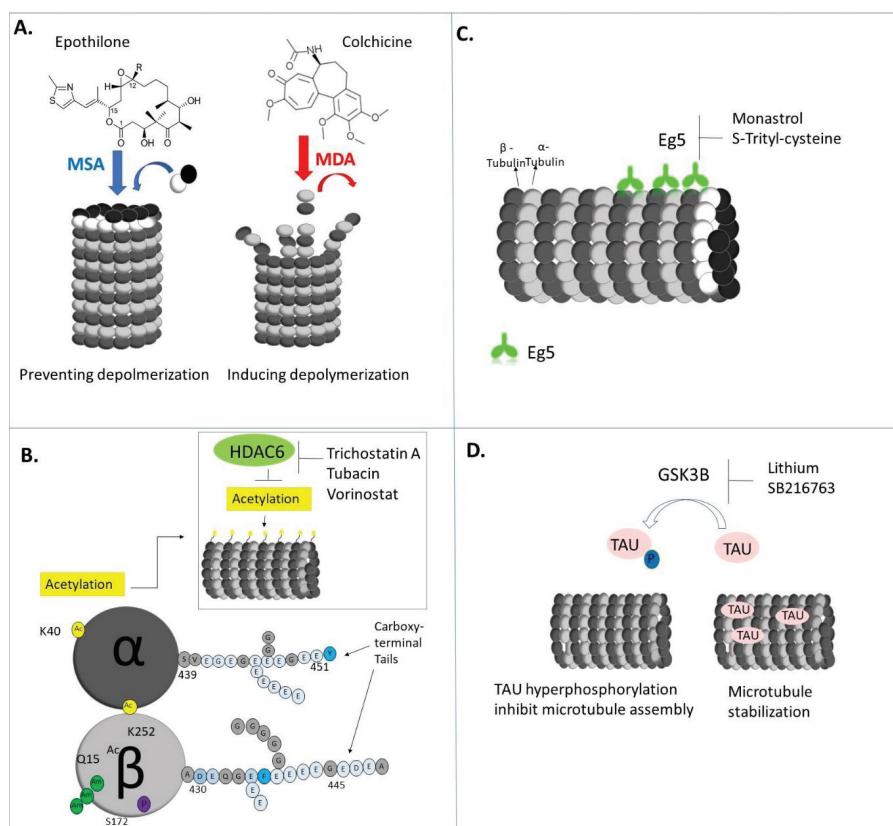


**Figure 2.** Mechanisms of action of microtubule modulatory compounds. (A) Compounds that can directly bind to tubulin or filament. MSA: microtubule-stabilizing agent, MDA: microtubule-destabilizing agent (B) Modulation of tubulin acetylation by HDAC inhibitors. (C) Eg5 inhibition by Monastrol and S-Trityl-cysteine (D) Modulation of signaling pathways through GSK3B kinase inhibitors. Ac: Acetylation, P: Phosphorylation



ones. PTMs are enzymatically catalyzed, thereby it is possible to alter some of the modifications by inhibiting/activating tubulin-modifying enzymes. One of the most studied PTM is acetylation, which takes place at the 40<sup>th</sup> lysine (K40) of a tubulin within the microtubule lumen (Janke & Kneussel, 2010). Acetylation is catalyzed by tubulin acetyltransferase (TAT1), whereas deacetylation is catalyzed by sirtuin 2 (SIRT2) and histone deacetylase 6 (HDAC6) enzymes. It has been reported that inhibition of HDAC6 by inhibitors such as tubacin, trichostatin A and vorinostat leads to an increase in tubulin acetylation and enhancing cell motility (Palazzo, Ackerman, & Gundersen, 2003) (Figure 2B). Additionally, in an *in vitro* ALS model, HDAC inhibitors restore axonal transport defects, suggesting that increasing microtubule acetylation could have therapeutic potential (Guo et al., 2017). Acetylated microtubules are considered to be stable and long-lived, however, microtubule stabilization is not promoted by tubulin acetylation, therefore other acetylation related mechanisms should be involved.

### Modulation of microtubule-related proteins

Several proteins play a role in regulating microtubule structure, therefore it is possible to modify it by inhibiting the activities of such proteins. For instance, kinesins are motor proteins that function in anterograde transport of membrane-bound organelles (Chen & Hancock, 2015). A member of the kinesin-5 family Eg5 is a plus-end kinesin and a key protein for spindle pole separation in many organisms, including humans. Monastrol and also S-Trityl-cysteine can selectively inhibit Eg5 protein, which causes mitotic arrest and apoptotic cell death due to defective spindle pole migration and the formation of radially aligned microtubules (Peterson & Mitchison, 2002)(Figure 2C). Several compounds were also identified to inhibit dyneins, another class of motor proteins, such as Ciliobrevin D and EHNA hydrochloride. These compounds affect the ATPase activity of dynein, therefore, are useful to address cellular functions of dynein proteins (Roossien, Miller, & Gallo, 2015).

### Alteration of signaling pathways

The pharmacological alteration of signaling pathways is another approach to modify microtubule structure. Glycogen synthase kinase-3 beta (GSK-3 $\beta$ ) is the major kinase that controlling microtubule structure and dynamics by differently

regulating multiple types of microtubule-associated proteins such as MAP1B, MAP2C, TAU, CRMP2 and APC (Xu, Ge, Liu, & Gong, 2015), (Trivedi, Marsh, Goold, Wood-Kaczmar, & Gordon-Weeks, 2005), (Sánchez, Pérez, & Avila, 2000). High GSK3 $\beta$  activity induces phosphorylation of CRMP2 and APC thus inhibiting their microtubule polymerization/stabilization activities (Zumbrunn J., 2001), (Yoshimura T., 2005) However, loss of GSK3 $\beta$  activity results in dephosphorylation of MAP1B at growth cone that leads to decrease in growth cone motility necessary for axonal growth (Trivedi et al., 2005). Inhibition of GSK3 $\beta$  by compounds like lithium (LiCl) diminished TAU phosphorylation that leads to enhance microtubule polymerization and stabilization in Alzheimer's disease models (Trivedi et al., 2005; Lei, Ayton, Bush, & Adlard, 2011; Engel et al., 2006) Another compound, SB216763, also reduced TAU phosphorylation levels in the neuronal cultures, the hippocampus of postnatal rats, which correlated with its neuroprotective potential (Selenica et al., 2007) (Figure 2D).

### Microfilaments and modulatory compounds

Microfilaments are the thinnest filaments (6 nm in diameter) of the cytoskeleton, which are composed of highly conserved globular actin proteins (G-actin). To form filamentous actin (F-actin), three G-actin proteins come together using ATP and subsequent binding of G-actin to the plus end leads to the formation of a helix having two chains. Similar to microtubules, F-actin shows polarity and plus end of the filament-barbed end-grows faster than the minus-pointed- end. Microfilaments are dynamic structures and both polymerization and depolymerization of actin subunits are regulated by several actin-binding proteins (Figure 3).

Actin filaments play an important role in the maintenance of cellular morphology as well as cell migration, cytokinesis, vesicle and organelle transport, and endocytosis. Therefore, modifying the actin cytoskeleton is a useful approach to understand the molecular mechanisms of actin-related biological processes. Besides, actin dysregulations are involved in the pathomechanisms of several diseases and targeting actin could have therapeutic potential for diseases such as cancer. There are several chemically diverse compounds, which are widely used as tools in cell biology but not in the clinic because of their cardiotoxic side effects (Bryce, Hardeman, Gun-

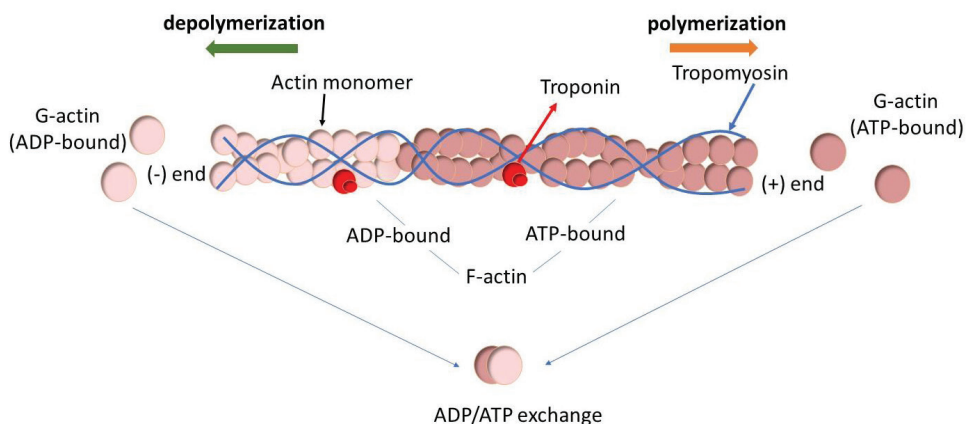


**Figure 3.** Actin filament structure and organization.

ning, & Lock, 2019). According to their targets, actin modifying compounds are grouped into three, as summarized below.

**Direct binding to G-actin or F-actin**

Some compounds alter filament polymerization by binding to either G-actin monomer or F actin. These small actin-binding compounds are roughly divided as stabilizers and destabilizers depending on their effect on the actin cytoskeleton

(Table 2). Stabilizers prevent depolymerization of F- actin and protecting it from proteolytic cleavage, while destabilizers inhibit filament formation thereby promote the depolymerization of filaments with a different mechanism (Coluccio & Tilney, 1984). One of the stabilizers is phalloidin, which is derived from *Amanita phalloides* (death cap mushroom), binds to actin filaments more tightly than monomers and prevents depolymerization (Figure 4A). There are fluorescent deriva-

Table 2. Well-known actin modifying compounds and its binding sites.				
Direct binding to G-actin or F- actin	Binding site		Compounds that modulate actin regulatory proteins	Target
	G- actin	F-actin		
<b>Stabilizers</b>			Wiskostatin, 187-1	N-WASP
<b>Cucurbitacin*</b>		+	CK-0944636,CK0993548 CK-666	Arp2/3 complex
<b>Jasplakinolide**</b>		+	Blebbistatin	Myosin II
<b>Chondramide**</b>		+	Migrastatin**	Fascin
<b>Dolastatin 11***</b>		+	TR-100, ATM1001, ATM3507	Tropomyosin
<b>Phalloidin****</b>		+	Doxazosin	Talin
<b>Destabilizers</b>			SMIFH2	Formins
<b>Cytochalasins****</b>	+	+	6-B345TTQ	Paxilin
<b>Swinholide***</b>		+	Cucurbitacin E and I*	Cofilin
<b>Staurosporine**</b>		+		
<b>Chaetoglobosins****</b>		+		
<b>Latrunculins***</b>	+			

Natural compounds originally derived from \* plants, \*\*bacteria, \*\*\*marine species and \*\*\*\* fungi

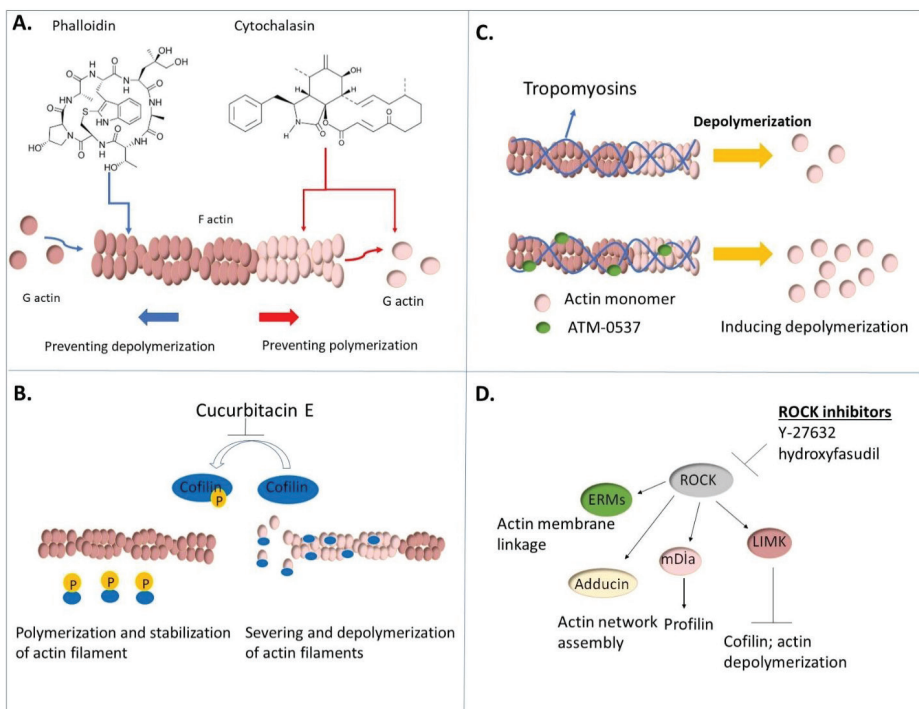


**Figure 4.** Mechanisms of action of actin modulatory compounds. (A) Compounds that can directly bind to G or F actin. (B) Inhibition of post-translational modification of an actin-binding protein, cofilin by compounds. (C) Inhibition of actin-binding protein, tropomyosin (D) Modulation of ROCK signaling pathway and downstream effectors through inhibitors.

tives of phalloidin, which are useful tools to visualize actin filaments in fixed tissues and also cultured cells (Gandalovičová et al., 2017). Cytochalasins, which are fungal toxins, are the most studied actin targeting agents that destabilize filaments by binding to the barbed end and also G-actin monomer thereby inhibiting F actin formation and polymerization (Figure 4A). Cytochalasins inhibit cytokinesis, cell motility and induce apoptosis. Currently, more than 60 different cytochalasins have been identified and some of them have been investigated as chemotherapeutics (Brown & Spudich, 1979).

### Modulation of actin-regulatory proteins

Actin dynamics can be modified chemically via inhibiting/altering activities of regulatory proteins (Table 2). For instance, N-WASP, a protein regulating actin polymerization, binds to Cdc42 and undergoes a conformational change, which is required for the activation of the Arp2/3 complex. Arp2/3 functions in the formation of new actin filaments as a branch from the existing ones. There are two compounds, namely 187-1 and wiskostatin, which inhibit conformational changes of N-WASP and prevent the activation of the Arp2/3 complex (Peterson & Mitchison, 2002; Zigmond, 2000; Carlier, 2001). Similarly, tropomyosin, a coiled-coil F-actin binding protein, is a key to the stability of actin filaments. Tropomyosin inhibition by using ATM3507, induce depolymerization of actin filament (Figure 4C). Inhibition of tropomyosins or myosins have been used to reduce the motility of tumor cells by either affecting actin or actomyosin contractility (Currier et al., 2017).

In addition, post-translational modifications of actin regulatory proteins have an impact on actin dynamics. Cofilin is an F-actin binding protein, which plays a role in depolymerization and severing of actin filaments. Phosphorylation of cofilin on serine 3 by LIM kinases inhibits its depolymerizing activity. Cucurbitacins E and I, which are derived from traditional Chinese medicinal plants -pumpkins and gourds- have been shown to inhibit phosphorylation of cofilin and increased its severing and depolymerizing activities (Figure 4B) (Currie et al., 2017; Nakashima et al., 2010).

### Alteration of signaling pathways

Actin filaments are regulated by signaling pathways. Among all, one of the key pathway regulating actin dynamics is Rho-associated kinases (ROCKs) which are serin/threonine kinases that phosphorylate various actin-regulating proteins like profilin, myosin light chain phosphatase (MLC) and LIM kinase (Amin et al., 2013). Therefore it involves various cellular processes in both neuronal and non-neuronal cells such as neurite elongation, stress fiber formation, cytokinesis, cell migration, and apoptosis. Small molecules, namely hydroxyfasudil and Y-27632 are useful tools for cell biology to inhibit ROCK for investigating alterations of both actin dynamics and actin related processes in physiological and pathological conditions (Figure 4D) (Brown & Spudich, 1981)(Schofield, Steels, & Bernard, 2012).

### Intermediate filaments and modulatory compounds

Intermediate filaments (IFs), are strong and flexible polymers (10 nm in diameter), which provide mechanical strength to

cells. Unlike microtubules and microfilaments, IFs are composed of different subunits. More than 70 proteins have been shown to form a filament structure in different cells. For filament assembly, two proteins interact with each other to form coiled-coil homo/heterodimers. Dimers associate with another one in an antiparallel fashion and form tetramers. End to end interaction of tetramers form protofilaments and laterally interacting eight protofilaments form the final intermediate filament structure. In contrast to microtubules and microfilaments, IFs are non-polar and generally exist in polymerized form. These structural properties make IFs generally not suitable as drug targets. Nevertheless, it has been identified that some compounds, such as withaferin A, which is derived from the Solanaceae family of plants, including *Withania somnifera* and *Acnistus arborescens*, and simvastatin target vimentin, a type III intermediate filament expressed in mesenchymal cells. Since vimentin is also expressed in cancer cells in epithelial-mesenchymal transition, therapeutic potential has been investigated for cancer. (Grin et al., 2012)(Trodden et al., 2018).

### CONCLUSION

The cytoskeleton is a dynamic network and involves almost all cellular processes. Structure and organization of cytoskeleton are still being investigated in a physiological and pathological context. Therefore, targeting cytoskeleton is a powerful approach not only for experimental purposes but also for the treatment of several diseases such as cancer and neurodegeneration. Currently, only microtubule targeted compounds are used in the clinic even though there is still a need for the development of new compounds because of their toxicity, and side effects, as well as the resistance of cancer cells. Increasing knowledge about the structure and organization of cytoskeletal elements is required to develop better modulatory drugs and can overcome the aforementioned limitations.

**Peer-review:** Externally peer-reviewed.

**Author Contributions:** Conception/Design of Study- P.Z., G.B.; Drafting Manuscript- P.Z., G.B.; Critical Revision of Manuscript- P.Z., G.B.; Final Approval and Accountability- P.Z., G.B.

**Conflict of Interest:** The authors have no conflict of interest to declare.

**Financial Disclosure:** Authors declared no financial support.

### REFERENCES






- Amin, E., Dubey, B. N., Zhang, S. C., Gremer, L., Dvorsky, R., Moll, J. M., ... & Ahmadian, M. R. (2013). Rho-kinase: regulation, (dys) function, and inhibition. *Biological Chemistry*, 394(11): 1399–1410. doi:10.1515/hsz-2013-0181.
- Bora, G., Sicularlı, C., Hensel, N., Claus, P., & Yurter, H. E. (2019). Investigations of Microtubule-associated Protein 2 Gene Expression in Spinal Muscular Atrophy. *The Journal of Pediatric Research*, 6(2), 148–154. doi: 10.4274/jpr.galenos.2019.71473
- Bora, G., Koyunoğlu, D., Sunguroğlu, M., & Yurter, H. E. (2019). Microtubule Structure, Organization and Defects: Spinal Muscular Atrophy and Amyotrophic Lateral Sclerosis. *Turkiye Klinikleri Journal of Medical Sciences*, 39(2), 221–230. doi: 10.5336/medsci.2018-63881

- Brown, S. S., & Spudich, J. A. (1979). Nucleation of polar actin filament assembly by a positively charged surface. *The Journal of Cell Biology*, 80, 499-504. doi: 10.1083/jcb.80.2.499
- Brown, S. S., & Spudich, J. A. (1981). Mechanism of action of cytochalasin: evidence that it binds to actin filament ends. *The Journal of Cell Biology*, 88(3), 487-491. doi: 10.1083/jcb.88.3.487
- Brunden, K. R., Yao, Y., Potuzak, J. S., Ferrer, N. I., Ballatore, C., James, M. J., ... Lee, V. M. Y. (2011). The characterization of microtubule-stabilizing drugs as possible therapeutic agents for Alzheimer's disease and related tauopathies. *Pharmacological Research*, 63(4), 341-351. https://doi.org/10.1016/j.phrs.2010.12.002
- Bryce, N. S., Hardeman, E. C., Gunning, P. W., & Lock, J. G. (2019). Chemical biology approaches targeting the actin cytoskeleton through phenotypic screening. *Current Opinion in Chemical Biology*, 51, 40-47. doi: 10.1016/j.cbpa.2019.02.013
- Carlier, M. F. (2001). Faculty of 1000 evaluation for A chemical inhibitor of N-WASP reveals a new mechanism for targeting protein interactions. *F1000 - Post-Publication Peer Review of the Biomedical Literature*. doi: 10.3410/f.1000267.14705
- Chen, Y., & Hancock, W. O. (2015). Kinesin-5 is a microtubule polymerase. *Nature Communications*, 6(1). doi: 10.1038/ncomms9160
- Colchicine for Amyotrophic Lateral Sclerosis - Full Text View. (n.d.). Retrieved from https://clinicaltrials.gov/ct2/show/NCT03693781
- Coluccio, L. M., & Tilney, L. G. (1984). Phalloidin enhances actin assembly by preventing monomer dissociation. *Journal of Cell Biology*, 99(2), 529-535. https://doi.org/10.1083/jcb.99.2.529
- Currier, M. A., Stehn, J. R., Swain, A., Chen, D., Hook, J., Eiffe, E., ... Cripe, T. P. (2017). Identification of Cancer-Targeted Tropomyosin Inhibitors and Their Synergy with Microtubule Drugs. *Molecular Cancer Therapeutics*, 16(8), 1555-1565. doi: 10.1158/1535-7163.mct-16-0873
- Dalbeth, N., Lauterio, T. J., & Wolfe, H. R. (2014). Mechanism of action of colchicine in the treatment of gout. *Clinical Therapeutics*, 36(10), 1465-1479. https://doi.org/10.1016/j.clinthera.2014.07.017
- Dubey, J., Ratnakaran, N., & Koushika, S. P. (2015). Neurodegeneration and microtubule dynamics: Death by a thousand cuts. *Frontiers in Cellular Neuroscience*, 9(September), 1-15. https://doi.org/10.3389/fncel.2015.00343
- Engel, T., Goñi-Oliver, P., Lucas, J. J., Avila, J., & Hernández, F. (2006). (Engel et al., 2006) pre-formed neurofibrillary tangles do not revert. *Journal of Neurochemistry*, 99(6), 1445-1455. https://doi.org/10.1111/j.1471-4159.2006.04139.x
- Evans, K. J., Gomes, E. R., Reisenweber, S. M., Gundersen, G. G., & Lauring, B. P. (2005). Linking axonal degeneration to microtubule remodeling by Spastin-mediated microtubule severing. *Journal of Cell Biology* 168, 599-606. https://doi.org/10.1083/jcb.200409058
- Gandalovičová, A., Rosel, D., Fernandes, M., Veselý, P., Heneberg, P., Čermák, V., ... Brábek, J. (2017). Migrastatics—Anti-metastatic and Anti-invasion Drugs: Promises and Challenges. *Trends in Cancer*, 3(6), 391-406. https://doi.org/10.1016/j.trecan.2017.04.008
- Grin, B., Mahammad, S., Wedig, T., Cleland, M. M., Tsai, L., Herrmann, H., & Goldman, R. D. (2012). Withaferin A alters intermediate filament organization, cell shape and behavior. *PLoS ONE*, 7(6), 1-13. https://doi.org/10.1371/journal.pone.0039065
- Guo, W., Naujock, M., Fumagalli, L., Vandoorne, T., Baatsen, P., Boon, R., ... Van Den Bosch, L. (2017). HDAC6 inhibition reverses axonal transport defects in motor neurons derived from FUS-ALS patients. *Nature Communications*, 8(1), 1-14. https://doi.org/10.1038/s41467-017-00911-y
- Hazan, J., Fonknechten, N., Mavel, D., Paternotte, C., Samson, D., Artiguenave, F., ... Weissenbach, J. (1999). Spastin, a new AAA protein, is altered in the most frequent form of autosomal dominant spastic paraplegia. *Nature Genetics*, 23(3), 296-303. doi: 10.1038/15472
- Janke, C., & Kneussel, M. (2010). Tubulin post-translational modifications: Encoding functions on the neuronal microtubule cytoskeleton. *Trends in Neurosciences*, 33(8), 362-372. https://doi.org/10.1016/j.tins.2010.05.001
- Lee, J. J., & Swain, S. M. (2008). The epothilones: Translating from the laboratory to the clinic. *Clinical Cancer Research*, 14(6), 1618-1624. https://doi.org/10.1158/1078-0432.CCR-07-2201
- Lei, P., Ayton, S., Bush, A. I., & Adlard, P. A. (2011). GSK-3 in neurodegenerative diseases. *International Journal of Alzheimer's Disease*, 2011. https://doi.org/10.4061/2011/189246
- Lodish, H., Berk, A., Matsudaira, P., Kaiser, C. A., Krieger, M., Scott, M. P., Zipursky, S. L., & Darnell, J. (2003). *Molecular Cell Biology*. New York: W. H. Freeman.
- Nakashima, S., Matsuda, H., Kurume, A., Oda, Y., Nakamura, S., Yamashita, M., & Yoshikawa, M. (2010). Cucurbitacin E as a new inhibitor of cofilin phosphorylation in human leukemia U937 cells. *Bioorganic and Medicinal Chemistry Letters*, 20(9), 2994-2997. https://doi.org/10.1016/j.bmcl.2010.02.062
- Niel, E., & Scherrmann, J. M. (2006). Colchicine today. *Joint Bone Spine*, 73(6), 672-678. https://doi.org/10.1016/j.jbspin.2006.03.006
- Overmoyer, B., Waintraub, S., Kaufman, P. A., Doyle, T., Moore, H., Modiano, M., ... Demario, M. (2005). Phase II trial of KOS-862 (epothilone D) in anthracycline and taxane pretreated metastatic breast cancer. *Journal of Clinical Oncology*, 23(16\_suppl), 778-778. doi: 10.1200/jco.2005.23.16\_suppl.778
- Palazzo, A., Ackerman, B., & Gundersen, G. G. (2003). Tubulin acetylation and cell motility. *Nature*, 421(6920), 230. https://doi.org/10.1038/421230a
- Peterson, J. R., & Mitchison, T. J. (2002). Small molecules, big impact: A history of chemical inhibitors and the cytoskeleton. *Chemistry and Biology*, 9(12), 1275-1285. https://doi.org/10.1016/S1074-5521(02)00284-3
- Roossien, D. H., Miller, K. E., & Gallo, G. (2015). Ciliobrevins as tools for studying dynein motor function. *Frontiers in Cellular Neuroscience*, 9(JULY), 1-10. https://doi.org/10.3389/fncel.2015.00252
- Sánchez, C., Pérez, M., & Avila, J. (2000). GSK3 $\beta$ -mediated phosphorylation of the microtubule-associated protein 2C (MAP2C) prevents microtubule bundling. *European Journal of Cell Biology*, 79(4), 252-260. https://doi.org/10.1078/S0171-9335(04)70028-X
- Schofield, A. V., Steels, R., & Bernard, O. (2012). Rho-associated coiled-coil kinase (ROCK) protein controls microtubule dynamics in a novel signaling pathway that regulates cell migration. *Journal of Biological Chemistry*, 287(52), 43620-43629. https://doi.org/10.1074/jbc.M112.394965
- Selenica, M. L., Jensen, H. S., Larsen, A. K., Pedersen, M. L., Helboe, L., Leist, M., & Lotharius, J. (2007). Efficacy of small-molecule glycogen synthase kinase-3 inhibitors in the postnatal rat model of tau hyperphosphorylation. *British Journal of Pharmacology*, 152(6), 959-979. doi: 10.1038/sj.bjp.0707471
- Steinmetz, M. O., & Prota, A. E. (2018). Microtubule-Targeting Agents: Strategies To Hijack the Cytoskeleton. *Trends in Cell Biology*, 28(10), 776-792. https://doi.org/10.1016/j.tcb.2018.05.001
- Trivedi, N., Marsh, P., Goold, R. G., Wood-Kaczmar, A., & Gordon-Weeks, P. R. (2005). Glycogen synthase kinase-3 $\beta$  phosphorylation of MAP1B at Ser1260 and Thr1265 is spatially restricted to growing axons. *Journal of Cell Science*, 118(5), 993-1005. https://doi.org/10.1242/jcs.01697
- Trogden, K. P., Battaglia, R. A., Kabiraj, P., Madden, V. J., Herrmann, H., & Snider, N. T. (2018). An image-based small-molecule screen identifies vimentin as a pharmacologically relevant target of simvastatin in cancer cells. *Federation of American Societies for Experimental Biology Journal*, 32(5), 2841-2854. https://doi.org/10.1096/fj.201700663R
- Xu, W., Ge, Y., Liu, Z., & Gong, R. (2015). Glycogen synthase kinase 3 $\beta$  orchestrates microtubule remodeling in compensatory glomerular adaptation to podocyte depletion. *Journal of Biological Chemistry*, 290(3), 1348-1363. https://doi.org/10.1074/jbc.M114.593830

- Yee, L., Lynch, T., Villalona-Calero, M., Rizvi, N., Gabrail, N., Sandler, A., ... Palmer, G. (2005). A phase II study of KOS-862 (epothilone D) as second-line therapy in non-small cell lung cancer. *Journal of Clinical Oncology*, *23*(16\_suppl), 7127–7127. doi: 10.1200/jco.2005.23.16\_suppl.7127
- Yoshimura, T., Kawano, Y., Arimura, N., Kawabata, S., Kikuchi, A., & Kaibuchi, K. (2005). GSK-3 $\beta$  regulates phosphorylation of CRMP-2 and neuronal polarity. *Cell*, *120*(1), 137–149. <https://doi.org/10.1016/j.cell.2004.11.012>
- Zemer, D., Pras, M., Sohar, E., Modan, M., Cabili, S., & Gafni, J. (1986). Colchicine in the prevention and treatment of the amyloidosis of Familial Mediterranean fever. *The New England Journal of Medicine*, *314*, 1001–1005. doi:10.1056/NEJM198604173141601
- Zhang, B., Carroll, J., Trojanowski, J. Q., Yao, Y., Iba, M., Potuzak, J. S., ... Brunden, K. R. (2012). The Microtubule-Stabilizing Agent, Epothilone D, Reduces Axonal Dysfunction, Neurotoxicity, Cognitive Deficits, and Alzheimer-Like Pathology in an Interventional Study with Aged Tau Transgenic Mice. *Journal of Neuroscience*, *32*(11), 3601–3611. doi: 10.1523/jneurosci.4922-11.2012
- Zigmond, S. H. (2000). How Wasp Regulates Actin Polymerization. *The Journal of Cell Biology*, *150*(6). doi: 10.1083/jcb.150.6.f117
- Zumbunn, J., Kinoshita, K., Hyman, A. A., & Näthke, I. S. (2001). Binding of the adenomatous polyposis coli protein to microtubules increases microtubule stability and is regulated by GSK3 $\beta$  phosphorylation. *Current Biology*, *11*(1), 44–49. doi: 10.1016/s0960-9822(01)00002-1.



# Vitamin-anticancer drug conjugates: a new era for cancer therapy

Ritesh P. Bhole<sup>1</sup> , Shradha Jadhav<sup>1</sup> , Yogesh B. Zambare<sup>1</sup> , Rupesh V. Chikhale<sup>2</sup> , Chandrakant G. Bonde<sup>3</sup> 

<sup>1</sup>Dr. D. Y. Patil Institute of Pharmaceutical Sciences and Research, Department of Pharmaceutical Chemistry & Pharmaceutical Quality Assurance, Pune, India

<sup>2</sup>University of East Anglia, Faculty of Pharmacy, Norwich Research Park, United Kingdom

<sup>3</sup>SPTM, School of Pharmacy, Department of Pharmaceutical Chemistry, Shirpur, India

**ORCID IDs of the authors:** R.P.B. 0000-0003-4088-7470; S.J. 0000-0002-6443-5009; Y.B.Z. 0000-0001-5115-0971; R.V.C. 0000-0001-5622-3981; C.G.B. 0000-0001-5712-1119

**Cite this article as:** Bhole, R. P., Jadhav, S., Zambare, Y. B., Chikhale, R. V., & Bonde, C. G. (2020). Vitamin-anticancer drug conjugates: A new era for cancer therapy. *Istanbul Journal of Pharmacy*, 50 (3), 312-322.

## ABSTRACT

**Background:** Following cardiovascular diseases, cancer is the world's second leading cause of death. Chemotherapy is the conventional gold technique for successful treatment of cancer. There are some drawbacks associated with traditional chemotherapy, namely, low aqueous solubility, limited biological half-life, production of multidrug resistance and non-specificity (lack of targeting ability) or dose-limiting cellular toxicity. To develop a targeted drug delivery for its anticancer effect is still a challenging task.

**Methods:** We developed literature review methods which included inclusion and exclusion criteria for identifying potentially relevant articles, articles search strategies, abstract review protocols and a comprehensive scoring system for published studies. This study contains a detailed survey of various reported methods such as folic acid-drug conjugates, Cobalamin-Drug Conjugate, Vitamin B12-Conjugated and Paclitaxel-Loaded Micelles etc., all of which were studied for their methods of preparation and possible impact on biological activity.

**Results:** Due to its specific ability to carry anticancer drugs directly to tumours, vitamin-mediated drug targeting has recently emerged as a novel concept. Solid tumour cancer has an unquenchable appetite for various essential vitamins, resulting in over-expression of the receptors involved in cell internalization of vitamins on the surface of cancer cells. So, the vitamin drug conjugates are specifically important for carrying the anticancer drugs directly to the tumour cells. Biotin, folic acid, vitamin B12 and riboflavin, the vitamin necessary for the division of all cells, especially cancer cells, have recently been examined as targeting agents.

**Conclusion:** Vitamin-Drug Conjugate methods were found to be the most suitable methods amongst all the other reported methods and they can be applied for current therapy against cancer.

**Keywords:** Cancer, chemotherapy, anticancer drug and vitamin

## INTRODUCTION

Cancer is the unchecked development of cells in the human body and these cells have the capacity to metastasize. If this spread is not managed, cancer will lead to death (Davis, 2019). It is a multicellular and multigenic disease that may occur with a complex etiology from any type of cell and organ (Baskar,

Lee, Yeo, & Yeoh, 2012). Cancer has become the world's second-largest cause of death after cardiovascular disease (Padma, 2015).

Mainstream modalities of treatment include surgery, radiotherapy, immunotherapy, hormonal therapy, laser therapy, and stem cell therapy. Surgery and radiotherapy are the most effec-

**Address for Correspondence:**  
Ritesh BHOLE, e-mail: ritesh.edu@gmail.com

Submitted: 13.01.2020  
Revision Requested: 10.03.2020  
Last Revision Received: 01.04.2020  
Accepted: 17.04.2020

This work is licensed under a Creative Commons Attribution 4.0 International License.



tive and common therapies for localized primary tumors and non-metastatic cancers. Cancer drugs (chemotherapy, biological and hormonal therapy) are used to treat metastatic cancer. Drugs spread to all tissues in the body, through the bloodstream (Pérez-Herrero, & Fernández-Medarde, 2015). Thus, for effective cancer treatment, chemotherapy is said to be as the gold standard strategy. Chemotherapy is based on chemotherapeutic drugs (i.e. toxic compounds) that act by inhibiting the cancer cells' rapid proliferation. There are some drawbacks associated with traditional chemotherapy, i.e. chemotherapeutic drugs with cancer cell suppression, which can also prevent the rapid growth needed to maintain normal cells, such as bone marrow, gastrointestinal tract and hair follicle cells, leading to undesirable side effects in cancer treatments (Seifu & Nath, 2019). Some other drawbacks in cancer treatment associated with free chemotherapeutic agents are low aqueous solubility, short biological half-life, production of multidrug resistance and non-specificity (lack of targeting capacity) or dose-limiting cellular toxicity.

Consequently, it is still difficult to target an anti-cancer drug selectively to cancerous cells and to achieve a breakthrough in cancer research. To achieve this goal, different approaches can be implemented. The most popular is to provide an effective carrier for a medication. Thanks to its ease of use and uncomplicated chemical modification, polymeric drug carriers are the most powerful (Pawar, Badhwar, Kharas, Khandare, & Vavia, 2012; Tripodo, Mandracchia, Collina, Rui, & Rossi, 2014). Such systems usually have the ability to accumulate by means of passive drug targeting in different organs as a result of their removal route or for active organotropism, and a more specific drug targeting can be accomplished by adding a carrier with specific targeting agents, such as vitamins, antibodies, peptides, magnetic particles or hormones (Cavallaro, Maniscalco, Campisi, Schillaci, & Giammona, 2007; Bareford, Avaritt, Ghandehari, Nan, & Swaan, 2013; Tripodo et al., 2014; Gibiansky & Gibiansky, 2014; Qu, Zhou, Chen, Chen, & Shen, 2015). The most commonly used method for drug targeting to specific cells is to attach a drug directly to targeting moiety to form a new chemical entity which is pharmacologically active, i.e. prodrug (Elsadek et al., 2010; Tripodo et al., 2014). In these conditions, the so-called vitamin-mediated drug targeting has recently emerged as a new concept for carrying anticancer drugs particular to tumours (Mahato, Tai, & Cheng, 2011; Bildstein, Dubernet, & Couvreur, 2011; Fortin & Berube, 2013). As it is well known, all living cells require vitamins for their survival, whereas rapidly dividing cells that are found in solid tumour cancer, have an unquenchable appetite for different essential vitamins, resulting in vitamin receptors being over-expressed on the surface of cancer cells. In addition, there has been a claim that the combination of an anticancer drug with a particular vitamin contributes to the development of vitamin-drug conjugates (Figure 1). This vitamin drug conjugate would lead to the targeting of a higher amount of drugs, i.e. a high dose to the targeted cancer cells. Biotin, folic acid, vitamin B12 and riboflavin, which are necessary for the division of all cells, in particular cancer cells, have recently been investigated as targeting agents (Chen et al., 2010; Russell, McTavish, & McEvan, 2011).

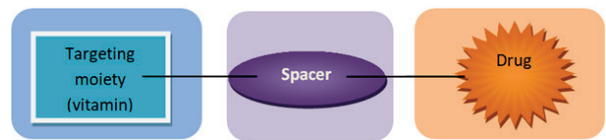


**Figure 1.** Vitamin drug conjugate.

### Vitamin-Drug Conjugates

A drug is linked directly or through a spacer with a targeting moiety to form a pharmacologically active new chemical entity to produce vitamin-drug conjugate.

Advantages: Vitamin drug conjugates will be nontoxic, and they will be specifically internalized into cancerous cells and release anticancer drugs without loss of potency. In addition, they will minimize the systemic toxicity by being stable in blood circulation, and provide a target specific activity by sparing the normal cell that will minimize any side effects (Ojima, Zuniga, Berger, & Seitz, 2012).

### Vitamin-9 (Folic Acid)-Drug Conjugates

Folic acid (FA) is more closely related to folate receptors (FR). Glycosylphosphatidylinositol (GPI)-linked membrane folate receptor was involved in folate-based chemotherapeutic drug receptor-mediated absorption (Rijnbouts, Jansen, Posthuma, Hynes, & Schornagel, 1996). This GPI-connected membrane protein collects the ligands from the extracellular matrix and transports them through the recycled endosomal pathway to the intracellular space (Figure 2). The folate receptors are also recognized as tumour antigens/biomarkers due to the fact that the folate receptors are commonly absent in normal tissues. This has led to the development of therapeutics and diagnosis approaches for the treatment of cancer (Leamon et al., 2007). Hence molecular payloads with a size range from radio-nuclides to large constructs of DNA and liposome have been

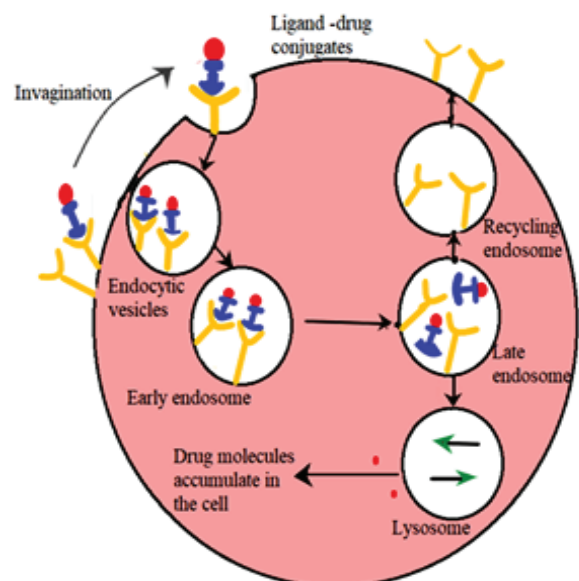


**Figure 2.** Receptor mediated endocytosis of folate-drug conjugate.

successfully delivered through the FR pathway within cancer cells. One particularly related approach is to attach powerful chemotherapy drugs to FA to form a small molecule drug conjugate or SMDCs. (Vlahov & Leamon, 2012).

### Folic acid-paclitaxel conjugates

Yuxuan et al., 2019, engineered the conjugates of folic acid-peptide-paclitaxel (FA-P3/P7-PTX), to resolve drug resistance, achieve targeted delivery to tumours, increase cellular absorption, and allow water-soluble conjugates. The synthesized (FA-P3/P7-PTX) conjugate was a folic acid-lytic peptide conjugate, in which lytic peptides I-3 and I-7 were used as molecular carriers and cell-disrupting peptides. 16-site cysteine-substituted I-3 and I-7 were named as P3 and P7, respectively, and served as a peptide backbone. The conjugates were tested for their efficacy and also showed higher anti-proliferative activity than free paclitaxel in MCF-7/PTX cells. Higher cellular uptake in MCF-7/PTX cells was shown by, FA-P3-PTX than P3-PTX, which was based on folate receptors present. FA-P7-PTX had a much stronger effect on cell toxicity, apoptosis and membrane disturbance behavior in MCC. Similar to FA-P3-PTX, FA-P7-PTX had more ability to suppress tumor growth than PTX. (Wang et al., 2011; Gaspar, Costa, Qeios, Pichon, & Souse, 2015; Dai et al., 2019).

### Folic acid-DAVLBH conjugates (Vintafolide)

Vintafolide (formerly EC145), the most active FA-SMDC, developed by Leamon et al., 2014, was a water-soluble conjugate that selectively delivers the medication desacetyl vinblastine monohydrate (DAVLBH) to tumours over-expressed to FR-alpha (Leamon et al., 2014). Preclinical studies have shown

a higher affinity of vintafolide to bind to FR $\alpha$ , and therefore have a very strong and selective action against FR $\alpha$ -positive xenografts as compared to untargeted DAVALBH (Vlahov et al., 2009).

Vintafolide consists of 4 part modules: 1) a folic acid moiety targeting FR $\alpha$ , 2) a hydrophilic peptide spacer, 3) an autoimmolative disulfide linker, and 4) a DAVALBH microtubule-stabilizing compound (Figure 3).

Leamon et al., 2014, conducted a study to assess the impact of changing three of the vintafolide's constituent elements out of the four. It was noted that by changing the spacer composition, given the spacer remained hydrophilic, the vintafolide's potency was minimally affected. By comparison, the bioreleasable linker such as glutathione (GluSH) in the endosomal setting is cleaved by the intracellular thiols which is of critical importance for the conjugate action and has been the most successful approach to activated drug release within the cell (Figure 4). As an example, self-immolative disulfide and acyl hydrazone were exercised both *in vitro* and *in vivo* activity, while vintafolide analogs showed more stable amide linkers and thioether linkers did not show (Leamon et al., 2014). In addition, it was shown that by replacing DAVALBH with other clinically approved vinca alkaloid drugs (such as vincristine, vinflunine, vinorelbine and vindesine) while retaining the cleavable disulfide linker, vintafolide was the only variant showing biological activity *in vitro* and *in vivo*. It was later hypothesized that other absence of activity in other vinca alkaloid was found due to alteration in the chemical structures, following disulfide reduction and linker release.

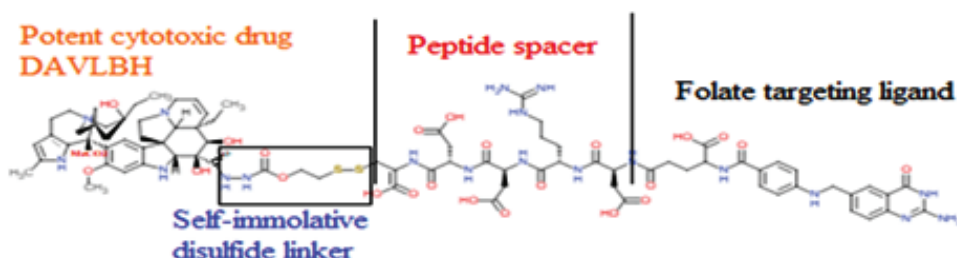


Figure 3. Chemical structure of folic acid-based SMDC vintafolide.

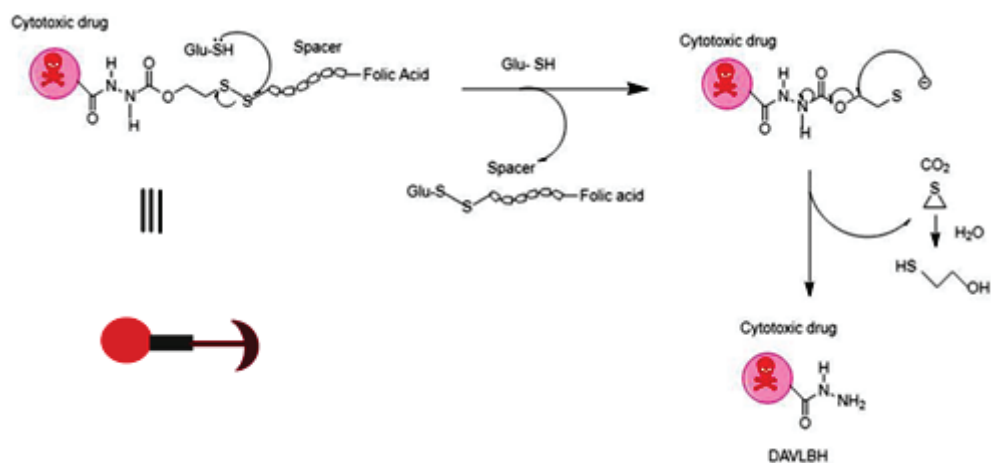


Figure 4. Drug release mechanism of vintafolide.

EC145 was the first clinically tested FA-SMDC. Vintafolide showed reliability, both as a single agent and in conjunction with doxorubicin, in two phase II tests (ovarian and non-small cell lung cancers) and in a controlled open-label Phase II test (platinum-resistant ovarian cancer). It entered the clinical trials phase-III for advanced platinum-resistant ovarian cancer in 2010 (Leamon et al., 2014). This FA-SMDC failed to meet the previously stated progression-free survival requirements and the trial was prematurely terminated due to this outcome. Despite expectations of doing otherwise, the Phase III trials were unable to demonstrate the dominance of the targeted FR therapy over conventional chemotherapy. Future studies and experiments therefore need to be performed for a good range of qualifying patients who may adequately benefit from anti-FR therapy. (Leamon et al., 2014; Sausville et al., 2007; Reddy et al., 2007; Naumann et al., 2013; Naumann & Coleman, 2011; Vlahov et al., 2009; Fernandez, Javaid, & Chudasama, 2018).

### Folate-taxoid conjugates

Seitz, 2015, developed a folate-taxoid conjugate of the next decade that is highly potent for use against drug-sensitive and drug-resistant cell lines of cancer. This folate-taxoid conjugate (Figure 5) contains both a highly potent taxoid, i.e. an analog of the chemotherapeutic drug Taxol, and also folic acid moiety. This SMDC has a hydrophilic PEGylated dipeptide spacer and an autoimmolative disulfide linker, similar to vintafolide (Seitz, Vineberg, Herlihy, Park, & Melief, 2015).

*In vitro* research was conducted to compare the behavior of the free taxoid and taxoid conjugate in FRa-positive and FRa-negative cells. For both cell lines, i.e., free (taxoid) SB-T-1214 was highly potent as expected. Moreover, taxoid conjugate demonstrated significant cytotoxicity to the FRa-positive cell lines. In addition, taxoid conjugate also showed more than a 1000-fold decline in toxicity to normal cells compared to the free drug (Fernandez et al., 2018).

Such FA-SMDCs are from a vast field of conjugates using a disulfide linker for cytotoxic drug release. It is particularly relevant to note that folate is conjugated to many other medications, such as camptothecins (Henne, Kularatne, Hakenjos, Carron, & Henne, 2013), tubulysins (Reddy et al., 2009; Bartouskova, Melichar, & Mohelnikova, 2015), mitomycins (Leamon et al., 2007), and maytansinoids, all of which were prepared and evaluated by disulfide linker.

### 5-Fluorouracil loaded PLGA-1, 3-diaminopropane-folic acid nanoparticles

Because of a low FA conjugation ratio, (Wang et al., 2015), developed a PLGA [poly (lactic co-glycolic acid)]-based drug delivery carrier with a targeting mood such as folic acid (FA) that has poor targeting performance. A crosslinker 1, 3-diaminopropane was used in this work to produce a FA-conjugated PLGA device and achieved a high 46.7% (mol / mol) conjugation level. The prepared biomaterial based on PLGA was then used for encapsulation into nanoparticles of 5-fluorouracil (5-FU). The IC<sub>50</sub> of 5-FU loaded PLGA-1, 3-diaminopropane-folic acid nanoparticles on HT-29 cancer cells was observed to be 5.69 mg/mL *in vitro* experiments and is smaller than that of 5-FU loaded PLGA nanoparticles and 5-FU with only 14.17 and 22.9 mg/mL, IC<sub>50</sub> respectively. The images of fluorescent microscopy showed that targeting nanoparticles have more affinity with cancer cells, and nanoparticles with FA are taken up in greater amount than pure drugs and untreated nanoparticles, by the cancer cells with HT-29. The 5-FU primed PLGA-1, 3-diaminopropane-folic acid nanoparticles are therefore one of the highly efficient methods for the targeted delivery of the drug to the cancer cells (Wang, Li, Chen, Gao, Zeng, & Kong, 2015).

### Folic acid- trimethyl chitosan- paclitaxel conjugates

He & Yin, 2017, developed a trimethyl chitosan (TMC-PTX) conjugated paclitaxel (PTX) modified with folic acid (FA), (FA-TMC-PTX) for oral and intravenous delivery of PTX. Modification of FA has been carried out to alleviate conjugate protein adsorption (Pawar et al., 2012; Henne et al., 2013, He & Yin, 2017).

### Folic acid coupled to the pegylated-liposomes of 5-fluorouracil

Pegylated-liposomes coupled with folic acid were produced by Gupta et al., 2007, and they increased the *in vitro* absorption by up to 11 times compared to non-coupled pegylated liposomes. The tumor-inhibitory effect of FA-SL (stabilized liposome) was significantly greater than that of free 5-FU and SL. Therefore, this device can be successfully used to target 5-FU to the tumour cells. (Gupta, Jain, Jain, & Jain, 2007).

### Abrabinogalactan-folic acid- drug conjugate

The FA-AG-GFLG-MTX conjugate, illustrated by Pinhasi et al., 2009, shows the distribution of a cytotoxic cargo to FR-over-expressing cells. They also showed, a target-activated release

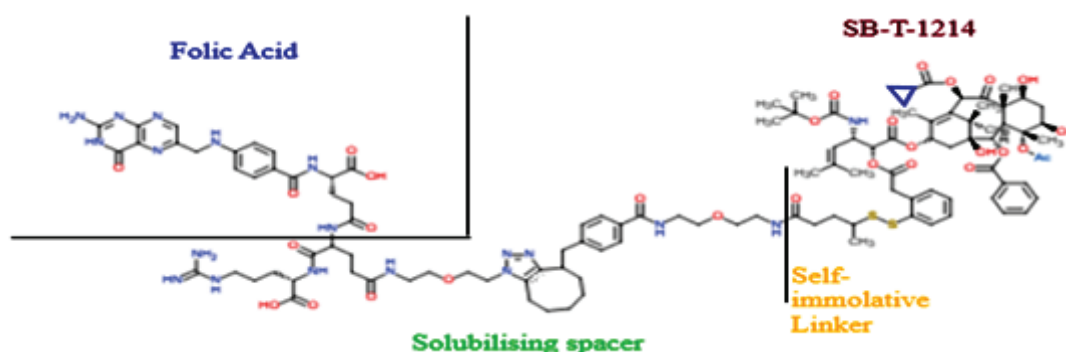


**Figure 5.** Structure of folate- taxoid conjugate.

mechanism by adding an endosomally cleavable peptide (GFLG) into the conjugate. Compared to normal cells, this conjugate showed a 6.3-fold increase in cytotoxic activity of cancer cells. This result creates a novel FA bound polymer nanoconjugate to transmit methotrexate to over-expressed cancer cells in FR. (Pinhassi et al., 2009).

### Cobalamin-Drug-Conjugate

The invention provides a cobalamin-drug conjugate in which cobalamin is indirectly covalently bound to an anti-tumour drug through a cleavable linker and one or more optional spacers, and is suitable for the treatment of tumour-related diseases. Cobalamin is covalently bound by the 5'-OH of the cobalamin ribose ring to a cleavable linker or the first spacer. The drug is connected to the cleavable linker's Second Spacer through an additional or current functional group on the surface. This conjugate then forms a transcobalamin complex (any of its isoforms). This complex binds to the receptor present on the cell membrane and is the result of cellular internalization, and the intracellular enzymes then separate the conjugates and activate the drug. Based on the conjugate form, the specific class or type of intracellular enzyme influences the cleavage. As there is a high demand of rising cells for cobalamin, tumour cells have more appetite than the normal cells. Compared to a free drug, the technology conjugate has an increased potency and reduced systemic toxicity. (Jung & Keller, 2012).

### VB12-Conjugated and PTX-Loaded Micelles (VB12-Sericin-PBLG (Poly (Gamma-Benzyl-L-Glutamate))-PTX)

Guo et al., 2018, introduced sericin micelles to reverse drug resistance in their previous research, but these sericin micelles could not selectively bind to the cells of gastric cancer (GC). They developed sericin micelles conjugated with vitamin B12 (VB12) for the targeted treatment of gastric cancer. Researchers studied their physicochemical properties, the function of antitumours, and the cellular uptake. It was shown that VB12-sericin-PBLG-PTX micelles have an acceptable particle size, have strong dispersion, and are bio-safe. Through following transcobalamin-II (CD320)-receptor-mediated endocytosis, the micelles were internalized cellularly with gastric targeting and improved cellular uptake capacities, they reversed drug resistance, and modified the mitochondrial transmembrane / apoptosis pathway (Guo et al., 2018).

### Vitamin B12-Metal Conjugates for the Therapeutic and Diagnostic Application

Vitamin B12 (cyanocobalamin) is an essential nutrient characterized by very poor bioavailability. Due to the rapid rate of proliferation of cancerous cells, they have a greater demand of nutrients including a greater vitamin B12 uptake compared to normal cells. Such a cyanocobalamin appetite can be used for site-specific delivery of the medication to tumour cells by conjugating the vitamin B12 (carrier) anticancer drug for therapeutic use or by conjugating a fluorophore or radionuclide diagnostic agent with vitamin B12 for diagnostic use. Vitamins such as B12 are transformed through biologically active cofactors, i.e. methylcobalamin (which is used to manufacture

methionine) and adenosylcobalamin (which is used as a coenzyme to generate energy through the synthesis of carboxylic acids), and it is noteworthy that the quickly dividing tumour cell needs higher amounts of methionine and energy for replication, allowing vitamin B12 to be more aimed at cancer.

### Therapeutic vitamin B12- metal conjugates

An impressive number of studies on platinum-based and other metal-based anticancer drugs were generated from the marketing and clinical establishment of anticancer drug cisplatin, but the main drawback associated with such treatment is low water solubility, low bioavailability, non-specific tumour cell binding, and higher toxicity. There has lately been a greater interest in the development of vitamin-metallo drug conjugates, but none of them have yet reached the clinical trial stage and have thus far only explored their therapeutic efficacy.

**Platinum:** Florea & Büsselberg, 2011, developed a strategy to address the issue of non-specific anticancer medication binding, such as cisplatin, and its severe side effects. Conjugating cisplatin to cyanocobalamin as an anticancer medication has been speculated as a possible way of improving tumour-specific attachment with a better clinical output. The metal containing scaffolds are directly linked by the nitrogen atom to the cyanogroup present on vitamin B12, producing a heterodinuclear derivative (B12-CoIII-CN-M), in which the present vitamin serves as a ligand. For vitamin B12 to be transformed into its cofactor (methylcobalamin or adenosylcobalamin) requires first of all the reduction of Co (III) to Co (II) by removing the main cyanogroup. Thus, when mixing a metal product with the moiety B12-CoIII-CN, the release of the cyanometal species (CN-M) will occur directly within the cells, so this vitamin B12-metal conjugate would be considered a prodrug.

*In vitro* cytotoxicity experiments on human ovarian adenocarcinoma A2780 cells and human breast adenocarcinoma MCF7 cells have shown that the isolated Pt (II)-cyanoderivative has a comparable anti-cancer action to cisplatin, thereby indicating that conjugate (B12-CoIII-CN-PtII) can be identified as a prodrug because it has the ability to release Pt II, a cytotoxic agent, directly into the body. Unfortunately, this hypothesis was not consistent with evidence that the initial conjugate was less cytotoxic than free cisplatin. (Ruiz-Sanchez, Konig, Ferrari, & Alberto, 2011; Tran, Sturup, Lambert, Gammelgaard, & Furger, 2016; Petteuzzo, Pigot, & Ronconi, 2017).

### Diagnostic vitamin B12-metal conjugates

Recent developments for diagnostic applications of vitamin B12-metal conjugates using radiodiagnostic or fluorescent samples are discussed below. A variety of biomolecules are used as a carrier for radionuclides, some of which have been approved by Food and Drug Administration, such as peptides and monoclonal antibodies. Among all of these, vitamins were researched as a target-specific delivery carrier in which vitamin B12 is the least studied.

**Gadolinium:** -Gadolinium (III) is a paramagnetic material that is used for magnetic resonance imaging (MRI) and may also be cytotoxic. Siega et al., 2009, formed two metal chelating ligands of vitamin B12, either diethylenetriamine-N, N,



N,N',N'',N'''-pentaacetic acid (DTPA) or triethylenetetramine-N, N'',N'',N'',N'',N''',N''''-hexaacetic acid (TTHA), and the corresponding gadolinium(III) combines Gd-1 and Gd-2 (Figure 6).

On human immortalized myelogenous leukemia K562 cells, in vitro cytotoxicity was performed; in which it was found that the Gd-1 conjugate emitted the Gd<sup>3+</sup> molecule, resulting in reduced cell viability. On the other hand, when the same test was performed of more stable Gd-2 ion, it did not show Gd<sup>3+</sup> cell internalization, and also no significant influence was observed on cell viability (Siega et al., 2009; Pettenuzzo et al., 2017).

### Vitamin D3-Drug Conjugates

Patil, Gawali, Patil, & Basu, (2014), developed nanoparticles of vitamin D3 to deliver some of the commonly used and clinically licensed anticancer drugs such as doxorubicin (a DNA-damaging agent), paclitaxel (a microtubule-stabilizing agent) and PI103 (a phosphatidylinositol-3-kinase inhibitor). Next, they developed vitamin D3-drug conjugates (Figure 7-compound no 3, 4 and 5), then the biocompatible vitamin D3 nanoparticles were synthesized from these conjugates using a process of hydration-extrusion solvent evaporation-lipid film (Figure 8).

Such vitamin D3-nanoparticles were examined in the drug release model. A gradual and continuous release of medications over a period of time and an accelerated release was

found at pH 5.5 relative to pH 7.4. Connections in vitamin-drug conjugates, i.e. vitamin-D3-PI103 conjugates, contain phenolic-ester connections, vitamin D3-paclitaxel conjugates contain ester connections, and amide-connected vitamin-D3-doxorubicin conjugates were more labile at pH 5.5 relative to pH 7.4, resulting in increased drug release at acid pH. In addition, the cellular absorption process of vitamin D3-NPs was studied in HeLa cells by treating them with vitD3-Dox-NPs. It was observed that internalization in HeLa cells was through a low pH lysosomal compartment, whereas free drug doxorubicin was internalized through the diffusion path. A similar endocytosis was expected for VitD3-paclitaxel-NPs and vitD3-PI103-NPs (Patil et al., 2014; Petros & DeSimone, 2010; Rajendran, Knolker & Simons, 2010; Iversen, Skotland, & Sandvig, 2011).

### Dual drug loaded vitamin D3 nanoparticles

One of cancer chemotherapy's most challenging problems is combating drug resistance. Drug cocktails can overcome drug resistance. Double vitamin D3 nanoparticles (i.e. a fair mixture of PI103 and doxorubicin or paclitaxel or cisplatin) were developed by Palvia et al. 2014, (Table 1). Nanoparticles dual drug release was observed to be higher at pH 5.5 relative to pH 7.4 at a slow rate over 72 hours in a prolonged fashion, and at 37°C and 40°C for more than 15 days. Cell death by dual drug loaded nanoparticles in human hepatocellular

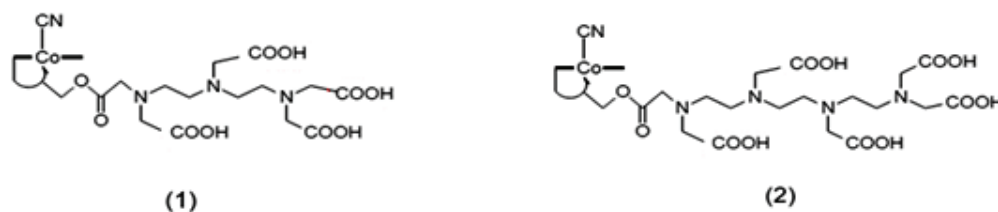


Figure 6. Vitamin B12-DTPA and vitamin B12-TTHA ligand.

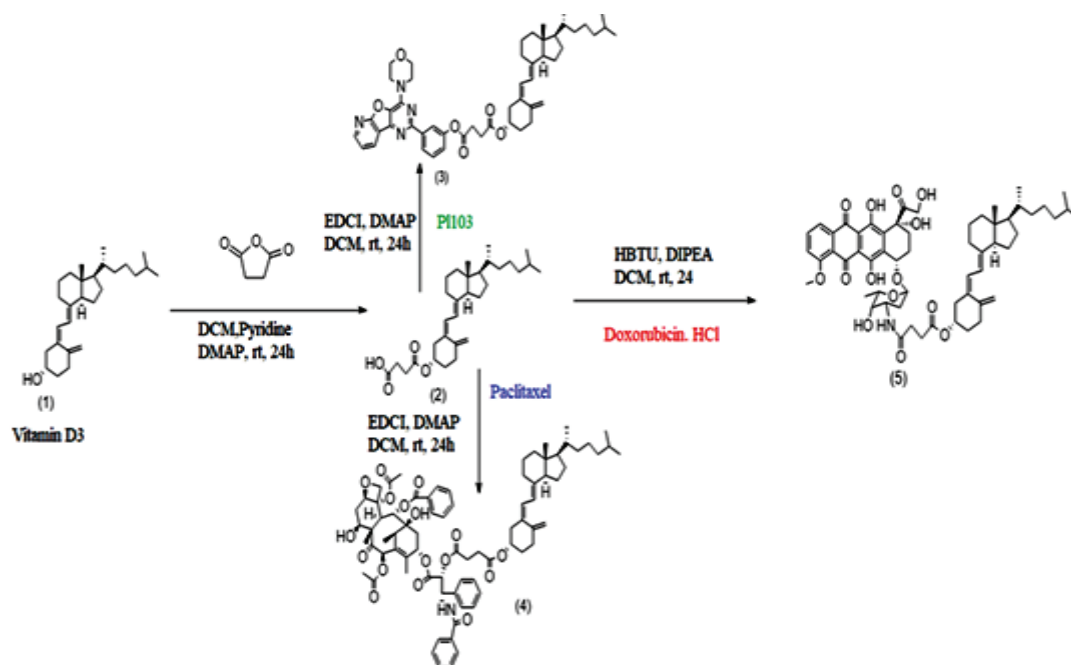


Figure 7. Synthetic scheme for vitamin D3- drug conjugate.

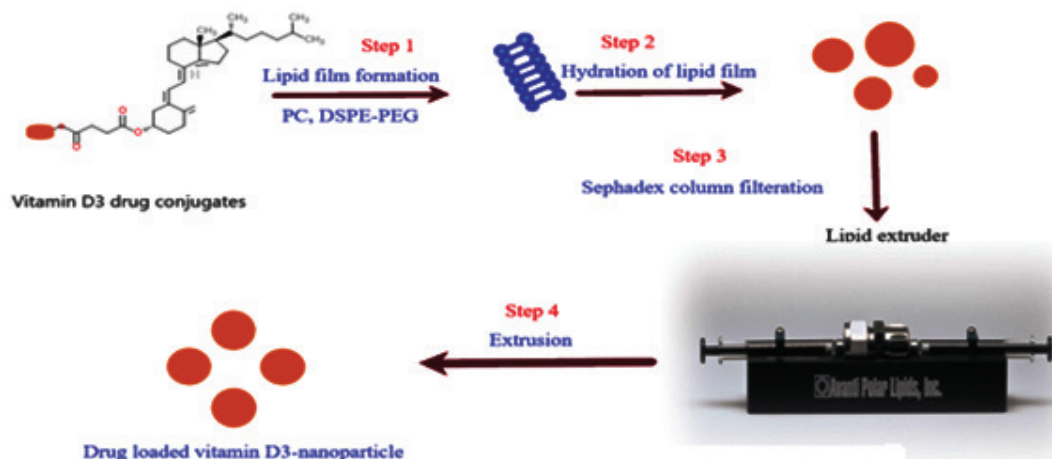


Figure 8. Synthetic scheme for vitamin D3 nanoparticles.

NANOPARTICLES	APPLICATION
VitD3-PI103-Dox-NP and VitD3-PI103-CDDP-NP.	Showed toxicity by inducing apoptosis, through DNA damaging.
VitD3-PI103-CDDP-NP.	Showed improved efficacy in 5-fluorouracil resistant Hep3B-5FU-R cells
VitD3-PI103-Proflavlin-NP.	Internalized cisplatin resistant Hep3B-R cells faster (3 mins) as compared to Hep3B cells.

(Palvai, Nagraj, Mapara, Chowdhury, & Basu, 2014).

carcinoma (Hep3B cell) was found to be increased at 24 hours compared to monotherapy (Persidis, 1999; Garraway & Janne, 2012; Parhi, Mohanty, & Sahoo, 2012; Palvai, Nagraj, Mapara, Chowdhury, & Basu, 2014).

### Vitamin-E-Drug-Conjugates

#### Vitamin-E analogue-neomycin conjugate for RNA-I drug

Iwata et al., 2015, synthesized a vitamin E-conjugated neomycin derivative to administer RNAi (RNA interference) medication to the cell of liver cancer and tested it for its biological and physicochemical properties. siRNA delivery studies were not entirely successful, but some of the neomycin derivatives showed significant RNAi activity in liver cancer cells. (Iwata et al., 2015).

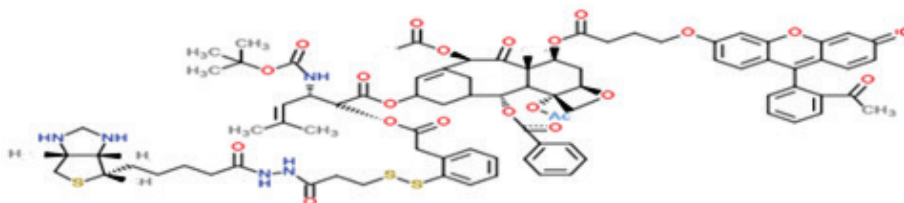


Figure 9. Chemical structure of biotin-SBT-1214-fluorescein conjugate.

### Biotin-Drug-Conjugates

#### Biotin-taxoid conjugates

Chen et al., 2010, developed a biotin (vitamin or vitamin B7)-taxoid conjugate for a tumour-targeted drug delivery system. These conjugates included biotin as a mood-targeted tumour, a mechanism-based self-immolative linker, and a cytotoxic agent (SB-T-1214) (Figure 9). They developed a tumour-specific mechanism for the delivery of drugs based on endocytosis mediated by vitamin receptors. Reports of L1210FR leukemia cells that over-express biotin receptors were performed. The result was an excellent site-specific delivery of the conjugates, reducing unwanted toxicity to healthy cells (Chen et al., 2010; Tripodo, Mandracchia, Collina, Rui, & Rossi, 2014).

#### Biotin-doxorubicin conjugates

Ibsen et al., 2010, developed and synthesized the biotin-doxorubicin conjugate in which the amine component of doxorubicin was derivatized with a photocell biotinylated spacer (Figure 10) (Tripodo et al., 2014).

Ibsen et al., 2010, demonstrated that the doxorubicin (i.e. active drug) is only released after the conjugates are internalized into the cancerous cells and then further activated via exposure to UV at 350 nm of the photocleavable group in the conjugate, leading to a decrease in the cytotoxic effects on normal cells.

The cell proliferation assay results clearly evidenced a lower cytotoxicity of conjugate than that of free doxorubicin (Sutherland & Griffin, 1981; Ibsen et al., 2010).

The brief summary of all the reported methods and their advantages over conventional chemotherapy is shown in Table 2.

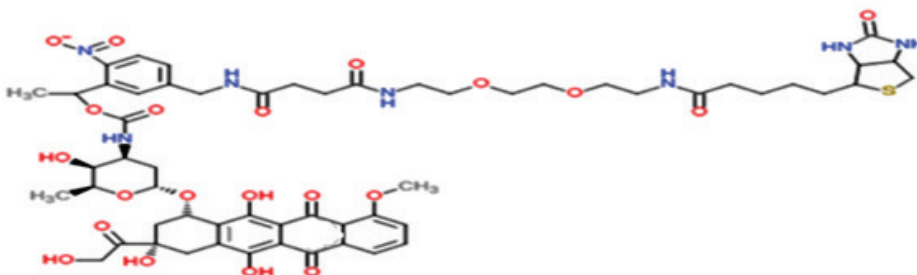


**Figure 10.** Chemical structure of biotin-doxorubicin conjugate.

<b>Table 2. Vitamin-drug conjugates and their advantages over chemotherapeutic drugs.</b>		
<b>Sr. No.</b>	<b>Method</b>	<b>Advantages over chemotherapeutic drugs</b>
1.	<b>Folic acid-Paclitaxel Conjugates.</b>	Conjugate showed higher anti-proliferative activity, Higher cellular uptake than free paclitaxel in MCF-7/PTX cells. FA-P7-PTX had a much stronger effect on cell toxicity, apoptosis and membrane disturbance behavior in MCC. FA-P3-PTX, FA-P7-PTX conjugates had more ability to suppress tumour growth than PTX. (Dai et al., 2019).
2.	<b>Folic acid-DAVLBH (desacetyl vinblastine monohydrate) conjugate / Vintafolide.</b>	Vintafolide showed higher affinity to bind FRA (folate receptor-alpha), and therefore has a very strong and selective action against FRA-positive xenografts as compared to untargeted DAVLBH. (Vlahov et al., 2009).
3.	<b>Folate-Taxoid Conjugates.</b>	Taxoid conjugate demonstrated significant cytotoxicity to the FRA-positive cell lines. In addition, taxoid conjugate also showed more than 1000-fold decline in toxicity to normal cells compared to the free drug (Fernandez et al., 2018).
4.	<b>5-Fluorouracil Loaded PLGA-1, 3-Diaminopropane-Folic Acid Nanoparticles</b>	Targeting nanoparticles have more affinity with cancer cells and nanoparticles with FA are taken up in greater amount than pure drugs and untreated nanoparticles, by the cancer cells with HT-29. (Wang et al., 2015).
5.	<b>Folic Acid- Trimethyl Chitosan- Paclitaxel Conjugates</b>	Folic acid modification in TMC-PTX alleviated the protein adsorption of conjugate. FA-TMC-PTX conjugate showed enhanced antitumor activity. (He & Yin, 2017; Pawar et al., 2012; Henne et al., 2013).
6.	<b>Folic Acid Coupled to the Pegylated-Liposomes of 5-Fluorouracil</b>	Pegylated-liposomes coupled with folic acid showed increased <i>in-vitro</i> absorption by up to 11 times compared to non-coupled pegylated liposomes. The tumour-inhibitory effect of FA-SL (stabilized liposome) was significantly greater than that of free 5-FU and SL. (Gupta et al., 2007).
7.	<b>Abrabinogalactan-Folic Acid- Drug Conjugate.</b>	This conjugate showed a 6.3-fold increase in cytotoxic activity of cancer cells compared to the normal cells (Pinhassi et al., 2009).
8.	<b>Cobalamin-Drug Conjugate.</b>	As there is a high demand of rising cells for cobalamine, tumor cells have more appetite than the normal cells. Compared to a free drug, the technology conjugate has an increased potency and reduced systemic toxicity. (Jung & Keller, 2012).
9.	<b>VB12-Conjugated And PTX-Loaded Micelles (VB12-Sericin-PBLG (Poly (Gamma-Benzyl-L-Glutamate))-PTX)</b>	Sericin micelles could not selectively bind to the cells of gastric cancer, the vitamin B12conjugated micelles were internalized cellularly with gastric targeting and improved cellular uptake capacities, reversed drug resistance, and modified the mitochondrial transmembrane / apoptosis pathway. (Guo et al., 2018).

**Table 2. Continued.**

10.	<b>Vitamin B12 – Metal Conjugates for the Therapeutic and Diagnostic Application</b>	<p><b>Therapeutic Vitamin B12- Metal Conjugates:-Platinum:</b> - A2780 cells and MCF7 cells have shown that the isolated Pt (II) - cyanoderivative has a comparable anti-cancer action to cisplatin, thereby indicating that conjugate (B12-CoIII-CN-PtII) can be identified as a prodrug because it has the ability to release Pt II (i.e. a cytotoxic agent) directly into the body. Unfortunately, this hypothesis was not consistent with evidence that the initial conjugate was less cytotoxic than free cisplatin (Ruiz-Sanchez et al., 2011).</p> <p><b>Diagnostic Vitamin B12-Metal Conjugates:-</b>  <b>Gadolinium:</b> -K562 cells, in vitro cytotoxicity was performed; in which it was found that the Gd-1 conjugate emitted the Gd<sup>3+</sup> molecule, resulting in reduced cell viability. On the other hand, when the same test was performed of more stable Gd-2 ion, it did not show Gd<sup>3+</sup> cell internalization, and also no significant influence was observed on cell viability . (Siega et al., 2009 &amp; Pettenuzzo et al., 2017).</p>
11.	<b>Vitamin D3- Drug Conjugates.</b>	Vitamin D3- Drug Conjugates showed increased drug release in acidic pH (5.5) as compared to pH 7.4. Conjugates showed internalization in HeLa cells through a low pH lysosomal compartment, whereas free drug doxorubicin was internalized through the diffusion path. (Patil et al., 2014).
12.	<b>Dual Drug Loaded Vitamin D3 Nanoparticles.</b>	Nanoparticles dual drug release was observed to be higher at pH 5.5 relative to pH 7.4 at a slow rate over 72 hours in a prolonged fashion, and at 37°C and 40°C for more than 15 days. Cell death by dual drug loaded nanoparticles in human hepatocellular carcinoma (Hep3B cell) was found to be increased at 24 hours compared to monotherapy (Palvai et al., 2014).
13.	<b>Vitamin-E Analogue-Neomycin Conjugate for RNA-I Drug.</b>	SiRNA delivery studies were not entirely successful, but some of the neomycin derivatives showed significant RNAi activity in liver cancer cells. (Iwata et al., 2015).
14.	<b>Biotin-Taxoid Conjugates.</b>	L1210FR leukaemia cells that over-express biotin receptors were performed. The result was an excellent site-specific delivery of the conjugates, reducing unwanted toxicity to healthy cells. (Chen et al., 2010).
15.	<b>Biotin-Doxorubicin Conjugates.</b>	A lower cytotoxicity of conjugate than that of the free doxorubicin was observed. (Ibsen, Zahavy, Wrasdilo, Berns, & Chan, 2010).

## CONCLUSION

Such vitamin-drug conjugates identify and manipulate the inherent morphological and physiological distinctions between normal cells/tissues and cancerous ones. For example, cancer cells that are rapidly growing overexpress cancer-specific receptors to increase nutrient and vitamin intakes. These receptors can be used as targets for the targeted delivery of cytotoxic drugs to cancer cells via receptor-mediated endocytosis (RME). Our review focuses on the conventional treatment of cancer and its advantages and disadvantages. It was noted that there are many novel approaches involved in overcoming these disadvantages. Out of several formulation therapies involved, methods such as conjugation with metal ions or conjugation with several vitamins etc. The Vitamin Drug conjugates were found to be a most effective therapy. Progress in Vitamin-drug conjugates, including some of the recent vitamin-drug conjugates for target specific delivery via vitamin-receptor mediated endocytosis mechanism, reduces the undesirable toxicity to healthy cells. Some of the vitamin-metallo drug conjugates are also given, which are used for therapeutic and diagnostic applications in cancer treatment. Out of all the methods reviewed, the vitamin B12 conjugate

method was found to be more specific, and also had a more positive impact on biological activity.

From the literature survey, the conjugation of vitamins with an anticancer agent is of great interest and is becoming a highly innovative approach to improving efficacy and reducing toxicity to healthy cells.

Although very few vitamin-drug conjugates have thus far been developed, this field is in constant growth, as there is a wider need for a targeted drug delivery for cancer therapy.

**Peer-review:** Externally peer-reviewed.

**Author Contributions:** Conception/Design of Study- R.P.B, C.G.B.; Data Acquisition- R.P.B., Y.B.Z.; Data Analysis/Interpretation- S.J., R.V.C., R.P.B.; Drafting Manuscript- R.P.B., S.J., C.G.B.; Critical Revision of Manuscript- R.V.C., R.P.B., Y.B.Z.; Final Approval and Accountability- R.P.B., S.J., Y.B.Z., R.V.C., C.G.B.; Technical or Material Support- R.P.B, C.G.B.; Supervision- R.P.B., S.J., Y.B.Z., R.V.C., C.G.B

**Conflict of Interest:** The authors have no conflict of interest to declare.

**Financial Disclosure:** Authors declared no financial support.

## REFERENCES

- Bareford, L. M., Avaritt, B. R., Ghandehari, H., Nan, A., & Swaan, P. W. (2013). Riboflavin-targeted polymer conjugates for breast tumor delivery. *Pharmaceutical Research*, 30(7), 1799–812. <http://dx.doi.org/10.1007/s11095-013-1024>.
- Bartouskova, M., Melichar, B., & Mohelnikova-Duchonova, B. (2015). Folate receptor: A potential target in ovarian cancer. *Pteridines*, 26(1), 1–2. <https://doi.org/10.1515/pterid-2014-0013>.
- Baskar, R., Lee, K. A., Yeo, R., & Yeoh, K. W. (2012). Cancer and radiation therapy: Current advances and future directions. *International Journal of Medical Sciences*, 9(3), 193. <http://dx.doi.org/10.7150/ijms.3635>.
- Bildstein, L., Dubernet, C., & Couvreur, P. (2011). Prodrug-based intracellular delivery of anticancer agents. *Advanced Drug Delivery Reviews*, 63(1–2), 3–23. <http://dx.doi.org/10.1016/j.addr.2010.12.005>.
- Cavallaro, G., Maniscalco, L., Campisi, M., Schillaci, D., & Giammona, G. (2007). Synthesis, characterization and in vitro cytotoxicity studies of a macromolecular conjugate of paclitaxel bearing oxytocin as targeting moiety. *European Journal of Pharmaceutics and Biopharmaceutics*, 66(2), 182–192. <http://dx.doi.org/10.1016/j.ejpb.2006.10.013>.
- Chen, S., Zhao, X., Chen, J., Chen, J., Kuznetsova, L., Wong, S. S., & Ojima, I. (2010). Mechanism-based tumor-targeting drug delivery system. Validation of efficient vitamin receptor-mediated endocytosis and drug release. *Bioconjugate Chemistry*, 21(5), 979–987. <http://dx.doi.org/10.1021/bc9005656>.
- Dai, Y., Cai, X., Bi, X., Liu, C., Yue, N., Zhu, Y. ... Qian, H. (2019). Synthesis and anti-cancer evaluation of folic acid-peptide-paclitaxel conjugates for addressing drug resistance. *European Journal of Medicinal Chemistry*, 171, 104–115. <http://dx.doi.org/10.1016/j.ejmech.2019.03.031>.
- Davis, C. (2019, September 18). *Cancer* [Web log post]. Retrieved from <http://www.medicinenet.com/cancer/article.htm#>.
- Elsadek, B., Graeser, R., Esser, N., Schäfer-Obodozie, C., Ajaj, K. A., Unger, C. ... Kratz, F. (2010). Development of a novel prodrug of paclitaxel that is cleaved by prostate-specific antigen: An in vitro and in vivo evaluation study. *European Journal of Cancer*, 46(18), 3434–3444. <http://dx.doi.org/10.1016/j.ejca.2010.08.018>.
- Fernandez, M., Javaid, F., & Chudasama, V. (2018). Advances in targeting the folate receptor in the treatment/imaging of cancers. *Chemical Science*, 9(4), 790–810. <https://doi.org/10.1039/C7SC04004K>.
- Florea, A. M., & Busselberg, D. (2011). Cisplatin as an anti-tumor drug: Cellular mechanisms of activity, drug resistance and induced side effects. *Cancers*, 3(1), 1351–1371. doi: 0.3390/cancers3011351
- Fortin, S., & Berube, G. (2013). Advances in the development of hybrid anticancer drugs. *Expert Opinion on Drug Discovery*, 8(8), 1029–1047. <http://dx.doi.org/10.1517/17460441.2013.798296>.
- Garraway, L. A., & Janne, P. A. (2012). Circumventing cancer drug resistance in the era of personalized medicine. *Cancer Discovery*, 2, 214–226. <http://dx.doi.org/10.1158/2159-8290.CD-12-0012>.
- Gaspar, V. M., Costa, E. C., Queiroz, J. A., Pichon, C., & Sousa, F. (2015). Folate-targeted multifunctional amino acid-chitosan nanoparticles for improved cancer therapy. *Pharmaceutical Research*, 32(2), 562–577. <http://dx.doi.org/10.1007/s11095-014-1486-0>.
- Gibiansky, L., & Gibiansky, E. (2014). Target-mediated drug disposition model and its approximations for antibody–drug conjugates. *Journal of Pharmacokinetics and Pharmacodynamics*, 41(1), 35–47. <http://dx.doi.org/10.1007/s10928-013-9344-y>.
- Gupta, Y., Jain, A., Jain, P., & Jain, S.K. (2007). Design and development of folate appended liposomes for enhanced delivery of 5-FU to tumor cells. *Journal of Drug Targeting*, 15(3), 231–240. <http://dx.doi.org/10.1080/10611860701289719>.
- Guo, W., Deng, L., Chen, Z., Chen, Z., Yu, J., Liu, H. ... Zhang, L. (2018). Vitamin B12-conjugated sericin micelles for targeting CD320-overexpressed gastric cancer and reversing drug resistance. *Nanomedicine*, 14(3), 353–370. <https://doi.org/10.2217/nnm-2018-0321>.
- He, R., & Yin, C. (2017). Trimethyl chitosan based conjugate for oral and intravenous delivery of paclitaxel. *Acta Biomaterial*, 53, 355–366. <http://dx.doi.org/10.1016/j.actbio.2017.02.012>.
- Henne, W. A., Kularatne, S. A., Hakenjos, J., Carron, J. D., & Henne, K. L. (2013). Synthesis and activity of a folate targeted mono-disperse PEG camptothecin conjugate. *Bioorganic & Medicinal Chemistry Letters*, 23(21), 5810–5813. <http://dx.doi.org/10.1016/j.bmcl.2013.08.113>.
- Ibsen, S., Zahavy, E., Wrasdilo, W., Berns, M., & Chan, M. (2010). A novel doxorubicin prodrug with controllable photolysis activation for cancer chemotherapy. *Pharmaceutical Research*, 27(9), 1848–1860. <http://dx.doi.org/10.1007/s11095-010-0183-x>.
- Iversen, T. G., Skotland, T., & Sandvig, K. (2011). Endocytosis and intracellular transport of nanoparticles: Present knowledge and need for future studies. *Nano today*, 6(2), 176–185. <http://dx.doi.org/10.1016/j.nantod.2011.02.003>.
- Iwata, R., Nakayama, F., Hirochi, S., Sato, K., Piao, W., Nishina, K. ... Wada, T. (2015). Synthesis and properties of vitamin E analog-conjugated neomycin for delivery of RNAi drugs to liver cells. *Bioorganic & Medicinal Chemistry Letters*, 25(4), 815–819. <http://dx.doi.org/10.1016/j.bmcl.2014.12.079>.
- Jung, J. H., & Keller, T. (2012). United States (12) Patent Application Publication (10) Pub. No.: US. 310126:A1.
- Leamon, C. P. (2008). Folate-targeted drug strategies for the treatment of cancer. *Current Opinion in Investigational Drugs*, 9(12), 1277–1286.
- Leamon, C. P., Vlahov I. R., Reddy, J. A., Vetzal, M., Santhapuram, H. K., You, F. ... Westrick, E. (2014). Folate-vinca alkaloid conjugates for cancer therapy: A structure-activity relationship. *Bioconjugate chemistry*, 25(3), 560–568. <http://dx.doi.org/10.1021/bc400441s>.
- Leamon, C. P., Reddy, J. A., Vlahov, I. R., Westrick, E., Dawson, A., Dorton, R. ... Wang, Y. (2007). Preclinical antitumor activity of a novel folate-targeted dual drug conjugate. *Molecular Pharmaceutics*, 4(5), 659–667. <https://doi.org/10.1021/mp070049c>.
- Mahato, R., Tai, W., & Cheng, K. (2011). Prodrugs for improving tumor-targetability and efficiency. *Advanced Drug Delivery Reviews*, 63(8), 659–670. <http://dx.doi.org/10.1016/j.addr.2011.02.002>.
- Naumann, R.W., & Coleman, R. L. (2011). Management strategies for recurrent platinum-resistant ovarian cancer. *Drugs*, 71(11), 1397–1412. <http://dx.doi.org/10.2165/11591720-000000000-00000>.
- Naumann, R. W., Coleman, R. L., Burger, R. A., Sausville, E. A., Kutarska, E., Ghamande, S. A. ... Gersh, R.H. (2013). PRECEDENT: A randomized phase II trial comparing vintafolide (EC145) and pegylated liposomal doxorubicin (PLD) in combination versus PLD alone in patients with platinum-resistant ovarian cancer. *Journal of Clinical Oncology*, 31(35), 4400–4406. <http://dx.doi.org/10.1200/JCO.2013.49.7685>.
- Ojima, I., Zuniga, E., Berger, W., & Seitz, J. (2012). Tumor-targeting drug delivery of new-generation taxoids. *Future Medicinal Chemistry*, 4(1), 33–50. <http://dx.doi.org/10.4155/fmc.11.167>.
- Padma, V. V. (2015). An overview of targeted cancer therapy. *Bio-Medicine*, 5(4). <http://dx.doi.org/10.7603/s40681-015-0019-4>.
- Patil, S., Gawali, S., Patil, S., & Basu, S. (2014). Synthesis, characterization and in vitro evaluation of novel vitamin D3 nanoparticles as a versatile platform for drug delivery in cancer therapy. *Journal of Material Chemistry B*, 5742. <https://doi.org/10.1039/C3TB21176B>.
- Palvai, S., Nagraj, J., Mapara, N., Chowdhury, R., & Basu, S. (2014). Dual drug loaded vitamin D3 nanoparticle to target drug resistance in cancer. *RSC Advances*, 4(100), 57271–57281. <http://dx.doi.org/10.1039/C4RA06475E>.



- Parhi, P., Mohanty, C., & Sahoo, S. K. (2012). Nanotechnology-based combinational drug delivery: an emerging approach for cancer therapy. *Drug Discovery Today*, 17(17-18), 1044–1052. <http://dx.doi.org/10.1016/j.drudis.2012.05.010>.
- Pawar, S. K., Badhwar, A. J., Kharas, F., Khandare, J. J., & Vavia, P. R. (2012). Design, synthesis and evaluation of N-acetyl glucosamine (NAG)–PEG–doxorubicin targeted conjugates for anticancer delivery. *International Journal of Pharmaceutics*, 436(1-2), 183–193. <http://dx.doi.org/10.1016/j.ijpharm.2012.05.078>.
- Pérez-Herrero, E., & Fernández-Medarde, A. (2015). Advanced targeted therapies in cancer: drug nanocarriers, the future of chemotherapy. *European Journal of Pharmaceutics and Biopharmaceutics*, 93, 52–79. <http://dx.doi.org/10.1016/j.ejpb.2015.03.018>.
- Persidis, A. (1999). Cancer multidrug resistance. *Nature Biotechnology*, 17(1), 94. <http://dx.doi.org/10.1038/5289>.
- Petros, R. A., & DeSimone, J. M. (2010). Strategies in the design of nanoparticles for therapeutic applications. *Nature Reviews Drug discovery*, 9(8), 615. <http://dx.doi.org/10.1038/nrd2591>.
- Pettenuzzo, A., Pigot, R., & Ronconi, L. (2017). Vitamin B12–metal conjugates for targeted chemotherapy and diagnosis: Current status and future prospects. *European Journal of Inorganic Chemistry*, (12), 1625–1638. <https://doi.org/10.1002/ejic.201601217>.
- Pinhassi, R. I., Assaraf, Y. G., Farber, S., Stark, M., Ickowicz, D., Drori, S. ... Livney, Y. D. (2009). Arabinoxylan– folic acid– drug conjugate for targeted delivery and target-activated release of anti-cancer drugs to folate receptor-overexpressing cells. *Biomacromolecules*, 11(1), 294–303. <http://dx.doi.org/10.1021/bm900853z>.
- Qu, C.Y., Zhou, M., Chen, Y. W., Chen, M. M., & Shen, F. (2015). Engineering of lipid prodrug-based, hyaluronic acid-decorated nanostructured lipid carriers platform for 5-fluorouracil and cisplatin combination gastric cancer therapy. *International Journal of Nanomedicine*, 10, 3911. <http://dx.doi.org/10.2147/IJN.S83211>.
- Rajendran, L., Knolker, H. J., & Simons, K. (2010). Subcellular targeting strategies for drug design and delivery. *Nature Reviews Drug Discovery*, 9(1), 29. <http://dx.doi.org/10.1038/nrd2897>.
- Reddy, J. A., Dorton, R., Westrick, E., Dawson, A., Smith, T., Xu, L. C. ... Leamon, C.P. (2007). Preclinical evaluation of EC145, a folate-vincristine alkaloid conjugates. *Cancer Research*, 67(9), 4434–4442. <http://dx.doi.org/10.1158/0008-5472.CAN-07-0033>.
- Reddy, J. A., Dorton, R., Dawson, A., Vetzl, M., Parker, N., Nicoson, J.S. ... Leamon, C.P. (2009). In vivo structural activity and optimization studies of folate– tubulysin conjugates. *Molecular Pharmaceutics*, 6(5), 1518–1525. <https://doi.org/10.1021/mp900086w>.
- Rijnboutt, S., Jansen, G., Posthuma, G., Hynes, J. B., & Schornagel, J. H. (1996). Endocytosis of GPI-linked membrane folate receptor- $\alpha$ . *The Journal of Cell Biology*, 132(1), 35–47. <http://dx.doi.org/10.1083/jcb.132.1.35>.
- Ruiz-Sánchez, P., König, C., Ferrari, S., & Alberto, R. (2011). Vitamin B 12 as a carrier for targeted platinum delivery: In vitro cytotoxicity and mechanistic studies. *Journal of Biological Inorganic Chemistry*, 16(1), 33–44. <http://dx.doi.org/10.1007/s00775-010-0697-z>.
- Russell-Jones, G., McTavish, K., & McEwan, J. (2011). Preliminary studies on the selective accumulation of vitamin-targeted polymers within tumors. *Journal of Drug Targeting*, 19(2), 133–139. <http://dx.doi.org/10.3109/10611861003734027>.
- Sausville, E., LoRusso, P., Quinn, M., Forman, K., Leamon, C., Morganstern, D. ... Messmann, R. (2007). A phase I study of EC145 administered weeks 1 and 3 of a 4-week cycle in patients with refractory solid tumors. *Journal of Clinical Oncology*, 25(18\_suppl), 2577. <http://dx.doi.org/10.1200/JCO.2011.41.4946>.
- Seifu, M. F., & Nath, L. K. (2019). Polymer-drug conjugates: novel carriers for cancer chemotherapy. *Polymer-Plastics Technology and Materials*, 58(2), 1158–1171. <https://doi.org/10.1080/0362559.2018.1466172>.
- Seitz, J. D., Vineberg, J. G., Herlihy, E., Park, B., & Melief, E. (2015). Design, synthesis and biological evaluation of a highly potent and cancer cell selective folate-taxoid conjugate. *Bioorganic & Medicinal Chemistry*, 23(12), 2187–2194. <http://dx.doi.org/10.1016/j.bmc.2015.02.057>.
- Siega, P., Wuerges, J., Arena, F., Gianolio, E., Fedosov, S.N., Dreos, R. ... Randaccio, L. (2009). Release of toxic Gd<sup>3+</sup> ions to tumour cells by vitamin B12 bioconjugates. *Chemistry–A European Journal*, 15(32), 7980–7989. <http://dx.doi.org/10.1002/chem.200802680>.
- Sutherland, J. C., & Griffin, K. P. (1981). Absorption spectrum of DNA for wavelengths greater than 300 nm. *Radiation Research*, 86(3), 399–410. <http://dx.doi.org/10.2307/3575456>.
- Tran, M. T., Stürup, S., Lambert, I. H., Gammelgaard, B., & Furger, E. (2016). Cellular uptake of metallatedcobalamins. *Metallomics*, 8(3), 298–304. <http://dx.doi.org/10.1039/c5mt00272a>.
- Tripodo, G., Mandracchia, D., Collina, S., Rui, M., & Rossi, D. (2014). New perspectives in cancer therapy: the biotin-antitumor molecule conjugates. *Medicinal Chemistry*, 8, 1–4. <http://dx.doi.org/10.4172/2161-0444.S1-004>.
- Vlahov, I. R., & Leamon, C. P. (2012). Engineering folate–drug conjugates to target cancer: from chemistry to clinic. *Bioconjugate Chemistry*, 23(7), 1357–1369. <http://dx.doi.org/10.1021/bc2005522>.
- Vlahov, I. R., Leamon, C. P., Parker, M. A., Howard, S. J., Santhapuram, H. K., Satyam, A., & Reddy, J. A. (2009). Inventors; Endocytel Inc, assignee. Vitamin receptor binding drug delivery conjugates, United States patent US 7,601,332.
- Wang, X., Li, J., Wang, Y., Koenig, L., Gjyzezi, A., Giannakakou, P. ... Shin, D. M. (2011). A folate receptor-targeting nanoparticle minimizes drug resistance in a human cancer model. *ACS Nano*, 5(8), 6184–6194. <http://dx.doi.org/10.1021/nn200739q>.
- Wang, Y., Li, P., Chen, L., Gao, W., & Zeng, F. (2015). Targeted delivery of 5-fluorouracil to HT-29 cells using high efficient folic acid-conjugated nanoparticles. *Drug Delivery*, 22(2), 191–198. <http://dx.doi.org/10.3109/10717544.2013.875603>.
- Yuxuan, D., Xingguang, C., Xinzhou, B., Chunxia, L., Na, Y., Ying, Z., Jiaqi, Z., & Mian, F. (2019). Synthesis and anti-cancer evaluation of folic acid-peptide- paclitaxel conjugates for addressing drug resistance. *European Journal of Medicinal Chemistry*, 171, 104–115. doi: 10.1016/j.ejmech.2019.03.031

# 50<sup>th</sup> Volume Index

## REVIEWER LIST - 2020

in issues April 2020 - December 2020

- A. Alper Öztürk  
Adriano G.Cruz  
Adriano Mollica  
Affe Mat  
Ahmet Ada  
Ali Sağırođlu  
Alper Okyar  
Ayfer Ülgenal  
Ayhan Savaşer  
Aylin Döğen  
Aylin Üstündağ  
Ayse Birteksöz Tan  
Aysel Berkkan  
Ayşe İstanbullu Tosun  
Ayşegül Peksel  
Bahar Sökmen  
Belen Şirinođlu Çapan  
Bengi Uslu  
Berna Özbek  
Berna Terziođlu  
Betül Arıca  
Betül Demirci  
Betül Sever Yılmaz  
Burcu Mesut  
CĂÇNdida Lopes Alves  
Çağrı Karaburun  
Çetin Taş  
Deniz Kaleli Durman  
Didem Şöhretođlu  
Dilek Bilgiç Alkaya  
Durişehvar Ünal  
Elif Özdemir  
Emine Alarçin  
Emirhan Nemutlu  
Eren Özçağlı  
Erkan Rayaman  
Erol Şener  
Esra Erođlu Özkan  
Ezgi Öztaş  
Fatih Göğer  
Feramuz Özdemir  
Genada Sinani  
Gergo Toth  
Gizem Bulut  
Gökçe Şeker Karatoprak  
Gökçe Topal Tanyılmaz  
Gökçen Yaşayan  
Gülay Ecevit-Genç
- Gülay Melikođlu,  
Gülderen Yılmaz  
Gülen Kaya  
Gülin Amasya  
Gülşah Gedik  
Günay Yetik Anacak  
HAKEM LİSTESİ  
Hasan Kırmızıbekmez  
Hassan Farghali  
Hassan Y.Boul-Enein  
Hülya Yılmaz Aydođan,  
Işık Özgüney  
İbrahim Çağatay Uzuner  
İlkay Alp Yıldırım  
İlkay Küçükğüzel  
İlkay Yıldız  
İman Fatemi  
İmren Esentürk  
İpek Süntar  
İsmail Öçsoy  
İsmail Yener  
Kritsanee Saramunee  
Leyla Bitiş  
M. F. Mahomoodally  
Malgorzata Dolowy  
Mariadhas Valan Arasu  
Marwa Ragab  
Mehdi Hassanshahian  
Mehdi Khoshneviszadeh  
Mehmet Alp  
Mehmet Boğa  
Mehmet Yaltrık  
Melike Sessevmez  
Meltem Ocak,  
Mine Özyazıcı  
Mohamed A Zayed  
Mohamed M.Abdel-Daim  
Mosad A.Ghareeb  
Muhammad Abuzar Ghaffari  
Muna Jalal Ali  
Murat Palabiyik  
Narin Öztürk  
Naveen Singhal  
Neslihan Saki  
Neslihan Üstündağ Okur  
Nihan Cankara  
Nur Tan  
Nuray Ari
- Nuray Ulusoy Güzeldemirci  
Nurten Özsoy  
Olgica Stefanovic,  
Oya Kerimođlu  
Özge Ülker  
Özgür Eşim  
Özlem Atlı Ekliođlu  
Özlem Bahadır Acıkara  
Özlem Saçan  
Özlem Saçan  
Panoraia Siafaka  
Pelin Yüksel Mayda  
Raffaele Capasso  
Raj Patil  
Refiye Yanardağ  
Rıza Binzet  
Santosh Karn  
Sara Thomas  
Sarvesh Bohrey  
Sedef Erdal  
Seher Birteksöz Tan  
Seher Karslı Cepciođlu  
Selma Şahin  
Sena Sezen  
Serap Sağlık Aslan  
Sevgi Karakuş  
Sıdika Toker  
Sibel Özden  
Sibel Özkan  
Sinem Ilgın  
Suna Erdođan  
Süleyman Demiryas  
Şengül Uysal  
Teresa Garnatj  
Tijen Önkol  
Tuğba Yılmaz Özden  
Tuğrul Körüklü  
Ufuk Kolak  
Ülkü Ündeger Bucurgat  
Violeta D.Mitic  
Vittthal Chaware  
Yeşim Karasulu  
Yeşim Kaya Yaşar  
Yeter Yeşil  
Zeliha Pala Kara  
Zeynep Aydoğmuş